Quantum Science and Technology

Renato Portugal

Quantum Walks and Search Algorithms

Second Edition

Springer

Quantum Science and Technology

Series editors

Raymond Laflamme, Waterloo, Canada
Gaby Lenhart, Sophia Antipolis, France
Daniel Lidar, Los Angeles, USA
Arno Rauschenbeutel, Vienna, Austria
Renato Renner, Zürich, Switzerland
Maximilian Schlosshauer, Portland, USA
Yaakov S. Weinstein, Princeton, USA
H. M. Wiseman, Brisbane, Australia

Aims and Scope

The book series Quantum Science and Technology is dedicated to one of today's most active and rapidly expanding fields of research and development. In particular, the series will be a showcase for the growing number of experimental implementations and practical applications of quantum systems. These will include, but are not restricted to: quantum information processing, quantum computing, and quantum simulation; quantum communication and quantum cryptography; entanglement and other quantum resources; quantum interfaces and hybrid quantum systems; quantum memories and quantum repeaters; measurement-based quantum control and quantum feedback; quantum nanomechanics, quantum optomechanics and quantum transducers; quantum sensing and quantum metrology; as well as quantum effects in biology. Last but not least, the series will include books on the theoretical and mathematical questions relevant to designing and understanding these systems and devices, as well as foundational issues concerning the quantum phenomena themselves. Written and edited by leading experts, the treatments will be designed for graduate students and other researchers already working in, or intending to enter the field of quantum science and technology.

More information about this series at http://www.springer.com/series/10039

Renato Portugal

Quantum Walks and Search Algorithms

Second Edition

Springer

Renato Portugal
National Laboratory of Scientific
Computing (LNCC)
Petrópolis, Brazil

ISSN 2364-9054 ISSN 2364-9062 (electronic)
Quantum Science and Technology
ISBN 978-3-319-97812-3 ISBN 978-3-319-97813-0 (eBook)
https://doi.org/10.1007/978-3-319-97813-0

Library of Congress Control Number: 2018950813

1st edition: © Springer Science+Business Media New York 2013
2nd edition: © Springer Nature Switzerland AG 2018
This work is subject to copyright. All rights are reserved by the Publisher, whether the whole or part of the material is concerned, specifically the rights of translation, reprinting, reuse of illustrations, recitation, broadcasting, reproduction on microfilms or in any other physical way, and transmission or information storage and retrieval, electronic adaptation, computer software, or by similar or dissimilar methodology now known or hereafter developed.
The use of general descriptive names, registered names, trademarks, service marks, etc. in this publication does not imply, even in the absence of a specific statement, that such names are exempt from the relevant protective laws and regulations and therefore free for general use.
The publisher, the authors and the editors are safe to assume that the advice and information in this book are believed to be true and accurate at the date of publication. Neither the publisher nor the authors or the editors give a warranty, express or implied, with respect to the material contained herein or for any errors or omissions that may have been made. The publisher remains neutral with regard to jurisdictional claims in published maps and institutional affiliations.

This Springer imprint is published by the registered company Springer Nature Switzerland AG
The registered company address is: Gewerbestrasse 11, 6330 Cham, Switzerland

To my father (in memoriam)

Preface

This is a textbook about *quantum walks* and *quantum search algorithms*. The readers will take advantage of the pedagogical aspects and learn the topics faster and make less effort than reading the original research papers, often too convoluted. The exercises and references allow the readers to deepen their knowledge on specific issues. Guidelines to use or to develop computer programs for simulating the evolution of quantum walks are also available.

Almost nothing can be extracted from this book if the reader is unfamiliar with the postulates of quantum mechanics, described in the second chapter, and the material on linear algebra described in Appendix A. Some extra bases are required: It is desirable that the reader has (1) notions of quantum computing, including the circuit model, references of which are provided at the end of Appendix A, (2) notions of graph theory, references of which are provided at the end of Appendix B, and (3) notions of classical algorithms and computational complexity. Any undergraduate or graduate student with this background can read this book. Some topics addressed in this second edition are currently active research areas with impact on the development of new quantum algorithms. Because of that, researchers working with quantum computing may find this book useful.

The second edition brings at least three main novelties: (1) a new chapter on the staggered quantum walk model—Chap. 8, (2) a new chapter on the element distinctness problem—Chap. 10, and (3) a new appendix on graph theory—Appendix B. Besides, the chapter on quantum-walk-based search algorithm—Chap. 9—was rewritten, the presentation has been simplified, and new material has been included.

Corrections, suggestions, and comments are welcome, which can be sent through Web page (qubit.lncc.br) or directly to the author by email (portugal@lncc.br).

Petrópolis, RJ, Brazil Renato Portugal

Acknowledgements

I am grateful to many people, including colleagues, graduate students, and the group of quantum computing of LNCC, friends and coauthors in research papers, projects, and conference organization. I am also grateful to many researchers for exchanging ideas in conferences and in collaborations. Some of them helped by reviewing, giving essential suggestions, and spending time on this project, in special, Drs. Stefan Boettcher, Norio Konno, Raqueline Santos, and Etsuo Segawa.

In January and February 2018, I gave a short course on quantum-walk-based search algorithms at the Tohoku University under the invitation of Dr. Etsuo Segawa. I thank the students and researchers that attended the course, who raised interesting discussion topics, helping to improve some chapters of the new edition of this book.

I thank Tom Spicer and Cindy Zitter from Springer for encouraging me to write the second edition, which turned out to be an opportunity for fixing many problems of the first edition and improving the book by adding new material. I hope to have introduced fewer problems this time.

I thank the support of the National Laboratory of Scientific Computing (LNCC), the funding agencies CNPq, CAPES, and FAPERJ, and the scientific societies SBMAC and SBC.

Last but not least, from the bottom of my heart, I thank my family, wife and sons, for giving support and amplifying my inner motivation.

Contents

1 Introduction 1

2 The Postulates of Quantum Mechanics 5
- 2.1 State Space 5
  - 2.1.1 State Space Postulate 7
- 2.2 Unitary Evolution 8
  - 2.2.1 Evolution Postulate 8
- 2.3 Composite Systems 11
- 2.4 Measurement Process 12
  - 2.4.1 Measurement Postulate 12
  - 2.4.2 Measurement in the Computational Basis 14
  - 2.4.3 Partial Measurement in the Computational Basis 16

3 Introduction to Quantum Walks 19
- 3.1 Classical Random Walk on the Line 19
- 3.2 Classical Discrete-Time Markov Chains 23
- 3.3 Coined Quantum Walks 25
  - 3.3.1 Coined Walk on the Line 26
- 3.4 Classical Continuous-Time Markov Chains 33
- 3.5 Continuous-Time Quantum Walks 35
  - 3.5.1 Continuous-Time Walk on the Line 35
  - 3.5.2 Why Must Time be Continuous? 38

4 Grover's Algorithm and Its Generalization 41
- 4.1 Grover's Algorithm 42
- 4.2 Quantum Circuit of Grover's Algorithm 44
- 4.3 Analysis of the Algorithm Using Reflection Operators 45
- 4.4 Analysis Using the Two-Dimensional Real Space 50
- 4.5 Analysis Using the Spectral Decomposition 52
- 4.6 Optimality of Grover's Algorithm 53
- 4.7 Search with Repeated Elements 59

4.7.1 Analysis Using Reflection Operators 60
4.7.2 Analysis Using the Reduced Space 62
4.8 Amplitude Amplification 63
4.8.1 The Technique 64

5 Coined Walks on Infinite Lattices 69
5.1 Hadamard Walk on the Line 69
5.1.1 Fourier Transform 71
5.1.2 Analytic Solution 75
5.1.3 Other Coins 78
5.2 Two-Dimensional Lattice 79
5.2.1 The Hadamard Coin 81
5.2.2 The Fourier Coin 82
5.2.3 The Grover Coin 83
5.2.4 Standard Deviation 84
5.3 Quantum Walk Packages 85

6 Coined Walks with Cyclic Boundary Conditions 89
6.1 Cycles 89
6.1.1 Fourier Transform 91
6.1.2 Analytic Solutions 94
6.1.3 Periodic Solutions 97
6.2 Finite Two-Dimensional Lattices 98
6.2.1 Fourier Transform 100
6.2.2 Analytic Solutions 104
6.3 Hypercubes 106
6.3.1 Fourier Transform 108
6.3.2 Analytic Solutions 114
6.3.3 Reducing a Hypercube to a Line Segment 115

7 Coined Quantum Walks on Graphs 125
7.1 Quantum Walks on Class-1 Regular Graphs 126
7.2 Coined Quantum Walks on Arbitrary Graphs 127
7.2.1 Locality 129
7.2.2 Grover Quantum Walk 130
7.2.3 Coined Walks on Cayley Graphs 131
7.2.4 Coined Walks on Multigraphs 132
7.3 Dynamics and Quasi-periodicity 132
7.4 Perfect State Transfer and Fractional Revival 137
7.5 Limiting Probability Distribution 139
7.5.1 Limiting Distribution Using the Fourier Basis 142
7.5.2 Limiting Distribution of QWs on Cycles 143
7.5.3 Limiting Distribution of QWs on Hypercubes 147
7.5.4 Limiting Distribution of QWs on Finite Lattices 150

7.6 Distance Between Distributions 152
7.7 Mixing Time 155
7.7.1 Instantaneous Uniform Mixing (IUM) 156

8 Staggered Model 159
8.1 Graph Tessellation Cover 159
8.2 The Evolution Operator 161
8.3 Staggered Walk on the Line 163
8.3.1 Fourier Analysis 167
8.3.2 Standard Deviation 169

9 Spatial Search Algorithms 175
9.1 Quantum-Walk-Based Search Algorithms 176
9.2 Analysis of the Time Complexity 178
9.2.1 Case $B = 0$ 182
9.2.2 Tulsi's Modification 183
9.3 Finite Two-Dimensional Lattices 186
9.3.1 Tulsi's Modification of the Two-Dimensional Lattice 191
9.4 Hypercubes 192
9.5 Grover's Algorithm as Spatial Search on Graphs 195
9.5.1 Grover's Algorithm in terms of the Coined Model 195
9.5.2 Grover's Algorithm in terms of the Staggered Model 197
9.5.3 Complexity Analysis of Grover's Algorithm 198

10 Element Distinctness 201
10.1 Classical Algorithms 202
10.2 Naïve Quantum Algorithms 202
10.3 The Optimal Quantum Algorithm 203
10.3.1 Analysis of the Algorithm 207
10.3.2 Number of Queries 216
10.3.3 Example 218

11 Szegedy's Quantum Walk 223
11.1 Discrete-Time Markov Chains 223
11.2 Markov Chain-Based Quantum Walk 224
11.3 Evolution Operator 227
11.4 Singular Values and Vectors of the Discriminant 228
11.5 Eigenvalues and Eigenvectors of the Evolution Operator 230
11.6 Quantum Hitting Time 234
11.7 Searching Instead of Detecting 237
11.8 Example: Complete Graphs 237
11.8.1 Probability of Finding a Marked Element 242

Appendix A: Linear Algebra for Quantum Computation 247
Appendix B: Graph Theory for Quantum Walks 271
Appendix C: Classical Hitting Time 281
References 289
Index 303

Chapter 1
Introduction

Quantum mechanics has changed the way we understand the physical world and has introduced new ideas that are difficult to accept, not because they are complex, but because they are different from what we are used to in our everyday lives. Those new ideas can be collected in four postulates or laws. It is hard to believe that Nature works according to those laws, and the difficulty starts with the notion of the superposition of contradictory possibilities. Do you accept the idea that a billiard ball could rotate around its axis in both directions at the same time?

Quantum computation was born from this kind of idea. We know that digital classical computers work with zeroes and ones and that the value of the bit cannot be zero and one at the same time. The classical algorithms must obey Boolean logic. So, if the coexistence of bit-0 and bit-1 is possible, which logic should the algorithms obey?

Quantum computation was born from a paradigm change. Information storage, processing, and transmission obeying quantum mechanical laws allowed the development of new algorithms, faster than the classical analogues, which can be implemented in physics laboratories. Nowadays, quantum computation is a well-established area with important theoretical results within the context of the theory of computing, as well as in terms of physics, and has raised huge engineering challenges to the construction of the quantum hardware.

The majority of people, who are not familiar with the area and talk about quantum computers, expect that the hardware development would obey the famous Moore's law, valid for classical computer development for fifty years. Many of those people are disappointed to learn about the enormous theoretical and technological difficulties to be overcome to harness and control quantum systems whose tendency is to behave classically. On the one hand, the quantum CPU must be large enough and must stay coherent long enough to allow at least thousands of steps in order to produce a nontrivial output.

The processing of classical computers is very stable. Depending on the calculation, an inversion of a single bit could invalidate the entire process. But we know that long computations, which require inversion of billions of bits, are performed without problems. Classical computers are unerring because its basic components

© Springer Nature Switzerland AG 2018

R. Portugal, *Quantum Walks and Search Algorithms*, Quantum Science and Technology, https://doi.org/10.1007/978-3-319-97813-0_1

are stable. Consider, for example, a mechanical computer. It would be very unusual for a mechanical device to change its position, especially if we put a spring to keep it stable in the desired position. The same is true for electronic devices, which remain in their states until an electrical pulse of sufficient power changes this. Electronic devices are built to operate at a power level well above the noise, and this noise is kept low by dissipating heat into the environment.

The laws of quantum mechanics require that the physical device must be isolated from the environment; otherwise the superposition vanishes, at least partially. It is too difficult a task to isolate macroscopic physical systems from their environment. Ultra-relativistic particles and gravitational waves pass through any blockade, penetrate into the most guarded places, obtain information, and convey it out of the system. This process is equivalent to a measurement of a quantum observable, which often collapses the superposition and slows down the quantum computer, making it almost, or entirely, equivalent to the classical one. Theoretical results show that there are no fundamental issues against the possibility of building quantum hardware. It is a matter of technological difficulty.

There is no point in building quantum computers if we are going to use them in the same way we use classical computers. Algorithms must be rewritten, and new techniques for simulating physical systems must be developed. The task is more difficult than for classical computers. So far, we do not have a quantum programming language. Also, quantum algorithms must be developed using concepts of linear algebra. Quantum computers with a large enough number of qubits are not available, as yet, slowing down the development of simulations. At the moment that the second edition of this book is to be released, Google and IBM and Intel have built universal quantum computers with 72 and 50 and 49 qubits, respectively, using superconducting electronic circuits which need temperatures as low as one-tenth of one Kelvin or around one-thirtieth of the temperature in deep space. Despite those impressive achievements, the coherence time announced by IBM is around 90 ms, not enough yet.

The quantum walk (QW) is a powerful technique for building quantum algorithms and for simulating complex quantum systems. Quantum walks were developed in the beginning as the quantum version of the classical random walk, which requires the tossing of a coin to determine the direction of the next step. The laws of quantum mechanics state that the evolution of an isolated quantum system is deterministic. Randomness shows up only when the system is measured and classical information is obtained. This explains why the name "quantum random walk" is seldom used. The coined model evolves at discrete time steps on a discrete space, which is modeled by a graph. The coined model is not the only discrete-time version of quantum walks. In fact, there is a coinless version called staggered model, which uses an evolution operator defined by partitioning the vertex set. Besides, there is a continuous-time version, which has been extensively studied.

The richness of the area has attracted the attention of the scientific community, and the interest has increased significantly in the last years. Good parameters to test this statement are shown in Fig. 1.1, which depicts the number of paper with the tag "quantum walk" either in the title or in the topics returned after querying the

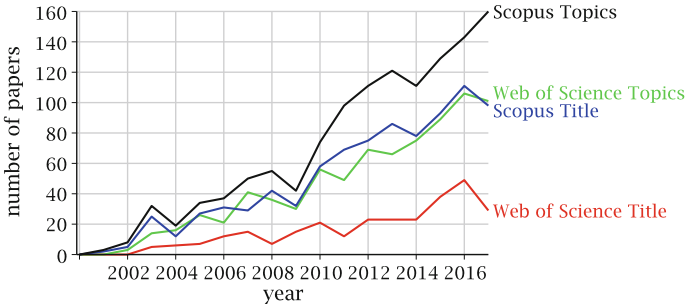

Fig. 1.1 Number of papers with the tag "quantum walk" in the title and in the topics returned by Scopus and Web of Science from 2000 to 2017

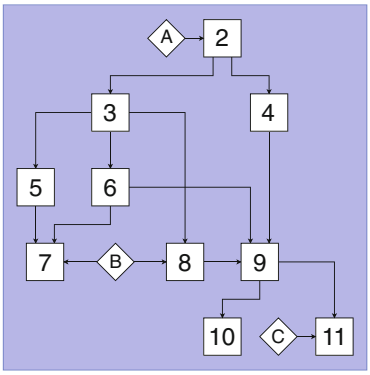

2	quantum mechanics
3	introduction to QW
4	Grover
5	QW on infinite lattices
6	QW on finite lattices
7	QW on graphs
8	staggered
9	search
10	element distinctness
11	Szegedy
A	linear algebra
B	graph theory
C	classical hitting time

Fig. 1.2 Flowchart of the chapter dependencies

databases Scopus and Web of Science. It is easy to see that the number of papers is increasing as a superlinear function.

This book starts by describing in Chap. 2 the set of postulates of quantum mechanics, which is one of the pillars of quantum computation. Chapter 2 is a gentle introduction to quantum walks with the goal of describing how the coined and the continuous-time models can be obtained by quantizing classical random walks and classical continuous-time Markov chains, respectively. Chapter 4 describes the Grover algorithm, its generalization when there is more than one marked element, and its optimality. At the heart of the Grover algorithm lies the amplitude amplification technique, which is addressed at the end of the chapter. Chapters 5 and 6 are devoted to the coined model on lattices and hypercubes. Quantum walks on infinite lattices and lattices with cyclic boundary conditions with one and two dimensions are analyzed in detail using the Fourier transform. Chapter 7 defines coined quantum walks on arbitrary graphs and analyzes the limiting probability distribution and mixing time. Chapter 8 is new to the second edition of this book and describes the staggered quantum walk model and the analytic calculation of the position standard deviation of a staggered walk

on the line. Chapter 9 describes quantum-walk-based spatial search algorithms and has been remodeled in this edition. Readers will benefit from the efficacious presentation. Chapter 10 is also new to this edition and describes the optimal algorithm that solves the element distinctness problem. Finally, Chap. 11 describes Szegedy's quantum walk model and the definition of quantum hitting time. The flowchart of Fig. 1.2 shows the chapter dependencies.

There are three appendices. Appendix A compiles the main definitions of linear algebra used in this book. Appendix B compiles the main definitions of graph theory used in the area of quantum walks. Appendix C addresses the classical hitting time, which is useful to the definition of Szegedy's model. The dependencies on the appendices are also shown in Fig. 1.2

Chapter 2
The Postulates of Quantum Mechanics

It is impossible to present quantum mechanics in few pages. Since the goal of this book is to describe quantum algorithms, we limit ourselves to the *principles* of quantum mechanics and describe them as "game rules." Suppose you have played checkers for many years and know several strategies, but you really do not know chess. Suppose now that someone describes the chess rules. Soon you will be playing a new game. Certainly, you will not master many chess strategies, but you will be able to play. This chapter has a similar goal. The postulates of a theory are its game rules. If you break the rules, you will be out of the game.

At best, we can focus on four postulates. The first describes the arena where the game goes on. The second describes the dynamics of the process. The third describes how we adjoin various systems. The fourth describes the process of physical measurement. All these postulates are described in terms of linear algebra. It is essential to have a solid understanding of the basic results in this area. Moreover, the postulate of composite systems uses the concept of tensor product, which is a method of combining two vector spaces to build a larger one. This concept must be mastered.

2.1 State Space

The *state* of a physical system describes its physical characteristics at a given time. Usually, we describe some possible features that the system can have because, otherwise, the physical problems would be too complex. For example, the spin state of a billiard ball can be characterized by a vector in $\mathbb{R}^3$. In this example, we disregard the linear velocity of the billiard ball, its color or any other characteristics that are not directly related to its rotation. The spin state is completely characterized by the axis direction, the rotation direction, and rotation intensity. The spin state can be described by three real numbers that are the entries of a vector, whose direction

© Springer Nature Switzerland AG 2018

R. Portugal, *Quantum Walks and Search Algorithms*, Quantum Science and Technology, https://doi.org/10.1007/978-3-319-97813-0_2

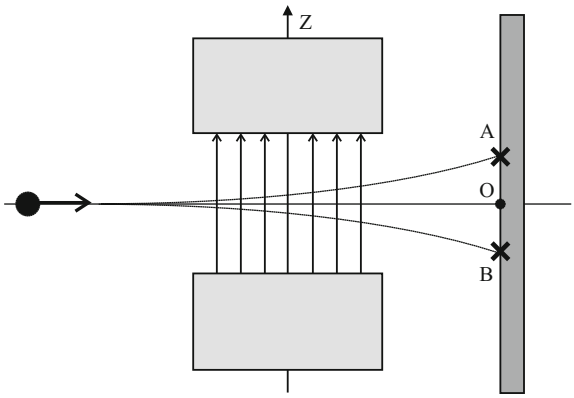

Fig. 2.1 Scheme of an experimental device to measure the spin state of an electron. The electron passes through a nonuniform magnetic field in the vertical direction. It hits A or B depending on the rotation direction. The distance of the points A and B from point O depends on the rotation speed. The results of this experiment are quite different from what we expect classically

characterizes the rotation axis, whose sign describes to which side of the billiard ball is spinning, and whose length characterizes the speed of rotation. In classical physics, the direction of the rotation axis can vary continuously, as well as the rotation intensity.

Does an *electron*, which is considered an elementary particle, i.e., not composed of other smaller particles, rotates like a billiard ball? The best way to answer this is by experimenting in real settings to check whether the electron in fact rotates and whether it obeys the laws of classical physics. Since the electron has charge, its rotation would produce magnetic fields that could be measured. Experiments of this kind were performed at the beginning of quantum mechanics, with beams of silver atoms, later on with beams of hydrogen atoms, and today they are performed with individual particles (instead of beams), such as electrons or photons. The results are different from what is expected by the laws of the classical physics.

We can send the electron through a magnetic field in the vertical direction (direction z), according to the scheme of Fig. 2.1. The possible results are shown. Either the electron hits the screen at the point A or point B. One never finds the electron at point O, which means no rotation. This experiment shows that the *spin* of the electron only admits two values: *spin up* and *spin down* both with the same intensity of "rotation." This result is quite different from what is expected classically since the direction of the rotation axis is quantized, admitting only two values. The rotation intensity is also quantized.

Quantum mechanics describes the electron spin as a unit vector in the Hilbert space $\mathbb{C}^2$. The *spin up* is described by the vector

$$|0\rangle = \begin{bmatrix} 1 \\ 0 \end{bmatrix}$$

and the *spin down* by the vector

$$|1\rangle = \begin{bmatrix} 0 \\ 1 \end{bmatrix}.$$

This seems a paradox because vectors $|0\rangle$ and $|1\rangle$ are orthogonal. Why use orthogonal vectors to describe *spin up* and *spin down*? In $\mathbb{R}^3$, if we add *spin up* and *spin down*, we obtain a rotationless particle because the sum of two opposite vectors of equal length gives the zero vector, which describes the absence of rotation. In the classical world, we cannot rotate a billiard ball to both sides at the same time. We have two mutually excluded situations, and we apply the law of excluded middle. The notions of spin up and spin down of billiard balls refer to $\mathbb{R}^3$, whereas quantum mechanics describes the behavior of the electron before the observation, that is, before entering the magnetic field, which aims to determine its state of rotation.

If the electron has not entered the magnetic field and if it is somehow isolated from the macroscopic environment, its spin state is described by a linear combination of vectors $|0\rangle$ and $|1\rangle$

$$|\psi\rangle = a_0|0\rangle + a_1|1\rangle, \tag{2.1}$$

where the coefficients a_0 and a_1 are complex numbers that satisfy the constraint

$$|a_0|^2 + |a_1|^2 = 1. \tag{2.2}$$

Since vectors $|0\rangle$ and $|1\rangle$ are orthogonal, the sum does not result in the zero vector. Excluded situations in classical physics can coexist in quantum mechanics. This coexistence is destroyed when we try to observe it using the device shown in Fig. 2.1. In the classical case, the spin state of an object is independent of the choice of the measuring apparatus and, in principle, has not changed after the measurement. In the quantum case, the spin state of the particle is a mathematical idealization which depends on the choice of the measuring apparatus to have a physical interpretation and, in principle, suffers irreversible changes after the measurement. The quantities $|a_0|^2$ and $|a_1|^2$ are interpreted as the probability of detection of spin up or down, respectively.

2.1.1 State Space Postulate

An *isolated physical system* has an associated Hilbert space, called the *state space*. The state of the system is fully described by a unit vector, called the *state vector* in that Hilbert space.

Notes

1. The postulate does not tell us the Hilbert space we should use for a given physical system. In general, it is not easy to determine the dimension of the Hilbert space of the system. In the case of electron spin, we use the Hilbert space of dimension 2

because there are only two possible results when we perform an experiment to determine the vertical electron spin. More complex physical systems admit more possibilities, which can be an infinite number.

2. A system is isolated or *closed* if it does not influence and is not influenced by the outside. In principle, the system need not be small, but it is easier to isolate small systems with few atoms. In practice, we can only deal with approximate isolated systems, so the state space postulate is an idealization.

The state space postulate is impressive, on the one hand, but deceiving, on the other hand. The postulate admits that classically incompatible states coexist in superposition, such as rotating to both sides simultaneously, but this occurs only in isolated systems, that is, we cannot see this phenomenon, as we are on the outside of the insulation (let us assume that we are not *Schrödinger's cat*). A second restriction demanded by the postulate is that quantum states must have unit norm. The postulate constraints show that the quantum superposition is not absolute, i.e., is not the way we understand the classical superposition. If quantum systems admit a kind of superposition that could be followed classically, the quantum computer would have available an exponential amount of parallel processors with enough computing power to solve the problems in *class NP-complete*.[1] It is believed that the quantum computer is exponentially faster than the classical computer only in a restricted class of problems.

2.2 Unitary Evolution

The goal of physics is not simply to describe the state of a physical system at a present time; rather the main objective is to determine the state of this system at future times. A theory makes predictions that can be verified or falsified by physical experiments. This is equivalent to determining the dynamical laws the system obeys. Usually, these laws are described by differential equations, which govern the time evolution of the system.

2.2.1 Evolution Postulate

The *time evolution* of an isolated quantum system is described by a *unitary transformation*. If the state of the quantum system at time t_1 is described by vector $|\psi_1\rangle$, the system state $|\psi_2\rangle$ at time t_2 is obtained from $|\psi_1\rangle$ by a unitary transformation U, which depends only on t_1 and t_2, as follows:

[1]The class NP-complete consists of the most difficult problems in the class NP (*nondeterministic polynomial*). The class NP is defined as the class of computational problems that have solutions whose correctness can be "quickly" verified.

$$|\psi_2\rangle = U|\psi_1\rangle. \tag{2.3}$$

Notes

1. The action of a unitary operator on a vector preserves its norm. Thus, if $|\psi\rangle$ is a unit vector, $U|\psi\rangle$ is also a unit vector.
2. A *quantum algorithm* is a prescription of a sequence of unitary operators applied to an initial state takes the form

$$|\psi_n\rangle = U_n \cdots U_1|\psi_1\rangle.$$

   The qubits in state $|\psi_n\rangle$ are measured, returning the result of the algorithm. Before measurement, we can obtain the initial state from the final state because unitary operators are invertible.
3. The evolution postulate is to be written in the form of a differential equation, called *Schrödinger equation*. This equation provides a method to obtain operator U once given the physical context. Since the goal of physics is to describe the dynamics of physical systems, the Schrödinger equation plays a fundamental role. The goal of computer science is to analyze and implement algorithms, so the computer scientist wants to know if it is possible to implement some form of a unitary operator previously chosen. Equation (2.3) is useful for the area of quantum algorithms.

Let us analyze a second experimental device. It will help to clarify the role of unitary operators in quantum systems. This device uses *half-silvered mirrors* with 45° incident light, which transmit 50% of incident light and reflect 50%. If a single photon hits the mirror at 45°, with probability 1/2, it keeps the direction unchanged, and with probability 1/2, it is reflected. These half-silvered mirrors have a layer of glass that can change the phase of the wave by 1/2 wavelength. The complete device consists of a source that can emit one photon at a time, two half-silvered mirrors, two fully reflective mirrors, and two photon detectors, as shown in Fig. 2.2. By tuning the device, the result of the experiment shows that 100% of the light reaches detector 2.

There is no problem explaining the result using the interference of electromagnetic waves in the context of the *classical physics* because there is a phase change in the

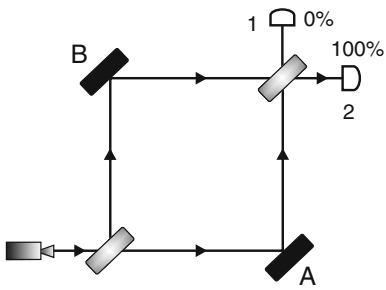

Fig. 2.2 Schematic drawing of an experimental device, which consists of a light source, two half-silvered mirrors, fully reflective mirrors A and B, detectors 1 and 2. The interference produced by the last half-silvered mirror makes all light to go to the detector 2

light beam that goes through one of the paths producing a destructive interference with the beam going to the detector 1 and constructive interference with the beam going to the detector 2. However, if the light intensity emitted by the source is decreased such that one photon is emitted at a time, this explanation fails. If we insist on using classical physics in this situation, we predict that 50% of the photons would be detected by detector 1 and 50% by detector 2 because the photon either goes through the mirror A or goes through B, and it is not possible to interfere since it is a single photon.

In *quantum mechanics*, if the set of mirrors is isolated from the environment, the two possible paths are represented by two orthonormal vectors $|0\rangle$ and $|1\rangle$, which generate the state space that describes the possible paths to reach the photon detector. Therefore, a photon can be in the superposition of "*path A*," described by $|0\rangle$, and "*path B*," described by $|1\rangle$. This is the application of the first postulate. The next step is to describe the dynamics of the process. How is this done and what are the unitary operators in the process? In this experiment, the dynamics are produced by the half-silvered mirrors, since they generate the paths. The action of the half-silvered mirrors on the photon must be described by a unitary operator U. This operator must be chosen so that the two possible paths are created in a balanced way, i.e.,

$$U|0\rangle = \frac{|0\rangle + \mathrm{e}^{\mathrm{i}\phi}|1\rangle}{\sqrt{2}}. \tag{2.4}$$

This is the most general case where paths A and B have the same probability to be followed because the coefficients have the same modulus. To complete the definition of operator U, we need to know its action on state $|1\rangle$. There are many possibilities, but the most natural choice that reflects the experimental device is $\phi = \pi/2$ and

$$U = \frac{1}{\sqrt{2}}\begin{bmatrix} 1 & \mathrm{i} \\ \mathrm{i} & 1 \end{bmatrix}. \tag{2.5}$$

The state of the photon after passing through the second half-silvered mirror is

$$\begin{aligned} U(U|0\rangle) &= \frac{\big(|0\rangle + \mathrm{i}\,|1\rangle\big) + \mathrm{i}\,\big(\mathrm{i}\,|0\rangle + |1\rangle\big)}{2} \\ &= \mathrm{i}\,|1\rangle. \end{aligned} \tag{2.6}$$

The intermediate step of the calculation was displayed on purpose. We can see that the paths described by $|0\rangle$ algebraically cancel, which can be interpreted as a destructive interference, while the $|1\rangle$-paths interfere constructively. The final result shows that the photon that took path B remains, going directly to the detector 2. Therefore, quantum mechanics predicts that 100% of the photons will be detected by detector 2.

2.3 Composite Systems

The *postulate of composite systems* states that the state space of a *composite system* is the *tensor product* of the state space of the components. If $|\psi_1\rangle, \ldots, |\psi_n\rangle$ describe the states of n isolated quantum systems, the state of the composite system is $|\psi_1\rangle \otimes \cdots \otimes |\psi_n\rangle$.

An example of a composite system is the memory of a *n-qubit* quantum computer. Usually, the memory is divided into sets of qubits, called *registers*. The state space of the computer memory is the tensor product of the state space of the registers, which is obtained by the repeated tensor product of the Hilbert space $\mathbb{C}^2$ of each *qubit*.

The state space of the memory of a 2-qubit quantum computer is $\mathbb{C}^4 = \mathbb{C}^2 \otimes \mathbb{C}^2$. Therefore, any unit vector in $\mathbb{C}^4$ represents the quantum state of two qubits. For example, the vector

$$|0, 0\rangle = \begin{bmatrix} 1 \\ 0 \\ 0 \\ 0 \end{bmatrix}, \tag{2.7}$$

which can be written as $|0\rangle \otimes |0\rangle$, represents the state of two electrons both with spin up. Analogous interpretation applies to $|0, 1\rangle$, $|1, 0\rangle$, and $|1, 1\rangle$. Consider now the unit vector in $\mathbb{C}^4$ given by

$$|\psi\rangle = \frac{|0, 0\rangle + |1, 1\rangle}{\sqrt{2}}. \tag{2.8}$$

What is the spin state of each electron in this case? To answer this question, we have to factor $|\psi\rangle$ as follows:

$$\frac{|0, 0\rangle + |1, 1\rangle}{\sqrt{2}} = \big(a|0\rangle + b|1\rangle\big) \otimes \big(c|0\rangle + d|1\rangle\big). \tag{2.9}$$

We can expand the right-hand side and match the coefficients setting up a system of equations to find a, b, c, and d. The state of the first qubit would be $a|0\rangle + b|1\rangle$ and second would be $c|0\rangle + d|1\rangle$. But there is a big problem: The system of equations has no solution, that is, there are no coefficients a, b, c, and d satisfying (2.9). Every state of a composite system that cannot be factored is called *entangled*. The quantum state is well-defined when we look at the composite system as a whole, but we cannot attribute the states to the parts.

A single qubit can be in a superposed state, but it cannot be entangled because its state is not composed of subsystems. The qubit should not be taken as a synonym of a particle because it is confusing. The state of a single particle can be entangled when we are analyzing more than a physical quantity related to it. For example, we may describe both the position and the rotation state. The position state may be entangled with the rotation state.

Exercise 2.1. Consider the states

$$|\psi_1\rangle = \frac{1}{2}\big(|0,0\rangle - |0,1\rangle + |1,0\rangle - |1,1\rangle\big),$$

$$|\psi_2\rangle = \frac{1}{2}\big(|0,0\rangle + |0,1\rangle + |1,0\rangle - |1,1\rangle\big).$$

Show that $|\psi_1\rangle$ is not entangled and $|\psi_2\rangle$ is entangled.

Exercise 2.2. Show that if $|\psi\rangle$ is an entangled state of two qubits, then the application of a unitary operator of the form $U_1 \otimes U_2$ necessarily generates an entangled state.

2.4 Measurement Process

In general, measuring a quantum system that is in the state $|\psi\rangle$ seeks to obtain classical information about this state. In practice, measurements are performed in laboratories using devices such as lasers, magnets, scales, and chronometers. In theory, we describe the process mathematically in a way that is consistent with what occurs in practice. Measuring a physical system that is in an unknown state, in general, disturbs this state irreversibly. In those cases, there is no way to know or recover the state before the measurement. If the state was not disturbed, no new information about it is obtained. Mathematically, the disturbance is described by an *orthogonal projector*. If the projector is over a one-dimensional space, it is said that the quantum state *collapsed* and is now described by the unit vector belonging to the one-dimensional space. In the general case, the projection is over a vector space of dimension greater than 1, and it is said that the collapse is partial or, in extreme cases, there is no change at all in the quantum state of the system.

The measurement requires the interaction between the quantum system with a macroscopic device, which violates the *state space postulate* because the quantum system is not isolated at this moment. We do not expect the evolution of the quantum state during the measurement process to be described by a unitary operator.

2.4.1 Measurement Postulate

A *projective measurement* is described by a Hermitian operator O, called *observable*, which acts on the state space of the system being measured. The observable O has a *diagonal representation*

$$O = \sum_{\lambda} \lambda P_{\lambda}, \tag{2.10}$$

where P_λ is the projector on the eigenspace of O associated with the eigenvalue λ. The possible results of the measurement of the observable O are the eigenvalues λ. If the system state at the time of measurement is $|\psi\rangle$, the probability of obtaining the result λ will be $\|P_\lambda|\psi\rangle\|^2$ or, equivalently,

$$p_\lambda = \langle\psi|P_\lambda|\psi\rangle. \tag{2.11}$$

If the result of the measurement is λ, the state of the quantum system immediately after the measurement is

$$\frac{1}{\sqrt{p_\lambda}} P_\lambda|\psi\rangle. \tag{2.12}$$

Notes

1. There is a correspondence between the physical layout of the devices in a physics lab and the observable O. When an experimental physicist measures a quantum system, he or she gets real numbers as result. Those numbers correspond to the eigenvalues λ of the Hermitian operator O.
2. The states $|\psi\rangle$ and $e^{i\phi}|\psi\rangle$ have the same *probability distribution* p_λ when one measures the same observable O. The states after the measurement differ by the same factor $e^{i\phi}$. The term $e^{i\phi}$ multiplying a quantum state is called *global phase factor* , whereas a term $e^{i\phi}$ multiplying a vector of a sum of vectors, such as $|0\rangle + e^{i\phi}|1\rangle$, is called *relative phase factor*. The real number ϕ is called *phase*.

Since the possible outcomes of a measurement of observable O obey a probability distribution, we can define the *expected value* of a measurement as

$$\langle O\rangle = \sum_\lambda p_\lambda \lambda, \tag{2.13}$$

and the *standard deviation* as

$$\Delta O = \sqrt{\langle O^2\rangle - \langle O\rangle^2}. \tag{2.14}$$

It is important to remember that the mean and standard deviation of an observable depend on the state that the physical system was in just before the measurement.

Exercise 2.3. Show that $\langle O\rangle = \langle\psi|O|\psi\rangle$.

Exercise 2.4. Show that if the physical system is in a state $|\psi\rangle$ that is an eigenvector of O, then $\Delta O = 0$, that is, there is no uncertainty about the result of the measurement of the observable O. What is the result of the measurement?

Exercise 2.5. Show that $\sum_\lambda p_\lambda = 1$ for any observable O and any state $|\psi\rangle$.

Exercise 2.6. Suppose that the physical system is in an arbitrary state $|\psi\rangle$. Show that $\sum_\lambda p_\lambda^2 = 1$ to an observable O if and only if $\Delta O = 0$.

2.4.2 Measurement in the Computational Basis

The *computational basis* of space $\mathbb{C}^2$ is the set $\{|0\rangle, |1\rangle\}$. For one qubit, the observable of the *measurement in the computational basis* is the Pauli matrix Z, whose spectral decomposition is

$$Z = (+1)P_{+1} + (-1)P_{-1}, \tag{2.15}$$

where $P_{+1} = |0\rangle\langle 0|$ and $P_{-1} = |1\rangle\langle 1|$. The possible results of the measurement are ± 1. If the state of the qubit is given by (2.1), the probabilities associated with possible outcomes are

$$p_{+1} = |a_0|^2, \tag{2.16}$$
$$p_{-1} = |a_1|^2, \tag{2.17}$$

whereas the states immediately after the measurement are $|0\rangle$ and $|1\rangle$, respectively. In fact, each of these states has a global phase that can be discarded. Note that

$$p_{+1} + p_{-1} = 1,$$

because state $|\psi\rangle$ has unit norm.

Before generalizing to n qubits, it is interesting to reexamine the process of measurement of a qubit with another observable given by

$$O = \sum_{k=0}^{1} k|k\rangle\langle k|. \tag{2.18}$$

Since the eigenvalues of O are 0 and 1, the above analysis holds if we replace $+1$ by 0 and -1 by 1. With this new observable, there is a one-to-one correspondence in the nomenclature of the measurement result and the final state. If the result is 0, the state after the measurement is $|0\rangle$. If the result is 1, the state after the measurement is $|1\rangle$.

The *computational basis* of the Hilbert space of n qubits in decimal notation is the set $\{|0\rangle, \ldots, |2^n - 1\rangle\}$. The *measurement in the computational basis* is associated with observable

$$O = \sum_{k=0}^{2^n-1} k\, P_k, \tag{2.19}$$

where $P_k = |k\rangle\langle k|$. An arbitrary state of n qubits is given by

$$|\psi\rangle = \sum_{k=0}^{2^n-1} a_k|k\rangle, \tag{2.20}$$

where amplitudes a_k satisfying the constraint

$$\sum_k |a_k|^2 = 1. \tag{2.21}$$

The measurement result is an integer k in the range $0 \leq k \leq 2^n - 1$ with a probability distribution given by

$$\begin{aligned} p_k &= \langle\psi|P_k|\psi\rangle \\ &= |\langle k|\psi\rangle|^2 \\ &= |a_k|^2. \end{aligned} \tag{2.22}$$

Equation (2.21) ensures that the sum of the probabilities is 1. The n-qubit state immediately after the measurement is

$$\frac{P_k|\psi\rangle}{\sqrt{p_k}} \simeq |k\rangle. \tag{2.23}$$

For example, suppose that the state of two qubits is given by

$$|\psi\rangle = \frac{1}{\sqrt{3}}\left(|0,0\rangle - \mathrm{i}\,|0,1\rangle + |1,1\rangle\right). \tag{2.24}$$

The probability that the result is 00, 01, or 11 in binary notation is $1/3$. Result 10 is never obtained because the associated probability is 0. If the measurement result is 00, the system state immediately after will be $|0,0\rangle$, similarly for 01 and 11. For the measurement in the computational basis, it makes sense to say that the result is *state* $|0,0\rangle$ because there is a one-to-one correspondence between eigenvalues and states of the computational basis.

The result of the measurement specifies on which vector of the computational basis state $|\psi\rangle$ is projected. The result does not provide the value of coefficient a_k, that is, none of the 2^n amplitudes a_k describing state $|\psi\rangle$ are revealed. Suppose we want to find number k as a result of an algorithm. This result should be encoded as one of the vectors of the computational basis, which spans the vector space to which state $|\psi\rangle$ belongs. It is undesirable, in principle, that the result itself is associated with one of the amplitudes. If the desired result is a noninteger real number, then the k most significant digits should be coded as a vector of the computational basis. After a measurement, we have a chance to get closer to k. A technique used in quantum algorithms is to amplify the value of a_k making it as close as possible to 1. A measurement at this point will return k with high probability. Therefore, the number that specifies a *ket*, for example, number k of $|k\rangle$ is a possible outcome of the algorithm, while the amplitudes of the quantum state are associated with the probability of obtaining a result.

The description of the measurement process of observable (2.19) is equivalent to simultaneous measurements or in a cascade of observables Z, that is, one observable Z for each qubit. The possible results of measuring Z are ± 1. Simultaneous measurements, or in a cascade of n qubits, result in a sequence of values ± 1. The relationship between a result of this kind and the one described before is obtained by replacing $+1$ by 0 and -1 by 1. We will have a binary number that can be converted into a decimal number which is one of the values k of (2.19).

For example, for three qubits the result may be $(-1, +1, +1)$, which is equivalent to $(1, 0, 0)$. Converting to base-10, the result is number 4. The state after the measurement is obtained using the projector

$$\begin{aligned} P_{-1,+1,+1} &= |1\rangle\langle 1| \otimes |0\rangle\langle 0| \otimes |0\rangle\langle 0| \\ &= |1, 0, 0\rangle\langle 1, 0, 0| \end{aligned} \tag{2.25}$$

over the state system of the three qubits followed by *renormalization*. The renormalization in this case replaces the coefficient by 1. The state after the measurement is $|1, 0, 0\rangle$. When using the computational basis, for both observables (2.19) and Z's, it makes sense to say that the result is $|1, 0, 0\rangle$ because we automatically know that the eigenvalues of Z in question are $(-1, +1, +1)$ and the number k is 4.

A simultaneous measurement of n observables Z is not equivalent to measure observable $Z \otimes \cdots \otimes Z$. The latter observable returns a single value, which can be $+1$ or -1, whereas measuring n observables Z, simultaneously or not, we obtain n values ± 1. Measurements on a cascade are performed with observable $Z \otimes I \otimes \cdots \otimes I$, $I \otimes Z \otimes \cdots \otimes I$, and so on. They can also be performed simultaneously. Usually, we use a more compact notation, Z_1, Z_2, successively, where Z_1 means that observable Z was used for the first qubit and the identity operator for the remaining ones. Since these observables commute, the order is irrelevant and the limitations imposed by the *uncertainty principle* do not apply. Measurement of observables of this kind is called *partial measurement* in the computational basis.

Exercise 2.7. Suppose that the state of a qubit is $|1\rangle$.

1. What are the mean value and standard deviation of the measurement of observable X?
2. What are the mean value and standard deviation of the measurement of observable Z? Compare with Exercise 2.4.

2.4.3 Partial Measurement in the Computational Basis

The term *measurement in the computational basis* of n qubits implies a measurement of all n qubits. However, it is possible to perform a *partial measurement*—to measure some qubits. The result in this case is not necessarily a state of the computational

basis. For example, we can measure the first qubit of a system described by the state $|\psi\rangle$ of (2.24). It is convenient to rewrite that state as follows:

$$|\psi\rangle = \sqrt{\frac{2}{3}}|0\rangle \otimes \frac{|0\rangle - \mathrm{i}|1\rangle}{\sqrt{2}} + \frac{1}{\sqrt{3}}|1\rangle \otimes |1\rangle. \tag{2.26}$$

We can see that the measurement result is either 0 or 1. The probability of obtaining 1 is $1/3$ because the only way to get 1 for a measurement of the first qubit is to obtain 1 as well, for the second qubit. Therefore, the probability of obtaining 0 is $2/3$, and the state immediately after the measurement in this case is

$$|0\rangle \otimes \frac{|0\rangle - \mathrm{i}|1\rangle}{\sqrt{2}}.$$

Only the qubits involved in the measurement are projected on the computational basis. The state of the remaining qubits is in superposition in general. In this example, when the result is 0, the state of the second qubit is a superposition, and when the result is 1, the state of the second qubit is $|1\rangle$.

If we have a system composed of subsystems A and B, a partial measurement of subsystem A is a measurement of the observable $O_A \otimes I_B$, where O_A is an observable of system A and I_B is the identity operator of system B. Physically, this means that the measuring apparatus interacted only with the subsystem A. Equivalently, a partial measurement interacting only with subsystem B is a measurement of the observable $I_A \otimes O_B$.

If we have a register of m qubits together with a register of n qubits, we can represent the computational basis in a compact form $\left\{|i, j\rangle : 0 \leq i \leq 2^m - 1, 0 \leq j \leq 2^n - 1\right\}$, where i and j are both represented in base-10. An arbitrary state is represented by

$$|\psi\rangle = \sum_{i=0}^{2^m-1} \sum_{j=0}^{2^n-1} a_{ij}|i, j\rangle. \tag{2.27}$$

Suppose we measure all qubits of the first register in the computational basis, that is, we measure observable $O_A \otimes I_B$, where

$$O_A = \sum_{k=0}^{2^m-1} k P_k. \tag{2.28}$$

The probability of obtaining k so that $0 \leq k \leq 2^m - 1$ is

$$\begin{aligned} p_k &= \langle\psi| (P_k \otimes I) |\psi\rangle \\ &= \sum_{j=0}^{2^n-1} \left|a_{kj}\right|^2. \end{aligned} \tag{2.29}$$

The set $\{p_0, \ldots, p_{2^m-1}\}$ is a probability distribution and therefore satisfies

$$\sum_{k=0}^{2^m-1} p_k = 1. \tag{2.30}$$

If the measurement result is k, the state immediately after the measurement will be

$$\frac{1}{\sqrt{p_k}}(P_k \otimes I)|\psi\rangle = \frac{1}{\sqrt{p_k}}|k\rangle\left(\sum_{j=0}^{2^n-1} a_{kj}|j\rangle\right). \tag{2.31}$$

Note that the state after the measurement is a superposition of the second register. A measurement of observable (2.28) is equivalent to measure observables $Z_1, \ldots, Z_m$.

Exercise 2.8. Suppose that the state of two qubits is given by

$$|\psi\rangle = \frac{3}{5\sqrt{2}}|0,0\rangle - \frac{3\,\mathrm{i}}{5\sqrt{2}}|0,1\rangle + \frac{2\sqrt{2}}{5}|1,0\rangle - \frac{2\sqrt{2}\,\mathrm{i}}{5}|1,1\rangle. \tag{2.32}$$

1. Describe completely the measurement process of observable Z_1, that is, obtain the probability of each outcome and the corresponding states after the measurement. Suppose that, after measuring Z_1, we measure Z_2. Describe all resulting cases.
2. Now invert the order of the observables and describe the whole process.
3. If the intermediate quantum states are disregarded, is there a difference when we invert the order of the observable? Note that the measurement of Z_1 and Z_2 may be performed simultaneously. One can move the qubits without changing the quantum state, which may be entangled or not, and put each of them into a measuring device, both adjusted to measure observable Z, as in Fig. 2.1.
4. For two qubits, the state after the measurement of the first qubit in the computational basis can be either $|0\rangle|\alpha\rangle$ or $|1\rangle|\beta\rangle$, where $|\alpha\rangle$ and $|\beta\rangle$ are states of the second qubit. In general, we have $|\alpha\rangle \neq |\beta\rangle$. Why is this not the case in the previous items?

Further Reading

The amount of good books about quantum mechanics is very large. For the first contact, we suggest [126, 257, 287]. Reference [287] uses the *Dirac notation* since the beginning, which is welcome in the context of *quantum computation*. For a more complete approach, we suggest [84]. For a more conceptual approach, we suggest [96, 252]. For those who are only interested in the application of quantum mechanics to quantum computation, we suggest [170, 234, 248, 272, 276].

Chapter 3
Introduction to Quantum Walks

Quantum walks are interesting for many a reason: (1) They are useful to build new *quantum algorithms*, (2) they can be directly implemented in laboratories without using a *quantum computer*, and (3) they can simulate many complex physical systems.

A quantum walk takes place on a *graph*, whose *vertices* are the places the walker may step and whose *edges* tell the possible directions the walker can choose to move. Space is discrete but time can be discrete or continuous.

In the discrete-time case, the motion consists in stepping from one vertex to the next over and over. Each step takes one time unit and it takes a long time to go far. The walker starts at some initial state and the dynamic in its simplest form is described by a unitary operator U^t, where U is the evolution operator and t is the number of steps. At the end, a measurement is performed to determine the walker's position.

In the continuous-time case, there is a *transition rate* controlling the jumping probability, which starts with a small value and increases continually so that the walker eventually steps on the next vertex. The dynamic is described by the unitary operator $U(t) = \exp(\mathrm{i}tH)$, where t is time and H is a *Hermitian* matrix, whose entries are nonzero only if they correspond to neighboring vertices.

In this chapter, we briefly review the area of *classical random walks* with a focus on the *expected distance* from the origin. Next, we give a gentle introduction to the *coined quantum walk model* and analyze the expected distance in the quantum case. The probability of finding the walker away from the origin is larger in the quantum case. We also give an introduction to the *continuous-time Markov chain*, which is used to obtain the *continuous-time quantum walk model*.

3.1 Classical Random Walk on the Line

One of the simplest examples of a random walk is the classical motion of a particle on the integer points of a line, where the direction is determined by an unbiased coin. Flip the coin, if the result is heads, the particle moves to the next vertex to the

© Springer Nature Switzerland AG 2018

R. Portugal, *Quantum Walks and Search Algorithms*, Quantum Science and Technology, https://doi.org/10.1007/978-3-319-97813-0_3

$t \backslash n$	-5	-4	-3	-2	-1	0	1	2	3	4	5
0						1					
1					$\frac{1}{2}$		$\frac{1}{2}$				
2				$\frac{1}{4}$		$\frac{1}{2}$		$\frac{1}{4}$			
3			$\frac{1}{8}$		$\frac{3}{8}$		$\frac{3}{8}$		$\frac{1}{8}$		
4		$\frac{1}{16}$		$\frac{1}{4}$		$\frac{3}{8}$		$\frac{1}{4}$		$\frac{1}{16}$	
5	$\frac{1}{32}$		$\frac{5}{32}$		$\frac{5}{16}$		$\frac{5}{16}$		$\frac{5}{32}$		$\frac{1}{32}$

Fig. 3.1 Probability of the particle being at the position n at time t, assuming the walk starts at the origin. The probability is zero in empty cells

right, and if it is tails, the particle moves to the next vertex to the left. This process is repeated over and over. We cannot know for sure where the particle will be at a later time, but we can calculate the probability p of being at a given point n at time t. Suppose the particle is at the origin at time $t = 0$. Then $p(t = 0, n = 0) = 1$, as shown in Fig. 3.1. For $t = 1$, the particle can be either at $n = -1$ with probability $1/2$ or at $n = 1$ with probability $1/2$. The probability of being at $n = 0$ becomes zero. By repeating this process over and over, we can confirm all probabilities described in Fig. 3.1.

The probability is given by (Exercise 3.1)

$$p(t, n) = \frac{1}{2^t} \binom{t}{\frac{t+n}{2}}, \tag{3.1}$$

where $\binom{a}{b} = \frac{a!}{(a-b)!b!}$. This equation is valid only if $t + n$ is even and $n \leq t$. If $t + n$ is odd or $n > t$, the probability is zero. For fixed t, $p(t, n)$ is a *binomial distribution*. For relatively large values of fixed t, the probability as a function of n has a familiar shape. Figure 3.2 depicts three curves that correspond to $t = 72$, $t = 180$, and $t = 450$. Strictly speaking, the curves are envelopes of the actual probability distribution because the probability is zero for odd n when t is even. Another way to interpret the curves is as the sum $p(t, n) + p(t + 1, n)$, that is, we have two overlapping distributions.

Note that the width of the curve increases and the height of the midpoint decreases when t increases. It is interesting to determine the *expected distance* from the origin. It is important to determine how far away from the origin we can find the particle as time goes by. The expected distance is a statistical quantity that captures this idea and is equal to the *position standard deviation* when the probability distribution is symmetrical. The *average position* (or *expected position*) is

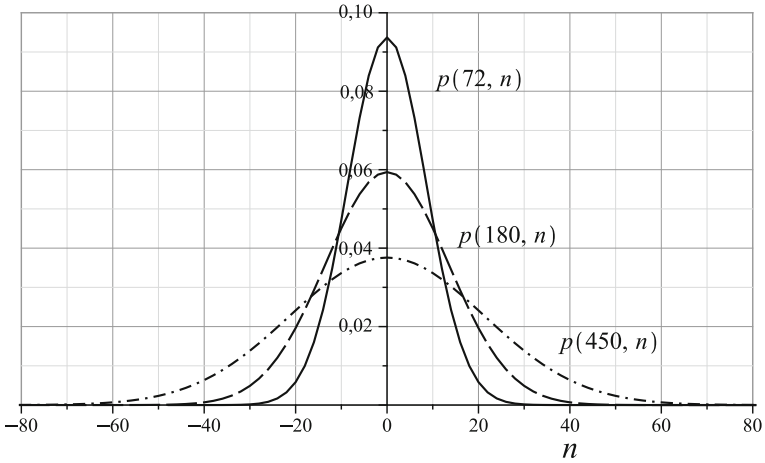

Fig. 3.2 Probability distribution of a classical random walk on a line for $t = 72$, $t = 180$ and $t = 450$

$$\langle n \rangle = \sum_{n=-\infty}^{\infty} n\, p(t, n).$$

Using the symmetry $p(t, n) = p(t, -n)$, we obtain

$$\langle n \rangle = 0. \tag{3.2}$$

Then, the standard deviation $\sigma(t)$ is

$$\sqrt{\langle n^2 \rangle - \langle n \rangle^2} = \sqrt{\sum_{n=-\infty}^{\infty} n^2\, p(t, n)}.$$

Using (3.1), we obtain (Exercise 3.2)

$$\sigma(t) = \sqrt{t}\,. \tag{3.3}$$

Another way to calculate the standard deviation is to convert the binomial distribution into an expression that is easier to handle analytically. By expanding the binomial factor of (3.1) in terms of factorials, and using Stirling's approximation for large t, the probability distribution of the random walk can be approximated by expression (Exercise 3.3)

$$p(t, n) \simeq \frac{2}{\sqrt{2\pi\, t}}\, \mathrm{e}^{-\frac{n^2}{2t}}. \tag{3.4}$$

For a fixed t, $p(t,n)/2$ is the *normal distribution* (also known as *Gaussian distribution*). Now, the calculation of the standard deviation is simpler because after converting the sum into an integral the standard deviation is the square root of

$$\frac{1}{\sqrt{2\pi t}} \int_{-\infty}^{\infty} n^2 \, \mathrm{e}^{-\frac{n^2}{2t}} \, \mathrm{d}n.$$

The normal distribution has two *inflection points*, which are the solutions of the equation $\partial^2 p(t,n)/\partial n^2 = 0$. The distance between the inflection points is $2\sqrt{t}$. The standard deviation is the distance between the midpoint and an inflection point.

Exercise 3.1. The goal of this exercise is to help to obtain (3.1). First show that at time t, the total number of possible paths of the particle is 2^t. At time t, the particle is at position n. Suppose that the particle has moved a steps to the right and b steps to the left. Find a and b as functions of t and n. Now focus on the steps towards the right direction. In how many ways can the particle move a steps to the right in t units of time? Or, equivalently, we have t objects, in how many ways can we select a objects? Show that the probability of the particle being at the position n is given by (3.1).

Exercise 3.2. The goal of this exercise is to help the calculation of the sum of (3.3). Change the dummy index to obtain a finite sum starting at $n = 0$ and running over even n when t is even and running over odd n when t is odd. After this manipulation, you can use (3.1). Rename the dummy index in order to use the identities

$$\sum_{n=0}^{t} \binom{2t}{n} = 2^{2t-1} + \frac{1}{2}\binom{2t}{t}, \quad \sum_{n=0}^{t} n \binom{2t}{n} = t2^{2t-1},$$
$$\sum_{n=0}^{t} n^2 \binom{2t}{n} = t^2 2^{2t-1} + t2^{2t-2} - \frac{t^2}{2}\binom{2t}{t}$$

and simplify the result to show that

$$\sum_{n=-\infty}^{\infty} n^2 \, p(t,n) = t.$$

Exercise 3.3. Show that (3.4) can be obtained from (3.1) using *Stirling's approximation*, which is given by

$$t! \approx \sqrt{2\pi t} \; t^t \, \mathrm{e}^{-t},$$

when $t \gg 1$. [Hint: Use Stirling's approximation and simplify the result trying to factor out the fraction n/t. Take the *natural logarithm* of the expression, expand the logarithm, and use the asymptotic expansion of the logarithm. Note that the terms of the type n^2/t^2 are much smaller than n^2/t. At the end, take the exponential of the result.]

3.2 Classical Discrete-Time Markov Chains

A *classical Markov chain* is a stochastic process that assumes values in a discrete set and obeys the following property: The next state of the chain depends only on the current state—it is not influenced by the past states. The next state is determined by some deterministic or random rule based only on the current state.

The Markov chain can be viewed as a directed graph where the states are represented by vertices and the transitions between states are represented by *arcs*. Note that the set of states is discrete, whereas the evolution time can be discrete or continuous. Then, the term discrete or continuous used here refers only to time.

Let us start by describing the *classical discrete-time Markov chain*. At each step, the Markov chain has an associated probability distribution. After choosing an order for the states, we describe the probability distribution with a vector. Let $\Gamma(X, E)$ be a graph with set of vertices $X = \{x_1, \ldots, x_n\}$ ($|X| = n$) and set of edges E. The probability distribution is described by a vector

$$\begin{bmatrix} p_1(t) \\ \vdots \\ p_n(t) \end{bmatrix},$$

where $p_i(t)$ is the probability of the walker being on vertex x_i at time t. If the process begins with the walker on the first vertex, we have $p_1(0) = 1$ and $p_i(0) = 0$ for $i = 2, \ldots, n$. In a Markov chain, we cannot tell precisely where the walker will be at future time steps. However, we can determine the probability distribution if we know the *transition matrix* M, also called *probability matrix* or *stochastic matrix*.

If the probability distribution is known at time t, we obtain the distribution at time $t + 1$ using

$$p_i(t+1) = \sum_{j=1}^{n} M_{i\,j}\, p_j(t). \tag{3.5}$$

To be sure that $p_i(t + 1)$ is a probability distribution, matrix M must satisfy the following properties: (1) The entries are nonnegative real numbers, and (2) the sum of the entries of any column is equal to 1. Using the vector notation, we have

$$\vec{p}(t+1) = M\,\vec{p}(t). \tag{3.6}$$

M is called *left stochastic matrix*. There is a corresponding description that uses a transposed vector of probabilities (row vector) and matrix M is on the right-hand side of $\vec{p}(t)$. In this case, the sum of the entries of each line of M must be 1.

If the walker is on vertex x_j, the probability to go to vertex x_i is M_{ij}. An interesting case using undirected graphs is

$$M_{ij} = \frac{1}{d_j},$$

where d_j is the *degree* of vertex x_j and $M_{ij} = 0$ if there is no edge linking x_j and x_i. In this case, the walker goes to one of the adjacent vertices with equal probability because the transition probability is the same for all vertices in the neighborhood of x_j. The stochastic matrix M and the *adjacency matrix* A obey equation $M_{ij} = A_{ij}/d_j$. The adjacency matrix of an undirected graph is a symmetric Boolean matrix specifying whether two vertices x_i and x_j are connected (entry A_{ij} is 1) or not (entry A_{ij} is 0).

Let us use the *complete graph* with n vertices as an example. All vertices are connected by undirected edges. Then, the degree of each vertex is $n-1$. The vertices do not have *loops*, so $M_{ii} = 0$ for all i. The stochastic matrix is

$$M = \frac{1}{n-1}\begin{bmatrix} 0 & 1 & 1 & \cdots & 1 \\ 1 & 0 & 1 & \cdots & 1 \\ 1 & 1 & 0 & \cdots & 1 \\ \vdots & \vdots & \vdots & \ddots & \vdots \\ 1 & 1 & 1 & \cdots & 0 \end{bmatrix}. \tag{3.7}$$

If the initial condition is a walker located on the first vertex, the probability distributions during the first steps are

$$\vec{p}(0) = \begin{bmatrix} 1 \\ 0 \\ \vdots \\ 0 \end{bmatrix}, \quad \vec{p}(1) = \frac{1}{n-1}\begin{bmatrix} 0 \\ 1 \\ \vdots \\ 1 \end{bmatrix}, \quad \vec{p}(2) = \frac{1}{(n-1)^2}\begin{bmatrix} n-1 \\ n-2 \\ \vdots \\ n-2 \end{bmatrix}.$$

The probability distribution at an arbitrary step t is (Exercise 3.4)

$$\vec{p}(t) = \begin{bmatrix} f_n(t-1) \\ f_n(t) \\ \vdots \\ f_n(t) \end{bmatrix}, \tag{3.8}$$

where

$$f_n(t) = \frac{1}{n}\left(1 - \frac{1}{(1-n)^t}\right). \tag{3.9}$$

Note that when $t \to \infty$ the probability distribution goes to the uniform distribution, which is the *limiting distribution* of this graph.

As a motivation for introducing the next section, we observe that (3.6) is a *recursive equation* that can be solved and written as

$$\vec{p}(t) = M^t\, \vec{p}(0), \tag{3.10}$$

where $\vec{p}(0)$ is the initial condition. This equation encodes all possible ways the walker can move after t steps. Note that only one possible way actually occurs in reality. A similar matrix structure is used in the next section to describe the quantum evolution. However, the vector of probabilities is replaced by a vector of amplitudes (complex numbers) and the stochastic matrix M is replaced by a unitary matrix. The physical interpretation of what happens in reality is clearly different from the stochastic process since in the quantum case it is not correct to say that only one of the possible ways occurs.

Exercise 3.4. The goal of this exercise is to obtain expression (3.8). By inspecting the stochastic matrix of the complete graph, show that $p_2(t) = p_3(t) = \cdots = p_n(t)$ and $p_1(t+1) = p_2(t)$. Considering that the sum of the entries of the vector of probabilities is 1, show that $p_2(t)$ satisfies the following recursive equation:

$$p_2(t) = \frac{1 - p_2(t-1)}{n-1}.$$

Using that $p_2(0) = 0$, solve the recursive equation and show that $p_2(t)$ is given by $f_n(t)$, as in (3.9).

Exercise 3.5. Obtain an expression for M^t in terms of function $f_n(t)$, where M is the stochastic matrix of the complete graph. Using M^t, show that $\vec{p}(t)$ obeys (3.8).

Exercise 3.6. Consider a cycle with n vertices and take as the initial condition a walker located on one of the vertices. Obtain the stochastic matrix of this graph. Describe the probability distribution for the first steps and compare with the values in Fig. 3.1. Obtain the distribution at an arbitrary time and find the limiting distribution for the odd cycle. [Hint: To find the distribution for the cycle, use the probability distribution of the line.]

Exercise 3.7. Let M be an arbitrary stochastic matrix. Show that M^t is a stochastic matrix for any positive integer t.

3.3 Coined Quantum Walks

The construction of quantum models and their equations is usually performed by a process called *quantization*. Momentum and energy are replaced by operators acting on a Hilbert space, whose size depends on the degree of freedom of the physical system. If a quantum system is totally isolated from interactions with the macroscopic world around, its state is described by a vector in the Hilbert space and its evolution is driven by a unitary operation. If the system has more than one component, the Hilbert space is the tensor product of the Hilbert spaces of the components. There is no room for *randomness* since the evolution of isolated quantum systems is unitary. Then, in principle, the name *quantum random walk* is contradictory. In the literature,

the term *quantum walk* has been used instead, but the evolution of quantum systems that are not totally isolated from the environment has some *stochasticity*. In addition, at some point we measure the quantum system to obtain macroscopic information about it. The description of this process uses probability distributions. It is natural to use the term "quantum walk" for unitary evolution and the term "quantum random walk" for non-unitary evolution.

3.3.1 Coined Walk on the Line

The first model of quantization of classical random walks that we discuss is the *discrete-time coined quantum walk model* or simply *coined model*. We use the line (a one-dimensional lattice) as a first example. In the quantum case, the walker's position n on the line is described by a vector $|n\rangle$ in a Hilbert space $\mathcal{H}_P$ of infinite dimension, the computational basis of which is $\left\{\left|n'\right\rangle : n' \in \mathbb{Z}\right\}$. The evolution of the walk depends on a quantum "coin." If one obtains "heads" after tossing the "coin" when the position of the walker is described by $|n\rangle$, then the next position is described by $|n+1\rangle$. If the result is "tails," the next position is described by $|n-1\rangle$. How do we include the "coin" in this scheme? We can think in physical terms. Suppose an electron is the walker and it is on a vertex of the line. The state of the electron is described not only by its position but also by the value of its spin, which may be up or down. The spin can determine the direction of the motion. If the position of the electron is $|n\rangle$ and its spin is up, it goes to $|n+1\rangle$; if its spin is down, it goes to $|n-1\rangle$. The Hilbert space of the system is $\mathcal{H} = \mathcal{H}_C \otimes \mathcal{H}_P$, where $\mathcal{H}_C$ is the two-dimensional Hilbert space associated with the "coin," whose computational basis is $\left\{|0\rangle,\ |1\rangle\right\}$. We can now define the "coin" as any unitary matrix C with dimension 2, which acts on vectors in Hilbert space $\mathcal{H}_C$. C is called *coin operator*.

The shift from $|n\rangle$ to $|n+1\rangle$ or $|n-1\rangle$ must be described by a unitary operator, called the *shift operator* S. It acts as follows:

$$S|0\rangle|n\rangle = |0\rangle|n+1\rangle, \tag{3.11}$$

$$S|1\rangle|n\rangle = |1\rangle|n-1\rangle. \tag{3.12}$$

If we know the action of S on the computational basis of $\mathcal{H}$, we have a complete description of this linear operator, and we obtain

$$S = |0\rangle\langle 0| \otimes \sum_{n=-\infty}^{\infty} |n+1\rangle\langle n| + |1\rangle\langle 1| \otimes \sum_{n=-\infty}^{\infty} |n-1\rangle\langle n|. \tag{3.13}$$

We can re-obtain (3.11) and (3.12) by applying S to the computational basis.

The quantum walk starts when we apply the operator $C \otimes I_P$ to the initial state, where I_P is the identity operator of the Hilbert space $\mathcal{H}_P$. This is analogous to tossing a coin in the classical case. C changes the coin state and the walker stays at

the same position. If the coin state is initially described by one of the states of the computational basis, the result is a superposition of states assuming that the coin is nontrivial. Each term in this superposition generates a shift in one direction. Consider the particle initially located at the origin $|n = 0\rangle$ and the coin state with spin up $|0\rangle$, that is,

$$|\psi(0)\rangle = |0\rangle|n = 0\rangle, \tag{3.14}$$

where $|\psi(0)\rangle$ denotes the state of the quantum walk at $t = 0$ and $|\psi(t)\rangle$ denotes the state at time t.

The most used coin is the *Hadamard* operator

$$H = \frac{1}{\sqrt{2}}\begin{bmatrix} 1 & 1 \\ 1 & -1 \end{bmatrix}. \tag{3.15}$$

One step consists of applying H to the coin state followed by the shift operator S, in the following way:

$$\begin{aligned} |0\rangle \otimes |0\rangle &\xrightarrow{H\otimes I} \frac{|0\rangle + |1\rangle}{\sqrt{2}} \otimes |0\rangle \\ &\xrightarrow{S} \frac{1}{\sqrt{2}}\big(|0\rangle \otimes |1\rangle + |1\rangle \otimes |-1\rangle\big). \end{aligned} \tag{3.16}$$

After the first step, the position of the particle is a superposition of $n = 1$ and $n = -1$. The superposition of positions is the result of the superposition generated by the coin operator. Note that the coin H is unbiased when applied to $|0\rangle$ because the probability to go to the right is equal to the probability to go to the left. The same is true if we apply H to $|1\rangle$. There is a difference between the signs of the amplitudes, but the sign plays no role in the calculation of the probability in this case. So we call H an unbiased coin.

In the quantum case, if we want to know the particle's position, we need to measure the quantum system when it is in state (3.16). If we perform a measurement in the computational basis, we have a 50% chance of finding the particle at $n = 1$ and a 50% chance of finding it at $n = -1$. This result is the same as the first step of the classical random walk with an unbiased coin. If we repeat this procedure over and over, that is, (1) we apply the coin operator, (2) we apply the shift operator, and (3) we perform a measurement in the computational basis, we obtain a classical random walk. Our goal is to use quantum features to obtain new results, which cannot be obtained in the classical context. When we measure the particle position after the first step, we destroy the correlations between different positions. On the other hand, if we apply the coin operator followed by the shift operator over and over without intermediary measurements, the quantum correlations between different positions generate constructive or destructive interference, creating a behavior characteristic of quantum walks that is different from the classical behavior. In this case, the probability distribution is not the normal distribution and the standard deviation is not $\sqrt{t}$.

The quantum walk dynamics are driven by the unitary operator

$$U = S\,(H \otimes I) \tag{3.17}$$

with no intermediary measurements. One step consists in applying U one time, which is equivalent to applying the coin operator followed by the shift operator. In the next step, we apply U again without measurements. After t steps, the state of the quantum walk is given by

$$|\psi(t)\rangle = U^t|\psi(0)\rangle. \tag{3.18}$$

Let us calculate the first few steps explicitly in order to compare with the first steps of a classical random walk. We take (3.14) as the initial condition. The first step is equal to (3.16). The second step is calculated using $|\psi(2)\rangle = U|\psi(1)\rangle$ and the third using $|\psi(3)\rangle = U|\psi(2)\rangle$:

$$\begin{aligned}
|\psi(1)\rangle &= \frac{1}{\sqrt{2}}\big(|1\rangle|-1\rangle + |0\rangle|1\rangle\big),\\
|\psi(2)\rangle &= \frac{1}{2}\Big(-|1\rangle|-2\rangle + (|0\rangle + |1\rangle)|0\rangle + |0\rangle|2\rangle\Big),\\
|\psi(3)\rangle &= \frac{1}{2\sqrt{2}}\Big(|1\rangle|-3\rangle - |0\rangle|-1\rangle + (2|0\rangle + |1\rangle)|1\rangle + |0\rangle|3\rangle\Big).
\end{aligned} \tag{3.19}$$

These few initial steps have already revealed that the quantum walk differs from the classical random walk in several aspects. We have used an unbiased coin, but the state $|\psi(3)\rangle$ is not symmetric with respect to the origin. Figure 3.3 shows the probability distribution up to the fifth step. Besides being asymmetric, the probability distributions are not concentrated around the origin. Compare with the probability distributions of Fig. 3.1.

We would like to find the probability distribution for a number of steps larger than 5. However, the calculation method we are using is not good enough. Suppose we want to calculate the probability distribution $p(100, n)$ after 100 steps. We cannot calculate $|\psi(100)\rangle$ by hand. We have to rely on some computational implementation.

$t \backslash n$	-5	-4	-3	-2	-1	0	1	2	3	4	5
0						1					
1					$\frac{1}{2}$		$\frac{1}{2}$				
2				$\frac{1}{4}$		$\frac{1}{2}$		$\frac{1}{4}$			
3			$\frac{1}{8}$		$\frac{1}{8}$		$\frac{5}{8}$		$\frac{1}{8}$		
4		$\frac{1}{16}$		$\frac{1}{8}$		$\frac{1}{8}$		$\frac{5}{8}$		$\frac{1}{16}$	
5	$\frac{1}{32}$		$\frac{5}{32}$		$\frac{1}{8}$		$\frac{1}{8}$		$\frac{17}{32}$		$\frac{1}{32}$

Fig. 3.3 Probability of finding the quantum particle on vertex n at time t, assuming that the walk starts at the origin with the quantum coin in state "spin up"

An efficient way of implementing quantum walks is to use recursive formulas for the amplitudes. The arbitrary state of the quantum walk in the computational basis is

$$|\psi(t)\rangle = \sum_{n=-\infty}^{\infty} \big(A_n(t)|0\rangle + B_n(t)|1\rangle\big)|n\rangle, \tag{3.20}$$

where the amplitudes satisfy the constraint

$$\sum_{n=-\infty}^{\infty} |A_n(t)|^2 + |B_n(t)|^2 = 1, \tag{3.21}$$

which means that $|\psi(t)\rangle$ has norm 1 at all steps. In Sect. 5.1 on p. 69, we show that when applying $H \otimes I$ followed by the shift operator to (3.20), we obtain the following recursive formulas for the amplitudes A and B:

$$A_n(t+1) = \frac{A_{n-1}(t) + B_{n-1}(t)}{\sqrt{2}},$$
$$B_n(t+1) = \frac{A_{n+1}(t) - B_{n+1}(t)}{\sqrt{2}}.$$

Using the initial condition

$$A_n(0) = \begin{cases} 1, & \text{if } n = 0; \\ 0, & \text{otherwise,} \end{cases}$$

and $B_n(0) = 0$ for all n, we can calculate iteratively $A_n(t)$ and $B_n(t)$ for t from 1 to 100. The probability distribution is obtained using

$$p(t, n) = |A_n(t)|^2 + |B_n(t)|^2 . \tag{3.22}$$

This approach is suitable to be implemented in the mainstream programming languages, such as `C`, `Fortran`, `Java`, `Python`, or `Julia`.

A second method to implement quantum walks is based on the explicit calculation of matrix U. We have to calculate the tensor product $H \otimes I$ using the formula described in Sect. A.15 on p. 263. The tensor product is also required to obtain a matrix representation of the shift operator as defined in (3.13). These operators act on vectors in an infinite vector space. However, the number of nonzero entries is finite. Then, these arrays must have dimensions slightly larger than 200×200 in order to calculate $|\psi(100)\rangle$. After calculating U, we calculate U^{100}, and the matrix product of U^{100} and the initial condition $|\psi(0)\rangle$, written as a column vector with a compatible number of entries. The result is $|\psi(100)\rangle$. Finally, we can calculate the probability distribution. This method can be implemented in computer algebra systems, such as `Mathematica`, `Maple`, or `Sage`, and is inefficient in general.

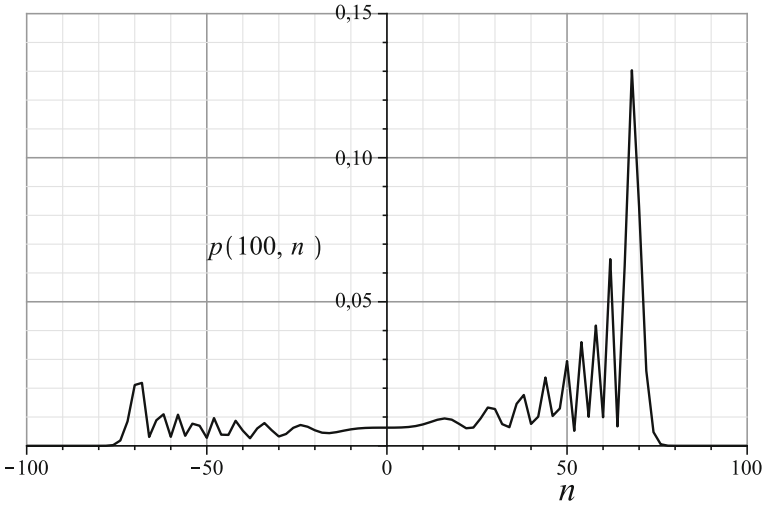

Fig. 3.4 Probability distribution after 100 steps of a quantum walk with the Hadamard coin starting from the initial condition $|\psi(0)\rangle = |0\rangle|n = 0\rangle$. The points where the probability is zero were excluded (n odd)

This method becomes more efficient if the programmer uses techniques to deal with sparse matrices and parallel programming.

Note that there is an alternate route that is to download a package for quantum walk simulations. In Sect. 5.3 on p. 85, we describe the main available packages, and we provide references that may help the user to obtain the desired results quicker than implementing by oneself.

By employing any of the above methods, the probability distribution after 100 steps depicted in Fig. 3.4 is eventually obtained. Analogous to the plot of the probability distribution of the classical random walk, we ignore the points corresponding to probabilities equal to zero. For instance, at $t = 100$, the probability is zero for all odd values of n—these points are not shown. If we observe the plot, we notice that the probability distribution is asymmetric. The probability of finding the particle on the right-hand side of the origin is larger than on the left-hand side. In particular, there is a peak for n around $100/\sqrt{2}$ and the probability at the peak is more than 10 times larger than the probability at the origin. The peak is always there, even for large t. This suggests that the quantum walk has a *ballistic* behavior, which means that the particle can be found away from the origin as if it is in a uniform rightward motion. It is natural to ask whether this pattern holds when the distribution is symmetric around the origin.

In order to obtain a symmetrical distribution, we must understand why the previous example has a tendency to go to the right. The Hadamard coin introduces a negative sign when applied to state $|1\rangle$. This means that there are more cancellations of terms when the coin state is $|1\rangle$ than of terms when the coin state is $|0\rangle$. Since the coin state $|0\rangle$ induces a motion to the right and $|1\rangle$ to the left, the final effect is the asymmetry

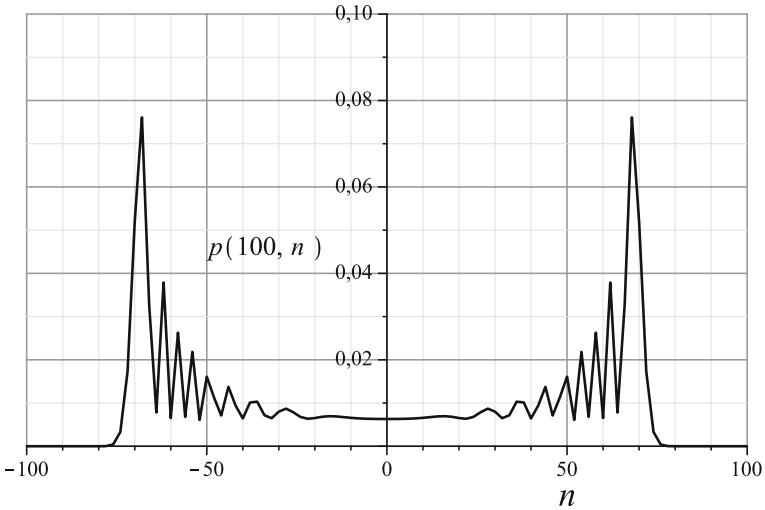

Fig. 3.5 Probability distribution after 100 steps of a Hadamard quantum walk starting from the initial condition (3.23)

with larger probabilities on the right-hand side of the origin. We would confirm this analysis if we calculate the resulting probability distribution when the initial condition is

$$|\psi(0)\rangle = -|1\rangle|n = 0\rangle.$$

In this case, the number of negative terms is greater than the number of positive terms and there are more cancellations of terms when the coin state is $|0\rangle$. The final result is a probability distribution that is the mirror image of the one depicted in Fig. 3.4. To obtain a symmetrical distribution, we must superpose the quantum walks resulting from these two initial conditions. This superposition should not cancel terms before the calculation of the probability distribution. The trick is to multiply the imaginary unit number to the second initial condition and add to the first initial condition in the following way:

$$|\psi(0)\rangle = \frac{|0\rangle - \mathrm{i}|1\rangle}{\sqrt{2}}|n = 0\rangle. \tag{3.23}$$

The entries of the Hadamard coin are real numbers. When we apply the evolution operator, terms with the imaginary unit are not converted into terms without the imaginary unit and vice versa. There are no cancellations of terms of the walk that goes to the right with the terms of the walk that goes to the left. At the end, the probability distributions are added. In fact, the result is depicted in Fig. 3.5. Note that the probability distribution is spread in the range $\left[-t/\sqrt{2}, t/\sqrt{2}\right]$, while the classical distribution is a Gaussian centered at the origin and visible in the range $\left[-2\sqrt{t}, 2\sqrt{t}\right]$.

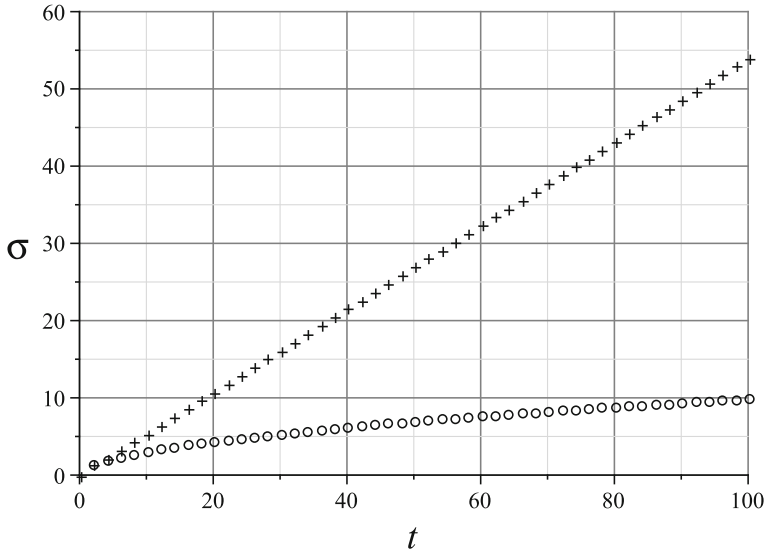

Fig. 3.6 Standard deviation of the quantum walk (*crosses*) and the classical random walk (*circles*) as a function of the number of steps

If the probability distribution is symmetric, the expected value of the position is zero, that is, $\langle n \rangle = 0$. The question now is how the standard deviation $\sigma(t)$ behaves as a function of time. The formula for the standard deviation when $\langle n \rangle = 0$ is

$$\sigma(t) = \sqrt{\sum_{n=-\infty}^{\infty} n^2 \, p(t, n)}, \tag{3.24}$$

where $p(t, n)$ is the probability distribution of the quantum walk with the initial condition given by (3.23). The analytical calculation is quite elaborate and is performed in another chapter. For now, we calculate $\sigma(t)$ numerically using a computational implementation. Figure 3.6 depicts the standard deviation as a function of time for the quantum walk (cross-shaped points) and classical random walk (circle-shaped points). In the classical case, we have $\sigma(t) = \sqrt{t}$. In the quantum case, we obtain a line with slope 0.54 approximately, that is, $\sigma(t) = 0.54\, t$.

It is remarkable that the position standard deviation is proportional to t. Compare with the following extreme situation. Suppose that the probability of the particle to go to the right is exactly 1. After t steps, it will certainly be found at $n = t$. This is called the *ballistic* case. It is the motion of a free particle with unit velocity. The standard deviation in this case is obtained by replacing $p(t, n)$ by $\delta_{t\,n}$ in (3.24). The result is $\sigma(t) = t$. The Hadamard quantum walk is ballistic, though its speed is almost half of the speed of the free particle. However, after a measurement the quantum particle

can be found either on the right-hand side or on the left-hand side of the origin, which is not possible in a classical ballistic motion.

Exercise 3.8. Obtain states $|\psi(4)\rangle$ and $|\psi(5)\rangle$ by continuing the sequence of the states of (3.19) and check that the probability distribution coincides with the one described in Fig. 3.3.

3.4 Classical Continuous-Time Markov Chains

The coined quantum walk model is not the only way to *quantize* classical random walks. In the next section, we describe another quantum walk model that does not use a coin. In this section, we describe the classical *continuous-time Markov chain*, which is used as the base model for the quantization.

When time is a continuous variable, the walker can go from vertex x_j to an adjacent vertex x_i at any time. One way to visualize the dynamics is to consider the probability as if it is a liquid seeping from x_j to x_i. At the beginning, the walker is on vertex x_j and it is likely to be found there during a short period. As time goes by, the probability of being found on one of the neighboring vertices increases and the probability of staying on x_j decreases, and eventually the walker moves ahead. We have a *transition rate* denoted by γ, which is constant for all vertices (*homogeneous rate*) and for all times (*uniform rate*). Then, the transition between neighboring vertices occurs with a probability γ per unit time. To address problems with continuous variables, we generally use an *infinitesimal* time interval, set up the differential equation of the problem, and solve the equation. If we take an infinitesimal time interval ϵ, the probability of the walker to go from vertex x_j to x_i is $\gamma\epsilon$. Let d_j be the degree of the vertex x_j, that is, vertex x_j has d_j neighboring vertices. It follows that the probability of the walker to be on one of the neighboring vertices after time ϵ is $d_j\gamma\epsilon$. Then, the probability of staying on x_j is $1 - d_j\gamma\epsilon$. In the continuous-time case, the entry $M_{ij}(t)$ of the transition matrix at time t is defined as the probability of the particle, which is on vertex x_j, to go to vertex x_i during the time interval t. Then,

$$M_{ij}(\epsilon) = \begin{cases} 1 - d_j\gamma\epsilon + O(\epsilon^2), & \text{if } i = j; \\ \gamma\epsilon + O(\epsilon^2), & \text{if } i \neq j. \end{cases} \tag{3.25}$$

Let us define an auxiliary matrix, called *generating matrix* given by

$$H_{ij} = \begin{cases} d_j\gamma, & \text{if } i = j; \\ -\gamma, & \text{if } i \neq j \text{ and adjacent;} \\ 0, & \text{if } i \neq j \text{ and non-adjacent.} \end{cases} \tag{3.26}$$

It is known that the probability of two independent events is the product of the probability of each event. The same occurs in a Markov chain because the next state of a Markov chain depends only on the current configuration of the chain. We can

multiply the transition matrix at different times. Then,

$$M_{ij}(t+\epsilon) = \sum_k M_{ik}(t) M_{kj}(\epsilon). \tag{3.27}$$

The index k runs over all vertices; however, this is equivalent to running only over the vertices adjacent to x_j. In fact, if there is no edge linking x_j and x_k, then $M_{kj}(\epsilon) = 0$.

By isolating the term $k = j$ and using the (3.25) and (3.26), we obtain

$$\begin{aligned} M_{ij}(t+\epsilon) &= M_{ij}(t) M_{jj}(\epsilon) + \sum_{k \neq j} M_{ik}(t) M_{kj}(\epsilon) \\ &= M_{ij}(t)(1 - \epsilon H_{jj}) - \epsilon \sum_{k \neq j} M_{ik}(t) H_{kj}. \end{aligned}$$

By moving the first term on the right-hand side to the left-hand side and dividing by ϵ, we obtain

$$\frac{\mathrm{d}M_{ij}(t)}{\mathrm{d}t} = -\sum_k H_{kj} M_{ik}(t). \tag{3.28}$$

The solution of this differential equation with initial condition $M_{ij}(0) = \delta_{ij}$ is

$$M(t) = \mathrm{e}^{-Ht}. \tag{3.29}$$

The verification is simple if we expand the exponential function in *Taylor series*. With the transition matrix in hand, we can obtain the probability distribution at time t. If the initial distribution is $\vec{p}(0)$, we have

$$\vec{p}(t) = M(t)\, \vec{p}(0). \tag{3.30}$$

It is interesting to compare this form of evolution with the one for the discrete-time Markov chain, given by (3.10).

Exercise 3.9. Show that the uniform vector is a 0-eigenvector of H. Use this to show that the uniform vector is a 1-eigenvector of $M(t)$. Show that $M(t)$ is a stochastic matrix for all $t \in \mathbb{R}$.

Exercise 3.10. What is the relationship between H and the Laplacian matrix of the graph?

Exercise 3.11. Show that the probability distribution satisfies the following differential equation:

$$\frac{\mathrm{d}p_i(t)}{\mathrm{d}t} = -\sum_k H_{ki}\, p_k(t).$$

3.5 Continuous-Time Quantum Walks

In the passage from the *classical random walk model* to the *coined model*, we use the *standard quantization process*, which consists in replacing the vector of probabilities by a state vector (a vector of probability amplitudes) and the transition matrix by a unitary matrix. It is also necessary to extend the position Hilbert space with the coin Hilbert space, which is accomplished with the tensor product because we need to obey the postulates of quantum mechanics.

In the passage from the *continuous-time Markov chain* to the *continuous-time quantum walk model*, we use again the standard quantization process. Note that the continuous-time Markov chain has no coin. Then, we simply convert the vector that describes the probability distribution to a state vector and the transition matrix to an equivalent unitary operator. We must pay attention to the following detail: Matrix H is Hermitian and matrix M is not unitary in general. There is a simple way to make M unitary, which is to replace H by $\mathrm{i}H$, that is, to multiply H by the *imaginary unit*. Let us define the evolution operator of the continuous-time quantum walk as

$$U(t) = \mathrm{e}^{-\mathrm{i}Ht}. \tag{3.31}$$

If the initial condition is $|\psi(0)\rangle$, the quantum state at time t is

$$|\psi(t)\rangle = U(t)|\psi(0)\rangle \tag{3.32}$$

and the probability distribution is

$$p_k = \left|\left\langle k \middle| \psi(t)\right\rangle\right|^2, \tag{3.33}$$

where k is a vertex label or a state of the Markov chain and $|k\rangle$ is the state of the computational basis corresponding to the vertex k.

3.5.1 Continuous-Time Walk on the Line

As a first application, let us consider the continuous-time quantum walk on the line. The vertices are integer points (discrete space). Equation (3.26) reduces to

$$H_{ij} = \begin{cases} 2\gamma, & \text{if } i = j; \\ -\gamma, & \text{if } i \neq j \text{ and adjacent;} \\ 0, & \text{if } i \neq j \text{ and non-adjacent.} \end{cases} \tag{3.34}$$

Then,

$$H|n\rangle = -\gamma\,|n-1\rangle + 2\gamma\,|n\rangle - \gamma\,|n+1\rangle. \tag{3.35}$$

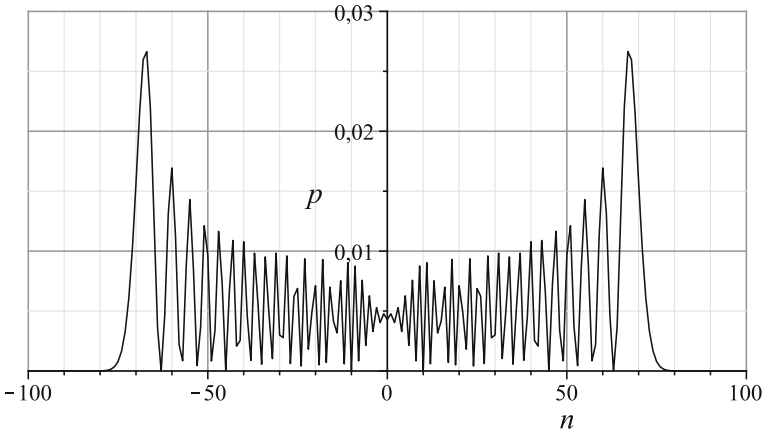

Fig. 3.7 Probability distribution at $t = 100$ with $\gamma = \left(2\sqrt{2}\right)^{-1}$ of a continuous-time quantum walk with initial condition $|\psi(0)\rangle = |0\rangle$

```
t = 100;
n = 100;
gamma = 1./(2.*Sqrt[2.]);
H = Table[If[i == j, 2.*gamma,
     If[i == j+1 || i == j-1, -gamma, 0]],
                    {i, 2*n+1}, {j, 2*n+1}];
expH = MatrixExp[-I*t*H];
Psi = expH.Table[If[i == n+1, 1, 0], {i, 2*n+1}];
ListLinePlot[Table[{i-1-n, Abs[Psi[[i]]]^2}, {i,2*n+1}]]
```

Fig. 3.8 Script in *Mathematica* that generates the probability distribution of the continuous-time quantum walk of Fig. 3.7

Fig. 3.9 Script in *Maple* that generates the probability distribution of the continuous-time quantum walk of Fig. 3.7

```
with(LinearAlgebra):
t := 100:
n := 100:
gamma0:= 1/(2.*sqrt(2.)):
H := Matrix(2*n+1, 2*n+1,
     (i,j) -> `if`(i=j, 2*gamma0,`if`(i=j+1 or
                    i=j-1, -gamma0, 0.))):
expH := MatrixExponential(-I*H*t):
Psi_t := expH . Vector([0$n, 1., 0$n]):
plot([seq([i-n, abs(Psi_t[i+1])^2], i=0..2*n)]);
```

The analytical calculation of operator $U(t)$ is guided in Exercise 3.12. The numerical calculation of this operator is relatively simple. Figure 3.7 shows the probability distribution of the continuous-time quantum walk at $t = 100$ for $\gamma = 1/\left(2\sqrt{2}\right)$ with the initial condition $|\psi(0)\rangle = |0\rangle$. This plot can be generated by the programs of Fig. 3.8 or Fig. 3.9.

The comparison of the curve of Fig. 3.7 with the curve of Fig. 3.5 is revealing. There are many common points between the evolution of discrete-time and continuous-time quantum walks; however, they differ in several details. From the global point of view, the probability distribution of the continuous-time walk has two major external peaks and a low probability near the origin, which is similar to the discrete-time case. In the coined walk, these features can be amplified or reduced by choosing an appropriate coin or changing the walker's initial condition. In the continuous-time walk, the dispersion is controlled by the constant γ. If one decreases γ, the distribution shrinks around the origin, maintaining the same pattern.

The most relevant comparison in this context refers to the standard deviation. How does the standard deviation of the continuous-time walk compare with the discrete-time walk? The probability distribution of the continuous-time walk is symmetric with respect to the origin in this case. Then, the expected position is zero, that is, $\langle n \rangle = 0$. The standard deviation $\sigma(t)$ is given by (3.24), where the probability distribution $p(t, n)$ is

$$p(t, n) = \left| \langle n | U(t) | \psi(0) \rangle \right|^2. \tag{3.36}$$

As before, we can calculate $\sigma(t)$ numerically. Figure 3.10 depicts the standard deviation as a function of time for the continuous-time quantum walk (solid line) and for the coined quantum walk (cross-shaped points). In the continuous-time case, we obtain a line with slope 0.5 approximately, or $\sigma(t) = 0.5\,t$. In the coined case, it is also a line with slope 0.54 approximately. Again, these values change if we change γ or the coin. What really matters is that the standard deviation is linear, that is, $\sigma(t)$ is proportional to t, contrasting with the classical case where $\sigma(t)$ is proportional to $\sqrt{t}$.

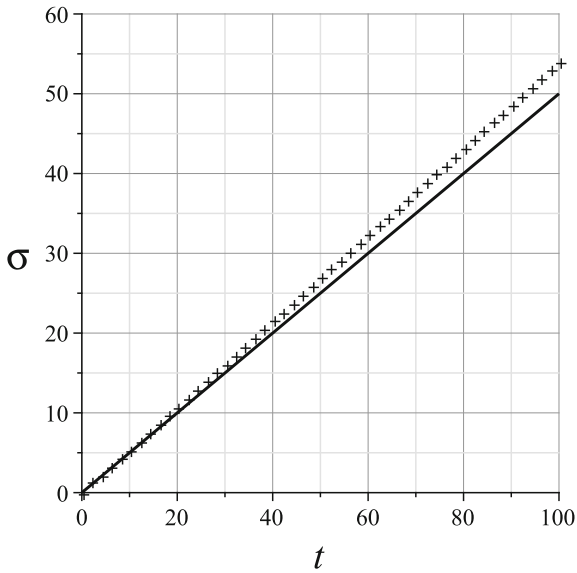

Fig. 3.10 Standard deviation as a function of time of the continuous-time quantum walk with $\gamma = \left(2\sqrt{2}\right)^{-1}$ (*solid line*) and the discrete-time quantum walk analyzed in Sect. 3.3 (*cross-shaped points*)

After analyzing two quantization models of classical random walks, the following question naturally arises: Are the coined and continuous-time models equivalent? In several applications, these models have very similar behavior. Both models have standard deviations that depend linearly on t and, with respect to algorithmic applications, they improve the time complexity for many problems when compared with classical algorithms. However, when we consider the smallest details, these models are not equivalent. We give references that address this issue in the Further Reading section.

Exercise 3.12. Show that for any real time t, matrix H of the continuous-time quantum walk on the line obeys

$$H^t|0\rangle = \gamma^t \sum_{n=-t}^{t} (-1)^n \binom{2t}{t-n} |n\rangle.$$

From this expression, compute $U(t)|0\rangle$ in terms of two nested sums. Invert the sums, use the identity

$$\mathrm{e}^{-2\,\mathrm{i}\,\gamma\,t} J_{|n|}(2\,\gamma\,t) = \mathrm{e}^{\frac{\pi \mathrm{i}}{2}|n|} \sum_{k=|n|}^{\infty} \frac{(-\mathrm{i}\gamma t)^k}{k!} \binom{2\,k}{k-n},$$

where J is the Bessel function of the first kind with integer n, to show that the wave function of the continuous-time walk on the line at time t is

$$|\psi(t)\rangle = \sum_{n=-\infty}^{\infty} \mathrm{e}^{\frac{\pi \mathrm{i}}{2}|n| - 2\,\mathrm{i}\,\gamma\,t} J_{|n|}(2\,\gamma\,t)\,|n\rangle.$$

Show that the probability distribution is

$$p(t,n) = \left| J_{|n|}(2\,\gamma\,t) \right|^2.$$

Use this result to depict the probability distributions with the same parameters of Fig. 3.7, both for continuous and discrete n.

3.5.2 Why Must Time be Continuous?

It is interesting to ask why a *Hamiltonian walk* must be continuous in time. The answer is related to *locality*. By definition, the dynamic of a quantum walk on a graph G must be local with respect to G. This means that the walker is forbidden to jump from vertex v_1 to v_2 if these vertices are non-adjacent. The walker must visit all vertices of a chain that links v_1 to v_2 before reaching v_2. Consider the expansion

$$\mathrm{e}^{-\mathrm{i}Ht} = I - \mathrm{i}Ht + \frac{(-\mathrm{i}t)^2}{2!} H^2 + \frac{(-\mathrm{i}t)^3}{3!} H^3 + \cdots.$$

Note that the action of H^a for $a \geq 2$ is non-local. For instance, if the walker is on vertex v, the action of H^2 moves the walker to the neighborhood of the neighborhood of v. One way to cancel out the action of H^a for $a \geq 2$ is to use an infinitesimal time because $\mathrm{e}^{-\mathrm{i}Ht}$ will be close to $(I - \mathrm{i}Ht)$, which is local. This explains why time must be continuous when H is defined by (3.26). Exercise 3.13 suggests an alternative route to explore this issue by restricting the choices of H.

Exercise 3.13. Try to convert the continuous-time model into a discrete-time model by using evolution operators $\mathrm{e}^{-\mathrm{i}\bar{H}t}$ with Hermitian operators $\bar{H}$ that obeys

$$\bar{H}^2 = aI + b\bar{H},$$

where $a, b \in \mathbb{R}$.

1. Show that $\mathrm{e}^{-\mathrm{i}\bar{H}t}$ is a local operator for any $t \in \mathbb{Z}$.
2. Show that if the quantum walk starts with a walker on vertex v, then the walker never goes beyond the neighborhood of v using the evolution operator $\mathrm{e}^{-\mathrm{i}\bar{H}t}$ with $t \in \mathbb{Z}$.
3. Conclude that (1) the attempt has failed and (2) we need more than one local operator in order to define a nontrivial discrete-time quantum walk model.

Further Reading

The concept of *quantum walk* was introduced in [9] from the physical viewpoint and in [133, 255] from the mathematical viewpoint. From the historical viewpoint, we can find precursor ideas dating back to 1940 in Feynman's *relativistic chessboard model*,[1] which connects the spin with the propagation of a particle in a *two-dimensional spacetime*. From now on we give references to the modern description of quantum walks.

A detailed analysis of coined quantum walks on the line is presented in [17, 247]. Coined quantum walks on arbitrary graphs are addressed in [8]. The link between *universal quantum computation* and coined quantum walks is addressed in [216]. A good reference for an initial contact with the coined quantum walk is the review article [172]. The most relevant references on quantum walks published before 2012 are provided by the review papers [13, 172, 175, 183, 274, 320] or by the review books [229, 319]. Some recent papers analyzing coined quantum walks are [31, 69, 124, 158, 239, 330, 348]. More references are provided in the next chapters.

The *continuous-time quantum walk* was introduced in [113]. The continuous-time quantum walk on the line was studied in [81]. The link between universal quantum computation and continuous-time quantum walks is addressed in [78]. Good references for an initial contact with the continuous-time quantum walk are the review article [246] or the review book [229]. The connection between the coined and continuous-time models is addressed in [79, 98, 99, 260, 294, 306]. Some recent papers analyzing continuous-time quantum walks are [39, 66, 86, 105, 117, 162, 163, 210, 212, 283, 310, 334, 339].

[1] https://en.wikipedia.org/wiki/Feynman_checkerboard.

Classical discrete-time Markov chains are described in [90, 240]. *Classical random walks* are addressed in many books such as [114, 154, 155]. Identities with *binomial* expressions used in Exercise 3.2 are described in [123] or can be deduced from the methods presented in [125]. *Stirling's approximation* is described in [114].

Chapter 4
Grover's Algorithm and Its Generalization

Grover's algorithm is a *search algorithm* originally designed to look for an element in an unsorted *quantum database* with no repeated elements. If the database elements are stored in a random order, the only available method to find a specific element is an exhaustive search. Usually, this is not the best way to use databases, especially if it is queried several times. It is better to sort the elements, which is an expensive task but performed only once. In the context of quantum computing, storing data in superposition or in an entangled state for a long period is not an easy task. Because of this, Grover's algorithm is described in this chapter via an alternate route, which shows its wide applicability.

Grover's algorithm can be generalized in order to search databases with repeated elements. The details of this generalization when we know the number of repetitions beforehand are worked out in this chapter since it is important in many applications. We also show that Grover's algorithm is *optimal* up to a multiplicative constant, that is, it is not possible to improve its *computational complexity*. If N is the number of database entries, the algorithm needs to query the database $O(\sqrt{N})$ times in order to find the marked element with high probability using $O(\log N)$ storage space. We describe a quantum circuit that shows that Grover's algorithm can be implemented with $O(\sqrt{N}\log N)$ *universal gates*.

At the heart of Grover's algorithm lies a technique called *amplitude amplification*, which can be used in many quantum algorithms. The amplitude amplification technique is presented in detail at the end of this chapter.

Grover's algorithm can be seen as a quantum-walk-based search on the complete graph with N vertices. The details are described in Sect. 9.5 on p. 195.

© Springer Nature Switzerland AG 2018

R. Portugal, *Quantum Walks and Search Algorithms*, Quantum Science and Technology, https://doi.org/10.1007/978-3-319-97813-0_4

4.1 Grover's Algorithm

Let N be 2^n for some positive integer n and suppose that $f : \{0, \ldots, N-1\} \to \{0, 1\}$ is a function whose image is $f(x) = 1$ if and only if $x = x_0$ for a fixed x_0, that is,

$$f(x) = \begin{cases} 1, & \text{if } x = x_0, \\ 0, & \text{otherwise.} \end{cases} \tag{4.1}$$

Suppose that point x_0 is unknown and we do wish to find it. It is allowed to evaluate f at any point in the domain. The problem is to find x_0 with the minimum number of evaluations. Function f is called *oracle* and point x_0 is called *marked element*.This is a search problem whose relation to a database search is clear.

Let us start by analyzing this problem from the classical viewpoint. We are not interested in the implementation details of f. On the contrary, we want to know how many times we need to apply f in order to find x_0. Supposing it is known no detail about f, our only option is to perform an exhaustive search by applying f to all points in the domain. Then, the *time complexity* of the best classical algorithm is $\Omega(N)$ because each evaluation costs some time, and we need at least N evaluations in the worst case.

A concrete way to describe this problem is to ask a programmer to select point x_0 at random and implement f using a programming language in a classical computer with a single processor. The programmer must compile the program to hide x_0—it is not allowed to read the code. The function domain is known to us and there is the following *promise*: Only one image point is 1, all others are 0. A program that solves this problem is described in Algorithm 1.

Algorithm 1: Classical search algorithm

Input: N and f as described in Eq. (4.1).
Output: x_0.

```
for x = 0 to N − 1 do
    if f(x) = 1 then
        print x
        stop
```

Now let us return to the quantum context. It is striking to know that Grover's algorithm is able to find x_0 by evaluating f less than N times, in fact, it evaluates $\left\lfloor \frac{\pi}{4}\sqrt{N} \right\rfloor$ times, which is asymptotically optimal. There is a quadratic gain in the time complexity in the transition from the classical to the quantum context. How can we put this problem concretely in the quantum context? Can we write a quantum program equivalent to Algorithm 1?

In the quantum context, we must use a unitary operator $\mathcal{R}_f$ that plays the role of the function f. There is a standard method to build $\mathcal{R}_f$. The method can be used to implement an arbitrary function. The quantum computer has two *registers*: The

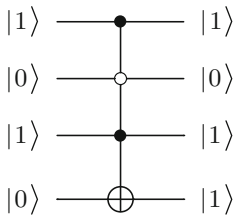

Fig. 4.1 Circuit of operator $\mathcal{R}_f$ when $x_0 = 5$ and $n = 3$. The bits of x_0 determine which control bits should be *empty* and which should be *full*. Only the programmer knows which quantum controls are empty and full. The goal of Grover's algorithm is to find out the correct configuration of the empty and full controls

first stores the domain points, and the second stores the image points. A complete description of $\mathcal{R}_f$ is given by its action on the computational basis, which is

$$\mathcal{R}_f|x\rangle|i\rangle = |x\rangle|i \oplus f(x)\rangle, \tag{4.2}$$

where operation $\oplus$ is the *binary sum* or *bitwise xor*. The standard method is based on the following recipe: (1) Repeat x to guarantee *reversibility*, and (2) add the image of x to the value inside the *ket* of the second register. For any function f, the resulting operator is unitary. For the oracle (4.1), the first register has n qubits and the second has one qubit and the associated Hilbert space has $(2N)$ dimensions. If the state of the first register is $|x\rangle$ and the state of the second register is $|0\rangle$, $\mathcal{R}_f$ evaluates $f(x)$ and stores the result in the second register, that is,

$$\mathcal{R}_f|x\rangle|0\rangle = \begin{cases} |x_0\rangle|1\rangle, & \text{if } x = x_0, \\ |x\rangle|0\rangle, & \text{otherwise.} \end{cases} \tag{4.3}$$

Now we ask a quantum programmer to implement $\mathcal{R}_f$. The programmer uses a *generalized Toffoli gate*. For example, the circuit of Fig. 4.1 implements $\mathcal{R}_f$ when $x_0 = 5$ and $n = 3$. Note that the state of the second register will change from $|0\rangle$ to $|1\rangle$ only if the entry of the first register is 5, otherwise it remains equal to $|0\rangle$ (see Sect. A.16 on p. 265).

Similar to the classical setting, we are not allowed to look at any implementation detail about $\mathcal{R}_f$, but we can apply this operator as many times as we wish. What is the algorithm that determines x_0 using $\mathcal{R}_f$ the minimum number of times?

Grover's algorithm uses a second unitary operator defined by

$$\mathcal{R}_{\mathrm{D}} = \left(2\,|\mathrm{D}\rangle\langle\mathrm{D}| - I_N\right) \otimes I_2, \tag{4.4}$$

where

$$|\mathrm{D}\rangle = \frac{1}{\sqrt{N}} \sum_{j=0}^{N-1} |j\rangle,$$

that is, $|\mathrm{D}\rangle$ the *diagonal state* of the first register (see Sect. A.16 on p. 265). The *evolution operator* that performs one step of the algorithm is

$$\mathcal{U} = \mathcal{R}_{\mathrm{D}}\,\mathcal{R}_f. \tag{4.5}$$

The initial condition is

$$|\psi_0\rangle = |\mathrm{D}\rangle|-\rangle, \tag{4.6}$$

where $|-\rangle = (|0\rangle - |1\rangle)/2$. The algorithm tells us to apply $\mathcal{U}$ iteratively $\left\lfloor \frac{\pi}{4}\sqrt{N} \right\rfloor$ times. Then, measure the first register in the computational basis and the result is x_0 with probability greater than or equal to $1 - \frac{1}{N}$ (see Algorithm 2).

Algorithm 2: Grover's algorithm

Input: N and f as described in Eq. (4.1).
Output: x_0 with probability greater than or equal to $1 - \frac{1}{N}$.

1. Use a 2-register quantum computer with $n + 1$ qubits;
2. Prepare the initial state $|\mathrm{D}\rangle|-\rangle$;
3. Apply $\mathcal{U}^t$, where $t = \left\lfloor \frac{\pi}{4}\sqrt{N} \right\rfloor$ and $\mathcal{U}$ is given by (4.5);
4. Measure the first register in the computational basis.

4.2 Quantum Circuit of Grover's Algorithm

Figure 4.2 depicts the circuit of Grover's algorithm. To check the correctness of this circuit, we have to show that $\mathcal{R}_{\mathrm{D}}$ has been correctly implemented. We use the equation

$$|\mathrm{D}\rangle = H^{\otimes n}|0\rangle,$$

in order to show that

$$\mathcal{R}_{\mathrm{D}} = -\left(H^{\otimes n}\left(I - 2\,|0\rangle\langle 0|\right) H^{\otimes n}\right) \otimes I_2.$$

The action of the operator $\left(I - 2\,|0\rangle\langle 0|\right)$ on $|x\rangle$ is $-|0\rangle$ if $x = 0$, and $|x\rangle$ if $x \neq 0$. This action is equal to the action of $\mathcal{R}_f$ when the marked element is $x_0 = 0$. Then, we can implement $\left(I - 2\,|0\rangle\langle 0|\right)$ with a generalized Toffoli acting on $(n + 1)$ qubits with n empty controls. There is a minus sign in the definition of $\mathcal{R}_{\mathrm{D}}$ in terms of $\left(I - 2\,|0\rangle\langle 0|\right)$. We disregard this minus sign because it is a global phase with no effect on the result. This shows that this is a correct implementation of Grover's algorithm and with high probability the output $(i_1, \ldots, i_n)$ is x_0 in base-2.

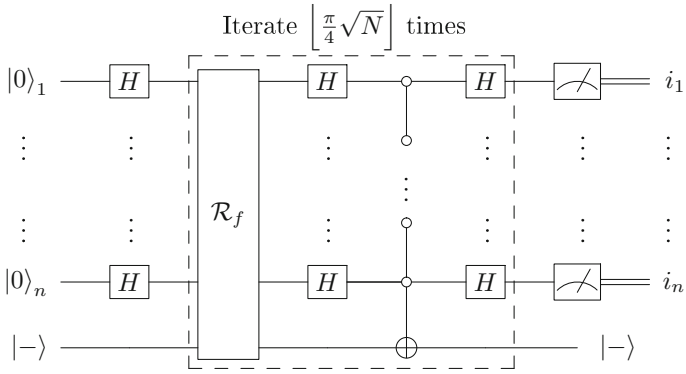

Fig. 4.2 Circuit of Grover's algorithm. The first register has n qubits initially in state $|0\rangle$. The second register has 1 qubit always in state $|-\rangle$. The dashed box is iterated $\lfloor (\pi/4)\sqrt{N} \rfloor$ times and its input is $|\mathrm{D}\rangle|-\rangle$. At the end, the first register is measured and the output is the binary digits $i_1, \ldots, i_n$, which are with high probability the digits of x_0 in base-2

From the circuit of Fig. 4.2, it is clear that the *query complexity* is $O(\sqrt{N})$. To be more precise, the number of queries is exactly the floor of $(\pi/4)\sqrt{N}$ because this is the number of times $\mathcal{R}_f$ is used in the circuit. Note that in the quantum case, instead of counting the number of times f is evaluated, we count the number of times $\mathcal{R}_f$ is used, which is equivalent to the number of times the quantum database is queried.

The *time complexity* is a bit larger than the query complexity. A generalized Toffoli gate with n controls can be implemented with $O(n)$ *universal gates* as shown in Sect. A.16 on p. 265. Then, the time complexity of Grover's algorithm is $O(\sqrt{N} \log N)$.

Exercise 4.1. Use Fig. 4.2 to depict the circuit of Grover's algorithm for the case $n = 3$ ($N = 8$) when the marked element is $x_0 = 5$ in the following cases:

1. Using generalized Toffoli gates.
2. Using Toffoli gates (no generalized gate is allowed).
3. Using universal gates (CNOT, X, H, T, and $T^\dagger$).

Implement the version using universal gates on a quantum computer.

4.3 Analysis of the Algorithm Using Reflection Operators

The evolution operator and the initial condition of Grover's algorithm have real entries. This means that the entire evolution takes place in a real vector subspace of a $(2N)$-dimensional Hilbert space. We can give a geometric interpretation to the algorithm and, in fact, visualize the evolution as a rotation of a vector on a two-dimensional vector space over the real numbers. The key to understanding the

algorithm is to note that the evolution operator $\mathcal{U}$ is the product of two *reflection operators*. It is easier to show this fact after noting that the state of the second register does not change during the algorithm. Initially, this state is $|-\rangle$ and it does not change under the action of $\mathcal{R}_{\mathrm{D}}$ as can be seen from (4.4). It does not change either under the action of $\mathcal{R}_f$ because if the state of the first register is $|x\rangle$ with $x \neq x_0$, from the definition of $\mathcal{R}_f$ — Eq. (4.3), the state $|x\rangle|-\rangle$ does not change. If $x = x_0$, the action of $\mathcal{R}_f$ on $|x_0\rangle|-\rangle$ is

$$\begin{aligned}\mathcal{R}_f\,|x_0\rangle|-\rangle &= \frac{\mathcal{R}_f|x_0\rangle|0\rangle - \mathcal{R}_f|x_0\rangle|1\rangle}{\sqrt{2}}\\ &= \frac{|x_0\rangle|1\rangle - |x_0\rangle|0\rangle}{\sqrt{2}}\\ &= -|x_0\rangle|-\rangle.\end{aligned}$$

There is a sign inversion, but the minus sign can be absorbed by the state of the first register and then the state to the second register is still $|-\rangle$. The state of the second register is always $|-\rangle$ if we give a proper destination to the minus sign when the input of the first register is $|x_0\rangle$.

On the one hand, the second register is necessary for the algorithm because it is the only way to define $\mathcal{R}_f$. On the other hand, we can discard it for the sake of simplicity in the analysis of the algorithm. We define the reduced versions R_f and R_{D} that act on the Hilbert space $\mathcal{H}^N$ and replace $\mathcal{R}_f$ and $\mathcal{R}_{\mathrm{D}}$, respectively. The definitions of the reduced operators are

$$R_f = -|x_0\rangle\langle x_0| + \sum_{x\neq x_0} |x\rangle\langle x| \tag{4.7}$$

and

$$R_{\mathrm{D}} = 2\,|\mathrm{D}\rangle\langle\mathrm{D}| - I_N. \tag{4.8}$$

The input to the algorithm is $|\mathrm{D}\rangle$, which is the reduced version of $|\mathrm{D}\rangle|-\rangle$, and the reduced version of the evolution operator is

$$U = R_{\mathrm{D}} R_f. \tag{4.9}$$

Note that the action of the reduced version R_f on $|x\rangle$ is the same as $\mathcal{R}_f$ on $|x\rangle|-\rangle$ for all x in the computational basis of $\mathcal{H}^N$.

Let us check that R_f is a reflection. Define the following vector spaces over the real numbers:

$$\begin{aligned}\mathcal{A} &= \mathrm{span}\{|x_0\rangle\},\\ \mathcal{B} &= \mathrm{span}\{|x\rangle : x \neq x_0\}.\end{aligned}$$

Note that $\dim \mathcal{A} = 1$, $\dim \mathcal{B} = N - 1$, and $\mathcal{A} \perp \mathcal{B}$. In other words, $\mathcal{B}$ is the real subspace of $\mathcal{H}^N$ that is orthogonal to the vector space spanned by $|x_0\rangle$. We state that

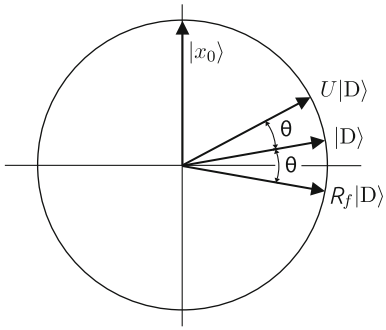

Fig. 4.3 The initial condition of Grover's algorithm is state $|\mathrm{D}\rangle$. After applying operator R_f, state $|\mathrm{D}\rangle$ is reflected through the hyperplane orthogonal to vector $|x_0\rangle$, represented by the horizontal line. After applying operator R_D, vector $R_f|\mathrm{D}\rangle$ is reflected through $|\mathrm{D}\rangle$. That is, one application of U rotates the initial vector through angle θ about the origin toward vector $|x_0\rangle$

R_f is a reflection through $\mathcal{B}$. The proof is the following: Let $|\psi\rangle$ be a real vector in $\mathcal{H}^N$. Then, there are $|\psi_a\rangle \in \mathcal{A}$ and $|\psi_b\rangle \in \mathcal{B}$ such that $|\psi\rangle = |\psi_a\rangle + |\psi_b\rangle$. The action of R_f on $|\psi\rangle$ inverts the sign of $|\psi_a\rangle$ and preserves the sign of $|\psi_b\rangle$. The geometric interpretation of this action is a reflection through $\mathcal{B}$, that is, $-|\psi_a\rangle + |\psi_b\rangle$ is the mirror image of $|\psi_a\rangle + |\psi_b\rangle$ and the mirror is the vector space $\mathcal{B}$. The mirror is always the vector space that is invariant.

Let us check that R_D is also a reflection. Using (4.8), we obtain $R_\mathrm{D}|\mathrm{D}\rangle = |\mathrm{D}\rangle$ and $R_\mathrm{D}\left|\mathrm{D}^\perp\right\rangle = -\left|\mathrm{D}^\perp\right\rangle$, where $\left|\mathrm{D}^\perp\right\rangle$ is any real vector orthogonal to $|\mathrm{D}\rangle$. Let $\mathcal{D}$ be the vector space spanned by $|\mathrm{D}\rangle$. $\mathcal{D}$ is invariant under the action of R_D and any vector orthogonal to $|\mathrm{D}\rangle$ inverts its sign under the action of R_D. Then, R_D is a reflection through $\mathcal{D}$.

From Fig. 4.3, we see that the action of U on the initial state $|\mathrm{D}\rangle$ returns a vector that is in the vector space spanned by $|x_0\rangle$ and $|\mathrm{D}\rangle$. This is checked in the following way: Note that $|\mathrm{D}\rangle$ is almost orthogonal to $|x_0\rangle$ if N is large. Start by considering the initial condition $|\mathrm{D}\rangle$ in Fig. 4.3, then apply R_f, then apply R_D, and then convince yourself that $U|\mathrm{D}\rangle$ is correctly represented. The same argumentation holds for successive applications of U. Therefore, the entire evolution takes place in a real two-dimensional subspace $\mathcal{W}$ of $\mathcal{H}^N$, where $\mathcal{W} = \mathrm{span}\left\{|\mathrm{D}\rangle, |x_0\rangle\right\}$.

We can further simplify the interpretation of R_f. Let $\left|x_0^\perp\right\rangle$ be the unit vector orthogonal to $|x_0\rangle$ that is in $\mathcal{W}$ and has the smallest angle with $|\mathrm{D}\rangle$. The expression for $\left|x_0^\perp\right\rangle$ in the computational basis is

$$\left|x_0^\perp\right\rangle = \frac{1}{\sqrt{N-1}} \sum_{x \neq x_0} |x\rangle. \tag{4.10}$$

Set $\left\{\left|x_0^\perp\right\rangle, |x_0\rangle\right\}$ is an orthonormal basis of $\mathcal{W}$. For vectors in $\mathcal{W}$, R_f can be interpreted as a reflection through the one-dimensional vector space spanned by $\left|x_0^\perp\right\rangle$.

Let $(\theta/2)$ be the angle between vectors $\left|x_0^{\perp}\right\rangle$ and $|\mathrm{D}\rangle$, that is, $(\theta/2)$ is the complement of the angle between $|x_0\rangle$ and $|\mathrm{D}\rangle$. So,

$$\begin{aligned}\sin\frac{\theta}{2} &= \cos\left(\frac{\pi}{2}-\frac{\theta}{2}\right)\\ &= \left\langle x_0\middle|\mathrm{D}\right\rangle\\ &= \frac{1}{\sqrt{N}}.\end{aligned} \tag{4.11}$$

Angle θ is very small when $N \gg 1$, i.e., when the function f has a large domain. Solving (4.11) for θ and calculating the asymptotic expansion, we obtain

$$\theta = \frac{2}{\sqrt{N}} + \frac{1}{3\,N\sqrt{N}} + O\left(\frac{1}{N^2}\right). \tag{4.12}$$

Starting from the initial condition $|\mathrm{D}\rangle$, one application of U rotates $|\mathrm{D}\rangle$ through approximately $2/\sqrt{N}$ radians about the origin toward $|x_0\rangle$. This application makes little progress, but definitely a good one because it can be repeated. At the time step (*running time*)

$$t_{\mathrm{run}} = \left\lfloor \frac{\pi}{4}\sqrt{N} \right\rfloor, \tag{4.13}$$

$|\mathrm{D}\rangle$ will have rotated through approximately $\pi/2$ radians. In fact, it will have rotated a little less, because the next term in the expansion (4.12) is positive. The probability of obtaining x_0 when we measure the first register is

$$p_{x_0} = \left|\langle x_0|U^{t_{\mathrm{run}}}|\mathrm{D}\rangle\right|^2. \tag{4.14}$$

The angle between $|x_0\rangle$ and the final state is about $2/\sqrt{N}$ and is at most $\theta/2$. Then,

$$p_{x_0} \geq \cos^2\left(\frac{\theta}{2}\right). \tag{4.15}$$

Using (4.11), we obtain

$$p_{x_0} \geq 1 - \frac{1}{N}. \tag{4.16}$$

The lower bound for the success probability shows that Grover's algorithm has a very high success probability when N is large.

To summarize, we have used the fact that U is a real operator and the product of two reflections to perform the algorithm analysis as an evolution in a real two-dimensional subspace of the Hilbert space. U is a rotation matrix on a two-dimensional vector space and the rotation angle is twice the angle between the vector spaces that are

invariant under the action of the reflection operators. The marked state $|x_0\rangle$ and initial condition $|\mathrm{D}\rangle$ are almost orthogonal when N is large. The strategy of the algorithm is to rotate the initial condition through $\pi/2$ radians about the origin and to perform a measurement in the computational basis. Since the angle between the final state and the marked state is small, the probability of obtaining x_0 as a result of the measurement is close to 1.

Exercise 4.2. Show that the success probability of Grover's algorithm is exactly 121/128 when $N = 8$ and is exactly 1 when $N = 4$ using a single iteration.

Exercise 4.3. Calculate the probability of Grover's algorithm returning x such that $x \neq x_0$, when $N \gg 1$. Check out that the sum of the probabilities, when we consider all cases $x \neq x_0$ and $x = x_0$, is asymptotically equal to 1.

Exercise 4.4. After discarding the second register, show that operator R_f given by (4.7) can be written as

$$R_f = I - 2\,|x_0\rangle\langle x_0|, \tag{4.17}$$

or equivalently as

$$R_f = 2\sum_{x\neq x_0} |x\rangle\langle x| - I.$$

Exercise 4.5. The goal of this exercise is to show that, when we analyze the evolution of Grover's algorithm in $\mathcal{W}$, operator R_f can be replaced by

$$R'_f = 2\,\left|x_0^{\perp}\right\rangle\left\langle x_0^{\perp}\right| - I_N,$$

which keeps $\left|x_0^{\perp}\right\rangle$ unchanged and inverts the sign of a vector orthogonal to $\left|x_0^{\perp}\right\rangle$. Show that the actions of R'_f and R_f are the same if we restrict their actions to real vectors in $\mathcal{W}$.

Exercise 4.6. The analysis of Grover's algorithm presented in this section is heavily based on Fig. 4.3. On the other hand, it is known that on real vector spaces the action of two successive reflections on a real vector $|\psi\rangle$ rotates $|\psi\rangle$ through an angle that is twice the angle between the invariant spaces. The goal of this exercise is to show algebraically in the specific setting of Grover's algorithm that one application of the evolution operator rotates the current state counterclockwise through angle θ, that is, toward the marked vector.

Show algebraically that the product of reflections $(R_{\mathrm{D}}\,R_f)$ rotates an arbitrary unit vector in the real plane spanned by $|x_0\rangle$ and $\left|x_0^{\perp}\right\rangle$ through angle θ that is twice the angle between the invariant spaces, i.e., $\arccos\left\langle \mathrm{D}\middle|x_0^{\perp}\right\rangle$. Show that the direction of the rotation depends on the order of the reflections. Show that $(R_{\mathrm{D}}\,R_f)$ rotates counterclockwise. [Hint: Take an arbitrary unit vector of the form $|\psi\rangle = a\left|x_0^{\perp}\right\rangle + b|x_0\rangle$, where $a^2 + b^2 = 1$. Calculate $\cos\theta = \langle\psi|R_{\mathrm{D}}\,R_f|\psi\rangle$. Use the trigonometric identity $\cos(\theta/2) = \sqrt{1+\cos\theta}/\sqrt{2}$.]

Exercise 4.7. Show that the entries of matrix R_f given by (4.7) are $(R_f)_{k\ell} = (-1)^{\delta_{kx_0}}\delta_{k\ell}$ and for matrix $\mathcal{R}_{\mathrm{D}}$ given by (4.8) are $(R_{\mathrm{D}})_{k\ell} = \frac{2}{N} - \delta_{k\ell}$. Show that the entries of U are

$$U_{k\ell} = (-1)^{\delta_{\ell x_0}}\left(\frac{2}{N} - \delta_{k\ell}\right).$$

4.4 Analysis Using the Two-Dimensional Real Space

There is an alternate route to analyze Grover's algorithm by considering orthogonal operators acting on $\mathbb{R}^2$.

Let us start with the initial condition. Define the unit vector

$$|\mathrm{d}\rangle = \frac{\sqrt{N-1}}{\sqrt{N}}\,|0\rangle + \frac{1}{\sqrt{N}}\,|1\rangle,$$

which is the two-dimensional version of $|\mathrm{D}\rangle$. Vector $|0\rangle$ plays the role of $\left|x_0^{\perp}\right\rangle$ and $|1\rangle$ plays the role of $|x_0\rangle$. Using (4.11), we obtain

$$|\mathrm{d}\rangle = \cos\frac{\theta}{2}\,|0\rangle + \sin\frac{\theta}{2}\,|1\rangle. \tag{4.18}$$

The two-dimensional version of R_{D} is

$$r_{\mathrm{d}} = 2|\mathrm{d}\rangle\langle\mathrm{d}| - I_2,$$

and, using the definition of $|\mathrm{d}\rangle$ and trigonometric identities, we obtain

$$r_{\mathrm{d}} = \begin{bmatrix} \cos\theta & \sin\theta \\ \sin\theta & -\cos\theta \end{bmatrix}.$$

The two-dimensional version of R_f is

$$r_f = \begin{bmatrix} 1 & 0 \\ 0 & -1 \end{bmatrix}$$

and the two-dimensional version of U is

$$u = r_{\mathrm{d}}\, r_f = \begin{bmatrix} \cos\theta & -\sin\theta \\ \sin\theta & \cos\theta \end{bmatrix}, \tag{4.19}$$

which is an orthogonal rotation matrix that rotates any vector counterclockwise through angle θ. Using induction on t and trigonometric identities, we obtain (Exercise 4.8)

$$u^t = \begin{bmatrix} \cos(\theta t) & -\sin(\theta t) \\ \sin(\theta t) & \cos(\theta t) \end{bmatrix}$$

for any positive integer t and

$$u^t|\mathrm{d}\rangle = \cos\left(\theta t + \frac{\theta}{2}\right)|0\rangle + \sin\left(\theta t + \frac{\theta}{2}\right)|1\rangle.$$

The running time of Grover's algorithm is the time step that maximizes the amplitude of $|1\rangle$, that is, it is t_{run} such that

$$\sin\left(\theta t_{\mathrm{run}} + \frac{\theta}{2}\right) = 1.$$

We have to solve the equation $\theta t_{\mathrm{run}} + \theta/2 = \pi/2$, which yields

$$t_{\mathrm{run}} = \frac{\pi}{2\theta} - \frac{1}{2}.$$

Using that $\theta \approx 2/\sqrt{N}$, we obtain the running time

$$t_{\mathrm{run}} = \left\lfloor \frac{\pi}{4}\sqrt{N} \right\rfloor.$$

The success probability, using the previous expressions of t_{run} and θ, is

$$p_{\mathrm{succ}} = \sin^2\left(\frac{\pi}{2} + \frac{1}{\sqrt{N}}\right),$$

whose asymptotic expansion is

$$p_{\mathrm{succ}} = 1 - \frac{1}{N} + O\left(\frac{1}{N^2}\right).$$

The mapping defined in Exercise 4.10 establishes a correspondence between the calculations in $\mathbb{R}^2$ and the calculations in $\mathcal{H}^N$.

Exercise 4.8. Show by induction on t that

$$u^t = \begin{bmatrix} \cos(\theta t) & -\sin(\theta t) \\ \sin(\theta t) & \cos(\theta t) \end{bmatrix}$$

for any positive integer t.

Exercise 4.9. Show that r_f and r_{d} are Hermitian and unitary operators. Can we conclude that $(r_{\mathrm{d}}\, r_f)$ is Hermitian? Show that any nonHermitian real unitary operator

has at least two nonreal eigenvalues. Show that the nonreal eigenvalues come in complex conjugate pairs.

Exercise 4.10. A vector $|\psi\rangle = a\,|0\rangle + b\,|1\rangle$ in $\mathcal{W}$ corresponds to a vector $|\Psi\rangle$ in $\mathcal{H}^N$, whose definition is

$$|\Psi\rangle = a\,\left|x_0^{\perp}\right\rangle + b\,|x_0\rangle.$$

This correspondence is established by a linear transformation from $\mathcal{W}$ to $\mathcal{H}^N$ so that $|0\rangle$ corresponds to $\left|x_0^{\perp}\right\rangle$ and $|1\rangle$ to $|x_0\rangle$. Show that if $|\psi\rangle$ is an eigenvector of u with eigenvalue λ, then the corresponding vector $|\Psi\rangle$ is an eigenvector of U with eigenvalue λ. Show that there are eigenvectors of U that cannot be obtained from u.

Exercise 4.11. Define a linear mapping $\phi : \mathcal{W} \mapsto \mathcal{H}^{2N}$ so that

$$\phi\big(a\,|0\rangle + b\,|1\rangle\big) = \big(a\,\left|x_0^{\perp}\right\rangle + b\,|x_0\rangle\big) \otimes |-\rangle$$

for $a, b \in \mathbb{C}$. Convince yourself that by using ϕ we can bypass the analysis of Grover's algorithm described in Sect. 4.3 and prove its correctness using only the method of this section.

4.5 Analysis Using the Spectral Decomposition

Another way to analyze the evolution of Grover's algorithm is via the *spectral decomposition* of u, given by (4.19). Instead of using $\mathbb{R}^2$, we have to use $\mathcal{H}^2$ (see Exercise 4.9). If we use the method described in Exercise 4.10, we obtain some eigenvectors of U from the eigenvectors of u. We cannot obtain all eigenvectors of U from u, but this is no problem because not all eigenvectors of U matter, and in fact the ones that matter are obtained from u. The remaining eigenvectors have no overlap with the initial condition.

The *characteristic polynomial* of u is

$$|\lambda I - u| = \lambda^2 - 2\,\lambda\cos\theta + 1, \tag{4.20}$$

and then the eigenvalues of u are $\mathrm{e}^{\pm \mathrm{i}\theta}$, where

$$\cos\theta = 1 - \frac{2}{N}. \tag{4.21}$$

A unit eigenvector of u associated with $\mathrm{e}^{\mathrm{i}\theta}$ is

$$|\alpha_1\rangle = \frac{|0\rangle - \mathrm{i}\,|1\rangle}{\sqrt{2}}, \tag{4.22}$$

and a unit eigenvector associated with $\mathrm{e}^{-\mathrm{i}\theta}$ is

$$|\alpha_2\rangle = \frac{|0\rangle + \mathrm{i}\,|1\rangle}{\sqrt{2}}. \tag{4.23}$$

Set $\left\{|\alpha_1\rangle, |\alpha_2\rangle\right\}$ is an orthonormal basis of $\mathcal{H}^2$.

To analyze the evolution of Grover's algorithm, we must find the expression of the initial condition $|\mathrm{d}\rangle$ in the eigenbasis of u. Using (4.18), we obtain

$$|\mathrm{d}\rangle = \frac{1}{\sqrt{2}}\left(\mathrm{e}^{\frac{\mathrm{i}\theta}{2}}|\alpha_1\rangle + \mathrm{e}^{-\frac{\mathrm{i}\theta}{2}}|\alpha_2\rangle\right). \tag{4.24}$$

The action of u^t on $|\mathrm{d}\rangle$ can be readily calculated when $|\mathrm{d}\rangle$ is written in the eigenbasis of u.[1] The result is

$$u^t|\mathrm{d}\rangle = \frac{1}{\sqrt{2}}\left(\mathrm{e}^{\mathrm{i}\left(\theta t+\frac{\theta}{2}\right)}|\alpha_1\rangle + \mathrm{e}^{-\mathrm{i}\left(\theta t+\frac{\theta}{2}\right)}|\alpha_2\rangle\right). \tag{4.25}$$

The probability of finding x_0 as a function of the number of steps is

$$\begin{aligned} p(t) &= \left|\langle 1|u^t|\mathrm{d}\rangle\right|^2 \\ &= \frac{1}{2}\left|\mathrm{e}^{\mathrm{i}\left(\theta t+\frac{\theta}{2}\right)}\left\langle 1\middle|\alpha_1\right\rangle + \mathrm{e}^{-\mathrm{i}\left(\theta t+\frac{\theta}{2}\right)}\left\langle 1\middle|\alpha_2\right\rangle\right|^2 \\ &= \sin^2\left(\theta t + \frac{\theta}{2}\right). \end{aligned} \tag{4.26}$$

From now on, the calculation is equal to the one in the previous section. The running time is

$$t_{\mathrm{run}} = \left\lfloor \frac{\pi}{4}\sqrt{N} \right\rfloor$$

and the asymptotic expansion of the success probability is

$$p_{\mathrm{succ}} = 1 - \frac{1}{N} + O\left(\frac{1}{N^2}\right).$$

4.6 Optimality of Grover's Algorithm

Grover's algorithm finds the marked element by querying the oracle $O\left(\sqrt{N}\right)$ times. Is it possible to develop an algorithm faster than Grover's algorithm? In this section, we show that Grover's algorithm is *optimal*, that is, no quantum algorithm can find the marked element with less than $\Omega\left(\sqrt{N}\right)$ evaluations of f using space $O(n)$ and with success probability greater than or equal to $1/2$.

[1] The calculation of u^t here is simpler than the calculation performed in Sect. 4.4 because there the solution of Exercise 4.8 is required.

This kind of proof should be as generic as possible. We use the standard quantum computing model in which an arbitrary algorithm is a sequence of unitary operators acting iteratively, starting with some initial condition, followed by a measurement at the end. We want to show that if the oracle is queried less than $\Omega\left(\sqrt{N}\right)$ times, the marked element is not found. Let us assume that to query the oracle we use $R_f = I - 2|x_0\rangle\langle x_0|$ as given by (4.17), where x_0 is the marked element. This is no restriction because the oracle must somehow distinguish the marked element, and in order to have other forms of oracles, let us allow the use of any unitary operators U_a and U_b that transform R_f to $U_a R_f U_b$ during the execution of the algorithm. More than that, U_a and U_b may change at each step.

Let $|\psi_0\rangle$ be the initial state. The state of the quantum computer after t steps is given by

$$|\psi_t\rangle = U_t R_f \ \ldots \ U_1 R_f U_0 |\psi_0\rangle, \tag{4.27}$$

where $U_1, \ldots, U_t$ are arbitrary unitary operators. There is no restriction on the efficiency of these operators. The strategy of the proof is to compare the state $|\psi_t\rangle$ with state

$$|\phi_t\rangle = U_t \ \ldots \ U_0 |\psi_0\rangle, \tag{4.28}$$

that is, the equivalent state without the application of the oracles. To make this comparison, we define the quantity

$$D_t = \frac{1}{N} \sum_{x_0=0}^{N-1} \left\| |\psi_t\rangle - |\phi_t\rangle \right\|^2, \tag{4.29}$$

which measures the deviation between $|\psi_t\rangle$ and $|\phi_t\rangle$ after t steps. The sum over x_0 is to average over all possible values of x_0 in order to avoid favoring any particular value. Note that $|\psi_t\rangle$ depends on x_0 and, in principle, $|\phi_t\rangle$ does not so depend. If D_t is too small after t steps, we cannot distinguish the marked element from the unmarked ones.

We will show that

$$c \leq D_t \leq \frac{4\,t^2}{N}, \tag{4.30}$$

where c is a strictly positive constant. From this result, we conclude that if we take the number of steps t with a functional dependence on N smaller than $\Omega\left(\sqrt{N}\right)$, for example, $N^{\frac{1}{4}}$, the first inequality is violated. This discordant case means that D_t is not big enough to allow us to distinguish the marked element. In the asymptotic limit, the violation of this inequality is more dramatic showing that, for this number of steps, a sequence of operators that distinguishes the marked element is equivalent to a sequence that does not so distinguish.

Let us start with inequality $D_t \leq 4\,t^2/N$. This inequality is valid for $t = 0$. By induction on t, we assume that the inequality is valid for t and show that it is valid for $t + 1$. Note that

$$
\begin{aligned}
D_{t+1} &= \frac{1}{N}\sum_{x_0=0}^{N-1}\left\| U_{t+1}R_f|\psi_t\rangle - U_{t+1}|\phi_t\rangle \right\|^2 \\
&= \frac{1}{N}\sum_{x_0=0}^{N-1}\left\| R_f|\psi_t\rangle - |\phi_t\rangle \right\|^2 \\
&= \frac{1}{N}\sum_{x_0=0}^{N-1}\left\| R_f(|\psi_t\rangle - |\phi_t\rangle) + (R_f - I)|\phi_t\rangle \right\|^2. \qquad (4.31)
\end{aligned}
$$

Using the square of the *triangle inequality*

$$
\left\| |\alpha\rangle + |\beta\rangle \right\|^2 \le \left\| |\alpha\rangle \right\|^2 + 2\,\| |\alpha\rangle \|\,\| |\beta\rangle \| + \left\| |\beta\rangle \right\|^2, \qquad (4.32)
$$

where

$$
|\alpha\rangle = R_f(|\psi_t\rangle - |\phi_t\rangle)
$$

and

$$
\begin{aligned}
|\beta\rangle &= (R_f - I)|\phi_t\rangle \\
&= -2\,\langle x_0|\phi_t\rangle\,|x_0\rangle,
\end{aligned}
$$

we obtain

$$
\begin{aligned}
D_{t+1} \le \frac{1}{N}\sum_{x_0=0}^{N-1}\Big(&\left\| |\psi_t\rangle - |\phi_t\rangle \right\|^2 + 4\left\| |\psi_t\rangle - |\phi_t\rangle \right\| \left|\langle x_0|\phi_t\rangle\right| \\
&+ 4\left|\langle x_0|\phi_t\rangle\right|^2\Big). \qquad (4.33)
\end{aligned}
$$

Using the *Cauchy–Schwarz inequality*

$$
\left|\langle \alpha|\beta\rangle\right| \le \| |\alpha\rangle \|\,\| |\beta\rangle \| \qquad (4.34)
$$

in the second term of inequality (4.33), where

$$
|\alpha\rangle = \sum_{x_0=0}^{N-1}\left\| |\psi_t\rangle - |\phi_t\rangle \right\| |x_0\rangle
$$

and

$$
|\beta\rangle = \sum_{x_0=0}^{N-1}\left|\langle x_0|\phi_t\rangle\right| |x_0\rangle
$$

and also using the fact that

$$\sum_{x_0=0}^{N-1} \left|\langle x_0|\phi_t\rangle\right|^2 = \langle\phi_t|\phi_t\rangle = 1,$$

we obtain

$$\begin{aligned} D_{t+1} &\leq D_t + \frac{4}{N}\left(\sum_{x_0=0}^{N-1} \left\| |\psi_t\rangle - |\phi_t\rangle \right\|^2\right)^{\frac{1}{2}} \left(\sum_{x_0'=0}^{N-1} \left|\langle x_0'|\phi_t\rangle\right|^2\right)^{\frac{1}{2}} + \frac{4}{N} \\ &\leq D_t + 4\sqrt{\frac{D_t}{N}} + \frac{4}{N}. \end{aligned} \tag{4.35}$$

Since we are assuming that $D_t \leq 4\,t^2/N$ from the inductive hypothesis, we obtain $D_{t+1} \leq 4\,(t+1)^2/N$.

We now show the harder inequality $c \leq D_t$. Let us define two new quantities given by

$$E_t = \frac{1}{N}\sum_{x_0=0}^{N-1} \left\| |\psi_t\rangle - |x_0\rangle \right\|^2, \tag{4.36}$$

$$F_t = \frac{1}{N}\sum_{x_0=0}^{N-1} \left\| |\phi_t\rangle - |x_0\rangle \right\|^2. \tag{4.37}$$

We obtain an inequality involving D_t, E_t, and F_t as follows:

$$\begin{aligned} D_t &= \frac{1}{N}\sum_{x_0=0}^{N-1} \Big\| \left(|\psi_t\rangle - |x_0\rangle\right) + \left(|x_0\rangle - |\phi_t\rangle\right) \Big\|^2 \\ &\geq E_t + F_t - \frac{2}{N}\sum_{x_0=0}^{N-1} \left\| |\psi_t\rangle - |x_0\rangle \right\| \left\| |\phi_t\rangle - |x_0\rangle \right\| \\ &\geq E_t + F_t - 2\sqrt{E_t\,F_t} \\ &= \left(\sqrt{F_t} - \sqrt{E_t}\right)^2, \end{aligned} \tag{4.38}$$

where, in the first inequality, we use the square of the *reverse triangle inequality*

$$\left\| |\alpha\rangle + |\beta\rangle \right\|^2 \geq \left\| |\alpha\rangle \right\|^2 - 2\,\| |\alpha\rangle \|\,\| |\beta\rangle \| + \left\| |\beta\rangle \right\|^2 \tag{4.39}$$

and, in the second inequality, we use the Cauchy–Schwarz inequality with vectors

$$|\alpha\rangle = \sum_{x_0=0}^{N-1} \left\| |\psi_t\rangle - |x_0\rangle \right\|\, |x_0\rangle,$$

$$|\beta\rangle = \sum_{x_0=0}^{N-1} \left\| |\phi_t\rangle - |x_0\rangle \right\| \, |x_0\rangle.$$

We now show that

$$F_t \geq 2 - 2\frac{1}{\sqrt{N}}.$$

Define θ_{x_0} as the phase of $\langle x_0|\phi_t\rangle$, that is,

$$\langle x_0|\phi_t\rangle = \mathrm{e}^{\mathrm{i}\theta_{x_0}} \left|\langle x_0|\phi_t\rangle\right|.$$

Define the state

$$|\theta\rangle = \frac{1}{\sqrt{N}} \sum_{x_0=0}^{N-1} \mathrm{e}^{\mathrm{i}\theta_{x_0}} |x_0\rangle. \tag{4.40}$$

So,

$$\begin{aligned} \langle\theta|\phi_t\rangle &= \frac{1}{\sqrt{N}} \sum_{x_0=0}^{N-1} \mathrm{e}^{-\mathrm{i}\theta_{x_0}} \langle x_0|\phi_t\rangle \\ &= \frac{1}{\sqrt{N}} \sum_{x_0=0}^{N-1} \left|\langle x_0|\phi_t\rangle\right|. \end{aligned} \tag{4.41}$$

Using the Cauchy–Schwarz inequality, we obtain $\left|\langle\theta|\phi_t\rangle\right| \leq 1$ and

$$\sum_{x_0=0}^{N-1} \left|\langle x_0|\phi_t\rangle\right| \leq \sqrt{N}. \tag{4.42}$$

To reach the desired result, we use the above inequality and the fact that the real part of $\langle x_0|\phi_t\rangle$ is smaller than or equal to $\left|\langle x_0|\phi_t\rangle\right|$:

$$\begin{aligned} F_t &= \frac{1}{N} \sum_{x_0=0}^{N-1} \left\| |\phi_t\rangle - |x_0\rangle \right\|^2 \\ &= 2 - \frac{2}{N} \sum_{x_0=0}^{N-1} \mathrm{Re}\left\{\langle x_0|\phi_t\rangle\right\} \\ &\geq 2 - \frac{2}{N} \sum_{x_0=0}^{N-1} \left|\langle x_0|\phi_t\rangle\right| \\ &\geq 2 - \frac{2}{\sqrt{N}}. \end{aligned} \tag{4.43}$$

Now we show that $E_t \leq (2-\sqrt{2})$. After t steps, the state of the quantum computer after the action of the oracles is $|\psi_t\rangle$. Similar to the calculation used for F_t, we have

$$\begin{aligned} E_t &= \frac{1}{N}\sum_{x_0=0}^{N-1} \left\| |\psi_t\rangle - |x_0\rangle \right\|^2 \\ &= 2 - \frac{2}{N}\sum_{x_0=0}^{N-1} \mathrm{Re}\left\{\langle x_0|\psi_t\rangle\right\}. \end{aligned}$$

Let us assume that the probability of a measurement to return x_0 is greater than or equal to $1/2$, that is, $\left|\langle x_0|\psi_t\rangle\right|^2 \geq 1/2$ for all x_0. Instead of using $1/2$, we can choose any fixed value between 0 and 1 (Exercise 4.12) and instead of using the computational basis, we use basis $\{\mathrm{e}^{\mathrm{i}\alpha_0}|0\rangle, \ldots, \mathrm{e}^{\mathrm{i}\alpha_{N-1}}|N-1\rangle\}$, where α_{x_0} for $0 \leq x_0 < N$ is defined as the phase of $\langle x_0|\psi_t\rangle$. This basis transformation does not change the inequalities that we have obtained so far and it does not change measurement results either. In this new basis (tilde basis), $\langle \tilde{x}_0|\psi_t\rangle$ is a real number, that is, $\mathrm{Re}\left\{\langle \tilde{x}_0|\psi_t\rangle\right\} = \left|\langle \tilde{x}_0|\psi_t\rangle\right|$. Therefore,

$$\begin{aligned} E_t &= 2 - \frac{2}{N}\sum_{x_0=0}^{N-1} \left|\langle \tilde{x}_0|\psi_t\rangle\right| \\ &\leq 2 - \frac{2}{N}\sum_{x_0=0}^{N-1} \frac{1}{\sqrt{2}} \\ &= 2 - \sqrt{2}. \end{aligned} \tag{4.44}$$

Using inequalities $E_t \leq (2-\sqrt{2})$ and $F_t \geq 2 - 2/\sqrt{N}$, we obtain

$$\begin{aligned} D_t &\geq \left(\sqrt{F_t} - \sqrt{E_t}\right)^2 \\ &\geq \left(\sqrt{2 - \frac{2}{\sqrt{N}}} - \sqrt{2-\sqrt{2}}\right)^2 \\ &= \left(\sqrt{2} - \sqrt{2-\sqrt{2}}\right)^2 + O\left(\frac{1}{\sqrt{N}}\right). \end{aligned} \tag{4.45}$$

This completes the proof of inequality $c \leq D_t$ for N large enough. Constant c must obey

$$0 < c < \left(\sqrt{2} - \sqrt{2-\sqrt{2}}\right)^2.$$

We conclude that an algorithm that is able to find the marked element must obey the inequalities (4.30). Therefore, $cN \leq 4t^2$ or equivalently $t = \Omega\left(\sqrt{N}\right)$.

Exercise 4.12. Show that if the probability of measurement to return x_0 is greater than or equal to p, then the constant c must obey

$$0 < c < \left(\sqrt{2} - \sqrt{2 - 2\sqrt{p}}\right)^2.$$

To achieve a success probability close to 1, the algorithm must be run $1/p$ times. Since p is constant, this does not change the total cost of $\Omega\left(\sqrt{N}\right)$.

Exercise 4.13. Instead of assuming that $\left|\langle x_0|\psi_t\rangle\right|^2 \geq \frac{1}{2}$ for all x_0, suppose that the uniform average probability is greater than or equal to $1/2$. Show that one still needs to query the oracle $\Omega\left(\sqrt{N}\right)$ times.

Exercise 4.14. In (4.27) and (4.28), unitary operators $U_0, \ldots, U_t$ can also distinguish the marked element. Is the proof valid if $U_i = U_i' R_f$ for all i?

Exercise 4.15. What is the value of $\left\| |\alpha\rangle - |\beta\rangle \right\|^2$ for orthogonal states $|\alpha\rangle$ and $|\beta\rangle$? Can you give an interpretation for F_t and explain why it is so close to 2? Is it important that E_t be smaller than 2?

4.7 Search with Repeated Elements

Grover's algorithm solves the following problem: Given a Boolean function f, find x_0 such that $f(x_0) = 1$ assuming that x_0 is the only domain point whose image is 1. In this section, we address a generalized version. Let f be a Boolean function as before, but the image of m domain points is 1. The case $m = 1$ is equal to the previous case. Let M be the set of points whose image is 1. The problem is to find an element in M by evaluating f. How many times f must be evaluated?

We can also put this version in a concrete way. We ask a quantum programmer to choose m points in the domain of f without telling us which are the points. We know m, but we do not know the points. For example, if the programmer chooses points 5 and 6, two *generalized Toffoli gates* are needed as shown in the circuit of Fig. 4.4. Note that the state of the second register changes from $|0\rangle$ to $|1\rangle$ only if the input of the first register is 5 or 6, otherwise the state remains unchanged.

The optimal quantum algorithm that solves this problem is a straightforward generalization of Grover's algorithm. As before, we use two registers, the first has n qubits and the second has 1 qubit, whose state is always $|-\rangle$. The form of operator $\mathcal{R}_f$ is similar to the one described in (4.3) and is defined by

$$\mathcal{R}_f|x\rangle|0\rangle = \begin{cases} |x\rangle|1\rangle, & \text{if } x \in M, \\ |x\rangle|0\rangle, & \text{otherwise.} \end{cases} \tag{4.46}$$

Operator $\mathcal{R}_\mathrm{D}$ does not change and is given by (4.4). Each step is driven by $\mathcal{U} = \mathcal{R}_\mathrm{D}\,\mathcal{R}_f$ and the initial condition is $|\mathrm{D}\rangle|-\rangle$, the same as before. The number of times operator

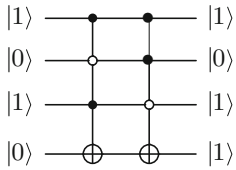

Fig. 4.4 Circuit that implements $\mathcal{R}_f$ for the case $f(5) = 1$, $f(6) = 1$, $f(x) = 0$ otherwise. Only the quantum programmer knows where the *full* and *empty* controls are. However, we know the number of generalized Toffoli gates that was used, in this case $m = 2$

$\mathcal{U}$ is applied is

$$t_{\text{run}} = \left\lfloor \frac{\pi}{4}\sqrt{\frac{N}{m}} \right\rfloor.$$

At the end, we measure the first register in the computational basis and the result is an element in M with probability greater than or equal to $1 - \frac{m}{N}$.

4.7.1 Analysis Using Reflection Operators

The analysis of the algorithm when $m > 1$ is similar to the analysis of Grover's algorithm. We discard the second register because its state is always $|-\rangle$ and we define R_f, which acts on $\mathcal{H}^N$, as

$$R_f = -\sum_{x \in M} |x\rangle\langle x| + \sum_{x \notin M} |x\rangle\langle x|. \tag{4.47}$$

We split $\mathcal{H}^N$ into two subspaces: $\mathcal{M} = \text{span}\{|x\rangle : x \in M\}$ and $\mathcal{M}^\perp = \text{span}\{|x\rangle : x \notin M\}$. R_f is a reflection through $\mathcal{M}^\perp$. We define two unit vectors in these subspaces, which are

$$|M\rangle = \frac{1}{\sqrt{m}} \sum_{x \in M} |x\rangle, \tag{4.48}$$

$$\left|M^\perp\right\rangle = \frac{1}{\sqrt{N-m}} \sum_{x \notin M} |x\rangle. \tag{4.49}$$

The evolution of the algorithm takes place in the two-dimensional vector space spanned by $|M\rangle$ and $\left|M^\perp\right\rangle$. These vectors play the same role as $|x_0\rangle$ and $\left|x_0^\perp\right\rangle$ in Grover's algorithm.

Let $(\theta/2)$ be the angle between the initial condition $|\text{D}\rangle$ and $\left|M^\perp\right\rangle$. Then,

$$\theta = 2 \arccos \langle M^{\perp} | \mathrm{D} \rangle .$$

Using (4.49), we obtain

$$\theta = 2 \arccos \sqrt{1 - \frac{m}{N}}.$$

Using trigonometric identities, we obtain

$$\theta = \arccos \left(1 - \frac{2m}{N} \right). \tag{4.50}$$

The asymptotic expansion when $N \gg m$ yields

$$\theta = 2\sqrt{\frac{m}{N}} + O\left(\frac{1}{N}\right). \tag{4.51}$$

Vector $|\mathrm{D}\rangle$ lies in the two-dimensional vector space spanned by $|M\rangle$ and $|M^{\perp}\rangle$ and is written as

$$|\mathrm{D}\rangle = \cos \frac{\theta}{2} \left| M^{\perp} \right\rangle + \sin \frac{\theta}{2} |M\rangle.$$

The evolution operator $U = R_{\mathrm{D}} R_f$ is a product of two reflections and rotates the initial condition counterclockwise through angle θ about the origin. We apply U repeatedly until the initial vector is rotated through $\pi/2$ radians. The number of times t_{run} we apply U obeys $\theta\, t_{\mathrm{run}} + \theta/2 = \pi/2$. When $N \gg m$, we obtain

$$t_{\mathrm{run}} = \left\lfloor \frac{\pi}{4} \sqrt{\frac{N}{m}} \right\rfloor .$$

The success probability is calculated in the same way as before: The angle between the final state and $|M\rangle$ is almost $(\theta/2)$ because the final state is almost orthogonal to $|\mathrm{D}\rangle$. Then,

$$\begin{aligned} p_{\mathrm{succ}} &\geq \cos^2 \left(\frac{\theta}{2} \right) \\ &= 1 - \frac{m}{N}. \end{aligned} \tag{4.52}$$

Exercise 4.16. Show that

$$U^t |\mathrm{D}\rangle = \sin \left(t\,\theta + \frac{\theta}{2} \right) |M\rangle + \cos \left(t\,\theta + \frac{\theta}{2} \right) \left| M^{\perp} \right\rangle,$$

where θ is given by (4.51). From this expression, find the best stopping point t_{run} for the algorithm and show that the success probability p_{succ} obeys (4.52).

Exercise 4.17. Show that $U^t|\mathrm{D}\rangle$ is orthogonal to $|\mathrm{D}\rangle$ for $t = \frac{\pi}{2\theta}$.

Exercise 4.18. What is the computational complexity in terms of the number of evaluations of function f of the best *classical algorithm* that finds an element in set M with probability $p \geq \frac{1}{2}$.

Exercise 4.19. Show that if $m = \frac{N}{2}$, a marked element is found with probability 1 using a single iteration. Find the best success probability when $m = \frac{N}{4}$.

Exercise 4.20. Analyze the algorithm when $m \geq \frac{N}{2}$. What happens to the number of steps and the success probability? Can we efficiently solve this problem with a classical algorithm?

4.7.2 Analysis Using the Reduced Space

Since the evolution of the algorithm when $m > 1$ takes place in the two-dimensional vector space spanned by $|M\rangle$ and $\left|M^{\perp}\right\rangle$, we define the reduced unitary operators r_{D} and r_f that act on a two-dimensional Hilbert space. The initial condition in the reduced space is

$$|\mathrm{d}\rangle = \cos\frac{\theta}{2}|0\rangle + \sin\frac{\theta}{2}|1\rangle, \tag{4.53}$$

where θ is given by (4.50). Note that $|\mathrm{d}\rangle$ is the same as the one in Eq. (4.18) except that θ has been redefined. Then, the evolution operator acting on the reduced space is

$$u = \begin{bmatrix} \cos\theta & -\sin\theta \\ \sin\theta & \cos\theta \end{bmatrix}, \tag{4.54}$$

which is the same as the one described in Eq. (4.19) except that θ has been redefined. The optimal running time can be found either by using induction on t or by performing the spectral decomposition, yielding

$$t_{\text{run}} = \frac{\pi}{2\theta} - \frac{1}{2},$$

whose asymptotic expansion when $N \gg m$ is

$$t_{\text{run}} = \frac{\pi}{4}\sqrt{\frac{N}{m}} + O\left(\frac{1}{\sqrt{N}}\right).$$

The success probability is calculated in the same way as before.

Exercise 4.21. Show that the eigenvectors of $U = R_{\mathrm{D}}\, R_f$ associated with the eigenvalues $\mathrm{e}^{\pm \mathrm{i}\theta}$ are

$$\frac{\left|M^{\perp}\right\rangle \mp \mathrm{i}|M\rangle}{\sqrt{2}},$$

where $|M\rangle$ and $\left|M^{\perp}\right\rangle$ are defined in (4.48) and (4.49), respectively.

4.8 Amplitude Amplification

The technique called *amplitude amplification* used in quantum algorithms is contrasted with the technique called *probability amplification* used in classical randomized algorithms. An algorithm is said to be randomized if, during its execution, it chooses a path at random, usually employing a *random number generator*. The algorithm can output different values in two separate rounds, using the same input on each round. For example, a randomized algorithm that outputs a factor of number N may return 3 when $N = 15$ and, in a second round with the same input, may return 5. This never happens in a deterministic algorithm. One of the reasons we need randomized algorithms is that in some problems in which we are faced with several options, it is best to take a random decision instead of spending time analyzing what is the best option.

The two most common classes of randomized algorithms are the *Monte Carlo* and *Las Vegas algorithms*. A brief description of these classes is as follows: Monte Carlo algorithms always return an output in a finite predetermined time, but it may be wrong. The probability of correct response may be small. Las Vegas algorithms return a correct output or an error message, but the running time may be long or infinite. It is usually required that the expected running time is finite. Monte Carlo algorithms can be converted into Las Vegas algorithms if a procedure that checks the correctness of the output is known. Las Vegas algorithms can be converted into Monte Carlo algorithms using the *Markov's inequality*.[2]

Here we deal with the class of Monte Carlo algorithms. Let p be the probability of returning the correct value. If a procedure that checks the correctness of the output is known, then we can amplify the success probability by running the algorithm many times with the same input each time. We have a collection of outputs, and we want to be sure that the correct result is in the collection. If the algorithm runs n times, the probability of returning a wrong result every time is $(1-p)^n$. Therefore, the probability of returning at least one correct result is $1-(1-p)^n$. This probability is approximately np if $p \ll 1$. In order to achieve a success probability close to 1 and independent of p, we must take $n = 1/p$ as a first approximation. To analyze the complexity of a Monte Carlo algorithm that returns the correct output with probability p, we must multiply the running time by $1/p$. If p does not depend on the input size,

[2]Markov's inequality provides an upper bound for the probability that a nonnegative function of a random variable is greater than or equal to some positive constant.

then multiplying by $1/p$ does not change the time complexity. Otherwise, this factor must be considered.

4.8.1 The Technique

In the quantum case, we amplify amplitudes and consequently the number of rounds is $1/\sqrt{p}$, that is, quadratically smaller compared with the method of probability amplification.

The technique of amplitude amplification can be described as follows:

Initial Setup

Suppose we have a quantum algorithm described by the unitary operator A, which can be implemented in a quantum computer with at least n qubits (main register) and aims to find a marked element. A *marked element* x is a point in the domain of a Boolean function $f : \{0, 1\}^n \to \{0, 1\}$ such that $f(x) = 1$. Suppose that this algorithm is not good enough because if we perform a measurement in the computational basis when the state of the quantum computer is $A|\psi_{\text{in}}\rangle$, we obtain a marked element with a small probability p, where $|\psi_{\text{in}}\rangle$ is the best initial state of the algorithm A. We wish to improve the success probability.

The Amplification

Using f and possibly some extra registers, we define operator U_f, whose action on the computational basis of the main register is

$$U_f|x\rangle = (-1)^{f(x)}|x\rangle. \tag{4.55}$$

There is a quantum procedure that allows us to find a marked element using $O\left(1/\sqrt{p}\right)$ applications of U_f and A, with the success probability approaching 1 when $n \to \infty$.

The *amplitude amplification technique* can be described as follows: Apply $U^{t_{\text{run}}}$ to state $|\psi\rangle$ and measure the main register in the computational basis, where

$$U = (2\,|\psi\rangle\langle\psi| - I)\,U_f, \tag{4.56}$$

and

$$|\psi\rangle = A|\psi_{\text{in}}\rangle, \tag{4.57}$$

and

$$t_{\text{run}} = \left\lfloor \frac{\pi}{4\sqrt{p}} \right\rfloor. \tag{4.58}$$

Note that there are no intermediary measurements. The evolution operator of the new algorithm is U, which must be iterated t_{run} times. In the quantum case, A is repeated around $1/\sqrt{p}$ times, and we measure the first register only one time at the end.

An Example

Grover's algorithm is the simplest example that employs the amplitude amplification technique. In this case, A is $H^{\otimes n}$, $|\psi_{\text{in}}\rangle$ is $|0\rangle^{\otimes n}$, and $A|0\rangle^{\otimes n}$ is $|\text{D}\rangle$. If we measure the main register when it is in state $|\text{D}\rangle$, we obtain a marked element with probability $p = m/N$, which is very bad when $N \gg m$. We wish to improve this probability. Then, we use the amplitude amplification technique, which turns out to be the same as the generalized Grover algorithm. The number of times we employ U_f and A to find a marked element is $O(1/\sqrt{p}) = O\left(\sqrt{N/m}\right)$.

In this example, A does not evaluate f. Then, the number of queries depends only on the number of times U_f is used.

Analysis

The analysis of the *amplitude amplification technique* is very similar to the analysis of the generalized version of Grover's algorithm. Let us disregard any extra register that is necessary to implement operator U_f. Suppose that $|\psi\rangle$ — see (4.57) — is

$$|\psi\rangle = \sum_{x\in\{0,1\}^n} \alpha_x |x\rangle. \tag{4.59}$$

The probability of finding a marked element after running algorithm A is

$$p = \sum_{f(x)=1} \left|\alpha_x\right|^2. \tag{4.60}$$

For now, let us assume that $0 < p < 1$. Define states

$$|\psi_0\rangle = \frac{1}{\sqrt{1-p}} \sum_{f(x)=0} \alpha_x |x\rangle, \tag{4.61}$$

$$|\psi_1\rangle = \frac{1}{\sqrt{p}} \sum_{f(x)=1} \alpha_x |x\rangle. \tag{4.62}$$

Using (4.59), we obtain

$$|\psi\rangle = \cos\frac{\theta}{2}\,|\psi_0\rangle + \sin\frac{\theta}{2}\,|\psi_1\rangle, \tag{4.63}$$

where

$$\sin\frac{\theta}{2} = \sqrt{p} \tag{4.64}$$

and $\theta \in (0, \pi)$.

One step is obtained by applying the evolution operator

$$U = R_\psi U_f, \tag{4.65}$$

where $R_\psi = 2\,|\psi\rangle\langle\psi| - I$. The initial condition is $|\psi\rangle = A|\psi_{\text{in}}\rangle$, where $|\psi_{\text{in}}\rangle$ is the initial state of the original algorithm. Let us focus on how many times we have to apply U_f to find a marked element with certainty when $n \to \infty$. The overall efficiency of the amplitude amplification technique depends on operator A, which must be considered eventually.

The evolution of the amplitude amplification technique takes place in the real plane spanned by vectors $|\psi_0\rangle$ and $|\psi_1\rangle$, which plays the same role as vectors $\left|M^\perp\right\rangle$ and $|M\rangle$ of Sect. 4.7.1. As in Exercise 4.16 on p. 61, the state of the quantum computer after t steps is given by

$$U^t|\psi\rangle = \cos\left(t\,\theta + \frac{\theta}{2}\right)|\psi_0\rangle + \sin\left(t\,\theta + \frac{\theta}{2}\right)|\psi_1\rangle. \tag{4.66}$$

As before, we choose t that maximizes the amplitude of $|\psi_1\rangle$, that is, $t = \pi/2\theta - 1/2$. We assume that p tends to zero when n increases. Using (4.64), the asymptotic running time is

$$t_{\text{run}} = \left\lfloor \frac{\pi}{4\sqrt{p}} \right\rfloor. \tag{4.67}$$

The number of applications of U_f is asymptotically the order of $1/\sqrt{p}$. The success probability is

$$\begin{aligned} p_{\text{succ}} &\approx \sin^2\left(\frac{\pi}{2} + \sqrt{p}\right) \\ &= 1 - p + O(p^2). \end{aligned} \tag{4.68}$$

The success probability is 1 in the asymptotic limit (large n).

Further Reading

The original version of Grover's algorithm is described in the conference paper [128] and in the journal paper [130]. References [129, 131] are also influential. The generalization of the algorithm for searching databases with repeated elements and a first version of the *counting algorithm* are described in [57]. The version of the counting algorithm using *phase estimation* is described in [244]. The geometric interpretation of Grover's algorithm is described in [7]. The analysis using spectral decomposition is discussed in [244] and its connection with the *abstract search algorithm* is briefly described in [19]. The proof of *optimality* of Grover's algorithm is presented in [42]. A more readable version is described in [57], and we have closely followed the proof presented in [248]. Reference [344] presents a more detailed proof. The role of entanglement in Grover's algorithm is addressed in [237]. The method of *amplitude amplification* is addressed in [59, 151, 170, 285].

Experimental proposals and realizations of Grover's algorithm are described in [47, 103, 110, 116, 167, 203, 325, 340]. Quantum circuit designs for Grover's algorithm are addressed in [25, 100, 132]. A modified version of Grover's algorithm that searches a marked state with full successful rate is presented in [214]. How

Grover's algorithm depends on the entanglement of the initial state is addressed in [49]. A quantum secret-sharing protocol based on Grover's algorithm is described in [153]. Study of dissipative decoherence on the accuracy of the Grover quantum search algorithm is addressed in [351]. Improvements in Grover's algorithm using phase matching are described in [206, 207]. Decoherence effects on Grover's algorithm using the depolarizing channel are presented in [288]. The geometry of entanglement of Grover's algorithm is addressed in [160].

Quantum secret-sharing protocol and quantum communication based on Grover's algorithm are presented in [137, 322]. Quantum search with certainty is discussed in [165, 311]. A workflow of Grover's algorithm using CUDA and GPGPU is described in [218]. Applications of quantum search to cryptography are described in [197, 343]. Quantum algorithms to check the resiliency property of a Boolean function are addressed in [71]. Quantum error correction for Grover's algorithm is presented in [55]. The entanglement nature of quantum states generated by Grover's search algorithm is investigated by means of algebraic geometry in [149]. Improvements on the success probability of Grover's algorithm are addressed in [219]. Quantum coherence depletion in Grover's algorithm is investigated in [298]. Reference [65] presents a generalized version of Grover's Algorithm for multiple phase inversion.

Grover's algorithm is described in many books, such as [30, 40, 43, 97, 140, 146, 170, 178, 209, 230, 234, 248, 276, 303, 328].

Chapter 5
Coined Walks on Infinite Lattices

The *coined quantum walk* on the line was introduced in Sect. 3.3 on p. 25 in order to highlight features that are strikingly different from the *classical random walk*. In this Chapter, we present in detail the analytic calculation of the state of the quantum walk on the line after an arbitrary number of steps. The calculation is a model for the study of quantum walks on many graphs, and the *Fourier transform* is the key to the success of this calculation.

We also analyze coined quantum walks on the *two-dimensional infinite lattice*. Since the evolution equations are very complex in this case, the analysis is performed numerically. Among new features that show up in the two-dimensional case, we highlight the fact that there are nonequivalent coins, which generate a wide class of probability distributions.

On infinite graphs, the quantum walk spreads indefinitely. One of the most interesting physical properties is the *expected distance* from the origin, which is measured by the *standard deviation* of the probability distribution. Both the line and the two-dimensional lattice have a standard deviation that is directly proportional to the number of steps in contrast to the standard deviation of the classical random walk, which is proportional to the square root of the number of steps.

Quantum walks can also be defined in higher dimensions, such as the *three-dimensional infinite lattice*. The standard deviation is also a linear function of time, and the quadratic speedup over the behavior of classical random walk is maintained.

5.1 Hadamard Walk on the Line

Consider a coined quantum walk on the integer points of the infinite line. The spatial part has an associated Hilbert space $\mathcal{H}_P$ of infinite dimension, whose computational basis is $\left\{|x\rangle : -\infty \leq x \leq \infty\right\}$. The coin space $\mathcal{H}_C$ has two dimensions and its computational basis is $\left\{|0\rangle, |1\rangle\right\}$ corresponding to two possible directions of motion,

© Springer Nature Switzerland AG 2018

R. Portugal, *Quantum Walks and Search Algorithms*, Quantum Science and Technology, https://doi.org/10.1007/978-3-319-97813-0_5

rightward or leftward. The full Hilbert space associated with the quantum walk is $\mathcal{H}_C \otimes \mathcal{H}_P$, whose computational basis is $\{|j, x\rangle : j \in \{0, 1\} : x \in \mathbb{Z}\}$, where $j = 0$ means rightward and $j = 1$ means leftward.[1]

The state of the walker at time t is described by

$$|\Psi(t)\rangle = \sum_{j=0}^{1} \sum_{x=-\infty}^{\infty} \psi_{j,x}(t)|j, x\rangle, \tag{5.1}$$

where the coefficients $\psi_{j,x}(t)$ are complex functions, called *probability amplitudes*, which obey for any time step t the *normalization condition*

$$\sum_{x=-\infty}^{\infty} p_x(t) = 1, \tag{5.2}$$

where

$$p_x(t) = \left|\psi_{0,x}(t)\right|^2 + \left|\psi_{1,x}(t)\right|^2 \tag{5.3}$$

is the probability distribution of a position measurement at the time step t in the computational basis.

The *shift operator* is

$$S = \sum_{j=0}^{1} \sum_{x=-\infty}^{\infty} \left|j, x + (-1)^j\right\rangle\langle j, x|. \tag{5.4}$$

After one application of S, x is incremented by one unit if $j = 0$, whereas x is decremented by one unit if $j = 1$. Equation (5.4) is equal to Eq. (3.13) of Sect. 3.3 on p. 25, as can be checked by expanding the sum over index j.

Let us use the *Hadamard coin*

$$H = \frac{1}{\sqrt{2}} \begin{bmatrix} 1 & 1 \\ 1 & -1 \end{bmatrix}. \tag{5.5}$$

Applying the *evolution operator* of the coined model

$$U = S\,(H \otimes I) \tag{5.6}$$

to state $|\Psi(t)\rangle$, we obtain

[1]Note that we use the order coin-position in $|j, x\rangle$, which is called the *coin-position notation*. There is an alternate order which is position-coin written as $|x, j\rangle$, which is called the *position-coin notation*. The notation's choice is a matter of taste.

$$
\begin{aligned}
|\Psi(t+1)\rangle &= \sum_{x=-\infty}^{\infty} S\left(\psi_{0,x}(t)H|0\rangle|x\rangle + \psi_{1,x}(t)H|1\rangle|x\rangle\right) \\
&= \sum_{x=-\infty}^{\infty} \frac{\psi_{0,x}(t)+\psi_{1,x}(t)}{\sqrt{2}} S|0\rangle|x\rangle + \frac{\psi_{0,x}(t)-\psi_{1,x}(t)}{\sqrt{2}} S|1\rangle|x\rangle \\
&= \sum_{x=-\infty}^{\infty} \frac{\psi_{0,x}(t)+\psi_{1,x}(t)}{\sqrt{2}} |0\rangle|x+1\rangle \\
&\qquad + \frac{\psi_{0,x}(t)-\psi_{1,x}(t)}{\sqrt{2}} |1\rangle|x-1\rangle.
\end{aligned}
$$

After expanding the left-hand side in the computational basis, we search for the corresponding coefficients on the right-hand side to obtain the walker's *evolution equations*

$$\psi_{0,x}(t+1) = \frac{\psi_{0,x-1}(t)+\psi_{1,x-1}(t)}{\sqrt{2}}, \tag{5.7}$$

$$\psi_{1,x}(t+1) = \frac{\psi_{0,x+1}(t)-\psi_{1,x+1}(t)}{\sqrt{2}}. \tag{5.8}$$

Our goal is to calculate the probability distribution analytically. However, (5.7) and (5.8) cannot be easily solved at least in the way they are presently described. Fortunately, in this case, there is an alternative way to address the problem. There is a special basis called *Fourier basis* that diagonalizes the shift operator. This will help in the diagonalization of the evolution operator.

Exercise 5.1 Instead of using operator H as coin, use the Pauli matrix X. Obtain the evolution equations of the walker on the line, and solve analytically taking as the initial condition a walker on the origin with an arbitrary coin state. Calculate the standard deviation.

5.1.1 Fourier Transform

The *Fourier transform* of a discrete function $f : \mathbb{Z} \to \mathbb{C}$ is a continuous function $\tilde{f} : [-\pi, \pi] \to \mathbb{C}$ defined by

$$\tilde{f}(k) = \sum_{x=-\infty}^{\infty} \mathrm{e}^{-\mathrm{i}kx} f(x), \tag{5.9}$$

where $\mathrm{i} = \sqrt{-1}$. The inverse transform is given by

$$f(x) = \int_{-\pi}^{\pi} \mathrm{e}^{\mathrm{i}kx} \tilde{f}(k) \ \frac{\mathrm{d}k}{2\pi}. \tag{5.10}$$

This is a special case of a more general class of Fourier transforms, which is useful in our context. Note that if x had units (e.g., meters), k should have the inverse unit (1/meters), since (kx) is the argument of the exponential function and therefore must be *dimensionless*. The physical interpretation of the variable k is the *wave number*.

In (5.1), the coefficients $\psi_{j,x}(t)$ are discrete functions of variable x. The Fourier transform of $\psi_{j,x}(t)$ is

$$\widetilde{\psi}_j(k,t) = \sum_{x=-\infty}^{\infty} \mathrm{e}^{-\mathrm{i}kx} \psi_{j,x}(t), \tag{5.11}$$

where k is a continuous variable defined in the interval $[-\pi, \pi]$. The goal now is to obtain the evolution equations for $\widetilde{\psi}_j(k,t)$. If we solve these new equations, we can obtain $\psi_{j,x}(t)$ via the inverse Fourier transform.

There is another way to use the Fourier transform. Instead of transforming the function $f : \mathbb{Z} \to \mathbb{C}$, we transform the computational basis of $\mathcal{H}_P$. We use the formula

$$\left|\tilde{k}\right\rangle = \sum_{x=-\infty}^{\infty} \mathrm{e}^{\mathrm{i}kx} |x\rangle \tag{5.12}$$

to define vectors $\left|\tilde{k}\right\rangle$, where k is a continuous variable defined in the interval $[-\pi, \pi]$, as before. Note that we are using the positive sign in the argument of the exponential. The problem with this method is that the norm of $\left|\tilde{k}\right\rangle$ is infinite. This can be solved by redefining $\left|\tilde{k}\right\rangle$ as follows

$$\left|\tilde{k}\right\rangle = \lim_{L\to\infty} \frac{1}{\sqrt{2L+1}} \sum_{x=-L}^{L} \mathrm{e}^{\mathrm{i}kx} |x\rangle. \tag{5.13}$$

The same change should be applied to (5.11) for the sake of consistency. Since the *normalization constant* is not relevant, we will continue to use (5.12) as the definition of $\left|\tilde{k}\right\rangle$ and (5.11) as the definition of $\widetilde{\psi}_j(k,t)$ to simplify the calculation. The Fourier transform defines a new orthonormal basis $\left\{|j\rangle\left|\tilde{k}\right\rangle : j \in \{0,1\}, -\pi \le k \le \pi\right\}$ called (extended) *Fourier basis*. In this basis, we can express the state of the quantum walk as

$$|\Psi(t)\rangle = \sum_{j=0}^{1} \int_{-\pi}^{\pi} \widetilde{\psi}_j(k,t)\, |j\rangle\left|\tilde{k}\right\rangle \frac{\mathrm{d}k}{2\pi}. \tag{5.14}$$

Note that in the above equation $|\Psi(t)\rangle$ is written in the Fourier basis, while in Eq. (5.1), $|\Psi(t)\rangle$ is written in the computational basis.

Exercise 5.2 Show that (5.1) and (5.14) are equivalent if the Fourier basis is defined by formula (5.12).

Let us calculate the action of the shift operator on the new basis, that is, the action of S on $|j\rangle|\tilde{k}\rangle$. Using (5.12) and the definition of S, we have

$$\begin{aligned} S|j\rangle|\tilde{k}\rangle &= \sum_{x=-\infty}^{\infty} \mathrm{e}^{\mathrm{i}kx} S|j,x\rangle \\ &= \sum_{x=-\infty}^{\infty} \mathrm{e}^{\mathrm{i}kx} |j\rangle|x+(-1)^j\rangle. \end{aligned}$$

Renaming index x so that $x' = x + (-1)^j$, we obtain

$$\begin{aligned} S|j\rangle|\tilde{k}\rangle &= \sum_{x'=-\infty}^{\infty} \mathrm{e}^{\mathrm{i}\,k\,(x'-(-1)^j)} |j\rangle|x'\rangle \\ &= \mathrm{e}^{-\mathrm{i}\,k\,(-1)^j} |j\rangle|\tilde{k}\rangle. \end{aligned} \tag{5.15}$$

The result shows that the action of the shift operator S on a state of the Fourier basis only changes its phase, that is, $|j\rangle|\tilde{k}\rangle$ is an eigenvector associated with the eigenvalue $\mathrm{e}^{-\mathrm{i}k(-1)^j}$. The next task is to find the eigenvectors of the evolution operator U. If we diagonalize U, we will be able to find an analytic expression for the state of the quantum walk as a function of time.

Applying U to vector $|j'\rangle|\tilde{k}\rangle$ and using (5.15), we obtain

$$\begin{aligned} U|j'\rangle|\tilde{k}\rangle &= S\left(\sum_{j=0}^{1} H_{j,j'}|j\rangle|\tilde{k}\rangle\right) \\ &= \sum_{j=0}^{1} \mathrm{e}^{-\mathrm{i}\,k\,(-1)^j} H_{j,j'}|j\rangle|\tilde{k}\rangle. \end{aligned} \tag{5.16}$$

The entries of U in the Fourier basis are

$$\langle j,\tilde{k}|U|j',\tilde{k}'\rangle = \mathrm{e}^{-\mathrm{i}\,k\,(-1)^j} H_{j,j'}\,\delta_{k,k'}. \tag{5.17}$$

For each k, we define operator $\widetilde{H}_k$, whose entries are

$$\widetilde{H}_{j,j'} = \mathrm{e}^{-\mathrm{i}\,k\,(-1)^j} H_{j,j'}. \tag{5.18}$$

In the matrix form, we have

$$\widetilde{H}_k = \begin{bmatrix} \mathrm{e}^{-\mathrm{i}\,k} & 0 \\ 0 & \mathrm{e}^{\mathrm{i}\,k} \end{bmatrix} \cdot H$$
$$= \frac{1}{\sqrt{2}} \begin{bmatrix} \mathrm{e}^{-\mathrm{i}\,k} & \mathrm{e}^{-\mathrm{i}\,k} \\ \mathrm{e}^{\mathrm{i}\,k} & -\mathrm{e}^{\mathrm{i}\,k} \end{bmatrix}. \tag{5.19}$$

Equation (5.17) shows that the nondiagonal part of operator U is associated with the coin space. The goal now is to diagonalize operator $\widetilde{H}_k$. If $|\alpha_k\rangle$ is an eigenvector of $\widetilde{H}_k$ with eigenvalue α_k, then $|\alpha_k\rangle\big|\tilde{k}\big\rangle$ is an eigenvector of U associated with the same eigenvalue α_k. To check this, note that (5.16) can be written as

$$U|j\rangle\big|\tilde{k}\big\rangle = \big(\widetilde{H}_k|j\rangle\big)\big|\tilde{k}\big\rangle. \tag{5.20}$$

The action of the shift operator S has been absorbed by $\widetilde{H}_k$ when U acts on $|j\rangle\big|\tilde{k}\big\rangle$. If $|\alpha_k\rangle$ is an eigenvector of $\widetilde{H}_k$ with eigenvalue α_k, we have

$$U|\alpha_k\rangle\big|\tilde{k}\big\rangle = \big(\widetilde{H}_k|\alpha_k\rangle\big)\big|\tilde{k}\big\rangle$$
$$= \alpha_k|\alpha_k\rangle\big|\tilde{k}\big\rangle. \tag{5.21}$$

Therefore, $|\alpha_k\rangle\big|\tilde{k}\big\rangle$ is an eigenvector of U associated with the eigenvalue α_k. This result shows that the diagonalization of the evolution operator reduces to the diagonalization of $\widetilde{H}_k$. U acts on an infinite-dimensional Hilbert space, while $\widetilde{H}_k$ acts on a two-dimensional space.

The characteristic polynomial of $\widetilde{H}_k$ is

$$p_{\widetilde{H}_k}(\lambda) = \lambda^2 + \mathrm{i}\sqrt{2}\,\lambda \sin k - 1. \tag{5.22}$$

The eigenvalues are the solutions of $p_{\widetilde{H}_k}(\lambda) = 0$, which are

$$\alpha_k = \mathrm{e}^{-\mathrm{i}\,\omega_k}, \tag{5.23}$$
$$\beta_k = \mathrm{e}^{\mathrm{i}\,(\pi+\omega_k)}, \tag{5.24}$$

where ω_k is an angle in the interval $[-\pi/2, \pi/2]$ that satisfies the equation

$$\sin\omega_k = \frac{1}{\sqrt{2}} \sin k. \tag{5.25}$$

The normalized eigenvectors are

$$|\alpha_k\rangle = \frac{1}{\sqrt{c^-}} \begin{bmatrix} \mathrm{e}^{-\mathrm{i}\,k} \\ \sqrt{2}\,\mathrm{e}^{-\mathrm{i}\,\omega_k} - \mathrm{e}^{-\mathrm{i}\,k} \end{bmatrix}, \tag{5.26}$$
$$|\beta_k\rangle = \frac{1}{\sqrt{c^+}} \begin{bmatrix} \mathrm{e}^{-\mathrm{i}\,k} \\ -\sqrt{2}\,\mathrm{e}^{\mathrm{i}\,\omega_k} - \mathrm{e}^{-\mathrm{i}\,k} \end{bmatrix}, \tag{5.27}$$

where

$$c^{\pm} = 2\left(1+\cos^2 k\right) \pm 2\,\cos k\,\sqrt{1+\cos^2 k}. \tag{5.28}$$

The spectral decomposition of U is

$$U = \int_{-\pi}^{\pi} \left(\mathrm{e}^{-\mathrm{i}\,\omega_k} \left|\alpha_k, \tilde{k}\right\rangle\left\langle\alpha_k, \tilde{k}\right| + \mathrm{e}^{\mathrm{i}\,(\pi+\omega_k)} \left|\beta_k, \tilde{k}\right\rangle\left\langle\beta_k, \tilde{k}\right| \right) \frac{\mathrm{d}k}{2\pi}. \tag{5.29}$$

The tth power of U is

$$U^t = \int_{-\pi}^{\pi} \left(\mathrm{e}^{-\mathrm{i}\,\omega_k\,t} \left|\alpha_k, \tilde{k}\right\rangle\left\langle\alpha_k, \tilde{k}\right| + \mathrm{e}^{\mathrm{i}\,(\pi+\omega_k)\,t} \left|\beta_k, \tilde{k}\right\rangle\left\langle\beta_k, \tilde{k}\right| \right) \frac{\mathrm{d}k}{2\pi}, \tag{5.30}$$

because a function applied to U is by definition applied directly to the eigenvalues when U is written in its eigenbasis. In this case, the function is $f(x) = x^t$ (see Sect. A.13 on p. 260).

5.1.2 Analytic Solution

Suppose that initially the walker is at the origin $x = 0$ and the coin state is $|0\rangle$. The initial condition is

$$|\psi(0)\rangle = |0\rangle|x = 0\rangle. \tag{5.31}$$

Using (5.30) we obtain

$$\begin{aligned} |\psi(t)\rangle &= U^t|\psi(0)\rangle \\ &= \int_{-\pi}^{\pi} \Big(\mathrm{e}^{-\mathrm{i}\,\omega_k\,t} \left|\alpha_k, \tilde{k}\right\rangle \left\langle \alpha_k, \tilde{k}\,\middle|0, 0\right\rangle \\ &\quad + \mathrm{e}^{\mathrm{i}\,(\pi+\omega_k)\,t} \left|\beta_k, \tilde{k}\right\rangle \left\langle \beta_k, \tilde{k}\,\middle|0, 0\right\rangle \Big) \frac{\mathrm{d}k}{2\pi}. \end{aligned} \tag{5.32}$$

Using (5.12), (5.26), and (5.27), we obtain

$$\left\langle \alpha_k, \tilde{k}\,\middle|0, 0\right\rangle = \frac{\mathrm{e}^{\mathrm{i}\,k}}{\sqrt{c^-}}, \tag{5.33}$$

$$\left\langle \beta_k, \tilde{k}\,\middle|0, 0\right\rangle = \frac{\mathrm{e}^{\mathrm{i}\,k}}{\sqrt{c^+}}. \tag{5.34}$$

Then,

$$|\psi(t)\rangle = \int_{-\pi}^{\pi} \left(\frac{\mathrm{e}^{-\mathrm{i}\,(\omega_k t - k)}}{\sqrt{c^-}} |\alpha_k\rangle + \frac{\mathrm{e}^{\mathrm{i}\,(\pi+\omega_k)\,t + \mathrm{i}\,k}}{\sqrt{c^+}} |\beta_k\rangle \right) \left|\tilde{k}\right\rangle \frac{\mathrm{d}k}{2\pi}. \tag{5.35}$$

The state of the walk is written in the eigenbasis of U. It is better to present it in the computational basis. As an intermediate step, we write the eigenvectors $|\alpha_k\rangle$ and $|\beta_k\rangle$ in the computational basis using (5.26) and (5.27) keeping intact vectors $|\tilde{k}\rangle$, which yields

$$|\psi(t)\rangle = \int_{-\pi}^{\pi} \left(\frac{\mathrm{e}^{-\mathrm{i}\,(\omega_k t - k)}}{c^-} \begin{bmatrix} \mathrm{e}^{-\mathrm{i}\,k} \\ \sqrt{2}\,\mathrm{e}^{-\mathrm{i}\,\omega_k} - \mathrm{e}^{-\mathrm{i}\,k} \end{bmatrix} + \frac{\mathrm{e}^{\mathrm{i}\,(\pi+\omega_k)\,t + \mathrm{i}\,k}}{c^+} \begin{bmatrix} \mathrm{e}^{-\mathrm{i}\,k} \\ -\sqrt{2}\,\mathrm{e}^{\mathrm{i}\,\omega_k} - \mathrm{e}^{-\mathrm{i}\,k} \end{bmatrix} \right) |\tilde{k}\rangle \, \frac{\mathrm{d}k}{2\pi}. \tag{5.36}$$

Using (5.14), coefficients $\widetilde{\psi}_j(k,t)$ are given by

$$\widetilde{\psi}_0(k,t) = \frac{\mathrm{e}^{-\mathrm{i}\omega_k t}}{c^-} + \frac{\mathrm{e}^{\mathrm{i}(\pi+\omega_k)t}}{c^+}, \tag{5.37}$$

$$\widetilde{\psi}_1(k,t) = \frac{\mathrm{e}^{-\mathrm{i}\omega_k t + \mathrm{i}k} \left(\sqrt{2}\,\mathrm{e}^{-\mathrm{i}\,\omega_k} - \mathrm{e}^{-\mathrm{i}\,k} \right)}{c^-} - \frac{\mathrm{e}^{\mathrm{i}(\pi+\omega_k)t + \mathrm{i}k} \left(\sqrt{2}\,\mathrm{e}^{\mathrm{i}\,\omega_k} + \mathrm{e}^{-\mathrm{i}\,k} \right)}{c^+}. \tag{5.38}$$

To simplify these expressions, it is convenient to use the identities

$$\frac{1}{c^\pm} = \frac{1}{2} \left(1 \mp \frac{\cos k}{\sqrt{1+\cos^2 k}} \right) \tag{5.39}$$

and

$$\sqrt{2}\,\mathrm{e}^{\pm\mathrm{i}\,\omega_k} \pm \mathrm{e}^{-\mathrm{i}\,k} = \frac{c^\pm}{2\sqrt{1+\cos^2 k}}. \tag{5.40}$$

We obtain

$$\widetilde{\psi}_0(k,t) = \frac{1}{2} \left(1 + \frac{\cos k}{\sqrt{1+\cos^2 k}} \right) \mathrm{e}^{-\mathrm{i}\,\omega_k t} + \frac{(-1)^t}{2} \left(1 - \frac{\cos k}{\sqrt{1+\cos^2 k}} \right) \mathrm{e}^{\mathrm{i}\,\omega_k t}, \tag{5.41}$$

$$\widetilde{\psi}_1(k,t) = \frac{\mathrm{e}^{\mathrm{i}k}}{2\sqrt{1+\cos^2 k}} \left(\mathrm{e}^{-\mathrm{i}\,\omega_k t} - (-1)^t \mathrm{e}^{\mathrm{i}\,\omega_k t} \right). \tag{5.42}$$

Coefficient $\psi_{j,x}$ in the computational basis is given by

$$\psi_{j,x}(t) = \int_{-\pi}^{\pi} \mathrm{e}^{\mathrm{i}kx}\, \widetilde{\psi}_j(k,t)\, \frac{\mathrm{d}k}{2\pi}. \tag{5.43}$$

Using Eqs. (5.41) and (5.42) and simplifying the integrals (Exercise 5.3), we obtain

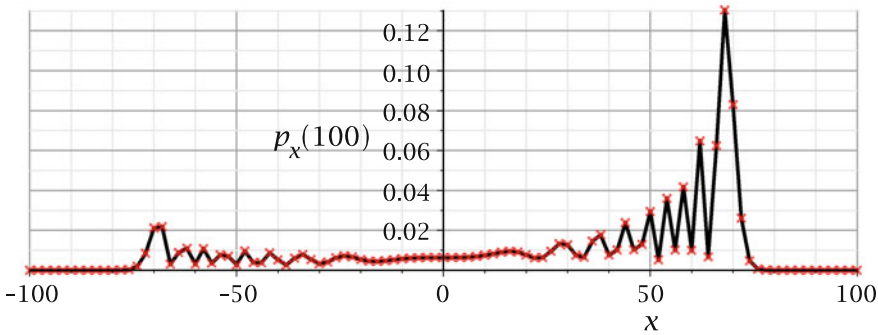

Fig. 5.1 Probability distribution of the quantum walk on the line after 100 steps obtained from the analytic expressions (5.44) and (5.45). The diagonal crosses × correspond to integer values of x

$$\psi_{0,x}(t) = \int_{-\pi}^{\pi} \left(1 + \frac{\cos k}{\sqrt{1+\cos^2 k}}\right) \mathrm{e}^{-\mathrm{i}\,(\omega_k t - kx)} \, \frac{\mathrm{d}k}{2\pi}, \tag{5.44}$$

$$\psi_{1,x}(t) = \int_{-\pi}^{\pi} \frac{\mathrm{e}^{\mathrm{i}k}}{\sqrt{1+\cos^2 k}} \, \mathrm{e}^{-\mathrm{i}\,(\omega_k t - kx)} \, \frac{\mathrm{d}k}{2\pi} \tag{5.45}$$

when $n + t$ is even and $\psi_{0,x}(t) = \psi_{1,x}(t) = 0$ when $n + t$ is odd.

For numerical values of x and t, we calculate $\psi_{0,x}(t)$ and $\psi_{1,x}(t)$ through numerical integration, and using (5.3) we calculate the probability distribution. The plot of Fig. 5.1 shows the probability distribution after 100 steps. Only the even points are displayed because the probability is zero at odd points. This curve is the same as the curve generated numerically with the same initial condition in Sect. 3.3 on p. 25.

Exercise 5.3 Show that the integrals

$$(\pm 1)^t \int_{-\pi}^{\pi} \left(1 \pm \frac{\cos k}{\sqrt{1+\cos^2 k}}\right) \mathrm{e}^{-\mathrm{i}(\pm\omega_k t - kx)} \, \frac{\mathrm{d}k}{2\pi}$$

are real numbers and equal to each other when $n + t$ is even and have opposite signs when $n + t$ is odd. Show the same for the integrals

$$(\pm 1)^{t+1} \int_{-\pi}^{\pi} \frac{\mathrm{e}^{\mathrm{i}k}}{\sqrt{1+\cos^2 k}} \, \mathrm{e}^{-\mathrm{i}(\pm\omega_k t - kx)} \, \frac{\mathrm{d}k}{2\pi}.$$

Use these facts to obtain (5.44) and (5.45) from (5.41) and (5.42).

Exercise 5.4 Calculate analytically the *probability amplitudes* of the Hadamard quantum walk with initial condition

$$|\psi(0)\rangle = \frac{|0\rangle + \mathrm{i}|1\rangle}{\sqrt{2}} |x = 0\rangle.$$

Depict the plot of the probability distribution and verify that it is symmetric about the origin. Let $f_x(t)$ be the following function:

$$f_x(t) = \begin{cases} \frac{2}{\pi t\left(1-\frac{x^2}{t^2}\right)\sqrt{1-\frac{2x^2}{t^2}}}, & |x| \leq \frac{t}{\sqrt{2}}; \\ 0, & \frac{t}{\sqrt{2}} < |x|. \end{cases}$$

Plot of $f_x(t)$ together with the probability distribution for some values of t and check that $f_x(t)$ is a good approximation, disregarding the rapid oscillation of the probability distribution.

5.1.3 Other Coins

A question that naturally arises is how general the results of the last section are. The evolution operator of the *coined quantum walk* is $U = S(C \otimes I)$, where S is the shift operator (5.4). The only degrees of freedom are the coin operator C and the initial condition. For the quantum walk on the line, these choices are not independent. An arbitrary coin operator, disregarding a global phase, has the form

$$C = \begin{bmatrix} \sqrt{\rho} & \sqrt{1-\rho}\,\mathrm{e}^{\mathrm{i}\theta} \\ \sqrt{1-\rho}\,\mathrm{e}^{\mathrm{i}\phi} & -\sqrt{\rho}\,\mathrm{e}^{\mathrm{i}(\theta+\phi)} \end{bmatrix}, \tag{5.46}$$

where $0 \leq \rho \leq 1$ and $0 \leq \theta, \phi \leq \pi$.

The coin state $|0\rangle$ induces a motion to the right, while $|1\rangle$ to the left. Note that

$$C|0\rangle = \sqrt{\rho}|0\rangle + \sqrt{1-\rho}\,\mathrm{e}^{\mathrm{i}\theta}|1\rangle. \tag{5.47}$$

Therefore, depending on ρ, the coin can increase the probability associated with "go to right" or "go to left." Angles θ and ϕ play no role in this probability. The *unbiased coin* is obtained by taking $\rho = 1/2$. The Hadamard coin is an example of an unbiased coin and the simplest one. An unbiased coin does not guarantee a *symmetric probability distribution*, because there is still freedom in the initial condition. The initial condition starting from the origin has the form

$$|\Psi(0)\rangle = \left(\cos\alpha\,|0\rangle + \mathrm{e}^{\mathrm{i}\beta}\,\sin\alpha\,|1\rangle\right)|0\rangle, \tag{5.48}$$

so we have two control parameters: α and β.

Considering unbiased coins and repeating the calculation of the quantum state for an arbitrary time using an arbitrary initial condition, we conclude that the change produced by parameters θ and ϕ can be fully achieved through appropriate choices of parameters α and β. In fact, the result is more general because if we fix the coin as a real operator ($\theta = \phi = 0$, ρ arbitrary), we can obtain all possible quantum walks by choosing an appropriate initial condition (Exercise 5.7). For some of these choices,

the probability distribution is symmetric, assuming that the walker starts from the origin. If we restrict ourselves to unbiased coins, the Hadamard walk with arbitrary initial condition encompasses all cases.

Exercise 5.5 Find a coin that generates a symmetric probability distribution using the initial condition

$$|\psi(0)\rangle = \frac{|0\rangle + |1\rangle}{\sqrt{2}}|x = 0\rangle.$$

Exercise 5.6 In the classical random walk, we can have a walker on the line that can move to the left, to the right, or stay in the same position. What is the quantum version of this classical walk? Find the shift operator and use the Grover coin to calculate the first steps using the initial condition $|\Psi(0)\rangle = |\mathrm{D}\rangle|0\rangle$. Obtain the answer in the computational basis. [Hint: Use a three-dimensional coin.]

Exercise 5.7 Using operator (5.46) as coin, show that the operator $\widetilde{C}_k$ associated with the Fourier space is given by

$$\widetilde{C}_k = \begin{bmatrix} \sqrt{\rho}\,\mathrm{e}^{-\mathrm{i}k} & \sqrt{1-\rho}\,\mathrm{e}^{\mathrm{i}(-k+\theta)} \\ \sqrt{1-\rho}\,\mathrm{e}^{\mathrm{i}(k+\phi)} & -\sqrt{\rho}\,\mathrm{e}^{\mathrm{i}(k+\theta+\phi)} \end{bmatrix}.$$

Verify that the operator (5.19) can be obtained by a suitable choice of parameters ρ, θ, and ϕ. Find the eigenvalues and eigenvectors of $\widetilde{C}_k$. Show that in the Fourier space, we can write

$$\left|\tilde{\Psi}_k(t)\right\rangle = (\widetilde{C}_k)^t \left|\tilde{\Psi}_k(0)\right\rangle,$$

where $\left|\tilde{\Psi}_k(0)\right\rangle$ is obtained from the Fourier transform of $|\Psi(0)\rangle$, given by (5.48). Show that parameters θ and β only appear in the expression of $\left|\tilde{\Psi}_k(0)\right\rangle$ in the form $\theta + \beta$. Therefore, we can take $\theta = 0$ and any possibility can be reproduced by choosing an appropriate β. Show that parameter ϕ plays the role of a global phase and is eliminated when we take the *inverse Fourier transform*. Conclude that by taking $\theta = \phi = 0$, that is,

$$C = \begin{bmatrix} \cos\lambda & \sin\lambda \\ \sin\lambda & -\cos\lambda \end{bmatrix},$$

where λ is an angle, all one-dimensional quantum walks are obtained by a suitable choice of the initial condition. If we restrict to unbiased coins, the Hadamard walk with arbitrary initial condition encompasses all cases.

5.2 Two-Dimensional Lattice

Consider a quantum walk on the nodes of the infinite two-dimensional lattice. The spatial part has an associated Hilbert space $\mathcal{H}_P$ of infinite dimension, whose computational basis is $\left\{|x, y\rangle : x, y \in \mathbb{Z}\right\}$. If the walker is on a lattice node, it has four

options to move and the coin decides which one. There are two ways to implement the coin: (1) It can be a single quantum system with four levels (a qudit) or (2) a composite quantum system each one with two levels (two qubits). We use the second way. The coin space $\mathcal{H}_C$ has four dimensions, and its computational basis is denoted by $\{|i_x, i_y\rangle : 0 \leq i_x, i_y \leq 1\}$. The total Hilbert space associated with the quantum walk is the coin-position space, which is given by $\mathcal{H}_C \otimes \mathcal{H}_P$. We use the *coin-position notation*.

The state of the walker at time t is described by

$$|\Psi(t)\rangle = \sum_{i_x, i_y=0}^{1} \sum_{x,y=-\infty}^{\infty} \psi_{i_x, i_y;\, x,y}(t) |i_x, i_y\rangle |x, y\rangle, \tag{5.49}$$

where the coefficients $\psi_{i_x, i_y;\, x,y}(t)$ are complex functions that obey the *normalization condition*

$$\sum_{i_x, i_y=0}^{1} \sum_{x,y=-\infty}^{\infty} \left|\psi_{i_x, i_y;\, x,y}(t)\right|^2 = 1, \tag{5.50}$$

for any time step t. The probability distribution is given by

$$p_{x,y}(t) = \sum_{i_x, i_y=0}^{1} |\psi_{i_x, i_y;\, x,y}(t)|^2. \tag{5.51}$$

The action of the shift operator S on the computational basis is described by

$$S|i_x, i_y\rangle |x, y\rangle = |i_x, i_y\rangle \left|x + (-1)^{i_x}, y + (-1)^{i_y}\right\rangle. \tag{5.52}$$

If $i_x = 0$ and $i_y = 0$, x and y are incremented by one unit, which means that if the walker leaves position $(0, 0)$, it will go to $(1, 1)$, that is, it goes through the main diagonal of the lattice. If $i_x = 0$ and $i_y = 1$, x is incremented by one unit, while y is decremented by one unit, indicating that the walker goes through the secondary diagonal to the right. Similarly, for cases $i_x = i_y = 1$ and $i_x = 1$, $i_y = 0$. If i_x and i_y are equal, the walker goes through the main diagonal. Otherwise, it goes through the secondary diagonal.

Applying the standard evolution operator

$$U = S\,(C \otimes I) \tag{5.53}$$

to the state at time t, we obtain

$$|\Psi(t+1)\rangle = \sum_{j_x, j_y=0}^{1} \sum_{x,y=-\infty}^{\infty} \psi_{j_x, j_y;\, x,y}(t)\, S\Big(C|j_x, j_y\rangle |x, y\rangle\Big)$$

$$= \sum_{j_x, j_y=0}^{1} \sum_{x,y=-\infty}^{\infty} \psi_{j_x, j_y; x,y}(t)\, S \left(\sum_{i_x, i_y=0}^{1} C_{i_x, i_y; j_x, j_y} \left| i_x, i_y \right\rangle |x, y\rangle \right)$$

$$= \sum_{i_x, i_y, j_x, j_y=0}^{1} \sum_{x,y=-\infty}^{\infty} \psi_{j_x, j_y; x,y}(t)\, C_{i_x, i_y; j_x, j_y} \left| i_x, i_y \right\rangle \left| x + (-1)^{i_x},\ y + (-1)^{i_y} \right\rangle.$$

By renaming $x + (-1)^{i_x}$, $y + (-1)^{i_y}$ to x, y, we obtain

$$|\Psi(t+1)\rangle = \sum_{i_x, i_y, j_x, j_y=0}^{1} \sum_{x,y=-\infty}^{\infty} C_{i_x, i_y; j_x, j_y} \times \psi_{j_x, j_y; x-(-1)^{i_x},\, y-(-1)^{i_y}}(t) \left| i_x, i_y \right\rangle |x, y\rangle. \tag{5.54}$$

After expanding the left-hand side of the above equation in the computational basis, we search for the corresponding coefficients on the right-hand side in order to obtain the walker's evolution equation

$$\psi_{i_x, i_y; x,y}(t+1) = \sum_{j_x, j_y=0}^{1} C_{i_x, i_y; j_x, j_y}\, \psi_{j_x, j_y; x+(-1)^{i_x},\, y+(-1)^{i_y}}(t). \tag{5.55}$$

This equation is too complex to be solved analytically for an arbitrary coin. In the next chapter, exact solutions are obtained using Fourier transform for the *flip-flop quantum walk* with the Grover coin on the *finite two-dimensional lattice*, which can be used to obtain information about the behavior of quantum walks on the infinite lattice. Here, we analyze (5.55) numerically by choosing three important nonequivalent coins: *Hadamard*, *Fourier*, and *Grover*.

Exercise 5.8 Show that if the coin operator is the tensor product of two operators $C = C_1 \otimes C_2$, then the evolution operator (5.53) can be factorized as the tensor product of two operators.

5.2.1 The Hadamard Coin

The Hadamard coin is $C = H \otimes H$, and its matrix representation is

$$C = \frac{1}{2} \begin{bmatrix} 1 & 1 & 1 & 1 \\ 1 & -1 & 1 & -1 \\ 1 & 1 & -1 & -1 \\ 1 & -1 & -1 & 1 \end{bmatrix}. \tag{5.56}$$

Let us use the initial condition

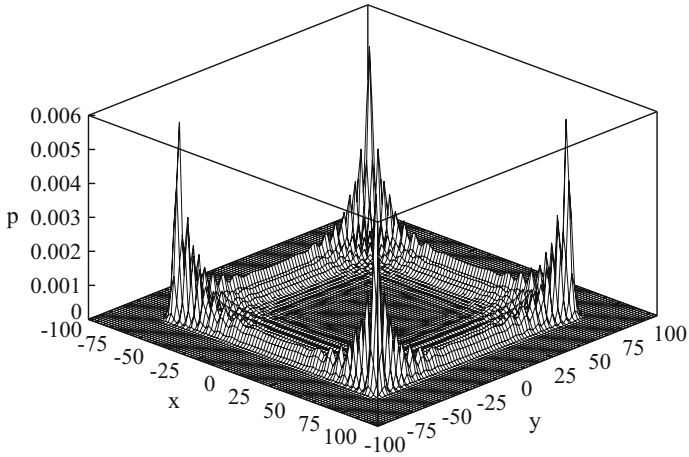

Fig. 5.2 Probability distribution of the quantum walk on the two-dimensional lattice with the Hadamard coin after 100 steps

$$|\Psi(0)\rangle = \frac{|0\rangle + \mathrm{i}|1\rangle}{\sqrt{2}} \otimes \frac{|0\rangle + \mathrm{i}|1\rangle}{\sqrt{2}} \otimes |x = 0, y = 0\rangle, \tag{5.57}$$

which is based on the initial condition used in Sect. 3.3 on p. 25 to obtain a symmetric probability distribution for the Hadamard coin. The plot of the probability distribution after 100 steps is shown in Fig. 5.2.

The dynamic in this example is equivalent to two diagonal *uncoupled quantum walks*. The analytic results obtained for the one-dimensional Hadamard walk do apply in this case. A detailed analysis of Fig. 5.2 shows the characteristics of the one-dimensional walk analyzed before.

5.2.2 The Fourier Coin

The entries of the N-dimensional Fourier coin are $[F_N]_{k\ell} = \omega^{k\ell}/\sqrt{N}$, where $\omega = \exp(2\pi\mathrm{i}/N)$. In the four-dimensional case, we have $C = F_4$ and its matrix representation is

$$F_4 = \frac{1}{2}\begin{bmatrix} 1 & 1 & 1 & 1 \\ 1 & \mathrm{i} & -1 & -\mathrm{i} \\ 1 & -1 & 1 & -1 \\ 1 & -\mathrm{i} & -1 & \mathrm{i} \end{bmatrix}. \tag{5.58}$$

Let us use the initial condition

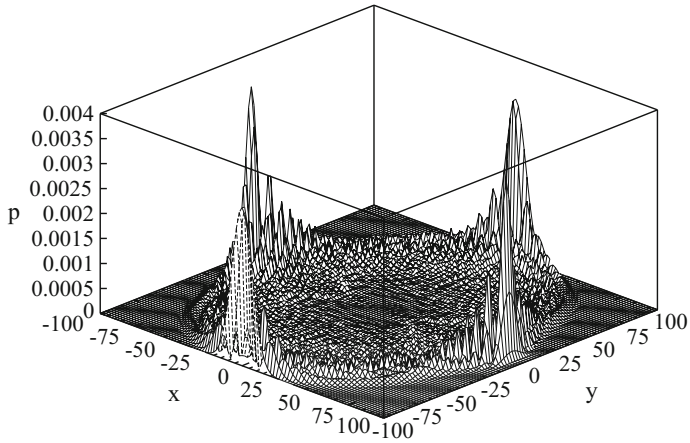

Fig. 5.3 Probability distribution of a quantum walk on the two-dimensional lattice with the Fourier coin

$$|\Psi(0)\rangle = \frac{1}{2}\left(|00\rangle + \frac{1-\mathrm{i}}{\sqrt{2}}|01\rangle + |10\rangle - \frac{1-\mathrm{i}}{\sqrt{2}}|11\rangle\right)|x=0, y=0\rangle. \tag{5.59}$$

The plot of the probability distribution after 100 steps is shown in Fig. 5.3.

The plot is *invariant* under a rotation through 180°, but it is not invariant under a rotation through 90°. The walk is symmetric in each direction, but the evolution toward the direction x is different from the evolution toward the direction y.

5.2.3 The Grover Coin

At last, we use the Grover coin given by

$$G = 2|\mathrm{D}\rangle\langle\mathrm{D}| - I, \tag{5.60}$$

where $|\mathrm{D}\rangle = \frac{1}{2}\sum_{i_x,i_y=0}^{1}\left|i_x, i_y\right\rangle$ is the diagonal state of $\mathcal{H}_C$. The matrix representation is

$$G = \frac{1}{2}\begin{bmatrix} -1 & 1 & 1 & 1 \\ 1 & -1 & 1 & 1 \\ 1 & 1 & -1 & 1 \\ 1 & 1 & 1 & -1 \end{bmatrix}. \tag{5.61}$$

The initial condition which has the largest standard deviation for the Grover coin is the state

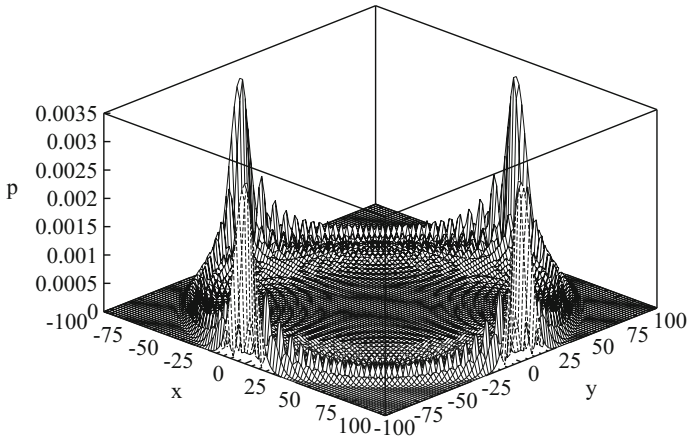

Fig. 5.4 Probability distribution of the quantum walk on the two-dimensional lattice with the Grover coin

$$|\Psi(0)\rangle = \frac{1}{2}\big(|00\rangle - |01\rangle - |10\rangle + |11\rangle\big)|x = 0, y = 0\rangle. \tag{5.62}$$

The plot of the probability distribution after 100 steps is shown in Fig. 5.4. The plot is *invariant* under a rotation through 90°, showing that the directions x and y are equivalent.

In Sect. 5.1.3, we have shown that all real coins in the one-dimensional case are equivalent in the sense that one can use the Hadamard coin and can obtain all alternative real-coined walks by changing the initial condition. This is not true in the two-dimensional case. The three coins that we analyzed are independent. They fall into three distinct classes.

5.2.4 Standard Deviation

The formula of the position standard deviation of the one-dimensional case was described in Sect. 3.3 on p. 25. In the two-dimensional case, the natural extension is

$$\sigma(t) = \sqrt{\sum_{x,y=-\infty}^{\infty} \left(x^2 + y^2\right)\, p_{x,y}(t)}, \tag{5.63}$$

which is valid when the *average* or *expected value* of the position is zero. The three lines in Fig. 5.5 are the standard deviation of the Hadamard (dashed line), Fourier (dotted line), and Grover (continuous line) coins as a function of t. Note that the Grover coin has the largest slope among the three coins. The Grover coin has some

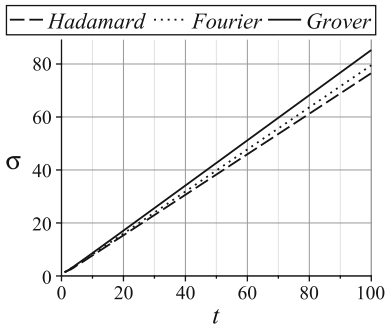

Fig. 5.5 Standard deviation of the quantum walk on the two-dimensional lattice for Hadamard, Fourier, and Grover coin as a function of the number of steps

advantages over the Fourier and Hadamard coins, besides the gain in the standard deviation, which can be useful in algorithmic applications. The Grover coin can be used in any dimension and is nontrivial for dimension greater than two. The Hadamard coin can only be used in dimensions that are a power of 2. It is interesting to use a coin that is somehow *distant* from the identity operator. The Grover coin is more distant from identity than the Fourier coin (Exercise 5.11).

The position standard deviation is $\sigma(t) = at$ asymptotically, where a is the slope. The choice of the initial condition can change a but cannot change the linear dependence σ as a function of t. Different from what was displayed in the previous examples, we can generate probability distributions strongly centered around the origin by choosing an appropriate initial condition.

Exercise 5.9 Are Fourier and Grover coins biased?

Exercise 5.10 Show that the standard deviation of the one- and two-dimensional Hadamard walks are equal.

Exercise 5.11 Use the distance formula based on the trace (see Sect. A.14 on p. 262) to show that the distance of the N-dimensional Grover coin to the identity operator is $\|G - I\| = 2\sqrt{N-1}$ and the distance of the N-dimensional Hadamard coin to the identity operator is $\|H^{\otimes \log_2 N} - I\| = \sqrt{2N}$ if N is a power of 2 and the distance of the N-dimensional Fourier coin to the identity operator is $\|F_N - I\| = \sqrt{2N}$ if N is a multiple of 4 plus 2.

5.3 Quantum Walk Packages

In this section, we list some packages that can be used to simulate quantum walks on graphs. It is necessary to spend some time to implement and to learn the basic commands of those packages. The user must judge whether it is better to spend time implementing one of them or to spend time developing codes.

QWalk [231]

QWalk aims to simulate the coined quantum walk dynamics on one- and two-dimensional lattices. The package is written in C and uses Gnuplot to plot the probability distribution. The user can choose the coin and the initial condition. There is an option to simulate decoherent dynamics based on *broken links*—also known as *percolation* [251, 280]. The links of the lattice can be broken at random at each step or the user can specify which edges will be missing during the evolution. QWalk allows the user to simulate quantum walks on any graph that is a subgraph of the two-dimensional lattice. Some plots in this section were made using QWalk. The package can be obtained from the *Computer Physics Communications library*.[2]

QwViz [46]

QwViz aims at plotting graphics for visualizing the probability distribution of quantum walks on graphs. The package is written in C and uses OpenGL to generate two- or three-dimensional graphics. The user must enter the adjacency matrix of the graph, and the package simulates the dynamics of the coined model to calculate the probability distribution. By default, the walker starts at vertex 1 with the coin in uniform superposition. The initial location can be changed by the user. It is possible to specify marked vertices, which tell the package to use quantum-walk-based search procedures starting from a uniform superposition of all vertices and using the Grover coin on the unmarked vertices and $(-I)$ on the marked vertices. The package can be obtained from the *Computer Physics Communications library*.[3]

PyCTQW [161]

PyCTQW aims to simulate large multi-particle continuous-time quantum walks using object-oriented Python and Fortran. The package takes advantage of modern HPC systems and runs using distributed memory. There are tools to visualize the probability distribution and tools for data analysis. The package can be obtained from the *Computer Physics Communications library*.[4]

Hiperwalk [201]

Hiperwalk (high-performance quantum walk) aims to simulate the quantum walk dynamics using high-performance computing (HPC). Hiperwalk uses OpenCL to run in parallel on accelerator cards, multicore CPU, or GPGPU. It is not required any knowledge of parallel programming, but the installation of the package dependencies is tricky, in special, OpenCL. Besides, Hiperwalk uses the *Neblina programming language*.[5] In the CUSTOM option, the input is an initial state $|\psi_0\rangle$ and a unitary operator U, which must be stored in two different files (only nonzero entries in order to take advantage of sparsity). Hiperwalk calculates $U^t|\psi_0\rangle$ for integer t using HPC and saves the output in a file. There are extra commands for the coined and staggered

[2] http://cpc.cs.qub.ac.uk/summaries/AEAX_v1_0.html.

[3] http://cpc.cs.qub.ac.uk/summaries/AEJN_v1_0.html.

[4] http://cpc.cs.qub.ac.uk/summaries/AEUN_v1_0.html.

[5] http://qubit.lncc.br/neblina.

models. The Hiperwalk manual[6] has a detailed description of the installation steps and some examples of applications.

QSWalk [112]

QSWalk is a *Mathematica* package that aims to simulate the time evolution of *quantum stochastic walks* on *directed weighted graphs*. The quantum stochastic walk is a generalization of the continuous-time quantum walk that includes the incoherent dynamics [327]. The dynamic uses the *Lindblad formalism* for *open quantum systems* using density matrices [61]. The package can be obtained from the *Computer Physics Communications library*.[7]

QSWalk.jl [120]

QSWalk.jl is a *Julia* package that aims to simulate the time evolution of *quantum stochastic walks* on *directed weighted graphs*. The authors claim that is faster than QSWalk [112] when used in large networks. Besides, it can be used for *nonmoralizing evolution*, which means that the evolution takes place on a directed acyclic graph and does not change to an evolution on the corresponding *moral graph* [104]. The package can be downloaded from *GitHub*.[8]

Further Reading

The seminal article to analyze quantum walks on the line is [247]. A thorough analysis is presented in [17, 68, 182, 190]. Reference [222] is one of the first to analyze walks in dimensions greater than one. Reference [313] performed an extensive examination of possible coins for walks on the two-dimensional lattice. The first papers about *decoherence* of coined quantum walks on the line are [176, 222, 280] and on the two-dimensional lattice are [191, 251]. The most relevant references on quantum walks on infinite graphs published before 2012 are provided by the review papers [13, 172, 175, 183, 274, 320] or by the review books [229, 319].

A partial list of recent references of quantum walks on lattices is as follows. An experimental investigation of Anderson localization of entangled photons is presented in [91]. Quantum walks on the Apollonian network are analyzed in [299]. The return probability of the open quantum random walk is described in [21]. Spatially dependent decoherence and anomalous diffusion are investigated in [258]. Survival probability with partially absorbing traps is analyzed in [122]. *Renormalization group* for quantum walks and the connection between the coined walk and *persistent random walk* is analyzed by Boettcher et al. in [51]. Environment-induced mixing processes are studied in [202]. Anderson localization with superconducting qubits is analyzed in [119]. Entanglement and disorder are investigated in [321]. Quantum percolation and transition point are analyzed in [74]. Decoherence models and their application to neutral atom experiments are described in [10]. History-dependent quantum walks as quantum lattice gas automata are analyzed in [296].

[6] http://qubit.lncc.br/qwalk/hiperwalk.pdf.

[7] http://dx.doi.org/10.17632/8rwd3j9zhk.1.

[8] https://github.com/QuantumWalks/QSWalk.jl.

Reference [277] shows that quantum walks falsify the idea of classical trajectories by analyzing the transport of cesium atoms on a one-dimensional optical lattice. Limit distributions of four states on the two-dimensional lattice are addressed in [221]. Localization and limit laws of three-state quantum walks on the two-dimensional lattice are analyzed in [220]. Ramsauer effect in the one-dimensional lattice with defects is presented in [198]. Quantum walks under artificial magnetic fields on lattices are addressed in [338]. Implementations in optical lattices are presented in [271]. Quantum walk on a cylinder is addressed in [62]. Analysis of the dynamics and energy spectra of aperiodic quantum walks is presented in [134]. Stationary amplitudes on higher-dimensional lattices are addressed in [181]. Analysis of phase disorder, localization, and entanglement are presented in [345]. Analysis of coherence on lattices is presented in [142]. Quantum walk with position-independent coin is addressed in [208]. Anderson localization of quantum walks on the line is addressed in [95]. Note that Anderson's seminal paper *"Absence of diffusion in certain random lattices"* is reference [22].

Besides the packages described in Sect. 5.3, there are some papers addressing the simulation of quantum walks, for instance, GPU-accelerated algorithms for many-particle continuous-time quantum walks [262], a simulator for discrete quantum walks on lattices [278], and Quandoop: a classical simulator of quantum walks on computer clusters [300].

Chapter 6
Coined Walks with Cyclic Boundary Conditions

In this chapter, we address coined quantum walks on three important finite graphs: *cycles*, *finite two-dimensional lattices*, and *hypercubes*: A cycle is a finite version of the line; a finite two-dimensional lattice is a two-dimensional version of the cycle in the form of a discrete *torus*; and a hypercube is a generalization of the *cube* to dimensions greater than three.

These graphs have spatial symmetries and can be analyzed via the *Fourier transform* method. We obtain analytic results that are useful in other chapters of this book. For instance, here we describe the spectral decomposition of the quantum walk evolution operators of two-dimensional lattices and hypercubes. The results are used in Chap. 9 in the analysis of the *time complexity* of *spatial search algorithms* using coined quantum walks on these graphs.

There are some interesting physical quantities of quantum walks on finite graphs that have different properties when compared with walks on infinite graphs, such as the *limiting distribution*, *mixing time*, and *hitting time*. The number of vertices is used as a parameter to describe bounds on the mixing and hitting times. Such number is not available in the infinite case.

6.1 Cycles

Suppose that the place on which the walker moves is the set of vertices of an N-cycle. If the walker moves N steps clockwise, it reaches the departure point. The same is true for the counterclockwise direction. The spatial part has associated an N-dimensional Hilbert space $\mathcal{H}^N$ with *computational basis* $\left\{|j\rangle : 0 \leq j \leq N-1\right\}$, where j is the vertex label. Vertex j is a neighbor of vertices $j-1$ and $j+1$ and only of them. The coin space has two dimensions because the walker can move clockwise or counterclockwise. Thus, the Hilbert space associated with the quantum walk is $\mathcal{H}^2 \otimes \mathcal{H}^N$, whose computational basis is $\left\{|s, j\rangle : 0 \leq s \leq 1, 0 \leq j \leq N-1\right\}$, where

© Springer Nature Switzerland AG 2018

R. Portugal, *Quantum Walks and Search Algorithms*, Quantum Science and Technology, https://doi.org/10.1007/978-3-319-97813-0_6

we set $s = 0$ as clockwise and $s = 1$ as counterclockwise. Under these conventions, the *shift operator* is

$$S|s, j\rangle = \left|s,\ j + (-1)^s\right\rangle. \tag{6.1}$$

After one application of S, j is incremented by one if $s = 0$, and j is decremented by one if $s = 1$. Arithmetic operations with variable j are performed modulo N.

The state at time t is described by

$$|\Psi(t)\rangle = \sum_{j=0}^{N-1} \psi_{0,j}(t)|0, j\rangle + \psi_{1,j}(t)|1, j\rangle, \tag{6.2}$$

where coefficients $\psi_{0,j}(t)$ and $\psi_{1,j}(t)$ are complex functions that obey the normalization condition

$$\left|\psi_{0,j}(t)\right|^2 + \left|\psi_{1,j}(t)\right|^2 = 1, \tag{6.3}$$

for any time step t.

Let us use the Hadamard coin operator

$$H = \frac{1}{\sqrt{2}}\begin{bmatrix} 1 & 1 \\ 1 & -1 \end{bmatrix}. \tag{6.4}$$

Applying the *standard evolution operator* of the coined model

$$U = S\,(H \otimes I) \tag{6.5}$$

to the state at time t, we obtain

$$\begin{aligned}
|\Psi(t+1)\rangle &= \sum_{j=0}^{N-1} S\left(\psi_{0,j}(t)H|0\rangle|j\rangle + \psi_{1,j}(t)H|1\rangle|j\rangle\right) \\
&= \sum_{j=0}^{N-1} \frac{\psi_{0,j}(t) + \psi_{1,j}(t)}{\sqrt{2}} S|0\rangle|j\rangle + \frac{\psi_{0,j}(t) - \psi_{1,j}(t)}{\sqrt{2}} S|1\rangle|j\rangle \\
&= \sum_{j=0}^{N-1} \frac{\psi_{0,j}(t) + \psi_{1,j}(t)}{\sqrt{2}} |0, j+1\rangle + \frac{\psi_{0,j}(t) - \psi_{1,j}(t)}{\sqrt{2}} |1, j-1\rangle.
\end{aligned}$$

Using (6.2) on the left-hand side of the above equation, that is, expanding the left-hand side in the computational basis, and equating with the corresponding coefficients on the right-hand side of the equation, we obtain the evolution equations

$$\psi_{0,j}(t+1) = \frac{\psi_{0,j-1}(t) + \psi_{1,j-1}(t)}{\sqrt{2}},$$
$$\psi_{1,j}(t+1) = \frac{\psi_{0,j+1}(t) - \psi_{1,j+1}(t)}{\sqrt{2}}.$$

These equations are very difficult to solve. However, they can be used for computational simulations, which help us to obtain quick results and to have a general idea about the behavior of the quantum walk. For instance, we can obtain numerically the probability distribution, which is given by

$$p_j(t) = \left|\psi_{0,j}(t)\right|^2 + \left|\psi_{1,j}(t)\right|^2, \tag{6.6}$$

and satisfies

$$\sum_{j=0}^{N-1} p_j(t) = 1$$

for any time step t.

6.1.1 Fourier Transform

The analytic expression of the quantum walk state on the N-cycle can be obtained when we use the *Fourier transform*. The Fourier transform of the spatial part of the computational basis is

$$\left|\tilde{k}\right\rangle = \frac{1}{\sqrt{N}} \sum_{j=0}^{N-1} \omega_N^{jk} |j\rangle, \tag{6.7}$$

where $\omega_N = \mathrm{e}^{\frac{2\pi \mathrm{i}}{N}}$ and the range of k is the same as j. The Fourier transform defines an *orthonormal basis* $\left\{\left|\tilde{k}\right\rangle : 0 \le k \le N-1\right\}$ of $\mathcal{H}^N$, which can be extended into the Hilbert space $\mathcal{H}^2 \otimes \mathcal{H}^N$ as the orthonormal basis $\{|s\rangle\left|\tilde{k}\right\rangle : 0 \le s \le 1, 0 \le k \le N-1\}$ called (extended) *Fourier basis*. In this new basis, the state of the walker is

$$|\Psi(t)\rangle = \sum_{s=0}^{1} \sum_{k=0}^{N-1} \widetilde{\psi}_{s,k}(t)\, |s\rangle\left|\tilde{k}\right\rangle, \tag{6.8}$$

where the coefficients are given by

$$\widetilde{\psi}_{s,k} = \frac{1}{\sqrt{N}} \sum_{j=0}^{N-1} \omega_N^{-jk} \psi_{s,j}. \tag{6.9}$$

The interpretation of this last equation is that the amplitude of a state on the Fourier basis is the *Fourier transform* of the amplitudes in the computational basis.

The vectors of the Fourier basis are eigenvectors of S. In fact, using (6.7) the action of S on $|s\rangle\left|\tilde{k}\right\rangle$ is

$$\begin{aligned} S|s\rangle\left|\tilde{k}\right\rangle &= \frac{1}{\sqrt{N}}\sum_{j=0}^{N-1}\omega_N^{jk}S|s,\,j\rangle \\ &= \frac{1}{\sqrt{N}}\sum_{j=0}^{N-1}\omega_N^{jk}|s\rangle\left|j+(-1)^s\right\rangle. \end{aligned}$$

Renaming the dummy index j so that $j' = j + (-1)^s$, we obtain

$$\begin{aligned} S|s\rangle\left|\tilde{k}\right\rangle &= \frac{1}{\sqrt{N}}\sum_{j'=0}^{N-1}\omega_N^{(j'-(-1)^s)k}|s\rangle\left|j'\right\rangle \\ &= \omega_N^{-(-1)^s k}|s\rangle\left|\tilde{k}\right\rangle. \end{aligned} \tag{6.10}$$

This result confirms our statement. However, our main goal is to *diagonalize* U, which depends on the coin operator.

Applying U to vector $\left|s'\right\rangle\left|\tilde{k}\right\rangle$ and using (6.10), we obtain

$$\begin{aligned} U\left|s'\right\rangle\left|\tilde{k}\right\rangle &= S\left(\left(H\left|s'\right\rangle\right)\left|\tilde{k}\right\rangle\right) \\ &= S\left(\sum_{s=0}^{1}H_{s,s'}|s\rangle\left|\tilde{k}\right\rangle\right) \\ &= \sum_{s=0}^{1}\omega_N^{-(-1)^s k}H_{s,s'}|s\rangle\left|\tilde{k}\right\rangle. \end{aligned}$$

The entries of U in the extended Fourier basis are

$$\left\langle s,\tilde{k}\middle|U\middle|s',\tilde{k}'\right\rangle = \omega_N^{-(-1)^s k}H_{s,s'}\,\delta_{kk'}. \tag{6.11}$$

For each k, define operator $\widetilde{H}^{(k)}$, whose entries are

$$\widetilde{H}^{(k)}_{s,s'} = \omega_N^{-(-1)^s k}H_{s,s'}. \tag{6.12}$$

In the matrix form, we have

$$\widetilde{H}^{(k)} = \begin{bmatrix} \omega_N^{-k} & 0 \\ 0 & \omega_N^{k} \end{bmatrix} \cdot H$$
$$= \frac{1}{\sqrt{2}} \begin{bmatrix} \omega_N^{-k} & \omega_N^{-k} \\ \omega_N^{k} & -\omega_N^{k} \end{bmatrix}. \tag{6.13}$$

Equation (6.11) shows that the nondiagonal part of U is associated with the coin space. For each k, we have a *reduced evolution operator* $\widetilde{H}^{(k)}$. The goal now is to diagonalize $\widetilde{H}^{(k)}$. If $|\alpha_k\rangle$ is an eigenvector of $\widetilde{H}^{(k)}$ with eigenvalue α_k, then $|\alpha_k\rangle\left|\tilde{k}\right\rangle$ is an eigenvector of U associated with the same eigenvalue α_k (Exercise 6.2).

The *characteristic polynomial* of $\widetilde{H}^{(k)}$ is

$$p_{\widetilde{H}}(\lambda) = \lambda^2 + \sqrt{2}\,\mathrm{i}\lambda \sin\kappa - 1,$$

where

$$\kappa = \frac{2\pi k}{N}. \tag{6.14}$$

By solving the equation $p_{\widetilde{H}}(\lambda) = 0$, we obtain the eigenvalues $\mathrm{e}^{-\mathrm{i}\theta_k}$ and $\mathrm{e}^{\mathrm{i}(\pi+\theta_k)}$, where θ_k is a solution of

$$\sin\theta_k = \frac{1}{\sqrt{2}} \sin\kappa. \tag{6.15}$$

The normalized eigenvectors are

$$|\alpha_k\rangle = \frac{1}{\sqrt{c_k^-}} \begin{bmatrix} 1 \\ \left(\sqrt{1+\cos^2\kappa} - \cos\kappa\right)\mathrm{e}^{\mathrm{i}\kappa} \end{bmatrix}, \tag{6.16}$$

$$|\beta_k\rangle = \frac{1}{\sqrt{c_k^+}} \begin{bmatrix} 1 \\ -\left(\sqrt{1+\cos^2\kappa} + \cos\kappa\right)\mathrm{e}^{\mathrm{i}\kappa} \end{bmatrix}, \tag{6.17}$$

where

$$c_k^{\pm} = 2\sqrt{1+\cos^2\kappa}\left(\sqrt{1+\cos^2\kappa} \pm \cos\kappa\right). \tag{6.18}$$

The spectral decomposition of U is

$$U = \sum_{k=0}^{N-1} \left(\mathrm{e}^{-\mathrm{i}\,\theta_k} \left|\alpha_k, \tilde{k}\right\rangle\left\langle\alpha_k, \tilde{k}\right| + \mathrm{e}^{\mathrm{i}\,(\pi+\theta_k)} \left|\beta_k, \tilde{k}\right\rangle\left\langle\beta_k, \tilde{k}\right|\right). \tag{6.19}$$

The tth power of U is

$$U^t = \sum_{k=0}^{N-1} \left(\mathrm{e}^{-\mathrm{i}\,\theta_k t} \left|\alpha_k, \tilde{k}\right\rangle\left\langle\alpha_k, \tilde{k}\right| + \mathrm{e}^{\mathrm{i}\,(\pi+\theta_k)t} \left|\beta_k, \tilde{k}\right\rangle\left\langle\beta_k, \tilde{k}\right|\right). \tag{6.20}$$

Exercise 6.1. Show the following properties of the Fourier transform:

1. $\left|\tilde{0}\right\rangle$ is the diagonal state of Hilbert space $\mathcal{H}^N$.
2. $\left\{\left|\tilde{k}\right\rangle : 0 \leq k \leq N-1\right\}$ is an orthonormal basis for Hilbert space $\mathcal{H}^N$.
3. $|0\rangle = \frac{1}{\sqrt{N}} \sum_{k=0}^{N-1} \left|\tilde{k}\right\rangle$.
4. $|j\rangle = \frac{1}{\sqrt{N}} \sum_{k=0}^{N-1} \omega_N^{-jk} \left|\tilde{k}\right\rangle$.

Exercise 6.2. Show that if $|\alpha_k\rangle$ is an eigenvector of $\widetilde{H}^{(k)}$ with eigenvalue α_k, then $|\alpha_k\rangle\left|\tilde{k}\right\rangle$ is an eigenvector of U associated with the same eigenvalue α_k.

Exercise 6.3. Show that $\left\{\left|\alpha_k, \tilde{k}\right\rangle, \left|\beta_k, \tilde{k}\right\rangle : 0 \leq k < N\right\}$ is an orthonormal basis of Hilbert space $\mathcal{H}^2 \otimes \mathcal{H}^N$.

6.1.2 Analytic Solutions

Consider initially a particle on vertex 0 with the coin pointing clockwise. The initial condition in the computational basis is

$$|\psi(0)\rangle = |0\rangle|0\rangle. \tag{6.21}$$

Using (6.20), we obtain

$$\begin{aligned} |\psi(t)\rangle &= U^t|\psi(0)\rangle \\ &= \sum_{k=0}^{N-1} \left(\mathrm{e}^{-\mathrm{i}\,\theta_k t} \left|\alpha_k, \tilde{k}\right\rangle \left\langle \alpha_k, \tilde{k} \middle| 0, 0\right\rangle + \mathrm{e}^{\mathrm{i}\,(\pi+\theta_k)t} \left|\beta_k, \tilde{k}\right\rangle \left\langle \beta_k, \tilde{k} \middle| 0, 0\right\rangle \right). \end{aligned}$$

Using (6.16), (6.17), and (6.7), we obtain

$$\left\langle \alpha_k, \tilde{k} \middle| 0, 0\right\rangle = \frac{1}{\sqrt{N\, c_k^-}}, \tag{6.22}$$

$$\left\langle \beta_k, \tilde{k} \middle| 0, 0\right\rangle = \frac{1}{\sqrt{N\, c_k^+}}. \tag{6.23}$$

Therefore,

$$|\psi(t)\rangle = \frac{1}{\sqrt{N}} \sum_{k=0}^{N-1} \left(\frac{\mathrm{e}^{-\mathrm{i}\,\theta_k t}}{\sqrt{c_k^-}} |\alpha_k\rangle + \frac{(-1)^t\, \mathrm{e}^{\mathrm{i}\,\theta_k t}}{\sqrt{c_k^+}} |\beta_k\rangle \right) \left|\tilde{k}\right\rangle. \tag{6.24}$$

To calculate the probability of finding the walker on any vertex of a cycle, we have to express the quantum state in the computational basis. Using (6.16), (6.17),

and the identity

$$\frac{1}{c_k^{\pm}} = \frac{1}{2}\left(1 \mp \frac{\cos\kappa}{\sqrt{1+\cos^2\kappa}}\right), \tag{6.25}$$

we obtain

$$|\psi(t)\rangle = \frac{1}{\sqrt{N}} \sum_{k=0}^{N-1} \begin{bmatrix} A_k(t) \\ B_k(t) \end{bmatrix} |\tilde{k}\rangle, \tag{6.26}$$

where

$$A_k(t) = \cos\theta_k t - \frac{\mathrm{i}\cos\kappa\ \sin\theta_k t}{\sqrt{1+\cos^2\kappa}}, \tag{6.27}$$

$$B_k(t) = -\frac{\mathrm{i}\,\mathrm{e}^{\mathrm{i}\kappa}\ \sin\theta_k t}{\sqrt{1+\cos^2\kappa}}, \tag{6.28}$$

which is valid when t is even. Using (6.7), we obtain

$$|\psi(t)\rangle = \frac{1}{N} \sum_{j=0}^{N-1} \begin{bmatrix} \sum_{k=0}^{N-1} A_k(t)\,\omega_N^{jk} \\ \sum_{k=0}^{N-1} B_k(t)\,\omega_N^{jk} \end{bmatrix} |j\rangle. \tag{6.29}$$

Using (6.6), we obtain the probability distribution

$$p_j(t) = \frac{1}{N^2}\left|\sum_{k=0}^{N-1} A_k(t)\,\omega_N^{jk}\right|^2 + \frac{1}{N^2}\left|\sum_{k=0}^{N-1} B_k(t)\,\omega_N^{jk}\right|^2. \tag{6.30}$$

This equation is valid for any N, but only for even t. Exercise 6.4 gives us hints that help us to obtain $A_k(t)$ and $B_k(t)$ when t is odd. When $j+t$ is odd and N is even, the probability distribution is zero. When N is odd, the probability distribution is nonzero for all vertices (for large enough t). Exercise 6.6 gives us hints that help us to prove those facts.

Consider j in the interval $[N/2, N-1]$. If we shift j by $(-N)$, the probability distribution of the N-cycle is equal to the probability distribution of the walk on the line when $t \le N$. This can be seen from the plot of the probability distribution (blue line) in Fig. 6.1 for the cycle with $N = 200$. Note that for j in the interval $[0, N/2]$, the plot of Fig. 6.1 is equal to the one of Fig. 5.1 of Sect. 5.1.2 on P. 75. If the remaining part of the plot is shifted leftward, the new plot becomes entirely equal to the plot of the quantum walk on the line.

On the line, the *wavefronts* move to opposite directions and go away forever. On even cycles, the *wavefronts* move toward each other, are close to each other at t around $N/2$, and collide, as can be seen in Fig. 6.1. On odd cycles, the wavefronts move toward each other but do not collide and, instead, they intertwine because there is an inverse relationship between the *parity* of j and the nonzero values of the probability.

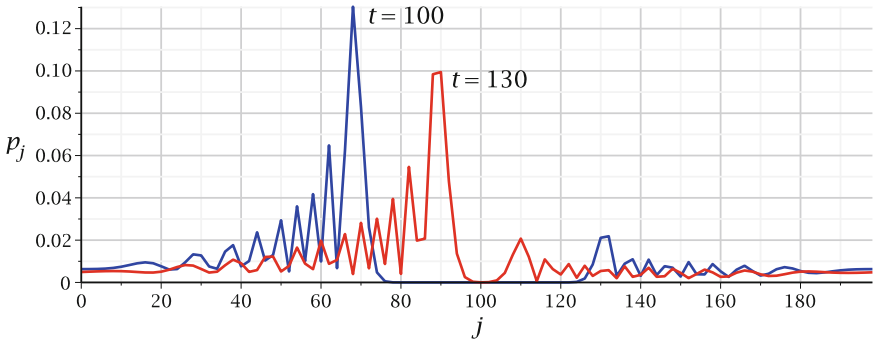

Fig. 6.1 Probability distribution of the quantum walk on the 200-cycle after 100 steps (blue line) and 130 steps (red line) with the initial condition $|\psi(0)\rangle = |0, 0\rangle$. Odd values of j are not shown because the probability is zero

These facts show that quantum walks on odd and even cycles have different behavior. A confirming evidence comes from the form of the *limiting distribution*, which is uniform for odd cycles for all initial conditions, while nonuniform and initial condition-dependent for even cycles. In terms of the graph structure, even cycles are *bipartite graphs*. The asymptotic behavior of *classical random walks* on bipartite graphs is different from the behavior on *nonbipartite graphs*. Part of this difference is inherited by the quantum context.

On the line, all unbiased quantum walks can be obtained from the Hadamard coin through a suitable choice of the initial condition. On a cycle, this is true for a period while there is no interference of the wavefronts. When the wavefronts collide or travel the whole circle, relative phase factors can produce constructive or destructive interference. These phase factors are introduced through the evolution operator and cannot be reproduced by choosing initial conditions.

Exercise 6.4. Show that, to obtain valid expressions for $A_k(t)$ and $B_k(t)$ for odd t, we have to interchange $\cos\theta_k t$ by $-\mathrm{i}\sin\theta_k t$ in (6.27) and (6.28).

Exercise 6.5. Show that

$$\frac{1}{N}\sum_{j=0}^{N-1} \mathrm{e}^{\mathrm{i}\, j\,(\kappa-\kappa')} = \delta_{\kappa\kappa'}.$$

Using the above identity and (6.30), show that

$$\sum_{j=0}^{N-1} p_j(t) = 1$$

for any even number of steps t. Using Exercise 6.4, show also for odd t.

Exercise 6.6. Consider N even. If t is even, show that

$$|\psi(t)\rangle = \frac{1}{N}\sum_{j=0}^{N-1}\left(1+(-1)^j\right)\begin{bmatrix}\sum_{k=0}^{N/2-1} A_k(t)\,\omega_N^{jk}\\ \sum_{k=0}^{N/2-1} B_k(t)\,\omega_N^{jk}\end{bmatrix}|j\rangle.$$

From this result, show that $p_j(t) = 0$ for odd j. Using Exercise 6.4, show that when t is odd, $p_j(t) = 0$ for even j. How can this result be interpreted in terms of the *parity* of N and the properties of the shift operator?

Exercise 6.7. The *flip-flop shift operator* is defined as

$$S|s, j\rangle = \left|s \oplus 1,\ j + (-1)^s\right\rangle,$$

where $\oplus$ is the binary sum modulo 2. Obtain the eigenvalues and eigenvectors of the evolution operator with the flip-flop shift operator and the state of the quantum walk $|\psi(t)\rangle$ at any time step t, and compare the results with the results obtained with the standard shift operator.

6.1.3 Periodic Solutions

In some cases, the evolution of a quantum walk can be periodic, that is, there is an integer T such that $|\psi(t+T)\rangle = |\psi(t)\rangle$ for any time step t. To obtain a periodic solution, we can use (6.20) that completely determines the state of the quantum walk at time t once given the initial condition. We must find T such that $U^T = I$. This implies that

$$\mathrm{e}^{-\mathrm{i}\theta_k T} = \mathrm{e}^{\mathrm{i}(\pi+\theta_k)T} = 1, \tag{6.31}$$

for all k. Therefore, T must be even and

$$\cos\theta_k T = 1,$$
$$\sin\theta_k T = 0,$$

that is, $\theta_k T = 2\pi j_k$, where each j_k must be an integer. Using (6.15), we obtain

$$\sin\frac{2\pi j_k}{T} = \frac{1}{\sqrt{2}}\sin\frac{2\pi k}{N}, \tag{6.32}$$

which must be valid for $0 \le k \le N-1$. This equation can be solved by exhaustive search, and we find solutions for $N = 2$ and $T = 2$; $N = 4$ and $T = 8$; $N = 8$ and $T = 24$.

Figure 6.2 shows the probability at vertex $v = 0$ as a function of time for the cycle with eight vertices. Note that the probability is periodic. The same holds for any other vertex.

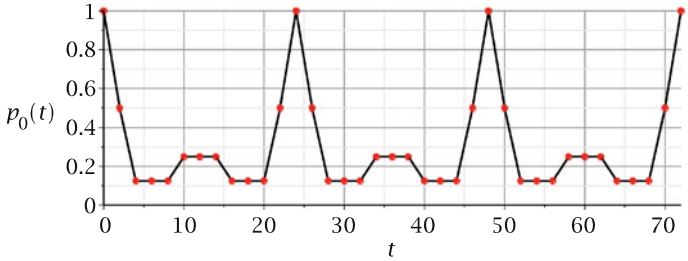

Fig. 6.2 Probability at vertex $v = 0$ as a function of time for the 8-cycle. The probability has period $T = 24$. The plot shows only the probability at even t

6.2 Finite Two-Dimensional Lattices

Suppose that N is a perfect square and consider the $\sqrt{N} \times \sqrt{N}$ square lattice with *periodic boundary conditions*, that is, a lattice with the shape of a *torus*. If the walker moves $\sqrt{N}$ steps toward x-direction, it returns to original position. The same holds for the y-direction. The vectors of the computational basis of the spatial part are $|x, y\rangle$, where $x, y \in \{0, \ldots, \sqrt{N} - 1\}$. The coin space has four dimensions. The vectors of the computational basis of the coin space are $|d, s\rangle$, with $0 \leq d, s \leq 1$, where d determines the direction of movement: $d = 0$ stands for x-direction and $d = 1$ stands for y-direction, and s determines the direction sign: $s = 0$ stands for positive direction and $s = 1$ stands for negative direction.

Under these conventions, we write the *shift operator* as

$$S|d, s\rangle|x, y\rangle = |d, s \oplus 1\rangle\left|x + (-1)^s \delta_{d0}, y + (-1)^s \delta_{d1}\right\rangle, \tag{6.33}$$

where the arithmetic operations with variables x and y are performed modulo $\sqrt{N}$. After one application of S, x is incremented by one and y remains unchanged if $d = 0$ and $s = 0$. When x changes, y remains unchanged, and vice versa. Note that the coin state changes from $|d, s\rangle$ to $|d, s \oplus 1\rangle$, that is, the direction is inverted after the shift. This inversion in the coin value is important for speeding up *search algorithms* on the two-dimensional lattice. This issue will be addressed in Sect. 9.3 on P. 186. Shift operators that invert the coin are called *flip-flop*.

We use the *Grover coin*, which is given by

$$G = 2|\mathrm{D}\rangle\langle\mathrm{D}| - I, \tag{6.34}$$

where $|\mathrm{D}\rangle = \frac{1}{2}\sum_{d,s=0}^{1} |d, s\rangle$ is the *diagonal state* of $\mathcal{H}^2 \otimes \mathcal{H}^2$. The *matrix representation* of G is

$$G = \frac{1}{2}\begin{bmatrix} -1 & 1 & 1 & 1 \\ 1 & -1 & 1 & 1 \\ 1 & 1 & -1 & 1 \\ 1 & 1 & 1 & -1 \end{bmatrix}. \tag{6.35}$$

The state of the walker at time t is described by

$$|\Psi(t)\rangle = \sum_{d,s=0}^{1} \sum_{x,y=0}^{\sqrt{N}-1} \psi_{d,s;\,x,y}(t)|d,s\rangle|x,y\rangle, \tag{6.36}$$

where the coefficients $\psi_{d,s;\,x,y}(t)$ are complex functions that obey the normalization condition

$$\sum_{d,s=0}^{1} \sum_{x,y=0}^{\sqrt{N}-1} \left|\psi_{d,s;\,x,y}(t)\right|^2 = 1, \tag{6.37}$$

for any time step t.

Applying the *standard evolution operator*

$$U = S\,(G \otimes I) \tag{6.38}$$

to the state at time t, we obtain

$$\begin{aligned}
|\Psi(t+1)\rangle &= \sum_{d',s'=0}^{1} \sum_{x,y=0}^{\sqrt{N}-1} \psi_{d',s';\,x,y}(t)\, S\Big(G\big|d',s'\big\rangle|x,y\rangle\Big) \\
&= \sum_{d',s'=0}^{1} \sum_{x,y=0}^{\sqrt{N}-1} \psi_{d',s';\,x,y}(t)\, S\left(\sum_{d,s=0}^{1} G_{d,s;\,d',s'}|d,s\rangle|x,y\rangle\right) \\
&= \sum_{d,s,d',s'=0}^{1} \sum_{x,y=0}^{\sqrt{N}-1} \psi_{d',s';\,x,y}(t)\, G_{d,s;\,d',s'} \\
&\qquad |d,s\oplus 1\rangle\big|x+(-1)^s\delta_{d0},\ y+(-1)^s\delta_{d1}\big\rangle.
\end{aligned}$$

We can rename the dummy indices of the sum from $x+(-1)^s\delta_{d0}$, $y+(-1)^s\delta_{d1}$, $s\oplus 1$ to x, y, s. Then,

$$\begin{aligned}
|\Psi(t+1)\rangle = \sum_{d,s,d',s'=0}^{1} \sum_{x,y=0}^{\sqrt{N}-1} & G_{d,s\oplus 1;\,d',s'} \\
& \times \psi_{d',s';\,x-(-1)^{s\oplus 1}\delta_{d0},\,y-(-1)^{s\oplus 1}\delta_{d1}}(t)|d,s\rangle|x,y\rangle.
\end{aligned}$$

Expanding the left-hand side of the above equation in the computational basis and equating coefficients alike, we obtain the *evolution equation*

$$\psi_{d,s;\,x,y}(t+1) = \sum_{d',s'=0}^{1} G_{d,s\oplus 1;\,d',s'}\, \psi_{d',s';\,x+(-1)^s\delta_{d0},\,y+(-1)^s\delta_{d1}}(t). \tag{6.39}$$

This equation is too complex to be solved the way it is written. In the one-dimensional case, we have learned that by taking the Fourier transform on the spatial part, we can diagonalize the shift operator. This allowed us to find analytically the state of the quantum walk at any time step. The same technique works here.

6.2.1 Fourier Transform

The Fourier transform of the spatial part of the computational basis is

$$\left|\tilde{k}, \tilde{\ell}\right\rangle = \frac{1}{\sqrt{N}} \sum_{x,y=0}^{\sqrt{N}-1} \omega^{xk+y\ell} |x, y\rangle, \tag{6.40}$$

where $\omega = \mathrm{e}^{\frac{2\pi \mathrm{i}}{\sqrt{N}}}$ and the ranges of variables k and ℓ are the same as x and y. The Fourier transform is the tensor product of the Fourier transform of each coordinate. The Fourier transform allows us to define a new orthonormal basis $\left\{|d, s\rangle\left|\tilde{k}, \tilde{\ell}\right\rangle : 0 \leq d, s \leq 1, 0 \leq k, \ell \leq \sqrt{N} - 1\right\}$ called the *Fourier basis*.

Let us calculate the action of the shift operator S on $|d, s\rangle\left|\tilde{k}, \tilde{\ell}\right\rangle$. Using (6.40), we have

$$\begin{aligned} S|d, s\rangle\left|\tilde{k}, \tilde{\ell}\right\rangle &= \frac{1}{\sqrt{N}} \sum_{x,y=0}^{\sqrt{N}-1} \omega^{xk+y\ell} S|d, s\rangle|x, y\rangle \\ &= \frac{1}{\sqrt{N}} \sum_{x,y=0}^{\sqrt{N}-1} \omega^{xk+y\ell} |d, s \oplus 1\rangle \otimes \\ &\qquad \left|x + (-1)^s \delta_{d0}, y + (-1)^s \delta_{d1}\right\rangle. \end{aligned}$$

To simplify the last equation, we rename the dummy indices so that $x' = x + (-1)^s \delta_{d0}$ and $y' = y + (-1)^s \delta_{d1}$. Then,

$$\begin{aligned} S|d, s\rangle\left|\tilde{k}, \tilde{\ell}\right\rangle &= \frac{1}{\sqrt{N}} \sum_{x',y'=0}^{\sqrt{N}-1} \omega^{(x'-(-1)^s \delta_{d0})k + (y'-(-1)^s \delta_{d1})\ell} \\ &\qquad \times |d, s \oplus 1\rangle\left|x', y'\right\rangle \\ &= \omega^{-(-1)^s (\delta_{d0} k + \delta_{d1} \ell)} |d, s \oplus 1\rangle\left|\tilde{k}, \tilde{\ell}\right\rangle. \end{aligned} \tag{6.41}$$

In the flip-flop case, the vectors of the Fourier basis are not eigenvectors of S. However, the result (6.41) is useful to diagonalize the evolution operator because we can factor out vector $\left|\tilde{k}, \tilde{\ell}\right\rangle$ leaving a four-dimensional subspace.

Applying U to vector $\left|d', s'\right\rangle\left|\tilde{k}, \tilde{\ell}\right\rangle$ and using (6.41), we obtain

$$\begin{aligned} U\left|d', s'\right\rangle\left|\tilde{k}, \tilde{\ell}\right\rangle &= S\left(\sum_{d,s=0}^{1} G_{d,s;\,d',s'}|d, s\rangle\left|\tilde{k}, \tilde{\ell}\right\rangle\right) \\ &= \sum_{d,s=0}^{1} \omega^{-(-1)^s(\delta_{d0}k+\delta_{d1}\ell)} G_{d,s;\,d',s'}|d, s\oplus 1\rangle\left|\tilde{k}, \tilde{\ell}\right\rangle \\ &= \sum_{d,s=0}^{1} \omega^{(-1)^s(\delta_{d0}k+\delta_{d1}\ell)} G_{d,s\oplus 1;\,d',s'}|d, s\rangle\left|\tilde{k}, \tilde{\ell}\right\rangle. \end{aligned}$$

The entries of U in the Fourier basis are

$$\left\langle d, s, \tilde{k}', \tilde{\ell}'\right|U\left|d', s', \tilde{k}, \tilde{\ell}\right\rangle = \omega^{(-1)^s(\delta_{d0}k+\delta_{d1}\ell)} G_{d,s\oplus 1;\,d',s'}\,\delta_{kk'}\delta_{\ell\ell'}. \tag{6.42}$$

For each k and ℓ, we define operator $\widetilde{G}$ with entries

$$\widetilde{G}_{d,s;\,d',s'} = \omega^{(-1)^s(\delta_{d0}k+\delta_{d1}\ell)} G_{d,s\oplus 1;\,d',s'}. \tag{6.43}$$

The matrix representation is

$$\widetilde{G} = \begin{bmatrix} 0 & \omega^{k} & 0 & 0 \\ \omega^{-k} & 0 & 0 & 0 \\ 0 & 0 & 0 & \omega^{\ell} \\ 0 & 0 & \omega^{-\ell} & 0 \end{bmatrix} \cdot G. \tag{6.44}$$

Equation (6.42) shows that the nondiagonal part of operator U is associated with the coin space. The goal now is to diagonalize operator $\widetilde{G}$. If $|\nu\rangle$ is an eigenvector of $\widetilde{G}$, then $|\nu\rangle\left|\tilde{k}, \tilde{\ell}\right\rangle$ is an eigenvector of U associated with the same eigenvalue.

If $k = 0$ and $\ell = 0$, matrix $\widetilde{G}$ reduces to

$$\widetilde{G}_{(k=0,\ell=0)} = \frac{1}{2}\begin{bmatrix} 1 & -1 & 1 & 1 \\ -1 & 1 & 1 & 1 \\ 1 & 1 & 1 & -1 \\ 1 & 1 & -1 & 1 \end{bmatrix}. \tag{6.45}$$

The determinant $\left|\lambda I - \widetilde{G}_{(k=0,\ell=0)}\right|$ is $(\lambda - 1)^3\,(\lambda + 1)$. Therefore, the eigenvalues are $(+1)$ with multiplicity 3 and (-1) with multiplicity 1. The eigenvectors associated with eigenvalue $(+1)$ are

$$\left|\nu_{00}^{1a}\right\rangle = \frac{1}{2}\begin{bmatrix}1\\1\\1\\1\end{bmatrix}, \left|\nu_{00}^{1b}\right\rangle = \frac{1}{\sqrt{2}}\begin{bmatrix}1\\-1\\0\\0\end{bmatrix}, \left|\nu_{00}^{1c}\right\rangle = \frac{1}{\sqrt{2}}\begin{bmatrix}0\\0\\1\\-1\end{bmatrix}. \tag{6.46}$$

The (-1)-eigenvector is

$$\left|\nu_{00}^{-1}\right\rangle = \frac{1}{2}\begin{bmatrix}1\\1\\-1\\-1\end{bmatrix}. \tag{6.47}$$

Note that $\left|\nu_{00}^{1a}\right\rangle = |\mathrm{D}\rangle$. The set of these eigenvectors is an orthonormal basis.

If $k \neq 0$ or $\ell \neq 0$, the determinant of $(\lambda I - \widetilde{G})$ is

$$\left|\lambda I - \widetilde{G}\right| = \left(\lambda^2 - 1\right)\left(\lambda^2 - \left(\cos\frac{2\pi k}{\sqrt{N}} + \cos\frac{2\pi \ell}{\sqrt{N}}\right)\lambda + 1\right). \tag{6.48}$$

Therefore, the eigenvalues of $\widetilde{G}$ are

$$\lambda = \begin{cases} \pm 1, \\ \mathrm{e}^{\pm \mathrm{i}\theta_{k\ell}}, \end{cases} \tag{6.49}$$

where

$$\cos\theta_{k\ell} = \frac{1}{2}\left(\cos\frac{2\pi k}{\sqrt{N}} + \cos\frac{2\pi \ell}{\sqrt{N}}\right). \tag{6.50}$$

Eigenvectors $|\nu\rangle = (a, b, c, d)$ are found as follows: We calculate vector $(\widetilde{G} - \lambda I)|\nu\rangle$ and equate each entry to zero. We have a system of four equations in variables a, b, c, d. We eliminate one of the equations, for example, the last one, and solve the system of equations in the three variables a, b, c. After that, choose d that normalizes the vector. This procedure for eigenvalue $(+1)$ yields eigenvector

$$\left|\nu_{k\ell}^{+1}\right\rangle = \frac{1}{n^{(+1)}}\begin{bmatrix}\omega^k\left(\omega^\ell - 1\right)\\ 1 - \omega^\ell \\ \omega^\ell\left(1 - \omega^k\right)\\ \omega^k - 1\end{bmatrix}. \tag{6.51}$$

For eigenvalue (-1), we have

$$\left|\nu_{k\ell}^{-1}\right\rangle = \frac{1}{n^{(-1)}} \begin{bmatrix} -\omega^k\left(1+\omega^\ell\right) \\ -\left(1+\omega^\ell\right) \\ \omega^\ell\left(1+\omega^k\right) \\ 1+\omega^k \end{bmatrix}. \tag{6.52}$$

Variables $n^{(\pm 1)}$ are normalization constants. For the other eigenvalues ($\pm\theta_{k\ell} \neq \pm 1$), we denote the eigenvectors by $\left|\nu_{k\ell}^{\pm\theta}\right\rangle$. The expression for the $+\theta$ case is

$$\left|\nu_{k\ell}^{+\theta}\right\rangle = \frac{\mathrm{i}}{2\sqrt{2}\sin\theta_{k\ell}} \begin{bmatrix} \mathrm{e}^{-\mathrm{i}\theta_{k\ell}} - \omega^k \\ \mathrm{e}^{-\mathrm{i}\theta_{k\ell}} - \omega^{-k} \\ \mathrm{e}^{-\mathrm{i}\theta_{k\ell}} - \omega^{\ell} \\ \mathrm{e}^{-\mathrm{i}\theta_{k\ell}} - \omega^{-\ell} \end{bmatrix}. \tag{6.53}$$

To obtain the fourth eigenvector, we replace θ by $-\theta$. Remember that θ depends on k and ℓ. The expression for $\sin\theta_{k\ell}$ can be obtained from (6.50).

If $k = \ell$ or $k = \sqrt{N} - \ell$, the eigenvectors simplify to the following expressions:

$$\left|\nu_{k,k}^{+\theta}\right\rangle = \frac{1}{\sqrt{2}} \begin{bmatrix} 1 \\ 0 \\ 1 \\ 0 \end{bmatrix}, \quad \left|\nu_{k,k}^{-\theta}\right\rangle = \frac{1}{\sqrt{2}} \begin{bmatrix} 0 \\ 1 \\ 0 \\ 1 \end{bmatrix},$$

$$\left|\nu_{k,\sqrt{N}-k}^{+\theta}\right\rangle = \frac{1}{\sqrt{2}} \begin{bmatrix} 1 \\ 0 \\ 0 \\ 1 \end{bmatrix}, \quad \left|\nu_{k,\sqrt{N}-k}^{-\theta}\right\rangle = \frac{1}{\sqrt{2}} \begin{bmatrix} 0 \\ 1 \\ 1 \\ 0 \end{bmatrix}. \tag{6.54}$$

Note that if $\sqrt{N}$ is even and $k = \ell = \frac{\sqrt{N}}{2}$, (6.50) implies that $\theta = \pi$. In this case, the eigenvectors of (6.54) have eigenvalue (-1). The basis is complete when we take the eigenvectors of (6.51) and (6.52). The eigenvalue (-1) has multiplicity 3 and eigenvalue 1 has multiplicity 1. Matrix $\widetilde{G}$ is the negative of the matrix described in (6.45).

The union of sets $\left\{\left|\nu_{k\ell}^{+1}\right\rangle\left|\tilde{k},\tilde{\ell}\right\rangle,\ \left|\nu_{k\ell}^{-1}\right\rangle\left|\tilde{k},\tilde{\ell}\right\rangle,\ \left|\nu_{k\ell}^{\pm\theta}\right\rangle\left|\tilde{k},\tilde{\ell}\right\rangle : 0 \leq k,\ell < \sqrt{N},\ (k,\ell) \neq (0,0)\right\}$ and $\left\{\left|\nu_{00}^{1a}\right\rangle\left|\tilde{0},\tilde{0}\right\rangle, \left|\nu_{00}^{1b}\right\rangle\left|\tilde{0},\tilde{0}\right\rangle, \left|\nu_{00}^{1c}\right\rangle\left|\tilde{0},\tilde{0}\right\rangle, \left|\nu_{00}^{-1}\right\rangle\left|\tilde{0},\tilde{0}\right\rangle\right\}$ is an orthonormal eigenbasis of U for Hilbert space $\mathcal{H}^2 \otimes \mathcal{H}^2 \otimes \mathcal{H}^{\sqrt{N}} \otimes \mathcal{H}^{\sqrt{N}}$. The associated eigenvalues are ± 1 and $\mathrm{e}^{\pm\mathrm{i}\theta_{k\ell}}$.

Exercise 6.8. Show the following properties of the Fourier transform:

1. $\left|\tilde{0},\tilde{0}\right\rangle$ is the diagonal state of Hilbert space $\mathcal{H}^{\sqrt{N}} \otimes \mathcal{H}^{\sqrt{N}}$.

2. $\left\{\left|\tilde{k}, \tilde{\ell}\right\rangle : 0 \le k, \ell \le \sqrt{N} - 1\right\}$ is an orthonormal basis for Hilbert space $\mathcal{H}^{\sqrt{N}} \otimes \mathcal{H}^{\sqrt{N}}$.
3. $|0, 0\rangle = \frac{1}{\sqrt{N}} \sum_{k,\ell=0}^{\sqrt{N}-1} \left|\tilde{k}, \tilde{\ell}\right\rangle$.

Exercise 6.9. Show that the norm of $\left|\nu_{k\ell}^{\pm 1}\right\rangle$ is

$$n^{(\pm 1)} = 2\sqrt{2}\left(1 \mp \cos\theta_{k\ell}\right)^{\frac{1}{2}}.$$

Obtain expressions $n^{(+1)} = 4\sin\frac{\theta_{k\ell}}{2}$ and $n^{(-1)} = 4\cos\frac{\theta_{k\ell}}{2}$.

Exercise 6.10. Show that $\left|\nu_{00}^{1a}\right\rangle$ is orthogonal to $\left|\nu_{k\ell}^{\pm 1}\right\rangle$.

Exercise 6.11. Verify that $\left|\nu_{k\ell}^{+\theta}\right\rangle$ given by (6.53) is a unit vector. Show that $\left|\nu_{k\ell}^{+\theta}\right\rangle$ is an eigenvector of $\widetilde{G}$ associated with eigenvalue $\mathrm{e}^{\mathrm{i}\theta_{k\ell}}$.

Exercise 6.12. Vector $\left|\nu_{k\ell}^{-\theta}\right\rangle$ is the complex conjugate of $\left|\nu_{k\ell}^{\theta}\right\rangle$?

Exercise 6.13. Show that

1. $|\mathrm{D}\rangle = \frac{\left|\nu_{k\ell}^{\theta}\right\rangle + \left|\nu_{k\ell}^{-\theta}\right\rangle}{\sqrt{2}}$,
2. $\left\langle \nu_{k\ell}^{\pm\theta} \middle| \mathrm{D}\right\rangle = \frac{1}{\sqrt{2}}$,
3. $\langle \mathrm{D}|\widetilde{G}|\mathrm{D}\rangle = \cos\theta_{k\ell}$.

6.2.2 Analytic Solutions

Let us calculate the state of the quantum walk at an arbitrary time step. Let us consider the initial state

$$|\Psi(0)\rangle = |\mathrm{D}\rangle|0, 0\rangle, \tag{6.55}$$

that is, a walker is initially located at vertex $(0, 0)$ and its coin state is the diagonal state.

Let us use the following notation for the eigenvalues and eigenvectors of U: $\left|\nu_{k\ell}^{j}\right\rangle\left|\tilde{k}, \tilde{\ell}\right\rangle$, where the eigenvalues are $\nu_{k\ell}^{j}$ with $1 \le j \le 4$. Then,

$$U = \sum_{j=1}^{4} \sum_{k,\ell=0}^{\sqrt{N}-1} \nu_{k\ell}^{j} \left|\nu_{k\ell}^{j}, \tilde{k}, \tilde{\ell}\right\rangle\left\langle \nu_{k\ell}^{j}, \tilde{k}, \tilde{\ell}\right|. \tag{6.56}$$

At time t, the state of the quantum walk will be given by

$$\begin{aligned} |\Psi(t)\rangle &= U^t|\Psi(0)\rangle \\ &= \sum_{j=1}^{4} \sum_{k,\ell=0}^{\sqrt{N}-1} (\nu_{k\ell}^{j})^t \left\langle \nu_{k\ell}^{j}, \tilde{k}, \tilde{\ell} \middle| \Psi(0)\right\rangle \left|\nu_{k\ell}^{j}\right\rangle\left|\tilde{k}, \tilde{\ell}\right\rangle, \end{aligned} \tag{6.57}$$

The state of the quantum walk at time t can be calculated explicitly. The task is reduced to calculate the entries of the initial condition in the eigenbasis of U and, after that, to calculate the tth power of the eigenvalues. We have already obtained explicit expressions for the eigenvalues and eigenvectors of U.

Using (6.57), we obtain

$$|\Psi(t)\rangle = \sum_{j=1}^{4} \sum_{k,\ell=0}^{\sqrt{N}-1} (\nu_{k\ell}^{j})^{t} \left\langle \nu_{k\ell}^{j} \middle| \mathrm{D} \right\rangle \left\langle \tilde{k}, \tilde{\ell} \middle| 0, 0 \right\rangle \left| \nu_{k\ell}^{j} \right\rangle \left| \tilde{k}, \tilde{\ell} \right\rangle. \tag{6.58}$$

Using (6.40), we have $\left\langle \tilde{k}, \tilde{\ell} \middle| 0, 0 \right\rangle = 1/\sqrt{N}$. Among all eigenvectors of $\widetilde{G}$, only $\left| \nu_{00}^{1a} \right\rangle$ and $\left| \nu_{k\ell}^{\pm\theta} \right\rangle$ are not orthogonal to $|\mathrm{D}\rangle$. Therefore, the above equation reduces to

$$\begin{aligned} |\Psi(t)\rangle = {} & \frac{(+1)^{t}}{\sqrt{N}} \left| \nu_{00}^{1a} \right\rangle \left| \tilde{0}, \tilde{0} \right\rangle + \frac{1}{\sqrt{N}} \sum_{\substack{k,\ell=0 \\ (k,\ell)\neq(0,0)}}^{\sqrt{N}-1} \left(\mathrm{e}^{\mathrm{i}\theta_{k\ell}} \right)^{t} \left\langle \nu_{k\ell}^{\theta} \middle| \mathrm{D} \right\rangle \left| \nu_{k\ell}^{\theta} \right\rangle \left| \tilde{k}, \tilde{\ell} \right\rangle \\ & + \left(\mathrm{e}^{-\mathrm{i}\theta_{k\ell}} \right)^{t} \left\langle \nu_{k\ell}^{-\theta} \middle| \mathrm{D} \right\rangle \left| \nu_{k\ell}^{-\theta} \right\rangle \left| \tilde{k}, \tilde{\ell} \right\rangle. \end{aligned} \tag{6.59}$$

Since $\left\langle \nu_{k\ell}^{\pm\theta} \middle| \mathrm{D} \right\rangle = 1/\sqrt{2}$, it follows that the state of the quantum walk at time t is

$$|\Psi(t)\rangle = \frac{1}{\sqrt{N}} |\mathrm{D}\rangle|\mathrm{D}\rangle + \frac{1}{\sqrt{2N}} \sum_{\substack{k,\ell=0 \\ (k,\ell)\neq(0,0)}}^{\sqrt{N}-1} \left(\mathrm{e}^{\mathrm{i}\theta_{k\ell}t} \left| \nu_{k\ell}^{\theta} \right\rangle + \mathrm{e}^{-\mathrm{i}\theta_{k\ell}t} \left| \nu_{k\ell}^{-\theta} \right\rangle \right) \left| \tilde{k}, \tilde{\ell} \right\rangle, \tag{6.60}$$

where $\left| \tilde{k}, \tilde{\ell} \right\rangle$, $\theta_{k\ell}$, and $\left| \nu_{k\ell}^{\pm\theta} \right\rangle$ are given by (6.40), (6.50), and (6.53), respectively.

Exercise 6.14. Show that (6.60) reduces to (6.55) when $t = 0$.

Exercise 6.15. The goal of this exercise is to analyze the quantum walk on a finite-dimensional lattice with a *shift operator* that does not invert the coin, usually called as *moving shift operator*.

1. Obtain the shift operator analogous to (6.41) without inverting the direction of the coin.
2. Show that the matrix $\widetilde{G}$, analogous to (6.43), is

$$\widetilde{G} = \begin{bmatrix} \omega^{k} & 0 & 0 & 0 \\ 0 & \omega^{-k} & 0 & 0 \\ 0 & 0 & \omega^{\ell} & 0 \\ 0 & 0 & 0 & \omega^{-\ell} \end{bmatrix} \cdot G. \tag{6.61}$$

3. Obtain the eigenvalues and eigenvectors of this new matrix $\widetilde{G}$.
4. Use (6.55) as the initial condition. Find the state of the quantum walk $|\Psi(t)\rangle$ at time t, analogous to (6.60).

6.3 Hypercubes

The n-dimensional *hypercube* is a *regular graph* of *degree* n with $N = 2^n$ vertices. The labels of the vertices are binary n-tuples. Two vertices are *adjacent* if and only if their corresponding n-tuples differ only by one bit, that is, their *Hamming distance* is equal to 1. The edges also have labels, which specify the entry of the tuples that has different bits, that is, if two vertices differ in the ath entry, the label of the edge connecting these vertices is a. The Hilbert space associated with a quantum walk on the n-dimensional hypercube is $\mathcal{H} = \mathcal{H}^n \otimes \mathcal{H}^{2^n}$. Vectors $|a\rangle|\vec{v}\rangle$, where $1 \leq a \leq n$ and $\vec{v}$ are binary n-tuples, form the computational basis of $\mathcal{H}$. Vector $|a\rangle$ is a coin state associated with the edge of label a, specifying the direction of movement. In this section, we use vector $|1\rangle$ as the first vector of the computational basis of the coin space. Vector $|\vec{v}\rangle$ is in the computational basis of $\mathcal{H}^{2^n}$ and specifies on which vertex the walker is.

Exercise 6.16. Make a sketch of the three-dimensional hypercube (cube) and label all vertices and edges.

The *shift operator* should move the walker from state $|a\rangle|\vec{v}\rangle$ to $|a\rangle|\vec{v} \oplus \vec{e}_a\rangle$, where $\vec{e}_a$ is the binary n-tuple with all entries zero except the ath entry, the value of which is 1. Operation $\oplus$ is the *binary sum* (*bitwise xor*). This shift has the following meaning: If the coin value is a and the walker position is $\vec{v}$, the walker will move through edge a to the adjacent vertex $|\vec{v} \oplus \vec{e}_a\rangle$. The coin is unchanged after the shift, characterizing a *flip-flop shift operator* because in binary arithmetic the inverse of a is a ($a \oplus a = 0$). Then,

$$S|a\rangle|\vec{v}\rangle = |a\rangle|\vec{v} \oplus \vec{e}_a\rangle. \tag{6.62}$$

An equivalent way of writing the shift operator is

$$S = \sum_{a=1}^{n} \sum_{\vec{v}=0}^{2^n-1} |a, \vec{v} \oplus \vec{e}_a\rangle\langle a, \vec{v}|. \tag{6.63}$$

The range of variable $\vec{v}$ (in the sum) is written in base-10. For example, the notation $\vec{v} = 2^n - 1$ means $\vec{v} = (1, \ldots, 1)$. We will use the decimal notation if its meaning is clear from the context.

We use the *Grover coin*, which is

$$G = 2|\mathrm{D}\rangle\langle\mathrm{D}| - I, \tag{6.64}$$

where $|\mathrm{D}\rangle = 1/\sqrt{n}\sum_{a=1}^{n}|a\rangle$ is the *diagonal state* of the coin space. The matrix representation is

$$G = \begin{bmatrix} \frac{2}{n}-1 & \frac{2}{n} & \cdots & \frac{2}{n} \\ \frac{2}{n} & \frac{2}{n}-1 & \cdots & \frac{2}{n} \\ \vdots & \vdots & \ddots & \vdots \\ \frac{2}{n} & \frac{2}{n} & \cdots & \frac{2}{n}-1 \end{bmatrix}. \tag{6.65}$$

The entries of G are $G_{ij} = \frac{2}{n} - \delta_{ij}$. The Grover coin is invariant under permutation of directions. That is, if the labels of edges were interchanged (keeping the labels of the vertices), the Grover coin would drive the walker along the same path. This is equivalent to keep the labels and to swap the rows and columns of G corresponding to the permutation of labels. The *Grover matrix* is unchanged by simultaneous permutation of rows and columns.

The state of the walker at time t is described by

$$|\Psi(t)\rangle = \sum_{a=1}^{n}\sum_{\vec{v}=0}^{2^n-1}\psi_{a,\vec{v}}(t)|a,\vec{v}\rangle, \tag{6.66}$$

where coefficients $\psi_{a,\vec{v}}(t)$ are complex functions that obey the *normalization condition*

$$\sum_{a=1}^{n}\sum_{\vec{v}=0}^{2^n-1}\left|\psi_{a,\vec{v}}(t)\right|^2 = 1. \tag{6.67}$$

Applying the *standard evolution operator*

$$U = S\,(G \otimes I) \tag{6.68}$$

to the state at time t, we obtain

$$\begin{aligned} |\Psi(t+1)\rangle &= \sum_{b=1}^{n}\sum_{\vec{v}=0}^{2^n-1}\psi_{b,\vec{v}}(t)\,S\Big(G|b\rangle|\vec{v}\rangle\Big) \\ &= \sum_{b=1}^{n}\sum_{\vec{v}=0}^{2^n-1}\psi_{b,\vec{v}}(t)\,S\Big(\sum_{a=1}^{n}G_{ab}|a\rangle|\vec{v}\rangle\Big) \\ &= \sum_{a,b=1}^{n}\sum_{\vec{v}=0}^{2^n-1}\psi_{b,\vec{v}}(t)\,G_{ab}|a\rangle|\vec{v}\oplus\vec{e}_a\rangle. \end{aligned}$$

Renaming the dummy index $\vec{v}$ to $\vec{v}\oplus\vec{e}_a$, we obtain

$$|\Psi(t+1)\rangle = \sum_{a,b=1}^{n} \sum_{\vec{v}=0}^{2^n-1} G_{ab}\, \psi_{b,\vec{v}\oplus\vec{e}_a}(t)\, |a\rangle|\vec{v}\rangle. \tag{6.69}$$

Writing $|\Psi(t+1)\rangle$ in the computational basis and equating coefficients alike, we obtain the evolution equation

$$\psi_{a,\vec{v}}(t+1) = \sum_{b=1}^{n} G_{ab}\, \psi_{b,\vec{v}\oplus\vec{e}_a}(t). \tag{6.70}$$

This equation is too complex to be solved the way it is written. For cycles and finite two-dimensional lattices, we have learned that we can diagonalize the shift operator by taking the Fourier transform of the spatial part. This technique has allowed us to analytically solve the evolution equation. The same technique works here.

6.3.1 Fourier Transform

The spatial *Fourier transform* for the n-dimensional hypercube is given by

$$\left|\beta_{\vec{k}}\right\rangle = \frac{1}{\sqrt{2^n}} \sum_{\vec{v}=0}^{2^n-1} (-1)^{\vec{k}\cdot\vec{v}} |\vec{v}\rangle, \tag{6.71}$$

where $\vec{k}\cdot\vec{v}$ is the inner product of *binary vectors* $\vec{k}$ and $\vec{v}$. The range of variable $\vec{k}$ is the same as variable $\vec{v}$. The Fourier vectors satisfy $\left\langle\beta_{\vec{k}}\middle|\beta_{\vec{k}'}\right\rangle = \delta_{\vec{k}\vec{k}'}$. As before, the Fourier transform defines a new orthonormal basis $\left\{|a\rangle\left|\beta_{\vec{k}}\right\rangle : 1 \le a \le n, 0 \le \vec{k} \le 2^n - 1\right\}$ called the (extended) *Fourier basis*.

We show that the shift operator is diagonal in the Fourier basis, that is, $|a\rangle\left|\beta_{\vec{k}}\right\rangle$ is an eigenvector of S. In fact, using (6.71), we have

$$\begin{aligned} S|a\rangle\left|\beta_{\vec{k}}\right\rangle &= \frac{1}{\sqrt{2^n}} \sum_{\vec{v}=0}^{2^n-1} (-1)^{\vec{k}\cdot\vec{v}}\, S|a, \vec{v}\rangle \\ &= \frac{1}{\sqrt{2^n}} \sum_{\vec{v}=0}^{2^n-1} (-1)^{\vec{k}\cdot\vec{v}}\, |a, \vec{v}\oplus\vec{e}_a\rangle \\ &= \frac{1}{\sqrt{2^n}} \sum_{\vec{v}=0}^{2^n-1} (-1)^{\vec{k}\cdot(\vec{v}\oplus\vec{e}_a)}\, |a, \vec{v}\rangle \\ &= (-1)^{\vec{k}\cdot\vec{e}_a} |a\rangle\left|\beta_{\vec{k}}\right\rangle. \end{aligned} \tag{6.72}$$

The inner product $\vec{k} \cdot \vec{e}_a$ is the ath entry of $\vec{k}$, which we denote by k_a. Therefore, $(-1)^{k_a}$ is the eigenvalue associated with eigenvector $|a\rangle\left|\beta_{\vec{k}}\right\rangle$.

We have shown that S is a diagonal operator in the extended basis, but this does not imply that the evolution operator is diagonal in this basis. If the coin operator is not diagonal, the evolution operator is not diagonal either. However, we want to diagonalize the evolution operator to explicitly calculate the state of the quantum walk at an arbitrary time t.

Applying U to vector $|b\rangle\left|\beta_{\vec{k}}\right\rangle$ and using (6.72), we obtain

$$\begin{aligned} U|b\rangle\left|\beta_{\vec{k}}\right\rangle &= S\left(\sum_{a=1}^{n} G_{ab}\,|a\rangle\left|\beta_{\vec{k}}\right\rangle\right) \\ &= \sum_{a=1}^{n}(-1)^{k_a} G_{ab}\,|a\rangle\left|\beta_{\vec{k}}\right\rangle. \end{aligned} \tag{6.73}$$

In the extended Fourier basis, the entries of U are

$$\left\langle a, \beta_{\vec{k}'}\right|U\left|b, \beta_{\vec{k}}\right\rangle = (-1)^{k_a} G_{ab}\,\delta_{\vec{k}\vec{k}'}. \tag{6.74}$$

Let us define operator $\widetilde{G}$ with entries $\widetilde{G}_{ab} = (-1)^{k_a} G_{ab}$ for arbitrary vectors $\vec{k}$ and $\vec{k}'$.

The goal now is to diagonalize operator $\widetilde{G}$. Let us start with the simplest case, which is $\vec{k} = \vec{0} = (0, \ldots, 0)$. In this case, operator $\widetilde{G}$ reduces to the Grover operator G. First, note that $G^2 = I$. So, the eigenvalues are ± 1. We know that $|\mathrm{D}\rangle$ is a 1-eigenvector of G. Let us focus now on the (-1)-eigenvectors. We must look for vectors $|\alpha\rangle$ such that $(G + I)|\alpha\rangle = 0$. Using (6.65), we conclude that $G + I$ is a matrix with all entries equal to $2/n$. It follows that any vector

$$\left|\alpha_a^{\vec{0}}\right\rangle = \frac{1}{\sqrt{2}}\left(|1\rangle - |a\rangle\right), \tag{6.75}$$

where $1 < a \leq n$, is an eigenvector of G associated with eigenvalue (-1). Counting the number of vectors, it follows that set $\left\{\left|\alpha_a^{\vec{0}}\right\rangle : 1 \leq a \leq n\right\}$, where $\left|\alpha_1^{\vec{0}}\right\rangle = |\mathrm{D}\rangle$, is a nonorthogonal eigenbasis of G.

Let us calculate the spectral decomposition when $\vec{k} = (1, \ldots, 1)$. In this case, we have $\widetilde{G} = -G$ and the (-1)-eigenvectors of G are $(+1)$-eigenvectors of $\widetilde{G}$ and vice versa. In summary, eigenvectors

$$\left|\alpha_a^{\vec{1}}\right\rangle = \frac{1}{\sqrt{2}}\left(|a\rangle - |n\rangle\right), \tag{6.76}$$

where $1 \leq a \leq n - 1$, are associated with eigenvalue $(+1)$ and $\left|\alpha_n^{\vec{1}}\right\rangle = |\mathrm{D}\rangle$ is associated with eigenvalue (-1).

Now let us consider a vector $\vec{k}$ with *Hamming weight* $0 < k < n$, that is, with k entries equal to 1 and $(n-k)$ equal to 0. Matrix $\widetilde{G}$ is obtained from G by inverting the signs of the rows corresponding to the entries of $\vec{k}$ that are equal to 1. Therefore, k rows of $\widetilde{G}$ invert signs compared to G. To find the (± 1)-eigenvectors, we split the Hilbert space as a sum of two vector spaces, the first associated with the rows that have not inverted the sign and the second associated with the rows that have inverted the sign. By permutating rows and columns, matrix $\widetilde{G}$ assumes the following form:

$$\widetilde{G} = \left[\begin{array}{ccc|ccc} \frac{2}{n}-1 & \frac{2}{n} & \cdots & & & \\ \frac{2}{n} & \frac{2}{n}-1 & & & \frac{2}{n} & \\ \vdots & & \ddots & & & \\ \hline & & & -\frac{2}{n}+1 & -\frac{2}{n} & \cdots \\ & -\frac{2}{n} & & -\frac{2}{n} & -\frac{2}{n}+1 & \\ & & & \vdots & & \ddots \end{array}\right], \tag{6.77}$$

where the first diagonal block is a $(n-k)$-square matrix and the second block is a k-square matrix. To find the 1-eigenvectors, we look for vectors $|\alpha\rangle$ such that $(\widetilde{G} - I)|\alpha\rangle = 0$. Note that

$$\widetilde{G} - I = \left[\begin{array}{ccc|c} \frac{2}{n}-2 & \frac{2}{n} & \cdots & \\ \frac{2}{n} & \frac{2}{n}-2 & & \frac{2}{n} \\ \vdots & & \ddots & \\ \hline & -\frac{2}{n} & & -\frac{2}{n} \end{array}\right]. \tag{6.78}$$

Therefore, vector[1] $|\alpha\rangle = (0, \ldots, 0 \mid 1, -1, 0, \ldots, 0)/\sqrt{2}$ is a 1-eigenvector. Vector $|\alpha\rangle$ has zero entries except at two positions corresponding to sign-inverted rows, the first position with $(+1)$ and the second with (-1). We can build $k-1$ vectors in this way. Following the same method, but using $(\widetilde{G} + I)$, we can find $(n-k-1)$ (-1)-eigenvectors with zero entries except for two positions corresponding to rows that have not inverted sign, with $(+1)$ and (-1). The total number of eigenvectors found so far is $(k-1) + (n-k-1) = n-2$ with eigenvalues (± 1). Therefore, it is missing two eigenvectors associated with the complex nonreal eigenvalues.

[1]The vertical bar separates the first $(n-k)$ entries from the last k entries.

The remaining two eigenvectors can be found as follows: If a matrix has the property that the sum of the entries of a row is invariant for all rows, a vector with entries equal to some number a is an eigenvector. In the case of matrix $\widetilde{G}$, this property is valid for blocks of size $(n-k)$ and k. Therefore, the form of the eigenvector should be $|\alpha\rangle = (a, \ldots, a \mid b, \ldots, b)$, that is, the first $(n-k)$ entries must have some a, and the k remaining entries must have some b. Without loss of generality, we take $b = 1$. Let $\mathrm{e}^{\mathrm{i}\omega_k}$ be the corresponding eigenvalue. Note that the eigenvalue depends on k (the Hamming weight of $\vec{k}$), but it does not depend explicitly on $\vec{k}$. We solve the matrix equation

$$\left[\begin{array}{ccc|ccc} \frac{2}{n} - 1 - \mathrm{e}^{\mathrm{i}\omega_k} & \frac{2}{n} & \cdots & & & \\ \frac{2}{n} & \frac{2}{n} - 1 - \mathrm{e}^{\mathrm{i}\omega_k} & & & \frac{2}{n} & \\ \vdots & & \ddots & & & \\ \hline & & & -\frac{2}{n} + 1 - \mathrm{e}^{\mathrm{i}\omega_k} & -\frac{2}{n} & \cdots \\ & -\frac{2}{n} & & -\frac{2}{n} + 1 - \mathrm{e}^{\mathrm{i}\omega_k} & -\frac{2}{n} & \\ & & & \vdots & & \ddots \end{array}\right] \left[\begin{array}{c} a \\ \vdots \\ a \\ \hline 1 \\ \vdots \\ 1 \end{array}\right] = 0,$$

which reduces to

$$\begin{cases} \left(1 - \frac{2k}{n} - \mathrm{e}^{\mathrm{i}\omega_k}\right) a + \frac{2k}{n} = 0, \\ -2\left(1 - \frac{k}{n}\right) a + 1 - \frac{2k}{n} - \mathrm{e}^{\mathrm{i}\omega_k} = 0. \end{cases} \tag{6.79}$$

Solving this system of equations, we obtain

$$\begin{cases} a = \pm \mathrm{i} \frac{\sqrt{\frac{k}{n}}}{\sqrt{1 - \frac{k}{n}}}, \\ \mathrm{e}^{\mathrm{i}\omega_k} = 1 - \frac{2k}{n} \mp 2\mathrm{i}\sqrt{\frac{k}{n}\left(1 - \frac{k}{n}\right)}. \end{cases} \tag{6.80}$$

Then,

$$\begin{cases} \cos\omega_k = 1 - \frac{2k}{n}, \\ \sin\omega_k = \mp 2\sqrt{\frac{k}{n}\left(1 - \frac{k}{n}\right)}. \end{cases} \tag{6.81}$$

Normalizing, the eigenvector associated with eigenvalue $\mathrm{e}^{\mathrm{i}\omega_k}$ is written as

$$\left|\tilde{\alpha}_1^{\vec{k}}\right\rangle = \frac{1}{\sqrt{2}} \begin{bmatrix} \frac{-\mathrm{i}}{\sqrt{n-k}} \\ \vdots \\ \frac{-\mathrm{i}}{\sqrt{n-k}} \\ \hline \frac{1}{\sqrt{k}} \\ \vdots \\ \frac{1}{\sqrt{k}} \end{bmatrix}, \tag{6.82}$$

and eigenvector $\left|\tilde{\alpha}_n^{\vec{k}}\right\rangle$ associated with eigenvalue $\mathrm{e}^{-\mathrm{i}\omega_k}$ is the complex conjugate of vector $\left|\tilde{\alpha}_1^{\vec{k}}\right\rangle$.

These eigenvectors were described by separating the rows that inverted sign from the rows that have remained unchanged. We must permute the entries of the eigenvectors to match the rows in their original positions. The variable that points out which rows have inverted sign is $\vec{k}$. If entry k_a is zero, it means that there was no sign inversion in the ath row, and if $k_a = 1$, then there was an inversion. The eigenvectors $\left|\tilde{\alpha}_1^{\vec{k}}\right\rangle$ and $\left|\tilde{\alpha}_n^{\vec{k}}\right\rangle$ associated with eigenvalues $\mathrm{e}^{\pm\mathrm{i}\omega_k}$ are written in the original basis as

$$\left|\tilde{\alpha}_1^{\vec{k}}\right\rangle = \frac{1}{\sqrt{2}} \sum_{a=1}^{n} \left(\frac{k_a}{\sqrt{k}} - \mathrm{i}\frac{1-k_a}{\sqrt{n-k}} \right) |a\rangle, \tag{6.83}$$

$$\left|\tilde{\alpha}_n^{\vec{k}}\right\rangle = \frac{1}{\sqrt{2}} \sum_{a=1}^{n} \left(\frac{k_a}{\sqrt{k}} + \mathrm{i}\frac{1-k_a}{\sqrt{n-k}} \right) |a\rangle, \tag{6.84}$$

for $0 < k < n$.

We now redefine eigenvectors $\left|\tilde{\alpha}_1^{\vec{k}}\right\rangle$ and $\left|\tilde{\alpha}_n^{\vec{k}}\right\rangle$ in order to change a global phase. Using (6.83) and (6.84), we have

$$\left\langle \mathrm{D} \middle| \tilde{\alpha}_1^{\vec{k}} \right\rangle = \frac{1}{\sqrt{2}} \left(\sqrt{\frac{k}{n}} - \mathrm{i}\sqrt{1-\frac{k}{n}} \right), \tag{6.85}$$

$$\left\langle \mathrm{D} \middle| \tilde{\alpha}_n^{\vec{k}} \right\rangle = \frac{1}{\sqrt{2}} \left(\sqrt{\frac{k}{n}} + \mathrm{i}\sqrt{1-\frac{k}{n}} \right). \tag{6.86}$$

From now on we use the eigenvectors

$$\left|\alpha_1^{\vec{k}}\right\rangle = \frac{\mathrm{e}^{\mathrm{i}\theta}}{\sqrt{2}} \sum_{a=1}^{n} \left(\frac{k_a}{\sqrt{k}} - \mathrm{i}\frac{1-k_a}{\sqrt{n-k}} \right) |a\rangle, \tag{6.87}$$

Table 6.1 Eigenvalues and eigenvectors of U for the hypercube, where ω_k is given by Eq. (6.82) and c_a is the coefficient of $|a\rangle$ in Eq. (6.87)

Hamming wgt	Eigenval	Eigenvec $\otimes\left\|\beta_{\vec{k}}\right\rangle$	Index a'	Multiplicity
$\|k\| = 0$	-1	$(\|0\rangle - \left\|a'\right\rangle)/\sqrt{2}$	$a' \in [1, n-1]$	$n-1$
	1	$\sum_{a=0}^{n-1} \|a\rangle/\sqrt{n}$	n	1
$1 \le \|k\| < n$	-1	$(\|0\rangle - \left\|a'\right\rangle)/\sqrt{2}$	$a' \in [1, n-\|k\|-1]$	$n-\|k\|-1$
	1	$\frac{(\|n-\|k\|\rangle - \|a'+1\rangle)}{\sqrt{2}}$	$a' \in [n-\|k\|, n-2]$	$\|k\|-1$
	$\mathrm{e}^{\mathrm{i}\,\omega_k}$	$\sum_{a=0}^{n-1} c_a \|a\rangle$	n	1
	$\mathrm{e}^{-\mathrm{i}\,\omega_k}$	$\sum_{a=0}^{n-1} c_a^* \|a\rangle$	$n-1$	1
$\|k\| = n$	1	$(\|0\rangle - \left\|a'\right\rangle)/\sqrt{2}$	$a' \in [1, n-1]$	$n-1$
	-1	$\sum_{a=0}^{n-1} \|a\rangle/\sqrt{n}$	n	1

$$\left|\alpha_n^{\vec{k}}\right\rangle = \frac{\mathrm{e}^{-\mathrm{i}\theta}}{\sqrt{2}} \sum_{a=1}^{n} \left(\frac{k_a}{\sqrt{k}} + \mathrm{i}\frac{1-k_a}{\sqrt{n-k}} \right) |a\rangle, \tag{6.88}$$

for $0 < k < n$, where $\cos\theta = \sqrt{k/n}$ and $k_a = \vec{k} \cdot \vec{e}_a$ is the ath entry of $\vec{k}$. For $0 < k < n$, we have

$$\left\langle \mathrm{D} \middle| \alpha_1^{\vec{k}} \right\rangle = \left\langle \mathrm{D} \middle| \alpha_n^{\vec{k}} \right\rangle = \frac{1}{\sqrt{2}}. \tag{6.89}$$

We conclude that set $\left\{ \left|\alpha_a^{\vec{k}}\right\rangle \left|\beta_{\vec{k}}\right\rangle : 1 \le a \le n, 0 \le \vec{k} \le 2^n - 1 \right\}$ is a nonorthogonal eigenbasis of U. The eigenvalues are ± 1 and $\mathrm{e}^{\pm \mathrm{i}\omega_k}$. Vectors $\left|\alpha_a^{\vec{k}}\right\rangle$ in the computational basis are given by (6.75), (6.76) for $k = 0$ and $k = n$; and $\left|\alpha_1^{\vec{0}}\right\rangle = \left|\alpha_n^{\vec{1}}\right\rangle = |\mathrm{D}\rangle$ are particular cases. For $0 < k < n$, $a = 1$ or $a = n$, $\left|\alpha_a^{\vec{k}}\right\rangle$ are given by (6.87) and (6.88). Vectors $\left|\beta_{\vec{k}}\right\rangle$ are given by (6.71). Table 6.1 compiles the list of eigenvalues and eigenvectors.

Exercise 6.17. Show the following properties of the Fourier transform:

1. $\left|\beta_{\vec{0}}\right\rangle$ is the diagonal state of Hilbert space $\mathcal{H}^{2^n}$.
2. $\left\{ \left|\beta_{\vec{k}}\right\rangle : 0 \le \vec{k} \le 2^n - 1 \right\}$ is an orthonormal basis for the Hilbert space $\mathcal{H}^{2^n}$.
3. $\left|\vec{0}\right\rangle = \frac{1}{\sqrt{2^n}} \sum_{\vec{k}=0}^{2^n-1} \left|\beta_{\vec{k}}\right\rangle$.

Exercise 6.18. Show that the eigenvectors of (6.87) and (6.88) are unit vectors.

Exercise 6.19. Show explicitly that $\left\{\left|\alpha_1^{\vec{k}}\right\rangle\left|\beta_{\vec{k}}\right\rangle, \left|\alpha_n^{\vec{k}}\right\rangle\left|\beta_{\vec{k}}\right\rangle : 1 \leq \vec{k} \leq 2^n - 2\right\}$ together with $|\mathrm{D}\rangle\left|\beta_{\vec{0}}\right\rangle$ and $|\mathrm{D}\rangle\left|\beta_{\vec{1}}\right\rangle$ is an orthonormal eigenbasis of U with eigenvalues $\mathrm{e}^{\pm \mathrm{i}\omega_k}$, 1, and (-1), respectively, for the eigenspace orthogonal to $|\mathrm{D}\rangle\left|\vec{0}\right\rangle$.

Exercise 6.20. Obtain explicit expressions for eigenvectors $\left|\alpha_a^{\vec{k}}\right\rangle$ when $0 < k < n$ and $0 < a < n$ associated with eigenvalues $\mathrm{e}^{\pm \mathrm{i}\omega_k}$.

6.3.2 Analytic Solutions

Now we calculate the state of the quantum walk at an arbitrary time step. Let us use state

$$|\Psi(0)\rangle = |\mathrm{D}\rangle\left|\vec{0}\right\rangle, \tag{6.90}$$

as initial condition, that is, initially the walker is located at vertex $\vec{v} = \vec{0}$ with the *diagonal state* in the *coin space*. This initial condition is invariant under permutation of edges. Suppose that $\phi_{a,\vec{k}}$ is an eigenvalue associated with eigenvector $\left|\phi_{a,\vec{k}}\right\rangle$ and suppose that the set of eigenvectors $\left|\phi_{a,\vec{k}}\right\rangle$ is an orthonormal basis. Using the *spectral decomposition* of U, we have

$$U = \sum_{a,\vec{k}} \phi_{a,\vec{k}} \left|\phi_{a,\vec{k}}\right\rangle\left\langle\phi_{a,\vec{k}}\right|. \tag{6.91}$$

At time t, the state of the quantum walk will be given by

$$\begin{aligned} |\Psi(t)\rangle &= U^t|\Psi(0)\rangle \\ &= \sum_{a,\vec{k}} \phi_{a,\vec{k}}^t \left\langle\phi_{a,\vec{k}}\middle|\Psi(0)\right\rangle \left|\phi_{a,\vec{k}}\right\rangle. \end{aligned} \tag{6.92}$$

The eigenvectors of U that have nonzero overlap with $|\Psi(0)\rangle$ are $\left|\alpha_1^{\vec{k}}\right\rangle\left|\beta_{\vec{k}}\right\rangle$ for $0 \leq \vec{k} < 2^n - 1$, where $\left|\alpha_1^{\vec{0}}\right\rangle = |\mathrm{D}\rangle$, which have eigenvalues $\mathrm{e}^{\mathrm{i}\omega_k}$, and $\left|\alpha_n^{\vec{k}}\right\rangle\left|\beta_{\vec{k}}\right\rangle$ for $0 < \vec{k} \leq 2^n - 1$, where $\left|\alpha_n^{\vec{1}}\right\rangle = |\mathrm{D}\rangle$, which have eigenvalues $\mathrm{e}^{-\mathrm{i}\omega_k}$. The set of those eigenvectors is an orthonormal basis for the eigenspace orthogonal to $|\Psi(0)\rangle$ (Exercise 6.19). Then, (6.92) reduces to

$$\begin{aligned} |\Psi(t)\rangle = &\sum_{\vec{k}=0}^{2^n-2} (\mathrm{e}^{\mathrm{i}\omega_k})^t \left\langle\alpha_1^{\vec{k}}\middle|\mathrm{D}\right\rangle\left\langle\beta_{\vec{k}}\middle|\vec{0}\right\rangle \left|\alpha_1^{\vec{k}}\right\rangle\left|\beta_{\vec{k}}\right\rangle + \\ &\sum_{\vec{k}=1}^{2^n-1} (\mathrm{e}^{-\mathrm{i}\omega_k})^t \left\langle\alpha_n^{\vec{k}}\middle|\mathrm{D}\right\rangle\left\langle\beta_{\vec{k}}\middle|\vec{0}\right\rangle \left|\alpha_n^{\vec{k}}\right\rangle\left|\beta_{\vec{k}}\right\rangle. \end{aligned} \tag{6.93}$$

Using (6.71), we have $\left\langle \beta_{\vec{k}} \middle| \vec{0} \right\rangle = 1/\sqrt{2^n}$. Using that $\left| \alpha_1^{\vec{0}} \right\rangle = |\mathrm{D}\rangle$ (1-eigenvector), $\left| \alpha_n^{\vec{1}} \right\rangle = |\mathrm{D}\rangle$ ((−1)-eigenvector), and Eqs. (6.89), the state of the quantum walk on the n-dimensional hypercube at time t is

$$\begin{aligned} |\Psi(t)\rangle = & \frac{1}{\sqrt{2^n}} \Big(|\mathrm{D}\rangle \left| \beta_{\vec{0}} \right\rangle + (-1)^t |\mathrm{D}\rangle \left| \beta_{\vec{1}} \right\rangle \Big) \\ & + \frac{1}{\sqrt{2^{n+1}}} \sum_{\vec{k}=1}^{2^n-2} \mathrm{e}^{\mathrm{i}\omega_k t} \left| \alpha_1^{\vec{k}} \right\rangle \left| \beta_{\vec{k}} \right\rangle \\ & + \frac{1}{\sqrt{2^{n+1}}} \sum_{\vec{k}=1}^{2^n-2} \mathrm{e}^{-\mathrm{i}\omega_k t} \left| \alpha_n^{\vec{k}} \right\rangle \left| \beta_{\vec{k}} \right\rangle. \end{aligned} \tag{6.94}$$

It is remarkable that we obtain an analytic expression for the quantum state at any time. This result allows us to obtain several other results such as the *limiting distribution* and the *mixing time* on the hypercube. The analytic result was obtained because we have used the Fourier transform. Note that only the eigenvectors that are nonorthogonal to $|\mathrm{D}\rangle \otimes I$ are used to obtain the expression of $|\Psi(t)\rangle$. This fact depends on the choice of initial condition. If the initial condition is in a subspace spanned by some eigenvectors of U, the state will remain in this subspace during the evolution. In the case of $|\Psi(t)\rangle$, the dimension of the subspace is $2^{n+1} - 2$ and is spanned by the orthonormal basis $\left\{ \left| \alpha_1^{\vec{k}} \right\rangle \left| \beta_{\vec{k}} \right\rangle : 0 \leq \vec{k} < 2^n - 1, \left| \alpha_n^{\vec{k}} \right\rangle \left| \beta_{\vec{k}} \right\rangle : 0 < \vec{k} \leq 2^n - 1 \right\}$. We will show in the next section that the evolution of the quantum walk with initial condition $|\mathrm{D}\rangle \left| \vec{0} \right\rangle$ uses a much smaller subspace.

6.3.3 Reducing a Hypercube to a Line Segment

Note the walker starts on vertex $\vec{0}$ and its coin state is the diagonal state. After the first step, the state is

$$\begin{aligned} |\Psi(1)\rangle &= S(G \otimes I) |\mathrm{D}\rangle \left| \vec{0} \right\rangle \\ &= \frac{1}{\sqrt{n}} \sum_{a=1}^{n} |a\rangle |\vec{e}_a\rangle \\ &= \frac{1}{\sqrt{n}} \Big(|1\rangle |1, 0, \ldots, 0\rangle + \cdots + |n\rangle |0, \ldots, 0, 1\rangle \Big). \end{aligned} \tag{6.95}$$

The quantum walk is described by a state that has the same amplitude for the vertices with the same *Hamming weight*. Since the *Grover coin* is not biased, it is interesting to ask whether this property will remain the same in the next steps. Applying U to $|\Psi(1)\rangle$, we obtain

$$|\Psi(2)\rangle = \frac{2-n}{n}|\mathrm{D}\rangle\left|\vec{0}\right\rangle + \frac{2}{n\sqrt{n}} \sum_{\substack{a,\,b=1\\ a\neq b}}^{n} |a\rangle|\vec{e}_a \oplus \vec{e}_b\rangle. \tag{6.96}$$

The terms with Hamming weight equal to zero have coefficient $(2-n)/n$. The terms with Hamming weight 2 have coefficient $2/n\sqrt{n}$. Again, the amplitudes are equal for the vertices with the same Hamming weight. However, in the next step we obtain

$$\begin{aligned}|\Psi(3)\rangle = {} & \frac{2-n}{n\sqrt{n}}\sum_{a=1}^{n}|a\rangle|\vec{e}_a\rangle + \frac{2(4-n)}{n^2\sqrt{n}} \sum_{\substack{a,\,b=1\\ a\neq b}}^{n} |a\rangle|\vec{e}_b\rangle \\ & + \frac{4}{n^2\sqrt{n}} \sum_{\substack{a,\,b,\,c=1\\ a\neq b\neq c\neq a}}^{n} |c\rangle|\vec{e}_a \oplus \vec{e}_b \oplus \vec{e}_c\rangle.\end{aligned} \tag{6.97}$$

The terms with Hamming weight 3 have coefficient $4/n^2\sqrt{n}$, and the terms with Hamming weight 1 are divided into two blocks, the first with coefficient $(2-n)/n\sqrt{n}$ corresponding to terms with vertices that satisfy $v_a = 1$ and with coefficient $2(4-n)/n^2\sqrt{n}$ corresponding to terms that satisfy $v_a = 0$. Since the n-dimensional hypercube and the evolution operator are symmetric under permutation of edges, it is interesting to ask again if the amplitudes corresponding to vertices $|a\rangle|\vec{v}\rangle$ with the same Hamming weight belonging to the block $v_a = 0$ will remain equal to each other in the next steps and the same regarding the amplitudes corresponding to the terms belonging to the block $v_a = 1$.

A formal way of showing that $|\Psi(t)\rangle$ has the symmetry above described is to consider the following permutation operation: A vector in the computational basis has the form $|a\rangle|v_1, \ldots, v_n\rangle$, where $1 \leq a \leq n$, and $\vec{v} = (v_1, \ldots, v_n)$ is a binary vector. The permutation of i and j is defined as follows: It converts vector $|a\rangle\left|v_1, \ldots, v_i, \ldots, v_j, \ldots, v_n\right\rangle$ into vector $|a\rangle\left|v_1, \ldots, v_j, \ldots, v_i, \ldots, v_n\right\rangle$ and vice versa if $a \neq i$ and $a \neq j$. If a is equal to i or j, a should also be permuted. If $|\Psi(t)\rangle$ is invariant under such a permutation for all i and j, then the coefficients in block $v_a = 0$ are equal and the same is true for the coefficients in block $v_a = 1$. Vice versa: If the coefficients are equal, $|\Psi(t)\rangle$ is invariant under such permutations for all i and j. In other words, this kind of permutation preserves the blocks, that is, a vector of a block does not move to another block and vice versa. Take, for example, these two states for $n = 2$:

$$|\psi\rangle = \frac{1}{\sqrt{2}}\big(|1\rangle|1, 0\rangle + |2\rangle|0, 1\rangle\big),$$
$$|\phi\rangle = \frac{1}{\sqrt{2}}\big(|1\rangle|0, 1\rangle + |1\rangle|1, 0\rangle\big).$$

State $|\psi\rangle$ is invariant. On the other hand, $|\phi\rangle$ is not invariant since the permutation of 1 and 2 converts $|\phi\rangle$ into $\big(|2\rangle|1,0\rangle + |2\rangle|0,1\rangle\big)/\sqrt{2}$.

Let us define a basis of invariant vectors under those permutations. This basis will span an invariant subspace $\mathcal{H}_{\text{inv}} \subset \mathcal{H}$. The basis of $\mathcal{H}_{\text{inv}}$ is obtained as follows: Select an arbitrary vector in the computational basis of Hilbert space $\mathcal{H}$, for example, vector $|1\rangle|1,0,0\rangle$, which is associated with a three-dimensional hypercube. Apply all allowed permutations to $|1\rangle|1,0,0\rangle$. The resulting set is $\big\{|1\rangle|1,0,0\rangle, |2\rangle|0,1,0\rangle$ $|3\rangle|0,0,1\rangle\big\}$. Add up all these vectors and normalize. The result is

$$|\lambda_1\rangle = \frac{1}{\sqrt{3}}\big(|1\rangle|1,0,0\rangle + |2\rangle|0,1,0\rangle + |3\rangle|0,0,1\rangle\big). \tag{6.98}$$

By construction, vector $|\lambda_1\rangle$ is invariant under the permutation operation. Now select another vector in the computational basis of $\mathcal{H}$ that is not in the previous set and repeat the process over and over until you have exhausted all possibilities. The resulting set is an invariant basis of $\mathcal{H}_{\text{inv}}$. This basis has vectors $|\rho_0\rangle, \ldots, |\rho_{n-1}\rangle$ and vectors $|\lambda_1\rangle$, $\ldots, |\lambda_n\rangle$, defined by

$$|\rho_v\rangle = \frac{1}{\sqrt{(n-v)\binom{n}{v}}} \sum_{\substack{a,\,\vec{v} \\ |\vec{v}| = v \\ v_a = 0}} |a,\vec{v}\rangle, \tag{6.99}$$

$$|\lambda_v\rangle = \frac{1}{\sqrt{v\binom{n}{v}}} \sum_{\substack{a,\,\vec{v} \\ |\vec{v}| = v \\ v_a = 1}} |a,\vec{v}\rangle, \tag{6.100}$$

where the sum runs over the vertices of the same Hamming weight v with the following constraint: $|a,\vec{v}\rangle$ is in $|\rho_v\rangle$ if ath entry of $\vec{v}$ is 0, otherwise it is in $|\lambda_v\rangle$. As usual, $\binom{n}{v}$ is the binomial expression $n!/(n-v)!v!$. The basis described by (6.99) and (6.100) is orthonormal and has $2n$ elements, which shows that the dimension of $\mathcal{H}_{\text{inv}}$ is $2n$.

Exercise 6.21. Obtain expressions (6.96) and (6.97) by applying $U = S(G \otimes I)$ to $|\Psi(1)\rangle$.

Exercise 6.22. Obtain all vectors invariant under permutation in a three-dimensional hypercube following the method used to obtain (6.98). Divide the set of vectors into two blocks: *right* and *left*. Vectors $|a\rangle|\vec{v}\rangle$ in block *right* have the property $v_a = 0$, and vectors in block *left* have the property $v_a = 1$. The names of the vectors should use ρ for vectors in block *right*, λ in block *left*, and the Hamming weight of the vertices v as a subindex. Verify the results of this process with vectors of (6.99) and (6.100).

Exercise 6.23. Show that:

1. $|\rho_0\rangle = |\mathrm{D}\rangle\left|\vec{0}\right\rangle$.
2. $|\lambda_n\rangle = |\mathrm{D}\rangle\left|\vec{1}\right\rangle$.
3. Vectors $|\rho_v\rangle$, $0 \leq v \leq n-1$, and $|\lambda_v\rangle$, $1 \leq v \leq n$ are orthonormal.

The initial condition $|\mathrm{D}\rangle\left|\vec{0}\right\rangle$ is in the vector space spanned by $|\rho_v\rangle$ and $|\lambda_v\rangle$ because $|\mathrm{D}\rangle\left|\vec{0}\right\rangle$ is equal to $|\rho_0\rangle$. One way to show that the state of the quantum walk remains on the space spanned by $|\rho_v\rangle$ and $|\lambda_v\rangle$ during the evolution is to show that the *evolution operator* can be written only in terms of $|\rho_v\rangle$ and $|\lambda_v\rangle$. First, we show that the shift operator can be written in this basis. Let us calculate the action of S on vector $|\rho_v\rangle$. Using (6.99), we have

$$\begin{aligned} S|\rho_v\rangle &= \frac{1}{\sqrt{(n-v)\binom{n}{v}}} \sum_{\substack{a,\,\vec{v} \\ |\vec{v}| = v \\ v_a = 0}} S|a,\vec{v}\rangle \\ &= \frac{1}{\sqrt{(n-v)\binom{n}{v}}} \sum_{\substack{a,\,\vec{v} \\ |\vec{v}| = v+1 \\ v_a = 1}} |a,\vec{v}\rangle \end{aligned}$$

Note that the action of S on $|a,\vec{v}\rangle$ replaces ath entry of $\vec{v}$ from 0 to 1. Therefore, the Hamming weight of this vertex increases one unit. Using the binomial expression, we show that $(n-v)\binom{n}{v} = (v+1)\binom{n}{v+1}$. Using this equation, we obtain

$$\begin{aligned} S|\rho_v\rangle &= \frac{1}{\sqrt{(v+1)\binom{n}{v+1}}} \sum_{\substack{a,\,\vec{v} \\ |\vec{v}| = v+1 \\ v_a = 1}} |a,\vec{v}\rangle \\ &= |\lambda_{v+1}\rangle. \end{aligned} \tag{6.101}$$

Similarly, we obtain

$$S|\lambda_v\rangle = |\rho_{v-1}\rangle. \tag{6.102}$$

Therefore, the shift operator can be written as

$$S = \sum_{v=0}^{n-1} |\lambda_{v+1}\rangle\langle\rho_v| + \sum_{v=1}^{n} |\rho_{v-1}\rangle\langle\lambda_v|. \tag{6.103}$$

The physical interpretation of the shift operator shows that the quantum walk takes place in the one-dimensional lattice with $n+1$ vertices, with the position being specified by v. The *chirality* is specified by ρ and λ and determines the direction of

the movement. Operator S shifts $|\rho_v\rangle$ rightward and inverts the chirality; and S shifts $|\lambda_v\rangle$ leftward and inverts the chirality. The boundary conditions are reflective since at $v = 0$ the walker has no overlap with $|\lambda_0\rangle$ and at $v = n$ it has no overlap with $|\rho_n\rangle$.

The coin operator can also be expressed in terms of basis $|\rho_v\rangle$ and $|\lambda_v\rangle$. Actually, the following results are valid:

$$G \otimes I\, |\rho_v\rangle = \cos\omega_v |\rho_v\rangle + \sin\omega_v |\lambda_v\rangle, \tag{6.104}$$

$$G \otimes I\, |\lambda_v\rangle = \sin\omega_v |\rho_v\rangle - \cos\omega_v |\lambda_v\rangle, \tag{6.105}$$

where

$$\cos\omega_v = 1 - \frac{2v}{n}, \tag{6.106}$$

$$\sin\omega_v = 2\sqrt{\frac{v}{n}\left(1 - \frac{v}{n}\right)}. \tag{6.107}$$

The proof of this result is oriented in Exercise 6.25. Equations (6.104) and (6.105) show that the action of the coin operator on the quantum walk on the one-dimensional finite lattice is a rotation through angle ω_v, which depends on point v. This is different from the standard quantum walk.

Exercise 6.24. Show that (6.102) is true.

Exercise 6.25. The goal of this exercise is to prove that the action of the Grover coin on basis $|\rho_v\rangle$ and $|\lambda_v\rangle$ is the one described in (6.104) and (6.105).

Show that

$$\sum_{\substack{a,\,\vec{v} \\ |\vec{v}| = v_0 \\ v_a = 0}} \left\langle \mathrm{D}, \vec{v}' \middle| a, \vec{v} \right\rangle = \frac{(n - v_0)}{\sqrt{n}} \delta_{v_0\, v'}.$$

[Hint: Show that if $|\vec{v}'| \neq v_0$, the result is zero. Fix a transposed vector $\left\langle \mathrm{D}, \vec{v}' \right|$ with $|\vec{v}'| = v_0$ and expand the sum. There are $(n - v_0)$ values of a satisfying $v_a = 0$ and $|\vec{v}\rangle = \left|\vec{v}'\right\rangle$. The $\sqrt{n}$ in the denominator comes from $\langle \mathrm{D}|a\rangle$.] Use this result to show that

$$\left\langle \mathrm{D}, \vec{v}' \middle| \rho_v \right\rangle = \sqrt{\frac{n - v}{n\binom{n}{v}}}\, \delta_{vv'}.$$

Show also that

$$|\mathrm{D}\rangle \sum_{|\vec{v}| = v} |\vec{v}\rangle = \sqrt{\frac{n - v}{n}\binom{n}{v}} |\rho_v\rangle + \sqrt{\frac{v}{n}\binom{n}{v}} |\lambda_v\rangle.$$

Use expressions $G = 2|\mathrm{D}\rangle\langle\mathrm{D}| - I_n$ and $I_{2^n} = \sum_{\vec{v}'} \left|\vec{v}'\right\rangle\left\langle\vec{v}'\right|$ to calculate $G \otimes I_{2^n}|\rho_v\rangle$ and compare the result with (6.104). Use the previous identities.

Using a similar procedure, show that (6.105) is true.

Exercise 6.26. From (6.104) and (6.105), obtain an expression for $G \otimes I$. Can this expression be factored out in $\mathcal{H}_{\mathrm{inv}}$? Define the computational basis of $\mathcal{H}_{\mathrm{inv}}$ as $\big\{|0, v\rangle, |1, v\rangle, 0 \le v \le n\big\}$, where $\{|0\rangle, |1\rangle\} \in \mathcal{H}^2$ and $|v\rangle \in \mathcal{H}^n$ such that $|0, v\rangle = |\rho_v\rangle$, $|1, v\rangle = |\lambda_v\rangle$. Obtain operator $C_v \in \mathcal{H}^2$ such that the coin operator has the form $\sum_{v=0}^{n} C_v \otimes |v\rangle\langle v|$. Give a physical interpretation for the action of the coin operator on this expression.

Using (6.103)–(6.105), we obtain the following expression for the evolution operator in basis $|\rho_v\rangle$ and $|\lambda_v\rangle$:

$$\begin{aligned} U &= S(G \otimes I) \\ &= \sum_{v=0}^{n-1} -\cos\omega_{v+1}|\rho_v\rangle\langle\lambda_{v+1}| + \sin\omega_{v+1}|\rho_v\rangle\langle\rho_{v+1}| \\ &\quad + \sum_{v=1}^{n} \sin\omega_{v-1}|\lambda_v\rangle\langle\lambda_{v-1}| + \cos\omega_{v-1}|\lambda_v\rangle\langle\rho_{v-1}|. \end{aligned} \tag{6.108}$$

Therefore, $\mathcal{H}_{\mathrm{inv}}$ is an invariant subspace under the action of U. Since the initial condition $|\rho_0\rangle = |\mathrm{D}\rangle\left|\vec{0}\right\rangle$ belongs to $\mathcal{H}_{\mathrm{inv}}$, the state of the quantum walk $|\Psi(t)\rangle$ will be in $\mathcal{H}_{\mathrm{inv}}$ during the evolution. The orthonormal basis $|\rho_v\rangle$, $|\lambda_v\rangle$ allows us to interpret physically the quantum walk on a hypercube as a quantum walk on the points of a finite line. From the state vector on the line, we can recover the state vector on the hypercube. However, the basis $|\rho_v\rangle$, $|\lambda_v\rangle$ is not the best one to obtain the evolution of the quantum walk because $|\rho_v\rangle$ and $|\lambda_v\rangle$ are not eigenvectors of the *reduced evolution operator*.

The strategy now is to find the spectral decomposition of U on $\mathcal{H}_{\mathrm{inv}}$. The goal is to find $(2n)$ linearly independent eigenvectors of U that are in the reduced space $\mathcal{H}_{\mathrm{inv}}$. We know that $\left\{\left|\alpha_1^{\vec{k}}\right\rangle\left|\beta_{\vec{k}}\right\rangle, \left|\alpha_n^{\vec{k}}\right\rangle\left|\beta_{\vec{k}}\right\rangle : 0 < \vec{k} \le 2^n - 1\right\}$ is an eigenbasis of U for a subspace where the quantum walk takes place. The associated eigenvalues are $\left\{\mathrm{e}^{\mathrm{i}\omega_k}, \mathrm{e}^{-\mathrm{i}\omega_k}\right\}$, where ω_k satisfies

$$\cos\omega_k = 1 - \frac{2k}{n}.$$

Eigenvectors $|\mathrm{D}\rangle\left|\beta_{\vec{0}}\right\rangle$ and $|\mathrm{D}\rangle\left|\beta_{\vec{1}}\right\rangle$ are in the space spanned by $|\lambda_v\rangle$ and $|\rho_v\rangle$ (see Exercises 6.27 and 6.28). However, the remaining eigenvectors are not. For example, $\left|\alpha_1^{\vec{k}}\right\rangle\left|\beta_{\vec{k}}\right\rangle$ explicitly depends on $\vec{k}$ and is not invariant under permutation of the entries of $\vec{k}$, as the ones described at the beginning of this section. Note that all eigenvectors of the kind $\left|\alpha_1^{\vec{k}}\right\rangle\left|\beta_{\vec{k}}\right\rangle$ with the same Hamming weight k have the same eigenvalue

$e^{i\omega_k}$. Since the sum of the eigenvectors with the same Hamming weight is also an eigenvector, we can generate a new eigenvector, which is invariant under permutation of the entries of $\vec{k}$ and, therefore, it will be in the subspace spanned by $|\rho_v\rangle$ and $|\lambda_v\rangle$. So, we define

$$\left|\omega_k^+\right\rangle = \frac{1}{\sqrt{\binom{n}{k}}} \sum_{|\vec{k}|=k} \left|\alpha_1^{\vec{k}}\right\rangle \left|\beta_{\vec{k}}\right\rangle, \tag{6.109}$$

for $0 \leq k < n$. Similarly, we define

$$\left|\omega_k^-\right\rangle = \frac{1}{\sqrt{\binom{n}{k}}} \sum_{|\vec{k}|=k} \left|\alpha_n^{\vec{k}}\right\rangle \left|\beta_{\vec{k}}\right\rangle, \tag{6.110}$$

for $0 < k \leq n$ associated with eigenvalue $e^{-i\omega_k}$. These eigenvectors are in $\mathcal{H}_{\text{inv}}$. The number of eigenvectors is the same as the dimension of $\mathcal{H}_{\text{inv}}$. Thus, set $\left\{\left|\omega_k^+\right\rangle : 0 \leq k \leq n-1, \left|\omega_k^-\right\rangle : 1 \leq k \leq n\right\}$ is an orthonormal eigenbasis of U for $\mathcal{H}_{\text{inv}}$ associated with eigenvalues $\left\{e^{i\omega_k}, e^{-i\omega_k}\right\}$.

The initial condition $|\mathrm{D}\rangle\left|\vec{0}\right\rangle$ can be expressed in this new eigenbasis if there are coefficients a_k and b_k such that

$$|\mathrm{D}\rangle\left|\vec{0}\right\rangle = \sum_{k=0}^{n-1} a_k \left|\omega_k^+\right\rangle + \sum_{k=1}^{n} b_k \left|\omega_k^-\right\rangle. \tag{6.111}$$

Since the eigenbasis is orthonormal, it follows that

$$\begin{aligned} a_k &= \left\langle \omega_k^+ \middle| \mathrm{D}, \vec{0} \right\rangle, \\ b_k &= \left\langle \omega_k^- \middle| \mathrm{D}, \vec{0} \right\rangle. \end{aligned}$$

Using that $\left\langle \alpha_1^k \middle| \mathrm{D} \right\rangle = \left\langle \alpha_n^k \middle| \mathrm{D} \right\rangle = 1/\sqrt{2}$, (6.109) and (6.110), we obtain

$$\begin{aligned} a_k &= \sqrt{\frac{1}{2^{n+1}} \binom{n}{k}}, \\ b_k &= \sqrt{\frac{1}{2^{n+1}} \binom{n}{k}}, \end{aligned}$$

for $0 < k < n$. Using (6.85) and (6.86), we obtain $a_0 = b_n = 1/\sqrt{2^n}$. So,

$$|\Psi(0)\rangle = \frac{1}{\sqrt{2^n}}\left(\left|\omega_0^+\right\rangle + \left|\omega_n^-\right\rangle\right) + \frac{1}{\sqrt{2^{n+1}}}\sum_{k=1}^{n-1}\sqrt{\binom{n}{k}}\left(\left|\omega_k^+\right\rangle + \left|\omega_k^-\right\rangle\right). \tag{6.112}$$

Then, the state of the quantum walk at time t is

$$|\Psi(t)\rangle = \frac{1}{\sqrt{2^n}}\left(\left|\omega_0^+\right\rangle + (-1)^t\left|\omega_n^-\right\rangle\right) + \frac{1}{\sqrt{2^{n+1}}}\sum_{k=1}^{n-1}\sqrt{\binom{n}{k}}\left(\mathrm{e}^{\mathrm{i}\omega_k t}\left|\omega_k^+\right\rangle + \mathrm{e}^{-\mathrm{i}\omega_k t}\left|\omega_k^-\right\rangle\right). \tag{6.113}$$

Exercise 6.27. Show that

$$\left|\alpha_1^{\vec{0}}\right\rangle\left|\beta_{\vec{0}}\right\rangle = |\mathrm{D}\rangle \otimes \frac{1}{\sqrt{2^n}}\sum_{\vec{v}=0}^{2^n-1}|\vec{v}\rangle = \frac{1}{\sqrt{2^n}}\left(\sum_{v=0}^{n-1}\sqrt{\binom{n-1}{v}}|\rho_v\rangle + \sum_{v=1}^{n}\sqrt{\binom{n-1}{v-1}}|\lambda_v\rangle\right).$$

Exercise 6.28. Show that

$$\left|\alpha_n^{\vec{1}}\right\rangle\left|\beta_{\vec{1}}\right\rangle = |\mathrm{D}\rangle \otimes \frac{1}{\sqrt{2^n}}\sum_{\vec{v}=0}^{2^n-1}(-1)^v|\vec{v}\rangle = \frac{1}{\sqrt{2^n}}\left(\sum_{v=0}^{n-1}(-1)^v\sqrt{\binom{n-1}{v}}|\rho_v\rangle + \sum_{v=1}^{n}(-1)^v\sqrt{\binom{n-1}{v-1}}|\lambda_v\rangle\right).$$

[Hint: Use the first identity of Exercise 6.25.]

Exercise 6.29. Show that $\left\{\left|\omega_k^+\right\rangle : 0 \le k \le n-1,\ \left|\omega_k^-\right\rangle : 1 \le k \le n\right\}$ is an orthonormal basis of $\mathcal{H}_{\mathrm{inv}}$ with eigenvalues $\mathrm{e}^{\pm\mathrm{i}\omega_k}$.

Further Reading

One of the seminal papers that has analyzed the quantum walk on cycles is [8]. References [35, 36, 313] are also useful. Periodic solutions were obtained in [312, 313]. The quantum walk on two-dimensional lattices was analyzed in [222, 313]. Periodic solutions can also be found on the two-dimensional lattice; see [302, 313]. Some earlier papers analyzing quantum walks on the n-dimensional hypercube are [233, 241]. Reference [173] showed that the quantum hitting time between two opposite vertices of a hypercube is exponentially smaller than the classical hitting time. More references about quantum walks in finite graphs published before 2012

are provided by the review papers [13, 172, 175, 183, 274, 320] or by the review books [229, 319].

Some recent references of quantum walks on cycles are as follows. Bounds for mixing time are addressed in [169]. Topological phases and bound states are addressed in [26]. Localization induced by an extra link in cycles is analyzed in [337]. Quantum walks with memory are presented in [118, 192]. Quantum state revivals are addressed in [106]. Lively quantum walks are studied in [286]. Transient temperature and mixing times are presented in [101]. Coherent dynamics are analyzed in [141]. Experimental proposals and implementations are presented in [48, 242]. Teleportation is studied in [324]. The topological classification of one-dimensional quantum walks is presented in [70].

Quantum walks on hypercubes are addressed in [227, 228]. Quantum walks on two-dimensional lattices are addressed in [27, 109, 143, 180]. Integrated photonic circuits for quantum walks on lattices are analyzed in [50]. Analysis of coined quantum walks on hierarchical graphs using renormalization is addressed in [52].

Chapter 7
Coined Quantum Walks on Graphs

In the previous chapters, we have addressed *coined quantum walks* on specific graphs of wide interest, such as lattices and hypercubes. In this chapter, we define coined quantum walks on arbitrary *graphs*. The concepts of graph theory reviewed in Appendix B are required here for a full understanding of the definition of the coined quantum walk. We split the presentation into *class* 1, and *class* 2 graphs. Class 1 comprises graphs whose *maximum degree* coincides with the *edge-chromatic number* and class 2 comprises the remaining ones. For graphs in class 1, we can use the standard *coin-position* or *position-coin notation*, and we can give the standard interpretation that the vertices are the positions and the edges are the directions. For graphs in class 2, on the other hand, we can use neither the *coin-position* nor *position-coin notation*; we have to use the *arc notation* and replace the simple graph by an associated *symmetric digraph*, whose underlying graph is the original graph. In this case, the walker steps on the arcs of the digraph. After those considerations, we are able to define formally coined quantum walks.

The *quantum walk dynamic* is determined by a *time-independent evolution operator* and an initial quantum state. The state of the quantum walk as a function of time is obtained from the repeated action of the evolution operator, starting from the initial state. In *finite* quantum systems, there is a *quasi-periodic* pattern during the time evolution, preventing the convergence to a *limiting distribution*. The quasi-periodic behavior is generated by eigenvalues of the evolution operator, whose arguments are noninteger multiples of 2π.

Perfect state transfer is a rare phenomenon that has applications for *quantum transport*. We give the definition of perfect state transfer not only for the coined model, but also for the *continuous-time* and *staggered* models.

We also address the concepts of *limiting probability distribution* and *mixing time* of quantum walks on *finite regular graphs*. A possible way to obtain limiting configurations is to define a new distribution called *average probability distribution*, which evolves stochastically and does not have the *quasi-periodic behavior*. We describe

© Springer Nature Switzerland AG 2018

R. Portugal, *Quantum Walks and Search Algorithms*, Quantum Science and Technology, https://doi.org/10.1007/978-3-319-97813-0_7

the limiting distribution of quantum walks on *cycles*, *finite lattices*, and *hypercubes* using the evolution operators and the initial conditions studied in previous chapters.

7.1 Quantum Walks on Class-1 Regular Graphs

Let $G(V, E)$ be a finite *d-regular graph* in *class* 1 with $N = |V|$ vertices. The labels of the vertices are 0 to $N - 1$, and the labels of the edges are 0 to $d - 1$, which correspond to an *edge coloring*. For graphs in class 1, the *edge-chromatic number* of G is $\Delta(G)$ and, for d-regular graphs, $\Delta(G) = d$. Regular graphs with an odd number of vertices are not included in class 1.

The Hilbert space associated with a coined quantum walk on G is $\mathcal{H} = \mathcal{H}^d \otimes \mathcal{H}^N$, where $\mathcal{H}^d$ is the coin space and $\mathcal{H}^N$ is the position space. The computational basis of $\mathcal{H}$ is the set of vectors $\{|a, v\rangle : 0 \leq a \leq d - 1,\ 0 \leq v \leq N - 1\}$. We use the *coin-position notation*. For graphs in class 1, we can assume that the walker steps on the vertices and we can interpret $|a, v\rangle$ as the state of a walker on position v with direction a.

The *evolution operator* of the *coined quantum walk* is

$$U = S\,(C \otimes I_N), \tag{7.1}$$

where C is the *coin operator*, which is a d-dimensional unitary matrix, and S is the *flip-flop shift operator* ($S^2 = I_{(dN)}$), which is defined by

$$S|a, v\rangle = \left|a, v'\right\rangle, \tag{7.2}$$

where vertices v and v' are adjacent and incident to edge a, that is, the label of the edge $\{v, v'\}$ is a.

The coin-position or position-coin notations can be used for graphs in class 1 that are nonregular, but in this case the coin is not separable as a tensor product of the form $(C \otimes I)$.

When we consider the graph embedded in a Euclidean space, we can define global directions for the motion, such as right or left, up or down, clockwise or counterclockwise. In these cases, we can define a shift operator with a subjacent physical meaning, called *moving shift operator*, which keeps the direction and $S^2 \neq I$. Examples are provided in Chap. 5. The quantum walk with moving shift operator can be converted into a quantum walk with flip-flop shift operator by redefining the coin operator.

The evolution operator (7.1) employs a *homogeneous coin*, that is, the same coin for all vertices. This can be generalized so that the coin may depend on the vertex. In this case, the coin is not separable as a tensor product $(C \otimes I)$. *Nonhomogeneous coins* are used in *quantum-walk-based search algorithms*.

Exercise 7.1. For graphs in class 1, define the action of an edge a on a vertex v as $a(v) = v'$, where v and v' are adjacent and incident to edge a. Note that $a(a(v)) = v$. This notation is consistent for regular graphs. In this notation, the shift operator is defined as

$$S|a, v\rangle = |a, a(v)\rangle,$$

where $0 \leq a < d$ and $0 \leq v < N$. If C is the Grover coin, show that

$$U|a, v\rangle = \left(\frac{2}{d} - 1\right)|a, a(v)\rangle + \frac{2}{d}\sum_{a' \neq a}\left|a', a'(v)\right\rangle.$$

Exercise 7.2. Analyze whether nonequivalent edge colorings produce nonsimilar evolution operators of quantum walks on d-regular graphs in class 1.

7.2 Coined Quantum Walks on Arbitrary Graphs

For graphs in *class* 2, such as regular graphs with an odd number of vertices, the *arc notation* reflects the quantum walk dynamic better than the *coin-position notation* (or the *position-coin notation*) used for graphs in *class* 1 in the previous section. One cannot label the edges of d-regular graphs in class 2 with d colors. This means that to use the *coin-position notation* and to assign directions, one must give different labels for the pairs of *symmetric arcs*. If v and v' are adjacent, the label (v, v') means from v to v' and the label (v', v) means from v' to v. Then, the concept of a simple graph is not adequate and some underlying arc notation, belonging to *directed graphs*, must be used. In this case, the physical interpretation of the actual position of the walker must change in order to match the mathematical description. Instead of walking on vertices, the walker steps on arcs, and instead of using a simple graph, we must use a *symmetric digraph*. For graphs in class 1, we have two set of labels, which can be used to represent the walker's positions (vertices) and the directions (edges). For graphs in class 2, the concept of a simple graph is not enough, and we need to consider the associated symmetric digraph, which has only one set of labels (v, v') representing both position and direction.

Let $G(V, E)$ be a simple graph with vertex set V and edge set E and let $N = |V|$ be the number of vertices. An *edge* is denoted by an unordered set $\{v, v'\}$, where v and v' are adjacent. An *arc* is denoted by an ordered pair (v, v'), where v is the *tail* and v' is the *head*. Let $\vec{G}(V, A)$ be a *directed graph* such that (v, v') and (v', v) are in $A(\vec{G})$ if and only if $\{v, v'\} \in G$. $\vec{G}$ and G have the same vertex set, and $\vec{G}$ is a *symmetric digraph*, whose underlying graph is G.

A coined quantum walk cannot be intrinsically defined on a simple graph G in *class* 2. The best we can do is to define the coined quantum walk on the symmetric digraph $\vec{G}$, whose underlying graph is G. The Hilbert space associated with the coined walk on $\vec{G}$ is spanned by the arc set, that is,

$$\mathcal{H}^{2|E|} = \operatorname{span}\{|(v, v')\rangle : (v, v') \in A(\vec{G})\}.$$

Since each edge of G is associated with two arcs of $\vec{G}$, we have $|A| = 2|E|$. The notation $|(v, v')\rangle$ is called *arc notation*.

The *evolution operator* of the *coined quantum walk* on $\vec{G}$ is

$$U = SC, \tag{7.3}$$

where S is the *flip-flop shift operator* defined by

$$S\,|(v, v')\rangle = |(v', v)\rangle \tag{7.4}$$

and C is the *coin operator* defined by

$$C = \bigoplus_{v \in V} C_v, \tag{7.5}$$

where C_v is a $d(v)$-dimensional unitary matrix and $d(v)$ is the *degree* of v. To write C as a direct sum, we are decomposing $\mathcal{H}^{2|E|}$ as

$$\mathcal{H}^{2|E|} = \bigoplus_{v \in V} \operatorname{span}\{|v, v'\rangle : (v, v') \in A(\vec{G})\}.$$

S is called *flip-flop* because $S^2 = I$. To demand that $S^2 = I$ is no loss of generality because the coin operator is a direct sum of arbitrary unitary operators. In fact, a coined quantum walk using the *moving shift operator* can be converted into the flip-flop case by defining a new coin $C' = PCP^{\mathrm{T}}$, where P is a permutation matrix. The coin operator C acts on $\mathcal{H}^{2|E|}$ and in general is not separable as a tensor product of smaller operators, unless the graph is regular and all C_v are equal. We can choose an ordering of the elements of the computational basis so that C is *block diagonal*. Let $V = \{0, \ldots, N-1\}$ be the vertex set and let us use the following ordering of the arc set: Take two different arcs (v_1, v_2) and (v_3, v_4). Arc (v_1, v_2) comes before arc (v_3, v_4) if $v_1 \leq v_3$ and when $v_1 = v_3$ if $v_2 < v_4$. The ordering of the vectors of the computational basis must change accordingly. On the other hand, the shift operator is not block diagonal. We can reverse the process, that is, we choose an ordering of the elements of the computational basis so that S is block diagonal while C is not block diagonal. In this case, $S = X^{\otimes|E|}$. In many applications, one can simply ignore such details.

Exercise 7.3. Show that $|A| = dN$ for d-regular graphs with N vertices.

Exercise 7.4. The goal of this exercise is to show that the coin-position notation cannot be used for graphs in class 2. Try to use the coin-position notation for a coined quantum walk on a triangle, which is a 2-regular graph in class 2. The dimension of the Hilbert space is 6. There is no problem to label the three vertices: v_1, v_2, v_3.

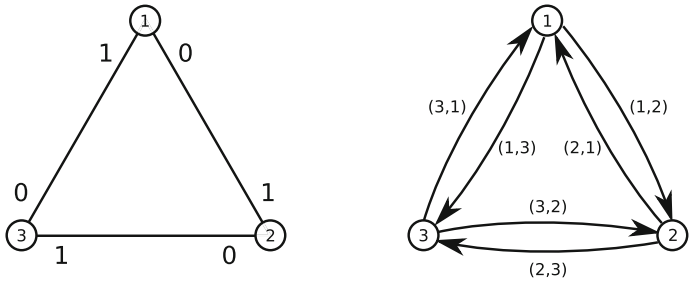

Fig. 7.1 Labeling of the left-hand graph is unfitting because each edge has two labels. The labeling of the right-hand digraph is appropriate

Now we have to give labels for the edges. We expect to give *one* label for each edge. Convince yourself that it is not possible to use only two labels (coin labels 0 and 1) because adjacent edges cannot have the same label (see the left-hand graph of Fig. 7.1 with an unfitting attempt). What can we do? We can use a notation based on the direction, such as $1 \to 2$, which means the walker on v_1 would move to v_2. Then, the computational basis would be $|1 \to 2, v_1\rangle$, $|1 \to 3, v_1\rangle$, $|2 \to 1, v_2\rangle$, $|2 \to 3, v_2\rangle$, $|3 \to 1, v_3\rangle$, $|3 \to 2, v_3\rangle$. Convince yourself that this is a disguised arc notation and is equivalent to the notation of the right-hand digraph of Fig. 7.1.

7.2.1 Locality

Is the evolution operator of the coined model a product of *local operators*? To answer this question, we have to define formally the concept of *local operator* so as it coincides, as much as possible, with the intuitive notion that the walker must move only to neighboring vertices (class 1) or neighboring arcs (class 2).[1] The problem is the following. For graphs in class 1, we assume that the walker steps on the vertices. Then, the coin operator does nothing to the walker's position. The usual escape is to say that the walker has an inner space, which is a useful interpretation for graphs in class 1, such as infinite lattices. For graphs in class 2, as we have pointed out, it is not possible to obtain an *edge coloring* with $\Delta(G)$ colors and there is no intrinsic way of describing the possible directions for the walker's shift unless we give different labels for the pairs of *symmetric arcs*. Note that the arc notation applies to both classes.

In a formal interpretation valid for any simple graph G, we define the coined walk on its associated symmetric digraph $\vec{G}$, whose underlying graph is G, and demand that the walker step on the arcs of $\vec{G}$. Both operators (coin and shift) move the walker. If the walker is on an arc (v, v'), the coin operator spreads the walker's position across the arcs whose tails are v, and the shift operator moves the walker to the opposite

[1] It is also allowed to stay put.

arc. Two arcs are *neighbors* if they are opposite or if their tails coincide. In this interpretation, the definition of *local operators* in the coined model is as follows.

Definition 7.1. An operator H on the Hilbert space spanned by the arc set of graph $\vec{G}$ is *local* when $\langle (v_3, v_4) | H | (v_1, v_2) \rangle \neq 0$ only if the pair of arcs (v_1, v_2) and (v_3, v_4) are neighbors.

Note that the shift S and the coin C are local operators. On the other hand, the evolution operator U is nonlocal. Note that U is usually a sparse matrix in the computational basis because $\langle (v_3, v_4) | U | (v_1, v_2) \rangle = 0$ when (v_3, v_4) is not a neighbor of a neighbor of (v_1, v_2).

7.2.2 Grover Quantum Walk

The *Grover quantum walk* is an important subcase when the coin operator is the direct sum of Grover operators, that is, each matrix C_v has entries

$$(C_v)_{k\ell} = \frac{2}{d(v)} - \delta_{k\ell}. \tag{7.6}$$

In the operator notation, the full coin matrix acts as

$$C\,|a\rangle = \sum_{\substack{a' \in A(\vec{G}) \\ \mathrm{tail}(a') = \mathrm{tail}(a)}} \left(\frac{2}{d(\mathrm{tail}(a))} - \delta_{a,a'} \right) |a'\rangle, \tag{7.7}$$

where $|a\rangle$ is a vector of the computational basis and $a \in A(\vec{G})$. The interpretation of this coin, which is the Grover coin in the arc notation, is as follows. If the walker is on arc a, the coin spread the walker's position across the arcs whose tails are $\mathrm{tail}(a)$.

The shift operator moves the walker to the set of arcs whose heads are $\mathrm{tail}(a)$. In this compact notation, the shift operator is

$$S|a\rangle = |\bar{a}\rangle, \tag{7.8}$$

where $\bar{a}$ is the opposite arc, that is, if $a = (v, v')$, then $\bar{a} = (v', v)$. The Grover walk is extensively used in quantum-walk-based search algorithms.

Exercise 7.5. Show that the evolution operator of the *Grover quantum walk* in the arc notation is

$$U = \sum_{a' \in A(\vec{G})} \sum_{\substack{a \in A(\vec{G}) \\ \mathrm{tail}(a) = \mathrm{tail}(a')}} \left(\frac{2}{d(\mathrm{tail}(a'))} - \delta_{a,a'} \right) |\bar{a}\rangle\langle a'|.$$

Show that for regular graphs in class 1, the above evolution operator reduces to the evolution operator of Exercise 7.1, by converting the arc notation into the coin-position notation. Use initially the conversion $\left|(v, v')\right\rangle \to \left|\{v, v'\}, v\right\rangle$.

7.2.3 Coined Walks on Cayley Graphs

Cayley graphs $\Gamma(G, S)$, where G is a group and S is a *symmetric generating set*, are interesting examples of regular graphs in which the *arc notation* comes naturally. If we consider the symmetric digraph $\vec{G}$, the labels of the arcs are $(g, g \cdot s)$, where $g \in G$ and $s \in S$. It is possible to use a kind of coin-position notation because $|(g, g \cdot s)\rangle$ can be denoted by $|s, g\rangle$ and $|(g \cdot s, g)\rangle$ by $\left|s^{-1}, g \cdot s\right\rangle$. In this case, the vertex labels are the group elements $g \in G$ and the arc labels can be guessed by the notation $|s, g\rangle$.[2]

The action of the flip-flop shift operator is

$$S|s, g\rangle = \left|s^{-1}, g \cdot s\right\rangle,$$

and of the Grover coin is

$$C|s, g\rangle = \left(\frac{2}{d} - 1\right)|s, g\rangle + \frac{2}{d}\sum_{\substack{s' \in S \\ s' \neq s}} \left|s', g\right\rangle,$$

where $d = |S|$. From those definitions, the action of the evolution operator $U = SC$ on the computational basis is

$$U|s, g\rangle = \left(\frac{2}{d} - 1\right)\left|s^{-1}, g \cdot s\right\rangle + \frac{2}{d}\sum_{\substack{s' \in S \\ s' \neq s}} \left|(s')^{-1}, g \cdot s'\right\rangle.$$

If all generators in S have the property $s = s^{-1}$, the Cayley graph is in class 1 and the true coin-position notation can be used and the generators $s \in S$ are edge labels. Note that this is not the only case in which the Cayley graph is in class 1.

The quantum walk on hypercubes analyzed in Sect. 6.3 on p. 106 is an explicit example of a walk on a Cayley graph of order $N = 2^n$ of the *abelian group* $\mathbb{Z}_2^n$ with n canonical generators $(1, 0, \ldots, 0), (0, 1, \ldots, 0), \ldots, (0, \ldots, 0, 1)$. Hypercubes are in class 1.

Quantum walks on odd cycles are examples of Cayley graphs of the group $\mathbb{Z}_N$ with generating set $S = \{1, -1\}$, which are in class 2.

[2]Note that the generators $s \in S$ cannot be used as edge labels in general. For instance, take the triangle, which is a Cayley graph $\Gamma(\mathbb{Z}_3, \{\pm 1\})$, and see Exercise 7.4.

7.2.4 Coined Walks on Multigraphs

The coined model achieves its full generality only on *multigraphs*. Coined quantum walk on simple graphs cannot describe instances of 2-*tessellable quantum walks* (see the definition in Chap. 8) on simple graphs that are the *line graphs* of bipartite multigraphs (with at least one *multiple edge*).

The definition of the coined model on multigraphs is very similar to the definition for graphs in class 2, but we need to give labels for all arcs without using the notation (v, v'), and we have to consider the *symmetric multidigraph* $\vec{G}$. The Hilbert space is spanned by the arc set, that is,

$$\mathcal{H} = \operatorname{span}\big\{|a\rangle : a \in A(\vec{G})\big\}.$$

The *evolution operator* is

$$U = S\,C, \tag{7.9}$$

where S is the *flip-flop shift operator* defined by

$$S\,|a\rangle = |\bar{a}\rangle, \tag{7.10}$$

where $\bar{a}$ is the arc opposite to a, and C is the *coin operator* defined by

$$C = \bigoplus_{v \in V} C_v, \tag{7.11}$$

where C_v is a $d(v)$-dimensional unitary matrix under the decomposition

$$\mathcal{H} = \bigoplus_{v \in V} \operatorname{span}\big\{|a\rangle : \operatorname{tail}(a) = v\big\}.$$

Exercise 7.6. Given a regular graph G in class 2, there are two ways to define a new graph G' that does not need the arc notation: (1) by adding a loop to each vertex of G, or (2) by adding a *leaf* to each vertex of G. Show that in both cases it is possible to assign $(\Delta(G) + 1)$ labels for the edges of G' and conclude that the coin-position notation can be used in a coined quantum walk on G'. Is the quantum walk dynamic on G' equivalent to the one on G?

7.3 Dynamics and Quasi-periodicity

In the last section, we have defined the evolution operator of the coined quantum walk. This section addresses the quantum walk dynamic. Most of the discussion from now on assume that G is a d-regular connected graph in class 1 with N vertices. We

use the coin-position notation because it is widespread in literature. However, the results apply to arbitrary graphs and to discrete-time quantum walks in general. It would not apply to the continuous model, which can have a noninteger time.

Suppose that the initial condition of a coined quantum walk is $|\psi(0)\rangle$. The dynamic of the coined model, or any discrete-time quantum walk, is described by the repeated action of the evolution operator. The state of the walker at time t is

$$|\psi(t)\rangle = U^t|\psi(0)\rangle, \tag{7.12}$$

where U is the *time-independent evolution operator*.

One may wonder whether state $|\psi(t)\rangle$ tends to a stationary state when t approaches infinity, that is, does $\lim_{t\to\infty} |\psi(t)\rangle$ exist? This limit does not exist because the norm $\big\| \, |\psi(t+1)\rangle - |\psi(t)\rangle \big\|$ is constant for all t, in fact,

$$\begin{aligned}\frac{1}{2}\big\||\psi(t+1)\rangle - |\psi(t)\rangle\big\|^2 &= \frac{1}{2}\big\|U^t(U-I)|\psi(0)\rangle\big\|^2 \\ &= 1 - \Re\big(\langle\psi(0)|U|\psi(0)\rangle\big).\end{aligned}$$

The result is time-independent because operator U is unitary. Since the real part of $\langle\psi(0)|U|\psi(0)\rangle$ is constant and strictly smaller than 1 for a given nontrivial evolution operator U, the above norm is a nonzero constant. The time-dependent state $|\psi(t)\rangle$ cannot tend toward a stationary state because the left-hand side would approach zero, which is a contradiction.

The probability of finding the walker on vertex v is given by

$$p_v(t) = \sum_{a=0}^{d-1} \big|\langle a, v|\psi(t)\rangle\big|^2. \tag{7.13}$$

When we consider all vertices of the graph, we have a probability distribution $p_v(t)$, which satisfies

$$\sum_{v=0}^{N-1} p_v(t) = 1.$$

We may ask ourselves again whether there is a limiting probability distribution in the general case, since the argumentation of the preceding paragraph does not directly exclude this possibility. Another way to answer such a question is by showing that the dynamics of quantum walks on finite graphs are quasi-periodic.

Quasi-periodic dynamic in the quantum walk literature is used with the meaning that there are an infinite number of time steps such that the quantum state is close to the initial state; besides, the repetitive structure is over varying timescales. Since this concept is an extension of the periodic behavior, let us start by defining the latter.

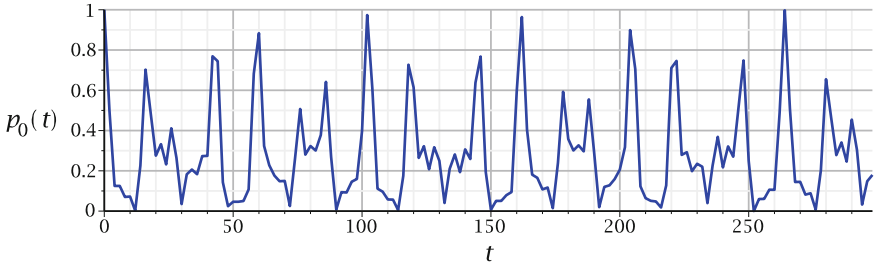

Fig. 7.2 Probability of finding the walker on vertex $v = 0$ as a function of t for a quantum walk on a 10-cycle

Definition 7.2 (Periodic dynamics). The dynamic (7.12) based on the repeated action of an evolution operator is *periodic* if there is a *fundamental period* $t_0 \in \mathbb{Z}^+$ and an angle α such that $U^{t_0} = \mathrm{e}^{\mathrm{i}\alpha} I$.

It follows from this definition that $\left|\langle\psi(nt_0)|\psi(0)\rangle\right|^2 = 1$ for all positive integer n and for any choice of the initial state $|\psi(0)\rangle$. The simplest extension of Definition 7.2 is as follows.

Definition 7.3 (Quasi-periodic dynamics). The dynamic (7.12) based on the repeated action of an evolution operator is *quasi-periodic* if for any positive number ϵ there is a time step t such that $\left\|U^t - I\right\| \leq \epsilon$.

Using the *norm* of linear operators (see Sect. A.14 on p. 262), this definition implies that, for any fixed positive ϵ, there is a time step t such that $\left|\langle\psi(t)|\psi(0)\rangle\right| \geq 1 - \epsilon$ (Exercise 7.7). Definition 7.3 also implies that there are an infinite number of time steps such that $\left|\langle\psi(t)|\psi(0)\rangle\right| \geq 1 - \epsilon$. In fact, if there is one such a t, then choose a new ϵ, for instance,

$$\epsilon' = \frac{1 - \left|\langle\psi(t)|\psi(0)\rangle\right|}{2}.$$

By Definition 7.3, there is a time step $t' \neq t$ such that $\left|\langle\psi(t')|\psi(0)\rangle\right| \geq 1 - \epsilon'$. This process can be repeated over and over. If t is the smallest time step such that $\left|\langle\psi(t)|\psi(0)\rangle\right| \geq 1 - \epsilon$, then $t' > t$.

Figure 7.2 shows the probability of finding the walker on the initial vertex as a function of the number of steps of a Hadamard walk on a 10-cycle. Note that the probability approaches 1 at many time steps, for instance, at time $t = 264$.

Let us show that the quantum walk dynamics on finite graphs are quasi-periodic. Suppose that $\left|\lambda_k^a\right\rangle$ for $0 \leq a \leq d-1$ and $0 \leq k \leq N-1$ is an orthonormal eigenbasis of U with eigenvalues $\mathrm{e}^{2\pi\mathrm{i}\lambda_k^a}$, where $0 \leq \lambda_k^a < 1$. The *spectral decomposition* of U is

$$U = \sum_{a=0}^{d-1} \sum_{k=0}^{N-1} \mathrm{e}^{2\pi\mathrm{i}\lambda_k^a} \left|\lambda_k^a\right\rangle\left\langle\lambda_k^a\right|. \tag{7.14}$$

The initial state can be written in the eigenbasis of U as

$$|\psi(0)\rangle = \sum_{a=0}^{d-1}\sum_{k=0}^{N-1} c_k^a \left|\lambda_k^a\right\rangle, \tag{7.15}$$

where $c_k^a = \left\langle\lambda_k^a \middle|\psi(0)\right\rangle$. Then,

$$|\psi(t)\rangle = \sum_{a=0}^{d-1}\sum_{k=0}^{N-1} c_k^a \, \mathrm{e}^{2\pi \mathrm{i}\lambda_k^a t}\left|\lambda_k^a\right\rangle. \tag{7.16}$$

For a given evolution operator U and initial condition $|\psi(0)\rangle$, the only time-dependent term in the last equation is $\mathrm{e}^{2\pi\mathrm{i}\lambda_k^a t}$. Then, the spectrum of U determines whether the dynamic is periodic or quasi-periodic.

Theorem 7.4 *The discrete-time quantum walk dynamic on finite graphs with evolution operator U is periodic if the arguments of the eigenvalues of U are rational multiples of 2π.*

Proof We use the eigenbasis of U to show that there is a t_0 such that $U^{t_0} = I$. If the phases[3] of the eigenvalues of U are $\lambda_k^a = n_k^a/d_k^a$ for coprime integers n_k^a, d_k^a for a finite number of values a and k, then the fundamental period is the *least common multiple* of the denominators d_k^a, that is, $t_0 = \mathrm{lcm}\{d_k^a : 0 \le a < d, 0 \le k < N\}$ because $\exp(2\pi\mathrm{i}\lambda_k^a t_0) = 1$ for all a and k. □

The condition of the theorem is sufficient but not necessary because we have not addressed the global phase (Exercise 7.8). Let us move on to quasi-periodicity, which is the main topic of this section.

Before addressing arbitrarily large finite Hilbert spaces, let us start with the two-dimensional case. In the eigenbasis of U, a two-dimensional U is *similar* to

$$\begin{bmatrix} \mathrm{e}^{2\pi\mathrm{i}\lambda_1} & 0 \\ 0 & \mathrm{e}^{2\pi\mathrm{i}\lambda_2} \end{bmatrix},$$

where $0 \le \lambda_1, \lambda_2 < 1$ are the phases of the eigenvalues. If λ_1 and λ_2 are rational, say $\lambda_1 = n_1/d_1$ and $\lambda_2 = n_2/d_2$ for integers n_1, n_2, d_1, and d_2, then U is periodic because $U^{(d_1 d_2)} = I$. If the numerators and denominators are coprime, then the least common multiple of d_1 and d_2 is the fundamental period. In general, λ_1 and λ_2 are real numbers. We can use the *continued fraction approximation* to find rational approximations n_1/d_1 and n_2/d_2 for λ_1 and λ_2 up to some digits. Then, $U^{(d_1 d_2)}$ is close to the identity up to some digits. If we choose a really small ϵ in Definition 7.3, then the rational approximations must be really tight.

Now we state some key lemmas.

[3] Here *phase* means the argument of a unit complex number over 2π. Note that in many papers the term phase is used as a synonym of *argument* of a unit complex number.

Lemma 7.5 *Given a unit complex number* $e^{i\theta}$*, where* $0 \le \theta < 2\pi$*, and a positive number* ϵ*, there exists* $t \in \mathbb{Z}^+$ *such that* $\left|e^{it\theta} - 1\right| \le \epsilon$.

Proof If θ is a rational multiple of 2π, then t is any integer multiple of the denominator of $\theta/2\pi$. To show the statement when θ is an irrational multiple of 2π, let n be an integer such that $n \ge 2\pi/\epsilon$ and, given any positive integer j, define $0 \le \theta(j) < 2\pi$ such that $j\,\theta \equiv \theta(j) \mod 2\pi$.[4] There exist two different integers j_1 and j_2 smaller than or equal to n such that $|\theta(j_1) - \theta(j_2)| \le 2\pi/n \le \epsilon$ because if we divide the unit circle into identical sectors such that each sector has angle ϵ (except possibly for one smaller sector) and if we take n different integers j, for instance, $j = 1, 2, \ldots, n$, then there is a sector with more than one $\theta(j)$. Then, $\theta(|j_2 - j_1|) \le \epsilon$ and the integer number $t = |j_2 - j_1|$ obeys $\theta(t) \le \epsilon$. Using that $\left|e^{it\theta} - 1\right| = \sqrt{2}\sqrt{1 - \cos\theta(t)} \le \sqrt{2}\sqrt{1 - \cos\epsilon} \le \epsilon$, we conclude the proof. □

In the proof of Lemma 7.5, we use a sequence $j = 1, 2, \ldots$ of consecutive integer numbers in order to find j_1 and j_2 with the desired property $\theta(|j_2 - j_1|) < \epsilon$. The proof works just as well if we use a sequence $j = i_1, i_2, \ldots$ of increasing integer numbers, not necessarily consecutive, that is, we are still able to find integers j_1 and j_2 with the desired property if we take n large enough. Another important fact is that if $e^{it\theta}$ is (ϵ/n)-close to 1 for a positive integer n, then each unit complex number of the sequence $e^{i\ell t\theta}$ for $\ell = 1, 2, .., n$ is at most ϵ-close to 1. We show this fact in the next lemma.

Lemma 7.6 *Given a positive number* ϵ *and unit complex numbers* $e^{i\theta_k}$ *for* $1 \le k \le N$ *and* $N \in \mathbb{Z}^+$*, there exists* $t \in \mathbb{Z}^+$ *such that*

$$\max_k \left|e^{it\theta_k} - 1\right| \le \epsilon.$$

Proof (*By induction on* N) Lemma 7.5 shows that the statement is true for $N = 1$. Now suppose it is true for N.

Given $\epsilon > 0$, let n be a positive integer such that $n \ge 2\pi/\epsilon$. Using the recursive condition, there exists $t \in \mathbb{Z}^+$ such that $\left|e^{it\theta_k} - 1\right| \le \frac{\epsilon}{2n}$, where k is the index of the maximum of $\left|e^{it\theta_{k'}} - 1\right|$ for $1 \le k' \le N$. Using that[5] $\frac{|\theta_k(t)|}{2} \le \left|e^{it\theta_k} - 1\right|$ when $-\pi < \theta_k(t) \le \pi$, we have $n|\theta_k(t)| \le \epsilon$. Then,

$$\left|e^{i\ell\theta_k(t)} - 1\right| \le \epsilon$$

for $\ell = 1, \ldots, n$. We have described an arbitrarily large finite sequence of integer numbers ℓt for $\ell = 1, \ldots, n$ such that $\left|e^{i\ell t\theta_k} - 1\right| \le \epsilon$.

Now we have to include the unit complex number $e^{i\theta_{N+1}}$ in the previous set $\{e^{i\theta_k} : 1 \le k \le N\}$. Using the proof of Lemma 7.5, we are able to find an integer number

[4]The notation $a \equiv b \mod 2\pi$ means that b (which can be an irrational number) is the remainder of the division of a by an integer multiple of 2π.

[5]Here we change the convention and we use $-\pi < \theta(t) \le \pi$ instead of $0 \le \theta(t) < 2\pi$.

$t' = |\ell_2 t - \ell_1 t|$ where $\ell_1, \ell_2 \leq n$ ($\ell_1 t$ and $\ell_2 t$ play the role of j_1 and j_2 in the proof of Lemma 7.5) such that $\left|\mathrm{e}^{\mathrm{i}t'\theta_{N+1}} - 1\right| \leq \epsilon$. We conclude that

$$\max_{k=1\ldots N+1} \left|\mathrm{e}^{\mathrm{i}t'\theta_k} - 1\right| \leq \epsilon,$$

which means that the statement of this lemma is true for $N + 1$. □

Theorem 7.7 *Discrete-time quantum walk dynamics on finite graphs are quasi-periodic.*

Proof On a finite graph with N vertices, the dynamic is obtained by the repeated action of a N-dimensional unitary operator U. In the eigenbasis of U, U is described by N unit complex numbers $\mathrm{e}^{\mathrm{i}\theta_k}$ for $1 \leq k \leq N$. Using Definition 7.3, Lemma 7.6, and the *norm* of linear operators described in Sect. A.14, we conclude that the dynamic is quasi-periodic. □

Note that not only discrete-time quantum walks are quasi-periodicity but also any finite quantum system that is driven by a time-independent evolution operator.

Exercise 7.7 Show that if $\left\|U^t - I\right\| \leq \epsilon$, then $\left|\left\langle\psi(t)\middle|\psi(0)\right\rangle\right| \geq 1 - \epsilon$.

Exercise 7.8 Improve the statement of Theorem 7.4 in order to describe a necessary and sufficient condition for periodic dynamics and prove the resulting proposition.

7.4 Perfect State Transfer and Fractional Revival

Perfect state transfer (PST) was analyzed in detail on *spin chains*, which is a row of qubits that interact with their neighbors via some time-independent Hamiltonian. Intuitively, PST means to transfer the state of a qubit in the chain at some point in time to another qubit at a future point in time. *Fractional revival* is a related concept, which is important for entanglement generation in spin chains.

These concepts have been naturally adapted to the area of quantum walks on graphs. However, the definitions depend on which quantum walk model one is using. Let us start by defining PST and fractional revival in the context of the *continuous-time quantum walk* (CTQW). The evolution operator in the continuous-time model on a graph $\Gamma(V, E)$ acts on the Hilbert space spanned by the graph vertices and is usually defined as $U(t) = \exp(-\mathrm{i}tA)$, where A is the adjacency matrix of Γ. There are alternative definitions, such as $U(t) = \exp(-\mathrm{i}tL)$, where L is the Laplacian matrix of Γ. In any case, the definition of perfect state transfer is as follows.

Definition 7.8 (Perfect state transfer in CTQW). Let $U(t)$ be the evolution operator of a continuous-time quantum walk on a graph $\Gamma(V, E)$. There is a *perfect state transfer* from vertex v to $v' \neq v$ at time $t_0 \in \mathbb{R}^+$ if $\left|\left\langle v'\middle|U(t_0)\middle|v\right\rangle\right| = 1$.

Note that if the walker is initially on vertex v, that is, $|v\rangle$ is the initial state, $U(t_0)|v\rangle$ is the walker's state at time t_0 and $\left|\langle v'|U(t_0)|v\rangle\right|^2$ is the probability of finding the walker on vertex v' at time t_0. Graph Γ admits PST from vertex v to v' at time t_0 if this probability is 1.

The definition of *fractional revival* is as follows.

Definition 7.9 (Fractional revival in CTQW). Let $U(t)$ be the evolution operator of a continuous-time quantum walk on a graph $\Gamma(V, E)$. There is a *fractional revival* at vertices v and $v' \neq v$ at time $t_0 \in \mathbb{R}^+$ if $U(t_0)|v\rangle = \alpha|v\rangle + \beta|v'\rangle$ for complex scalars α and $\beta \neq 0$ with $|\alpha|^2 + |\beta|^2 = 1$.

The definitions of PST and fractional revival for the *staggered quantum walk* are similar to the ones for CTQW because the Hilbert space of both models is spanned by the graph vertices. A 2-*tessellable quantum walk* is defined by the evolution operator

$$U = \mathrm{e}^{\mathrm{i}\theta_1 H_1}\mathrm{e}^{\mathrm{i}\theta_0 H_0},$$

where $\theta_0, \theta_1 \in \mathbb{R}$, H_0 and H_1 are Hamiltonians associated with two *tessellations* of a *tessellation cover* (see Chap. 8 for details). Since θ_0 and θ_1 are real parameters, they can be adjusted in order to create the conditions that admit PST and fractional revival.

Definition 7.10 (Perfect state transfer in the staggered model). Let U be the evolution operator of a staggered quantum walk on a graph $\Gamma(V, E)$. There is a *perfect state transfer* from vertex v to $v' \neq v$ at time $t_0 \in \mathbb{Z}^+$ if $\left|\langle v'|U^{t_0}|v\rangle\right| = 1$.

Definition 7.11 (Fractional revival in the staggered model). Let U be the evolution operator of a staggered quantum walk on a graph $\Gamma(V, E)$. There is a *fractional revival* at vertices v and $v' \neq v$ at time $t_0 \in \mathbb{Z}^+$ if $U^{t_0}|v\rangle = \alpha|v\rangle + \beta|v'\rangle$ for complex scalars α and $\beta \neq 0$ with $|\alpha|^2 + |\beta|^2 = 1$.

The definitions of PST and fractional revival in the coined model are the most complex ones.

Definition 7.12 (Perfect state transfer in the coined model). Let U be the evolution operator of a coined quantum walk on a d-regular graph $\Gamma(V, E)$ in class 1 described in the coin-position notation. There is a *perfect state transfer* from vertex v to $v' \neq v$ at time $t_0 \in \mathbb{Z}^+$ if

$$\sum_{a'=0}^{d-1}\sum_{a'=0}^{d-1}\left|\langle a', v'|U^{t_0}|a, v\rangle\right| = 1.$$

Next definition uses the *partial inner product*.

Definition 7.13 (Fractional revival in the coined model). Let U be the evolution operator of a coined quantum walk on a graph $\Gamma(V, E)$ in class 1 described in the

coin-position notation. There is a *fractional revival* at vertices v and $v' \neq v$ at time $t_0 \in \mathbb{Z}^+$ if there is a coin value $0 \leq a < d$ such that

$$\sum_{a=0}^{d-1} \langle a' | U^{t_0} | a, v \rangle = \alpha |v\rangle + \beta |v'\rangle$$

for complex scalars α and $\beta \neq 0$ with $|\alpha|^2 + |\beta|^2 = 1$.

We give at the end of this chapter references that describe graphs that admit perfect state transfer for all these definitions and graphs that admit fractional revival in the continuous-time case.

Exercise 7.9 Define perfect state transfer and fractional revival for coined quantum walks on graphs in class 2.

7.5 Limiting Probability Distribution

Classical random walks on connected *nonbipartite* graphs have *limiting* or *stationary distributions* that do not depend on the initial condition. In the quantum context, it is interesting to ask whether there is a stationary probability distribution when the quantum walk evolves up to $t \to \infty$. If there is, how does the limiting distribution depend on the *initial condition*?

We have shown in Sect. 7.3 that there is a time $t > 0$ such that $|\psi(t)\rangle$ is arbitrarily close to the initial condition. Due to the cyclic nature of the evolution, the same procedure can be used to find an infinite number of times such that the quantum state is close to the initial condition. Since this is a characteristic of discrete-time quantum walks on finite graphs, we can ask ourselves if there is some way to define limiting distributions.

The *average probability distribution* is defined as

$$\bar{p}_v(T) = \frac{1}{T} \sum_{t=0}^{T-1} p_v(t). \tag{7.17}$$

Note that $\bar{p}_v(T)$ is a probability distribution because $0 \leq \bar{p}_v(T) \leq 1$ and

$$\sum_{v=0}^{N-1} \bar{p}_v(T) = 1$$

for all T. We can give the following physical interpretation for $\bar{p}_v(T)$. Take an integer t *randomly* distributed between 0 and $T-1$. Let the quantum walk evolve from the initial condition until that time t. Perform a measurement in the computational basis to determine the position of the walker. Keeping T fixed, repeat the process over and

over. Analyzing the results, we can determine how many times the walker has been found on each vertex. Dividing these values by the total number of repetitions, we obtain a probability distribution close to $\bar{p}_v(T)$, which can be improved by increasing the number of repetitions.

The interpretation of $\bar{p}_v(T)$ uses *projective measurements*. Therefore, $\bar{p}_v(T)$ evolves *stochastically*. Now we have a good reason to believe that $\bar{p}_v(T)$ converges to a limiting distribution when T tends to infinity. Define

$$\pi(v) = \lim_{T\to\infty} \bar{p}_v(T). \tag{7.18}$$

This limit exists and can be explicitly calculated once given the initial condition. We can obtain a useful formula for calculating the limiting distribution and at the same time prove its existence for regular graphs in class 1.

Using (7.13) and (7.17), we obtain

$$\bar{p}_v(T) = \frac{1}{T}\sum_{t=0}^{T-1}\sum_{b=0}^{d-1}\left|\langle b, v|\psi(t)\rangle\right|^2.$$

Using (7.16), we obtain

$$\bar{p}_v(T) = \frac{1}{T}\sum_{t=0}^{T-1}\sum_{b=0}^{d-1}\left|\sum_{a=0}^{d-1}\sum_{k=0}^{N-1} c_k^a\, \mathrm{e}^{2\pi \mathrm{i}\lambda_k^a t}\,\langle b, v|\lambda_k^a\rangle\right|^2.$$

After some algebraic manipulations, we obtain

$$\begin{aligned}\bar{p}_v(T) = &\sum_{a,a',b=0}^{d-1}\sum_{k,k'=0}^{N-1} c_k^a\left(c_{k'}^{a'}\right)^*\langle b, v|\lambda_k^a\rangle\left\langle\lambda_{k'}^{a'}\middle|b, v\right\rangle \\ &\times\frac{1}{T}\sum_{t=0}^{T-1}\mathrm{e}^{2\pi\mathrm{i}(\lambda_k^a-\lambda_{k'}^{a'})t}.\end{aligned} \tag{7.19}$$

To obtain the limiting distribution, we have to calculate the limit

$$\lim_{T\to\infty}\frac{1}{T}\sum_{t=0}^{T-1}\left(\mathrm{e}^{2\pi\mathrm{i}(\lambda_k^a-\lambda_{k'}^{a'})}\right)^t.$$

Using the formula of the geometric series, we obtain

$$\frac{1}{T}\sum_{t=0}^{T-1}\left(\mathrm{e}^{2\pi\mathrm{i}(\lambda_k^a-\lambda_{k'}^{a'})}\right)^t = \begin{cases}\dfrac{\mathrm{e}^{2\pi\mathrm{i}(\lambda_k^a-\lambda_{k'}^{a'})T}-1}{T\left(\mathrm{e}^{2\pi\mathrm{i}(\lambda_k^a-\lambda_{k'}^{a'})}-1\right)}, & \text{if } \lambda_k^a \neq \lambda_{k'}^{a'};\\ 1, & \text{if } \lambda_k^a = \lambda_{k'}^{a'}.\end{cases} \tag{7.20}$$

If $\lambda_k^a \neq \lambda_{k'}^{a'}$, the result is a *complex number*, whose *modulus* obeys

$$\left| \frac{\mathrm{e}^{2\pi \mathrm{i}(\lambda_k^a - \lambda_{k'}^{a'})T} - 1}{T\left(\mathrm{e}^{2\pi \mathrm{i}(\lambda_k^a - \lambda_{k'}^{a'})} - 1\right)} \right|^2 = \frac{1}{T^2} \frac{1 - \cos 2\pi(\lambda_k^a - \lambda_{k'}^{a'})T}{1 - \cos 2\pi(\lambda_k^a - \lambda_{k'}^{a'})}$$
$$\leq \frac{1}{T^2} \frac{1}{1 - \cos 2\pi(\lambda_k^a - \lambda_{k'}^{a'})}.$$

Taking the limit $T \to \infty$, we obtain that the modulus of this complex number is zero. Then,

$$\lim_{T\to\infty} \frac{1}{T} \sum_{t=0}^{T-1} \left(\mathrm{e}^{2\pi \mathrm{i}(\lambda_k^a - \lambda_{k'}^{a'})}\right)^t = \begin{cases} 0, \text{ if } \lambda_k^a \neq \lambda_{k'}^{a'}; \\ 1, \text{ if } \lambda_k^a = \lambda_{k'}^{a'}. \end{cases} \tag{7.21}$$

Using this result in (7.19), we obtain the following expression for the limiting distribution:

$$\pi(v) = \sum_{a,a'=0}^{d-1} \sum_{\substack{k,k'=0 \\ \lambda_k^a = \lambda_{k'}^{a'}}}^{N-1} c_k^a \left(c_{k'}^{a'}\right)^* \sum_{b=0}^{d-1} \langle b, v | \lambda_k^a \rangle \left\langle \lambda_{k'}^{a'} \middle| b, v \right\rangle. \tag{7.22}$$

The sum runs over the pairs of indices (a, k) and (a', k') that correspond to equal eigenvalues $\lambda_k^a = \lambda_{k'}^{a'}$. If all eigenvalues are different, that is, $\lambda_k^a \neq \lambda_{k'}^{a'}$ for all (a, k) and (a', k'), the expression of the limiting distribution simplifies to

$$\pi(v) = \sum_{a=0}^{d-1} \sum_{k=0}^{N-1} |c_k^a|^2 \, p_{a,k}(v), \tag{7.23}$$

where

$$p_{a,k}(v) = \sum_{b=0}^{d-1} \left| \langle b, v | \lambda_k^a \rangle \right|^2. \tag{7.24}$$

Note that the limiting distribution depends on c_k^a, which are the coefficients of the initial state in the eigenbasis of U. Therefore, the limiting distribution depends on the initial condition in the general case.

Exercise 7.10 Let U be the evolution operator of a quantum walk as discussed in Sect. 7.1. Suppose that the limiting distribution is the same for any initial condition of type $|a, v\rangle$. Show that the limiting distribution is uniform on the vertices of the graph.

7.5.1 Limiting Distribution Using the Fourier Basis

In the previous chapters, we have been successful in analyzing quantum walks using the *Fourier basis*, which we denote by $\left|\tilde{k}\right\rangle$, because the evolution operator can be written using a *reduced operator*, which acts on the coin space. If $\left\{\left|\alpha_{a,k}\right\rangle\right\}$ is an orthonormal eigenbasis with eigenvalues $\alpha_{a,k}$ of the *reduced operator*, then $\left\{\left|\alpha_{a,k}, \tilde{k}\right\rangle\right\}$ is an orthonormal eigenbasis of the evolution operator, which replaces $\{\left|\lambda_k^a\right\rangle\}$ in (7.14)–(7.16) and the eigenvalues of the evolution operator are $\alpha_{a,k}$, the same as the reduced operator.

In the Fourier basis, the expression of the limiting distribution is simpler. When all eigenvalues are different, (7.24) reduces to

$$p_{a,k}(v) = \sum_{b=0}^{d-1} \left|\left\langle b\middle|\alpha_{a,k}\right\rangle\right|^2 \left|\left\langle v\middle|\tilde{k}\right\rangle\right|^2. \tag{7.25}$$

If the term $\left|\left\langle v\middle|\tilde{k}\right\rangle\right|^2$ is equal to $1/N$, we use the fact that

$$\sum_{b=0}^{d-1} \left|\left\langle b\middle|\alpha_{a,k}\right\rangle\right|^2 = 1$$

because each vector $\left|\alpha_{a,k}\right\rangle$ has unit norm, to conclude that $p_{a,k}(v) = 1/N$ for all v. Using this result in (7.23) and that the initial condition has unit norm, we obtain the uniform distribution

$$\pi(v) = \frac{1}{N}. \tag{7.26}$$

Among all graphs we have analyzed in Chap. 6, only cycles with odd number of vertices have distinct eigenvalues. Therefore, the limiting distribution is uniform in cycles with odd number of vertices, regardless of the initial condition.

Let us return to (7.22), which is valid in the general case in the Fourier basis. Renaming the original eigenvectors, we obtain

$$\pi(v) = \sum_{a,a'=0}^{d-1} \sum_{\substack{\vec{k},\vec{k}'=0 \\ \alpha_{a,\vec{k}}=\alpha_{a',\vec{k}'}}}^{N-1} c_{a,\vec{k}}\, c^*_{a',\vec{k}'} \sum_{b=0}^{d-1} \left\langle \alpha_{a',\vec{k}'}\middle|b\right\rangle\left\langle b\middle|\alpha_{a,\vec{k}}\right\rangle\left\langle v\middle|\tilde{k}\right\rangle\left\langle \tilde{k}'\middle|v\right\rangle. \tag{7.27}$$

Using the *completeness relation*, we obtain

$$\pi(v) = \sum_{a,a'=0}^{d-1} \sum_{\substack{\vec{k},\vec{k}'=0 \\ \alpha_{a,\vec{k}}=\alpha_{a',\vec{k}'}}}^{N-1} c_{a,\vec{k}}\, c^*_{a',\vec{k}'} \left\langle \alpha_{a',\vec{k}'}\middle|\alpha_{a,\vec{k}}\right\rangle\left\langle v\middle|\tilde{k}\right\rangle\left\langle \tilde{k}'\middle|v\right\rangle. \tag{7.28}$$

We will use this equation to calculate the limiting distribution of quantum walks on even cycles, two-dimensional finite lattices, and hypercubes.

Exercise 7.11 Show that the expression of $\pi(v)$ in (7.28) satisfies

$$\sum_{v=0}^{N-1} \pi(v) = 1.$$

7.5.2 Limiting Distribution of QWs on Cycles

In this section, we compute the limiting distribution of coined quantum walks on cycles. We need the expressions of the eigenvalues and eigenvectors of the evolution operator in order to use (7.28). For the Hadamard coin, the eigenvalues are

$$\alpha_{0,\vec{k}} = \mathrm{e}^{-\mathrm{i}\theta_k}, \tag{7.29}$$

$$\alpha_{1,\vec{k}} = \mathrm{e}^{\mathrm{i}(\pi+\theta_k)} = -\mathrm{e}^{\mathrm{i}\theta_k}, \tag{7.30}$$

where θ_k is a solution of equation

$$\sin\theta_k = \frac{1}{\sqrt{2}} \sin\frac{2\pi k}{N}, \tag{7.31}$$

as described in Sect. 6.1.1 on p. 91. The analysis of eigenvalue collisions for different values of k plays an important role in determining the sum in the expression of $\pi(v)$.

Figure 7.3 shows the eigenvalues for cycles with $N = 13$ and $N = 14$. The eigenvalues are confined to two regions of the unit circle. In fact, from (7.31), we have

$$|\sin\theta_k| \leq \frac{1}{\sqrt{2}}.$$

Then, $\theta_k \in [-\frac{\pi}{4}, \frac{\pi}{4}]$ or $\theta_k \in [\frac{3\pi}{4}, \frac{5\pi}{4}]$. If $-\theta_k$ is a solution of (7.31), then $\pi + \theta_k$ also is, since $\sin(\pi + \theta_k) = \sin(-\theta_k)$. Each eigenvalue of the form $\mathrm{e}^{-\mathrm{i}\theta_k}$ in the first sector $[-\frac{\pi}{4}, \frac{\pi}{4}]$ matches another (different) eigenvalue of the form $\mathrm{e}^{\mathrm{i}(\pi+\theta_k)}$ symmetrically opposite in the second sector.

The behavior of the eigenvalues depends on the parity of N. Two eigenvalues are equal if

$$\sin\frac{2\pi k}{N} = \sin\frac{2\pi k'}{N}.$$

This equation implies that $k = k'$ or $k + k' = \frac{N}{2}$ or $k + k' = \frac{3N}{2}$. If N is odd, only the first of these equations is satisfied and hence all eigenvalues are different. If N is

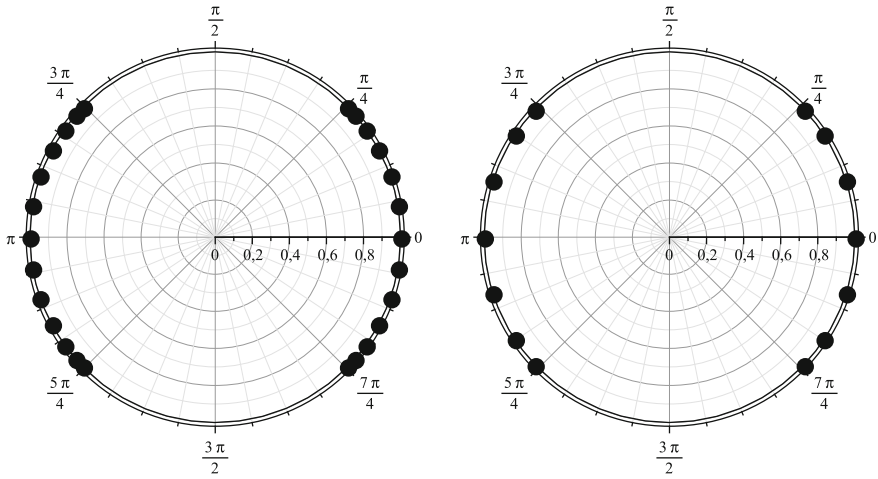

Fig. 7.3 Eigenvalues of the evolution operator for cycles with $N = 13$ and $N = 14$

even, there are 2 equal eigenvalues with different k's, unless $k = N/4$ or $k = 3N/4$; this only occurs when 4 divides N.

Since all eigenvalues are different for cycles with odd number of vertices, the limiting distribution is uniform for any initial condition. In the rest of this section, we address the case N even.

The eigenvectors of the reduced operator are $\left|\alpha_{0,\tilde{k}}\right\rangle = |\alpha_k\rangle$ and $\left|\alpha_{1,\tilde{k}}\right\rangle = |\beta_k\rangle$, which are given by (6.16) and (6.17), respectively. Using $\left|\tilde{k}\right\rangle$ given by (6.7), we obtain

$$\left\langle v\middle|\tilde{k}\right\rangle\left\langle\tilde{k}'\middle|v\right\rangle = \frac{\omega_N^{v(k-k')}}{N}.$$

To adapt (7.28) for the cycle, we must take $d = 2$. Expanding the sum over variables a and a', we obtain

$$\begin{aligned}\pi(v) = \frac{1}{N} \sum_{\substack{k,k'=0 \\ \mathrm{e}^{-\mathrm{i}\theta_k} = \mathrm{e}^{-\mathrm{i}\theta_{k'}}}}^{N-1} c_{0,k}\, c_{0,k'}^{*} \left\langle\alpha_{k'}\middle|\alpha_k\right\rangle \omega_N^{v(k-k')} \\ + \frac{1}{N} \sum_{\substack{k,k'=0 \\ \mathrm{e}^{\mathrm{i}(\pi+\theta_k)} = \mathrm{e}^{\mathrm{i}(\pi+\theta_{k'})}}}^{N-1} c_{1,k}\, c_{1,k'}^{*} \left\langle\beta_{k'}\middle|\beta_k\right\rangle \omega_N^{v(k-k')}.\end{aligned} \tag{7.32}$$

The cross terms $a = 0$, $a' = 1$, and vice versa do not contribute to any term because the eigenvalues $\mathrm{e}^{-\mathrm{i}\theta_k}$ and $\mathrm{e}^{\mathrm{i}(\pi+\theta_k)}$ are never the same for any values of k and k', since $\mathrm{e}^{-\mathrm{i}\theta_k}$ is either in quadrant I or quadrant IV, as we can see in Fig. 7.3, while $\mathrm{e}^{\mathrm{i}(\pi+\theta_{k'})}$ is quadrant II or quadrant III. On the other hand, $\mathrm{e}^{-\mathrm{i}\theta_k}$ is equal to $\mathrm{e}^{-\mathrm{i}\theta_{k'}}$, if $k' = k$

or $k' = N/2 - k$, as discussed in Sect. 6.1.1. Therefore, the double sums in $\pi(v)$ reduces to simple sums each generating three terms: $k' = k, k' = N/2 - k \mod N$, and $k = N/2 - k' \mod N$. When $k' = k$, the sums can be easily calculated, using that $|\alpha_k\rangle$, $|\beta_k\rangle$, and $|\psi(0)\rangle$ are unit vectors, generating term $1/N$ in (7.33). The sums under the constraints $k' = N/2 - k \mod N$ and $k = N/2 - k' \mod N$ are complex conjugate to each other. They can be simplified using the symmetries of the eigenvalues. Moreover, we can always take an initial condition such that $c_{0,k}$ and $c_{1,k}$ are real numbers because the phase factors of $c_{0,k}$ and $c_{1,k}$ can be absorbed in the eigenvectors. Eventually, (7.32) reduces to

$$\pi(v) = \frac{1}{N} + \frac{1}{N}\Re\left(\sum_{\substack{k=0\\ k\neq\frac{N}{4},\frac{3N}{4}}}^{N-1} c_{0,k}\, c_{0,\frac{N}{2}-k} \left\langle \alpha_{\frac{N}{2}-k} \middle| \alpha_k \right\rangle \omega_N^{v\left(2k-\frac{N}{2}\right)}\right) + \frac{1}{N}\Re\left(\sum_{\substack{k=0\\ k\neq\frac{N}{4},\frac{3N}{4}}}^{N-1} c_{1,k}\, c_{1,\frac{N}{2}-k} \left\langle \beta_{\frac{N}{2}-k} \middle| \beta_k \right\rangle \omega_N^{v\left(2k-\frac{N}{2}\right)}\right), \tag{7.33}$$

where $\Re(\,)$ is the real part and the subindices must be evaluated modulo N to include case $k > N/2$. Note that if 4 divides N, we delete the terms $k = N/4$ and $k = 3N/4$, since the eigenvalue is unique for these values of k.

Using that $\omega_N = \exp(2\pi \mathrm{i}/N)$, we obtain

$$\omega_N^{v\left(2k-\frac{N}{2}\right)} = (-1)^v \mathrm{e}^{\frac{4\pi \mathrm{i} k v}{N}}. \tag{7.34}$$

Using (6.16) and (6.17), we obtain

$$\left\langle \alpha_{\frac{N}{2}-k} \middle| \alpha_k \right\rangle = \left\langle \beta_{\frac{N}{2}-k} \middle| \beta_k \right\rangle = \frac{1 - \mathrm{e}^{\frac{4\pi \mathrm{i} k}{N}}}{2\sqrt{1 + \cos^2 \frac{2\pi k}{N}}}. \tag{7.35}$$

Substituting this result into (7.33), we obtain the limiting distribution of the quantum walk on the cycle with (real) initial conditions

$$\pi(v) = \frac{1}{N} + \frac{(-1)^v}{2N} \sum_{\substack{k=0\\ k\neq\frac{N}{4},\frac{3N}{4}}}^{N-1} \left(c_{0,k}\, c_{0,\frac{N}{2}-k} + c_{1,k}\, c_{1,\frac{N}{2}-k}\right) \times \frac{\cos\frac{4\pi k v}{N} - \cos\frac{4\pi k(v+1)}{N}}{\sqrt{1 + \cos^2 \frac{2\pi k}{N}}}. \tag{7.36}$$

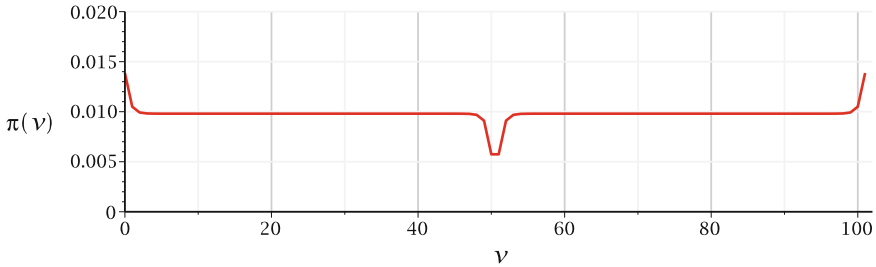

Fig. 7.4 Limiting probability distribution of the quantum walk on a cycle with $N = 102$ using the Hadamard coin and initial condition $|\psi(0)\rangle = |0\rangle|0\rangle$

This expression is general in the sense that any limiting distribution of a coined walk on the cycle with the Hadamard coin can be obtained from it. The subindices are evaluated modulo N.

The last step is to find coefficients $c_{0,k}$ and $c_{1,k}$ of the initial condition in the eigenbasis of the evolution operator. Taking $t = 0$ in (6.24), we obtain

$$|\psi(0)\rangle = \sum_{k=0}^{N-1} \left(\frac{1}{\sqrt{N c_k^-}} |\alpha_k\rangle |\tilde{k}\rangle + \frac{1}{\sqrt{N c_k^+}} |\beta_k\rangle |\tilde{k}\rangle \right). \tag{7.37}$$

Therefore,

$$c_{0,k} = \frac{1}{\sqrt{N c_k^-}},$$
$$c_{1,k} = \frac{1}{\sqrt{N c_k^+}}.$$

Using (6.18), we obtain

$$c_{0,k}\, c_{0,\frac{N}{2}-k} + c_{1,k}\, c_{1,\frac{N}{2}-k} = \frac{1}{N\sqrt{1+\cos^2 \frac{2\pi k}{N}}}. \tag{7.38}$$

Therefore, the limiting distribution of the quantum walk on the cycle with the Hadamard coin and initial condition $|\psi(0)\rangle = |0\rangle|0\rangle$ is

$$\pi(v) = \frac{1}{N} + \frac{(-1)^v}{2N^2} \sum_{\substack{k=0 \\ k \neq \frac{N}{4}, \frac{3N}{4}}}^{N-1} \frac{\cos \frac{4\pi k v}{N} - \cos \frac{4\pi k (v+1)}{N}}{1+\cos^2 \frac{2\pi k}{N}}. \tag{7.39}$$

Figure 7.4 shows the limiting probability distribution $\pi(v)$ of the quantum walk on a cycle with $N = 102$. The central peak pointing downward is typical for even N, that are nondivisible by 4. When N is divisible by 4, the peak points upward.

Exercise 7.12 Show that

$$\cos\frac{4\pi k v}{N} - \cos\frac{4\pi k\,(v+1)}{N} = 2\sin\frac{2\pi k}{N}\sin\frac{2\pi k}{N}(2v+1).$$

From this equality, obtain an equivalent expression for $\pi(v)$.

Exercise 7.13 Show that the expression of $\pi(v)$ in (7.39) satisfies

$$\sum_{v=0}^{N-1}\pi(v) = 1.$$

Exercise 7.14 Show that

$$\pi(0) \simeq \frac{\sqrt{2}}{N},$$

when $N \gg 1$.

Exercise 7.15 Show that

$$\pi(v) \simeq \frac{c_1(v)\sqrt{2} - c_2(v)}{N},$$

when $v \ll N$ and $1 \ll N$, where

$$c_1(v) = \frac{2+\sqrt{2}}{4}(d_+)^v + \frac{2-\sqrt{2}}{4}(d_-)^v,$$

$$c_2(v) = \frac{3\,(d_+)^{2\,v} + 1 + \sqrt{2}}{2\sqrt{2}\,(d_+)^v} - \frac{3\,(d_-)^{2\,v} + 1 - \sqrt{2}}{2\sqrt{2}\,(d_-)^v} - 1,$$

and $d_\pm = 3 \pm 2\sqrt{2}$.

7.5.3 Limiting Distribution of QWs on Hypercubes

The spectral decomposition of the evolution operator for the hypercube is described in Sect. 6.3 on p. 106. If the initial condition is

$$|\psi(0)\rangle = |\mathrm{D}\rangle|\vec{v} = 0\rangle,$$

the state of the quantum walk at time t is given by (6.94). Replacing $t = 0$ into this equation, we obtain the initial condition in the eigenbasis of the evolution operator

$$|\psi(0)\rangle = \frac{1}{\sqrt{2^n}}\Big(|\mathrm{D}\rangle\big|\beta_{\vec{0}}\big\rangle + |\mathrm{D}\rangle\big|\beta_{\vec{1}}\big\rangle\Big) + \frac{1}{\sqrt{2^{n+1}}}\sum_{\vec{k}=1}^{2^n-2}\Big(\Big|\alpha_1^{\vec{k}}\Big\rangle\big|\beta_{\vec{k}}\big\rangle + \Big|\alpha_n^{\vec{k}}\Big\rangle\big|\beta_{\vec{k}}\big\rangle\Big). \tag{7.40}$$

Therefore,

$$c_{1,\vec{k}} = c_{n,\vec{k}} = \begin{cases} \frac{1}{\sqrt{2^n}}, & \vec{k} = 0,\ \vec{k} = n; \\ \frac{1}{\sqrt{2^{n+1}}}, & 0 < \vec{k} < n, \end{cases} \tag{7.41}$$

and all other values are zero. Equation (7.28) assumes the form

$$\pi(\vec{v}) = \sum_{\substack{\vec{k},\vec{k}'=0 \\ k=k'}}^{N-1} c_{1,\vec{k}}c_{1,\vec{k}'}\,\Big\langle\alpha_1^{\vec{k}'}\Big|\alpha_1^{\vec{k}}\Big\rangle\big\langle\vec{v}\big|\beta_{\vec{k}}\big\rangle\big\langle\beta_{\vec{k}'}\big|\vec{v}\big\rangle + \sum_{\substack{\vec{k},\vec{k}'=0 \\ k=k'}}^{N-1} c_{n,\vec{k}}c_{n,\vec{k}'}\,\Big\langle\alpha_n^{\vec{k}'}\Big|\alpha_n^{\vec{k}}\Big\rangle\big\langle\vec{v}\big|\beta_{\vec{k}}\big\rangle\big\langle\beta_{\vec{k}'}\big|\vec{v}\big\rangle. \tag{7.42}$$

Note that parameter a starts at 1 and goes up to n in the convention used in the description of the hypercube in Sect. 6.3. The cross terms do not appear because $\Big\langle\alpha_n^{\vec{k}'}\Big|\alpha_1^{\vec{k}}\Big\rangle = 0$. The collision between the eigenvectors is guaranteed by restricting $k = k'$ in the sum, where k is the *Hamming weight* of $\vec{k}$.

Using (6.83) and (6.84), we obtain

$$\Big\langle\alpha_1^{\vec{k}'}\Big|\alpha_1^{\vec{k}}\Big\rangle = \Big\langle\alpha_n^{\vec{k}'}\Big|\alpha_n^{\vec{k}}\Big\rangle = \frac{n\,(\vec{k}\cdot\vec{k}') + k(n-2k)}{2k(n-k)}. \tag{7.43}$$

Using (6.71), we obtain

$$\big\langle\vec{v}\big|\beta_{\vec{k}}\big\rangle = \frac{1}{\sqrt{2^n}}(-1)^{\vec{k}\cdot\vec{v}}. \tag{7.44}$$

Using these results in (7.42), we obtain

$$\pi(\vec{v}) = \frac{2}{2^{2n}} + \frac{1}{2^{2n}}\sum_{\substack{\vec{k},\vec{k}'=0 \\ (k=k'\neq 0,n)}}^{2^n-1}(-1)^{(\vec{k}+\vec{k}')\cdot\vec{v}}\,\frac{n\,(\vec{k}\cdot\vec{k}') + k(n-2k)}{2k(n-k)}. \tag{7.45}$$

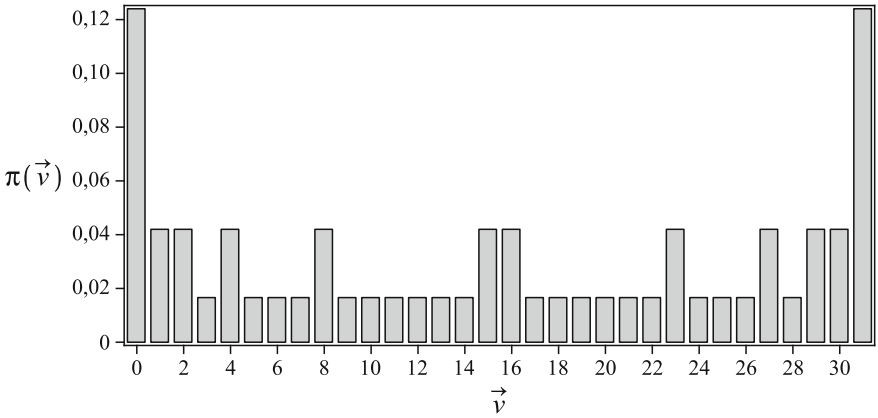

Fig. 7.5 Limiting distribution of the coined quantum walk on the hypercube with $N = 2^5$. The labels of the vertices are in the decimal notation

Figure 7.5 depicts the limiting distribution of the coined quantum walk on the hypercube with $N = 32$ vertices, obtained from (7.45). Note that the distribution has the same value for different vertices. In particular, the distribution is equal for all vertices of the same Hamming weight. This suggests that π depends only on the Hamming weight of $\vec{v}$. We can see that the graph is symmetric with respect to the central vertical axis. This suggests that the limiting distribution has the following invariance: $\pi(v) = \pi(2^n - 1 - v)$, which can be confirmed with all points on the graph.

Since the limiting distribution depends only on the Hamming weight of the vertices, we can define a new probability distribution of a walk on the line. The new expression is

$$\pi(v) = \binom{n}{v} \pi(\vec{v}). \tag{7.46}$$

The binomial coefficient gives the number of vertices that have the same Hamming weight. The new distribution satisfies

$$\sum_{v=0}^{n} \pi(v) = 1.$$

Figure 7.6 depicts the distribution of the quantum walk on the hypercube with 2^{32} vertices.

Exercise 7.16 Show that

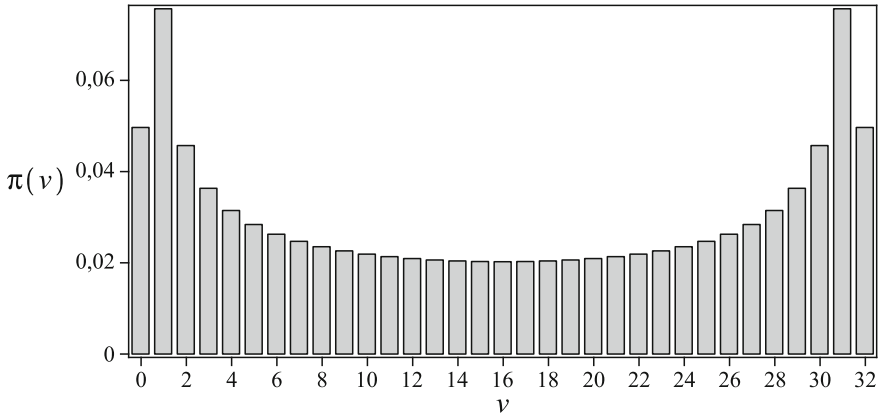

Fig. 7.6 Limiting distribution as function of the Hamming weight on the hypercube with $N = 2^{32}$, given by (7.46)

$$\begin{aligned}\pi(0) &= \frac{1}{4^n} + \frac{\Gamma\left(n+\frac{1}{2}\right)}{2\sqrt{\pi}\, n\, \Gamma(n)} \\ &= \frac{1}{4^n}\left(1 + \frac{(2n)!}{2(n!)^2}\right)\end{aligned}$$

where Γ is the *gamma function*.

7.5.4 Limiting Distribution of QWs on Finite Lattices

A two-dimensional finite lattice is an interesting example where the limiting distribution can be found analytically. The details of the calculation of the spectral decomposition of the evolution operator are presented in Sect. 6.2 on p. 98. If the initial condition is

$$|\psi(0)\rangle = |\mathrm{D}\rangle|x = 0, y = 0\rangle,$$

the state of the quantum walk at time t in the eigenbasis of the evolution operator is

$$\begin{aligned}|\psi(t)\rangle &= \frac{1}{\sqrt{N}}|\mathrm{D}\rangle|\mathrm{D}\rangle \\ &+ \frac{1}{\sqrt{2N}} \sum_{\substack{k_x,k_y=0 \\ (k_x,k_y)\neq(0,0)}}^{\sqrt{N}-1} \left(\mathrm{e}^{\mathrm{i}\theta t}\left|\nu^{\theta}_{k_x,k_y}\right\rangle + \mathrm{e}^{-\mathrm{i}\theta t}\left|\nu^{-\theta}_{k_x,k_y}\right\rangle\right)\left|\tilde{k}_x, \tilde{k}_y\right\rangle.\end{aligned}$$

From this expression, we can see that the eigenvectors of U that generate the subspace where the quantum walk evolves are $|\mathrm{D}\rangle|\mathrm{D}\rangle$, $\left|\nu^{\pm\theta}_{k_x,k_y}\right\rangle\left|\tilde{k}_x,\tilde{k}_y\right\rangle$, $0 \le k_x, k_y \le \sqrt{N}-1$, $(k_x, k_y) \neq (0,0)$.

Equation (7.22) assumes the form

$$\begin{aligned}
\pi(x,y) = {} & \left|c_{0,0}\right|^2 \left(\sum_{d,s=0}^{1} \left|\langle d,s|\mathrm{D}\rangle\right|^2\right) \left|\langle x,y|\mathrm{D}\rangle\right|^2 \\
& + \sum_{\substack{k_x,k_y=0 \\ (k_x,k_y)\neq(0,0)}}^{\sqrt{N}-1} \sum_{\substack{k'_x,k'_y=0 \\ (k'_x,k'_y)\neq(0,0) \\ \theta=\theta'}}^{\sqrt{N}-1} c^{+}_{k_x,k_y} \left(c^{+}_{k'_x,k'_y}\right)^* \\
& \times \sum_{d,s=0}^{1} \left\langle d,s|\nu^{\theta}_{k_x,k_y}\right\rangle \left\langle \nu^{\theta'}_{k'_x,k'_y}|d,s\right\rangle \left\langle x,y|\tilde{k}_x,\tilde{k}_y\right\rangle \left\langle \tilde{k}'_x,\tilde{k}'_y|x,y\right\rangle \\
& + c^{-}_{k_x,k_y} \left(c^{-}_{k'_x,k'_y}\right)^* \\
& \times \sum_{d,s=0}^{1} \left\langle d,s|\nu^{-\theta}_{k_x,k_y}\right\rangle \left\langle \nu^{-\theta'}_{k'_x,k'_y}|d,s\right\rangle \left\langle x,y|\tilde{k}_x,\tilde{k}_y\right\rangle \left\langle \tilde{k}'_x,\tilde{k}'_y|x,y\right\rangle, \quad (7.47)
\end{aligned}$$

where $\theta' = \theta(k'_x, k'_y)$. Note that we have simply rewritten the terms of (7.22) without performing simplifications. The label a in (7.22) is converted to d, s. The index k of eigenvectors is converted to k_x, k_y. The sum over the new indices is restricted to terms with nonzero c_{k_x,k_y}. Coefficients c_{k_x,k_y} are obtained by taking $t = 0$ in the equation of $|\psi(t)\rangle$ because for $t = 0$ we have the decomposition of the initial condition in the eigenbasis of the evolution operator. Then, we obtain

$$c_{0,0} = \frac{1}{\sqrt{N}}, \quad (7.48)$$

$$c^{+}_{k_x,k_y} = c^{-}_{k_x,k_y} = \frac{1}{\sqrt{2N}}. \quad (7.49)$$

Using the completeness relation $I_4 = \sum_{d,s=0}^{1} |d,s\rangle\langle d,s|$, we obtain

$$\sum_{d,s=0}^{1} \left\langle d,s|\nu^{\pm\theta}_{k_x,k_y}\right\rangle \left\langle \nu^{\pm\theta'}_{k'_x,k'_y}|d,s\right\rangle = \left\langle \nu^{\pm\theta'}_{k'_x,k'_y}|\nu^{\pm\theta}_{k_x,k_y}\right\rangle. \quad (7.50)$$

Using (6.40), we obtain

$$\left\langle x,y|\tilde{k}_x,\tilde{k}_y\right\rangle = \frac{1}{\sqrt{N}}\,\omega^{xk_x+yk_y}, \quad (7.51)$$

where $\omega = \mathrm{e}^{\frac{2\pi \mathrm{i}}{\sqrt{N}}}$.

Using these partial results in (7.47) and simplifying, we obtain

$$\pi(x, y) = \frac{1}{N^2} + \frac{1}{N^2} \sum_{\substack{k_x, k_y = 0 \\ (k_x, k_y) \neq (0,0)}}^{\sqrt{N}-1} \sum_{\substack{k'_x, k'_y = 0 \\ (k'_x, k'_y) \neq (0,0) \\ \theta(k'_x, k'_y) = \theta(k_x, k_y)}}^{\sqrt{N}-1} \left\langle \nu^{\theta'}_{k'_x, k'_y} \middle| \nu^{\theta}_{k_x, k_y} \right\rangle \times \mathrm{e}^{\frac{2\pi \mathrm{i}}{\sqrt{N}} \left(x(k_x - k'_x) + y(k_y - k'_y) \right)}. \tag{7.52}$$

We have used $\left\langle \nu^{\theta'}_{k'_x, k'_y} \middle| \nu^{\theta}_{k_x, k_y} \right\rangle = \left\langle \nu^{-\theta'}_{k'_x, k'_y} \middle| \nu^{-\theta}_{k_x, k_y} \right\rangle$, which can be verified using (6.53). The first term is absorbed in the sum. In the double sum, (k_x, k_y) need not be equal to (k'_x, k'_y), but the combination of values must be such that $\theta' = \theta$. Using that $\cos\theta' = \cos\theta$, we obtain

$$\left\langle \nu^{\theta'}_{k'_x, k'_y} \middle| \nu^{\theta}_{k_x, k_y} \right\rangle = \frac{1 - 2\cos^2\theta(k_x, k_y) + \cos\theta(k_x - k'_x, k_y - k'_y)}{2\sin^2\theta(k_x, k_y)}. \tag{7.53}$$

The simplification of this equation requires detailed knowledge of the collisions of the eigenvalues, that is, the relations about k'_x, k'_y such that $\theta(k'_x, k'_y) = \theta(k_x, k_y)$.

7.6 Distance Between Distributions

If we have more than one probability distribution of quantum walks on a graph with N vertices, it is interesting to define the notion of closeness between them. To use terms *close* or *far*, we have to define a *metric*. Let p and q be two probability distributions, that is, $0 \leq p_v \leq 1$, $0 \leq q_v \leq 1$, and

$$\sum_{v=1}^{N} p_v = \sum_{v=1}^{N} q_v = 1. \tag{7.54}$$

The definition that is usually used for *distance* is

$$D(p, q) = \frac{1}{2} \sum_{v=1}^{N} |p_v - q_v|, \tag{7.55}$$

known as *total variation distance* or L_1. This definition satisfies

1. $0 \leq D(p, q) \leq 1$,
2. $D(p, q) = 0$ if and only if $p = q$,
3. $D(p, q) = D(q, p)$, (symmetry)

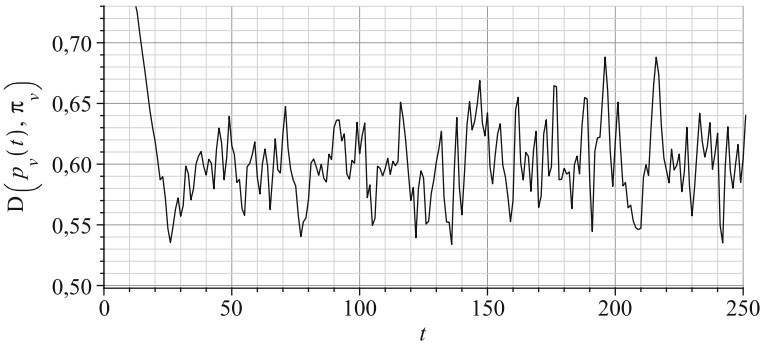

Fig. 7.7 Distance between the distribution $p_v(t)$ and the limiting distribution π_v as a function of time for a cycle with 102 vertices. The graph has a quasi-periodic pattern

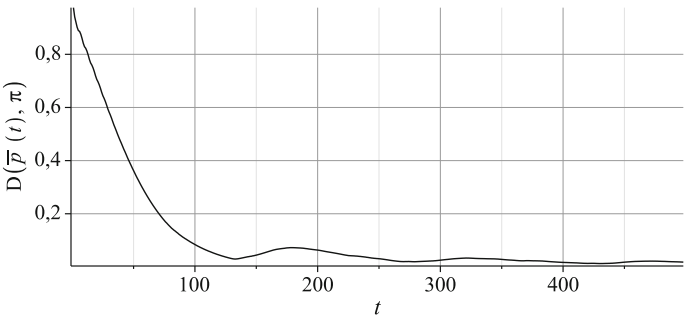

Fig. 7.8 Distance between the average distribution $\bar{p}_v(t)$ and the limiting distribution π_v as a function of time for a cycle with 102 vertices

4. $D(p, q) \leq D(p, r) + D(r, q)$. (triangle inequality)

We can improve our understanding of the unitary evolution by analyzing the distance between distribution $p_v(t)$ and the limiting distribution π_v. Figure 7.7 shows the typical behavior of this distance as a function of time for an even cycle with 102 vertices and initial condition $|\psi(0)\rangle = |0\rangle|0\rangle$. The plot shows the *quasi-periodic* behavior discussed in Sect. 7.5 manifesting in the distance between the instantaneous and the limiting distribution.

It is much more interesting to analyze the distance between the *average distribution* $\bar{p}_v(t)$ and the *limiting distribution* π_v as a function of time because we have a notion of convergence, since the limiting distribution is reached from the average distribution in the limit $t \to \infty$. Figure 7.8 shows $D(\bar{p}(t), \pi)$ as a function of time for a cycle with 102 vertices using the Hadamard coin and initial condition $|\psi(0)\rangle = |0\rangle|0\rangle$. The curve does not have a quasi-periodic pattern, in fact, disregarding the oscillation, we have the impression that the curve obeys a power law such as $1/t^a$, where a is a positive number. This kind of conjecture can be checked by plotting the curve using the axes in a log scale. If the result is a straight line, the slope

is a. Suppose that

$$D(\bar{p}(t), \pi) = \frac{b}{t^a}$$

for some b. Taking the logarithm of both sides, we obtain

$$\log D(\bar{p}(t), \pi) = -a \log t + \log b.$$

If the conjecture is true and we plot $\log D(\bar{p}(t), \pi)$ as a function of $\log t$, we obtain a straight line with negative slope. The base of the logarithm plays no role if we want to check the conjecture. It is only relevant when we wish to obtain b. Figure 7.9 shows the log–log plot of $D(\bar{p}(t), \pi)$ as a function of t. It seems that the curve oscillates around a straight line. To find the line equation, we select the two representative points, for instance, $(10, 0.7)$ and $(10^4, 0.0007)$. Then,

$$\begin{aligned} a &\simeq -\frac{\log 0.0007 - \log 0.7}{\log 10^4 - \log 10} \\ &\simeq 1.0, \end{aligned}$$

and b can be easily found. The line equation is $7.0/t$ approximately.

In the nontrivial cases, we can analytically show that $D(\bar{p}(t), \pi)$ has a dominant inverse power law behavior for any graph. Using (7.19) and (7.21), we obtain

$$\begin{aligned} \bar{p}_v(t) - \pi(v) = &\sum_{a,a',b=0}^{d-1} \sum_{k,k'=0}^{N-1} c_k^a \left(c_{k'}^{a'}\right)^* \langle b, v | \lambda_k^a \rangle \left\langle \lambda_{k'}^{a'} | b, v \right\rangle \\ &\times \left(\frac{1}{t} \sum_{t=0}^{t-1} \mathrm{e}^{2\pi \mathrm{i}(\lambda_k^a - \lambda_{k'}^{a'})t} - \delta_{\lambda_k^a, \lambda_{k'}^{a'}} \right). \end{aligned}$$

The terms of the sum corresponding to $\lambda_k^a = \lambda_{k'}^{a'}$ vanish. Using (7.20) and (7.55), we obtain

$$\begin{aligned} D(\bar{p}(t), \pi) = \frac{1}{2t} \sum_{v=1}^{N} \Bigg| &\sum_{a,a'=0}^{d-1} \sum_{\substack{k,k'=0 \\ \lambda_k^a \neq \lambda_{k'}^{a'}}}^{N-1} c_k^a \left(c_{k'}^{a'}\right)^* \frac{\mathrm{e}^{2\pi \mathrm{i}(\lambda_k^a - \lambda_{k'}^{a'})t} - 1}{\mathrm{e}^{2\pi \mathrm{i}(\lambda_k^a - \lambda_{k'}^{a'})} - 1} \\ &\times \sum_{b=0}^{d-1} \left\langle \lambda_{k'}^{a'} | b, v \right\rangle \langle b, v | \lambda_k^a \rangle \Bigg|. \end{aligned} \tag{7.56}$$

The factor $1/t$ is responsible for the inverse power law. The only term that depends on t in the sum is $\mathrm{e}^{2\pi \mathrm{i}(\lambda_k^a - \lambda_{k'}^{a'})t} - 1$, the modulus of which is a bounded periodic function. The linear combination of terms of this kind produces the oscillatory pattern around the straight line shown in Fig. 7.9.

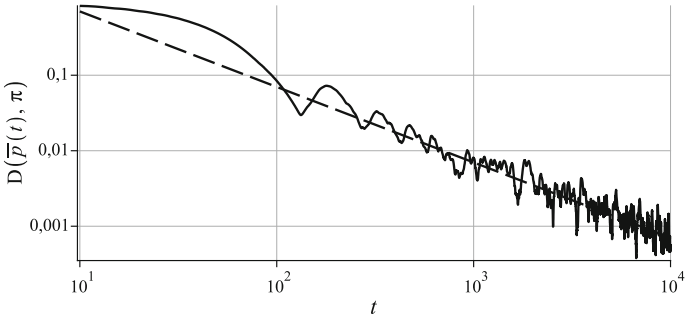

Fig. 7.9 Log–log plot of the distance between the average distribution $\bar{p}_v(t)$ and the limiting distribution π_v as a function of time for the cycle with 102 vertices up to $t = 10^4$. The equation of the *dashed line* is $7.0/t$

Exercise 7.17 Show that in odd cycles, the distance between the limiting distribution and the initial distribution starting from any vertex is

$$D\big(p(0), \pi\big) = 1 - \frac{1}{N}. \tag{7.57}$$

Note that when $N \gg 1$ this distance is close to the maximum distance.

Exercise 7.18 Simplify (7.56) for walks that can be analyzed in the Fourier basis.

Exercise 7.19 Obtain an explicit expression for (7.56) for walks on (odd and even) cycles with the Hadamard coin using the initial condition $|\psi(t)\rangle = |0\rangle|0\rangle$. Reproduce Fig. 7.8 using the analytical result.

7.7 Mixing Time

We have learned that the *average distribution* $\bar{p}_v(t)$ tends to the *limiting distribution* π_v. Usually, the approach is not monotonic, but there is a moment, that we denote by τ_ϵ, such that the distance between the distributions is smaller than or equal to the threshold ϵ and does not become larger.

Formally, the *quantum mixing time* is defined as

$$\tau_\epsilon = \min\big\{T \mid \forall t \geq T,\ D\big(\bar{p}_v(t), \pi_v\big) \leq \epsilon\big\}, \tag{7.58}$$

which can be interpreted as the number of steps it takes for the probability distribution to approach its final configuration. The quantum mixing time depends on the initial condition in general.

The mixing time captures the notion of the velocity in which the limiting distribution is reached. A small mixing time means that the limiting distribution is quickly

Table 7.1 Quantum and classical mixing times for the N-cycle, the two-dimensional lattice, and the hypercube with N vertices

τ_ϵ	N-cycle	2D lattice	Hypercube
Quantum	$O\left(\frac{N \log N}{\epsilon}\right)$	$O\left(\frac{\sqrt{N} \log N}{\epsilon}\right)$	$O\left(\frac{\log N}{\epsilon}\right)$
Classical	$O\left(N^2 \log \frac{1}{\epsilon}\right)$	$O\left(N \log \frac{1}{\epsilon}\right)$	$O\left(\log N \log \frac{\log N}{\epsilon}\right)$

reached. The mixing time τ_ϵ depends on parameter ϵ. If $D\left(\bar{p}_v(t), \pi_v\right)$ obeys an inverse power law as a function of time, then τ_ϵ obeys an inverse power law as a function of ϵ. Parameter ϵ is not the only one. In finite graphs, the number of vertices is a key parameter to assess the characteristics of the mixing time. It is interesting to compare the *quantum mixing time* with the *classical mixing time* of a *classical random walk* on the same graph. The definition of the classical mixing time is the same as (7.58), but instead of using the average probability distribution of the quantum walk the definition employs the probability distribution of the classical random walk.

In general, it is not possible to obtain closed analytical expressions for the mixing time in terms of the number of vertices. We can obtain upper or lower *bounds* or we can analyze numerically. Table 7.1 summarizes some results about quantum and classical mixing times for comparison. The quantum mixing times were obtained using numerical methods. The N-cycle with even N, the $(\sqrt{N} \times \sqrt{N})$-lattice with even $\sqrt{N}$, and hypercubes are bipartite graphs. The classical random walk in those cases must be the *lazy random walk*, which is defined in such way that the walker moves to one of its nearest neighbors or stays fixed with equal probability. This guarantees that there is a classical limiting distribution, which is uniform for those graphs.

The logarithm term in the classical mixing time shows that the limiting distribution is reached surprisingly rapidly by the classical random walk for a fixed N. On the other hand, the scaling with the graph size for cycles and lattices is smaller for the quantum mixing time.

7.7.1 Instantaneous Uniform Mixing (IUM)

The uniform probability distribution is interesting because it allows unbiased sampling from the vertex set. In general, such distribution cannot be obtained except instantaneously. Now we formally define *instantaneous uniform mixing* for the continuous-time, staggered, and coined models.

Definition 7.14 (IUM in the CTQW). Let $U(t)$ be the evolution operator of a continuous-time quantum walk on a graph $\Gamma(V, E)$. There is an *instantaneous uniform mixing* at time t_0 if all entries of $U(t_0)$ have the same absolute value.

Definition 7.15 (IUM in the staggered model). Let U be the evolution operator of a staggered quantum walk on a graph $\Gamma(V, E)$. There is an *instantaneous uniform mixing* at time t_0 if all entries of U^{t_0} have the same absolute value.

Definition 7.16 (IUM in the coined model). Let U be the evolution operator of a coined quantum walk on a graph $\Gamma(V, E)$ in class 1 described in the coin-position notation. There is an *instantaneous uniform mixing* at time t_0 if the entries of matrix

$$M_{vv'} = \sum_{a=0}^{d(v)-1} \sum_{a'=0}^{d(v')-1} \left\langle a', v' \middle| U^{t_0} \middle| a, v \right\rangle$$

have the same absolute value.

We give at the end of this chapter references that describe graphs that admit instantaneous uniform mixing. This concept is closely related to the concept of *perfect state transfer*.

Further Reading

The definition of the *coined quantum walk* on graphs presented in this chapter is based on many references, especially on [8, 193, 194, 275]. Reference [8] is one of the earliest papers presenting the definition of quantum walks on graphs and to draw attention to this area. References [193, 194] have given key contributions by calling attention to the importance of the *edge colorability* and Ref. [275] to the *arc notation* and to the *underlying symmetric digraph*. The contributions of early papers on the coined quantum walk on graphs were reviewed in [13, 172, 175, 183, 229, 274, 320], which provide relevant references.

Perfect state transfer on spin chains was introduced by Bose [54] in the context of quantum communication. His goal was to analyze how a state placed on one spin of the chain would be transmitted and received later on a distant spin. Usually, the *fidelity* between those states is smaller than 1, but it is interesting to analyze which kind of array would admit fidelity equal to 1 [83, 177]. The relation of PST in spin chains and Anderson localization was addressed in [281]. This problem has found a fertile ground in the area of quantum walks, especially, in the continuous-time case [12, 23, 33, 45, 67, 85, 87, 88, 156, 166, 174, 253, 352]. There some results on PST in the coined model [32, 171, 216, 301, 346] and one recent result on PST in the staggered model [89]. *Fractional revival* was analyzed in Refs. [44, 73, 106].

Reference [8] has provided a definition of the *limiting distribution* and the *quantum mixing time*. The limiting distribution of coined quantum walks on cycles was calculated in [8, 35, 36, 286, 336], on hypercubes in [169, 233], and on two-dimensional finite lattices in [232]. The mixing time in cycles was analyzed in [8, 202], in hypercubes in [233, 241]. Classical mixing times are analyzed in [240], which has a detailed study of the classical mixing time of random walks on hypercubes.

Reference [275] established a connection between coined walks on graphs and the Ihara zeta function. Reference [188] also analyzed the connection with zeta function.

Many relevant topics are analyzed using coined quantum walks on graphs. A short list is the following: walks on Cayley graphs [194], numerical quasi-periodicity [279], graph isomorphism [63, 284], localization [186, 295, 341], hitting time [227, 228], quantum transport [27, 56], walks on Möbius strip [205], quantum walks using quaternions instead of complex numbers [185], quantum walk with memory [204], abelian quantum walk [92].

Chapter 8
Staggered Model

The *staggered model* is the set of quantum walks based on the notion of *graph tessellation*, which is a new concept in *graph theory*. The evolution operator of a staggered quantum walk is obtained from a *graph tessellation cover*. A graph tessellation is a partition of the vertex set into *cliques*, and a graph tessellation cover is a set of tessellations whose union covers the edge set. A clique is a subset of the vertex set that induces a complete subgraph. Two vertices in a clique are neighbors, and the cliques of a tessellation specify which vertices are reachable after one local step once given the location of the walker.

In this chapter, we formally define the concept of graph tessellation cover and describe how to obtain the evolution operator of the staggered model. As a concrete example, we describe a staggered quantum walk on the line. Using the staggered Fourier transform, we diagonalize the evolution operator and calculate analytically the standard deviation of the walker's position.

8.1 Graph Tessellation Cover

Let $G(V, E)$ be a *connected simple graph*, where $V(G)$ is the vertex set and $E(G)$ is the edge set. A *clique* of G is a subset of the vertex set that induces a complete subgraph. For example, consider the *Hajós graph* depicted in Fig. 8.1 (first graph). The set of vertices $\{0, 1, 2\}$ is a clique of size 3, denoted by 3-clique, but set $\{0, 1, 2, 4\}$ is not a clique because it is missing an edge connecting vertices 1 and 4. A clique can have two vertices, such as $\{0, 1\}$, or a single vertex, such as $\{0\}$. The latter examples are not *maximal cliques*. On the other hand, set $\{0, 1, 2\}$ is a maximal clique because it is not contained in a larger clique.

A *partition* of the vertex set into cliques is a collection of disjoint cliques so that the union of these cliques is the vertex set. For example, the set $\mathcal{T}_1 =$

© Springer Nature Switzerland AG 2018

R. Portugal, *Quantum Walks and Search Algorithms*, Quantum Science and Technology, https://doi.org/10.1007/978-3-319-97813-0_8

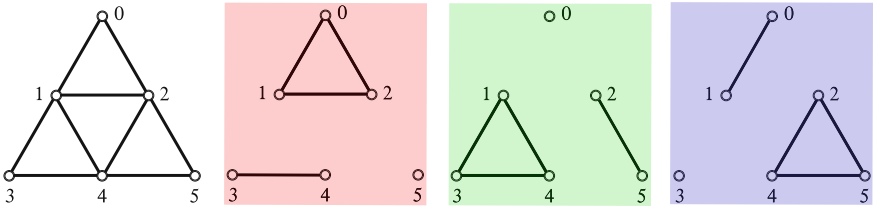

Fig. 8.1 Hajós graph and the depiction of three tessellations

$\{\{0, 1, 2\}, \{3, 4\}, \{5\}\}$ is a partition of the Hajós graph into cliques because $\{0, 1, 2\} \cup \{3, 4\} \cup \{5\}$ is the vertex set and the cliques are nonoverlapping sets.

Definition 8.1. A *graph tessellation* $\mathcal{T}$ is a partition of the vertex set into cliques. An edge *belongs* to the tessellation $\mathcal{T}$ if and only if its endpoints belong to the same clique in $\mathcal{T}$. The set of edges belonging to $\mathcal{T}$ is denoted by $\mathcal{E}(\mathcal{T})$. An element of the tessellation is called a *polygon* (or *tile*). The *size* of a tessellation $\mathcal{T}$ is the number of polygons in $\mathcal{T}$.

Set $\mathcal{T}_1 = \{\{0, 1, 2\}, \{3, 4\}, \{5\}\}$ is a tessellation of the Hajós graph. This tessellation contains the following set of edges $\mathcal{E}(\mathcal{T}_1) = \{\{0, 1\}, \{0, 2\}, \{1, 2\}, \{3, 4\}\}$. The *trivial tessellation* is the tessellation with cliques of size 1. The trivial tessellation of the Hajós graph is $\mathcal{T}_{\text{trivial}} = \{\{0\}, \{1\}, \{2\}, \{3\}, \{4\}, \{5\}\}$ and $\mathcal{E}(\mathcal{T}_{\text{trivial}}) = \emptyset$. A tessellation has size 1 only if G is complete, and in this case, the tessellation contains all edges.

Definition 8.2. Given a graph G with edge set $E(G)$, a *graph tessellation cover* of size k of G is a set of k tessellations $\mathcal{T}_1, \ldots, \mathcal{T}_k$, whose union covers the edges, that is, $\cup_{i=1}^{k} \mathcal{E}(\mathcal{T}_i) = E(G)$.

A tessellation cover of the Hajós graph is $\{\mathcal{T}_1, \mathcal{T}_2, \mathcal{T}_3\}$, where

$$\begin{aligned}
\mathcal{T}_1 &= \{\{0, 1, 2\}, \{3, 4\}, \{5\}\},\\
\mathcal{T}_2 &= \{\{1, 3, 4\}, \{2, 5\}, \{0\}\},\\
\mathcal{T}_3 &= \{\{2, 4, 5\}, \{0, 1\}, \{3\}\}.
\end{aligned}$$

Note that $\mathcal{E}(\mathcal{T}_1) \cup \mathcal{E}(\mathcal{T}_2) \cup \mathcal{E}(\mathcal{T}_3)$ is the edge set as can be seen in Fig. 8.1, which describes each tessellation separately with their respective edges.

Definition 8.3. A graph G is called *k-tessellable* if there is a tessellation cover of size at most k. The size of a smallest tessellation cover of G is called *tessellation cover number* and is denoted by $T(G)$.

We have provided a tessellation cover of size 3 for the Hajós graph. Then, it is 3-tessellable. An exhaustive inspection shows that it is not possible to find a tessellation cover of size 2 or 1. Then, $T(\text{Hajós}) = 3$.

Exercise 8.1. Find the maximal cliques of a N-cycle, and show that this graph is 2-tessellable if N is even and is 3-tessellable if N is odd. Find the *clique graph* of a N-cycle, and show the clique graph is 2-colorable if N is even and is 3-colorable if N is odd.

Exercise 8.2. Show that one maximal clique is contained in no tessellation of any minimum tessellation cover of the Hajós graph. Show that the clique graph of the Hajós graph is 4-*colorable*.

Exercise 8.3. Let G be a triangle-free graph. Show that if the *edge-chromatic number* $\chi'(G)$ of G is 3, then G is 3-tessellable.

Exercise 8.4. Let G be a graph. Show that $T(G) \leq \chi'(G)$.

Exercise 8.5. The *wheel graph* is the graph W_n for $n > 2$ with vertex set $\{0, 1, 2, \ldots, n\}$ and edge set $\{\{0, n\}, \{1, n\}, \ldots, \{n-1, n\}, \{0, 1\}, \{1, 2\}, \ldots, \{n-2, n-1\}, \{n-1, 0\}\}$. Show that W_n is $(n/2)$-tessellable if n is even. Show that the chromatic number of the clique graph $K(W_n)$ is n. By adding new edges to W_n, try to provide examples of graph classes that are $(n/3)$-tessellable such that the chromatic number of the clique graph of graphs in this new class is still n. By adding new edges to W_n, can you provide an example of a 3-tessellable graph class with the chromatic number of the clique graph equal to n?

8.2 The Evolution Operator

Let $G(V, E)$ be a connected simple graph so that $|V| = N$. Let $\mathcal{H}^N$ be the N-dimensional Hilbert space spanned by the computational basis $\{|v\rangle : v \in V\}$, that is, each vertex $v \in V$ is associated with a vector $|v\rangle$ of the computational basis. In the staggered model, there is a one-to-one correspondence between the set of vertex labels and states of the computational basis. There is neither coin space nor any other auxiliary space.

How do I obtain the evolution operator of the staggered model? The first step is to find a tessellation cover of G. From now on we suppose that a tessellation cover $\{\mathcal{T}_1, \ldots, \mathcal{T}_k\}$ of size k is known. There is a method to associate a tessellation $\mathcal{T}$ with a Hermitian operator H acting on $\mathcal{H}^N$. Suppose that tessellation $\mathcal{T}$ has p polygons each one denoted by α_j, that is, $\mathcal{T} = \{\alpha_j : 1 \leq j \leq p\}$. We associate a unit vector with each polygon as follows

$$|\alpha_j\rangle = \frac{1}{\sqrt{|\alpha_j|}} \sum_{\ell \in \alpha_j} |\ell\rangle, \tag{8.1}$$

where $|\alpha_j|$ is the number of vertices in polygon α_j. The Hermitian operator associated with $\mathcal{T}$ is defined by

$$H = 2\sum_{j=1}^{p} |\alpha_j\rangle\langle\alpha_j| - I. \tag{8.2}$$

For instance, the polygons of tessellation $\mathcal{T}_1 = \{\{0, 1, 2\}, \{3, 4\}, \{5\}\}$ of the Hajós graph are associated with the vectors

$$\begin{aligned}
|\alpha_1\rangle &= \frac{1}{\sqrt{3}}\left(|0\rangle + |1\rangle + |2\rangle\right), \\
|\alpha_2\rangle &= \frac{1}{\sqrt{2}}\left(|3\rangle + |4\rangle\right), \\
|\alpha_3\rangle &= |5\rangle,
\end{aligned}$$

and tessellation $\mathcal{T}_1$ is associated with the Hermitian operator

$$H_1 = \begin{bmatrix} -\frac{1}{3} & \frac{2}{3} & \frac{2}{3} & 0 & 0 & 0 \\ \frac{2}{3} & -\frac{1}{3} & \frac{2}{3} & 0 & 0 & 0 \\ \frac{2}{3} & \frac{2}{3} & -\frac{1}{3} & 0 & 0 & 0 \\ 0 & 0 & 0 & 0 & 1 & 0 \\ 0 & 0 & 0 & 1 & 0 & 0 \\ 0 & 0 & 0 & 0 & 0 & 1 \end{bmatrix}.$$

The evolution operator of the staggered model[1] associated with a tessellation cover $\{\mathcal{T}_1, \ldots, \mathcal{T}_k\}$ is

$$U = \mathrm{e}^{\mathrm{i}\theta_k H_k} \ldots \mathrm{e}^{\mathrm{i}\theta_1 H_1}, \tag{8.3}$$

where θ_j for $1 \leq j \leq k$ are angles and H_j is associated with tessellation $\mathcal{T}_j$ for each j. Note that $\mathrm{e}^{\mathrm{i}\theta_j H_j}$ is unitary because H_j is Hermitian. Besides, since $H_j^2 = I$, each term in (8.3) can be expanded as

$$\mathrm{e}^{\mathrm{i}\theta_j H_j} = \cos\theta_j\, I + \mathrm{i}\sin\theta_j\, H_j. \tag{8.4}$$

The evolution operator of any quantum walk model on a graph G must be the product of *local operators* with respect to G. The formal definition of local operator in the staggered model is as follows.

Definition 8.4. A linear operator H is *local* with respect to a graph G when $\langle v_2|H|v_1\rangle = 0$ if vertices v_1 and v_2 ($v_1 \neq v_2$) are nonadjacent.

Let us show that operator H given by (8.2) associated with tessellation $\mathcal{T}$ is a *local operator*. Suppose that v_1 and v_2 are nonadjacent. A vertex belongs to exactly one polygon of a tessellation $\mathcal{T}$. If v_1 belongs to polygon $\alpha_1 \in \mathcal{T}$, then v_2 does not belong

[1] In the literature, when at least one angle θ_j is not $\pi/2$, the model is called *staggered model with Hamiltonians*.

to polygon α_1 because v_2 is not adjacent to v_1. Then, $\langle v_2|H|v_1\rangle = 2\langle\alpha_1|v_1\rangle\langle v_2|\alpha_1\rangle - \langle v_2|v_1\rangle = 0$. Using (8.4), we conclude that the same argumentation is true for $e^{i\theta H}$. Then, U given by (8.3) is a product of local unitary operators.

A staggered quantum walk based on a tessellation cover of size k (or on a k-tessellable graph) is called *k-tessellable quantum walk*.

Exercise 8.6. Show that if vectors $|\alpha_j\rangle$ given by Eq. (8.1) are associated with polygons α_j of a tessellation $\mathcal{T}$, then $\langle\alpha_j|\alpha_{j'}\rangle = \delta_{jj'}$. Show that operator H defined in Eq. (8.2) is Hermitian and unitary. Show that $H^2 = I$.

Exercise 8.7. Prove that if $H^2 = I$, then $\exp(i\theta H) = \cos(\theta)\, I + i\sin(\theta)\, H$.

Exercise 8.8. Consider the complete graph K_N. Let $\mathcal{T}$ a tessellation of K_N consisting of a single set that covers all vertices. Show that operator H defined in Eq. (8.2) is the *Grover operator*.

Exercise 8.9. Show that the $(+1)$-eigenvectors $|\psi_x\rangle$ of H, given by (8.2), obey the following properties: (1) If the ith entry of $|\psi_x\rangle$ for a fixed x is nonzero, then the ith entries of the other $(+1)$-eigenvectors of H are zero, and (2) vector $\sum_x |\psi_x\rangle$ has no zero entry.

Exercise 8.10. Let $\{\mathcal{T}_1, \ldots, \mathcal{T}_k\}$ be a graph tessellation cover of graph $G(V, E)$. Let $G_j(V, E_j)$ be a subgraph of $G(V, E)$, where $E_j = \mathcal{E}(\mathcal{T}_j)$ for $1 \le j \le k$.

1. Show that an entry of the *adjacency matrix* A_j of G_j is zero if and only if the corresponding entry of H, given by (8.2), is zero.

2. Define the operator W by

$$W = e^{i\theta_k A_k} \ldots e^{i\theta_1 A_1},$$

where θ_j are angles. Show that W is the product of local unitary operators. Conclude that W is the evolution operator of a well-defined *discrete-time quantum walk*.

8.3 Staggered Walk on the Line

One of the simplest examples of a 2-tessellable staggered quantum walk is on the one-dimensional infinite lattice. A minimum tessellation cover of the one-dimensional lattice is the set of two tessellations depicted in Fig. 8.2. The first tessellation is $\mathcal{T}_0 = \{\alpha_x : x \in \mathbb{Z}\}$ where $\alpha = \{2x, 2x+1\}$, and the second is $\mathcal{T}_1 = \{\beta_x : x \in \mathbb{Z}\}$ where $\beta_x = \{2x+1, 2x+2\}$. Note that the union of the cliques is the vertex set for each tessellation, that is,

$$\bigcup_{x=-\infty}^{\infty} \alpha_x = \bigcup_{x=-\infty}^{\infty} \beta_x = \mathbb{Z},$$

Fig. 8.2 One-dimensional lattice with two tessellations α (red) and β (blue). For a fixed x, polygon $\alpha_x = \{2x, 2x+1\}$ is the set of vertices incident to the red edge with label α_x. Polygon $\beta_x = \{2x+1, 2x+2\}$ is the set of vertices incident to the blue edge with label β_x

and, very importantly, the tessellation cover $\{\mathcal{T}_0, \mathcal{T}_1\}$ covers the edge set because the red edges are in tessellation $\mathcal{T}_0$ and the blue edges are in $\mathcal{T}_1$, as can be seen in Fig. 8.2. This shows that the one-dimensional lattice is 2-tessellable.

The evolution operator for the case with $\theta_0 = \theta_1 = \theta$ is given by

$$U = \mathrm{e}^{\mathrm{i}\theta H_1}\mathrm{e}^{\mathrm{i}\theta H_0}, \tag{8.5}$$

where

$$H_0 = 2\sum_{x=-\infty}^{\infty} |\alpha_x\rangle\langle\alpha_x| - I, \tag{8.6}$$

$$H_1 = 2\sum_{x=-\infty}^{\infty} |\beta_x\rangle\langle\beta_x| - I, \tag{8.7}$$

and

$$|\alpha_x\rangle = \frac{|2x\rangle + |2x+1\rangle}{\sqrt{2}}, \tag{8.8}$$

$$|\beta_x\rangle = \frac{|2x+1\rangle + |2x+2\rangle}{\sqrt{2}}. \tag{8.9}$$

U acts on Hilbert space $\mathcal{H}$, whose computational basis is $\left\{|x\rangle : x \in \mathbb{Z}\right\}$.

We start the analysis of this walk by calculating the probability distribution after t time steps, which is given by

$$p(x,t) = \left|\left\langle x \middle| \psi(t)\right\rangle\right|^2, \tag{8.10}$$

where

$$|\psi(t)\rangle = U^t|\psi(0)\rangle, \tag{8.11}$$

and $|\psi(0)\rangle$ is the initial state. To calculate $p(x,t)$, we split the vertex set into even and odd nodes, so that

$$|\psi(t)\rangle = \sum_{x=-\infty}^{\infty} \left(\psi_{2x}(t)\,|2x\rangle + \psi_{2x+1}(t)\,|2x+1\rangle\right), \tag{8.12}$$

where $\psi_{2x}(t)$ are the amplitudes at even nodes and $\psi_{2x+1}(t)$ at odd nodes. Then,

$$p(2x,t) = |\psi_{2x}(t)|^2 ,$$
$$p(2x+1,t) = |\psi_{2x+1}(t)|^2 .$$

Now we obtain recursive equations for $\psi_{2x}(t)$ and $\psi_{2x+1}(t)$. Note that

$$\psi_{2x}(t) = \langle 2x | U | \psi(t-1) \rangle$$

and using the expression of U and Eq. (8.12), we obtain

$$\psi_{2x}(t) = \sum_{x'} \psi_{2x'}(t-1) \langle 2x | \mathrm{e}^{\mathrm{i}\theta H_1} \mathrm{e}^{\mathrm{i}\theta H_0} | 2x' \rangle + \sum_{x'} \psi_{2x'+1}(t-1) \langle 2x | \mathrm{e}^{\mathrm{i}\theta H_1} \mathrm{e}^{\mathrm{i}\theta H_0} | 2x'+1 \rangle .$$

Using the completeness relation

$$I = \sum_{x''} \left(|2x''\rangle\langle 2x''| + |2x''+1\rangle\langle 2x''+1| \right)$$

between $\mathrm{e}^{\mathrm{i}\theta H_1}$ and $\mathrm{e}^{\mathrm{i}\theta H_0}$, we obtain

$$\begin{aligned}\psi_{2x}(t) = &\sum_{x'x''} \psi_{2x'}(t-1) \langle 2x | \mathrm{e}^{\mathrm{i}\theta H_1} | 2x'' \rangle \langle 2x'' | \mathrm{e}^{\mathrm{i}\theta H_0} | 2x' \rangle + \\ &\sum_{x'x''} \psi_{2x'}(t-1) \langle 2x | \mathrm{e}^{\mathrm{i}\theta H_1} | 2x''+1 \rangle \langle 2x''+1 | \mathrm{e}^{\mathrm{i}\theta H_0} | 2x' \rangle + \\ &\sum_{x'x''} \psi_{2x'+1}(t-1) \langle 2x | \mathrm{e}^{\mathrm{i}\theta H_1} | 2x'' \rangle \langle 2x'' | \mathrm{e}^{\mathrm{i}\theta H_0} | 2x'+1 \rangle + \\ &\sum_{x'x''} \psi_{2x'+1}(t-1) \langle 2x | \mathrm{e}^{\mathrm{i}\theta H_1} | 2x''+1 \rangle \langle 2x''+1 | \mathrm{e}^{\mathrm{i}\theta H_0} | 2x'+1 \rangle .\end{aligned}$$

Exercise 8.11. Show that $H_0|2x\rangle = |2x+1\rangle$ and $H_1|2x\rangle = |2x-1\rangle$. Using $H_0^2 = H_1^2 = I$, calculate $H_0|2x+1\rangle$ and $H_1|2x-1\rangle$.

Using Eqs. (8.6)–(8.9) and Exercise 8.11, we obtain

$$\langle 2x \,|\mathrm{e}^{\mathrm{i}\theta H_0}|\, 2x' \rangle = \langle 2x+1 \,|\mathrm{e}^{\mathrm{i}\theta H_0}|\, 2x'+1 \rangle = \cos\theta \; \delta_{xx'},$$
$$\langle 2x \,|\mathrm{e}^{\mathrm{i}\theta H_0}|\, 2x'+1 \rangle = \langle 2x+1 \,|\mathrm{e}^{\mathrm{i}\theta H_0}|\, 2x' \rangle = \mathrm{i}\sin\theta \; \delta_{xx'},$$

for the local operator of the red tessellation and

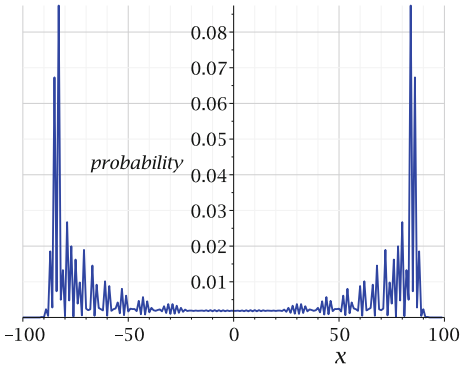

Fig. 8.3 Probability distribution after 50 steps with $\theta = \pi/3$ and initial condition $(|0\rangle + |1\rangle)/\sqrt{2}$

$$\begin{aligned}\left\langle 2x \left| e^{i\theta H_1} \right| 2x' \right\rangle = \left\langle 2x+1 \left| e^{i\theta H_1} \right| 2x'+1 \right\rangle &= \cos\theta\ \delta_{xx'},\\ \left\langle 2x \left| e^{i\theta H_1} \right| 2x'+1 \right\rangle &= i\sin\theta\ \delta_{x,x'+1},\\ \left\langle 2x+1 \left| e^{i\theta H_1} \right| 2x' \right\rangle &= i\sin\theta\ \delta_{x,x'-1},\end{aligned}$$

for the local operator of the blue tessellation. Replacing those results in the last expression of $\psi_{2x}(t)$, we obtain

$$\begin{aligned}\psi_{2x}(t) = &\cos^2\theta\ \psi_{2x}(t-1) - \sin^2\theta\ \psi_{2x-2}(t-1) + \\ &i\cos\theta\ \sin\theta\left(\psi_{2x+1}(t-1) + \psi_{2x-1}(t-1)\right).\end{aligned} \tag{8.13}$$

Analogously, the recursive equation for the amplitudes at the odd sites is

$$\begin{aligned}\psi_{2x+1}(t) = &i\cos\theta\ \sin\theta\left(\psi_{2x}(t-1) + \psi_{2x+2}(t-1)\right) + \\ &\cos^2\theta\ \psi_{2x+1}(t-1) - \sin^2\theta\ \psi_{2x+3}(t-1).\end{aligned} \tag{8.14}$$

Let us choose the initial condition

$$|\psi(0)\rangle = \frac{|0\rangle + |1\rangle}{\sqrt{2}}, \tag{8.15}$$

that is, the only nonzero amplitudes at $t = 0$ are $\psi_0(0) = \psi_1(0) = 1/\sqrt{2}$. Using Eqs. (8.13) and (8.14), we obtain the probability distribution depicted in Fig. 8.3.

Exercise 8.12. Obtain Eq. (8.14).

8.3.1 Fourier Analysis

In order to find the *spectral decomposition* of the evolution operator, we perform a basis change that takes advantage of the system symmetries. The general method is the following. The first step is to find a *graph tessellation cover*. The next step is to split the vertex set into subsets of equivalent vertices. For example, vertex 0 and vertex 2 on the line are equivalent because both have a red polygon to the right and a blue polygon to the left, as can be seen in Fig. 8.2. In fact, all even vertices are equivalent and the same holds for the odd vertices. The final step is to add up the computational basis vectors corresponding to the vertices of each subset using the Fourier amplitudes.

Let us define the Fourier basis by the vectors

$$\left|\tilde{\psi}_0^k\right\rangle = \sum_{x=-\infty}^{\infty} \mathrm{e}^{-2xk\mathrm{i}} \left|2x\right\rangle, \tag{8.16}$$

$$\left|\tilde{\psi}_1^k\right\rangle = \sum_{x=-\infty}^{\infty} \mathrm{e}^{-(2x+1)k\mathrm{i}} \left|2x+1\right\rangle, \tag{8.17}$$

where $k \in [-\pi, \pi]$. For a fixed k, those vectors define a plane that is invariant under the action of each local evolution operator, which is confirmed in the following way. There are k-dependent parameters $a(k)$, $b(k)$, $c(k)$, $d(k)$ so that

$$H_0\left|\tilde{\psi}_0^k\right\rangle = a(k)\left|\tilde{\psi}_0^k\right\rangle + b(k)\left|\tilde{\psi}_1^k\right\rangle,$$
$$H_0\left|\tilde{\psi}_1^k\right\rangle = c(k)\left|\tilde{\psi}_0^k\right\rangle + d(k)\left|\tilde{\psi}_1^k\right\rangle.$$

This means that in the subspace spanned by $\left|\tilde{\psi}_0^k\right\rangle$ and $\left|\tilde{\psi}_1^k\right\rangle$, H_0 reduces to a two-dimensional matrix

$$\tilde{H}_0^k = \begin{bmatrix} a(k) & c(k) \\ b(k) & d(k) \end{bmatrix}.$$

The k-dependent parameters $a(k)$, $b(k)$, $c(k)$, $d(k)$ can be obtained by acting H_0 on $\left|\tilde{\psi}_0^k\right\rangle$ and $\left|\tilde{\psi}_1^k\right\rangle$. After some algebraic manipulations, we obtain

$$\tilde{H}_0^k = \begin{bmatrix} 0 & \mathrm{e}^{-\mathrm{i}k} \\ \mathrm{e}^{\mathrm{i}k} & 0 \end{bmatrix}. \tag{8.18}$$

Analogously, we can repeat the process for H_1 in order to obtain a two-dimensional matrix $\tilde{H}_1^k$. After the algebraic manipulations, we conclude that $\tilde{H}_1^k = \tilde{H}_0^{(-k)}$.

The plane spanned by $\left|\tilde{\psi}_0^k\right\rangle$ and $\left|\tilde{\psi}_1^k\right\rangle$ for a fixed k is also invariant under the action of $U_0 = \mathrm{e}^{\mathrm{i}\theta H_0}$ and $U_1 = \mathrm{e}^{\mathrm{i}\theta H_1}$. The reduced 2×2 matrices $\tilde{U}_0^k$ and $\tilde{U}_1^k$ can be obtained

by using the fact that $(\tilde{H}_0^k)^2 = (\tilde{H}_1^k)^2 = I$. In fact, $\tilde{U}_0^k = \cos\theta\, I_2 + \mathrm{i}\sin\theta\, \tilde{H}_0^k$, and then

$$\tilde{U}_0^k = \begin{bmatrix} \cos\theta & \mathrm{i}\sin\theta\,\mathrm{e}^{-\mathrm{i}k} \\ \mathrm{i}\sin\theta\,\mathrm{e}^{\mathrm{i}k} & \cos\theta \end{bmatrix} \tag{8.19}$$

and $\tilde{U}_1^k = \tilde{U}_0^{(-k)}$. Finally, the reduced version of the full evolution operator U is obtained from the expression $\tilde{U}_k = \tilde{U}_1^k \tilde{U}_0^k$, yielding

$$\tilde{U}_k = \begin{bmatrix} \cos^2\theta - \sin^2\theta\ \mathrm{e}^{2\mathrm{i}k} & \mathrm{i}\sin 2\theta\ \cos k \\ \mathrm{i}\sin 2\theta\ \cos k & \cos^2\theta - \sin^2\theta\ \mathrm{e}^{-2\mathrm{i}k} \end{bmatrix}. \tag{8.20}$$

The connection between the two-dimensional reduced space and the original Hilbert space is established by

$$U\left|\tilde{\psi}_\ell^k\right\rangle = \sum_{\ell'=0}^{1} \left\langle \ell' \middle| \tilde{U}_k \middle| \ell \right\rangle \left|\tilde{\psi}_{\ell'}^k\right\rangle, \tag{8.21}$$

or in the operator form

$$U = \int_{-\pi}^{\pi} \left(\sum_{\ell,\ell'=0}^{1} \left\langle \ell' \middle| \tilde{U}_k \middle| \ell \right\rangle \left|\tilde{\psi}_{\ell'}^k\right\rangle \left\langle \tilde{\psi}_\ell^k \right| \right) \frac{\mathrm{d}k}{2\pi}. \tag{8.22}$$

Since all information conveyed by U can be obtained from $\tilde{U}_k$ for $k \in [-\pi, \pi]$, we can calculate the eigenvalues and eigenvectors of U from the eigenvalues and eigenvectors of $\tilde{U}_k$. In fact, the eigenvalues of U are the eigenvalues of $\tilde{U}_k$ (Exercise 8.13).

The eigenvalues of $\tilde{U}_k$ are $\mathrm{e}^{\pm\mathrm{i}\lambda}$, where

$$\cos\lambda = \cos^2\theta - \sin^2\theta\ \cos 2k. \tag{8.23}$$

The nontrivial normalized eigenvectors of $\tilde{U}_k$ are

$$\left|v_k^\pm\right\rangle = \frac{1}{\sqrt{C^\pm}} \begin{pmatrix} \sin 2\theta\ \cos k \\ \sin^2\theta\ \sin 2k \pm \sin\lambda \end{pmatrix}, \tag{8.24}$$

where

$$C^\pm = 2\ \sin\lambda\,(\sin\lambda \pm \sin^2\theta\ \sin 2k). \tag{8.25}$$

The normalized eigenvectors of the evolution operator U associated with eigenvalues $\mathrm{e}^{\pm\mathrm{i}\lambda}$ are

$$\left|V_k^\pm\right\rangle = \frac{1}{\sqrt{C^\pm}} \left(\sin 2\theta \cos k \left|\tilde{\psi}_0^k\right\rangle + (\sin^2\theta \sin 2k \pm \sin\lambda) \left|\tilde{\psi}_1^k\right\rangle \right), \tag{8.26}$$

and we can write

$$U = \int_{-\pi}^{\pi} \left(\mathrm{e}^{\mathrm{i}\lambda} \left| V_k^+ \right\rangle \left\langle V_k^+ \right| + \mathrm{e}^{-\mathrm{i}\lambda} \left| V_k^- \right\rangle \left\langle V_k^- \right| \right) \frac{\mathrm{d}k}{2\pi}. \tag{8.27}$$

If we take $|\psi(0)\rangle = |0\rangle$ as the initial condition, the quantum walk state at time t is given by

$$|\psi(t)\rangle = \sum_{x=-\infty}^{\infty} \left(\psi_{2x}(t) \, |2x\rangle + \psi_{2x+1}(t) \, |2x+1\rangle \right), \tag{8.28}$$

where (Exercise 8.15)

$$\psi_{2x}(t) = \sin^2 2\theta \int_{-\pi}^{\pi} \cos^2 k \left(\frac{\mathrm{e}^{\mathrm{i}(\lambda t - 2kx)}}{C^+} + \frac{\mathrm{e}^{-\mathrm{i}(\lambda t + 2kx)}}{C^-} \right) \frac{\mathrm{d}k}{2\pi}, \tag{8.29}$$

and

$$\psi_{2x+1}(t) = \mathrm{i} \sin 2\theta \int_{-\pi}^{\pi} \frac{\cos k \sin \lambda t}{\sin \lambda} \, \mathrm{e}^{-\mathrm{i}(2x+1)k} \, \frac{\mathrm{d}k}{2\pi}. \tag{8.30}$$

The probability distribution is obtained by calculating $p_{2x}(t) = |\psi_{2x}(t)|^2$ and $p_{2x+1}(t) = |\psi_{2x+1}(t)|^2$. The probability distribution is asymmetric in this case (localized initial condition).

Exercise 8.13. Show that the eigenvalues of U are the eigenvalues of $\tilde{U}_k$ and if $|\nu\rangle$ is an eigenvector of $\tilde{U}_k$, then

$$\sum_{\ell=0}^{1} \langle \ell | \nu \rangle \left| \tilde{\psi}_\ell^k \right\rangle$$

is an eigenvector of U.

Exercise 8.14. Use Eq. (8.22) to show that

$$U^t = \int_{-\pi}^{\pi} \left(\sum_{\ell,\ell'=0}^{1} \left\langle \ell' \middle| \tilde{U}_k^t \middle| \ell \right\rangle \left| \tilde{\psi}_{\ell'}^k \right\rangle \left\langle \tilde{\psi}_\ell^k \right| \right) \frac{\mathrm{d}k}{2\pi}.$$

Exercise 8.15. Using $\psi_{2x}(t) = \left\langle 2x \middle| U^t \middle| 0 \right\rangle$ and $\psi_{2x+1}(t) = \left\langle 2x+1 \middle| U^t \middle| 0 \right\rangle$, Eqs. (8.16), (8.17), and (8.23)–(8.27), obtain (8.29) and (8.30).

8.3.2 Standard Deviation

Let X be a *random variable* that assumes values in a *sample space* S. X has an associated probability distribution p, so that X assumes value $x \in S$ with probability $p(X = x)$. In *probability theory*, the *characteristic function* $\varphi_X(k)$ is an alternative

way of describing X and is defined as the *expected value* of $\mathrm{e}^{\mathrm{i}kX}$, that is

$$\varphi_X(k) = \mathbb{E}\big[\mathrm{e}^{\mathrm{i}kX}\big].$$

The nth *moment* of X can be calculated by differentiating $\varphi_X(k)$ n times at $k = 0$ (Exercise 8.16), that is

$$\mathbb{E}[X^n] = (-\mathrm{i})^n \left.\frac{\mathrm{d}^n \varphi_X(k)}{\mathrm{d}k^n}\right|_{k=0}. \tag{8.31}$$

In the context of the staggered quantum walk on the line, if X is the position operator, then $X|x\rangle = x|x\rangle$, that is, $|x\rangle$ is an eigenvector of X, whose eigenvalue is x (the walker's position). If the quantum state of the walker at time t is $|\psi(t)\rangle$, X has an associated probability distribution given by

$$p(X = x) \;=\; \big|\big\langle x\big|\psi(t)\big\rangle\big|^2 .$$

Since X is Hermitian, we can define the unitary operator $\exp(\mathrm{i}kX)$, which plays the role of the characteristic function and can be used to calculate the nth moment of the quantum walk.

In *quantum mechanics*, if the state of the system is $|\psi(t)\rangle$, the expected value of operator $\mathrm{e}^{\mathrm{i}kX}$ at time t is

$$\mathbb{E}[\mathrm{e}^{\mathrm{i}kX}]\big|_t = \big\langle\psi(t)\big|\mathrm{e}^{\mathrm{i}kX}\big|\psi(t)\big\rangle .$$

Using $|\psi(t)\rangle = U^t|\psi(0)\rangle$, the above equation simplifies to

$$\varphi_X(k)\Big|_t = \big\langle\psi(0)\big|(U^\dagger)^t \mathrm{e}^{\mathrm{i}kx} U^t\big|\psi(0)\big\rangle .$$

From now on we assume that the initial condition is localized at the origin, that is,

$$|\psi(0)\rangle = |0\rangle. \tag{8.32}$$

Using Eqs. (8.16) and (8.17), we show that $\left\langle\tilde{\psi}_\ell^k\middle|0\right\rangle = \delta_{\ell\,0}$ for any k. Using Exercise 8.14, we obtain

$$U^t|0\rangle = \int_{-\pi}^{\pi} \sum_{\ell=0}^{1} \left\langle\ell\middle|\tilde{U}_{k'}^t\middle|0\right\rangle \left|\tilde{\psi}_\ell^{k'}\right\rangle \frac{\mathrm{d}k'}{2\pi}. \tag{8.33}$$

Using Eqs. (8.16) and (8.17) again, we show that $\mathrm{e}^{\mathrm{i}kx}\left|\tilde{\psi}_\ell^{k'}\right\rangle = \left|\tilde{\psi}_\ell^{(k'-k)}\right\rangle$. Then,

$$\mathrm{e}^{\mathrm{i}kx}\,U^t|0\rangle = \int_{-\pi}^{\pi} \sum_{\ell=0}^{1} \left\langle \ell \middle| \tilde{U}_{k'}^t \middle| 0 \right\rangle \left| \tilde{\psi}_\ell^{(k'-k)} \right\rangle \frac{\mathrm{d}k'}{2\pi}. \tag{8.34}$$

The complex conjugate of Eq. (8.33) is

$$\langle 0|(U^\dagger)^t = \int_{-\pi}^{\pi} \sum_{\ell'=0}^{1} \left\langle 0 \middle| (\tilde{U}_{k''}^t)^\dagger \middle| \ell' \right\rangle \left\langle \tilde{\psi}_{\ell'}^{k''} \right| \frac{\mathrm{d}k''}{2\pi}. \tag{8.35}$$

Multiplying Eqs. (8.35) and (8.34), using $\left\langle \tilde{\psi}_{\ell'}^{k''} \middle| \tilde{\psi}_\ell^{(k'-k)} \right\rangle = \delta_{\ell\ell'}\,\delta(k+k''-k')$, where $\delta(k+k''-k')$ is the Dirac delta function, and using

$$\int_{-\pi}^{\pi} \left\langle \ell \middle| \tilde{U}_{k'}^t \middle| 0 \right\rangle \delta(k+k''-k')\,\frac{\mathrm{d}k'}{2\pi} = \left\langle \ell \middle| \tilde{U}_{k+k''}^t \middle| 0 \right\rangle, \tag{8.36}$$

we obtain the characteristic function at time t

$$\varphi_X(k)\Big|_t = \int_{-\pi}^{\pi} \langle 0|(\tilde{U}_{k'}^t)^\dagger \tilde{U}_{k+k'}^t|0\rangle\,\frac{\mathrm{d}k'}{2\pi}. \tag{8.37}$$

Using Eq. (8.31) and the fact that

$$\frac{\mathrm{d}f(k+k')}{\mathrm{d}k}\bigg|_{k=0} = \frac{\mathrm{d}f(k')}{\mathrm{d}k'},$$

we obtain an expression for the nth moment at time t

$$\mathbb{E}\left[X^n\right]\Big|_t = (-\mathrm{i})^n \int_{-\pi}^{\pi} \langle 0|\,(\tilde{U}_k^t)^\dagger\,\frac{\mathrm{d}^n \tilde{U}_k^t}{\mathrm{d}k^n}\,|0\rangle\,\frac{\mathrm{d}k}{2\pi}. \tag{8.38}$$

Let $\Lambda_k = \left[\left|v_k^+\right\rangle, \left|v_k^-\right\rangle\right]$ be the matrix of the normalized eigenvectors of $\tilde{U}_k$. Then,

$$\tilde{U}_k = \Lambda_k D\left[\mathrm{e}^{\pm\mathrm{i}\lambda}\right]\Lambda_k^\dagger,$$

where $D\left[\mathrm{e}^{\pm\mathrm{i}\lambda}\right]$ is the 2×2 diagonal matrix of the eigenvalues of $\tilde{U}_k$. Likewise,

$$\tilde{U}_k^t = \Lambda_k D\left[\mathrm{e}^{\pm\mathrm{i}\lambda t}\right]\Lambda_k^\dagger$$

because $\Lambda_k^\dagger\Lambda_k = I$. The derivative of $\tilde{U}_k^t$ with respect to k would produce three terms (product rule) but we consider only the term with the derivative of $D\left[\mathrm{e}^{\pm\mathrm{i}\lambda t}\right]$, that is

$$\frac{\mathrm{d}^n \tilde{U}_k^t}{\mathrm{d}k^n} = \Lambda_k \frac{\mathrm{d}^n D\left[\mathrm{e}^{\pm \mathrm{i}\lambda t}\right]}{\mathrm{d}k^n} \Lambda_k^\dagger + O\left(t^{n-1}\right),$$

because the derivative of Λ_k with respect to k does not depend of t and can be disregarded for large t when compared with the derivative of $D\left[\mathrm{e}^{\pm \mathrm{i}\lambda t}\right]$. Since $D\left[\mathrm{e}^{\pm \mathrm{i}\lambda t}\right]$ is a diagonal matrix, the last equation reduces to

$$\frac{\mathrm{d}^n \tilde{U}_k^t}{\mathrm{d}k^n} = \Lambda_k \begin{bmatrix} \mathrm{i}^n t^n \left(\frac{\mathrm{d}\lambda}{\mathrm{d}k}\right)^n \mathrm{e}^{\mathrm{i}\lambda t} & 0 \\ 0 & (-\mathrm{i})^n t^n \left(\frac{\mathrm{d}\lambda}{\mathrm{d}k}\right)^n \mathrm{e}^{-\mathrm{i}\lambda t} \end{bmatrix} \Lambda_k^\dagger + O\left(t^{n-1}\right).$$

Again, we are keeping only the dominant term for large t. When n is even, the last equation reduces to

$$\frac{\mathrm{d}^n \tilde{U}_k^t}{\mathrm{d}k^n} = \mathrm{i}^n t^n \left(\frac{\mathrm{d}\lambda}{\mathrm{d}k}\right)^n \tilde{U}_k^t + O\left(t^{n-1}\right).$$

Replacing in (8.38), we obtain

$$\mathbb{E}\left[X^{2n}\right]\Big|_t = t^{2n} \int_{-\pi}^{\pi} \left(\frac{\mathrm{d}\lambda}{\mathrm{d}k}\right)^{2n} \frac{\mathrm{d}k}{2\pi} + O\left(t^{2n-1}\right). \tag{8.39}$$

Using (8.23), we obtain

$$\frac{\mathrm{d}\lambda}{\mathrm{d}k} = -\frac{2\sin^2\theta \sin 2k}{\sin\lambda}. \tag{8.40}$$

The second moment is

$$\mathbb{E}\left[X^2\right] = 4\left(1 - |\cos\theta|\right) t^2 + O(t). \tag{8.41}$$

The odd moments are given by (Exercise 8.17)

$$\mathbb{E}\left[X^{2n-1}\right] = \frac{1}{2t}\,\mathbb{E}\left[X^{2n}\right] + O\left(t^{2n-2}\right). \tag{8.42}$$

The standard deviation is defined as

$$\sigma = \sqrt{\mathbb{E}[X^2] - \mathbb{E}[X]^2}. \tag{8.43}$$

Using (8.42), we obtain

$$\sigma = \sqrt{\mathbb{E}[X^2]}\sqrt{1 - \frac{\mathbb{E}[X^2]}{4t^2}}. \tag{8.44}$$

It simplifies asymptotically to

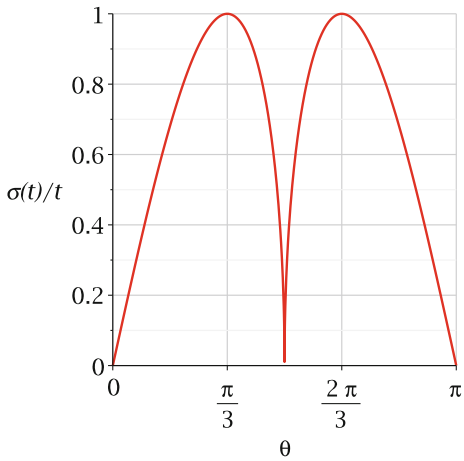

Fig. 8.4 Plot of the asymptotic slope of the standard deviation as a function of θ

$$\sigma = 2\sqrt{|\cos\theta|}\sqrt{1-|\cos\theta|}\; t. \tag{8.45}$$

The standard deviation is proportional to t asymptotically, and the slope depends on θ. It is interesting to find θ that corresponds to the maximum slope. Figure 8.4 shows that there are two critical values $\theta_{\max} = \pi/3$ and $2\pi/3$, which are found by calculating the derivative of $\sigma(t)/t$ with respect to θ and equating to zero, yielding equations $\cos(\theta_{\max}) = \pm 1/2$. The slope is 1 when θ is equal to the critical values.

When $\theta = 0$, $\pi/2$, and π, the standard deviation does not depend on t. These are limiting cases that result in no spreading of the wave function. Either the walker stays put ($\theta = 0$ or π) or the walker moves but the first and second moments are equal.

Exercise 8.16. Use the Taylor expansion of the exponential function and the linearity of the expectation operator $\mathbb{E}$ to obtain Eq. (8.31).

Exercise 8.17. The goal of this exercise is to calculate the odd moments. Use Eqs. (8.24) and (8.40) to show that

$$\langle 0|\Lambda_k \begin{bmatrix} 1 & 0 \\ 0 & -1 \end{bmatrix} \Lambda_k^\dagger |0\rangle = \frac{1}{2}\frac{\mathrm{d}\lambda}{\mathrm{d}k}.$$

Using this result to show that

$$\langle 0| \left(\tilde{U}_k^t\right)^\dagger \frac{\mathrm{d}^{2n-1}\tilde{U}_k^t}{\mathrm{d}k^{2n-1}} |0\rangle = \mathrm{i}^{2n-1} t^{2n-1} \left(\frac{\mathrm{d}\lambda}{\mathrm{d}k}\right)^{2n} + O\left(t^{2n-2}\right).$$

Use this result, Eqs. (8.38) and (8.39), to obtain Eq. (8.42).

Further Reading

Earlier papers that addressed the idea of having a *coinless* quantum walk are [20, 111, 135, 236, 256, 266, 293, 307]. The *staggered model*, which is based on the concept of *graph tessellation*, was introduced in [269]. Staggered quantum walks on graphs were analyzed in [264], which characterized 2-tessellable graphs. The version with Hamiltonians was presented in [267], and an experimental proposal using superconducting resonators was presented in [243]. Search algorithms on two-dimensional finite lattices using the staggered model with Hamiltonians was addressed in [268]. The spectrum of the evolution operator of 2-tessellable walks was analyzed in [184, 189]. The connection among the discrete-time models (staggered, coined, and Szegedy's model) was addressed in Refs. [187, 263, 270]. The connection between the continuous-time and staggered models was addressed in [89], which shows that for some graphs there is a discretization of the continuous-time evolution operator into a product of local operators that corresponds to a tessellation cover of the original graph. Using this connection, [89] presented graphs that admit *perfect state transfer* in the staggered model.

The definition of *graph tessellation cover* encompasses at the same time the sets of vertices and edges in a dual way, and besides, it employs the concept of *clique* widely studied in graph theory. For that reason, graph theorists may have interest in addressing this issue. For instance, Ref. [5] analyzed the graph tessellation as a problem in graph theory and obtained results regarding characterization, bounds, and hardness.

Chapter 9
Spatial Search Algorithms

An interesting problem in the area of algorithms is the *spatial search problem*, which aims to find one or more marked points in a finite physical region that can be modeled by a graph, for instance, a *two-dimensional finite lattice*, so that the vertices of the graph are the places one can search and the edges are the pathways one can use to move from one vertex to an adjacent one. The quantum version of this problem was analyzed by *Benioff* in a very concrete way. He imagined a *quantum robot* that moves to adjacent vertices in a time unit. The position of the robot can be a superposition of a finite number of places (vertices). How many steps does the robot need to take in order to find a *marked vertex* with high probability? In this problem, we suppose that the robot only finds the marked vertex by stepping on it and the robot has no hint about the direction of the marked vertex and no compass and no memory.

We compare the time that the quantum robot takes to find a marked vertex with the time a *classical random robot* takes. In the classical case, if the robot is on a vertex and there are d incident edges, a d-sided dice is tossed to determine which edge to use as the pathway to the next vertex. After reaching the next vertex, the process starts over. This means that the classical robot wanders aimlessly around the graph in hoping to step on a marked vertex. The dynamic is modeled by a *random walk*: The initial condition is usually the uniform probability distribution and the average time to find a marked vertex is called the *hitting time*. For instance, on the two-dimensional lattice (or *grid*) with N vertices and cyclic boundary conditions,[1] if there is only one marked vertex, the hitting time is $O(N \ln N)$. If the walker departs from a random vertex walking at random on the lattice, the walker will visit on average $O(N \ln N)$ vertices before stepping on the marked vertex.

On a finite two-dimensional lattice, a quantum robot can do better. It can find a marked site quicker than the classical random robot. In fact, the quantum robot finds a marked site taking $O(\sqrt{N \ln N})$ steps when the dynamic is described by a quantum walk, which replaces the role performed by the classical random walk. In

[1] A two-dimensional lattice with cyclic boundary conditions has the form a discrete *torus*.

© Springer Nature Switzerland AG 2018

R. Portugal, *Quantum Walks and Search Algorithms*, Quantum Science and Technology, https://doi.org/10.1007/978-3-319-97813-0_9

the quantum case, besides calculating the number of steps, we need to calculate the *success probability*, which usually decreases when the system size increases.

In this chapter, we describe in detail how to build quantum algorithms for the spatial search problem on graphs based on discrete-time quantum walks and how to analyze their time complexity. Coined quantum walks on two-dimensional lattices and on *hypercubes* are used as examples. At the end, we show that Grover's algorithm can be seen as a spatial search problem on the *complete graph* with loops using the *coined model* and on the complete graph without loops using the *staggered model*.

9.1 Quantum-Walk-Based Search Algorithms

Consider a graph Γ, where $V(\Gamma)$ is the set of vertices and $|V(\Gamma)| = N$. Let $\mathcal{H}^N$ be the N-dimensional Hilbert space associated with the graph, that is, the computational basis of $\mathcal{H}^N$ is $\{|v\rangle \,:\, 0 \leq v \leq N-1\}$. We use the *state space postulate* of *quantum mechanics* to make this association because the vertices are the possible places the particle can be in the classical sense. Then, each location is associated with a vector from an orthonormal basis. The postulate states that the "position" of the particle when the system is isolated from the environment can be a superposition of the basis vectors.

How do we mark vertices in a graph? Borrowing the idea from Grover's algorithm, we have to use the unitary operator that acts as the identity on the states corresponding to the unmarked vertices and inverts the sign of the states corresponding to the marked vertices. Let M be the set of marked vertices. Then, the unitary operator we need is

$$R = I - 2\sum_{v \in M} |v\rangle\langle v|. \tag{9.1}$$

This operator plays the same role of the oracle of Grover's algorithm, as described in Chap. 4. We focus on the case with only one marked vertex because the multimarked case depends heavily on the arrangement of the marked vertices even on translation-invariant graphs. There is no loss of generality by choosing the label of the marked vertex as 0 because we can mark an arbitrary vertex and choose the labels of the vertices after. In this case, the oracle is written as

$$R = I - 2|0\rangle\langle 0|. \tag{9.2}$$

The next step is to build an evolution operator U associated with the graph. We suppose at this stage that no vertex is marked. A quantum walk model is a recipe to build this kind of unitary operator U and, in this case, U is a product of local operators. The dimension of U in the coined model is larger than N. We address this issue later on when we consider two-dimensional lattices. For now, we suppose that U is defined on Hilbert space $\mathcal{H}^N$.

The evolution operator U' of a *quantum-walk-based search algorithm* is

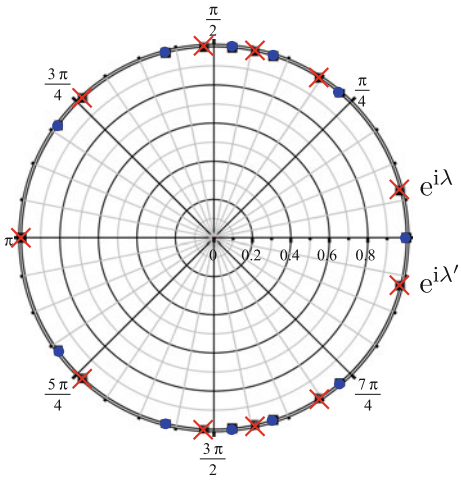

Fig. 9.1 Eigenvalues of U (blue points) and U' (red crosses) for the two-dimensional lattice with 25 vertices. Note that the eigenvalues are interlaced. The eigenvalues $e^{i\lambda}$ and $e^{i\lambda'}$ are the closest to 1 and they tend to 1 when N increases

$$U' = UR, \tag{9.3}$$

which is called *modified evolution operator* to distinguish from U. In this context, the walker starts at an initial state[2] $|\psi(0)\rangle$ and evolves driven by U', that is, the walker's state after t steps is $|\psi(t)\rangle = (U')^t|\psi(0)\rangle$.

Summing up, the *spatial search algorithm* on a graph uses a modified evolution operator $U' = UR$, where U is the standard evolution operator of a quantum walk on the graph with no marked vertex and R is the unitary operator that inverts the sign of the marked vertex, given by Eq. (9.2). There is a slight variation of this method, which employs the modified evolution operator $U' = U^a R$, where a is an integer that may depend on N. This variation is employed in the algorithm for solving the *element distinctness problem*, which is described in Chap. 10.

Most spatial search algorithms can be described asymptotically (large N) using only two eigenvectors of the modified evolution operator U'. One of them is associated with the eigenvalue with the smallest positive argument. Let $\exp(i\lambda_1)$, ..., $\exp(i\lambda_k)$ be the eigenvalues U' such that $\lambda_1, ..., \lambda_k \in [-\pi, \pi]$. Select the smallest positive element of the set $\{\lambda_1, ..., \lambda_k\}$. Let us call this smallest element by λ and the unit eigenvector by $|\lambda\rangle$, that is, $U'|\lambda\rangle = \exp(i\lambda)|\lambda\rangle$ and $\langle\lambda|\lambda\rangle = 1$. Eigenvalue $e^{i\lambda}$ is shown in Fig. 9.1 for the two-dimensional lattice with 25 vertices. Now select the largest negative element of the set $\{\lambda_1, ..., \lambda_k\}$. Let us call this largest negative element by λ' and the unit eigenvector by $|\lambda'\rangle$, that is, $U'|\lambda'\rangle = \exp(i\lambda')|\lambda'\rangle$ and $\langle\lambda'|\lambda'\rangle = 1$. In most spatial search algorithms, $\lambda' = -\lambda$ and vectors $|\lambda\rangle$ and $|\lambda'\rangle$ are the only eigenvectors of U' that we need to analyze the performance of the algorithm. If the graph on which the quantum walk takes place is simple enough, such as the complete graph, we can calculate λ and λ' without much effort. For an arbitrary graph, we describe a technique we call *principal eigenvalue technique*, which allows

[2]The uniform superposition is the most used initial state because it is an unbiased one.

to find λ and λ'. This technique requires the knowledge of the eigenvectors of U that have nonzero overlap with the marked vertex. Besides, the technique can be applied only if three conditions, described in the next section, are fulfilled.

9.2 Analysis of the Time Complexity

The complexity analysis of the spatial search algorithm is based on two quantities: The *running time* and the *success probability*. The expression of the probability of finding the marked vertex 0 after t steps is

$$p(t) = \left|\langle 0|\psi(t)\rangle\right|^2, \tag{9.4}$$

where $|\psi(t)\rangle$ is the state of the search algorithm after t steps. Since $|\psi(t)\rangle = (U')^t|\psi(0)\rangle$, where $|\psi(0)\rangle$ is the initial state, we have

$$p(t) = \left|\langle 0|(U')^t|\psi(0)\rangle\right|^2. \tag{9.5}$$

The goal now is to determine the optimal number of steps t_{opt}, which is the one that maximizes $p(t)$. The running time is t_{opt} and the success probability is $p(t_{\text{opt}})$.

We will not attempt to calculate the spectral decomposition of U' but instead we focus on the eigenvectors $|\lambda\rangle$ and $|\lambda'\rangle$. The eigenspace spanned by the other eigenvectors will be disregarded, which cause some supposedly small error. If the error is large, we cannot use the *principal eigenvalue technique*. The spectral decomposition of U' would be

$$U' = \mathrm{e}^{\mathrm{i}\lambda}|\lambda\rangle\langle\lambda| + \mathrm{e}^{\mathrm{i}\lambda'}|\lambda'\rangle\langle\lambda'| + U_{\text{tiny}}, \tag{9.6}$$

where U_{tiny} acts nontrivially only on the subspace orthogonal to the plane spanned by $\{|\lambda\rangle, |\lambda'\rangle\}$. After raising the previous equation to power t we obtain

$$(U')^t = \mathrm{e}^{\mathrm{i}\lambda t}|\lambda\rangle\langle\lambda| + \mathrm{e}^{\mathrm{i}\lambda' t}|\lambda'\rangle\langle\lambda'| + U_{\text{tiny}}^t. \tag{9.7}$$

Now we do the sandwich with vectors $|0\rangle$ and $|\psi(0)\rangle$, obtaining

$$p(t) = \left|\mathrm{e}^{\mathrm{i}\lambda t}\,\langle 0|\lambda\rangle\langle\lambda|\psi(0)\rangle + \mathrm{e}^{\mathrm{i}\lambda' t}\,\langle 0|\lambda'\rangle\langle\lambda'|\psi(0)\rangle + \epsilon\right|^2, \tag{9.8}$$

where $\epsilon = \langle 0|U_{\text{tiny}}^t|\psi(0)\rangle$. The *principal eigenvalue technique* can be applied when $|\epsilon|$ is much smaller than the absolute value of the remaining terms in the asymptotic limit (large N). From now on we will disregard ϵ and in the applications for specific graphs, we show that the above condition is fulfilled by proving that $\lim_{N\to\infty}|\epsilon| = 0$.

We need to find λ, λ', the inner products $\langle 0|\lambda\rangle$, $\langle\lambda|\psi(0)\rangle$, and their primed versions. We focus our attention on the calculation of λ because λ' and the inner products

will be obtained as a byproduct. Our goal now is to find λ supposing that we have already obtained the spectral decomposition of U, that is, we suppose that the set of vectors $|\psi_k\rangle$ is an orthonormal eigenbasis of U and $\exp(\mathrm{i}\phi_k)$ are the corresponding eigenvalues, that is $U|\psi_k\rangle = \exp(\mathrm{i}\phi_k)|\psi_k\rangle$. Then, we have $I = \sum_k |\psi_k\rangle\langle\psi_k|$. Making the sandwich with vectors $|0\rangle$ and $|\lambda\rangle$, we obtain

$$\langle 0|\lambda\rangle = \sum_k \langle 0|\psi_k\rangle\langle\psi_k|\lambda\rangle, \tag{9.9}$$

where the sum runs over all values of k. Using expression $\langle\psi_k|U'|\lambda\rangle = \langle\psi_k|UR|\lambda\rangle$, we obtain (Exercise 9.1)

$$\langle\psi_k|\lambda\rangle = \frac{2\langle 0|\lambda\rangle\langle\psi_k|0\rangle}{1-\mathrm{e}^{\mathrm{i}(\lambda-\phi_k)}}, \tag{9.10}$$

which is valid if $\lambda \neq \phi_k$. Using the above equation in (9.9), we obtain

$$\sum_k \frac{2\left|\langle 0|\psi_k\rangle\right|^2}{1-\mathrm{e}^{\mathrm{i}(\lambda-\phi_k)}} = 1. \tag{9.11}$$

The sum must be restricted to k such that $\phi_k \neq \lambda$. For simplicity, we assume that $\phi_k \neq \lambda$ for all k and leave the general case as an exercise. Using that $2/(1-\mathrm{e}^{\mathrm{i}a}) = 1 + \mathrm{i}\sin a/(1-\cos a)$, the imaginary part of Eq. (9.11) implies that

$$\sum_k \left|\langle 0|\psi_k\rangle\right|^2 \frac{\sin(\lambda-\phi_k)}{1-\cos(\lambda-\phi_k)} = 0. \tag{9.12}$$

If the eigenvectors of U that have nonzero overlap with $|0\rangle$ are known, we can calculate λ using the last equation, at least via numerical methods.

To proceed analytically, we suppose that $\lambda \ll \phi_{\min}$ when $N \gg 1$, where $\phi_{\min}$ is the smallest positive value of ϕ_k. We can check the validity of those assumptions in specific applications, confirming the process in hindsight. We have to split the sum (9.12) into two parts:

$$\sum_{\phi_k=0} \left|\langle 0|\psi_k\rangle\right|^2 \frac{\sin\lambda}{1-\cos\lambda} + \sum_{\phi_k\neq 0} \left|\langle 0|\psi_k\rangle\right|^2 \frac{\sin(\lambda-\phi_k)}{1-\cos(\lambda-\phi_k)} = 0, \tag{9.13}$$

corresponding to the sum of terms such that $\phi_k = 0$ and $\phi_k \neq 0$, respectively. Since we are assuming that $\lambda \ll 1$ for large N, the Maclaurin expansion of the term in the first sum is

$$\frac{\sin\lambda}{1-\cos\lambda} = \frac{2}{\lambda} + O(\lambda). \tag{9.14}$$

Assuming $\lambda \ll \phi_{\min}$ for large N, the Taylor expansion of the term in the second sum is

$$\frac{\sin(\lambda-\phi_k)}{1-\cos(\lambda-\phi_k)} = -\frac{\sin\phi_k}{1-\cos\phi_k} - \frac{\lambda}{1-\cos\phi_k} + O(\lambda^2), \tag{9.15}$$

which is valid if $\phi_k \neq 0$.

Using those expansions, Eq. (9.13) reduces to

$$A - B\,\lambda - C\,\lambda^2 = O(\lambda^3), \tag{9.16}$$

where

$$A = 2\sum_{\phi_k=0} \left|\langle 0|\psi_k\rangle\right|^2, \tag{9.17}$$

$$B = \sum_{\phi_k\neq 0} \frac{\left|\langle 0|\psi_k\rangle\right|^2 \sin\phi_k}{1-\cos\phi_k}, \tag{9.18}$$

$$C = \sum_{\phi_k\neq 0} \frac{\left|\langle 0|\psi_k\rangle\right|^2}{1-\cos\phi_k}. \tag{9.19}$$

We can find λ by solving Eq. (9.16), since all quantities necessary to calculate A, B, and C are supposedly known.

Our goal now is to find $\langle 0|\lambda\rangle$. Making a sandwich with $|\lambda\rangle$ on both sides of $I = \sum_k |\psi_k\rangle\langle\psi_k|$, we obtain $1 = \sum_k \left|\langle\psi_k|\lambda\rangle\right|^2$. Using (9.10), we obtain

$$\frac{1}{\left|\langle 0|\lambda\rangle\right|^2} = \sum_k \frac{4\left|\langle 0|\psi_k\rangle\right|^2}{\left|1-\mathrm{e}^{\mathrm{i}(\lambda-\phi_k)}\right|^2}. \tag{9.20}$$

Without loss of generality, we may assume that $\langle 0|\lambda\rangle$ is a positive real number. In fact, if $\langle 0|\lambda\rangle = a\,\mathrm{e}^{\mathrm{i}b}$, where a and b are real numbers and a is positive, we redefine $|\lambda\rangle$ as $\mathrm{e}^{-\mathrm{i}b}|\lambda\rangle$. We are allowed to do this redefinition because a multiple of an eigenvector is also an eigenvector and in this case the norm of the eigenvector does not change. After this redefinition and using that $\left|1-\mathrm{e}^{\mathrm{i}a}\right|^2 = 2(1-\cos a)$, we obtain

$$\frac{1}{\langle 0|\lambda\rangle} = \sqrt{\sum_k \frac{2\left|\langle 0|\psi_k\rangle\right|^2}{1-\cos(\lambda-\phi_k)}}, \tag{9.21}$$

which shows that we have attained our goal since all quantities on the right-hand side of the previous equation are known. This expression can be simplified further. In fact, splitting the sum into two parts, one sum of terms such that $\phi_k = 0$ and another sum of terms such that $\phi_k \neq 0$, expanding in Taylor series and using Eqs. (9.17)–(9.19), we obtain

$$\langle 0|\lambda\rangle = \frac{|\lambda|}{\sqrt{2}\sqrt{A+C\lambda^2}} + O(\lambda). \tag{9.22}$$

Our goal now is to find $\langle\lambda|\psi(0)\rangle$. We choose $|\psi(0)\rangle$ as an eigenvector of U with eigenvalue 1.[3] In this case, we can replace in Eq. (9.10) $|\psi_k\rangle$ by $|\psi(0)\rangle$ and ϕ_k by 0 to obtain

$$\langle\psi(0)|\lambda\rangle = \frac{2\langle 0|\lambda\rangle\langle\psi(0)|0\rangle}{1-\mathrm{e}^{\mathrm{i}\lambda}}. \tag{9.23}$$

Using $2/(1-\mathrm{e}^{\mathrm{i}\lambda}) = 1 + \mathrm{i}\sin\lambda/(1-\cos\lambda)$, we obtain

$$\langle\psi(0)|\lambda\rangle = \langle\psi(0)|0\rangle\langle 0|\lambda\rangle\left(1+\frac{\mathrm{i}\sin\lambda}{1-\cos\lambda}\right), \tag{9.24}$$

which can be simplified further by using Eq. (9.14). All quantities on the right-hand side of the previous equation are known. In fact, $\langle 0|\lambda\rangle$ is given by Eq. (9.22) and λ is given by Eq. (9.16).

The same procedure described in the last paragraphs can be used to calculate λ', $\langle 0|\lambda'\rangle$, and $\langle\psi(0)|\lambda'\rangle$, completing our main goal, which is to obtain all quantities required to calculate $p(t)$ [see Eq. (9.8)].

Exercise 9.1 The goal of this exercise is to obtain Eq. (9.10).

1. Show that if there is only one marked vertex with label 0, then $R|\lambda\rangle = |\lambda\rangle - 2\langle 0|\lambda\rangle|0\rangle$.
2. Show that $\langle\psi_k|\,U = \mathrm{e}^{\mathrm{i}\phi_k}\langle\psi_k|$.
3. Using 1. and 2. show that $\langle\psi_k|UR|\lambda\rangle = \mathrm{e}^{\mathrm{i}\phi_k}\left(\langle\psi_k|\lambda\rangle - 2\langle 0|\lambda\rangle\langle\psi_k|0\rangle\right)$.
4. Show that $\langle\psi_k|U'|\lambda\rangle = \mathrm{e}^{\mathrm{i}\lambda}\langle\psi_k|\lambda\rangle$.
5. Using the previous items and $\langle\psi_k|U'|\lambda\rangle = \langle\psi_k|UR|\lambda\rangle$, obtain Eq. (9.10).

Exercise 9.2 Show that

$$\frac{2}{1-\mathrm{e}^{\mathrm{i}a}} = 1 + \frac{\mathrm{i}\sin a}{1-\cos a}$$

for any angle $a \neq 0$ and

$$\left|1-\mathrm{e}^{\mathrm{i}a}\right|^2 = 2(1-\cos a)$$

for any angle a.

Exercise 9.3 Show that there is one and only one eigenvalue λ. Extend this result to λ'. [Hint: Let $f(\lambda)$ be the left-hand side of Eq. (9.12). Show that $\lim_{\lambda\to 0^+} f(\lambda) = +\infty$ and $\lim_{\lambda\to\phi_{\min}^-} f(\lambda) = -\infty$, where $\phi_{\min}$ is the positive argument of the eigenvalue of U nearest to 1. Next show that $f(\lambda)$ is a monotonically decreasing function.]

[3] If the dimension of the 1-eigenspace of U with nonzero overlap with $|0\rangle$ is greater than one, $|\psi(0)\rangle$ is the diagonal state of this 1-eigenspace.

9.2.1 Case $B = 0$

If the eigenvalues of U come in complex-conjugate pairs, that is, both $e^{i\phi_k}$ and $e^{-i\phi_k}$ are eigenvalues, and the corresponding values of $\left|\langle 0|\psi_k\rangle\right|$ are equal, for instance, when the eigenvector associated with $e^{-i\phi_k}$ is the complex conjugate of the eigenvector associated with $e^{i\phi_k}$, B is zero because Eq. (9.18) contains $\sin(\phi_k)$, which is an antisymmetric function.

When $B = 0$, Eq. (9.16) reduces to

$$\lambda = -\lambda' = \frac{\sqrt{A}}{\sqrt{C}}, \tag{9.25}$$

Equation (9.22) reduces to

$$\langle 0|\lambda\rangle = \langle 0|\lambda'\rangle = \frac{1}{2\sqrt{C}}, \tag{9.26}$$

and Eq. (9.24) reduces to

$$\langle\psi(0)|\lambda\rangle = \langle\lambda'|\psi(0)\rangle = \langle\psi(0)|0\rangle\left(\frac{1}{2\sqrt{C}} + \frac{i}{\sqrt{A}}\right). \tag{9.27}$$

Substituting those results into Eq. (9.8), we obtain

$$p(t) = \frac{\left|\langle 0|\psi(0)\rangle\right|^2}{A\,C}\sin^2\lambda t. \tag{9.28}$$

The running time is the optimal t, which is

$$t_{\text{opt}} = \left\lfloor\frac{\pi}{2\lambda}\right\rfloor \tag{9.29}$$

and the asymptotic success probability is

$$p_{\text{succ}} = \frac{\left|\langle 0|\psi(0)\rangle\right|^2}{A\,C}. \tag{9.30}$$

An important case is when $|\psi(0)\rangle$ is the diagonal state and the only (modulo a multiplicative constant) $(+1)$-eigenvector of U that has nonzero overlap with $|0\rangle$. In this case, $A = 2\left|\langle 0|\psi(0)\rangle\right|^2 = 2/N$ and the running time is

$$t_{\text{opt}} = \left\lfloor\frac{\pi\sqrt{NC}}{2\sqrt{2}}\right\rfloor, \tag{9.31}$$

and the success probability is

$$p_{\text{succ}} = \frac{1}{2\,C}. \tag{9.32}$$

In this case, the complexity of the algorithm is determined by C. For the two-dimensional lattice, $C = O(\ln N)$. The running time is $O\left(\sqrt{N \ln N}\right)$ and the success probability is $O(1/\ln N)$. The best scenario we can hope for is $C = O(1)$, which achieves the Grover lower bound, that is, the running time is $t_{\text{opt}} = O\left(\sqrt{N}\right)$ with constant success probability.

Exercise 9.4 Show that if U has real entries, then $B = 0$.

Exercise 9.5 Use the *amplitude amplification technique* to show that it is possible to obtain a quantum circuit that outputs the marked element with success probability $O(1)$ in $O(C\sqrt{N})$ steps when $|\psi(0)\rangle$ is the diagonal state and the only $(+1)$-eigenvector of U that has nonzero overlap with $|0\rangle$.

9.2.2 Tulsi's Modification

Tulsi described a modification of quantum-walk-based search algorithms that is useful when the success probability tends to zero when N increases. The goal of Tulsi's modification is to define a new evolution operator that on the one hand has the same *running time* of the original algorithm and on the other hand has a constant *success probability* by obtaining a new C so that $C^{\text{NEW}} = O(1)$.

Augment the Hilbert space by one qubit, that is, $\mathcal{H}^{\text{NEW}} = \mathcal{H}^2 \otimes \mathcal{H}^N$ and define a new evolution operator

$$U'' = U^{\text{NEW}} R^{\text{NEW}}, \tag{9.33}$$

where

$$U^{\text{NEW}} = (Z \otimes I_N)\, C_0(U), \tag{9.34}$$

Z is the Pauli matrix σ_z, $C_0(U)$ is the controlled operation that applies U to the state of the second register only if the control (first register) is set to 0, and

$$R^{\text{NEW}} = I_{2N} - 2\left|0^{\text{NEW}}\right\rangle\left\langle 0^{\text{NEW}}\right|, \tag{9.35}$$

where

$$\left|0^{\text{NEW}}\right\rangle = |\eta\rangle|0\rangle \tag{9.36}$$

and $|\eta\rangle$ is a 1-qubit state given by

$$|\eta\rangle = \sin\eta\,|0\rangle + \cos\eta\,|1\rangle, \tag{9.37}$$

where η is a small angle that will be tuned to amplify the success probability. The new initial condition is

$$\left|\psi^{\text{NEW}}(0)\right\rangle = |0\rangle|\psi(0)\rangle. \tag{9.38}$$

The *principal eigenvalue technique* can be employed because oracle R^{NEW} has the same form of oracle R. To calculate A^{NEW}, B^{NEW}, and C^{NEW}, which are given by Eqs. (9.17)–(9.19), we need to know the eigenvalues and eigenvectors of U^{NEW} that have nonzero overlap with $\left|0^{\text{NEW}}\right\rangle$. It is straightforward to check that

$$U^{\text{NEW}}|0\rangle|\psi_k\rangle = \mathrm{e}^{\mathrm{i}\phi_k}|0\rangle|\psi_k\rangle, \tag{9.39}$$

$$U^{\text{NEW}}|1\rangle|\psi_k\rangle = -|1\rangle|\psi_k\rangle, \tag{9.40}$$

where vectors $|\psi_k\rangle$ are the eigenvectors of U. Then, $\{|0\rangle|\psi_k\rangle, |1\rangle|\psi_k\rangle : 0 \le k < N\}$ is an orthonormal eigenbasis of U^{NEW}. Note that the $(+1)$-eigenvectors of U^{NEW} are $|0\rangle|\psi_k\rangle$ for all k such that $\phi_k = 0$, that is, $|\psi_k\rangle$ is a $(+1)$-eigenvector of U.

Suppose that $B^{\text{NEW}} = 0$ (see Exercise 9.9 for the case $B^{\text{NEW}} \neq 0$). The new values of A and C are

$$A^{\text{NEW}} = 2\sin^2(\eta) \sum_{\phi_k=0} \left|\langle 0|\psi_k\rangle\right|^2, \tag{9.41}$$

$$C^{\text{NEW}} = \frac{\cos^2(\eta)}{2} \sum_{\text{all } k} \left|\langle 0|\psi_k\rangle\right|^2 + \sin^2(\eta) \sum_{\phi_k\neq 0} \frac{\left|\langle 0|\psi_k\rangle\right|^2}{1-\cos\phi_k}. \tag{9.42}$$

It is expected that η be small to counteract the increase of the second term as a function of N. In this case, we have

$$A^{\text{NEW}} = \eta^2 A + O\left(\eta^3\right), \tag{9.43}$$

$$C^{\text{NEW}} = \frac{1}{2} + \eta^2 C + O\left(\eta^3\right). \tag{9.44}$$

The new running time t_{opt} is $\pi/2\lambda^{\text{NEW}}$, which reduces to

$$t_{\text{opt}} = \frac{\pi}{2}\sqrt{\frac{C}{A} + \frac{1}{2\eta^2 A}}. \tag{9.45}$$

Using Eq. (9.30) and $\left\langle 0^{\text{NEW}}\middle|\psi^{\text{NEW}}(0)\right\rangle = \sin(\eta)\left\langle 0\middle|\psi(0)\right\rangle$, the new success probability reduces to

$$p_{\text{succ}} = \frac{2\left|\langle 0|\psi(0)\rangle\right|^2}{A\left(1+2\eta^2 C\right)}. \tag{9.46}$$

If there is only one $(+1)$-eigenvector of U with nonzero overlap with $|0\rangle$ (modulo a multiplicative constant), we have $A = 2\left|\langle 0|\psi(0)\rangle\right|^2$. For this case, η that minimizes

$t_{\text{opt}}/p_{\text{succ}}$ is

$$\eta = \frac{1}{2\sqrt{C}}, \tag{9.47}$$

and the running time would be

$$t_{\text{opt}} = \left\lfloor \frac{\pi\sqrt{3}}{2}\sqrt{\frac{C}{A}} \right\rfloor \tag{9.48}$$

and the asymptotic success probability

$$p_{\text{succ}} = \frac{2}{3}.$$

As a final step, one would amplify the probability by running Tulsi's algorithm $(1/p_{\text{succ}})$ times (with intermediate measurements) in order to boost the final success probability.

An alternate strategy is to find η that minimizes $t_{\text{opt}}/\sqrt{p_{\text{succ}}}$, which is $\eta = 1/\sqrt{2C}$ yielding the running time

$$t_{\text{opt}} = \left\lfloor \frac{\pi\sqrt{2}}{2}\sqrt{\frac{C}{A}} \right\rfloor \tag{9.49}$$

and success probability $p_{\text{succ}} = 1/2$. As a final step, one would use the *amplitude amplification technique* to boost the final success probability, which means that Tulsi's algorithm would be repeated $(1/\sqrt{p_{\text{succ}}})$ times (with no intermediate measurements).

A bad strategy would be to adjust η in order to obtain a success probability very close to 1. The strategy is bad because the running time would increase too much.

Exercise 9.6 Show all the details needed to obtain Eqs. (9.41) and (9.42) from Eqs. (9.17) and (9.19) when $B = 0$.

Exercise 9.7 Find η so that the success probability is $p_{\text{succ}} = 3/4$ when there is only one $(+1)$-eigenvector of U that has nonzero overlap with $|0\rangle$; find the running time and compare to (9.48).

Exercise 9.8 Show that the circuit of Fig. 9.2 describes the unitary operator (9.33) (case $B = 0$).

Exercise 9.9 Show that the circuit of Fig. 9.3 describes a modification of the original evolution operator U' when $B \neq 0$ that finds the marked element with a new running time close to the running time of the original algorithm and new success probability $O(1)$.

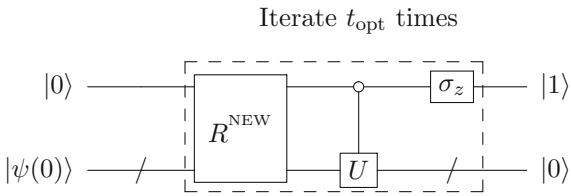

Fig. 9.2 Tulsi's modification when $B = 0$. The first register has one qubit and the second represents a N-dimensional Hilbert space. The output $|1\rangle|0\rangle \in \mathcal{H}^2 \otimes \mathcal{H}^N$ is obtained with probability $O(1)$, where $|0\rangle$ represents the market vertex

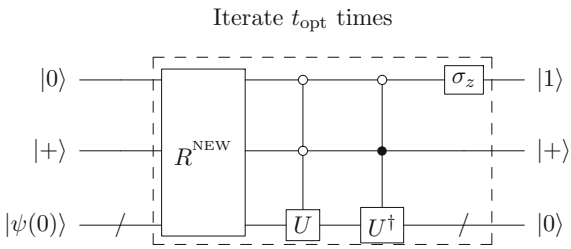

Fig. 9.3 Tulsi's modification when $B \neq 0$. The first and the second registers have one qubit (each one) and the third register represents a N-dimensional Hilbert space. The output $|1\rangle|+\rangle|0\rangle \in \mathcal{H}^2 \otimes \mathcal{H}^2 \otimes \mathcal{H}^N$ is obtained with probability $O(1)$, where $|0\rangle$ represents the market vertex

9.3 Finite Two-Dimensional Lattices

As an application of the previous results, we analyze the search for a marked vertex in the $\sqrt{N} \times \sqrt{N}$ square lattice with periodic boundary conditions. The evolution operator of a coined quantum walk with no marked vertex is

$$U = S\,(G \otimes I), \tag{9.50}$$

where G is the Grover coin and S is the flip-flop shift operator. The details are described in Sect. 6.2 on p. 98.

A search algorithm on the lattice is driven by the modified evolution operator

$$U' = U R', \tag{9.51}$$

where

$$R' = I - 2\left|0'\right\rangle\left\langle 0'\right| \tag{9.52}$$

and

$$\left|0'\right\rangle = |\mathrm{D}_C\rangle|0, 0\rangle, \tag{9.53}$$

when there is only one marked vertex with label $(0, 0)$. The *principal eigenvalue technique* can be employed because oracle R' has the same form of oracle R. Note that here the Hilbert space is larger because it has been augmented by the coin space.

The initial state $|\psi(0)\rangle$ is the uniform superposition of all states of the computational basis, that is,

$$|\psi(0)\rangle = |\mathrm{D}_C\rangle|\mathrm{D}_P\rangle, \tag{9.54}$$

where $|\mathrm{D}_C\rangle$ is the diagonal state of the coined space and $|\mathrm{D}_P\rangle$ is the diagonal state of the position space. This state can be generated by $O\left(\sqrt{N}\right)$ steps (Exercise 9.10).

The results of Sect. 9.2 can be readily employed as soon as we calculate A, B, and C given by Eqs. (9.17)–(9.19). We need to know the eigenvalues and eigenvectors of U that have nonzero overlap with $\left|0'\right\rangle$. An orthonormal eigenbasis of U is described in Sect. 6.2 on p. 103. We list the eigenvectors that have nonzero overlap with $\left|0'\right\rangle$. The only eigenvector with eigenvalue 1 is $\left|\nu_{0,0}^{1a}\right\rangle\left|\tilde{0}, \tilde{0}\right\rangle$, which is equal to the initial condition $|\psi(0)\rangle$. The remaining eigenvectors are $\left|\nu_{k\ell}^{\pm\theta}\right\rangle\left|\tilde{k}, \tilde{\ell}\right\rangle$ for $0 \le k, l < \sqrt{N}$ and $(k, l) \neq (0, 0)$, where

$$\left|\nu_{k\ell}^{\pm\theta}\right\rangle = \frac{\mathrm{i}}{2\sqrt{2}\sin\theta_{k\ell}} \begin{bmatrix} \mathrm{e}^{\mp\mathrm{i}\theta_{k\ell}} - \omega^{k} \\ \mathrm{e}^{\mp\mathrm{i}\theta_{k\ell}} - \omega^{-k} \\ \mathrm{e}^{\mp\mathrm{i}\theta_{k\ell}} - \omega^{\ell} \\ \mathrm{e}^{\mp\mathrm{i}\theta_{k\ell}} - \omega^{-\ell} \end{bmatrix}, \tag{9.55}$$

which have eigenvalues $\mathrm{e}^{\pm\mathrm{i}\theta_{k\ell}}$, where $\theta_{k\ell}$ are given by

$$\cos\theta_{k\ell} = \frac{1}{2}\left(\cos\frac{2\pi k}{\sqrt{N}} + \cos\frac{2\pi\ell}{\sqrt{N}}\right), \tag{9.56}$$

and $\omega = \mathrm{e}^{\frac{2\pi\mathrm{i}}{\sqrt{N}}}$. Vector $\left|\tilde{k}, \tilde{\ell}\right\rangle$ is the Fourier transform given by Eq. (6.40) on p. 100.

Note that the eigenvalues and eigenvectors of U come in complex-conjugate pairs, this means that $B = 0$. Converting the notation of Sect. 9.2 into the notation of the two-dimensional lattice, $\phi_k \to \theta_{k\ell}$, $|\psi_k\rangle \to \left|\nu_{k\ell}^{\pm\theta}\right\rangle\left|\tilde{k}, \tilde{\ell}\right\rangle$, $\sum_k \to \sum_{k\ell}$, and using that $\left\langle 0'\right| = \langle \mathrm{D}_C|\langle 0, 0|$, we obtain

$$\begin{aligned} A &= 2\left|\left\langle 0'\middle|\psi(0)\right\rangle\right|^2, \\ B &= 0, \\ C &= \sum_{\substack{k,\ell=0 \\ (k,\ell)\neq(0,0)}}^{\sqrt{N}-1} \frac{\left(\left|\langle \mathrm{D}_C|\nu_{k\ell}^{+\theta}\rangle\right|^2 + \left|\langle \mathrm{D}_C|\nu_{k\ell}^{-\theta}\rangle\right|^2\right)\left|\left\langle 00\middle|\tilde{k}\tilde{\ell}\right\rangle\right|^2}{1 - \cos\theta_{k\ell}}. \end{aligned}$$

From Exercise 6.13 on p. 104, we have

$$\left|\left\langle \mathrm{D}_C \middle| \nu_{k\ell}^{\pm\theta} \right\rangle\right|^2 = \frac{1}{2}, \tag{9.57}$$

and, from the definition of the Fourier transform, we have

$$\left|\left\langle 0, 0 \middle| \tilde{k}, \tilde{\ell} \right\rangle\right|^2 = \frac{1}{N}. \tag{9.58}$$

Using the above equations, (9.54), and (9.56), we obtain

$$\begin{aligned} A &= \frac{2}{N}, \\ B &= 0, \\ C &= \frac{1}{N} \sum_{\substack{k,\ell=0 \\ (k,\ell)\neq(0,0)}}^{\sqrt{N}-1} \frac{1}{1 - \frac{1}{2}\left(\cos\frac{2\pi k}{\sqrt{N}} + \cos\frac{2\pi \ell}{\sqrt{N}}\right)}. \end{aligned}$$

Using Exercise 9.11, we have

$$C = c \ln N + O(1), \tag{9.59}$$

where c is a number bounded by $2/\pi^2 \leq c \leq 1$. Numerical calculations show that $c = 0.33$ approximately. Since $B = 0$, the probability of finding the marked vertex as a function of the number of steps is given by Eq. (9.28). For the two-dimensional square lattice with odd $\sqrt{N}$, Eqs. (9.28) and (9.25) reduce to

$$p(t) = \frac{1}{2c \ln N} \sin^2\left(\frac{\sqrt{2}\, t}{\sqrt{c}\sqrt{N \ln N}}\right). \tag{9.60}$$

The running time is

$$t_{\mathrm{opt}} = \left\lfloor \frac{\pi\sqrt{c}\sqrt{N \ln N}}{2\sqrt{2}} \right\rfloor \tag{9.61}$$

and the success probability is

$$p_{\mathrm{succ}} = \frac{1}{2c \ln N} + O\left(N^{-1}\right). \tag{9.62}$$

Note that the running time is good enough because it is the square root of the classical hitting time. On the other hand, the success probability seems disappointing because it tends to zero when N increases. Since it goes to zero logarithmically in terms of N, the situation is not too bad and can be saved.

Exercise 9.10 Show that the uniform state $|\psi(0)\rangle = |\mathrm{D}_C\rangle|\mathrm{D}_P\rangle$ of the two-dimensional lattice can be generated with $O\left(\sqrt{N}\right)$ steps using local operators.

Exercise 9.11 The goal of this exercise is to calculate asymptotic bounds for

$$S_N = \sum_{\substack{k,\ell=0 \\ (k,\ell)\neq(0,0)}}^{\sqrt{N}-1} \frac{1}{1-\frac{1}{2}\left(\cos\frac{2\pi k}{\sqrt{N}} - \cos\frac{2\pi \ell}{\sqrt{N}}\right)}.$$

Using that

$$\frac{1-\cos a}{2} = \sin^2\frac{a}{2},$$

show that

$$S_N = \sum_{\substack{k,\ell=0 \\ (k,\ell)\neq(0,0)}}^{n-1} \frac{1}{\sin^2\frac{\pi k}{n} + \sin^2\frac{\pi \ell}{n}},$$

where $n = \sqrt{N}$. Using the symmetries of the expression inside the sum, show that

$$S_N = 4 \sum_{\substack{k,\ell=0 \\ (k,\ell)\neq(0,0)}}^{\lfloor \frac{n}{2} \rfloor} \frac{1}{\sin^2\frac{\pi k}{n} + \sin^2\frac{\pi \ell}{n}} + O(N)$$

when n is odd. Using that

$$\frac{4a^2}{\pi^2} \leq \sin^2 a \leq a^2,$$

for $0 \leq a \leq \pi/2$, show that

$$\frac{4\left(k^2+\ell^2\right)}{n^2} \leq \sin^2\frac{\pi k}{n} + \sin^2\frac{\pi \ell}{n} \leq \frac{\pi^2\left(k^2+\ell^2\right)}{n^2}$$

and

$$\frac{4n^2}{\pi^2} \sum_{\substack{k,\ell=0 \\ (k,\ell)\neq(0,0)}}^{\lfloor \frac{n}{2} \rfloor} \frac{1}{k^2+\ell^2} \leq S_N \leq n^2 \sum_{\substack{k,\ell=0 \\ (k,\ell)\neq(0,0)}}^{\lfloor \frac{n}{2} \rfloor} \frac{1}{k^2+\ell^2}$$

when n is odd up to $O(N)$ terms.

The goal now is to find bounds for

$$\sum_{\substack{k,\ell=0 \\ (k,\ell)\neq(0,0)}}^{\lfloor \frac{n}{2} \rfloor} \frac{1}{k^2+\ell^2}.$$

Using that $0 \leq (k-\ell)^2$, show that $2k\ell \leq k^2+\ell^2$ and then

$$\frac{(k+\ell)^2}{2} \leq k^2+\ell^2 \leq (k+\ell)^2.$$

From those inequalities, show that

$$\sum_{\substack{k,\ell=0\\(k,\ell)\neq(0,0)}}^{\lfloor \frac{n}{2} \rfloor} \frac{1}{(k+\ell)^2} \leq \sum_{\substack{k,\ell=0\\(k,\ell)\neq(0,0)}}^{\lfloor \frac{n}{2} \rfloor} \frac{1}{k^2+\ell^2} \leq \sum_{\substack{k,\ell=0\\(k,\ell)\neq(0,0)}}^{\lfloor \frac{n}{2} \rfloor} \frac{2}{(k+\ell)^2}.$$

Using tables of series,[4] one can find that

$$\sum_{\substack{k,\ell=0\\(k,\ell)\neq(0,0)}}^{\lfloor \frac{n}{2} \rfloor} \frac{1}{(k+\ell)^2} = \gamma + \frac{\pi^2}{6} + 2\,\Psi\left(\frac{n+3}{2}\right) + (n+1)\,\Psi\left(1, \frac{n+3}{2}\right) - n\Psi\,(1, n+1) - 2\,\Psi\left(1, \frac{n+1}{2}\right) - \Psi\,(n+1)\,,$$

where Ψ is the *polygamma function*. Show that the asymptotic expansion of the right-hand side of the last equation for odd n is

$$\sum_{\substack{k,\ell=0\\(k,\ell)\neq(0,0)}}^{\lfloor \frac{n}{2} \rfloor} \frac{1}{(k+\ell)^2} = \ln(n) + 1 + \gamma + \frac{\pi^2}{6} - 2\,\ln(2) + O\left(n^{-1}\right),$$

where γ is the *Euler number*.

Using the above results, show that

$$\frac{2}{\pi^2} N \ln N \leq S_N \leq N \ln N$$

up to $O\,(N)$ terms.

Exercise 9.12 The goal of this exercise is to show that the three required conditions for employing the *principal eigenvalue technique* described in Sect. 9.2 are fulfilled for the two-dimensional lattice.

1. Show that $|\psi(0)\rangle$ is an eigenvector of U with eigenvalue 1.
2. Show that the dominant term in the asymptotic expansion of $\theta_{k\ell}$ is

$$\theta_{k\ell} = \frac{\sqrt{2}\,\pi\,\sqrt{k^2+l^2}}{\sqrt{N}} + O\left(N^{-1}\right).$$

[4] http://www-elsa.physik.uni-bonn.de/~dieckman/InfProd/InfProd.html.

Use this expansion to show that the smallest positive argument among the eigenvalues of U is $\phi_{\min} = \theta_{k=0,\ell=1}$. Show that $\lambda \ll \phi_{\min}$ for large N.
3. Show that

$$\left|\langle\psi(0)|\lambda\rangle\right|^2 + \left|\langle\psi(0)|\lambda'\rangle\right|^2 = 1 + O\left(N^{-1}\right).$$

Use this result to show that ϵ (see Eq. (9.8)) can be disregarded for large N.

Exercise 9.13 The goal of this exercise is to show that the modified evolution operator U' can be seen as the evolution of a coined quantum walk with a *nonhomogeneous coin*. Show that Eq. (9.51) can be written as $U' = SC'$, where S is the flip-flop shift operator and C' is a nonhomogeneous coin operator, which is the Grover operator G on unmarked vertices and $(-I)$ on the marked vertex.

Exercise 9.14 Use the results of Exercise 6.15 and the principal eigenvalue technique to show that a quantum walk on the two-dimensional lattice with the *moving shift operator* (no inversion of the coin after the shift) needs $\Omega(N)$ time steps to find a marked vertex. Can Tulsi's modification improve this case?

9.3.1 Tulsi's Modification of the Two-Dimensional Lattice

Augment the Hilbert space of the two-dimensional lattice by one qubit, that is, $\mathcal{H}^{\text{NEW}} = \mathcal{H}^2 \otimes \mathcal{H}^4 \otimes \mathcal{H}^N$ and define a new evolution operator

$$U'' = U^{\text{NEW}} R^{\text{NEW}}, \tag{9.63}$$

where

$$U^{\text{NEW}} = (Z \otimes I_N)\, C_0(U), \tag{9.64}$$

U is given by Eq. (9.50), and

$$R^{\text{NEW}} = I_{2N} - 2\left|0^{\text{NEW}}\right\rangle\left\langle 0^{\text{NEW}}\right|, \tag{9.65}$$

where

$$\left|0^{\text{NEW}}\right\rangle = |\eta\rangle|\mathrm{D}_C\rangle|0, 0\rangle \tag{9.66}$$

and $|\eta\rangle$ is a 1-qubit state given by

$$|\eta\rangle = \sin\eta\,|0\rangle + \cos\eta\,|1\rangle, \tag{9.67}$$

where

$$\sin\eta = \frac{1}{2\sqrt{c\ln N}}. \tag{9.68}$$

The new initial condition is

$$\left|\psi^{\text{NEW}}(0)\right\rangle = |0\rangle|\mathrm{D}_C\rangle|\mathrm{D}_P\rangle. \tag{9.69}$$

Using the results of Sect. 9.2.2, the success probability as a function of the number of steps is

$$p(t) \;=\; \frac{2}{3}\,\sin^2\left(\frac{\sqrt{2}\,t}{\sqrt{3\,c\,N\ln N}}\right). \tag{9.70}$$

The running time is

$$t_{\text{opt}} \;=\; \left\lfloor \frac{\pi\sqrt{3c}}{2\sqrt{2}}\sqrt{N\ln N}\right\rfloor \tag{9.71}$$

and the success probability is $p_{\text{succ}} \;=\; 2/3 + O\left(N^{-1}\right)$.

9.4 Hypercubes

As a second application of the *principal eigenvalue technique*, we analyze the search for a marked vertex in the n-dimensional hypercube, which has $N = 2^n$ vertices whose labels are $\vec{v}$, for $0 \le v \le N-1$. The evolution operator of a coined quantum walk with no marked vertex is

$$U \;=\; S\,(G \otimes I_N), \tag{9.72}$$

where $G \in \mathcal{H}^n$ is the Grover coin and $S \in \mathcal{H}^n \otimes \mathcal{H}^N$ is the flip-flop shift operator, which was described in Sect. 6.3 on p. 106.

A search algorithm on the n-dimensional hypercube is driven the modified evolution operator

$$U' = U\,R', \tag{9.73}$$

where

$$R' = I - 2\left|0'\right\rangle\left\langle 0'\right| \tag{9.74}$$

and

$$\left|0'\right\rangle = |\mathrm{D}_C\rangle\left|\vec{0}\right\rangle, \tag{9.75}$$

when there is only one marked vertex with label $\vec{0} = (0, \ldots, 0)$. The *principal eigenvalue technique* can be employed because oracle R' has the same form of oracle R. Note that here the Hilbert space is larger because it has been augmented by the coin space.

The initial state $|\psi(0)\rangle$ is the uniform superposition of all states of the computational basis, that is,

$$|\psi(0)\rangle = |\mathrm{D}_C\rangle|\mathrm{D}_P\rangle, \tag{9.76}$$

where $|\mathrm{D}_C\rangle$ is the diagonal state of the coined space and

$$|\mathrm{D}_P\rangle = \frac{1}{\sqrt{N}}\sum_{\vec{v}=0}^{N-1}|\vec{v}\rangle$$

is the diagonal state of the position space. State $|\psi(0)\rangle$ can be generated with $O\left(\sqrt{N}\right)$ steps (Exercise 9.15).

Exercise 9.15 Show that the uniform state $|\psi(0)\rangle = |\mathrm{D}_C\rangle|\mathrm{D}_P\rangle$ of the n-dimensional hypercube can be generated with $O\left(\sqrt{N}\right)$ steps using local operators.

The results of Sect. 9.2 can be readily employed as soon as we calculate A, B, and C given by Eqs. (9.17)–(9.19). To calculate those quantities, we need to know the eigenvalues and eigenvectors of U that have nonzero overlap with $\left|0'\right\rangle$. An eigenbasis of U is described in Sect. 6.3.1 on p. 112. From Exercise 6.19, we know that an orthonormal basis of eigenvectors of U for the eigenspace orthogonal to $|\mathrm{D}\rangle\left|\vec{0}\right\rangle$ is $\left\{\left|\alpha_1^{\vec{k}}\right\rangle\left|\beta_{\vec{k}}\right\rangle, \left|\alpha_n^{\vec{k}}\right\rangle\left|\beta_{\vec{k}}\right\rangle : 1 \le \vec{k} \le 2^n - 2\right\}$ together with $|\mathrm{D}\rangle\left|\beta_{\vec{0}}\right\rangle$ and $|\mathrm{D}\rangle\left|\beta_{\vec{1}}\right\rangle$ with eigenvalues $\mathrm{e}^{\pm \mathrm{i}\omega_k}$, 1, and (-1), respectively, where $\left|\beta_{\vec{k}}\right\rangle$ is given by

$$\left|\beta_{\vec{k}}\right\rangle \equiv \frac{1}{\sqrt{2^n}}\sum_{\vec{v}=0}^{2^n-1}(-1)^{\vec{k}\cdot\vec{v}}|\vec{v}\rangle, \tag{9.77}$$

and

$$\left|\alpha_1^{\vec{k}}\right\rangle = \frac{\mathrm{e}^{\mathrm{i}\theta}}{\sqrt{2}}\sum_{a=1}^{n}\left(\frac{k_a}{\sqrt{k}} - \mathrm{i}\frac{1-k_a}{\sqrt{n-k}}\right)|a\rangle, \tag{9.78}$$

$$\left|\alpha_n^{\vec{k}}\right\rangle = \frac{\mathrm{e}^{-\mathrm{i}\theta}}{\sqrt{2}}\sum_{a=1}^{n}\left(\frac{k_a}{\sqrt{k}} + \mathrm{i}\frac{1-k_a}{\sqrt{n-k}}\right)|a\rangle, \tag{9.79}$$

and $\cos\theta = \sqrt{k/n}$ and $k_a = \vec{k}\cdot\vec{e}_a$ is the a-th entry of $\vec{k}$ and $\cos\omega_k = 1 - 2k/n$.

Note that there is only one eigenvector with eigenvalue 1, which is the uniform superposition $|\mathrm{D}_C\rangle\left|\beta_{\vec{0}}\right\rangle$, implying that $A = 2/N$. Besides, the eigenvalues and eigenvectors of U come in complex-conjugate pairs, implying that $B = 0$. Converting the notation of Sect. 9.2 into the notation of the n-dimensional hypercube, $\phi_k \to \omega_k$, $|\psi_k\rangle \to \left|\alpha^{\vec{k}}\right\rangle\left|\beta_{\vec{k}}\right\rangle$, $\sum_k = \sum_{\vec{k}=0}^{N-1}$, and using that $\left\langle 0'\right| = \langle \mathrm{D}_C|\left\langle\vec{0}\right|$, we obtain

$$
\begin{aligned}
A &= \frac{2}{N}, \\
B &= 0, \\
C &= \sum_{\vec{k}=1}^{N-2} \frac{\left(\left|\left\langle \mathrm{D}|\alpha_1^{\vec{k}}\right\rangle\right|^2 + \left|\left\langle \mathrm{D}|\alpha_n^{\vec{k}}\right\rangle\right|^2\right)\left|\left\langle \vec{0}|\beta_{\vec{k}}\right\rangle\right|^2}{1-\cos\omega_k} + \frac{\left|\left\langle \vec{0}|\beta_{\vec{1}}\right\rangle\right|^2}{2}.
\end{aligned}
$$

Equation (6.89) on p. 113 states that

$$
\left\langle \mathrm{D}|\alpha_1^{\vec{k}}\right\rangle = \left\langle \mathrm{D}|\alpha_n^{\vec{k}}\right\rangle = \frac{1}{\sqrt{2}}. \tag{9.80}
$$

Besides, using Eq. (9.77) we have $\left\langle \vec{0}|\beta_{\vec{k}}\right\rangle = 1/\sqrt{N}$ for all $\vec{k}$. Simplifying C, we obtain

$$
C = \frac{n}{2N}\sum_{k=1}^{n}\frac{1}{k}\binom{n}{k}. \tag{9.81}
$$

From Exercise 9.16, we have

$$
C = \frac{c}{2} + O\left(N^{-1}\right), \tag{9.82}
$$

where c is a number bounded by $1 \le c \le 4$. Numerical calculations show that $c = 2$ approximately. Since $B = 0$, the probability of finding the marked vertex as a function of the number of steps is given by Eq. (9.28) and, since there is only one $(+1)$-eigenvector, the success probability as a function of the number of steps is

$$
p(t) = \frac{1}{c}\sin^2\left(\frac{2t}{\sqrt{cN}}\right). \tag{9.83}
$$

The running time is

$$
t_{\mathrm{opt}} = \left\lfloor \frac{\pi\sqrt{cN}}{4} \right\rfloor \tag{9.84}
$$

and the success probability is

$$
p_{\mathrm{succ}} = \frac{1}{c} + O\left(n^{-1}\right). \tag{9.85}
$$

Note that the running time is $O(\sqrt{N})$, achieving the Grover lower bound with constant success probability.

Exercise 9.16 The goal of this exercise is to calculate asymptotic bounds for C given by Eq. (9.81). Show that

$$\frac{1}{n}\binom{n}{k} \leq \frac{1}{k}\binom{n}{k} \leq \frac{2}{n}\binom{n+1}{k+1}$$

for $1 \leq k \leq n$. Use

$$\sum_{k=1}^{n}\binom{n}{k} = N - 1$$

to conclude that

$$1 + O\left(\frac{1}{N}\right) \leq \frac{n}{N}\sum_{k=1}^{n}\frac{1}{k}\binom{n}{k} \leq 4 + O\left(\frac{n}{N}\right).$$

Exercise 9.17 Show that all conditions for employing the *principal eigenvalue technique* described in Sect. 9.2 are fulfilled for hypercubes.

Exercise 9.18 Show that Eq. (9.73) can be written as $U' = SC'$, where S is the flip-flop shift operator and C' is a *nonhomogeneous coin*, which is the Grover operator G on unmarked vertices and $(-I)$ on the marked vertex. Conclude that the modified evolution operator U' can be seen as the evolution of a coined quantum walk with a nonhomogeneous coin.

Exercise 9.19 Explain why the algorithm described in this section cannot be improved by using Tulsi's modification.

9.5 Grover's Algorithm as Spatial Search on Graphs

In this section, we describe Grover's algorithm as a coined quantum walk on the *complete graph* with *loops* and as a staggered quantum walk on the *loopless complete graph*. We also use the *principal eigenvalue technique* to describe an alternate way to analyze the complexity of Grover's algorithm.

9.5.1 Grover's Algorithm in terms of the Coined Model

Grover's algorithm can be seen as a spatial search algorithm on the *complete graph* with *loops*. All vertices of the complete graph are connected by undirected edges as shown by the left-hand complete graph of Fig. 9.4, which has $N = 3$ vertices and labels 0, ..., $N - 1$. In order to define a coined quantum walk on the complete graph with loops, we have to convert each *undirected edge* as two opposing *arcs* (*directed edges*) and to label the *arcs* using the notation (v_1, v_2), for $0 \leq v_1, v_2 \leq N - 1$, where v_1 is the *tail* and v_2 is the *head*. In terms of the *coined model*, v_1 is the position

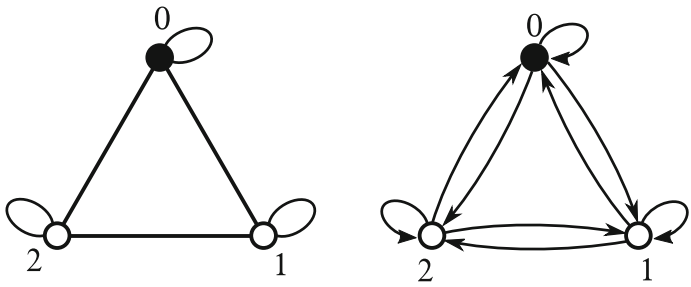

Fig. 9.4 Complete graph with $N = 3$ vertices. The left-hand graph has undirected edges. The right-hand graph has 9 arcs the labels of which are (v_1, v_2), where v_1 is the tail and v_2 is the head

and v_2 is the coin value, which coincides with the label of the next vertex following the arc.

The Hilbert space associated with the graph is spanned by the arcs, that is,

$$\mathcal{H}^{N^2} = \text{span}\{|v_1, v_2\rangle \,:\, 0 \leq v_1, v_2 \leq N-1\}.$$

We use the interpretation of $|v_1, v_2\rangle$ in which v_1 is the position and v_2 is the coin value and in terms of the coined model, we are using the *position-coin notation* instead of the *arc notation* because the loops allow to specify N directions unambiguously on complete graphs with odd (or even) number of vertices. The *flip-flop shift operator* is defined as

$$S|v_1, v_2\rangle = |v_2, v_1\rangle \tag{9.86}$$

and the coin operator is

$$C = I_N \otimes G, \tag{9.87}$$

where $G = 2|\mathrm{D}\rangle\langle\mathrm{D}| - I$ is the N-dimensional Grover coin and $|\mathrm{D}\rangle$ is the diagonal state of the coin space. The evolution operator of the coined quantum walk on the complete graph with loops and no marked vertex is

$$U \;=\; S\,(I \otimes G). \tag{9.88}$$

Suppose now that vertex 0 is marked. The oracle is

$$R' = (I_N - 2|0\rangle\langle 0|) \otimes I_N. \tag{9.89}$$

This oracle is equivalent to

$$R' = I_{N^2} - 2\sum_v |0, v\rangle\langle 0, v|, \tag{9.90}$$

which can be interpreted as an operator that marks all arcs leaving vertex 0 including the loop. The modified evolution operator is

$$U' = UR', \tag{9.91}$$

which can be written as

$$U' = S(R \otimes G), \tag{9.92}$$

where $R = I_N - 2|0\rangle\langle 0|$.

The initial state of the spatial search algorithm is $|\psi(0)\rangle = |\mathrm{D}_P\rangle|\mathrm{D}_C\rangle$, where $|\mathrm{D}_P\rangle$ is the diagonal state of the position space and $|\mathrm{D}_C\rangle$ is the diagonal state of the coin space. Following step-by-step, we can show that after an even number of steps ($2t$), we have

$$(U')^{2t}|\psi(0)\rangle = (GR)^t|\mathrm{D}_P\rangle \otimes R(GR)^{t-1}|\mathrm{D}_C\rangle. \tag{9.93}$$

Note that the operator (GR) and the initial state $|\mathrm{D}_P\rangle$ are the evolution operator and the initial state used in Grover's algorithm. We can obtain the same result of Grover's algorithm by taking $t = \left\lfloor \frac{\pi}{4}\sqrt{N} \right\rfloor$ and measuring the walker's position. In the coined case, the running time of the quantum-walk-based algorithm is twice the running time of Grover's algorithm.

Exercise 9.20 Show that $U'|\psi(0)\rangle = |\mathrm{D}\rangle \otimes R|\mathrm{D}\rangle$ and $(U')^2|\psi(0)\rangle = GR|\mathrm{D}\rangle \otimes R|\mathrm{D}\rangle$. Using induction, obtain Eq. (9.93).

Exercise 9.21 Show that Eq. (9.92) can be written as $U' = SC'$, where C' is a *non-homogeneous coin*, which is the Grover operator G on unmarked vertices and $(-G)$ on the marked vertex.

Exercise 9.22 Take the initial condition $|\psi(0)\rangle = |\mathrm{D}_P\rangle|\phi\rangle$, where $|\phi\rangle$ is the state of the coin space. Show that the same result of Grover's algorithm is reobtained.

Exercise 9.23 Show that a quantum walk driven by evolution operator (9.88) is *periodic*. What is the *fundamental period*?

9.5.2 Grover's Algorithm in terms of the Staggered Model

Grover's algorithm can be seen as a spatial quantum search using the *staggered quantum walk model* on the *complete graph*. To show this fact, we employ a two-step procedure. First, we find the evolution operator of the staggered quantum walk on the complete graph with N vertices. The complete graph is the only *connected graph* that is *1-tessellable*. The *tessellation cover* has only one *tessellation*, which has only one *polygon* containing all vertices. The vector associated with this polygon is

$$|\mathrm{D}\rangle = \frac{1}{\sqrt{N}} \sum_{v=0}^{N-1} |v\rangle, \tag{9.94}$$

which belongs to the Hilbert space $\mathcal{H}^N$ and is the diagonal state of the computational basis $\{|v\rangle : 0 \leq v \leq N-1\}$. The computational basis has a one-to-one correspondence with the set of vertex labels. Choosing $\theta = \pi/2$, Eq. (8.3) on p. 162 describes the following evolution operator, modulo a global phase,

$$U = 2|\mathrm{D}\rangle\langle\mathrm{D}| - I. \tag{9.95}$$

Second, we multiply U by oracle R obtaining a modified evolution operator

$$U' = U\,R, \tag{9.96}$$

where

$$R = I_N - 2|0\rangle\langle 0|. \tag{9.97}$$

Note that the operator U' and the initial state $|\mathrm{D}\rangle$ are the evolution operator and the initial state used in Grover's algorithm. We can obtain the same result of Grover's algorithm by taking $t = \left\lfloor \frac{\pi}{4}\sqrt{N} \right\rfloor$, applying $(U')^t$ to the initial state, and measuring the walker's position.

9.5.3 Complexity Analysis of Grover's Algorithm

To use the *principal eigenvalue technique* for Grover's algorithm (as a staggered quantum walk on the complete graph), we must be able to find the eigenvectors of U that have nonzero overlap with $|0\rangle$. U is given by Eq. (9.95) and, since $U^2 = I$, U has only two eigenvalues: $(+1)$ with multiplicity 1 and (-1) with multiplicity $N-1$. The eigenvector associated with $(+1)$ is $|\psi_0\rangle = |\mathrm{D}\rangle$ and the eigenvectors associated with (-1) are orthogonal to $|\psi_0\rangle$. Since we need only the eigenvectors of U that have nonzero overlap with $|0\rangle$ (we suppose that the marked vertex has label 0), the only eigenvector with eigenvalue (-1) that we need is

$$|\psi_1\rangle = \frac{\sqrt{N-1}}{\sqrt{N}}|0\rangle - \frac{1}{\sqrt{N(N-1)}} \sum_{j=1}^{N-1} |j\rangle. \tag{9.98}$$

Eigenvectors of U that are orthogonal to $|\psi_0\rangle$ and $|\psi_1\rangle$ have no overlap with $|0\rangle$ (Exercise 9.24).

Now we calculate A, B, and C given by Eqs. (9.17)–(9.19) using that $\phi_0 = 0$, $\phi_1 = \pi$, and $\langle 0|\psi_k\rangle = 0$ for $k \geq 2$. The result is

$$\begin{aligned} A &= \frac{2}{N}, \\ B &= 0, \\ C &= \frac{1}{2} - \frac{1}{3N}. \end{aligned} \tag{9.99}$$

Since $B = 0$, we use Eqs. (9.25)–(9.30) and $|\psi(0)\rangle = |\mathrm{D}\rangle$ to obtain

$$t_{\mathrm{opt}} = \left\lfloor \frac{\pi}{4}\sqrt{N} \right\rfloor \tag{9.100}$$

and

$$p_{\mathrm{succ}} = 1 + O\left(N^{-1}\right), \tag{9.101}$$

which coincide with the results of Grover's algorithm.

Exercise 9.24 Check that $U|\psi_1\rangle = -|\psi_1\rangle$ and $\langle\psi_1|\psi_1\rangle = 1$, where U by Eq. (9.95) and $|\psi_1\rangle$ is given by Eq. (9.98). Show that if $|\psi\rangle$ is an eigenvector of U with eigenvalue (-1) and $\langle\psi_1|\psi\rangle = 0$, then $\langle 0|\psi\rangle = 0$.

Exercise 9.25 Show that the three required conditions for employing the *principal eigenvalue technique* described in Sect. 9.2 are fulfilled for the analysis of Grover's algorithm, that is:
1. Show that $|\psi(0)\rangle$ is an eigenvector of U with eigenvalue 1.
2. Show that $\lambda \ll \phi_{\mathrm{min}}$ for large N.
3. Show that

$$\left|\langle\psi(0)|\lambda\rangle\right|^2 + \left|\langle\psi(0)|\lambda'\rangle\right|^2 = 1 + O\left(N^{-1}\right)$$

and use this result to show that ϵ (see Eq. (9.8)) can be disregarded for large N.

Exercise 9.26 Explain why Grover's algorithm cannot be improved by using Tulsi's modification without using the argumentation that Grover's algorithm is optimal.

Further Reading

The idea of *spatial search algorithms* started with Benioff [41], who showed that a direct application of *Grover's algorithm* does not improve the time complexity of a searching algorithm on *lattices* compared to classical algorithms. A more efficient algorithm was presented by Aaronson and Ambainis [1], who used a "divide-and-conquer" strategy that splits the grid into several subgrids and searches each of them. Shenvi, Kempe, and Whaley [297] described a search algorithm on *hypercubes* using coined quantum walks, which is one of the first contributions in the area of quantum-walk-based search algorithms together with Ambainis's algorithm for the element distinctness problem [14]. Tulsi [316] created a modification of *quantum-walk-based search algorithms* that improves the *success probability* and described those algorithms comprehensively.

Many important quantum-walk-based algorithms were analyzed on the *two-dimensional square lattice* with N vertices and one marked vertex. Ambainis

et al. [19] described an algorithm with time complexity $O\left(\sqrt{N}\log N\right)$ and Tulsi [315] described an algorithm with time complexity $O\left(\sqrt{N\log N}\right)$ by adding an extra qubit. Ambainis et al. [18] described an algorithm with time complexity $O\left(\sqrt{N\log N}\right)$ that does not use the *amplitude amplification technique* but requires classical post-processing. Hein and Tanner [144] analyzed quantum search on higher dimensional lattices. Search algorithms on the hexagonal and triangular lattices are described in [3, 4].

Relevant earlier references on quantum-walk-based algorithms are reviewed in [13, 183, 229, 274, 320]. A short list of important recent results for lattices and graphs in general based on the coined quantum walk model is the following: Errors in quantum-walk-based search algorithms were analyzed in [349]. Hamilton et al. [136] proposed experimental implementation using many walkers. Wong [330, 331] analyzed quantum-walk-based search on two-dimensional lattices with self-loops using his previous work [329] on lackadaisical quantum walks. Multimarked search is addressed by Yu-Chao et al. [350] Hoyer and Komeili [152]. Wong and Santos analyzed quantum search on cycles with multiple marked vertices [333]. Reitzner et al. [273] (see also [179]) used the scattering quantum walk model to search a path in graphs. Xi-Ling et al. [335] used the scattering quantum walk model to develop search algorithm on strongly regular graphs. Lovett et al. analyzed factors affecting the efficiency of coined quantum walk search algorithms in [217].

There are many results using the continuous-time quantum walk model and a *very short* list is the following: Childs and Goldstone [82] analyzed search on lattices using the continuous-time quantum walk model. Agliari, Blumen, and Mülken [6] analyzed quantum walk searching on fractal structures using continuous-time model. Quantum search on hexagonal lattices was described in [115]. Quantum search on trees was analyzed in [261]. General results on searching using the continuous-time quantum walk model are presented in [72, 238, 249, 329, 332].

Results using alternative models are described in [108, 317].

Chapter 10
Element Distinctness

The *element distinctness problem* is the problem of determining whether the elements of a list are distinct. For example, suppose we have a list x with $N = 9$ elements, which are in the range $[20, 50]$, such as $x = (25, 27, 39, 43, 39, 35, 30, 42, 28)$. Note that the third and the fifth elements are equal. We say that the elements in positions 3 and 5 collide. As a *decision problem*, the goal is to answer "yes" if there is a collision or "no" if there is no collision. In order to simplify the description of the quantum algorithm that solves this problem, we assume that there is either one 2-collision or none. If there is a collision, then there are indices i_1 and i_2 such that $x_{i_1} = x_{i_2}$. With a small overhead, we can find explicitly the indices i_1 and i_2 when the algorithm returns "yes."

We use the *quantum query model* to measure the hardness of this problem. In this model, we are interested in the number of times we have queried an element of the list, or equivalently, given a black box function $f : \{1, \ldots, N\} \to X$, where X is a finite set, we want to determine whether there are two distinct inputs $i_1, i_2 \in \{1, \ldots, N\}$ such that $f(i_1) = f(i_2)$. Given an index i, each time we check x_i or we use f, it counts one query. To solve this problem in a classical computer, we need to query all elements, one at a time in a serial processor, which takes $\Omega(N)$ queries. In the quantum case, we need $O(N^{2/3})$ queries, which is the best we can do.

Exercise 10.1. Show that the *element distinctness problem* is as hard as *unstructured search*. [Hint: Consider the following problem, which is easier than the element distinctness problem. Suppose that if there is a colliding pair $\{i_1, i_2\}$, then x_{i_1} is the first element of the list. Search for x_{i_2} in the remaining list.]

© Springer Nature Switzerland AG 2018

R. Portugal, *Quantum Walks and Search Algorithms*, Quantum Science and Technology, https://doi.org/10.1007/978-3-319-97813-0_10

10.1 Classical Algorithms

The best-known classical algorithm using the minimum number of queries has the following steps:

1. Query all elements of list x and store in the memory.
2. Sort the elements.
3. Traverse the sorted list checking whether any entry is repeated.

Step 1 requires exactly N queries. Step 2 takes $O(N \ln N)$ time steps. Step 3 takes $O(N)$ time steps. Then, the classical algorithm solves the element distinctness problem with N queries for lists with N entries. The time complexity is $O(N \ln N)$.

10.2 Naïve Quantum Algorithms

Before describing the optimal quantum algorithm, which is the main part of this chapter, let us address simpler attempts.

Using Grover's Algorithm

Let us use Grover's algorithm to solve the *element distinctness problem*. The search space is the set of all pairs $\{i, j\}$ for $0 \le i < j < N$. A pair is marked if $x_i = x_j$. The size of the search space is $O(N^2)$, and there is at most one marked element. Using Grover's algorithm, we need $O(N)$ queries to find a collision.

Using Amplitude Amplification

There is an algorithm with query complexity of $O(N^{3/4})$ combining Grover's algorithm with the *amplitude amplification technique*. Let us partition the set of indices into sets S_1 and S_2 with sizes n and $N - n$, respectively, where n will be determined later, for now, consider $n \ll N$ when $N \gg 1$. Suppose that the elements of S_1 were selected at random from the set of indices $\{1, \ldots, N\}$ and S_2 is the complement of S_1. In the first step, query all x_i for $i \in S_1$. In the second step, use Grover's algorithm to search for a colliding index on S_2, that is, find $j \in S_2$ such that $x_j = x_i$. The first step takes n queries, and the second step takes $(\pi/4)\sqrt{N-n}$ queries, which is around $\sqrt{N}$ queries. To balance the number of queries in each step, we set $n = \sqrt{N}$. The number of queries in the two-step algorithm is around $2\sqrt{N}$. The algorithm succeeds only if the colliding indices are in different sets. For large N, the success probability is around $2/\sqrt{N}$ (Exercise 10.2).

We can boost the success probability to $O(1)$ by using the amplitude amplification method. We have to run the two-step algorithm $\sqrt{\sqrt{N}/2}$ times. The total number of queries is $O\left(\sqrt{N}\sqrt{\sqrt{N}}\right) = O\left(N^{3/4}\right)$.

Exercise 10.2. Let N be a perfect square, $S_1 \subseteq \{1, \ldots, N\}$ such that $|S_1| = \sqrt{N}$, and $S_2 = \{1, \ldots, N\} \setminus S_1$. Select two different elements $i_1, i_2 \in \{1, \ldots, N\}$. If the

elements of S_1 are chosen at random, show that the probability that the two elements belong to different sets is around $2/\sqrt{N}$.

10.3 The Optimal Quantum Algorithm

The algorithm we describe in this section uses an extensive notation, which requires extra attention from the reader. Let us start with a list of basic definitions:

- $[N] = \{1, \ldots, N\}$
- $r = \left\lfloor N^{\frac{2}{3}} \right\rfloor$
- $\mathcal{S}_r$ = set of all r-subsets of $[N]$
- $\mathcal{V} = \{(S, y) \,:\, S \in \mathcal{S}_r,\ y \in [N] \setminus S\}$
- $\mathcal{H} = \operatorname{span}\{|S, y\rangle \,:\, (S, y) \in \mathcal{V}\}$

Note that $|\mathcal{S}_r| = \binom{N}{r}$ and $|\mathcal{V}| = \binom{N}{r}(N - r)$, where $\binom{N}{r}$ is the *binomial coefficient*. Let us provide an example of those definitions. If the number of elements in the list is $N = 4$, then

$$
\begin{aligned}
[N] &= \{1, 2, 3, 4\},\\
r &= 2,\\
\mathcal{S}_r &= \big\{\{1, 2\},\ \{1, 3\},\ \{1, 4\},\ \{2, 3\},\ \{2, 4\},\ \{3, 4\}\big\},\\
\mathcal{V} &= \Big\{\big(\{1, 2\}, 3\big),\ \big(\{1, 2\}, 4\big),\ \big(\{1, 3\}, 2\big),\ \big(\{1, 3\}, 4\big),\ \big(\{1, 4\}, 2\big),\ \big(\{1, 4\}, 3\big),\\
&\qquad \big(\{2, 3\}, 1\big),\ \big(\{2, 3\}, 4\big),\ \big(\{2, 4\}, 1\big),\ \big(\{2, 4\}, 3\big),\ \big(\{3, 4\}, 1\big),\ \big(\{3, 4\}, 2\big)\Big\},\\
\mathcal{H} &= \operatorname{span}\Big\{|\{1, 2\}, 3\rangle,\ |\{1, 2\}, 4\rangle,\ |\{1, 3\}, 2\rangle,\ |\{1, 3\}, 4\rangle,\ |\{1, 4\}, 2\rangle,\ |\{1, 4\}, 3\rangle,\\
&\qquad |\{2, 3\}, 1\rangle,\ |\{2, 3\}, 4\rangle,\ |\{2, 4\}, 1\rangle,\ |\{2, 4\}, 3\rangle,\ |\{3, 4\}, 1\rangle,\ |\{3, 4\}, 2\rangle\Big\}.
\end{aligned}
$$

The Hilbert space $\mathcal{H}$ is spanned by $|\mathcal{V}|$ vectors. We use the notation $|S, y\rangle$ for the vectors of the computational basis, where S is a set in $\mathcal{S}_r$ and y is in $[N]$ but not in S. Note that we have not given the list of elements yet. In fact, $[N]$ is simply the set of indices. Let us consider $x = (39, 45, 39, 28)$, which means that the colliding indices are $i_1 = 1$ and $i_2 = 3$. An element $(S, y) \in \mathcal{V}$ is called marked if $\{i_1, i_2\} \subseteq S$. Indices i_1, i_2 are also called marked indices. In the example, $\big(\{1, 3\}, 2\big)$ and $\big(\{1, 3\}, 4\big)$ are the marked elements; 1 and 3 are the marked indices.

Let $\Gamma(\mathcal{V}, E)$ be the graph where each vertex has label $(S, y) \in \mathcal{V}$ and vertices (S, y) and (S', y') are *adjacent* if and only if $S = S'$ or $S \cup \{y\} = S' \cup \{y'\}$. When $N = 4$, graph Γ is depicted in Fig. 10.1. If two vertices are adjacent because $S = S'$, the edge incident to these vertices has the blue color and if the vertices are adjacent because $S \cup \{y\} = S' \cup \{y'\}$, the edge has the red color.

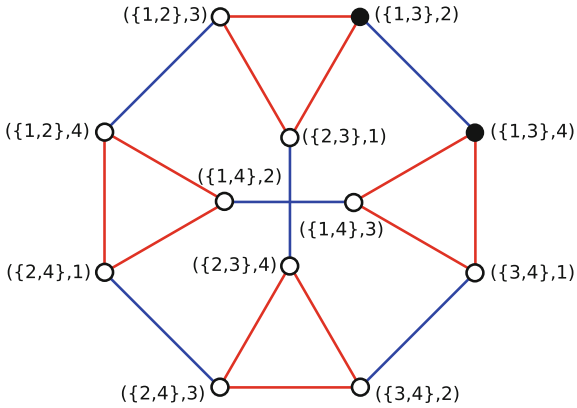

Fig. 10.1 Graph $\Gamma(\mathcal{V}, E)$ when $N = 4$. Vertices (S, y) and (S', y') such that $S = S'$ are linked by blue edges and vertices such that $S \cup \{y\} = S' \cup \{y'\}$ are linked by red edges

Let us focus on the set of blue edges. We start by defining a subset of vertices that are adjacent by blue edges. For each $S \in \mathcal{S}_r$, define

$$\alpha_S = \{(S, y) \in \mathcal{V} : y \in [N] \setminus S\}. \tag{10.1}$$

We state that α_S is a *clique* of size $(N - r)$. In fact, a subset of vertices is a clique if all vertices in the subset are adjacent. By definition, α_S is a subset of vertices and all vertices in α_S are adjacent because they share the same S. The size of the clique is $(N - r)$ because the *cardinality* of set $[N] \setminus S$ is $(N - r)$.

Each α_S is a clique, and it is straightforward to check that the union of α_S for all S in $\mathcal{S}_r$ is the vertex set $\mathcal{V}$, that is,

$$\mathcal{V} = \bigcup_{S \in \mathcal{S}_r} \alpha_S.$$

Besides, $\alpha_S \cap \alpha_{S'} = \emptyset$ if $S \neq S'$. In the terminology of the *staggered quantum walk model*, the set

$$\mathcal{T}_\alpha = \{\alpha_S : S \in \mathcal{S}_r\}$$

is a tessellation of Γ. The size of tessellation α is $|\mathcal{T}_\alpha| = \binom{N}{r}$. The blue edges in Fig. 10.1 are in $\mathcal{T}_\alpha$.

For each $S \in \mathcal{S}_r$, define the α-polygon vector

$$|\alpha_S\rangle = \frac{1}{\sqrt{N - r}} \sum_{y \in [N] \setminus S} |S, y\rangle. \tag{10.2}$$

It is straightforward to check that $\langle \alpha_S | \alpha_{S'} \rangle = \delta_{SS'}$. Now define

$$U_\alpha = 2\sum_{S\in\mathcal{S}_r} |\alpha_S\rangle\langle\alpha_S| - I, \tag{10.3}$$

which is the unitary and Hermitian operator associated with tessellation α.

Now we focus on the set of red edges. We start by defining a subset of vertices that are adjacent by red edges. Define a decomposition of the vertex set $\mathcal{V}$ induced by the equivalence relation $\sim$, where $(S, y)\sim(S', y')$ if and only if $S \cup \{y\} = S' \cup \{y'\}$. An equivalence class is defined by $[S, y] = \left\{(S', y') \in \mathcal{V} : (S', y')\sim(S, y)\right\}$ and the quotient set by $\mathcal{V}/\sim = \{[S, y] : (S, y) \in \mathcal{V}\}$. Note that the cardinality of each equivalence class is $(r + 1)$ and of the quotient set is $\binom{N}{r+1}$. For each element $[S, y]$ in the quotient set, define

$$\beta_{[S,y]} = \{(S', y') \in \mathcal{V} : (S', y')\sim(S, y)\}. \tag{10.4}$$

Set $\beta_{[S,y]}$ is obtained from a cyclic rotation of the elements of $S \cup \{y\}$. We state that $\beta_{[S,y]}$ is a *clique* of size $(r + 1)$. In fact, all vertices (S', y') in $\beta_{[S,y]}$ are adjacent because $S' \cup \{y'\} = S \cup \{y\}$. The size of $\beta_{[S,y]}$ is $(r + 1)$ because the cardinality of set $S \cup \{y\}$ is $(r + 1)$.

Each $\beta_{[S,y]}$ is a clique, and it is straightforward to check that the union of $\beta_{[S,y]}$ for all $[S, y]$ in quotient set $\mathcal{V}/\sim$ is the vertex set $\mathcal{V}$, that is,

$$\mathcal{V} = \bigcup_{[S,y]\in\mathcal{V}/\sim} \beta_{[S,y]}.$$

Besides, $\beta_{[S,y]} \cap \beta_{[S',y']} = \emptyset$ if $[S, y] \neq [S', y']$. In the terminology of the *staggered quantum walk model*, the set

$$\mathcal{T}_\beta = \{\beta_{[S,y]} : [S, y] \in \mathcal{V}/\sim\}$$

is a tessellation of Γ. The size of tessellation β is $\left|\mathcal{T}_\beta\right| = \binom{N}{r+1}$. The red edges in Fig. 10.1 are in $\mathcal{T}_\beta$.

For each $[S, y] \in \mathcal{V}/\sim$, define the β-polygon vector

$$\left|\beta_{[S,y]}\right\rangle = \frac{1}{\sqrt{r+1}} \sum_{y'\in S\cup\{y\}} \left|S \cup \{y\} \setminus \{y'\}, y'\right\rangle. \tag{10.5}$$

Note that $\left|\beta_{[S,y]}\right\rangle$ is the uniform superposition of the equivalence class that contains (S, y). It is straightforward to check that $\left\langle\beta_{[S,y]}\middle|\beta_{[S',y']}\right\rangle = \delta_{[S,y],[S',y']}$. Define

$$U_\beta = 2\sum_{[S,y]\in\mathcal{V}/\sim} \left|\beta_{[S,y]}\right\rangle\left\langle\beta_{[S,y]}\right| - I, \tag{10.6}$$

which is the unitary and Hermitian operator associated with tessellation β.

One step of the staggered quantum walk on graph Γ (with unmarked vertices) is driven by the evolution operator

$$U = U_\beta U_\alpha. \tag{10.7}$$

To search a marked vertex, we need to define a reflection operator R with the following property:

$$R|S, y\rangle = \begin{cases} -|S, y\rangle, & \text{if } (S, y) \text{ is marked,} \\ |S, y\rangle, & \text{otherwise.} \end{cases} \tag{10.8}$$

A vertex (S, y) is marked if $\{i_1, i_2\} \subseteq S$, where $\{i_1, i_2\}$ is the colliding pair of indices, that is, $x_{i_1} = x_{i_2}$. We assume that there is either one collision or none. The only way to implement this operator is by querying elements of the list, which can be stored in extra registers. We postpone the discussion about the number of queries, which is presented in Sect. 10.3.2 in order to simplify the description of the core of the algorithm. Define

$$R = I - 2 \sum_{\substack{(S,y)\in\mathcal{V} \\ \{i_1,i_2\}\subseteq S}} |S, y\rangle\langle S, y|. \tag{10.9}$$

The evolution operator that solves the element distinctness problem is

$$\mathcal{U} = U^{t_2} R, \tag{10.10}$$

where

$$t_2 = \frac{\pi\sqrt{r}}{2\sqrt{2}}. \tag{10.11}$$

Since t_2 must be an integer, we round the result and take the nearest integer. The initial condition is the uniform superposition of all vertices

$$|\psi(0)\rangle = \frac{1}{\sqrt{\binom{N}{r}(N-r)}} \sum_{(S,y)\in\mathcal{V}} |S, y\rangle. \tag{10.12}$$

Before measuring, one must apply $\mathcal{U}^{t_1}$ to the initial condition where

$$t_1 = \frac{\pi}{4}\sqrt{r}, \tag{10.13}$$

which needs to be rounded. The final state is

$$|\psi(t_1)\rangle = \left(U^{t_2} R\right)^{t_1} |\psi(0)\rangle. \tag{10.14}$$

After measuring the position of the walker, the result is a basis state $|S, y\rangle$ so that $\{i_1, i_2\} \subseteq S$ with probability $1 - O\left(1/N^{1/3}\right)$. As a final step, we use the classical algorithm to check whether there is a 2-collision in S.

Exercise 10.3. The size of tessellation α is denoted by $|\mathcal{T}_\alpha|$. A polygon in this tessellation has size $(N - r)$. Show that the product of $|\mathcal{T}_\alpha|$ and the polygon size is the number of vertices of Γ.

Exercise 10.4. Show that U_α given by Eq. (10.3) can be expressed as

$$U_\alpha = \left(\frac{2}{N-r} - 1\right) I + \frac{2}{N-r} \sum_{S \in \mathcal{S}_r} \sum_{\substack{y, y' \in [N] \setminus S \\ y \neq y'}} \left|S, y'\right\rangle\langle S, y|. \tag{10.15}$$

Exercise 10.5. Show that the size of tessellation β is $\left|\mathcal{T}_\beta\right| = \binom{N}{r+1}$ and the size of a polygon in this tessellation is $(r + 1)$. Show that the product of the polygon size and the tessellation size is the number of vertices of Γ.

Exercise 10.6. Show that U_β given by Eq. (10.6) can be expressed as

$$U_\beta = \frac{1-r}{1+r} I + \frac{2}{r+1} \sum_{S \in \mathcal{S}_r} \sum_{\substack{y' \in S, \\ y \in [N] \setminus S}} \left|S \cup \{y\} \setminus \{y'\}, y'\right\rangle\langle S, y|. \tag{10.16}$$

Exercise 10.7. Show that α_S and $\beta_{[S,y]}$ are *maximal cliques*.

Exercise 10.8. The goal of this exercise is to build part of the graph $\Gamma(\mathcal{V}, E)$ when $N = 5$. Show that $r = 2$. Start with vertex $(\{1, 2\}, 3)$ and obtain all blue-adjacent vertices and link them with blue edges. This set of vertices is a maximal clique. Now take one vertex of this maximal clique and obtain all red-adjacent vertices and link them with red edges. Repeat this process for all vertices of the first clique. At this point, the graph has one blue maximal clique and three red maximal cliques. Convince yourself that this process can be repeated over and over until the full graph is obtained.

10.3.1 Analysis of the Algorithm

The probability of finding a marked vertex as a function of the number of steps t is

$$p(t) = \sum_{\substack{(S,y) \in \mathcal{V} \\ \{i_1, i_2\} \subseteq S}} \left|\left\langle S, y \middle| \psi(t) \right\rangle\right|^2, \tag{10.17}$$

where

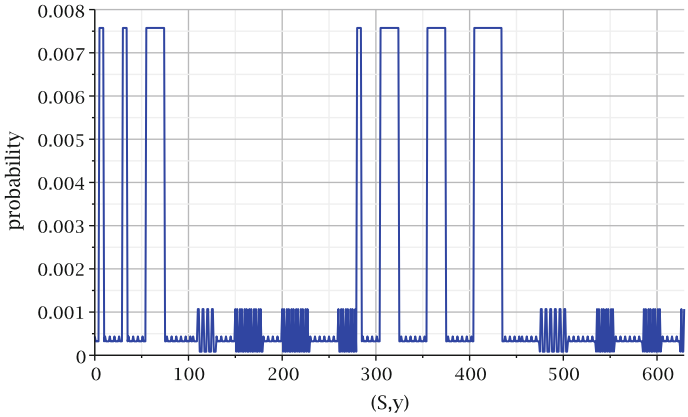

Fig. 10.2 Plot of the probability distribution of $|\psi(t_1)\rangle$ with $N = 9$, $r = 4$, and marked elements $\{i_1, i_2\} = \{2, 5\}$. The probability has 5 values ($\times 10^{-3}$): 7.57, 1.07, 0.43, 0.32, and 0.083

$$|\psi(t)\rangle = \left(U^{t_2} R\right)^t |\psi(0)\rangle, \tag{10.18}$$

U is given by (10.7), and R by (10.9). Parameter t_2 will be determined in this section. Figure 10.2 shows the probability distribution of $|\psi(t = 2)\rangle$ with $N = 9$, $r = 4$, and marked elements $\{i_1, i_2\} = \{2, 5\}$. Note that the probability distribution has only 5 values. For instance, there are 105 values 0.0076 approximately and they correspond to the marked vertices. This pattern is the same for any number of steps and any N, which strongly suggests that the vertices can be grouped according to some characteristic. Now we show that the analysis of the algorithm can be performed in a five-dimensional subspace of the original Hilbert space, that is, we will define five-dimensional reduced matrices U_{RED} and R_{RED} that are able to describe the action of U and R.

Let $\{i_1, i_2\}$ be the indices of the elements that are equal, that is, $x_{i_1} = x_{i_2}$, which is the only collision. We call i_1 and i_2 as marked indices. Define 5 types of sets (subsets of $\mathcal{V}$) in the following way:

η_0 – Set of vertices (S, y) such that S has exactly 2 marked indices.
η_1 – Set of vertices (S, y) such that S has no marked index and y is not a marked index.
η_2 – Set of vertices (S, y) such that S has no marked index and y is a marked index.
η_3 – Set of vertices (S, y) such that S has exactly 1 marked index and y is not a marked index.
η_4 – Set of vertices (S, y) such that S has exactly 1 marked index and y is a marked index.

Table 10.1 has a short description of sets η_ℓ for $0 \le \ell \le 4$ and their cardinalities.

Define 5 unit vectors

Table 10.1 Short description of sets η_ℓ for $0 \le \ell \le 4$ and their cardinalities

Set			Cardinality
η_0	$\lvert S \cap \{i_1, i_2\}\rvert = 2$	$y \notin \{i_1, i_2\}$	$\lvert\eta_0\rvert = \binom{N-2}{r-2}(N-r)$
η_1	$\lvert S \cap \{i_1, i_2\}\rvert = 0$	$y \notin \{i_1, i_2\}$	$\lvert\eta_1\rvert = \binom{N-2}{r}(N-r-2)$
η_2	$\lvert S \cap \{i_1, i_2\}\rvert = 0$	$y \in \{i_1, i_2\}$	$\lvert\eta_2\rvert = 2\binom{N-2}{r}$
η_3	$\lvert S \cap \{i_1, i_2\}\rvert = 1$	$y \notin \{i_1, i_2\}$	$\lvert\eta_3\rvert = 2\binom{N-2}{r-1}(N-r-1)$
η_4	$\lvert S \cap \{i_1, i_2\}\rvert = 1$	$y \in \{i_1, i_2\}$	$\lvert\eta_4\rvert = 2\binom{N-2}{r-1}$

$$|\eta_\ell\rangle = \frac{1}{\sqrt{|\eta_\ell|}} \sum_{(S,y)\in\eta_\ell} |S, y\rangle. \tag{10.19}$$

Note that $\langle\eta_k|\eta_\ell\rangle = \delta_{k\ell}$ because sets η_ℓ are nonintersecting. Those vectors define a five-dimensional subspace of the Hilbert space, which is invariant under the action of U, that is, there are 25 entries $(U_{\text{RED}})_{kj}$ such that

$$U|\eta_\ell\rangle = \sum_{k=0}^{4} (U_{\text{RED}})_{k\ell} |\eta_k\rangle, \tag{10.20}$$

where

$$U_{\text{RED}} = \begin{bmatrix} \frac{r-3}{r+1} & 0 & 0 & \frac{4\sqrt{2}\sqrt{r-1}\sqrt{a-1}}{(r+1)a} & \frac{2\sqrt{2}\sqrt{r-1}(2-a)}{(r+1)a} \\ 0 & \frac{a-4}{a} & \frac{2\sqrt{2}\sqrt{a-2}}{a} & 0 & 0 \\ 0 & \frac{2\sqrt{2}(1-r)\sqrt{a-2}}{(r+1)a} & \frac{(r-1)(a-4)}{(r+1)a} & \frac{2\sqrt{r}(a-2)}{(r+1)a} & \frac{4\sqrt{r}\sqrt{a-1}}{(r+1)a} \\ 0 & \frac{4\sqrt{2}\sqrt{r}\sqrt{a-2}}{(r+1)a} & \frac{2\sqrt{r}(4-a)}{(r+1)a} & \frac{(r-1)(a-2)}{(r+1)a} & \frac{2(r-1)\sqrt{a-1}}{(r+1)a} \\ \frac{2\sqrt{2}\sqrt{r-1}}{r+1} & 0 & 0 & \frac{2(3-r)\sqrt{a-1}}{(r+1)a} & \frac{(r-3)(a-2)}{(r+1)a} \end{bmatrix}$$

and $a = N - r$ (Exercise 10.9). A vector $|v\rangle = [v_0, v_1, v_2, v_3, v_4]^T$ in the five-dimensional subspace spanned by $\{|0\rangle, |1\rangle, |2\rangle, |3\rangle, |4\rangle\}$ is mapped to the large Hilbert space as $|V\rangle = v_0|\eta_0\rangle + v_1|\eta_1\rangle + v_2|\eta_2\rangle + v_3|\eta_3\rangle + v_4|\eta_4\rangle$, that is,

$$|V\rangle = \sum_{\ell=0}^{4} \langle\ell|v\rangle |\eta_\ell\rangle. \tag{10.21}$$

The eigenvalues of U_{RED} are eigenvalues of U, and the eigenvectors of U_{RED} are mapped to eigenvectors of U (Exercise 10.12). The converse is not true, that is, there are eigenvalues of U that are not eigenvalues of U_{RED} and there are eigenvectors of U

that cannot be obtained from eigenvectors of U_{RED}. The space reduction is useful only if the initial state of the algorithm comes from a reduced vector. Using Eq. (10.19), we can check that the sum of vectors $\sqrt{|\eta_\ell|}\,|\eta_\ell\rangle$ is the uniform superposition of vectors of the computational basis of the large Hilbert space. Using the normalization factor of vector $|\psi(0)\rangle$ given by Eq. (10.12), define vector

$$|\psi_0\rangle = \sum_{\ell=0}^{4} \langle \ell | \psi_0 \rangle \, |\ell\rangle \tag{10.22}$$

in the five-dimensional reduced space, where

$$\langle \ell | \psi_0 \rangle = \frac{\sqrt{|\eta_\ell|}}{\sqrt{\binom{N}{r}(N-r)}}. \tag{10.23}$$

It is straightforward to check that $|\psi_0\rangle$ is mapped to $|\psi(0)\rangle$ (Exercise 10.13). This means that the action of U on $|\psi(0)\rangle$ can be obtained from the action of U_{RED} on $|\psi_0\rangle$.

The goal now is to find the spectral decomposition of U_{RED}. The characteristic polynomial of U_{RED} is

$$\left|\lambda I_5 - U_{\text{RED}}\right| = (\lambda - 1)\left(\lambda^2 - 2\lambda\cos\omega_1 + 1\right)\left(\lambda^2 - 2\lambda\cos\omega_2 + 1\right), \tag{10.24}$$

where

$$\cos\omega_1 = 1 - \frac{2\,N}{(r+1)(N-r)}, \tag{10.25}$$

$$\cos\omega_2 = 1 - \frac{4\,(N-1)}{(r+1)(N-r)}. \tag{10.26}$$

The eigenvalues of U_{RED} are 1, $\mathrm{e}^{\mathrm{i}\omega_1}$, $\mathrm{e}^{\mathrm{i}\omega_2}$, $\mathrm{e}^{\mathrm{i}\omega_3}$, and $\mathrm{e}^{\mathrm{i}\omega_4}$, where $\omega_3 = -\omega_1$ and $\omega_4 = -\omega_2$.

The $(+1)$-eigenvector is

$$|\psi_0\rangle = \frac{1}{\sqrt{N}\sqrt{N-1}} \begin{bmatrix} \sqrt{r}\,\sqrt{r-1} \\ \sqrt{N-r-2}\,\sqrt{N-r-1} \\ \sqrt{2}\,\sqrt{N-r-1} \\ \sqrt{2}\sqrt{r}\,\sqrt{N-r-1} \\ \sqrt{2}\sqrt{r} \end{bmatrix}, \tag{10.27}$$

which coincides with vector $|\psi_0\rangle$ given by Eq. (10.22) (Exercise 10.14), that is, the initial state in the reduced space is a $(+1)$-eigenvector of U_{RED}. The eigenvector associated with $\mathrm{e}^{\mathrm{i}\omega_1}$ is

$$|\psi_1\rangle = \frac{1}{2\sqrt{a}\sqrt{N}\sqrt{N-2}} \begin{bmatrix} 2\,a\sqrt{r-1} \\ -2\sqrt{r}\sqrt{a-2}\sqrt{a-1} + 2\,\mathrm{i}\sqrt{N}\sqrt{a-2} \\ -2\sqrt{2}\sqrt{r}\sqrt{a-1} - \mathrm{i}\sqrt{2}\sqrt{N}\,(a-2) \\ \sqrt{2}\sqrt{a-1}\,(N-2\,r) + \mathrm{i}\sqrt{2}\sqrt{r}\sqrt{N} \\ \sqrt{2}\,(N-2\,r) - \mathrm{i}\sqrt{2}\sqrt{r}\sqrt{N}\sqrt{a-1} \end{bmatrix},$$

where $a = N - r$. The eigenvector associated with $\mathrm{e}^{\mathrm{i}\omega_3}$ is the complex conjugate of $|\psi_1\rangle$ that is, $|\psi_3\rangle = |\psi_1\rangle^*$. The eigenvector associated with $\mathrm{e}^{\mathrm{i}\omega_2}$ is

$$|\psi_2\rangle = \frac{1}{2\sqrt{a}\sqrt{N-1}\sqrt{N-2}} \begin{bmatrix} \sqrt{2}\,a\sqrt{a-1} \\ \sqrt{2}\sqrt{r}\sqrt{a-2}\sqrt{r-1} - 2\,\mathrm{i}\sqrt{r}\sqrt{N-1} \\ 2\,\sqrt{r}\sqrt{r-1} + \mathrm{i}\sqrt{2}\sqrt{r}\sqrt{N-1}\sqrt{a-2} \\ 2\,(1-a)\,\sqrt{r-1} + \mathrm{i}\sqrt{2}\sqrt{a-2}\sqrt{N-1} \\ -\sqrt{2}\sqrt{a-1}\left(\sqrt{2}\sqrt{r-1} + \mathrm{i}\sqrt{a-2}\sqrt{N-1}\right) \end{bmatrix}.$$

The eigenvector associated with $\mathrm{e}^{\mathrm{i}\omega_4}$ is $|\psi_4\rangle = |\psi_2\rangle^*$. This completes the spectral decomposition of U_{RED}. It can be checked (Exercise 10.15) that the eigenvectors satisfy the completeness relation $I_5 = \sum_{j=0}^{4} |\psi_j\rangle\langle\psi_j|$ and

$$U_{\text{RED}} = |\psi_0\rangle\langle\psi_0| + \sum_{j=1}^{4} \mathrm{e}^{\mathrm{i}\omega_j} |\psi_j\rangle\langle\psi_j|. \tag{10.28}$$

It is still missing to check the effect of R on a vector that comes from a reduced vector in order to confirm that R maintains invariant the subspace. The reduction scheme works only if R maps the initial state $|\psi(0)\rangle$ into a vector that can be obtained from a vector in the reduced space. R inverts the sign of the marked states, which are states $|S, y\rangle$ such that $|S \cap \{i_1, i_2\}| = 2$. R does nothing on the other states. Set η_0 comprises the marked vertices, then $R|\eta_0\rangle = -|\eta_0\rangle$ and $R|\eta_\ell\rangle = |\eta_\ell\rangle$ if $\ell \neq 0$. Then, R preserves the structure of the reduced space. The reduced version of R is

$$R_{\text{RED}} = I_5 - 2|0\rangle\langle 0|. \tag{10.29}$$

The evolution operator of the algorithm in the original Hilbert space is $\mathcal{U} = U^{t_2} R$. On the five-dimensional subspace, the reduced evolution operator is

$$\mathcal{U}_{\text{RED}} = (U_{\text{RED}})^{t_2} R_{\text{RED}} \tag{10.30}$$

and can be written as

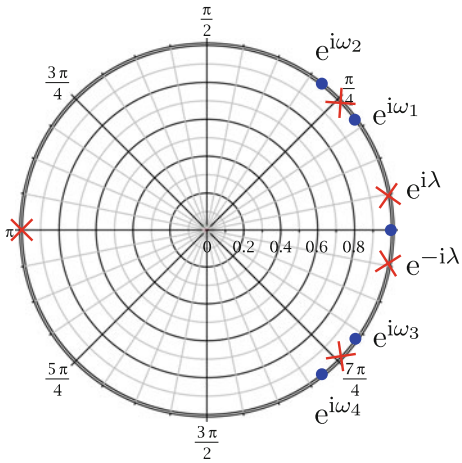

Fig. 10.3 Eigenvalues of U_{RED} (blue point) and $\mathcal{U}_{\text{RED}}$ (red cross) for $N = 50$. The eigenvalue of $\mathcal{U}_{\text{RED}}$ with the smallest positive argument is denoted by $e^{i\lambda}$

$$\mathcal{U}_{\text{RED}} = \left(|\psi_0\rangle\langle\psi_0| + \sum_{j=1}^{4} e^{it_2\omega_j}|\psi_j\rangle\langle\psi_j|\right)R_{\text{RED}}, \tag{10.31}$$

where R_{RED} is given by (10.29). To obtain the state in the reduced subspace that is mapped to the full final state $|\psi(t_1)\rangle$, we have to calculate

$$|\psi_f\rangle = \left(\mathcal{U}_{\text{RED}}\right)^{t_1}|\psi_0\rangle, \tag{10.32}$$

where $|\psi_0\rangle$ is the initial state in the reduced space. Note that $|\psi_0\rangle$ is not an eigenvector of $\mathcal{U}_{\text{RED}}$. The success probability is (Exercise 10.16)

$$p_{\text{succ}} = \left|\langle 0|\psi_f\rangle\right|^2. \tag{10.33}$$

Figure 10.3 shows the eigenvalues of U_{RED} (blue point) and $\mathcal{U}_{\text{RED}}$ (red cross) for $N = 50$. The eigenvalues that are not real tend to 1 when N goes to infinity, and they are interlaced for all values of N. It is interesting to compare the behavior of those eigenvalues with the behavior of the complex eigenvalues of the evolution operator of Grover's algorithm.

To calculate the success probability, we employ the *principal eigenvalue technique* described in Sect. 9.2 on p. 178, which requires the fulfillment of three conditions (Exercise 10.17). The coefficients A, B, and C given by Eqs. (9.17)–(9.19) on p. 180 are

$$A = 2\left|\langle 0|\psi_0\rangle\right|^2, \tag{10.34}$$

$$B = -\sum_{k=1}^{4} \frac{\left|\langle 0|\psi_k\rangle\right|^2 \sin\left(\omega_k t_2\right)}{1-\cos(\omega_k t_2)}, \tag{10.35}$$

$$C = \sum_{k=1}^{4} \frac{\left|\langle 0|\psi_k\rangle\right|^2}{1-\cos(\omega_k t_2)}. \tag{10.36}$$

Note that the nontrivial eigenvalues of $(U_{\text{RED}})^{t_2}$ are $\mathrm{e}^{\mathrm{i}\omega_k t_2}$ for $1 \le k \le 4$. Using that $\omega_3 = -\omega_1$ and $\omega_4 = -\omega_2$, we obtain $B = 0$. Simplifying Eqs. (10.34)–(10.36), we obtain

$$A = \frac{2\,r\,(r-1)}{N\,(N-1)}, \tag{10.37}$$

$$B = 0, \tag{10.38}$$

$$C = \frac{N-r}{N-2}\left(\frac{N-r-1}{(N-1)(1-\cos(\omega_2 t_2))} + \frac{2\,(r-1)}{N(1-\cos(\omega_1 t_2))}\right). \tag{10.39}$$

Using Eq. (9.28) on p. 182, the success probability as a function of the number of steps t is given by

$$p(t) = \frac{\left|\langle 0|\psi_0\rangle\right|^2}{A\,C}\,\sin^2\lambda t, \tag{10.40}$$

where

$$\lambda = \frac{\sqrt{A}}{\sqrt{C}}. \tag{10.41}$$

The largest success probability is obtained by taking $t = 2\pi/\lambda$ and choosing t_2 that minimizes C. Recall from Sect. 9.2 that the minimization of C plays a key role to improve the algorithm's efficiency. Since the last term of C in (10.39) tends to 0 for large N, we discard the last term, and the best t_2 is the one that maximizes $(1-\cos(\omega_2 t_2))$, which is $t_2 = \pi/\omega_2$. Using (10.26), the asymptotic expansion of π/ω_2 yields

$$t_2 = \frac{\pi}{\omega_2} = \frac{\pi\sqrt{r}}{2\sqrt{2}} + O\,(1)\,. \tag{10.42}$$

Using this value of t_2 and calculating the asymptotic expansion of C, we obtain

$$C = \frac{1}{2} + \cot^2\left(\frac{\pi}{2\sqrt{2}}\right)\frac{1}{\sqrt{r}} + O\left(r^{-1}\right) \tag{10.43}$$

and the probability as a function of time reduces to

$$p(t) = \left(1 - \cot^2\left(\frac{\pi}{2\sqrt{2}}\right)\frac{2}{\sqrt{r}}\right)\sin^2\left(\frac{2t}{\sqrt{r}}\right). \tag{10.44}$$

The optimal t is

$$t_1 = \frac{\pi}{4}\sqrt{r} + O(1) \tag{10.45}$$

and

$$p_{\text{succ}} = 1 - \cot^2\left(\frac{\pi}{2\sqrt{2}}\right)\frac{2}{\sqrt{r}} + O\left(r^{-1}\right). \tag{10.46}$$

Exercise 10.9. Use matrices u_α from Exercise 10.10 and u_β from Exercise 10.11 to find U_{RED}.

Exercise 10.10. The goal of this exercise is to find a five-dimensional matrix associated with U_α.

Use Eq. (10.2) to show that

$$\langle \alpha_S | \eta_\ell \rangle = \frac{c_\ell}{\sqrt{|\eta_\ell|}\sqrt{N-r}},$$

where $c_0 = (N-r)\delta_{|S\cap\{i_1,i_2\}|=2}$, $c_1 = (N-r-2)\delta_{|S\cap\{i_1,i_2\}|=0}$, $c_2 = 2\delta_{|S\cap\{i_1,i_2\}|=0}$, $c_3 = (N-r-1)\delta_{|S\cap\{i_1,i_2\}|=1}$, $c_4 = \delta_{|S\cap\{i_1,i_2\}|=1}$, where $\delta_{|S\cap\{i_1,i_2\}|=j}$ is equal to 1 if $|S \cap \{i_1, i_2\}| = j$ and 0 otherwise.

Show that

$$\sum_{\substack{S\in\mathcal{S}_r \\ |S\cap\{i_1,i_2\}|=0}} |\alpha_S\rangle = \frac{1}{\sqrt{N-r}}\left(\sqrt{|\eta_1|}\,|\eta_1\rangle + \sqrt{|\eta_2|}\,|\eta_2\rangle\right)$$

and find similar equations when $|S \cap \{i_1, i_2\}| = 1$ and $|S \cap \{i_1, i_2\}| = 2$.

Use the above equations and Eq. (10.3) to find the entries $(u_\alpha)_{kj}$ of

$$U_\alpha|\eta_\ell\rangle = \sum_{k=0}^{4}(u_\alpha)_{k\ell}|\eta_k\rangle.$$

Check your results with

$$u_\alpha = \begin{bmatrix} 1 & 0 & 0 & 0 & 0 \\ 0 & \frac{a-4}{a} & \frac{2\sqrt{2}\sqrt{a-2}}{a} & 0 & 0 \\ 0 & \frac{2\sqrt{2}\sqrt{a-2}}{a} & \frac{4-a}{a} & 0 & 0 \\ 0 & 0 & 0 & \frac{a-2}{a} & \frac{2\sqrt{a-1}}{a} \\ 0 & 0 & 0 & \frac{2\sqrt{a-1}}{a} & \frac{2-a}{a} \end{bmatrix},$$

where $a = N - r$.

Exercise 10.11. The goal of this exercise is to find a five-dimensional matrix associated with U_β. Show that

$$\langle \beta_{[S,y]} | \eta_\ell \rangle = \frac{d_\ell}{\sqrt{|\eta_\ell|}\sqrt{r+1}},$$

where $d_0 = (r-1)\delta_{k2}$, $d_1 = (r+1)\delta_{k0}$, $d_2 = \delta_{k1}$, $d_3 = r\delta_{k1}$, $d_4 = 2\delta_{k2}$, where $k = |(S \cup \{y\}) \cap \{i_1, i_2\}|$.

Define the following sets

$$D_k = \{[S, y] \in \mathcal{V}/\sim \; : \; |(S \cup \{y\}) \cap \{i_1, i_2\}| = k\}$$

for $0 \le k \le 2$ and show that

$$\sum_{[S,y]\in D_0} |\beta_{[S,y]}\rangle = \frac{1}{\sqrt{r+1}}\sqrt{|\eta_1|}\,|\eta_1\rangle,$$
$$\sum_{[S,y]\in D_1} |\beta_{[S,y]}\rangle = \frac{1}{\sqrt{r+1}}\left(\sqrt{|\eta_2|}\,|\eta_2\rangle + \sqrt{|\eta_3|}\,|\eta_3\rangle\right),$$
$$\sum_{[S,y]\in D_2} |\beta_{[S,y]}\rangle = \frac{1}{\sqrt{r+1}}\left(\sqrt{|\eta_0|}\,|\eta_0\rangle + \sqrt{|\eta_4|}\,|\eta_4\rangle\right).$$

Use those equations and (10.6) to find the entries $(u_\beta)_{k\ell}$ of

$$U_\beta|\eta_\ell\rangle = \sum_{k=0}^{4}(u_\beta)_{k\ell}|\eta_k\rangle.$$

Check your results with

$$u_\beta = \begin{bmatrix} \frac{r-3}{r+1} & 0 & 0 & 0 & \frac{2\sqrt{2}\sqrt{r-1}}{r+1} \\ 0 & 1 & 0 & 0 & 0 \\ 0 & 0 & \frac{1-r}{r+1} & \frac{2\sqrt{r}}{r+1} & 0 \\ 0 & 0 & \frac{2\sqrt{r}}{r+1} & \frac{r-1}{r+1} & 0 \\ \frac{2\sqrt{2}\sqrt{r-1}}{r+1} & 0 & 0 & 0 & \frac{3-r}{r+1} \end{bmatrix}.$$

Exercise 10.12. Use Eqs. (10.20) and (10.21) to show that the eigenvalues of U_{RED} are eigenvalues of U and the eigenvectors of U_{RED} are mapped to eigenvectors of U.

Exercise 10.13. Show that $\eta_{\ell_1} \cap \eta_{\ell_2} = \emptyset$ if $\ell_1 \neq \ell_2$ and $\cup_{\ell=0}^{4}\eta_\ell = \mathcal{V}$. Use those facts and Eq. (10.21) to show that $|\psi_0\rangle$ is mapped to $|\psi(0)\rangle$.

Exercise 10.14. Show that vector $|\psi_0\rangle$ given by Eq. (10.27) is equal to the vector described by Eqs. (10.22) and (10.23).

Exercise 10.15. Show that the eigenvectors of U_{RED} satisfy the completeness relation $I_5 = \sum_{j=0}^{4} |\psi_j\rangle\langle\psi_j|$ and Eq. (10.28).

Exercise 10.16. Show that p_{succ} given by Eq. (10.33) is equal to p_{succ} given by Eq. (10.17).

Exercise 10.17. Show that the *principal eigenvalue technique* can be applied to the algorithm of element distinctness, that is, check or show that:

1. The initial condition is a $(+1)$-eigenvector of the nonmodified evolution operator.
2. The phase λ of the principal eigenvalue $e^{i\lambda}$ of the modified evolution operator $\mathcal{U}_{\text{RED}}$ is much smaller than the phase of the principal eigenvalue $e^{i\omega_1 t_2}$ of the nonmodified evolution operator U_{RED}, that is, $\lambda \ll \omega_1 t_2$ when $N \gg 1$.
3. Show that
$$\left|\langle\psi_0|\lambda\rangle\right|^2 + \left|\langle\psi_0|\lambda'\rangle\right|^2 = 1 - O\left(1/\sqrt{r}\right)$$
and use this result to show that $|\epsilon|$ (see Eq. (9.8) on p. 178) can be disregarded for large N.

10.3.2 Number of Queries

The complexity analysis of Sect. 10.3.1 does not take into account the number of times the list of elements is queried. In order to fill this gap, we give the complete description of the algorithm and highlight the steps that perform queries. The algorithm uses two registers. A vector of the computation basis has the form

$$|S, y\rangle \otimes \left|x'_1, \ldots, x'_{r+1}\right\rangle,$$

where (S, y) is a vertex label and $x'_i \in [M]$, where M is an upper bound for the values of the list elements. The Hilbert spaces of the registers have $\binom{N}{r}(N-r)$ and M^{r+1} dimensions, respectively.

Initial Setup

The initial condition is

$$|\psi(0)\rangle|0, \ldots, 0\rangle, \tag{10.47}$$

where $|\psi(0)\rangle$ is given by Eq. (10.12). The first step is to query each x_i for $i \in S$. Suppose that $S = \{i_1, \ldots, i_r\}$, then the next state is

$$\frac{1}{\sqrt{\binom{N}{r}(N-r)}} \sum_{(S,y)\in\mathcal{V}} |S, y\rangle\left|x_{i_1}, \ldots, x_{i_r}, 0\right\rangle, \tag{10.48}$$

where x_i is the ith element of the list. The elements of S and the first r slots of the second register are in one-to-one correspondence. The number of queries in this step is r, and it is performed only once.

Main Block

1. Repeat this block of two steps the following number of times: $t_1 = \left\lfloor \frac{\pi}{4}\sqrt{r} \right\rceil$, where $\lfloor \cdot \rceil$ is the nearest integer.

   (a) Apply a conditional phase flip operator $\mathcal{R}$ that inverts the phase of $|S, y\rangle |x'_1, \ldots, x'_{r+1}\rangle$ if and only if both marked indices i_1 and i_2 are in S, that is,

$$\mathcal{R}|S, y\rangle |x'_1, \ldots, x'_{r+1}\rangle = \begin{cases} -|S, y\rangle |x'_1, \ldots, x'_{r+1}\rangle, & \text{if } i_1, i_2 \in S, \\ |S, y\rangle |x'_1, \ldots, x'_{r+1}\rangle, & \text{otherwise.} \end{cases}$$

   (b) Repeat Subroutine 1 the following number of times: $t_2 = \left\lfloor \frac{\pi\sqrt{r}}{2\sqrt{2}} \right\rceil$.

2. Measure the first register and check whether S has a 2-collision using a classical algorithm.

Subroutine 1

1. Apply operator U_α given by (10.3) to the first register.
2. Apply oracle $\mathcal{O}$ defined by

$$\mathcal{O}|S, y\rangle |x'_1, \ldots, x'_{r+1}\rangle = |S, y\rangle |x'_1, \ldots, x'_{r+1} \oplus x_y\rangle,$$

   which queries element x_y and adds x_y to x'_{r+1} in the last slot of the second register.
3. Apply operator U_β^{EXT}, which is an extension of (10.6), defined by

$$U_\beta^{\text{EXT}} = 2 \sum_{x'_1, \ldots, x'_{r+1}} \sum_{[S,y] \in \mathcal{V}/\sim} \left| \beta_{[S,y]}^{x'_1, \ldots, x'_{r+1}} \right\rangle \left\langle \beta_{[S,y]}^{x'_1, \ldots, x'_{r+1}} \right| - I,$$

   where

$$\left| \beta_{[S,y]}^{x'_1, \ldots, x'_{r+1}} \right\rangle = \frac{1}{\sqrt{r+1}} \sum_{y' \in S \cup \{y\}} |S \cup \{y\} \setminus \{y'\}, y'\rangle |\pi(x'_1), \ldots, \pi(x'_{r+1})\rangle \tag{10.49}$$

   and π is a permutation of the slots of the second register induced by the permutation of the indices of the first register.
4. Apply oracle $\mathcal{O}$.

Note that when the input is given by (10.48), the output of step 2 of Subroutine 1 has the elements of S and the first r slots of the second register in one-to-one

correspondence and the last slot of the second register is x_y. This one-to-one correspondence is maintained for each term in sum (10.49) and $\pi(x'_{r+1}) = x_{y'}$. This means that for the analysis of the algorithm the second register is "redundant" in the sense that it can be reproduced if we know S and y in the state $|S, y\rangle$ of the first register. When we eliminate the second register, as we have done earlier, U_β^{EXT} becomes U_β and $U_\alpha \otimes I$ becomes U_α.

The number of quantum queries is the number of times oracle $\mathcal{O}$ is used plus the number of queries in the initial setup. This yields $(2\,t_1 t_2 + r)$, which is $O\left(N^{2/3}\right)$. There is an overhead of r classical queries after the measurement, which is also $O\left(N^{2/3}\right)$.

Note that no queries are required in the action of the conditional phase flip $\mathcal{R}$. This is a central point in the algorithm because oracle $\mathcal{O}$ updates the information in the second register by querying only one element. When the walker moves from one vertex (S, y) to the next (S', y'), under the action of either U_α or U_β, sets S and S' differ by one element at most. This setup minimizes the number of queries. Operator U_α plays the role of a coin by diffusing the values of y that are not in S and operator U_β plays the role of the shift by moving the new values of y into S.

Exercise 10.18. Use the approximation

$$\ln \binom{N}{r} \approx r \ln \frac{N}{r}$$

valid when $N \gg r \gg 1$ to show that the algorithm uses $O\left(r\left(\ln N + \ln M\right)\right)$ qubits of memory.

Exercise 10.19. The goal of this exercise is to apply *Tulsi's modification* described in Sect. 9.2.2 on p. 183 in order to propose a new optimal algorithm for the element distinctness problem.

Set $t_2 = 1$, that is, use the evolution operator

$$\mathcal{U}_0 = U R,$$

and show that the success probability as a function of the number of steps tends to zero when N increases. Show that Tulsi's modification of $\mathcal{U}_0$ with $\eta \approx 1/(2\sqrt{r})$ can enhance the success probability to $O(1)$ by taking $O(r)$ steps. Show that the number of queries is $O(N^{2/3})$. Check that the three conditions are fulfilled.

10.3.3 Example

The algorithm presented in this chapter is so complex that an example is welcome. Take the list $x = (39, 45, 39, 28)$ with $N = 4$ elements. Then, $r = 2$. Let us focus on Subroutine 1. Consider state

$$|\psi_0\rangle = |\{1, 2\}, 3\rangle|39, 45, 0\rangle,$$

which belongs to the initial state (10.48). Let us start with Step 1 of Subroutine 1, that is, apply U_α. The action of U_α on $|S, y\rangle$ keeps the same S and outputs a sum of all $y \notin S$, that is

$$|\psi_1\rangle = c_0|\{1, 2\}, 3\rangle|39, 45, 0\rangle + c_1|\{1, 2\}, 4\rangle|39, 45, 0\rangle.$$

In this case, $c_0 = 0$ and $c_1 = 1$ because the blue polygons in Fig. 10.1 have two vertices only. Next step applies oracle $\mathcal{O}$, which outputs

$$|\psi_2\rangle = |\{1, 2\}, 4\rangle|39, 45, 28\rangle.$$

At this point, the entire first and second registers are in one-to-one correspondence at a cost of one query only.

Next step is to apply U_β^{EXT} to $|\psi_2\rangle$. The action of U_β^{EXT} on $|\{y_1, \ldots, y_r\}, y\rangle$ outputs all cyclic permutations of $(\{y_1, \ldots, y_r\}, y)$, that is, $|\{y, y_1, \ldots, y_{r-1}\}, y_r\rangle$, $|\{y_r, y, y_1, \ldots, y_{r-2}\}, y_{r-1}\rangle$, and so on.[1] Besides, the elements in the slots of the second register also permute. Then,

$$\begin{aligned}|\psi_3\rangle =& c_0|\{1, 2\}, 4\rangle|39, 45, 28\rangle + \\ & c_1|\{1, 4\}, 2\rangle|39, 28, 45\rangle + \\ & c_2|\{2, 4\}, 1\rangle|45, 28, 39\rangle,\end{aligned}$$

where $c_1 = -1/3$ and $c_1 = c_2 = 2/3$. Note that the one-to-one correspondence is kept because the second register was also permuted. We have to query one more time to clear the last slot of the second register before applying U_α. Apply oracle $\mathcal{O}$ again, which outputs

$$\begin{aligned}|\psi_4\rangle =& c_0|\{1, 2\}, 4\rangle|39, 45, 0\rangle + \\ & c_1|\{1, 4\}, 2\rangle|39, 28, 0\rangle + \\ & c_2|\{2, 4\}, 1\rangle|45, 28, 0\rangle.\end{aligned}$$

That is exactly what we need to go back to Step 1 of Subroutine 1, which applies U_α, and Step 2, and so on t_2 times.

Let us analyze the Main Block. If we apply the conditional phase flip $\mathcal{R}$ to $|\psi_4\rangle$, nothing changes because there are no states with repeated entries in the second register. On the other hand, if we apply Subroutine 1 to state

$$\left|\psi_0'\right\rangle = |\{1, 2\}, 4\rangle|39, 45, 0\rangle,$$

[1] Set S must be stored in a unique way independent of how it was created by choosing a suitable data structure. In the example, we display S sorted in increasing order, that is, after performing the cyclic permutation, S is sorted.

the output of Step 4 prime will be (4 → 3 and 28 → 39 in Step 4)

$$\begin{aligned}\left|\psi_4'\right\rangle =& c_0'|\{1,2\},3\rangle|39,45,0\rangle+\\ & c_1'|\{1,3\},2\rangle|39,39,0\rangle+\\ & c_2'|\{2,3\},1\rangle|45,39,0\rangle,\end{aligned}$$

and the action of $\mathcal{R}$ will invert the sign of term $|\{1,3\},2\rangle|39,39,0\rangle$. Notice that the same result is obtained by applying R given by Eq. (10.9) to the first register.

This example helps to understand why we can disregard the second register in the analysis of Sect. 10.3. Oracle $\mathcal{O}$ is necessary for querying the elements of the list, which allows operator $\mathcal{R}$ to invert the phase of the marked states. If we suppose that operator R as described by Eq. (10.9) is available, we can calculate the *running time* and the *success probability* by disregarding the second register, that is, by eliminating $\mathcal{O}$ and by replacing $\mathcal{R}$ by R.

Further Reading

The element distinctness problem has a long history. In classical computing, the optimal lower bound for the model of comparison-based branching programs was obtained by Yao [342]. Classical lower bounds have been obtained in general models in Refs. [34, 127].

A related problem is the *collision problem*, where a two-to-one function f is given and we have to find x and y such that $f(x) = f(y)$. Quantum lower bounds for the collision problem were obtained by Aaronson and Shi [2] and by Kutin [196]. Brassard, Høyer, and Tapp [60] solved the collision problem in $O(N^{1/3})$ quantum steps achieving the lower bound. If the element distinctness problem can be solved with N queries, then the collision problem can be solved with $O(\sqrt{N})$ queries [2].

Quantum lower bounds for the element distinctness problem were obtained by Aaronson and Shi [2] and Ambainis [15]. Buhrman et al. [64] described a quantum algorithm that uses $O(N^{3/4})$ queries. Ambainis's optimal algorithm for the element distinctness problem firstly appeared in [14] and was published in [16]. Ambainis's algorithm used a new quantum walk framework on a *bipartite graph*, which was generalized by Szegedy [307]. In a strict sense, Ambainis' quantum walk is not is not an instance of *Szegedy's model*, because the graph employed by Ambainis is a nonsymmetric bipartite graph.[2] On the other hand, a new efficient algorithm for the element distinctness problem was described by using an instance of Szegedy's model on the duplicated graph of the *Johnson graph* by Santha [290]. None of those versions have obtained the optimal values for t_1 and t_2, which were given for the first time in [265]. The material of this chapter was based on [265], which addressed the general case (k-collision). Since Szegedy's model is entirely included in the *staggered model*, the version using the Johnson graph can also be converted into a 2-*tessellable* staggered quantum walk using the *line graph* of the bipartite graph obtained from the duplication of the Johnson graph.

[2]It is important to stress that Ambainis's algorithm employs a quantum walk on a bipartite graph that is neither a Johnson graph nor the duplication of a Johnson graph.

Ambainis's algorithm was used to build a quantum algorithm for *triangle finding* by Magniez, Santha, and Szegedy [226] and to *subset finding* by Childs and Eisenberg [80]. Santha [290] surveyed the application of Szegedy's quantum walk to the element distinctness problem and for other related search problems, such as matrix product verification and group commutativity. Tani [309] described implementations of quantum-walk-based algorithms for claw finding. Childs [79] described the element distinctness algorithm in terms of the continuous-time quantum walk model [113]. Belovs [37] applied *learning graphs* to present quantum algorithms with a smaller number of queries for the k-distinctness problem. Belovs et al. [38] presented quantum walk algorithms for the 3-collision element distinctness problem with $O(N^{5/7})$. Rosmanis [282] addressed quantum adversary lower bounds for the element distinctness problem. Kaplan [168] used the element distinctness algorithm in the context of quantum attacks against iterated block ciphers. Jeffery, Magniez, and de Wolf [164] analyzed parallel quantum queries for the element distinctness problem. Abreu et al. [94] described a useful simulator for Ambainis's algorithm.

The description of the evolution operator of the element distinctness algorithm in the staggered model [264, 269] appeared in Abreu's master thesis [93].

Chapter 11
Szegedy's Quantum Walk

In this chapter, we describe Szegedy's model, which is a collection of *discrete-time coinless* quantum walks on *symmetric bipartite digraphs*. A symmetric bipartite digraph can be obtained from an underlying digraph by a *duplication process*. The underlying digraph defines a *classical Markov chain* , and Szegedy's model is usually said to be the quantized version of this Markov chain.

Before entering the quantum context, we review some relevant classical concepts, which are the *discrete-time classical Markov chains* and the *hitting time*. The most known formula for calculating the *classical hitting time* uses the *stationary distribution*. However, there is an alternative formula that does not rely on the stationary distribution and requires the use of *sinks*, which are vertices with *outdegree* zero. This formula can be generalized to the quantum context.

We start by describing Szegedy's model on *symmetric bipartite graphs*, which are obtained from underlying simple graphs via a *duplication process*. Then, we address digraphs that have at least one sink (or *marked vertex*). The duplication process produces a *bipartite digraph*. Szegedy's quantum walk takes place on the bipartite digraph, and the *quantum hitting time* is defined using this quantum walk. We show how the evolution operator is obtained from the *stochastic matrix* of the underlying digraph, and we exemplify the whole scheme using the *complete graph*.

11.1 Discrete-Time Markov Chains

In this section, we review discrete-time Markov chains in a way that complements the topics addressed in Sect. 3.2 on p. 23. A detailed review of the *classical hitting time* is left to Appendix C. A classical discrete-time *stochastic process* is a sequence of random variables $X_0, X_1, X_2, \ldots$ denoted by $\{X_t : t \in \mathbb{N}\}$. X_t is the *state* of the stochastic process at time t and X_0 is the initial state. We suppose that the *state space*

© Springer Nature Switzerland AG 2018

R. Portugal, *Quantum Walks and Search Algorithms*, Quantum Science and Technology, https://doi.org/10.1007/978-3-319-97813-0_11

$\mathcal{S}$ is discrete, for instance, $\mathcal{S} = \mathbb{N}$. A *Markov chain* is a stochastic process, whose future depends only on the present state, that is,

$$\text{Prob}(X_{t+1} = j \mid X_t = i, X_{t-1} = i_{n-1}, \ldots, X_0 = i_0) = \text{Prob}(X_{t+1} = j \mid X_t = i)$$

for all $t \geq 0$ and $i_0, \ldots, i, j \in \mathcal{S}$. Define $p_{ij} = \text{Prob}(X_{t+1} = j \mid X_t = i)$ and assume that p_{ij} does not depend on t (*time-homogeneous Markov chain*). Matrix P with entries p_{ij} for $i, j \in \mathcal{S}$ is called the *transition matrix* (or *right stochastic matrix*) of the chain and has the following properties: $p_{ij} \geq 0$ and $\sum_{j \in \mathcal{S}} p_{ij} = 1$ for all $i \in \mathcal{S}$.

Any time-homogeneous Markov chain can be represented by a digraph (directed graph) $\Gamma(V, A)$, where the vertex set V is the state space $\mathcal{S}$ and A is the arc set. Arc (i, j) is in A if and only if $p_{ij} > 0$. If the transition matrix is symmetric, then the digraph representing the Markov chain reduces to a simple graph. A *random walk* on Γ can be cast into the Markov chain formalism.

A state i is called *absorbing* if $p_{ii} = 1$. In this case, $p_{ij} = 0$ for all $j \neq i$, which means that if the Markov chain reaches state i, it will be stuck there forever because the probability to go to any other state different from i is zero. In terms of graph representation, an absorbing state is represented by a *sink*, which is a vertex that has *outdegree* equal to zero.

11.2 Markov Chain-Based Quantum Walk

Szegedy's quantum walk is defined on a bipartite digraph obtained by duplicating a digraph (called *underlying digraph*) associated with a discrete-time Markov chain. For simplicity, in this section we address the case with no marked vertices, which has only simple graphs. Figure 11.1 shows an example of a bipartite graph (second graph) obtained from the simple graph (first graph) of a Markov chain with three states $\mathcal{S} = \{0, 1, 2\}$. If x_1 is adjacent to x_2 and x_3 in the underlying graph, then x_1 must be adjacent only to y_2 and y_3 in the bipartite graph. The same must hold for x_2 and x_3. The description of the *duplication process* in a general setting is as follows. Each edge $\{x_i, x_j\}$ of the underlying graph, which connects the adjacent vertices x_i

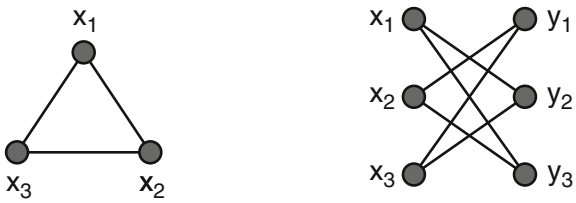

Fig. 11.1 Example of an underlying graph with three vertices and the bipartite graph generated by the *duplication process*. In this case, there is no marked vertex. The classical random walk is defined on the first graph and the quantum walk is defined on the second graph

and x_j, corresponds to two edges $\{x_i, y_j\}$ and $\{y_i, x_j\}$ in the bipartite graph. The reverse process can also be defined, that is, we can obtain the underlying graph from the bipartite graph.

Consider a bipartite graph with sets X and Y of equal cardinalities obtained from the duplication process. Let x and y be vertices of X and Y, respectively. Define p_{xy} as the inverse of the degree of vertex x, if y is *adjacent* to x, otherwise $p_{xy} = 0$. For example, if x is adjacent to only two vertices y_1 and y_2 in set Y, then $p_{xy_1} = p_{xy_2} = 1/2$. Analogously, we define q_{yx} as the inverse of the degree of vertex y. The entries p_{xy} and q_{yx} satisfy

$$\sum_{y \in Y} p_{xy} = 1 \quad \forall x \in X, \tag{11.1}$$

$$\sum_{x \in X} q_{yx} = 1 \quad \forall y \in Y. \tag{11.2}$$

Note that $p_{xy} = q_{xy}$ and p_{xy} are symmetric since the bipartite graph is undirected and there is an identification between X and Y.

The quantum walk on the bipartite graph has an associated Hilbert space $\mathcal{H}^{n^2} = \mathcal{H}^n \otimes \mathcal{H}^n$, where $n = |X| = |Y|$.[1] The computational basis of the first factor is $\{|x\rangle : x \in X\}$ and of the second is $\{|y\rangle : y \in Y\}$. The computational basis of $\mathcal{H}^{n^2}$ is $\{|x, y\rangle : x \in X, y \in Y\}$. Instead of using probability matrices P and Q of the classical random walk, the entries of which are p_{xy} and q_{yx}, we define operators $A : \mathcal{H}^n \to \mathcal{H}^{n^2}$ and $B : \mathcal{H}^n \to \mathcal{H}^{n^2}$ as follows:

$$A = \sum_{x \in X} |\alpha_x\rangle\langle x|, \tag{11.3}$$

$$B = \sum_{y \in Y} |\beta_y\rangle\langle y|, \tag{11.4}$$

where

$$|\alpha_x\rangle = |x\rangle \otimes \left(\sum_{y \in Y} \sqrt{p_{xy}}\, |y\rangle \right), \tag{11.5}$$

$$|\beta_y\rangle = \left(\sum_{x \in X} \sqrt{q_{yx}}\, |x\rangle \right) \otimes |y\rangle. \tag{11.6}$$

The dimensions of A and B are $n^2 \times n$. Another way to write (11.3) and (11.4) is

[1] The sizes of X and Y need not necessarily be equal. The terminology *bipartite quantum walk* would be more precise to describe this case.

$$A|x\rangle = |\alpha_x\rangle, \tag{11.7}$$
$$B|y\rangle = \left|\beta_y\right\rangle, \tag{11.8}$$

that is, multiplying matrix A by the xth vector of the computational basis of $\mathcal{H}^n$ is the xth column of A. Therefore, the columns of matrix A are the vectors $|\alpha_x\rangle$ and the columns of matrix B are the vectors $\left|\beta_y\right\rangle$. Using (11.5) and (11.6) along with (11.1) and (11.2), we obtain

$$\left\langle\alpha_x\middle|\alpha_{x'}\right\rangle = \delta_{xx'}, \tag{11.9}$$
$$\left\langle\beta_y\middle|\beta'_y\right\rangle = \delta_{yy'}. \tag{11.10}$$

Then, we have

$$A^{\mathrm{T}}A = I_n, \tag{11.11}$$
$$B^{\mathrm{T}}B = I_n. \tag{11.12}$$

These equations imply that the actions of A and B preserve the norm of vectors. So, if $|\mu\rangle$ is a unit vector in $\mathcal{H}^n$, then $A|\mu\rangle$ is a unit vector in $\mathcal{H}^{n^2}$. The same regarding B.

Let us investigate the product in the reverse order. Using (11.3) and (11.4), we obtain

$$AA^{\mathrm{T}} = \sum_{x\in X} |\alpha_x\rangle\langle\alpha_x|, \tag{11.13}$$
$$BB^{\mathrm{T}} = \sum_{y\in Y} \left|\beta_y\right\rangle\left\langle\beta_y\right|. \tag{11.14}$$

Using (11.11) and (11.12), we have $(AA^{\mathrm{T}})^2 = AA^{\mathrm{T}}$ and $(BB^{\mathrm{T}})^2 = BB^{\mathrm{T}}$. So, let us define the projectors

$$\Pi_A = AA^{\mathrm{T}}, \tag{11.15}$$
$$\Pi_B = BB^{\mathrm{T}}. \tag{11.16}$$

Equations (11.13) and (11.14) show that Π_A projects a vector in $\mathcal{H}^{n^2}$ on subspace $\mathcal{A} = \mathrm{span}\left\{|\alpha_x\rangle : x \in X\right\}$ and Π_B projects on subspace $\mathcal{B} = \mathrm{span}\left\{\left|\beta_y\right\rangle : y \in Y\right\}$.

After obtaining the projectors, we can define the associated *reflection operators*, which are

$$\mathcal{R}_A = 2\,\Pi_A - I_{n^2}, \tag{11.17}$$
$$\mathcal{R}_B = 2\,\Pi_B - I_{n^2}. \tag{11.18}$$

$\mathcal{R}_A$ reflects a vector in $\mathcal{H}^{n^2}$ through subspace $\mathcal{A}$. We can check this in the following way: $\mathcal{R}_A$ leaves invariant any vector in $\mathcal{A}$, that is, if $|\psi\rangle \in \mathcal{A}$, then $\mathcal{R}_A|\psi\rangle = |\psi\rangle$, as can be confirmed by (11.17). On the other hand, $\mathcal{R}_A$ inverts the sign of any vector

orthogonal to $\mathcal{A}$, that is, if $|\psi\rangle \in \mathcal{A}^{\perp}$ or $|\psi\rangle$ is in the *kernel* of $\mathcal{A}$, then $\mathcal{R}_A|\psi\rangle = -|\psi\rangle$. A vector in $\mathcal{H}^{n^2}$ can be written as a linear combination of a vector in $\mathcal{A}$ and another one in $\mathcal{A}^{\perp}$. The action of $\mathcal{R}_A$ leaves the component in $\mathcal{A}$ unchanged and inverts the sign of the component in $\mathcal{A}^{\perp}$. Geometrically, this is a *reflection* through $\mathcal{A}$, as if $\mathcal{A}$ is the mirror and $\mathcal{R}_A|\psi\rangle$ is the image of $|\psi\rangle$. The same is true for $\mathcal{R}_B$ with respect to subspace $\mathcal{B}$.

Now let us analyze the relation between subspaces $\mathcal{A}$ and $\mathcal{B}$. The best way is to analyze the angles between vectors in basis $\{|\alpha_x\rangle : x \in X\}$ and vectors in $\{|\beta_y\rangle : y \in Y\}$. Define the *inner product matrix* C so that $C_{xy} = \langle\alpha_x|\beta_y\rangle$. Using (11.5) and (11.6), we can express the entries of C in terms of the transition probabilities as $C_{xy} = \sqrt{p_{xy}q_{yx}}$. In matrix form, we write

$$C = A^{\mathrm{T}}B, \tag{11.19}$$

which can be obtained from (11.3) and (11.4). C is a n-dimensional matrix called *discriminant*, which is not *normal* in general. The eigenvalues and eigenvectors of C do not play an important role in this context. On the other hand, the *singular values and vectors* of C, which are quantities conceptually close to eigenvalues and eigenvectors, do play. They coincide with the ones of the Markov chain *transition matrix* for the symmetric case and will be analyzed ahead.

Exercise 11.1. The goal of this exercise is to generalize the formulas of this section when the cardinality of set X is different from the cardinality of set Y. Let $|X| = m$ and $|Y| = n$. What are the dimensions of matrices A, B, and C in this case? What formulas of this section explicitly change?

Exercise 11.2. Consider the complete bipartite graph when X has a single element and Y has two elements. Show that $\mathcal{R}_A$ is the Pauli matrix σ_x and $\mathcal{R}_B$ is the identity matrix I_2.

11.3 Evolution Operator

We are now ready to define a bipartite quantum walk associated with transition matrix P of the underlying graph. Let us define the *evolution operator* as

$$W_P = \mathcal{R}_B\,\mathcal{R}_A, \tag{11.20}$$

where $\mathcal{R}_A$ and $\mathcal{R}_B$ are the reflection operators given by (11.17) and (11.18). At time t, the state of the quantum walk is $(W_P)^t$ applied to the initial state. Note that the structure of this walk is different from the structure of the *coined quantum walk*, which employs a coin and a shift operator. The new definition has some advantages. In particular, the *quantum hitting time* can be naturally defined as a generalization of the *classical hitting time*. It can be shown that the quantum hitting time for this

quantum walk on a finite bipartite graph is quadratically smaller than the classical hitting time of a random walk on the underlying graph.

The analysis of the evolution of the quantum walk can be performed if we know the *spectral decomposition* of W_P. The spectral decomposition associated with the nontrivial eigenvalues can be calculated in terms of the *singular values and vectors* of matrix C defined by (11.19), as discussed in the following sections.

Exercise 11.3. The goal of this exercise is to determine the conditions that makes state

$$|\psi(0)\rangle = \frac{1}{\sqrt{n}} \sum_{\substack{x \in X \\ y \in Y}} \sqrt{p_{xy}}|x, y\rangle$$

be a 1-eigenvector of W_P. Show that the action of $\mathcal{R}_A$ leaves $|\psi(0)\rangle$ invariant. Does the action of $\mathcal{R}_B$ leave $|\psi(0)\rangle$ invariant? Under what conditions?

11.4 Singular Values and Vectors of the Discriminant

The *singular value decomposition theorem* states that there are unitary matrices U and V such that

$$C = UDV^\dagger, \tag{11.21}$$

where D is a n-dimensional diagonal matrix with nonnegative real entries. Usually, the diagonal elements are sorted with the largest element occupying the first position. These elements are called singular values and are uniquely determined once given matrix C. In the general case, matrices U and V are not uniquely determined. They can be determined by applying the spectral theorem to matrix $C^\dagger C$. $C^\dagger C$ is a positive semidefinite Hermitian matrix, that is, its eigenvalues are nonnegative real numbers. Then, $C^\dagger C$ admits a spectral decomposition and the square root $\sqrt{C^\dagger C}$ is well defined. Written on the basis of eigenvectors of $C^\dagger C$, $\sqrt{C^\dagger C}$ is a diagonal matrix where each diagonal element is the square root of the corresponding eigenvalue of $C^\dagger C$.

Let λ_i^2 and $|\nu_i\rangle$ be the *eigenvalues* and *eigenvectors* of $C^\dagger C$. Assume that $\left\{|\nu_i\rangle : 1 \leq i \leq n\right\}$ is an orthonormal basis. Then,

$$C^\dagger C = \sum_{i=1}^{n} \lambda_i^2 \, |\nu_i\rangle\langle\nu_i| \tag{11.22}$$

and

$$\sqrt{C^\dagger C} = \sum_{i=1}^{n} \lambda_i \, |\nu_i\rangle\langle\nu_i|. \tag{11.23}$$

Now we show how to find U and V. For each i such that $\lambda_i > 0$, define

$$|\mu_i\rangle = \frac{1}{\lambda_i} C|\nu_i\rangle. \tag{11.24}$$

Using Eqs. (11.11), (11.12), and that $\left\{|\nu_i\rangle : 1 \leq i \leq n\right\}$ is an orthonormal basis, we obtain

$$\left\langle \mu_i \middle| \mu_j \right\rangle = \delta_{ij}, \tag{11.25}$$

for all i, j such that λ_i and λ_j are positive. For the eigenvectors in the *kernel* of $\sqrt{C^\dagger C}$, define $\left|\mu'_j\right\rangle = \left|\nu_j\right\rangle$. However, with this extension we generally lose the orthogonality between vectors $|\mu_i\rangle$ and $\left|\mu'_j\right\rangle$. We can apply the *Gram–Schmidt orthonormalization process* to redefine vectors $\left|\mu'_j\right\rangle$ such that they are orthogonal to the vectors that do not belong to the kernel, and we call them $\left|\mu_j\right\rangle$. In the end, we can obtain a complete set satisfying orthonormality condition (11.25). With vectors $|\nu_i\rangle$ and $|\mu_i\rangle$, we obtain U and V using equations

$$U = \sum_{i=1}^{n} |\mu_i\rangle\langle i|, \tag{11.26}$$

$$V = \sum_{i=1}^{n} |\nu_i\rangle\langle i|. \tag{11.27}$$

$|\nu_i\rangle$ and $|\mu_i\rangle$ are the singular vectors, and λ_i are the corresponding singular values. They obey the following equations:

$$C|\nu_i\rangle = \lambda_i\, |\mu_i\rangle, \tag{11.28}$$

$$C^{\mathrm{T}}|\mu_i\rangle = \lambda_i\, |\nu_i\rangle, \tag{11.29}$$

for $1 \leq i \leq n$. Note that $|\mu_i\rangle$ and $|\nu_i\rangle$ have a dual behavior. In fact, they are called the *left* and *right singular vectors*, respectively.

By left multiplying (11.28) by A and (11.29) by B, we obtain

$$\Pi_A\, B|\nu_i\rangle = \lambda_i\, A|\mu_i\rangle, \tag{11.30}$$

$$\Pi_B\, A|\mu_i\rangle = \lambda_i\, B|\nu_i\rangle. \tag{11.31}$$

We have learned earlier that the action of operators A and B preserves the norm of the vectors. Since $|\mu_i\rangle$ and $|\nu_i\rangle$ are unit vectors, $A|\mu_i\rangle$ and $B|\nu_i\rangle$ are also unit vectors. The action of projectors either decreases the norm of vectors or maintains it invariant. Using (11.30), we conclude that the singular values satisfy inequalities $0 \leq \lambda_i \leq 1$. Therefore, λ_i can be written as $\lambda_i = \cos\theta_i$, where $0 \leq \theta_i \leq \pi/2$. The geometric interpretation of θ_i is the angle between vectors $A|\mu_i\rangle$ and $B|\nu_i\rangle$. In fact, using (11.19) and (11.28) we obtain that the inner product of $A|\mu_i\rangle$ and $B|\nu_i\rangle$ is

$$\lambda_i = \cos\theta_i = \langle\mu_i|A^{\mathrm{T}}\,B|\nu_i\rangle. \tag{11.32}$$

Exercise 11.4. Show that U and V given by (11.26) and (11.27) are unitary. Show that (11.21) is satisfied for these U and V.

Exercise 11.5. Show that if $\lambda_i \neq \lambda_j$, then the vector space spanned by $A|\mu_i\rangle$ and $B|\nu_i\rangle$ is orthogonal to the vector space spanned by $A\big|\mu_j\big\rangle$ and $B\big|\nu_j\big\rangle$.

Exercise 11.6. The objective of this exercise is to use matrix $CC^\dagger$ instead of $C^\dagger C$ to obtain the singular values and vectors of C.

1. Show that if $|\nu\rangle$ is an eigenvector of $C^\dagger C$ associated with the eigenvalue λ^2, then $C|\nu\rangle$ is an eigenvector of $CC^\dagger$ with the same eigenvalue.
2. Use $C^\dagger$ to define vectors $|\mu_i\rangle$ in (11.24) and interchange the roles of $|\mu_i\rangle$ and $|\nu_i\rangle$ to define U and V.
3. Show that the new matrices U and V are unitary and satisfy (11.21).

11.5 Eigenvalues and Eigenvectors of the Evolution Operator

Recall that $\mathcal{A}$ and $\mathcal{B}$ are the vector spaces spanned by vectors $|\alpha_x\rangle$ and $\big|\beta_y\big\rangle$, respectively. Note that the set of vectors $A\big|\mu_j\big\rangle$ for $1 \leq j \leq n$ is an orthonormal basis of $\mathcal{A}$ and the set of vectors $B\big|\nu_j\big\rangle$ for $1 \leq j \leq n$ is an orthonormal basis of $\mathcal{B}$. Let us start with the spectrum of W_P.

Lemma 11.1. (Konno, Sato, Segawa) *The characteristic polynomial of W_P is*

$$\det(\lambda I_N - W_P) = (\lambda - 1)^{N-2n} \det\big((\lambda+1)^2 I_n - 4\,\lambda\, C^T C\big).$$

Proof. Exercise 11.7 □

Lemma 11.1 shows that there are at least $(N-2n)$ $(+1)$-eigenvalues and the remaining $2n$ eigenvalues of W_P can be obtained from equation

$$\det\big((\lambda+1)^2 I_n - 4\,\lambda\, C^{\mathrm{T}} C\big) = 0.$$

Using that $I_n = \sum_{j=1}^n \big|\nu_j\big\rangle\big\langle\nu_j\big|$ and Eq. (11.22), we obtain

$$\det\left(\sum_{j=1}^n \big((\lambda+1)^2 - 4\,\lambda\,\lambda_j^2\big)\big|\nu_j\big\rangle\big\langle\nu_j\big|\right) = 0.$$

Then,

$$\prod_{j=1}^n \big(\lambda^2 - 2\,(2\lambda_j^2 - 1)\lambda + 1\big) = 0.$$

For each j, we obtain two eigenvalues of W_P, which are

$$\lambda = (2\lambda_j^2 - 1) \pm 2\lambda_j \sqrt{\lambda_j^2 - 1}.$$

Using that $\lambda_j = \cos\theta_j$, we obtain

$$\lambda = \mathrm{e}^{\pm 2\mathrm{i}\theta_j}.$$

This result shows that the eigenvalues of the evolution operator W_P are either $(+1)$ or can be obtained from the transition matrix of the underlying graph.

The next lemmas are also useful.

Lemma 11.2. *1. If $|\psi\rangle \in \mathcal{A} \cap \mathcal{B} + \mathcal{A}^\perp \cap \mathcal{B}^\perp$, then $W_P|\psi\rangle = |\psi\rangle$.*
2. If $|\psi\rangle \in \mathcal{A} \cap \mathcal{B}^\perp + \mathcal{A}^\perp \cap \mathcal{B}$, then $W_P|\psi\rangle = -|\psi\rangle$.

Proof. If $|\psi\rangle \in \mathcal{A} \cap \mathcal{B}$, then $|\psi\rangle$ is invariant under the action of both $\mathcal{R}_A$ and $\mathcal{R}_B$ and is a $(+1)$-eigenvector of W_P. If $|\psi\rangle \in \mathcal{A}^\perp \cap \mathcal{B}^\perp$, then both $\mathcal{R}_A$ and $\mathcal{R}_B$ inverts the sign of $|\psi\rangle$, which is therefore a $(+1)$-eigenvector of W_P. If $|\psi\rangle \in \mathcal{A} \cap \mathcal{B}^\perp$, then $|\psi\rangle$ is invariant under the action of $\mathcal{R}_A$ and inverts the sign under $\mathcal{R}_B$ and is a (-1)-eigenvector of W_P. If $|\psi\rangle \in \mathcal{A}^\perp \cap \mathcal{B}$, then $|\psi\rangle$ is invariant under the action of $\mathcal{R}_B$ and inverts the sign under $\mathcal{R}_A$ and is a (-1)-eigenvector of W_P. □

Lemma 11.3. *Let* $\dim(\mathcal{A} \cap \mathcal{B}) = k$. *Then,*

$$\dim(\mathcal{A}^\perp \cap \mathcal{B}^\perp) = N - 2n + k.$$

Proof. Using that $\mathcal{H} = (\mathcal{A} + \mathcal{B}) \oplus (\mathcal{A} + \mathcal{B})^\perp$ and $(\mathcal{A} + \mathcal{B})^\perp = \mathcal{A}^\perp \cap \mathcal{B}^\perp$, we obtain $\dim \mathcal{H} = \dim(\mathcal{A} + \mathcal{B}) + \dim(\mathcal{A}^\perp \cap \mathcal{B}^\perp)$. Then, $N = 2n - \dim(\mathcal{A} \cap \mathcal{B}) + \dim(\mathcal{A}^\perp \cap \mathcal{B}^\perp)$. The result follows when we use $\dim(\mathcal{A} \cap \mathcal{B}) = k$. □

The following theorem holds.

Theorem 11.4. (Szegedy) *The spectrum of W_P obeys:*

1. *The eigenvalues of W_P with $0 < \theta_j \le \pi/2$ are $e^{\pm 2i\theta_j}$ for $j = 1, \ldots, n-k$, where k is the multiplicity of singular value 1. The corresponding normalized eigenvectors are*
$$\left|\theta_j^\pm\right\rangle = \frac{1}{\sqrt{2}\,\sin\theta_j}\left(A\left|\mu_j\right\rangle - e^{\pm i\theta_j} B\left|\nu_j\right\rangle\right). \tag{11.33}$$
2. *$\mathcal{A} \cap \mathcal{B} + \mathcal{A}^\perp \cap \mathcal{B}^\perp$ is the $(+1)$-eigenspace of W_P. $\mathcal{A} \cap \mathcal{B}$ is spanned by $A\left|\mu_j\right\rangle$, where $\left|\mu_j\right\rangle$ are the left singular vectors of C with singular value 1.*
3. *$\mathcal{A} \cap \mathcal{B}^\perp + \mathcal{A}^\perp \cap \mathcal{B}$ is the (-1)-eigenspace of W_P. $\mathcal{A} \cap \mathcal{B}^\perp$ is spanned by $A\left|\mu_j\right\rangle$, where $\left|\mu_j\right\rangle$ are the left singular vectors of C with singular value 0, and $\mathcal{A}^\perp \cap \mathcal{B}$ is spanned by $B\left|\nu_j\right\rangle$, where $\left|\nu_j\right\rangle$ are the right singular vectors of C with singular value 0.*

Proof. Let us start with Item 1. Let $1 \leq j \leq n-k$ be a fixed integer and assume that $0 < \theta_j \leq \pi/2$. This means that vectors $A\left|\mu_j\right\rangle$ and $B\left|\nu_j\right\rangle$ are noncollinear. Using the definition of W_P, we obtain

$$\begin{aligned} W_P\, A\left|\mu_j\right\rangle &= -A\left|\mu_j\right\rangle + 2\lambda_j B\left|\nu_j\right\rangle, \\ W_P\, B\left|\nu_j\right\rangle &= -2\lambda_j A\left|\mu_j\right\rangle + (4\lambda_j^2 - 1) B\left|\nu_j\right\rangle. \end{aligned}$$

Using that $2\lambda_j = \left(\mathrm{e}^{\mathrm{i}\theta_j} + \mathrm{e}^{-\mathrm{i}\theta_j}\right)$, we have

$$4\lambda_j^2 - 1 = \mathrm{e}^{2\mathrm{i}\theta_j} + \mathrm{e}^{-2\mathrm{i}\theta_j} + 1.$$

Using the above equations, we obtain

$$W_P\left(A\left|\mu_j\right\rangle - \mathrm{e}^{\pm\mathrm{i}\theta_j} B\left|\nu_j\right\rangle\right) = \mathrm{e}^{\pm 2\mathrm{i}\theta_j}\left(A\left|\mu_j\right\rangle - \mathrm{e}^{\pm\mathrm{i}\theta_j} B\left|\nu_j\right\rangle\right).$$

Now we check that

$$\begin{aligned} \left\|A\left|\mu_j\right\rangle - \mathrm{e}^{\pm\mathrm{i}\theta_j} B\left|\nu_j\right\rangle\right\|^2 &= \left(\left\langle\mu_j\right| A^{\mathrm{T}} - \mathrm{e}^{\mp\mathrm{i}\theta_j}\left\langle\nu_j\right| B^{\mathrm{T}}\right)\left(A\left|\mu_j\right\rangle - \mathrm{e}^{\pm\mathrm{i}\theta_j} B\left|\nu_j\right\rangle\right) \\ &= 2 - \mathrm{e}^{\pm\mathrm{i}\theta_j}\left\langle\mu_j\right| A^{\mathrm{T}} B\left|\nu_j\right\rangle - \mathrm{e}^{\mp\mathrm{i}\theta_j}\left\langle\nu_j\right| B^{\mathrm{T}} A\left|\mu_j\right\rangle \\ &= 2\,\sin^2\theta_j. \end{aligned}$$

Then, $\left|\theta_j^{\pm}\right\rangle$ are unit eigenvectors of W_P with eigenvalues $\mathrm{e}^{\pm 2\mathrm{i}\theta_j}$. From Lemma 11.1, $\mathrm{e}^{\pm 2\mathrm{i}\theta_j}$ with $0 < \theta_j < 1$ are the only eigenvalues with nonzero complex part. The corresponding eigenvectors do not belong to the intersecting spaces described in Items 2 and 3. On the other hand, if $\theta_j = \pi/2$ (singular value 0), then the corresponding eigenvectors are in $\mathcal{A} \cap \mathcal{B}^{\perp} + \mathcal{A}^{\perp} \cap \mathcal{B}$ because $A\left|\mu_j\right\rangle$ and $B\left|\nu_j\right\rangle$ are orthogonal (Exercise 11.8). The remaining eigenvectors have eigenvalue 1 ($\theta_j = 0$).

Let us address Item 2. Using Lemma 11.2, we know that any vector in $\mathcal{A} \cap \mathcal{B} + \mathcal{A}^{\perp} \cap \mathcal{B}^{\perp}$ is a $(+1)$-eigenvector. The reverse is also true. In fact, using the proof of Item 1, we know that there are k $(+1)$-eigenvectors in $\mathcal{A} \cap \mathcal{B}$ and from Lemma 11.3, there are $(N - 2n + k)$ $(+1)$-eigenvectors in $\mathcal{A}^{\perp} \cap \mathcal{B}^{\perp}$. Then, $\mathcal{A} \cap \mathcal{B} + \mathcal{A}^{\perp} \cap \mathcal{B}^{\perp}$ is the $(+1)$-eigenspace of W_P. If $A\left|\mu_j\right\rangle \in \mathcal{A} \cap \mathcal{B}$, then $A\left|\mu_j\right\rangle = B\left|\nu_j\right\rangle$ and $\theta_j = 0$ ($\lambda_j = 1$). There are exactly k linearly independent vectors $A\left|\mu_j\right\rangle$, where k is the multiplicity of singular value 1 and $k = \dim(\mathcal{A} \cap \mathcal{B})$. Those vectors span $\mathcal{A} \cap \mathcal{B}$.

Let us address Item 3. Using Lemma 11.2, we know that any vector in $\mathcal{A} \cap \mathcal{B}^{\perp} + \mathcal{A}^{\perp} \cap \mathcal{B}$ is a (-1)-eigenvector. The reverse is also true. In fact, using the proof of Item 1, all (-1)-eigenvectors have $\theta_j = \pi/2$ and belong either to $\mathcal{A} \cap \mathcal{B}^{\perp}$ or to $\mathcal{A}^{\perp} \cap \mathcal{B}$. Then, $\mathcal{A} \cap \mathcal{B}^{\perp} + \mathcal{A}^{\perp} \cap \mathcal{B}$ is the (-1)-eigenspace of W_P. The set of vectors $A\left|\mu_j\right\rangle$ spans $\mathcal{A} \cap \mathcal{B}^{\perp}$ and the set of vectors $B\left|\nu_j\right\rangle$ spans $\mathcal{A}^{\perp} \cap \mathcal{B}$. □

Table 11.1 summarizes the results of the spectral decomposition of W_P obtained via Theorem 11.4. There are $2(n-k)$-eigenvectors of W_P associated with eigenvalues $\mathrm{e}^{\pm 2\mathrm{i}\theta_j}$ when $\theta_j > 0$. The expressions of those eigenvectors are given by Eq. (11.33).

Table 11.1 Eigenvalues and normalized eigenvectors of W_P obtained from the singular values and vectors of C, where k is the multiplicity of the singular value 1 of C and n is the dimension of C

Eigenvalue	Eigenvector	Range
$e^{\pm 2i\theta_j}$	$\left\|\theta_j^{\pm}\right\rangle = \frac{A\|\mu_j\rangle - e^{\pm i\theta_j} B\|\nu_j\rangle}{\sqrt{2}\sin\theta_j}$	$1 \le j \le n-k$
1	$\left\|\theta_j\right\rangle = A\left\|\mu_j\right\rangle$	$n-k+1 \le j \le n$
1	$\left\|\theta_j\right\rangle =$ no expression	$2n-k+1 \le j \le n^2$

Angles θ_j are obtained from the singular values λ_j using $\cos\theta_j = \lambda_j$. The eigenvectors $\left|\theta_j\right\rangle$, for $2n-k+1 \le j \le n^2$, cannot be obtained by the method described in this section, but we know that they have eigenvalue 1

Note that Theorem 11.4 can be used to find eigenvectors of the evolution operator W_P only when the singular values and vectors of the discriminant matrix can be explicitly found. In most cases, the calculation of the singular values and vectors is too difficult a task. Besides, the above theorem does not describe the $(N-2n+k)$ $(+1)$-eigenvectors that span $\mathcal{A}^\perp \cap \mathcal{B}^\perp$. However, the $(+1)$-eigenvectors are not needed in the calculation of the *quantum hitting time*.

Exercise 11.7. The goal of this exercise is to prove Lemma 11.1. Two properties of the determinant are useful here: (1) $\det(\lambda M) = \lambda^n \det(M)$ for any $n \times n$ matrix M and any scalar λ, (2) $\det(\lambda I_n - M_1 M_2) = \det(\lambda I_m - M_2 M_1)$ for any $n \times m$ matrix M_1 and $m \times n$ matrix M_2.

Using the definition of W_P, show that

$$\det(\lambda I - W_P) = (\lambda - 1)^{n^2} \det\left(I - \frac{2BB^T(2AA^T - I)M_-}{\lambda - 1}\right)\det(M_+),$$

where

$$M_\pm = I_{n^2} \pm \frac{2}{\lambda \mp 1} AA^T,$$

and (show this)

$$M_+ M_- = I_{n^2}$$

and (show this too)

$$\det(M_+) = \left(\frac{\lambda+1}{\lambda-1}\right)^n.$$

Using those results to show that

$$\det(\lambda I - W_P) = (\lambda-1)^{n^2-n}(\lambda+1)^n \det\left(I - \frac{2}{\lambda-1} BB^T\left(\frac{2\lambda}{\lambda+1} AA^T - I\right)\right).$$

To conclude the proof, use Eq. (11.19) and property (2) described in the beginning of this exercise.

Exercise 11.8. Show that if the singular value λ_j is equal to 0, then $A|\mu_j\rangle$ and $B|\nu_j\rangle$ are orthonormal (-1)-eigenvectors of W_P. Show that the (-1)-eigenvectors that span $\mathcal{A} \cap \mathcal{B}^\perp + \mathcal{A}^\perp \cap \mathcal{B}$ can be written as

$$\frac{A|\mu_j\rangle \pm \mathrm{i}B|\nu_j\rangle}{\sqrt{2}}.$$

11.6 Quantum Hitting Time

The quantum walk defined earlier does not search any specific vertex because we have not marked any vertex yet. This section is devoted to describing how Szegedy's quantum walk finds a marked vertex. There are two tasks: (1) Some vertices must be marked (let M be the set of marked vertices) and (2) a running time must be defined.

The empty vertex of the first graph in Fig. 11.2 is called *marked vertex* because it is a *sink* with a *loop*. To obtain the bipartite digraph (second graph), we follow the same duplication process described at the beginning of Sect. 11.2. All edges incident to a marked vertex are incident arcs, and an extra edge connecting twin marked vertices is added.

The quantum hitting time is defined using Szegedy's quantum walk on the bipartite digraph, and it is driven by the evolution operator $W_{P'}$, where P' is the modified stochastic matrix given by

$$p'_{xy} = \begin{cases} p_{xy}, & x \notin M; \\ \delta_{xy}, & x \in M, \end{cases} \tag{11.34}$$

where p_{xy} are the entries of the stochastic matrix P of the bipartite simple graph and M is the set of marked vertices. When we use operator $W_{P'}$ on the bipartite digraph, the probabilities associated with the marked vertices increase periodically. To find a marked vertex, we must measure the position of the walker as soon as the probability of being in M is high. The quantum hitting time tells when we measure the walker's position.

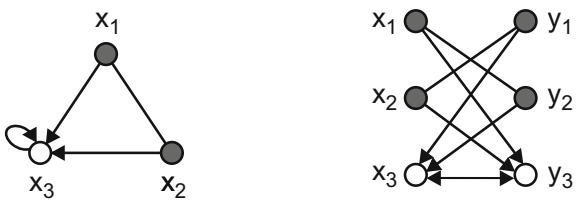

Fig. 11.2 Example of the *duplication process* with a *marked vertex*. A marked vertex is a *sink* in the underlying digraph with a self loop. The *bipartite digraph* is generated by the duplication process. The *classical hitting time* defined on the first digraph can be compared with the *quantum hitting time* of a Szegedy's quantum walk on the second digraph

The initial condition of Szegedy's quantum walk is

$$|\psi(0)\rangle = \frac{1}{\sqrt{n}} \sum_{\substack{x \in X \\ y \in Y}} \sqrt{p_{xy}}|x, y\rangle. \tag{11.35}$$

Note that $|\psi(0)\rangle$ is defined using the stochastic matrix of the underlying graph with unmarked vertices and is invariant under the action of W_P, that is, $|\psi(0)\rangle$ is a 1-eigenvector of W_P. However, $|\psi(0)\rangle$ is not an eigenvector of $W_{P'}$ in general. Now let us define the quantum hitting time.

Definition 11.5 (Quantum Hitting Time). The *quantum hitting time* $H_{P',M}$ of a quantum walk on the bipartite digraph with the associated evolution operator $W_{P'}$ starting from the initial condition $|\psi(0)\rangle$ is defined as the smallest number of steps T such that

$$F(T) \geq 1 - \frac{m}{n},$$

where m is the number of marked vertices, n is the number of vertices of the underlying digraph, and

$$F(T) = \frac{1}{T+1} \sum_{t=0}^{T} \left\| |\psi(t)\rangle - |\psi(0)\rangle \right\|^2, \tag{11.36}$$

where $|\psi(t)\rangle$ is the quantum state at step t, that is, $|\psi(t)\rangle = (W_{P'})^t|\psi(0)\rangle$.

Value $(1 - m/n)$ is taken as reference because it is the distance between the uniform probability distribution and the uniform probability distribution on the marked vertices. This distance can be confirmed by using (7.55) of Sect. 7.6 on p. 152.

The quantum hitting time depends only on the eigenspaces of $W_{P'}$ that are associated with eigenvalues different from 1. Or, similarly, the quantum hitting time depends only on the singular values of C different from 1. Let us show this fact. Table 11.1 summarizes the results on the eigenvalues and eigenvectors of the evolution operator. Using the notation of this table, we can write the initial condition of the quantum walk in the eigenbasis as follows:

$$|\psi(0)\rangle = \sum_{j=1}^{n-k} \left(c_j^+ \left|\theta_j^+\right\rangle + c_j^- \left|\theta_j^-\right\rangle \right) + \sum_{j=n-k+1}^{n^2-n+k} c_j |\theta_j\rangle, \tag{11.37}$$

where coefficients $c_j^{\pm}$ are given by

$$c_j^{\pm} = \left\langle \theta_j^{\pm} | \psi(0) \right\rangle, \tag{11.38}$$

and satisfy the constraint

$$\sum_{j=1}^{n-k}\left(\left|c_j^+\right|^2+\left|c_j^-\right|^2\right)+\sum_{j=n-k+1}^{n^2-n+k}\left|c_j\right|^2=1. \tag{11.39}$$

Applying $W_{P'}^t$ to $|\psi(0)\rangle$, we obtain

$$|\psi(t)\rangle=\sum_{j=1}^{n-k}\left(c_j^+\mathrm{e}^{2\mathrm{i}\theta_j t}\left|\theta_j^+\right\rangle+c_j^-\mathrm{e}^{-2\mathrm{i}\theta_j t}\left|\theta_j^-\right\rangle\right)+\sum_{j=n-k+1}^{n^2-n+k}c_j\left|\theta_j\right\rangle. \tag{11.40}$$

When we take the difference $|\psi(t)\rangle-|\psi(0)\rangle$, the terms associated with the eigenvalue 1 are eliminated.

Since vectors $\left|\theta_j^\pm\right\rangle$ are complex conjugates and $|\psi(0)\rangle$ is real, it follows from (11.38) that $\left|c_j^+\right|^2=\left|c_j^-\right|^2$. We will denote both $\left|c_j^+\right|^2$ and $\left|c_j^-\right|^2$ by $\left|c_j\right|^2$ such that the subindex j characterizes the coefficient. Using (11.37) and (11.40), we obtain

$$\left\||\psi(t)\rangle-|\psi(0)\rangle\right\|^2=4\sum_{j=1}^{n-k}\left|c_j\right|^2\left(1-T_{2t}(\cos\theta_j)\right), \tag{11.41}$$

where T_n is the nth *Chebyshev polynomial of the first kind* defined by $T_n(\cos\theta)=\cos n\theta$. $F(T)$ defined in (11.36) can be explicitly calculated. The result is

$$F(T)=\frac{2}{T+1}\sum_{j=1}^{n-k}\left|c_j\right|^2\Big(2T+1-U_{2T}(\cos\theta_j)\Big), \tag{11.42}$$

where U_n are the *Chebyshev polynomials of the second kind* defined by

$$U_n(\cos\theta)=\frac{\sin(n+1)\theta}{\sin\theta}.$$

Function $F(T)$ is continuous, and we can select a range $[0,T]$ containing point $1-m/n$ where $F(T)$ can be inverted to obtain the quantum hitting time by employing the following equation:

$$H_{P,M}=\left\lceil F^{-1}\left(1-\frac{m}{n}\right)\right\rceil. \tag{11.43}$$

In principle, it is not necessary to define the hitting time as an integer value since it is an average. If we remove the *ceiling function* from the above equation, we have a valid definition. In the example using a complete graph in Sect. 11.8, we use this alternative definition.

11.7 Searching Instead of Detecting

The quantum walk defined by the evolution operator $W_{P'}$ was designed such that the probability of finding a marked element increases during some time. Since the evolution is unitary, the probability of finding a marked element will have an oscillatory pattern. Then, determining the *running time* (execution time) of the algorithm is crucial. If the measurement is delayed, the success probability may be very low. The quantum hitting time must be close to the time $t_{\max}$ where the probability reaches the maximum for the first time.

In order to determine $t_{\max}$ and calculate the success probability, we need to find the analytical expression of $|\psi(t)\rangle$. Subtracting (11.40) of (11.37), we obtain

$$|\psi(t)\rangle = |\psi(0)\rangle + \sum_{j=1}^{n-k} \left(c_j^+ \left(\mathrm{e}^{2\mathrm{i}\theta_j t} - 1\right) \left|\theta_j^+\right\rangle + c_j^- \left(\mathrm{e}^{-2\mathrm{i}\theta_j t} - 1\right) \left|\theta_j^-\right\rangle \right). \tag{11.44}$$

The probability of finding a marked element is calculated with the *projector* on the vector space spanned by the marked elements, which is

$$\begin{aligned} \mathcal{P}_M &= \sum_{x \in M} |x\rangle\langle x| \otimes I \\ &= \sum_{x \in M} \sum_{y} |x, y\rangle\langle x, y|. \end{aligned} \tag{11.45}$$

The probability at time t is given by $\langle\psi(t)|\mathcal{P}_M|\psi(t)\rangle$.

In this context, we highlight: (1) The problem of determining whether the set of the marked elements is empty, called *detection problem* and (2) the problem of finding a marked element, called *finding problem*. In the general case, the detection problem is simpler than the finding problem because it does not require calculating the probability of finding a marked element. The detection problem only requires the calculation of the hitting time. The calculation of the probability of finding a marked element requires the knowledge of $|\psi(t)\rangle$, while the calculation of the hitting time requires knowledge of $|\psi(t)\rangle - |\psi(0)\rangle$. In the latter case, we need not calculate the $(+1)$-eigenvectors.

11.8 Example: Complete Graphs

The purpose of this section is to calculate the quantum hitting time using *complete graphs* as the underlying graph. Let n be the number of vertices. All vertices are adjacent in a complete graph. If the walker is in one vertex, it can go to $n - 1$ vertices. Therefore, the stochastic matrix is

$$P = \frac{1}{n-1}\begin{bmatrix} 0 & 1 & 1 & \cdots & 1 \\ 1 & 0 & 1 & \cdots & 1 \\ 1 & 1 & 0 & \cdots & 1 \\ \vdots & \vdots & \vdots & \ddots & \vdots \\ 1 & 1 & 1 & \cdots & 0 \end{bmatrix}. \tag{11.46}$$

Multiplying P by $(n-1)$, we obtain a matrix with all entries equal to 1 minus the identity matrix. Therefore, we can write P as follows:

$$P = \frac{1}{n-1}\left(n\left|u^{(n)}\right\rangle\left\langle u^{(n)}\right| - I_n\right), \tag{11.47}$$

where $\left|u^{(j)}\right\rangle$ is defined by

$$\left|u^{(j)}\right\rangle = \frac{1}{\sqrt{j}}\sum_{i=1}^{j}|i\rangle. \tag{11.48}$$

We number the vertices from 1 to n, such that in this section the computational basis of the Hilbert space $\mathcal{H}^n$ is $\left\{|1\rangle, \ldots, |n\rangle\right\}$. We suppose that the marked vertices are the last m vertices, that is, $x \in M$ if and only if $n - m < x \leq n$.

In the definition of the quantum hitting time, the evolution operator uses the modified stochastic matrix P' defined in (11.34) instead of the underlying matrix P. The entries of matrix P' are

$$p'_{xy} = \begin{cases} \frac{1-\delta_{xy}}{n-1}, & 1 \leq x \leq n-m; \\ \delta_{xy}, & n-m < x \leq n. \end{cases} \tag{11.49}$$

All vectors and operators in Sect. 11.2 must be calculated using P'. Operator C in (11.19) is important because their singular values and vectors are used to calculate some eigenvectors of the evolution operator $W_{P'}$. In Sect. 11.2, we have learned that the entries C_{xy} are given by $\sqrt{p'_{xy}q_{yx}}$. Here we are setting $q_{yx} = p'_{yx}$. In a complete graph, we have $p_{xy} = p_{yx}$. However, $p'_{xy} \neq p'_{yx}$, if x and y are in M. Using (11.49) and analyzing the entries of C, we conclude that

$$C = \begin{bmatrix} P_{\overline{M}} & 0 \\ 0 & I_m \end{bmatrix}, \tag{11.50}$$

where $P_{\overline{M}}$ is the matrix obtained from P by eliminating m rows and m columns corresponding to the marked vertices. We find the singular values and vectors of C through the spectral decomposition of $P_{\overline{M}}$.

The algebraic expression of $P_{\overline{M}}$ is

$$P_{\overline{M}} = \frac{1}{n-1}\left((n-m)\left|u^{(n-m)}\right\rangle\left\langle u^{(n-m)}\right| - I_{n-m}\right), \tag{11.51}$$

where $\left|u^{(n-m)}\right\rangle$ is obtained from (11.48). Its characteristic polynomial is

$$\det(P_{\overline{M}} - \lambda I) = \left(\lambda - \frac{n-m-1}{n-1}\right)\left(\lambda + \frac{1}{n-1}\right)^{n-m-1}. \tag{11.52}$$

The eigenvalues are $\frac{n-m-1}{n-1}$ with multiplicity 1 and $\frac{-1}{n-1}$ with multiplicity $n-m-1$. Note that if $m \geq 1$, then 1 is not an eigenvalue of $P_{\overline{M}}$. The eigenvector associated with eigenvalue $\frac{n-m-1}{n-1}$ is

$$|\nu_{n-m}\rangle := \left|u^{(n-m)}\right\rangle \tag{11.53}$$

and the eigenvectors associated with the eigenvalue $\frac{-1}{n-1}$ are

$$|\nu_i\rangle := \frac{1}{\sqrt{i+1}}\left(\left|u^{(i)}\right\rangle - \sqrt{i}\,|i+1\rangle\right), \tag{11.54}$$

where $1 \leq i \leq n-m-1$. The set $\left\{|\nu_i\rangle, 1 \leq i \leq n-m\right\}$ is an orthonormal basis of eigenvectors of $P_{\overline{M}}$. The verification is oriented in Exercise 11.9.

Exercise 11.9. The objective of this exercise is to explicitly check the orthonormality of the spectral decomposition of $P_{\overline{M}}$.

1. Use (11.51) to verify that $P_{\overline{M}}\left|u^{n-m}\right\rangle = \frac{n-m-1}{n-1}\left|u^{n-m}\right\rangle$.
2. Show that $\left\langle u^{(n-m)}\middle|\nu_i\right\rangle = 0$, for $1 \leq i \leq n-m-1$. Use this fact and (11.51) to verify that $P_{\overline{M}}|\nu_i\rangle = \frac{-1}{n-1}|\nu_i\rangle$.
3. Show that $\left\langle u^{(i)}\middle|i+1\right\rangle = 0$ and conclude that $\left\langle u^{(i)}\middle|u^{(i)}\right\rangle = 1$, for $1 \leq i \leq n-m-1$. Use this fact to show that $\left\langle \nu_i\middle|\nu_i\right\rangle = 1$.
4. Suppose that $i < j$. Show that $\left\langle u^{(i)}\middle|u^{(j)}\right\rangle = \sqrt{\frac{i}{j}}$ and $\left\langle u^{(i)}\middle|j+1\right\rangle = 0$. Use these facts to show that $\left\langle \nu_i\middle|\nu_j\right\rangle = 0$.

Matrix C is Hermitian. Therefore, the nontrivial singular values λ_i of C defined in (11.23) are obtained by taking the modulus of the eigenvalues of $P_{\overline{M}}$. The right singular vectors $|\nu_i\rangle$ are the eigenvectors of $P_{\overline{M}}$, and the left singular vectors are obtained from (11.24). If an eigenvalue of $P_{\overline{M}}$ is negative, the left singular vector is the negative of the corresponding eigenvector of $P_{\overline{M}}$. These vectors must be augmented with m zeros to have the dimension compatible with C. Finally, submatrix I_m in (11.50) adds to the list the singular value 1 with multiplicity m and the associated singular vectors $|j\rangle$, where $n-m+1 \leq j \leq n$. Table 11.2 summarizes these results.

Eigenvalues and eigenvectors of $W_{P'}$ that can be obtained from the singular values and vectors of C are described in Table 11.1. Table 11.3 reproduces these results for a complete graph. It is still missing $n^2 - 2n + m$ 1-eigenvectors.

The initial condition is given by (11.35), which reduces to

$$|\psi(0)\rangle = \frac{1}{\sqrt{n(n-1)}} \sum_{x,y=1}^{n} (1-\delta_{xy})|x\rangle|y\rangle. \tag{11.55}$$

Table 11.2 Right and left singular values and vectors of matrix C

Singular value	Right singular vector	Left singular vector	Range
$\cos\theta_1 = \frac{1}{n-1}$	$\lvert\nu_j\rangle$	$-\lvert\nu_j\rangle$	$1 \le j \le n-m-1$
$\cos\theta_2 = \frac{n-m-1}{n-1}$	$\lvert\nu_{n-m}\rangle$	$\lvert\nu_{n-m}\rangle$	$j = n-m$
$\cos\theta_3 = 1$	$\lvert j\rangle$	$\lvert j\rangle$	$n-m+1 \le j \le n$

Vectors $|\nu_{n-m}\rangle$ and $|\nu_i\rangle$ are given by (11.53) and (11.54). Angles θ_1, θ_2, and θ_3 are defined from the singular values

Table 11.3 Eigenvalues and normalized eigenvectors of $W_{P'}$ obtained from the singular values and vectors of C

Eigenvalue	Eigenvector	Range
$e^{\pm 2i\theta_1}$	$\left\lvert\theta_j^{\pm}\right\rangle = \frac{-\left(A+e^{\pm i\theta_1}B\right)\lvert\nu_j\rangle}{\sqrt{2}\sin\theta_1}$	$1 \le j \le n-m-1$
$e^{\pm 2i\theta_2}$	$\lvert\theta_{n-m}^{\pm}\rangle = \frac{\left(A-e^{\pm i\theta_2}B\right)\lvert\nu_{n-m}\rangle}{\sqrt{2}\sin\theta_2}$	$j = n-m$
1	$\lvert\theta_j\rangle = A\lvert j\rangle$	$n-m+1 \le j \le n$

Only the eigenvectors of $W_{P'}$ that are not orthogonal to the initial condition $|\psi(0)\rangle$ play a role in the dynamic. Exercise 11.10 guides the proof that the eigenvectors $\left|\theta_j\right\rangle$, $n-m+1 \le j \le n$, are orthogonal to the initial condition. Exercise 11.11 guides the proof that the eigenvectors $\left|\theta_j^{\pm}\right\rangle$, $1 \le j \le n-m-1$, are also orthogonal to the initial condition. The remaining eigenvectors are $\left|\theta_{n-m}^{\pm}\right\rangle$, associated with the positive eigenvalue of $P_{\overline{M}}$, and the 1-eigenvectors, which has not been addressed yet. Therefore, the initial condition $|\psi(0)\rangle$ can be written as

$$|\psi(0)\rangle = c^{+}\left|\theta_{n-m}^{+}\right\rangle + c^{-}\left|\theta_{n-m}^{-}\right\rangle + |\beta\rangle, \tag{11.56}$$

where coefficients $c^{\pm}$ are given by (see Exercise 11.12)

$$c^{\pm} = \frac{\sqrt{n-m}\,\left(1-e^{\mp i\theta_2}\right)}{\sqrt{2n}\,\sin\theta_2}, \tag{11.57}$$

where θ_2 is defined by

$$\cos\theta_2 = \frac{n-m-1}{n-1}. \tag{11.58}$$

Vector $|\beta\rangle$ is the component of $|\psi(0)\rangle$ in the 1-eigenspace. The calculation of a basis of eigenvectors for this eigenspace is hardworking; we postpone this calculation for now.

Exercise 11.10. To show that $\left\langle\theta_j\middle|\psi(0)\right\rangle = 0$ when $n-m+1 \le j \le n$, use the expression for A given by (11.3) and the expression for $|\alpha_x\rangle$ given by (11.5), where p_{xy} and q_{xy} are given by (11.49). Show that

$$\langle\theta_j|\psi(0)\rangle = \sum_{x\in M}\langle\alpha_x|\psi(0)\rangle.$$

Use (11.55) to show that $\langle\alpha_x|\psi(0)\rangle = 0$ if $x \in M$.

Exercise 11.11. To show that $\left\langle\theta_j^{\pm}\middle|\psi(0)\right\rangle = 0$, for $1 \le j \le n-m-1$, use the expressions of A and B given by (11.3) and (11.4), and the expressions for $|\alpha_x\rangle$ and $\left|\beta_y\right\rangle$ given by (11.5) and (11.6), where p_{xy} and q_{xy} are given by (11.49). Equation (11.54) and Exercise 11.9 must also be used. The expression of $|\psi(0)\rangle$ is given by (11.55).

Exercise 11.12. The purpose of this exercise is to guide the calculation of coefficients $c^{\pm}$ in (11.56), which are defined by

$$c^{\pm} = \langle\theta_{n-m}^{\pm}|\psi(0)\rangle.$$

Using (11.55) and (11.64), cancel out the orthogonal terms and simplify the result.

Applying $W_{P'}^t$ to $|\psi(0)\rangle$—given by (11.56)—using that $\left|\theta_{n-m}^{\pm}\right\rangle$ are eigenvectors associated with eigenvalues $\mathrm{e}^{\pm 2\mathrm{i}\theta_2}$, and $|\beta\rangle$ is in the 1-eigenspace, we obtain

$$\begin{aligned}|\psi(t)\rangle &= W_{P'}^t|\psi(0)\rangle \\ &= c^+\mathrm{e}^{2\mathrm{i}\theta_2 t}\left|\theta_{n-m}^+\right\rangle + c^-\mathrm{e}^{-2\mathrm{i}\theta_2 t}\left|\theta_{n-m}^-\right\rangle + |\beta\rangle,\end{aligned} \tag{11.59}$$

Using the expression of $|\psi(t)\rangle$ and (11.36), we can calculate $F(T)$. The difference $|\psi(t)\rangle - |\psi(0)\rangle$ can be calculated as follows: Using (11.56) and (11.59), we obtain

$$|\psi(t)\rangle - |\psi(0)\rangle = c^+(\mathrm{e}^{2\mathrm{i}\theta_2 t}-1)\left|\theta_{n-m}^+\right\rangle + c^-(\mathrm{e}^{-2\mathrm{i}\theta_2 t}-1)\left|\theta_{n-m}^-\right\rangle \tag{11.60}$$

and using (11.57), we obtain

$$\begin{aligned}\Big\||\psi(t)\rangle - |\psi(0)\rangle\Big\|^2 &= \left|c^+(\mathrm{e}^{2\mathrm{i}\theta_2 t}-1)\right|^2 + \left|c^-(\mathrm{e}^{-2\mathrm{i}\theta_2 t}-1)\right|^2 \\ &= \frac{4(n-1)(n-m)}{n(2n-m-2)}\left(1 - T_{2t}\left(\frac{n-m-1}{n-1}\right)\right),\end{aligned}$$

where T_n are the *Chebyshev polynomials of the first kind*. Taking the average and using

$$\sum_{t=0}^{T} T_{2t}\left(\frac{n-m-1}{n-1}\right) = \frac{1}{2} + \frac{1}{2}U_{2T}\left(\frac{n-m-1}{n-1}\right) \tag{11.61}$$

we obtain

$$F(T) = \frac{2\,(n-1)\,(n-m)\left(2\,T + 1 - U_{2T}\left(\frac{n-m-1}{n-1}\right)\right)}{n\,(2\,n-m-2)\,(T+1)}, \tag{11.62}$$

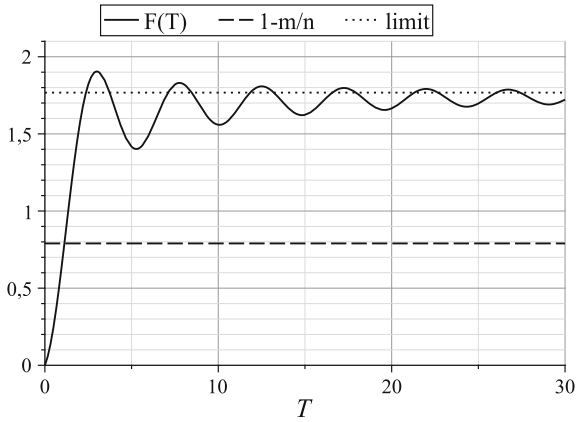

Fig. 11.3 Graph of function $F(T)$ (*solid line*), the line $1-\frac{m}{n}$ (*dashed line*), and the line $\frac{4(n-1)(n-m)}{n(2n-m-2)}$ (*dotted line*) for $n=100$ and $m=21$. The quantum hitting time is the time T such that $F(T)=1-\frac{m}{n}$, which is about 1.13

where U_n are the *Chebyshev polynomials of the second kind*. The graph in Fig. 11.3 shows the behavior of function $F(T)$. $F(T)$ grows rapidly passing through the dashed line, which represents $1-m/n$, and oscillates about the limiting value $\frac{4(n-1)(n-m)}{n(2n-m-2)}$.

For $n \gg m$, we obtain the hitting time $H_{P,M}$ by inverting the *Laurent series* of the equation $F(T)=1-\frac{m}{n}$. The first terms are

$$H_{P,M}=\frac{j_0^{-1}\left(\frac{1}{2}\right)}{2}\sqrt{\frac{n}{2m}}-\frac{\sqrt{1-\frac{1}{4}\,j_0^{-1}\left(\frac{1}{2}\right)^2}}{1+2\sqrt{1-\frac{1}{4}\,j_0^{-1}\left(\frac{1}{2}\right)^2}}+O\left(\frac{1}{\sqrt{n}}\right), \tag{11.63}$$

where j_0 is a *spherical Bessel function of the first kind* or the *unnormalized sync function*, and $j_0^{-1}\left(\frac{1}{2}\right)$ is approximately 1.9.

Exercise 11.13. The purpose of this exercise is to obtain (11.61). Use the trigonometric representation of T_n and convert the cosine into a sum of exponentials of complex arguments. Use the formula of the *geometric series* $\sum_{t=0}^{T} a^t=\frac{a^{T+1}-1}{a-1}$ to simplify the sum. Convert the result to the form of Chebyshev polynomials of the second kind.

11.8.1 Probability of Finding a Marked Element

The quantum hitting time is used in search algorithms as the running time. It is important to calculate the success probability when we use the hitting time. The calculation of the probability of finding a marked element as a function of time is more elaborated than the calculation of the hitting time because we explicitly calculate $|\psi(t)\rangle$, that is, we calculate the vectors $\left|\theta_{n-m}^{\pm}\right\rangle$ and $|\beta\rangle$ that appear in (11.59).

Using (11.3) and (11.4), we obtain

$$\left|\theta_{n-m}^{\pm}\right\rangle = \frac{1}{\sqrt{2}\sin\theta_2}\left(A - \mathrm{e}^{\pm\mathrm{i}\theta_2}B\right)\left|u^{(n-m)}\right\rangle$$
$$= \frac{1}{\sqrt{2(n-m)}\sin\theta_2}\left(\sum_{x=1}^{n-m}|\alpha_x\rangle - \mathrm{e}^{\pm\mathrm{i}\theta_2}\sum_{y=1}^{n-m}\left|\beta_y\right\rangle\right).$$

Using (11.5), (11.6), and (11.49), we obtain

$$\left|\theta_{n-m}^{\pm}\right\rangle = \frac{1}{\sqrt{2(n-1)(n-m)}\,\sin\theta_2}\left(\left(1-\mathrm{e}^{\pm\mathrm{i}\theta_2}\right)\sum_{x,y=1}^{n-m}\left(1-\delta_{xy}\right)|x\rangle|y\rangle\right.$$
$$\left.+\sum_{x=1}^{n-m}\sum_{y=n-m+1}^{n}|x\rangle|y\rangle - \mathrm{e}^{\pm\mathrm{i}\theta_2}\sum_{x=n-m+1}^{n}\sum_{y=1}^{n-m}|x\rangle|y\rangle\right). \tag{11.64}$$

Using (11.57) and (11.58), the expression for the quantum state at time t reduces to

$$|\psi(t)\rangle = \frac{1}{\sqrt{n(n-1)}}\left(\frac{2(n-1)T_{2t}\left(\frac{n-m-1}{n-1}\right)}{2n-m-2}\sum_{x,y=1}^{n-m}\left(1-\delta_{xy}\right)|x\rangle|y\rangle\right.$$
$$+\left(\frac{(n-1)T_{2t}\left(\frac{n-m-1}{n-1}\right)}{2n-m-2} - U_{2t-1}\left(\frac{n-m-1}{n-1}\right)\right)\sum_{x=1}^{n-m}\sum_{y=n-m+1}^{n}|x\rangle|y\rangle$$
$$\left.+\left(\frac{(n-1)T_{2t}\left(\frac{n-m-1}{n-1}\right)}{2n-m-2} + U_{2t-1}\left(\frac{n-m-1}{n-1}\right)\right)\sum_{x=n-m+1}^{n}\sum_{y=1}^{n-m}|x\rangle|y\rangle\right)$$
$$+|\beta\rangle. \tag{11.65}$$

Vector $|\beta\rangle$ can be determined from (11.56), since we know $|\psi(0)\rangle$ and $\left|\theta_{n-m}^{\pm}\right\rangle$. The result is

$$|\beta\rangle = \frac{1}{\sqrt{n(n-1)}}\left(\frac{-m}{2n-m-2}\sum_{x,y=1}^{n-m}\left(1-\delta_{xy}\right)|x\rangle|y\rangle\right.$$
$$+\frac{n-m-1}{2n-m-2}\sum_{x=1}^{n-m}\sum_{y=n-m+1}^{n}\left(|x\rangle|y\rangle+|y\rangle|x\rangle\right)$$
$$\left.+\sum_{x,y=n-m+1}^{n}\left(1-\delta_{xy}\right)|x\rangle|y\rangle\right). \tag{11.66}$$

The probability of finding a marked element $p_M(t)$ after performing a measurement with projectors $\mathcal{P}_M$ and $I-\mathcal{P}_M$, where $\mathcal{P}_M$ is the projector on the vector space spanned by the marked elements

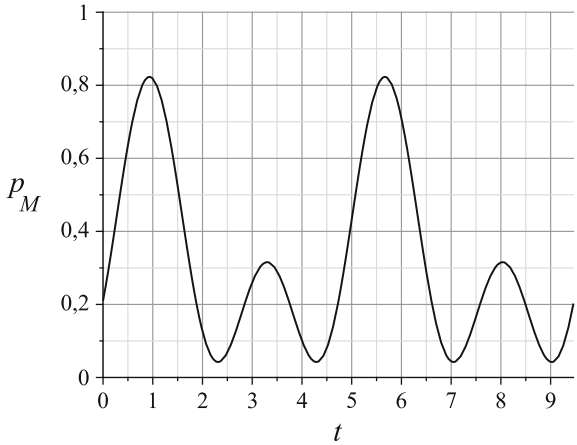

Fig. 11.4 Graph of the probability of finding a marked vertex as a function of time for $n = 100$ and $m = 21$. The initial value is $\frac{m}{n}$, and the probability has period $\frac{\pi}{\theta_2}$

$$\begin{aligned}\mathcal{P}_M &= \sum_{x=n-m+1}^{n} |x\rangle\langle x| \otimes I \\ &= \sum_{x=n-m+1}^{n} \sum_{y=1}^{n} |x, y\rangle\langle x, y|,\end{aligned} \tag{11.67}$$

is given by $\langle\psi(t)|\mathcal{P}_M|\psi(t)\rangle$. Using (11.65), we obtain

$$\begin{aligned}p_M(t) = \frac{m(m-1)}{n(n-1)} + \frac{m(n-m)}{n(n-1)} \Bigg(&\frac{n-1}{2n-m-2} T_{2t}\left(\frac{n-m-1}{n-1}\right) \\ &+ U_{2t-1}\left(\frac{n-m-1}{n-1}\right) + \frac{n-m-1}{2n-m-2}\Bigg)^2\end{aligned} \tag{11.68}$$

the graph of which is shown in Fig. 11.4 for $n = 100$ and $m = 21$.

We can determine the critical points of $p_M(t)$ by differentiating with respect to time. The first maximum point occurs at time

$$t_{\max} = \frac{\arctan\left(\dfrac{\sqrt{2n-m-2}}{\sqrt{m}}\right)}{2\arccos\left(\dfrac{n-m-1}{n-1}\right)}, \tag{11.69}$$

the asymptotic expansion of which is

$$t_{\max} = \frac{\pi}{4}\sqrt{\frac{n}{2m}} - \frac{1}{4} + O\left(\sqrt{\frac{m}{n}}\right). \tag{11.70}$$

Using (11.68), we obtain

$$p_M(t_{\max}) = \frac{1}{2} + \sqrt{\frac{m}{2\,n}} + O\left(\frac{m}{n}\right). \tag{11.71}$$

For any n or m, the probability of finding the marked vertex is greater than $\frac{1}{2}$ if the measurement is performed at time $t_{\max}$. The time $t_{\max}$ is less than the hitting time—see (11.63) because $\frac{\pi}{4\sqrt{2}} \approx 0.56$ and $\frac{j_0^{-1}(\frac{1}{2})}{2\sqrt{2}} \approx 0.67$. The success probability of an algorithm that uses the quantum hitting time as the running time will be smaller than the probability at time $t_{\max}$. Evaluating p_M at time $H_{P,M}$ and taking the asymptotic expansion, we obtain

$$p_M(H_{P,M}) = \frac{1}{8}\, j_0^{-1}\left(\frac{1}{2}\right)^2 + O\left(\frac{1}{\sqrt{n}}\right). \tag{11.72}$$

The first term is about 0.45 and does not depend on n or m. This shows that the quantum hitting time is a good parameter for the running time of the searching algorithm.

Exercise 11.14. Using (11.68), show that

1. $p_M(0) = \frac{m}{n}$.
2. $p_M(t)$ is a periodic function with period $\frac{\pi}{\theta_2}$.
3. the maximum points for $t \geq 0$ are given by

$$t_j = \frac{1}{2\theta_2} \arctan\left(\frac{1+\cos\theta_2}{\sin\theta_2}\right) + \frac{j\pi}{2\theta_2},$$

where $j = 0, 1, \ldots$.

Exercise 11.15. Show that in the asymptotic limit $n \gg m$, the expression of the success probability is

$$p_M(t) = \frac{1}{2}\sin^2(2t\theta_2) + O\left(\frac{1}{\sqrt{n}}\right).$$

Further Reading

The quantum walk model described in this chapter was introduced by Szegedy in [307]. The definition of the *quantum hitting time* presented in Sect. 11.6 was based on [307]. Reference [308] is also useful. Lemma 11.1 was proved by Konno, Sato, and Segawa [189]. The theory of classical Markov chains is described in many references, for instance, [11, 215, 235, 245].

Szegedy's quantum walk has many points in common with the bipartite quantum walk introduced by Ambainis to obtain the optimal algorithm for the *element distinctness problem* [14]. Despite the overlap, Ambainis' quantum walk cannot be considered an instance of Szegedy's model in a *strict* sense because the graph employed

by Ambainis is a nonsymmetric bipartite graph and the searching uses an oracle, while the searching in Szegedy's model uses sinks in symmetric bipartite digraphs. It is more precise to state that Ambainis' quantum walk is an instance of a bipartite quantum walk. Szegedy's model on the duplicated graph of the *Johnson graph* was used by Santha [290] to obtain a new alternate algorithm for the element distinctness problem. A new version of the element distinctness was described in [265] by converting the original Ambainis' algorithm into an instance of a 2-*tessellable* staggered quantum walk. The new version is simpler and describes the optimal values for obtaining an asymptotic 100% success probability. Since Szegedy's model is entirely included in the staggered model [269], the version using the Johnson graph can also be converted into a 2-*tessellable staggered quantum walk* by using the *line graph* of the bipartite graph obtained from the duplication of a Johnson graph.

An extension of Szegedy's model for ergodic Markov chains was introduced in [195, 224, 225]. The main problem that these references address is to show that the *hitting time* is of the order of the *detection time*. Reference [224] uses *Tulsi's modification* [315] to amplify the probability of finding a marked element, but can only be applied to symmetrical ergodic Markov chains. Reference [195] proposed a more general algorithm which is able to find a marked element with a quadratic speedup. Szegedy's model helped the development of new quantum algorithms faster than their classical counterparts. Reference [226] presented an algorithm for finding triangles in a graph. Reference [223] described an algorithm to test the commutativity of *black box groups*. The calculation of the quantum hitting time in complete graphs was presented in [292]. Master's thesis [159] presented an overview of the Szegedy's hitting time and the algorithm to test the commutativity of groups.

Quantum circuits for Szegedy's quantum walks were presented in References [77, 213]. Large sparse electrical networks were analyzed in [323] using Szegedy's quantum walk. Reference [157] analyzed a quantum walk similar to Szegedy's quantum walk on the path. Chiang and Gomez [76] analyzed the hitting time with perturbations. References [211, 254] used Szegedy's walk to the quantum Pagerank algorithm for determining the relative importance of nodes in a graph. Segawa [295] analyzed recurrent properties of the underlying random walk and the localization of the corresponding Szegedy's quantum walk. Higuchi et al. [145] analyzed the relation between a twisted version of Szegedy's model with the Grover walk. Dunjko and Briegel [107] analyzed mixing times in Szegedy's model. Santos [291] analyzed Szegedy's searching model with queries (oracle-based instead of sink-based searching). Ohno [250] addressed the unitary equivalence of one-dimensional quantum walks and presented a necessary and sufficient condition for a one-dimensional quantum walk to be a Szegedy walk. Wong [330] used Szegedy's model to obtain a coined quantum walk on weighted graphs. Ho et al. [147] derived the time-averaged distribution of Szegedy's walk in relation to the Ehrenfest model. Reference [29] analyzed limiting probability distribution of Szegedy's quantum walk.

Appendix A
Linear Algebra for Quantum Computation

The goal of this appendix is to compile the definitions, notations, and facts of linear algebra that are important for this book. Quantum computation has inherited linear algebra from quantum mechanics as the supporting language for describing this area. It is essential to have a solid knowledge of the basic results of linear algebra to understand quantum computation and quantum algorithms. If the reader does not have this base knowledge, we suggest reading some basic references recommended at the end of this appendix.

A.1 Vector Spaces

A *vector space* V over the field of complex numbers $\mathbb{C}$ is a nonempty set of elements called vectors together with two operations called vector addition and multiplication of a vector by a scalar in $\mathbb{C}$. The addition operation is associative and commutative and satisfies the following axioms:

- There is an element $\mathbf{0} \in V$, such that, for each $\mathbf{v} \in V$, $\mathbf{v} + \mathbf{0} = \mathbf{0} + \mathbf{v} = \mathbf{v}$ (existence of neutral element).
- For each $\mathbf{v} \in V$, there exists $\mathbf{u} = (-1)\mathbf{v}$ in V such that $\mathbf{v} + \mathbf{u} = \mathbf{0}$ (existence of inverse element).

$\mathbf{0}$ is called zero vector. The scalar multiplication operation satisfies the following axioms:

- $a.(b.\mathbf{v}) = (a.b).\mathbf{v}$ (associativity),
- $1.\mathbf{v} = \mathbf{v}$ (1 is the neutral element of multiplication),
- $(a + b).\mathbf{v} = a.\mathbf{v} + b.\mathbf{v}$ (distributivity over sum of scalars),
- $a.(\mathbf{v} + \mathbf{w}) = a.\mathbf{v} + a.\mathbf{w}$ (distributivity over vector addition).

where $\mathbf{v}, \mathbf{w} \in V$ and $a, b \in \mathbb{C}$.

A vector space can be infinite, but in most applications in *quantum computation*, *finite vector spaces* are used and are denoted by $\mathbb{C}^n$, where n is the number of

© Springer Nature Switzerland AG 2018

R. Portugal, *Quantum Walks and Search Algorithms*, Quantum Science and Technology, https://doi.org/10.1007/978-3-319-97813-0

dimensions. In this case, the vectors have n complex entries. In this book, we rarely use infinite spaces, and in these few cases, we are interested only in finite subspaces. In the context of *quantum mechanics*, *infinite vector spaces* are used more frequently than finite spaces.

A *basis* for $\mathbb{C}^n$ consists of exactly n linearly independent vectors. If $\{\mathbf{v}_1, \ldots, \mathbf{v}_n\}$ is a basis for $\mathbb{C}^n$, then an arbitrary vector $\mathbf{v}$ can be written as

$$\mathbf{v} = \sum_{i=1}^{n} a_i \mathbf{v}_i ,$$

where coefficients a_i are complex numbers. The *dimension* of a vector space is the number of basis vectors and is denoted by $\dim(V)$.

A.2 Inner Product

The *inner product* is a binary operation $(\cdot, \cdot) : V \times V \mapsto \mathbb{C}$, which obeys the following properties:

1. $(\cdot, \cdot)$ is linear in the second argument

$$\left(\mathbf{v}, \sum_{i=1}^{n} a_i \mathbf{v}_i\right) = \sum_{i=1}^{n} a_i \left(\mathbf{v}, \mathbf{v}_i\right) .$$

2. $(\mathbf{v}_1, \mathbf{v}_2) = (\mathbf{v}_2, \mathbf{v}_1)^*$.
3. $(\mathbf{v}, \mathbf{v}) \geq 0$. The equality holds if and only if $\mathbf{v} = \mathbf{0}$.

In general, the inner product is not linear in the first argument. The property in question is called *conjugate-linear*.

There is more than one way to define an inner product on a vector space. In $\mathbb{C}^n$, the most used inner product is defined as follows: If

$$\mathbf{v} = \begin{bmatrix} a_1 \\ \vdots \\ a_n \end{bmatrix}, \quad \mathbf{w} = \begin{bmatrix} b_1 \\ \vdots \\ b_n \end{bmatrix},$$

then

$$(\mathbf{v}, \mathbf{w}) = \sum_{i=1}^{n} a_i^* b_i .$$

This expression is equivalent to the matrix product of the transpose–conjugate vector $\mathbf{v}^\dagger$ and $\mathbf{w}$.

Two vectors $\mathbf{v}_1$ and $\mathbf{v}_2$ are *orthogonal* if the inner product $(\mathbf{v}_1, \mathbf{v}_2)$ is zero. We also introduce the notion of *norm* using the inner product. The norm of $\mathbf{v}$, denoted by $\|\mathbf{v}\|$, is defined as

$$\|\mathbf{v}\| = \sqrt{(\mathbf{v}, \mathbf{v})}.$$

A *normalized vector* or *unit vector* is a vector whose norm is equal to 1. A basis is said *orthonormal* if all vectors are normalized and mutually orthogonal.

A finite vector space with an inner product is called a *Hilbert space* and denoted by $\mathcal{H}$. In order to an infinite vector space be a Hilbert space, it must obey additional properties besides having an inner product. Since we deal primarily with finite vector spaces, we use the term *Hilbert space* as a synonym for *vector space with an inner product*. A *vector subspace* (or simply subspace) W of a finite Hilbert space V is also a Hilbert space. The set of vectors orthogonal to all vectors of W is the Hilbert space $W^\perp$ called *orthogonal complement*. V is the direct sum of W and $W^\perp$, that is, $V = W \oplus W^\perp$. A N-dimensional Hilbert space is denoted by $\mathcal{H}^N$ to highlight its dimension. A Hilbert space associated with a system A is denoted by $\mathcal{H}_A$ or simply $\mathcal{A}$. If $\mathcal{A}$ is a subspace of $\mathcal{H}$, then $\mathcal{H} = \mathcal{A} + \mathcal{A}^\perp$, which means that any vector in $\mathcal{H}$ can be written as a sum of a vector in $\mathcal{A}$ and a vector in $\mathcal{A}^\perp$.

Exercise A.1. Let $\mathcal{A}$ and $\mathcal{B}$ be subspaces of $\mathcal{H}$. Show that $\dim(\mathcal{A} + \mathcal{B}) = \dim(\mathcal{A}) + \dim(\mathcal{B}) - \dim(\mathcal{A} \cap \mathcal{B})$, $\left(\mathcal{A} + \mathcal{B}\right)^\perp = \mathcal{A}^\perp \cap \mathcal{B}^\perp$, and $\left(\mathcal{A} \cap \mathcal{B}\right)^\perp = \mathcal{A}^\perp + \mathcal{B}^\perp$.

Exercise A.2. Give one example of subspaces $\mathcal{A}$ and $\mathcal{B}$ of $\mathbb{C}^3$ such that $(\mathcal{A} \cap \mathcal{B})^\perp \neq \mathcal{A} \cap \mathcal{B}^\perp + \mathcal{A}^\perp \cap \mathcal{B} + \mathcal{A}^\perp \cap \mathcal{B}^\perp$.

A.3 The Dirac Notation

In this review of linear algebra, we use the *Dirac* or *bra–ket notation*, which was introduced by the English physicist Paul Dirac in the context of quantum mechanics to aid algebraic manipulations. This notation is very easy to grasp. Several alternative notations for vectors are used, such as $\mathbf{v}$ and $\vec{v}$. The Dirac notation uses $|v\rangle$. Up to this point, instead of using boldface or an arrow over letter v, we put letter v between a vertical bar and a right angle bracket. If we have an indexed basis, that is, $\{\mathbf{v}_1, \ldots, \mathbf{v}_n\}$, in the Dirac notation we use the form $\{|v_1\rangle, \ldots, |v_n\rangle\}$ or $\{|1\rangle, \ldots, |n\rangle\}$. Note that if we are using a single basis, letter $\mathbf{v}$ is unnecessary in principle. Computer scientists usually start counting from 0. So, the first basis vector is usually called $\mathbf{v}_0$. In the Dirac notation we have

$$\mathbf{v}_0 = |0\rangle.$$

Vector $|0\rangle$ is not the zero vector; it is only the first vector in a collection of vectors. The zero vector is an exception, whose notation is not modified. Here we use the notation $\mathbf{0}$.

Suppose that vector $|v\rangle$ has the following entries in a basis

$$|v\rangle = \begin{bmatrix} a_1 \\ \vdots \\ a_n \end{bmatrix}.$$

The dual vector is denoted by $\langle v|$ and is defined by

$$\langle v| = \begin{bmatrix} a_1^* & \cdots & a_n^* \end{bmatrix}.$$

Vectors and their duals can be seen as column and row matrices, respectively. The matrix product of $\langle v|$ and $|v\rangle$, denoted by $\langle v|v\rangle$, is

$$\langle v|v\rangle = \sum_{i=1}^{n} a_i^* a_i,$$

which coincides with $(|v\rangle, |v\rangle)$. Then, the norm of a vector in the Dirac notation is

$$\big\| |v\rangle \big\| = \sqrt{\langle v|v\rangle}.$$

If $\{|v_1\rangle, \ldots, |v_n\rangle\}$ is an orthonormal basis, then

$$\langle v_i|v_j\rangle = \delta_{ij},$$

where δ_{ij} is the *Kronecker delta*. We use the terminology *ket* for the vector $|v\rangle$ and *bra* for the dual vector $\langle v|$. Keeping consistency, we use the terminology *bra–ket* for $\langle v|v\rangle$.

It is also very common to see the matrix product of $|v\rangle$ and $\langle v|$, denoted by $|v\rangle\langle v|$, known as the *outer product*, whose result is a $n \times n$ matrix

$$\begin{aligned} |v\rangle\langle v| &= \begin{bmatrix} a_1 \\ \vdots \\ a_n \end{bmatrix} \cdot \begin{bmatrix} a_1^* & \cdots & a_n^* \end{bmatrix} \\ &= \begin{bmatrix} a_1 a_1^* & \cdots & a_1 a_n^* \\ & \ddots & \\ a_n a_1^* & \cdots & a_n a_n^* \end{bmatrix}. \end{aligned}$$

The key to the Dirac notation is to always view *kets* as column matrices, *bras* as row matrices, and recognize that a sequence of *bras* and *kets* is a matrix product, hence associative, but noncommutative.

A.4 Computational Basis

The *computational basis* of $\mathbb{C}^n$ is $\{|0\rangle, \ldots, |n-1\rangle\}$, where

$$|0\rangle = \begin{bmatrix} 1 \\ 0 \\ \vdots \\ 0 \end{bmatrix}, \ldots, |n-1\rangle = \begin{bmatrix} 0 \\ 0 \\ \vdots \\ 1 \end{bmatrix}.$$

This basis is also known as *canonical basis*. A few times we use the numbering of the computational basis beginning with $|1\rangle$ and ending with $|n\rangle$. In this book, when we use a small-caption *Latin letter* within a *ket* or *bra*, we are referring to the computational basis. Then, the following expression is always valid

$$\langle i | j \rangle = \delta_{ij}.$$

The normalized sum of all computational basis vectors defines vector

$$|\mathrm{D}\rangle = \frac{1}{\sqrt{n}} \sum_{i=0}^{n-1} |i\rangle,$$

which we call *diagonal state*. When $n = 2$, the diagonal state is given by $|\mathrm{D}\rangle = |+\rangle$, where

$$|+\rangle = \frac{|0\rangle + |1\rangle}{\sqrt{2}}.$$

Exercise A.3. Calculate explicitly the values of $|i\rangle\langle j|$ and

$$\sum_{i=0}^{n-1} |i\rangle\langle i|$$

in $\mathbb{C}^3$.

A.5 Qubit and the Bloch Sphere

The *qubit* is a *unit vector* in vector space $\mathbb{C}^2$. An arbitrary qubit $|\psi\rangle$ is represented by

$$|\psi\rangle = \alpha\,|0\rangle + \beta\,|1\rangle,$$

where coefficients α and β are complex numbers and obey the constraint

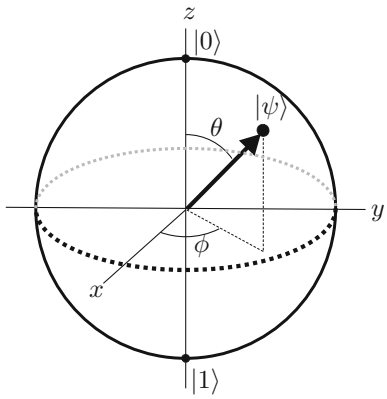

Fig. A.1 Bloch sphere. The state $|\psi\rangle$ of a qubit is represented by a point on the sphere

$$|\alpha|^2 + |\beta|^2 = 1.$$

The set $\{|0\rangle,\ |1\rangle\}$ is the computational basis of $\mathbb{C}^2$, and $\alpha,\ \beta$ are called amplitudes of state $|\psi\rangle$. The term *state* (or *state vector*) is used as a synonym for *unit vector in a Hilbert space*.

In principle, we need four real numbers to describe a qubit, two for α and two for β. The constraint $|\alpha|^2 + |\beta|^2 = 1$ reduces to three numbers. In quantum mechanics, two vectors that differ from a *global phase factor* are considered equivalent. A global phase factor is a complex number of unit modulus multiplying the state. By eliminating this factor, a qubit can be described by two real numbers θ and ϕ as follows:

$$|\psi\rangle = \cos\frac{\theta}{2}\,|0\rangle + \mathrm{e}^{i\phi}\sin\frac{\theta}{2}\,|1\rangle,$$

where $0 \le \theta \le \pi$ and $0 \le \phi < 2\pi$. In the notation above, state $|\psi\rangle$ can be represented by a point on the surface of a sphere of unit radius called *Bloch sphere*. Numbers θ and ϕ are spherical angles that locate the point that describes $|\psi\rangle$, as shown in Fig. A.1. The vector showed there is given by

$$\begin{bmatrix} \sin\theta\cos\phi \\ \sin\theta\sin\phi \\ \cos\theta \end{bmatrix}.$$

When we disregard global phase factors, there is a one-to-one correspondence between the quantum states of a qubit and the points on the Bloch sphere. State $|0\rangle$ is the *north pole* of the sphere because it is obtained by taking $\theta = 0$. State $|1\rangle$ is the *south pole*. States

$$|\pm\rangle = \frac{|0\rangle \pm |1\rangle}{\sqrt{2}}$$

are the intersection points of the x-axis and the sphere; states $(|0\rangle \pm \mathrm{i}|1\rangle)/\sqrt{2}$ are the intersection points of the y-axis with the sphere.

The representation of *classical bits* in this context is given by the poles of the Bloch sphere, and the representation of the *probabilistic classical bit*, that is, 0 with probability p and 1 with probability $1-p$, is given by the point on z-axis with coordinate $2p-1$. The interior of the Bloch sphere is used to describe states of a qubit in the presence of *decoherence*.

Exercise A.4. Using the Dirac notation, show that opposite points on the Bloch sphere correspond to orthogonal states.

Exercise A.5. Suppose you know that the state of a qubit is either $|+\rangle$ with probability p or $|-\rangle$ with probability $1-p$. If this is the best you know about the state of the qubit, where on the Bloch sphere would you represent this qubit?

A.6 Linear Operators

Let V and W be vector spaces, $\{|v_1\rangle, \ldots, |v_n\rangle\}$ a basis for V, and $\mathcal{A}$ a function $\mathcal{A} : V \mapsto W$ that satisfies

$$\mathcal{A}\left(\sum_i a_i|v_i\rangle\right) = \sum_i a_i \mathcal{A}(|v_i\rangle),$$

for any complex numbers a_i. $\mathcal{A}$ is called a *linear operator* from V to W. The term *linear operator on* V means that both the domain and codomain of $\mathcal{A}$ are V. The composition of linear operators $\mathcal{A} : V_1 \mapsto V_2$ and $\mathcal{B} : V_2 \mapsto V_3$ is also a linear operator $\mathcal{C} : V_1 \mapsto V_3$ obtained through the composition of their functions: $\mathcal{C}(|v\rangle) = \mathcal{B}(\mathcal{A}(|v\rangle))$. The sum of two linear operators, both from V to W, is defined by formula $(\mathcal{A}+\mathcal{B})(|v\rangle) = \mathcal{A}(|v\rangle) + \mathcal{B}(|v\rangle)$.

The *identity operator* $\mathcal{I}$ on V is a linear operator such that $\mathcal{I}(|v\rangle) = |v\rangle$ for all $|v\rangle \in V$. The *null operator* $\mathcal{O}$ on V is a linear operator such that $\mathcal{O}(|v\rangle) = \mathbf{0}$ for all $|v\rangle \in V$.

The *rank* of a linear operator $\mathcal{A}$ on V is the dimension of the image of $\mathcal{A}$. The *kernel* or *nullspace* or *support* of a linear operator $\mathcal{A}$ on V is the set of all vectors $|v\rangle$ such that $\mathcal{A}(|v\rangle) = \mathbf{0}$. The dimension of the kernel is called the *nullity* of the operator. The *rank–nullity theorem* states that $\mathrm{rank}(\mathcal{A}) + \mathrm{nullity}(\mathcal{A}) = \dim(V)$.

Fact

If we specify the action of a linear operator $\mathcal{A}$ on a basis of vector space V, the action of $\mathcal{A}$ on any vector in V can be determined by using the linearity property.

A.7 Matrix Representation

Linear operators are represented by matrices. Let $\mathcal{A} : V \mapsto W$ be a linear operator. Let $\{|v_1\rangle, \ldots, |v_n\rangle\}$ and $\{|w_1\rangle, \ldots, |w_m\rangle\}$ be orthonormal bases for V and W, respectively. The *matrix representation* of $\mathcal{A}$ is obtained by applying $\mathcal{A}$ to every vector in the basis of V and expressing the result as a linear combination of basis vectors of W, as follows:

$$\mathcal{A}\left(\left|v_j\right\rangle\right) = \sum_{i=1}^{m} a_{ij}|w_i\rangle,$$

where index j run from 1 to n. Therefore, a_{ij} are entries of a $m \times n$ matrix, which we call A. In this case, expression $\mathcal{A}\left(\left|v_j\right\rangle\right)$, which means function $\mathcal{A}$ applied to argument $\left|v_j\right\rangle$, is equivalent to the matrix product $A\left|v_j\right\rangle$. Using the outer product notation, we have

$$A = \sum_{i=1}^{m}\sum_{j=1}^{n} a_{ij}|w_i\rangle\langle v_j|.$$

Using the above equation and the fact that the basis of V is orthonormal, we can verify that the matrix product of A and $\left|v_j\right\rangle$ is equal to $\mathcal{A}\left(\left|v_j\right\rangle\right)$. The key to this calculation is to use the associativity of matrix multiplication:

$$\begin{aligned}\left(|w_i\rangle\langle v_j|\right)|v_k\rangle &= |w_i\rangle\left(\langle v_j|v_k\rangle\right)\\ &= \delta_{jk}|w_i\rangle.\end{aligned}$$

In particular, the matrix representation of the identity operator $\mathcal{I}$ in any orthonormal basis is the identity matrix I and the matrix representation of the null operator $\mathcal{O}$ in any orthonormal basis is the *zero matrix*.

If the linear operator $\mathcal{C}$ is the composition of the linear operators $\mathcal{B}$ and $\mathcal{A}$, the matrix representation of $\mathcal{C}$ is obtained by multiplying the matrix representation of $\mathcal{B}$ with that of $\mathcal{A}$, that is, $C = BA$.

When we fix orthonormal bases for the vector spaces, there is a one-to-one correspondence between linear operators and matrices. In $\mathbb{C}^n$, we use the computational basis as a reference basis, so that the terms *linear operator* and *matrix* are taken as synonyms. We also use the term *operator* as a synonym for *linear operator*.

Exercise A.6. Suppose B is an operator whose action on the computational basis of the n-dimensional vector space V is

$$B|j\rangle = \left|\psi_j\right\rangle,$$

where $\left|\psi_j\right\rangle$ are vectors in V for all j.

1. Obtain the expression of B using the outer product.
2. Show that $\left|\psi_j\right\rangle$ is the jth column in the matrix representation of B.

3. Suppose that B is the Hadamard operator

$$H = \frac{1}{\sqrt{2}} \begin{bmatrix} 1 & 1 \\ 1 & -1 \end{bmatrix}.$$

Redo the previous items using operator H.

A.8 Diagonal Representation

Let A be an operator on V. If there exists an orthonormal basis $\{|v_1\rangle, \ldots, |v_n\rangle\}$ of V such that

$$A = \sum_{i=1}^{n} \lambda_i |v_i\rangle\langle v_i|,$$

we say that A admits a *diagonal representation* or, equivalently, A is *diagonalizable*. The complex numbers λ_i are the *eigenvalues* of A and $|v_i\rangle$ are the corresponding *eigenvectors*. A vector $|\psi\rangle$ is an *eigenvector* of A if there is a scalar λ, called *eigenvalue*, so that

$$A|\psi\rangle = \lambda|\psi\rangle.$$

Any multiple of an eigenvector is also an eigenvector. If two eigenvectors are associated with the same eigenvalue, then any linear combination of these eigenvectors is an eigenvector. The number of linearly independent eigenvectors associated with the same eigenvalue is the *multiplicity* of that eigenvalue. We use the short notation "λ-eigenvectors" for eigenvectors associated with eigenvalues λ.

If there are eigenvalues with multiplicity greater than one, the diagonal representation is factored out as follows:

$$A = \sum_{\lambda} \lambda P_\lambda,$$

where index λ runs only on the distinct eigenvalues and P_λ is the projector on the eigenspace of A associated with eigenvalue λ. If λ has multiplicity 1, $P_\lambda = |v\rangle\langle v|$, where $|v\rangle$ is the unit eigenvector associated with λ. If λ has multiplicity 2 and $|v_1\rangle, |v_2\rangle$ are linearly independent unit eigenvectors associated with λ, $P_\lambda = |v_1\rangle\langle v_1| + |v_2\rangle\langle v_2|$ and so on. The projectors P_λ satisfy

$$\sum_{\lambda} P_\lambda = I.$$

An alternative way to define a diagonalizable operator is by requiring that A is *similar* to a diagonal matrix. Matrices A and A' are similar if $A' = M^{-1}AM$ for some invertible matrix M. We have interest only in the case when M is a unitary matrix.

The term *diagonalizable* used here is narrower than the one used in the literature because we are demanding that M be a unitary matrix.

The *characteristic polynomial* of a matrix A, denoted by $p_A(\lambda)$, is the monic polynomial

$$p_A(\lambda) = \det(\lambda I - A).$$

The roots of $p_A(\lambda)$ are the eigenvalues of A. Usually, the best way to calculate the eigenvalues of a matrix is via the characteristic polynomial. For a two-dimensional matrix U, the characteristic polynomial is given by

$$p_U(\lambda) = \lambda^2 - \mathrm{tr}(U)\,\lambda + \det(U).$$

If U is a real unitary matrix, the eigenvalues have the form $\mathrm{e}^{\pm \mathrm{i}\omega}$ and the characteristic polynomial is given by

$$p_U(\lambda) = \lambda^2 - 2\lambda\cos\omega + 1.$$

Exercise A.7. Suppose that A is a diagonalizable operator with eigenvalues ± 1. Show that

$$P_{\pm 1} = \frac{I \pm A}{2}.$$

A.9 Completeness Relation

The *completeness relation* is so useful that it deserves to be highlighted. Let $\{|v_1\rangle, \ldots, |v_n\rangle\}$ be an orthonormal basis of V. Then,

$$I = \sum_{i=1}^{n} |v_i\rangle\langle v_i|.$$

The completeness relation is the diagonal representation of the identity matrix.

Exercise A.8. If $\{|v_1\rangle, \ldots, |v_n\rangle\}$ is an orthonormal basis, it is straightforward to show that

$$A = \sum_{i=1}^{m}\sum_{j=1}^{n} a_{ij}|w_i\rangle\langle v_j|$$

implies

$$A|v_j\rangle = \sum_{i=1}^{m} a_{ij}|w_i\rangle.$$

Prove the reverse, that is, given the above expressions for $A|v_j\rangle$, use the completeness relation to obtain A. [Hint: Multiply the last equation by $\langle v_j|$ and sum over j.]

A.10 Cauchy–Schwarz Inequality

Let V be a Hilbert space and $|v\rangle, |w\rangle \in V$. Then,

$$\left|\langle v|w\rangle\right| \leq \sqrt{\langle v|v\rangle\langle w|w\rangle}.$$

A more explicit way of presenting the Cauchy–Schwarz inequality is

$$\left|\sum_i v_i w_i\right|^2 \leq \left(\sum_i |v_i|^2\right)\left(\sum_i |w_i|^2\right),$$

which is obtained when we take $|v\rangle = \sum_i v_i^* |i\rangle$ and $|w\rangle = \sum_i w_i |i\rangle$.

A.11 Special Operators

Let A be a linear operator on Hilbert space V. Then, there exists a unique linear operator $A^\dagger$ on V, called *adjoint operator*, that satisfies

$$(|v\rangle, A|w\rangle) = \left(A^\dagger|v\rangle, |w\rangle\right),$$

for all $|v\rangle, |w\rangle \in V$.

The matrix representation of $A^\dagger$ is the transpose–conjugate matrix $(A^*)^T$. The main properties of the *dagger* or *transpose–conjugate* operation are

1. $(A\,B)^\dagger = B^\dagger A^\dagger$
2. $|v\rangle^\dagger = \langle v|$
3. $\left(A|v\rangle\right)^\dagger = \langle v|A^\dagger$
4. $\left(|w\rangle\langle v|\right)^\dagger = |v\rangle\langle w|$
5. $\left(A^\dagger\right)^\dagger = A$
6. $\left(\sum_i a_i A_i\right)^\dagger = \sum_i a_i^* A_i^\dagger$

The last property shows that the dagger operation is *conjugate-linear* when applied on a linear combination of operators.

Normal Operator

An operator A on V is *normal* if $A^\dagger A = A A^\dagger$.

Spectral Theorem

An operator A on V is diagonalizable if and only if A is normal.

Unitary Operator

An operator U on V is *unitary* if $U^\dagger U = U U^\dagger = I$.

Facts about Unitary Operators

Unitary operators are normal. They are diagonalizable with respect to an orthonormal basis. Eigenvectors of a unitary operator associated with different eigenvalues are orthogonal. The eigenvalues have unit modulus, that is, they have the form $e^{i\alpha}$, where α is a real number . Unitary operators preserve the inner product, that is, the inner product of $U|v_1\rangle$ and $U|v_2\rangle$ is equal to the inner product of $|v_1\rangle$ and $|v_2\rangle$. The action of a unitary operator on a vector preserves its norm.

Hermitian Operator

An operator A on V is *Hermitian* or *self-adjoint* if $A^\dagger = A$.

Facts about Hermitian Operators

Hermitian operators are normal. They are diagonalizable with respect to an orthonormal basis. Eigenvectors of a Hermitian operator associated with different eigenvalues are orthogonal. The eigenvalues of a Hermitian operator are real numbers. A real symmetric matrix is Hermitian.

Orthogonal Projector

An operator P on V is an *orthogonal projector* if $P^2 = P$ and $P^\dagger = P$.

Facts about Orthogonal Projectors

The eigenvalues are equal to 0 or 1. If P is an orthogonal projector, then the *orthogonal complement* $I - P$ is also an orthogonal projector. Applying a projector to a vector either decreases its norm or maintains invariant. In this book, we use the term *projector* as a synonym for *orthogonal projector*. We use the term *nonorthogonal projector* explicitly to distinguish this case. An example of a nonorthogonal projector on a qubit is $P = |1\rangle(\langle 0| + \langle 1|)$. Note that P is not normal in this example.

Positive Operator

An operator A on V is said *positive* if $\langle v|A|v\rangle \geq 0$ for any $|v\rangle \in V$. If the inequality is strict for any nonzero vector in V, then the operator is said *positive definite*.

Facts about Positive Operators

Positive operators are Hermitian. The eigenvalues are nonnegative real numbers.

Exercise A.9. Consider matrix

$$M = \begin{bmatrix} 1 & 0 \\ 1 & 1 \end{bmatrix}.$$

1. Show that M is not normal.
2. Show that the eigenvectors of M generate a one-dimensional space.

Exercise A.10. Consider matrix

$$M = \begin{bmatrix} 1 & 0 \\ 1 & -1 \end{bmatrix}.$$

1. Show that the eigenvalues of M are ± 1.
2. Show that M is not unitary nor Hermitian.
3. Show that the eigenvectors associated with distinct eigenvalues of M are not orthogonal.
4. Show that M has a diagonal representation.

Exercise A.11. 1. Show that the product of two unitary operators is a unitary operator.
2. The sum of two unitary operators is necessarily a unitary operator? If not, give a counterexample.

Exercise A.12. 1. Show that the sum of two Hermitian operators is a Hermitian operator.
2. The product of two Hermitian operators is necessarily a Hermitian operator? If not, give a counterexample.

Exercise A.13. Show that $A^\dagger A$ is a positive operator for any operator A.

A.12 Pauli Matrices

The *Pauli matrices* are

$$\begin{aligned}
\sigma_0 = I &= \begin{bmatrix} 1 & 0 \\ 0 & 1 \end{bmatrix}, \\
\sigma_1 = \sigma_x &= X = \begin{bmatrix} 0 & 1 \\ 1 & 0 \end{bmatrix}, \\
\sigma_2 = \sigma_y &= Y = \begin{bmatrix} 0 & -i \\ i & 0 \end{bmatrix}, \\
\sigma_3 = \sigma_z &= Z = \begin{bmatrix} 1 & 0 \\ 0 & -1 \end{bmatrix}.
\end{aligned}$$

These matrices are unitary and Hermitian, and hence their eigenvalues are equal to ± 1. Putting in another way: $\sigma_j^2 = I$ and $\sigma_j^\dagger = \sigma_j$ to $j = 0, \ldots, 3$.

The following facts are extensively used:

$$X|0\rangle = |1\rangle, \;\; X|1\rangle = |0\rangle,$$

$$Z|0\rangle = |0\rangle, \;\; Z|1\rangle = -|1\rangle.$$

Pauli matrices form a basis for the vector space of 2×2 matrices. Therefore, an arbitrary operator that acts on a qubit can be written as a linear combination of Pauli matrices.

Exercise A.14. Consider the representation of the state $|\psi\rangle$ of a qubit on the Bloch sphere. What is the representation of states $X|\psi\rangle$, $Y|\psi\rangle$, and $Z|\psi\rangle$ relative to $|\psi\rangle$? What is the geometric interpretation of the action of the Pauli matrices on the Bloch sphere?

A.13 Operator Functions

If we have an operator A on V, we ask whether it is possible to calculate $\sqrt{A}$, that is, to find an operator whose square is A? It is more interesting to ask ourselves whether it makes sense to use an operator as an argument of an arbitrary function $f : \mathbb{C} \mapsto \mathbb{C}$, such as the exponential or logarithmic function. If f is analytic, we use the Taylor expansion of $f(x)$ and replace x by A. This will not work for the square root function. There is an alternate route for lifting f if operator A is normal. Using the diagonal representation, A can be written in the form

$$A = \sum_i a_i |v_i\rangle\langle v_i|,$$

where a_i are the eigenvalues and the set $\{|v_i\rangle\}$ is an orthonormal basis of eigenvectors of A. We extend the application of a function $f : \mathbb{C} \mapsto \mathbb{C}$ to the set of normal operators as follows. If A is a normal operator, then

$$f(A) = \sum_i f(a_i)|v_i\rangle\langle v_i|.$$

The result is an operator defined on the same vector space V.

If the goal is to calculate $\sqrt{A}$, first A must be diagonalized, that is, we must determine a unitary matrix U such that $A = U D U^\dagger$, where D is a diagonal matrix. Then, we use the fact that $\sqrt{A} = U\sqrt{D}\,U^\dagger$, where $\sqrt{D}$ is calculated by taking the square root of each diagonal element.

If U is the evolution operator of an isolated quantum system whose state is $|\psi(0)\rangle$ initially, the state at time t is given by

$$|\psi(t)\rangle \;=\; U^t|\psi(0)\rangle.$$

Usually, the most efficient way to calculate state $|\psi(t)\rangle$ is to obtain the diagonal representation of the unitary operator U, described as

$$U = \sum_i \lambda_i |v_i\rangle\langle v_i|,$$

and to calculate the tth power of U, which is

$$U^t = \sum_i \lambda_i^t |v_i\rangle\langle v_i|.$$

The system state at time t will be

$$|\psi(t)\rangle = \sum_i \lambda_i^t \left\langle v_i \middle| \psi(0) \right\rangle |v_i\rangle.$$

The *trace* of a matrix is another type of operator function. In this case, the result of applying the trace function is a complex number defined as

$$\mathrm{tr}(A) = \sum_i a_{ii},$$

where a_{ii} is the ith diagonal element of A. In the Dirac notation,

$$\mathrm{tr}(A) = \sum_i \langle v_i|A|v_i\rangle,$$

where $\{|v_1\rangle, \ldots, |v_n\rangle\}$ is an orthonormal basis of V. The trace function satisfies the following properties:

1. (Linearity) $\mathrm{tr}(aA + bB) = a\,\mathrm{tr}(A) + b\,\mathrm{tr}(B)$,
2. (Commutativity) $\mathrm{tr}(AB) = \mathrm{tr}(BA)$,
3. (Cyclic property) $\mathrm{tr}(A\,B\,C) = \mathrm{tr}(C\,A\,B)$.

The third property follows from the second one. Properties 2 and 3 are valid when A, B, and C are not square matrices (AB, ABC, and CAB must be square matrices).

The trace function is invariant under the *similarity transformation*, that is, $\mathrm{tr}(M^{-1}AM) = \mathrm{tr}(A)$, where M is an invertible matrix. This implies that the trace does not depend on the basis choice for the matrix representation of A.

A useful formula involving the trace of operators is

$$\mathrm{tr}(A|\psi\rangle\langle\psi|) = \left\langle \psi \middle| A \middle| \psi \right\rangle,$$

for any $|\psi\rangle \in V$ and any A on V. This formula is easily proved using the cyclic property of the trace function.

Exercise A.15. Using the method of applying functions to matrices described in this section, find all matrices M such that

$$M^2 = \begin{bmatrix} 5 & 4 \\ 4 & 5 \end{bmatrix}.$$

Exercise A.16. If f is analytic and A is normal, show that $f(A)$ using the Taylor expansion is equal to $f(A)$ using the spectral decomposition.

A.14 Norm of a Linear Operator

Given a vector space V over the complex numbers, a *norm* on V is a function $\| \ \| : V \to \mathbb{R}$ with the following properties:

- $\|a|\psi\rangle\| = |a| \, \||\psi\rangle\|$,
- $\||\psi\rangle + |\psi'\rangle\| \leq \||\psi\rangle\| + \||\psi'\rangle\|$,
- $\||\psi\rangle\| \geq 0$,
- $\||\psi\rangle\| = 0$ if and only if $|\psi\rangle = \mathbf{0}$,

for all $a \in \mathbb{C}$ and all $|\psi\rangle, |\psi'\rangle \in V$,

The set of all linear operators on a Hilbert space $\mathcal{H}$ is a vector space over the complex numbers because it obeys the properties demanded by the definition described in Sect. A.1. It is possible to define more than one norm on a vector space, and let us start with the following norm.

Let A be a linear operator on a Hilbert space $\mathcal{H}$. The *norm* of A is defined as

$$\|A\| = \max_{\langle\psi|\psi\rangle=1} \left|\langle\psi|A|\psi\rangle\right|,$$

where the maximum is over all normalized states $|\psi\rangle \in \mathcal{H}$.

The next norm is induced from an *inner product*. The *Hilbert–Schmidt inner product* (also known as *Frobenius inner product*) of two linear operators A and B is

$$(A, B) = \mathrm{tr}\left(A^\dagger B\right).$$

Now, we can define another norm (*trace norm*) of a linear operator A on a Hilbert space $\mathcal{H}$ as

$$\|A\|_{\mathrm{tr}} = \sqrt{\mathrm{tr}\left(A^\dagger A\right)}.$$

In a *normed vector space*, the *distance* between vectors $|\psi\rangle$ and $|\psi'\rangle$ is given by $\||\psi\rangle - |\psi'\rangle\|$. Then, it makes sense to speak about *distance between linear operators* A and B, which is the nonnegative number $\|A - B\|$.

Exercise A.17. Show that $\|U\| = 1$ if U is a unitary operator.

Exercise A.18. Show that the inner product $(A, B) = \mathrm{tr}(A^\dagger B)$ satisfies the properties described in Sect. A.2.

Exercise A.19. Show that $\|U\|_{\mathrm{tr}} = \sqrt{n}$ if U is a unitary operator on $\mathbb{C}^n$.

Exercise A.20. Show that both norms defined in this section satisfy the properties described at the beginning of this section.

A.15 Tensor Product

Let V and W be finite Hilbert spaces with basis $\{|v_1\rangle, \ldots, |v_m\rangle\}$ and $\{|w_1\rangle, \ldots, |w_n\rangle\}$, respectively. The *tensor product* of V and W, denoted by $V \otimes W$, is a (mn)-dimensional Hilbert space with basis $\{|v_1\rangle \otimes |w_1\rangle, |v_1\rangle \otimes |w_2\rangle, \ldots, |v_m\rangle \otimes |w_n\rangle\}$. The tensor product of a vector in V and a vector in W, such as $|v\rangle \otimes |w\rangle$, also denoted by $|v\rangle|w\rangle$ or $|v, w\rangle$ or $|v\, w\rangle$, is calculated explicitly via the Kronecker product, defined ahead. An arbitrary vector in $V \otimes W$ is a linear combination of vectors $|v_i\rangle \otimes \big|w_j\big\rangle$, that is, if $|\psi\rangle \in V \otimes W$, then

$$|\psi\rangle = \sum_{i=1}^{m} \sum_{j=1}^{n} a_{ij} |v_i\rangle \otimes \big|w_j\big\rangle.$$

The tensor product is *bilinear*, that is, linear with respect to each argument:

1. $|v\rangle \otimes \big(a\,|w_1\rangle + b\,|w_2\rangle\big) \;=\; a\,|v\rangle \otimes |w_1\rangle + b\,|v\rangle \otimes |w_2\rangle,$
2. $\big(a\,|v_1\rangle + b\,|v_2\rangle\big) \otimes |w\rangle \;=\; a\,|v_1\rangle \otimes |w\rangle + b\,|v_2\rangle \otimes |w\rangle.$

A scalar can always be factored out to the beginning of the expression:

$$a\big(|v\rangle \otimes |w\rangle\big) \;=\; \big(a|v\rangle\big) \otimes |w\rangle \;=\; |v\rangle \otimes \big(a|w\rangle\big).$$

The tensor product of a linear operator A on V and B on W, denoted by $A \otimes B$, is a linear operator on $V \otimes W$ defined by

$$\big(A \otimes B\big)\big(|v\rangle \otimes |w\rangle\big) \;=\; \big(A|v\rangle\big) \otimes \big(B|w\rangle\big).$$

In general, an arbitrary linear operator on $V \otimes W$ cannot be factored out as the tensor product of the form $A \otimes B$, but it can be written as a linear combination of operators of the form $A_i \otimes B_j$. The above definition is easily extended to operators $A : V \mapsto V'$ and $B : W \mapsto W'$. In this case, the tensor product of these operators is $(A \otimes B) : (V \otimes W) \mapsto (V' \otimes W')$.

In quantum mechanics, it is very common to use operators in the form of external products, for example, $A = |v\rangle\langle v|$ and $B = |w\rangle\langle w|$. The tensor product of A and B is represented by the following equivalent ways:

$$\begin{aligned} A \otimes B &= \big(|v\rangle\langle v|\big) \otimes \big(|w\rangle\langle w|\big) \\ &= |v\rangle\langle v| \otimes |w\rangle\langle w| \\ &= |v, w\rangle\langle v, w|. \end{aligned}$$

If A_1, A_2 are operators on V and B_1, B_2 are operators on W, then

$$(A_1 \otimes B_1) \cdot (A_2 \otimes B_2) = (A_1 \cdot A_2) \otimes (B_1 \cdot B_2).$$

The inner product of $|v_1\rangle \otimes |w_1\rangle$ and $|v_2\rangle \otimes |w_2\rangle$ is defined as

$$\big(|v_1\rangle \otimes |w_1\rangle\,,\ |v_2\rangle \otimes |w_2\rangle\big) = \big\langle v_1 \big| v_2 \big\rangle \big\langle w_1 \big| w_2 \big\rangle.$$

The inner product of vectors written as a linear combination of basis vectors is calculated by applying the linear property to the second argument and the *conjugate-linear* property on the first argument of the inner product. For example,

$$\left(\left(\sum_{i=1}^{n} a_i |v_i\rangle\right) \otimes |w_1\rangle\,,\ |v\rangle \otimes |w_2\rangle\right) = \left(\sum_{i=1}^{n} a_i^* \big\langle v_i \big| v \big\rangle\right) \big\langle w_1 \big| w_2 \big\rangle.$$

The inner product definition implies that

$$\big\| \, |v\rangle \otimes |w\rangle \, \big\| = \big\| \, |v\rangle \, \big\| \cdot \big\| \, |w\rangle \, \big\|.$$

In particular, the tensor product of unit norm vectors is a unit norm vector.

When we use matrix representations of operators, the tensor product is calculated explicitly via the *Kronecker product*. Let A be a $m \times n$ matrix and B a $p \times q$ matrix. Then,

$$A \otimes B = \begin{bmatrix} a_{11}B & \cdots & a_{1n}B \\ & \ddots & \\ a_{m1}B & \cdots & a_{mn}B \end{bmatrix}.$$

The dimension of the resulting matrix is $mp \times nq$. The Kronecker product is used for matrices of any dimension, particularly for two vectors,

$$\begin{bmatrix} a_1 \\ a_2 \end{bmatrix} \otimes \begin{bmatrix} b_1 \\ b_2 \end{bmatrix} = \begin{bmatrix} a_1 \begin{bmatrix} b_1 \\ b_2 \end{bmatrix} \\ a_2 \begin{bmatrix} b_1 \\ b_2 \end{bmatrix} \end{bmatrix} = \begin{bmatrix} a_1 b_1 \\ a_1 b_2 \\ a_2 b_1 \\ a_2 b_2 \end{bmatrix}.$$

The tensor product is an associative and distributive operation, but noncommutative, that is, $|v\rangle \otimes |w\rangle \neq |w\rangle \otimes |v\rangle$ if $v \neq w$. Most operations on a tensor product are performed term by term, such as

$$(A \otimes B)^\dagger = A^\dagger \otimes B^\dagger.$$

If both operators A and B are special operators of the same type, as the ones defined in Sect. A.11, then the tensor product $A \otimes B$ is also a special operator of the same type. For example, the tensor product of Hermitian operators is a Hermitian operator.

The trace of a Kronecker product of matrices is

$$\mathrm{tr}(A \otimes B) = \mathrm{tr}A \ \mathrm{tr}B,$$

while the determinant is

$$\det(A \otimes B) = (\det A)^m \, (\det B)^n,$$

where n is the dimension of A and m of B.

If the *diagonal state* of the vector space V is $|\mathrm{D}\rangle_V$ and of space W is $|\mathrm{D}\rangle_W$, then the diagonal state of space $V \otimes W$ is $|\mathrm{D}\rangle_V \otimes |\mathrm{D}\rangle_W$. Therefore, the diagonal state of space $V^{\otimes n}$ is $|\mathrm{D}\rangle^{\otimes n}$, where $V^{\otimes n}$ means $V \otimes \cdots \otimes V$ with n terms.

Exercise A.21. Let H be the Hadamard operator

$$H = \frac{1}{\sqrt{2}} \begin{bmatrix} 1 & 1 \\ 1 & -1 \end{bmatrix}.$$

Show that

$$\langle i | H^{\otimes n} | j \rangle = \frac{(-1)^{i \cdot j}}{\sqrt{2^n}},$$

where n represents the number of qubits and $i \cdot j$ is the binary inner product, that is, $i \cdot j = i_1 j_1 + \cdots + i_n j_n \mod 2$, where $(i_1, \ldots, i_n)$ and $(j_1, \ldots, j_n)$ are the binary decompositions of i and j, respectively.

A.16 Quantum Gates, Circuits, and Registers

A *quantum circuit* is a pictorial way to describe a *quantum algorithm*. The input lies on the left-hand side of the circuit and the *quantum information* flows unchanged through the wires, from the left to right, until finding a *quantum gate*, which is a square box with the name of a unitary operator. The quantum gate represents the action of the unitary operator, which transforms the quantum information and releases it to the wire on the right-hand side. For example, the algebraic expression $|+\rangle = H|0\rangle$

is represented by the circuit[1]

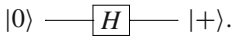

If a measurement is performed, the representation is

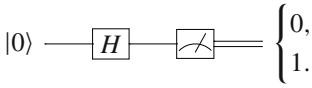

A *meter* represents a measurement in the computational basis, and a double wire conveys the *classical information* that comes out of the meter. In the example, the state of the qubit right before the measurement is $(|0\rangle + |1\rangle)/\sqrt{2}$. If the qubit state is projected on $|0\rangle$ after the measurement, the output is 0, otherwise 1.

The *controlled NOT gate* (CNOT or $C(X)$) is a 2-qubit gate defined by

$$\text{CNOT}\,|k\rangle|\ell\rangle = |k\rangle X^k|\ell\rangle,$$

and represented by the circuit

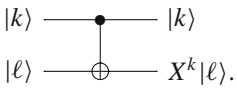

The qubit marked with the black full point is called *control qubit*, and the qubit marked with the $\oplus$ sign is called the *target qubit*.

The *Toffoli gate* $C^2(X)$ is a 3-qubit controlled gate defined by

$$C^2(X)\,|j\rangle|k\rangle|\ell\rangle = |j\rangle|k\rangle X^{jk}|\ell\rangle,$$

and represented by the circuit

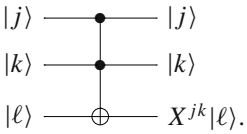

The Toffoli gate has two control qubits and one target qubit.

These gates can be generalized. The *generalized Toffoli gate* $C^n(X)$ is a $(n+1)$-qubit controlled gate defined by

$$C^n(X)\,|j_1\rangle...|j_n\rangle|j_{n+1}\rangle = |j_1\rangle...|j_n\rangle X^{j_1...j_n}|j_{n+1}\rangle.$$

When defined using the computational basis, the state of the target qubit inverts if and only if all control qubits are set to one. There is another case in which the state of the target qubit inverts if and only if all control qubits are set to zero. In this case, the control qubits are depicted by *empty controls* (empty white points) instead of *full controls* (full black points), such as

[1]The circuits were generated with package Q-circuit.

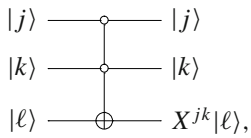

whose algebraic representation is

$$|j_1\rangle|j_2\rangle|j_3\rangle \longmapsto |j_1\rangle|j_2\rangle X^{(1-j_1)(1-j_2)}|j_3\rangle.$$

It is possible to mix full and empty controls. Those kinds of controlled gates are called *generalized Toffoli gates*.

A *register* is a set of qubits treated as a composite system. In many quantum algorithms, the qubits are divided into two registers: one for the main calculation from where the result comes out and one for the draft (calculations that will be discarded).

Suppose we have a register with two qubits. The computational basis is

$$|0,0\rangle = \begin{bmatrix}1\\0\\0\\0\end{bmatrix} \quad |0,1\rangle = \begin{bmatrix}0\\1\\0\\0\end{bmatrix} \quad |1,0\rangle = \begin{bmatrix}0\\0\\1\\0\end{bmatrix} \quad |1,1\rangle = \begin{bmatrix}0\\0\\0\\1\end{bmatrix}.$$

An arbitrary state of this register is

$$|\psi\rangle = \sum_{i=0}^{1}\sum_{j=0}^{1} a_{ij}|i,j\rangle$$

where coefficients a_{ij} are complex numbers that satisfy the constraint

$$|a_{00}|^2 + |a_{01}|^2 + |a_{10}|^2 + |a_{11}|^2 = 1.$$

To help to generalize to n qubits, it is usual to compress the notation by converting the base-2 notation to the base-10 notation. The computational basis for a two-qubit register in the base-10 notation is $\{|0\rangle, |1\rangle, |2\rangle, |3\rangle\}$. In the base-2 notation, we can determine the number of qubits by counting the number of digits inside the *ket*; for example, $|011\rangle$ refers to three qubits. In the base-10 notation, we cannot determine what is the number of qubits of the register. The number of qubits is implicit. At any point, we can go back, write the numbers in the base-2 notation, and the number of qubits will be clear. In the compact notation, an arbitrary state of a n-qubit register is

$$|\psi\rangle = \sum_{i=0}^{2^n-1} a_i|i\rangle$$

where coefficients a_i are complex numbers that satisfy the constraint

$$\sum_{i=0}^{2^n-1} |a_i|^2 = 1.$$

The *diagonal state* of a n-qubit register is the tensor product of the diagonal state of each qubit, that is, $|\mathrm{D}\rangle = |+\rangle^{\otimes n}$.

A set of *universal quantum gates* is a finite set of gates that generates any unitary operator through tensor and matrix products of gates in the set. Since the number of possible quantum gates is uncountable even in the 1-qubit case, we require that any quantum gate can be approximated by a sequence of universal quantum gates. One simple set of *universal gates* is CNOT, H, X, T (or $\pi/8$ gate), and $T^\dagger$, where

$$T = \begin{bmatrix} 1 & 0 \\ 0 & \mathrm{e}^{\frac{\mathrm{i}\pi}{4}} \end{bmatrix}.$$

To calculate the *time complexity* of a quantum algorithm, we have to implement a circuit of the algorithm in terms of universal gates in the best way possible. The time complexity is determined by the depth of the circuit.

For instance, Fig. A.2 shows the decomposition of the Toffoli gate into universal gates. The right-hand circuit has only universal gates (15 gates) and depth 12.

A Toffoli gate with empty controls can be decomposed in terms of a standard Toffoli gate and X gates as depicted in the right-hand circuit of Fig. A.3.

Figure A.4 shows the decomposition of a 6-qubit generalized Toffoli gate with five full controls into Toffoli gates. If the generalized Toffoli gate has n controls, we use $(n-2)$ *ancilla*[2] qubits initially in state $|0\rangle$. The ancilla qubits are interlaced with the controls starting from the second control.

Exercise A.22. Show that the diagonal state of a n-qubit register is $|\mathrm{D}\rangle = |+\rangle^{\otimes n}$ or equivalently $|\mathrm{D}\rangle = H^{\otimes n}|0, \ldots, 0\rangle$.

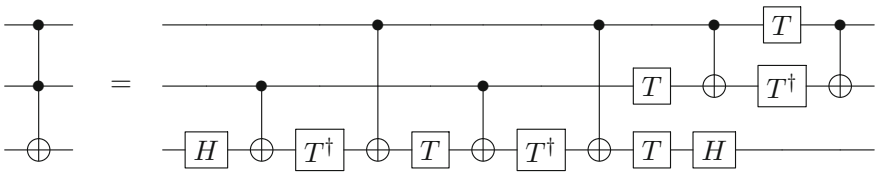

Fig. A.2 Decomposition of a Toffoli gates into universal gates

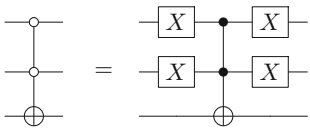

Fig. A.3 Converting empty controls into full controls

[2]Ancilla means auxiliary.

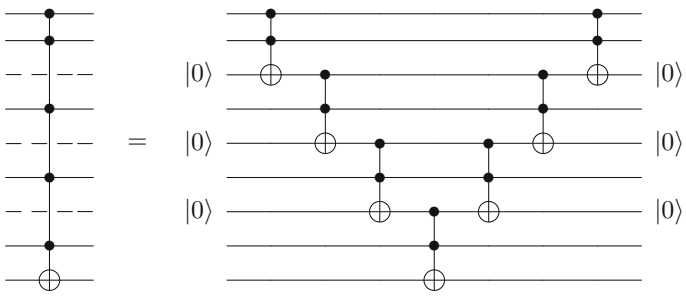

Fig. A.4 Decomposition of a generalized 6-qubit Toffoli gate into Toffoli gates. This decomposition can be easily extended for generalized Toffoli gates with any number of control qubits

Exercise A.23. Let f be a function with domain $\{0, 1\}^n$ and codomain $\{0, 1\}^m$. Consider a 2-register quantum computer with n and m qubits, respectively. Function f can be implemented by using operator U_f defined in the following way:

$$U_f|x\rangle|y\rangle = |x\rangle|y \oplus f(x)\rangle,$$

where x has n bits, y has m bits, and $\oplus$ is the binary sum (bitwise *xor*).

1. Show that U_f is a unitary operator for any f.
2. If $n = m$ and f is injective, show that f can be implemented on a 1-register quantum computer with n qubits.

Exercise A.24. Show that the circuits of Fig. A.4 are equivalent. Find the number of universal gates in the decomposition of a generalized Toffoli gate with n_1 empty controls and n_2 full controls. Find the depth of the circuit.

Exercise A.25. Show that the controlled Hadamard $C(H)$ can be decomposed into universal gates as depicted in the following circuit.

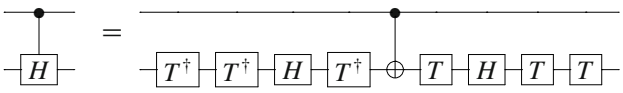

Further Reading

There are many good books on linear algebra. For an initial contact, Refs. [24, 28, 200, 305] are good options; for a more advanced approach, Refs. [148, 150, 199] are good options; for those who have mastered the basics and are only interested in the application of linear algebra to quantum computation, Ref. [248] is recommended, especially for the decomposition of unitary gates into *universal gates*. Linear algebra for quantum algorithms is addressed in [209]. The *Dirac notation* is clearly and comprehensively presented in [287].

Appendix B
Graph Theory for Quantum Walks

Graph theory is a large area of mathematics with a wide range of applications, especially in computer science. It is impossible to overstate the importance of graph theory for quantum walks. In fact, graph theory for quantum walks is as important as linear algebra for quantum computation.

In the quantum walk setting, the graph represents positions and directions for the walker's shift. It is not mandatory to use the graph vertices as the walker's position. Any interpretation is accepted if it employs the graph structure so that the physical meaning reflects the graph components. For example, it makes no sense to have a quantum walk model in which the walker can jump over some vertices, for instance, a model on the line in which the walker can jump from vertex 1 to vertex 3, skipping vertex 2. If it is allowed to jump from vertex 1 to vertex 3, it means that there is an edge or arc linking vertex 1 to vertex 3 and the underlying graph is not the line.

A solid basis on graph theory is required to understand the area of quantum walk. This appendix focuses on the main definitions of graph theory used in this work with some brief examples and should not be used as the first contact with graph theory. At the end of this appendix, introductory and advanced references for starters and for further reading are given.

B.1 Basic Definitions

A *simple graph* $\Gamma(V, E)$ is defined by a set $V(\Gamma)$ of vertices or nodes and a set $E(\Gamma)$ of edges so that each edge links two vertices and two vertices are linked by at most one edge. Two vertices linked by an edge are called *adjacent* or *neighbors*. The *neighborhood* of a vertex $v \in V$, denoted by $N(v)$, is the set of vertices adjacent to v. Two edges that share a common vertex are also called adjacent. A *loop* is an edge whose endpoints are equal. *Multiple edges* are edges having the same pair of endpoints. A simple graph has no loops nor multiple edges. In simple graphs, the edges can be named by the endpoints like an unordered set $\{v, v'\}$, where v and v' are vertices.

© Springer Nature Switzerland AG 2018

R. Portugal, *Quantum Walks and Search Algorithms*, Quantum Science and Technology, https://doi.org/10.1007/978-3-319-97813-0

The *degree* of vertex v is the number of edges incident to the vertex and is denoted by $d(v)$. The *maximum degree* is denoted by $\Delta(\Gamma)$, and the *minimum degree* is denoted by $\delta(\Gamma)$. A graph is *d-regular* if all vertices have degree d, that is, each vertex has exactly d neighbors. The *handshaking lemma* states that every graph has an even number of vertices with odd degree, which is a consequence of the *degree sum formula*

$$\sum_{v \in V} d(v) = 2|E|.$$

A *path* is a list $v_0, e_1, v_1, \ldots, e_k, v_k$ of vertices and edges such that edge e_i has endpoints v_{i-1} and v_i. A *cycle* is a closed path.

A graph is *connected* when there is a path between every pair of vertices; otherwise it is called *disconnected*. An example of connect graph is the *complete graph*, which denoted by K_N where N is the number of vertices, and is a simple graph in which every pair of distinct vertices is connected by an edge.

A subgraph $\Gamma'(V', E')$, where $V' \subset V$ and $E' \subset E$, is an *induced subgraph* of $\Gamma(V, E)$ if it has exactly the edges that appear in Γ over the same vertex set. If two vertices are adjacent in Γ, they are also adjacent in the induced subgraph. It is common to use the term subgraph in place of induced subgraph.

A graph Γ is *H-free* if Γ has no induced subgraph *isomorphic* to graph H. Take for instance a *diamond graph*, which is a graph with four vertices and five edges consisting of a K_4 minus one edge or two triangles sharing a common edge. A graph is *diamond-free* if no induced subgraph is isomorphic to a *diamond graph*.

The *adjacency matrix* M of a simple graph $\Gamma(V, E)$ is the symmetric square matrix whose rows and columns are indexed by the vertices and whose entries are

$$M_{vv'} = \begin{cases} 1, & \text{if } \{v, v'\} \in E(\Gamma), \\ 0, & \text{otherwise.} \end{cases}$$

The *Laplacian matrix* L of a simple graph $\Gamma(V, E)$ is the symmetric square matrix whose rows and columns are indexed by the vertices and whose entries are

$$L_{vv'} = \begin{cases} d(v), & \text{if } v = v', \\ -1, & \text{if } \{v, v'\} \in E(\Gamma), \\ 0, & \text{otherwise.} \end{cases}$$

Note that $L = D - A$, where D is the diagonal matrix whose rows and columns are indexed by the vertices and whose entries are $D_{vv'} = d(v)\delta_{vv'}$. The symmetric normalized Laplacian matrix is defined as $L^{\text{sym}} = D^{-1/2} L D^{-1/2}$.

Most of the times in this book, the term *graph* is used in place of *simple graph*. We also use the term *simple graph* to stress that the graph is undirected and has no loops nor multiple edges.

B.2 Multigraph

A *multigraph* is an extension of the definition of graph that allows multiple edges. Many books use the term graph as a synonym of multigraph. In a simple graph, the notation $\{v, v'\}$ is an edge label. In a multigraph, $\{v, v'\}$ does not characterize an edge and the edges can have their own identity or not. For quantum walks, we need to give labels for each edge (each one has its own identity). Formally, an *undirected labeled multigraph* $G(V, E, f)$ consists of a vertex set V, an edge *multiset* E, and an injective function $f : E \to \Sigma$, whose codomain Σ is an alphabet for the edge labels.

B.3 Bipartite Graph

A *bipartite graph* is a graph whose vertex set V is the union of two disjoint sets X and X' so that no two vertices in X are adjacent and no two vertices in X' are adjacent. A *complete bipartite graph* is a bipartite graph such that every possible edge that could connect vertices in X and X' is part of the graph and is denoted by $K_{m,n}$, where m and n are the cardinalities of sets X and X', respectively. $K_{m,n}$ is the graph that $V(K) = X \cup X'$ and $E(K) = \{\{x, x'\} : x \in X, x' \in X'\}$.

Theorem B.1. (König) *A graph is bipartite if and only if it has no odd cycle.*

B.4 Intersection Graph

Let $\{S_1, S_2, S_3, \ldots\}$ be a family of sets. The *intersection graph* of this family of sets is a graph whose vertices are the sets and two vertices are adjacent if and only if the intersection of the corresponding sets is nonempty, that is, $G(V, E)$ is the intersection graph of family $\{S_1, S_2, S_3, \ldots\}$ if $V = \{S_1, S_2, S_3, \ldots\}$ and $E(G) = \{\{S_i, S_j\} : S_i \cap S_j \neq \emptyset\}$ for all $i \neq j$.

B.5 Clique, Stable Set, and Matching

A *clique* is a subset of vertices of a graph such that its induced subgraph is complete. A *maximal clique* is a clique that cannot be extended by including one more adjacent vertex, that is, it is not contained in a larger clique. A *maximum clique* is a clique of maximum possible size. A clique of size d is called a *d-clique*. A set with one vertex is a clique. Some references in graph theory use the term "clique" as synonym of *maximal clique*. We avoid this notation here.

A *clique partition* of a graph Γ is a set of cliques of Γ that contains each edge of Γ exactly once. A *minimum clique partition* is a clique partition with the smallest set of cliques. A *clique cover* of a graph Γ is a set of cliques of Γ that contains each edge of Γ at least once. A *minimum clique cover* is a clique cover with the smallest set of cliques.

A *stable set* is a set of pairwise nonadjacent vertices.

A *matching* $M \subseteq E$ is a set of edges without pairwise common vertices. An edge $m \in M$ *matches* the endpoints of m. A *perfect matching* is a matching that matches all vertices of the graph.

B.6 Graph Operators

Let $\mathcal{C}$ be the set of all graphs. A graph operator $\mathcal{O} : \mathcal{C} \longrightarrow \mathcal{C}$ is a function that maps an arbitrary graph $G \in \mathcal{C}$ to another graph $G' \in \mathcal{C}$.

B.6.1 Clique Graph Operator

A *clique graph* $K(\Gamma)$ of a graph Γ is a graph such that every vertex represents a maximal clique of Γ and two vertices of $K(\Gamma)$ are adjacent if and only if the underlying maximal cliques in Γ share at least one vertex in common.

The clique graph of a *triangle-free graph* G is isomorphic to the line graph of G.

B.6.2 Line Graph Operator

A *line graph* (or *derived graph* or *interchange graph*) of a graph Γ (called *root graph*) is another graph $L(\Gamma)$ so that each vertex of $L(\Gamma)$ represents an edge of Γ and two vertices of $L(\Gamma)$ are adjacent if and only if their corresponding edges share a common vertex in Γ.

The line graph of a multigraph is a simple graph. On the other hand, given a simple graph G, it is possible to determine whether G is the line graph of a multigraph H, for instance, via the following theorems:

Theorem B.2. (Bermond and Meyer) *A simple graph G is a line graph of a multigraph if and only if there exists a family of cliques C in G such that*

1. *Every edge $\{v, v'\} \in E(G)$ belongs to at least one clique $c_i \in C$.*
2. *Every vertex $v \in V(G)$ belongs to exactly two cliques $c_i, c_j \in C$.*

A graph is *reduced* from a multigraph if the graph is obtained from a multigraph by merging multiple edges into single edges.

Theorem B.3. (Bermond and Meyer) *A simple graph is a line graph of a multigraph H if and only if the graph reduced from H is the line graph of a simple graph.*

It is possible to determine whether G is the line graph of a *bipartite multigraph* via the following theorem.

Theorem B.4. (Peterson) *A simple graph G is a line graph of a bipartite multigraph if and only if $K(G)$ is bipartite.*

B.6.3 Subdivision Graph Operator

A *subdivision* (or *expansion*) of a graph G is a new graph resulting from the subdivision of one or more edges in G. The *barycentric subdivision* subdivides all edges of the graph or a *multigraph* and produces a new bipartite simple graph. If the original graph is $G(V, E)$, the *barycentric subdivision* generates a new graph $BS(G) = \Gamma(V', E')$, whose vertex set is $V'(\Gamma) = V(G) \cup E(G)$ and an edge $\{v, e\}$, where $v \in V$ and $e \in E$, belongs to $E'(\Gamma)$ if and only if v is incident to e.

B.6.4 Clique–Insertion Operator

The *clique–insertion operator* replaces each vertex v of a graph G by a maximal $d(v)$-clique, creating a new graph $CI(G)$. Figure B.1 shows an example of a clique insertion, which replaces a vertex of degree 5 by a 5-clique. Note that the new clique is a maximal clique. Using the degree sum formula, the number of vertices of the clique–inserted graph is $|V(CI(G))| = 2|E(G)|$.

There is a relation between the clique–inserted graph and the line graph of the subdivision graph (called *para-line graph*).

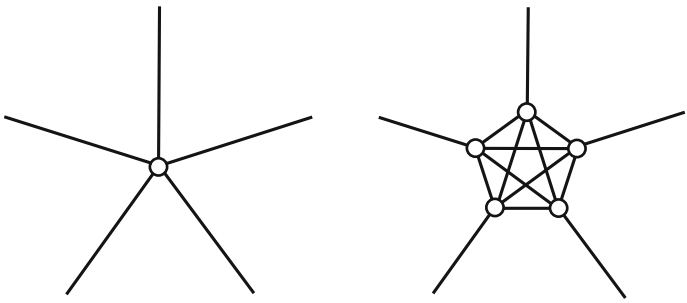

Fig. B.1 Example of a clique insertion. A degree-5 vertex (left-hand graph) is replaced by a 5-clique (right-hand graph)

Theorem B.5. (Sampathkumar) *The para-line graph of G is isomorphic to the clique–inserted graph $CI(G)$.*

B.7 Coloring

A *coloring* of a graph is a labeling of the vertices with colors so that no two vertices sharing the same edge have the same color. The smallest number of colors needed to color a graph Γ is called *chromatic number*, denoted by $\chi(\Gamma)$. A graph that can be assigned a coloring with k colors is *k-colorable* and is *k-chromatic* if its chromatic number is exactly k.

Theorem B.6. (Brooks) $\chi(\Gamma) \leq \Delta(\Gamma)$ *for a graph* Γ*, unless* Γ *is a complete graph or an odd cycle.*

The complete graph with N vertices has $\chi(\Gamma) = N$ and $\Delta(\Gamma) = N - 1$. Odd cycles have $\chi(\Gamma) = 3$ and $\Delta(\Gamma) = 2$. For these graphs the bound $\chi(\Gamma) \leq \Delta(\Gamma) + 1$ is the best possible. In all other cases, the bound $\chi(\Gamma) \leq \Delta(\Gamma)$ is given by Brooks' theorem.

The concept of coloring can be applied to the edge set of a loop free graph. An *edge coloring* is a coloring of the edges so that no vertex is incident to two edges of the same color. The smallest number of colors needed for an edge coloring is called the *chromatic index* or *edge-chromatic number*, denoted by $\chi'(\Gamma)$.

Theorem B.7. (Vizing) *A graph* Γ *of maximal degree* $\Delta(\Gamma)$ *has edge-chromatic number* $\Delta(\Gamma)$ *or* $\Delta(\Gamma) + 1$*, that is,* $\Delta(\Gamma) \leq \chi'(\Gamma) \leq \Delta(\Gamma) + 1$.

Since at least $\Delta(\Gamma)$ colors are always necessary for edge coloring, the set of all graphs may be partitioned into two classes: (1) *class* 1 graphs for which $\Delta(\Gamma)$ colors are sufficient and (2) *class* 2 graphs for which $\Delta(\Gamma) + 1$ colors are necessary. Examples of graphs in class 1 are: complete graphs K_N for even N, bipartite graphs. Examples of graph in class 2 are: regular graphs with an odd number of vertices $N > 1$ (includes complete graphs K_N for odd $N \geq 3$), Petersen graph. To determine whether an arbitrary graph is in class 1 is *NP-complete*. There are asymptotic results in literature showing that the proportion of graphs in class 2 is very small.

Given a graph Γ in class 2, we describe two ways to modify the graph in order to create a new graph in class 1: (1) Add a *leaf* to each vertex of Γ, or (2) make an identical copy of Γ and add edges connecting the pairs of identical vertices.

B.8 Diameter

The *geodesic distance* (simply *distance*) between two vertices in graph $G(V, E)$ is the number of edges in a shortest path connecting them. The *eccentricity* $\epsilon(v)$ of a

vertex v is the greatest geodesic distance between v and any other vertex, that is, it is how far a vertex is from the vertex most distant from it in the graph. The *diameter* d of a graph is $d = \max_{v \in V} \epsilon(v)$, that is, it is the maximum eccentricity of any vertex in the graph or the greatest distance between any pair of vertices.

B.9 Directed Graph

A *directed graph* or *digraph* G is defined by a vertex set $V(G)$, an arc set $A(G)$, and a function assigning each arc an ordered pair of vertices. We use the notation (v, v') for an ordered pair of vertices, where v is the *tail* and v' is the *head*, and (v, v') is called *directed edge* or simply *arc*. A digraph is a *simple digraph* if each ordered pair is the head and tail of at most one arc. The *underlying graph* of a digraph G is the graph obtained by considering the arcs of G as unordered pairs.

If (v, v') and (v', v) are in $A(G)$, the set with (v, v') and (v', v) is called a *pair of symmetric arcs*. A *symmetric directed graph* G or *symmetric digraph* is a digraph whose arc set comprises pairs of symmetric arcs, that is, if $(v, v') \in A(G)$, then $(v', v) \in A(G)$. Figure B.2 depicts an example of a symmetric digraph G and its underlying simple graph H.

The *outdegree* $d^+(v)$ is the number of arcs with tail v. The *indegree* $d^-(v)$ is the number of arcs with head v. The definitions of *out-neighborhood*, *in-neighborhood*, *minimum* and *maximum indegree* and *outdegree* are straightforward generalizations of the corresponding undirected ones. A *local sink* or simply *sink* is a vertex with outdegree zero, and a *local source* or simply *source* is a vertex with indegree zero. A *global sink* is a vertex which is reached by all other vertices. A *global source* A is a vertex which reaches all other vertices.

A *directed cycle graph* is a directed version of a cycle graph, where all edges are oriented in the same direction. A *directed acyclic graph* is a finite directed graph with no directed cycles. The *moral graph* of a directed acyclic graph G is a simple graph that is obtained from the underlying simple graph of G by adding edges between all pairs of vertices that have a common child (in G).

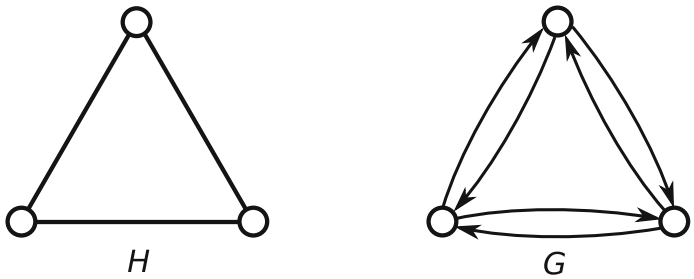

Fig. B.2 Example of a symmetric digraph G and its underlying simple graph H

B.10 Some Named Graphs

B.10.1 Johnson Graphs

Let $[N]$ be the set $\{1, \ldots, N\}$. There are $\binom{N}{k}$ k-subsets of $[N]$, where a k-subset is a subset of $[N]$ with k elements. Let us define the Johnson graph $J(N, k)$. The vertices of $J(N, k)$ are the k-subsets of $[N]$, and two vertices are adjacent if and only if their intersection has size $(k-1)$. If $k = 1$, $J(N, 1)$ is the complete graph K_N. $J(N, k)$ and $J(N, N-k)$ are the same graphs after renaming the vertices. $J(N, k)$ is a regular graph with degree $k\,(N-k)$. The diameter of $J(N, k)$ is $\min(k, N-k)$.

B.10.2 Kneser Graphs

Let $[N]$ be the set $\{1, \ldots, N\}$. A k-subset is a subset of $[N]$ with k elements. The *Kneser graph* $KG_{N,k}$ is the graph whose vertices are the k-subsets, and two vertices are adjacent if and only if the two corresponding sets are disjoint. If $k = 1$, $KG_{N,1}$ is the complete graph K_N. $KG_{N,k}$ is a regular graph with degree $\binom{N-k}{k}$. The diameter of $KG_{N,k}$ is $\lceil (k-1)/(N-2k) \rceil + 1$. The *Petersen graph*, depicted in Fig. B.3, is a Kneser graph $KG_{5,2}$. It is in class 2 because it is 3-regular and its edge-chromatic number is 4.

B.10.3 Cayley Graphs

A *Cayley graph* $\Gamma(G, S)$ encodes the structure of a *group* G described by a *generating set* S in the context of *abstract algebra*.

Definition B.8. A *group* is a nonempty set G together with a binary operation $\cdot$ (called product), which satisfies the following requirements:

- (Closure) For all a, b in G, $a \cdot b$ is also in G.
- (Associativity) For all a, b, c in G, $(a \cdot b) \cdot c = a \cdot (b \cdot c)$.

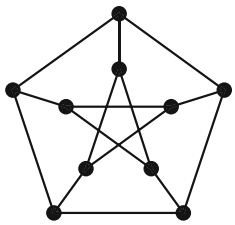

Fig. B.3 Petersen graph

- (Identity) There exists an identity element e in G such that, for every element a in G, $a \cdot e = e \cdot a = a$.
- (Inverse) For each a in G, there exists an element b in G, such that $a \cdot b = b \cdot a = e$, where e is the identity element. Element b is denoted by a^{-1}.

The *order* of a group is its number of elements. A group is finite if its order is finite. A group is *commutative* or *abelian* if the binary operation is commutative. A *generating set* of a group G is a subset $S \subset G$ such that every element of G can be expressed as the product of finitely many elements of S and their inverses. From now on, we suppose that S is finite. S is called *symmetric* if $S = S^{-1}$, that is, whenever $s \in S$, s^{-1} is also in S.

A *subgroup* of a group G is a subset H of G such that H is a group with the same product operation of G. No proper subgroup of group G can contain a generating set of G.

The Cayley graph $\Gamma(G, S)$ is a directed graph defined as follows. The vertex set $V(\Gamma)$ is G, and the arc (a, b) is in $A(\Gamma)$ if and only if $b = a \cdot s$ for some $s \in S$, where $a, b \in G$.

If S is symmetric and $e \neq S$, the Cayley graph $\Gamma(G, S)$ is a $|S|$-regular simple graph. It is a difficult problem to decide whether a Cayley graph of a group described by a symmetric generating set is in class 1 or class 2. There is a remarkable conjecture studied over decades:

Conjecture B.9. (Stong) *All undirected Cayley graphs of groups of even order are in class 1.*

Further Reading

Graph theory has many applications, and it is easy to get lost and waste time after taking some wrong direction. No danger comes from those introductory books [53, 139, 314, 326]. Before starting to read an advanced book, check whether it is really necessary to go further. In the context of quantum walks, the survey [58] is useful. Harary's book [138] is excellent (there is a new edition by CRC Press). Other suggestions are [75, 102, 121]. Wikipedia (English version) is an excellent place to obtain quickly the definition or the main properties of a concept in graph theory, and `http://www.graphclasses.org` is a Web site used by researchers in graph theory. Some results compiled in this Appendix are described in papers [259, 289, 304, 318, 347].

Appendix C
Classical Hitting Time

Consider a connected, nondirected, and non-bipartite *graph* $\Gamma(X, E)$, where $X = \{x_1, \ldots, x_n\}$ is the vertex set and E is the edge set. The *hitting time* of a *classical random walk* on this graph is the *expected time* for the walker to reach a marked vertex for the first time, once given the initial conditions. We may have more than one marked vertex defined by a subset $M \in X$. In this case, the hitting time is the expected time for the walker to reach a vertex in M for the first time.

If $p_{x\,x'}(t)$ is the probability of the walker to reach x' for the first time at time t having left x at $t = 0$, the hitting time from vertex x to x' is

$$H_{x\,x'} = \sum_{t=0}^{\infty} t\; p_{x\,x'}(t). \tag{C.1}$$

Define $H_{x\,x} = 0$ when the departure and arrival vertices are the same.

For example, the probability $p_{x\,x'}(t)$ at time $t = 1$ when $x \neq x'$ for the *complete graph* with n vertices is $1/(n-1)$, because the walker has $n-1$ possible vertices to move in the first step. To arrive at vertex x' at time $t = 2$ for the first time, the walker must visit one of $n-2$ vertices different from x and x'. The probability is $(n-2)/(n-1)$. After this visit, it must go directly to vertex x', which occurs with probability $1/(n-1)$. Therefore, $p_{x\,x'}(2) = (n-2)/(n-1)^2$. Generalizing this argumentation, we obtain $p_{x\,x'}(t) = (n-2)^{t-1}/(n-1)^t$. Then,

$$H_{x\,x'} = \sum_{t=0}^{\infty} t\,\frac{(n-2)^{t-1}}{(n-1)^t}.$$

Using the identity $\sum_{t=0}^{\infty} t\alpha^t = \alpha/(1-\alpha)^2$, which is valid for $0 < \alpha < 1$, we obtain

$$H_{x\,x'} = n - 1. \tag{C.2}$$

Usually, the hitting time depends on x and x', but the complete graph is an exception. In the general case, $H_{x\,x'}$ can be different from $H_{x'x}$.

© Springer Nature Switzerland AG 2018

R. Portugal, *Quantum Walks and Search Algorithms*, Quantum Science and Technology, https://doi.org/10.1007/978-3-319-97813-0

The notion of hitting time from a vertex to a subset can be formalized as follows: Suppose that M is a nonempty subset of X with cardinality m and define $p_{xM}(t)$ as the probability that the walker reaches any of the vertices in M for the first time at time t having left x at $t = 0$. The hitting time from x to M is

$$H_{xM} = \sum_{t=0}^{\infty} t\, p_{xM}(t). \tag{C.3}$$

Again, we define $H_{xM} = 0$ if $x \in M$.

Let us use an extended notion of hitting time when the walker starts from a probability distribution. In the former case, the probability to depart from vertex x is 1 and the probability to depart from any other vertex is 0. Suppose that the walker starts with a distribution σ, that is, at the initial time the probability of the walker to be at vertex x is σ_x. The most used initial distributions are the *uniform distribution* $\sigma_x = 1/n$ and the *stationary distribution*, which is defined ahead. In any case, the initial distribution must satisfy $\sum_{x \in X} \sigma_x = 1$. The hitting time from σ to M is

$$H_{\sigma M} = \sum_{x \in X} \sigma_x\, H_{xM}. \tag{C.4}$$

That is, $H_{\sigma M}$ is the *expected value* of the hitting time H_{xM} from x to M weighted with distribution σ.

Exercise C.1. Show that for the complete graph

$$H_{xM} = \frac{n-1}{m}$$

if $x \notin M$.

Exercise C.2. Show that for the complete graph

$$H_{\sigma M} = \frac{(n-m)(n-1)}{mn}$$

if σ is the uniform distribution. Why $H_{\sigma M} \approx H_{xM}$ for $n \gg m$?

C.1 Hitting Time Using the Stationary Distribution

Equations (C.1) and (C.3) are troublesome for the practical calculation of the hitting time of random walks on graphs. Fortunately, there are alternative methods. The best-known method uses a recursive method. Let us illustrate this method using the complete graph. We want to calculate $H_{xx'}$. The walker departs from x and moves directly to x' with probability $1/(n-1)$ spending one time unit. With probability

$(n-2)/(n-1)$, the walker moves to vertex x'' different from x' and therefore it spends one time unit plus the expected time to go from x'' to x', which is $H_{x\,x'}$. We have established the following recursive equation:

$$H_{x\,x'} = \frac{1}{n-1} + \frac{n-2}{n-1}\left(1 + H_{x\,x'}\right), \tag{C.5}$$

the solution of which is equal to (C.2).

This method works for an arbitrary graph. If V_x is the *neighborhood* of x, the cardinality of V_x is the *degree* of x denoted by $d(x)$. To help this calculation, we assume that the distance between x and x' is greater than 1. So, the walker will depart from x and will move to the neighboring vertex x'' with probability $1/d(x)$ spending one time unit. Now, we must add this result to the expected time to move from x'' to x'. This has to be performed for all vertices x'' in the neighborhood of x. We obtain

$$H_{x\,x'} = \frac{1}{d(x)} \sum_{x'' \in V_x} \left(1 + H_{x''\,x'}\right). \tag{C.6}$$

Equation (C.5) is a special case of (C.6), because for the complete graph $d(x) = n-1$ and $H_{x''\,x'} = H_{x\,x'}$ unless $x'' = x'$. The case $x'' = x'$ generates the first term in (C.5). The remaining $n-2$ cases generate the second term. This shows that (C.6) is general and the distance between x and x' need not be greater than 1. However, we cannot take $x = x'$ (distance 0) since the left-hand side is zero and the right-hand side is not.

The goal now is to solve (C.6) in terms of the hitting time $H_{x\,x'}$. This task is facilitated if (C.6) is converted to the matrix form. If H is a square n-dimensional matrix with entries $H_{x\,x'}$, the left-hand side will be converted into H and the right-hand side must be expanded. Using that

$$p_{x\,x'} = \begin{cases} \frac{1}{d(x)}, & \text{if } x' \text{ is adjacent to } x; \\ 0, & \text{otherwise,} \end{cases} \tag{C.7}$$

we obtain the following matrix equation:

$$H = J + PH + D, \tag{C.8}$$

where J is a matrix with all entries equal to 1, P is the *right stochastic matrix*, and D is a diagonal matrix that should be introduced to validate the matrix equation for the diagonal elements. P is also called *transition matrix* or *probability matrix*, as we have discussed in Chap. 3.

The diagonal matrix D can be calculated using the *stationary distribution* π, which is the distribution that satisfies equation $\pi^T \cdot P = \pi^T$. It is also called *limiting* or *equilibrium distribution*. For connected, nondirected, and non-bipartite graphs $\Gamma(X, E)$, there is always a limiting distribution. By left multiplying (C.8) by π^T, we obtain

$$D_{xx} = -\frac{1}{\pi_x},$$

where π_x is the xth entry of π.

Equation (C.8) can be written as $(I - P)H = J + D$. When we try to find H using this equation, we deal with the fact that $(I - P)$ is a noninvertible matrix, because $\mathbf{1}$ is a 0-eigenvector of $(I - P)$, where $\mathbf{1}$ is the vector with all entries equal to 1. This means that equation $(I - P)X = J + D$ has more than one solution X. In fact, if matrix X is a solution, then $X + \mathbf{1} \cdot v^T$ is also a solution for any vector v. However, having at hand a solution X of this equation does not guarantee that we have found H. There is a way to verify whether X is a correct solution by using that H_{xx} must be zero for all x. A solution of equation $(I - P)X = J + D$ is

$$X = \left(I - P + \mathbf{1} \cdot \pi^T\right)^{-1} (J + D), \tag{C.9}$$

as can be checked by solving Exercise C.3. Now we add a term of type $\mathbf{1} \cdot v^T$ to cancel out the diagonal entries of X, and we obtain

$$H = X - \mathbf{1} \cdot v^T, \tag{C.10}$$

where the entries of vector v are the diagonal entries of X, that is, $v_x = X_{xx}$.

Exercise C.3. Let

$$M = I - P + \mathbf{1} \cdot \pi^T.$$

1. Show that M is invertible.
2. Using equations $\pi^T \cdot P = \pi^T$, $P \cdot \mathbf{1} = \mathbf{1}$, and

$$M^{-1} = \sum_{t=0}^{\infty} (I - M)^t,$$

   show that

$$M^{-1} = \mathbf{1} \cdot \pi^T + \sum_{t=0}^{\infty} \left(P^t - \mathbf{1} \cdot \pi^T\right).$$

3. Show that solution (C.9) satisfies equation $(I - P)X = J + D$.
4. Show that matrix H given by (C.10) satisfies $H_{xx} = 0$.

Exercise C.4. Find the stochastic matrix of the complete graph with n vertices. Using the fact that the stationary distribution is uniform in this graph, find matrix X using (C.9) and then find matrix H using (C.10). Check the results with (C.2).

C.2 Hitting Time Without the Stationary Distribution

There is an alternative method for calculating the hitting time that does not use the stationary distribution. We describe the method using $H_{\sigma M}$ as defined in (C.4). The vertices in M are called *marked vertices*. Consider the *symmetric digraph* whose underlying graph is $\Gamma(X, E)$. Now we define a *modified digraph*, which is obtained from the symmetric digraph by converting all *arcs* leaving the marked vertices into *loops*, while maintaining unchanged the incoming ones. This means that if the walker reaches a marked vertex, the walker will stay there forever. To calculate the hitting time, the original undirected graph and the modified digraph are equivalent. However, the stochastic matrices are different. Let us denote the stochastic matrix of the modified graph by P', whose entries are

$$p'_{xy} = \begin{cases} p_{xy}, & x \notin M; \\ \delta_{xy}, & x \in M. \end{cases} \tag{C.11}$$

What is the probability of finding the walker in $X \backslash M$ at time t before visiting M? Let $\sigma^{(0)}$ be the initial probability distribution on the vertices of the original graph viewed as a row vector. Then, the distribution after t steps is

$$\sigma^{(t)} = \sigma^{(0)} \cdot P^t. \tag{C.12}$$

Let $\mathbf{1}$ be the column n-vector with all entries equal to 1. Define $\mathbf{1}_{X \backslash M}$ as the column n-vector with $n - m$ entries equal to 1 corresponding to the vertices that are in $X \backslash M$ and m entries equal to zero corresponding to the vertices are in M. The probability of finding the walker in $X \backslash M$ at time t is $\sigma^{(t)} \cdot \mathbf{1}_{X \backslash M}$. However, this expression is not useful for calculating the hitting time, because the walker has already visited M. We want to find the probability of the walker being in $X \backslash M$ at time t having not visited M. This result is obtained if we use matrix P' instead of P in (C.12). In fact, if the evolution is driven by matrix P' and the walker has visited M, it remains imprisoned in M forever. Therefore, if the walker is found in $X \backslash M$, it has certainly not visited M. The probability of finding the walker in $X \backslash M$ at time t without having visited M is $\sigma^{(0)} \cdot (P')^t \cdot \mathbf{1}_{X \backslash M}$.

In (C.3), we have calculated the average time to reach a marked vertex for the first time employing the usual formula for calculating weighted averages. When the variable t assumes nonnegative integer values, there is an alternative formula for calculating this average. This formula applies to this context because time t is the number of steps. Let T be the number of steps to reach a marked vertex for the first time, and let $p(T \geq t)$ be the probability of reaching M for the first time for any number of steps T equal to or greater than t. If the initial condition is distribution σ, the hitting time can be equivalently defined by formula

$$H_{\sigma M} = \sum_{t=1}^{\infty} p(T \geq t). \tag{C.13}$$

To verify the equivalence of this new formula with the previous one, note that

$$p(T \geq t) = \sum_{j=t}^{\infty} p(T = j), \tag{C.14}$$

where $p(T = t)$ is the probability of reaching M for the first time with exactly t steps. Using (C.14) and (C.13), we obtain

$$\begin{aligned} H_{\sigma\, M} &= \sum_{j=1}^{\infty} \sum_{t=1}^{j} p(T = j) \\ &= \sum_{j=1}^{\infty} j\, p(T = j). \end{aligned} \tag{C.15}$$

This last equation is equivalent to (C.3).

We can give another interpretation for probability $p(T \geq t)$. If the walker reaches M at $T \geq t$, then in the first $t - 1$ steps it will still be in $X \backslash M$, that is, it will be on one of the unmarked vertices without having visited M. We have learned in a previous paragraph that the probability of the walker being in $X \backslash M$ at time t without having visited M is $\sigma^{(0)} \cdot (P')^{t-1} \cdot \mathbf{1}_{X \backslash M}$. Then,

$$p(T \geq t) = \sigma^{(0)} \cdot (P')^{t-1} \cdot \mathbf{1}_{X \backslash M}. \tag{C.16}$$

Define $P_{\overline{M}}$ as a square $(n - m)$-matrix obtained from P by deleting the rows and columns corresponding to vertices of M. Define $\sigma_{\overline{M}}$ and $\mathbf{1}_{\overline{M}}$ using the same procedure. Analyzing the entries that do not vanish after multiplying the matrices on the right-hand side of (C.16), we conclude that

$$p(T \geq t) = \sigma_{\overline{M}}^{(0)} \cdot P_{\overline{M}}^{t-1} \cdot \mathbf{1}_{\overline{M}}. \tag{C.17}$$

Using the above equation and (C.13), we obtain

$$\begin{aligned} H_{\sigma\, M} &= \sigma_{\overline{M}}^{(0)} \cdot \left(\sum_{t=0}^{\infty} P_{\overline{M}}^{t} \right) \cdot \mathbf{1}_{\overline{M}} \\ &= \sigma_{\overline{M}}^{(0)} \cdot \left(I - P_{\overline{M}} \right)^{-1} \cdot \mathbf{1}_{\overline{M}}. \end{aligned} \tag{C.18}$$

Matrix $(I - P_{\overline{M}})$ is always invertible for connected, nondirected, and non-bipartite graphs. This result follows from the fact that $\mathbf{1}$ is not an eigenvector of $P_{\overline{M}}$, and hence $(I - P_{\overline{M}})$ has no eigenvalue equal to 0.

The strategy used to obtain (C.18) is used to define the *quantum hitting time* in *Szegedy's model*.

Exercise C.5. Use (C.18) to find the hitting time of a random walk on the complete graph with n vertices, and compare the results with Exercises C.1 and C.2.

Further Reading

The classical hitting time is described in many references, for instance, [11, 215, 235, 245]. The last chapter of [235] describes in detail the *Perron–Frobenius theorem*, which is important in the context of this appendix.

References

1. Aaronson, S., Ambainis, A.: Quantum search of spatial regions. In: Theory of Computing, pp. 200–209 (2003)
2. Aaronson, S., Shi, Y.: Quantum lower bounds for the collision and the element distinctness problems. J. ACM **51**(4), 595–605 (2004)
3. Abal, G., Donangelo, R., Forets, M., Portugal, R.: Spatial quantum search in a triangular network. Math. Struct. Comput. Sci. **22**(03), 521–531 (2012)
4. Abal, G., Donangelo, R., Marquezino, F.L., Portugal, R.: Spatial search on a honeycomb network. Math. Struct. Comput. Sci. **20**(6), 999–1009 (2010)
5. Abreu, A., Cunha, L., Fernandes, T., de Figueiredo, C., Kowada, L., Marquezino, F., Posner, D., Portugal, R.: The graph tessellation cover number: extremal bounds, efficient algorithms and hardness. In: Bender, M.A., Farach-Colton, M., Mosteiro, M.A. (eds.) LATIN 2018. Lecture Notes in Computer Science, vol. 10807, pp. 1–13. Springer, Berlin (2018)
6. Agliari, E., Blumen, A., Mülken, O.: Quantum-walk approach to searching on fractal structures. Phys. Rev. A **82**, 012305 (2010)
7. Aharonov, D.: Quantum computation - a review. In: Stauffer, D. (ed.) Annual Review of Computational Physics, vol. VI, pp. 1–77. World Scientific, Singapore (1998)
8. Aharonov, D., Ambainis, A., Kempe, J., Vazirani, U.: Quantum walks on graphs. In: Proceedings of the 33th STOC, pp. 50–59. ACM, New York (2001)
9. Aharonov, Y., Davidovich, L., Zagury, N.: Quantum random walks. Phys. Rev. A **48**(2), 1687–1690 (1993)
10. Alberti, A., Alt, W., Werner, R., Meschede, D.: Decoherence models for discrete-time quantum walks and their application to neutral atom experiments. New J. Phys. **16**(12), 123052 (2014)
11. Aldous, D., Fill, J.A.: Reversible Markov chains and random walks on graphs (2002). http://www.stat.berkeley.edu/~aldous/RWG/book.html
12. Alvir, R., Dever, S., Lovitz, B., Myer, J., Tamon, C., Xu, Y., Zhan, H.: Perfect state transfer in laplacian quantum walk. J. Algebr. Comb. **43**(4), 801–826 (2016)
13. Ambainis, A.: Quantum walks and their algorithmic applications. Int. J. Quantum Inf. **01**(04), 507–518 (2003)
14. Ambainis, A.: Quantum walk algorithm for element distinctness. In: Proceedings 45th Annual IEEE Symposium on Foundations of Computer Science FOCS, pp. 22–31. Washington (2004)
15. Ambainis, A.: Polynomial degree and lower bounds in quantum complexity: collision and element distinctness with small range. Theory Comput. **1**, 37–46 (2005)
16. Ambainis, A.: Quantum walk algorithm for element distinctness. SIAM J. Comput. **37**(1), 210–239 (2007)

© Springer Nature Switzerland AG 2018

R. Portugal, *Quantum Walks and Search Algorithms*, Quantum Science and Technology, https://doi.org/10.1007/978-3-319-97813-0

17. Ambainis, A., Bach, E., Nayak, A., Vishwanath, A., Watrous, J.: One-dimensional quantum walks. In: Proceedings of the 33th STOC, pp. 60–69. ACM, New York (2001)
18. Ambainis, A., Bačkurs, A., Nahimovs, N., Ozols, R., Rivosh, A.: Search by quantum walks on two-dimensional grid without amplitude amplification. In: Proceedings of the 7th TQC, Tokyo, Japan, pp. 87–97. Springer, Berlin (2013)
19. Ambainis, A., Kempe, J., Rivosh, A.: Coins make quantum walks faster. In: Proceedings of the 16th Annual ACM-SIAM Symposium on Discrete Algorithms SODA, pp. 1099–1108 (2005)
20. Ambainis, A., Portugal, R., Nahimov, N.: Spatial search on grids with minimum memory. Quantum Inf. Comput. **15**, 1233–1247 (2015)
21. Ampadu, C.: Return probability of the open quantum random walk with time-dependence. Commun. Theor. Phys. **59**(5), 563 (2013)
22. Anderson, P.W.: Absence of diffusion in certain random lattices. Phys. Rev. **109**, 1492–1505 (1958)
23. Angeles-Canul, R.J., Norton, R.M., Opperman, M.C., Paribello, C.C., Russell, M.C., Tamon, C.: Quantum perfect state transfer on weighted join graphs. Int. J. Quantum Inf. **7**(8), 1429–1445 (2009)
24. Apostol, T.M.: Calculus, Volume 1: One-Variable Calculus with an Introduction to Linear Algebra. Wiley, New York (1967)
25. Arunachalam, S., De Wolf, R.: Optimizing the number of gates in quantum search. Quantum Inf. Comput. **17**(3–4), 251–261 (2017)
26. Asbóth, J.K.: Symmetries, topological phases, and bound states in the one-dimensional quantum walk. Phys. Rev. B **86**, 195414 (2012)
27. Asbóth, J.K., Edge, J.M.: Edge-state-enhanced transport in a two-dimensional quantum walk. Phys. Rev. A **91**, 022324 (2015)
28. Axler, S.: Linear Algebra Done Right. Springer, New York (1997)
29. Balu, R., Liu, C., Venegas-Andraca, S.E.: Probability distributions for Markov chain based quantum walks. J. Phys. A: Math. Theor. **51**(3), 035301 (2018)
30. Barnett, S.: Quantum Information. Oxford University Press, New York (2009)
31. Barr, K., Fleming, T., Kendon, V.: Simulation methods for quantum walks on graphs applied to formal language recognition. Nat. Comput. **14**(1), 145–156 (2015)
32. Barr, K.E., Proctor, T.J., Allen, D., Kendon, V.M.: Periodicity and perfect state transfer in quantum walks on variants of cycles. Quantum Inf. Comput. **14**(5–6), 417–438 (2014)
33. Bašić, M.: Characterization of quantum circulant networks having perfect state transfer. Quantum Inf. Process. **12**(1), 345–364 (2013)
34. Beame, P., Saks, M., Sun, X., Vee, E.: Time-space trade-off lower bounds for randomized computation of decision problems. J. ACM **50**(2), 154–195 (2003)
35. Bednarska, M., Grudka, A., Kurzynski, P., Luczak, T., Wójcik, A.: Quantum walks on cycles. Phys. Lett. A **317**(1–2), 21–25 (2003)
36. Bednarska, M., Grudka, A., Kurzynski, P., Luczak, T., Wójcik, A.: Examples of non-uniform limiting distributions for the quantum walk on even cycles. Int. J. Quantum Inf. **2**(4), 453–459 (2004)
37. Belovs, A.: Learning-graph-based quantum algorithm for k-distinctness. In: IEEE 53rd Annual Symposium on Foundations of Computer Science, pp. 207–216 (2012)
38. Belovs, A., Childs, A.M., Jeffery, S., Kothari, R., Magniez, F.: Time-efficient quantum walks for 3-distinctness. In: Proceedings of the 40th International Colloquium ICALP, Riga, Latvia, 2013, pp. 105–122. Springer, Berlin (2013)
39. Benedetti, C., Buscemi, F., Bordone, P., Paris, M.G.A.: Non-Markovian continuous-time quantum walks on lattices with dynamical noise. Phys. Rev. A **93**, 042313 (2016)
40. Benenti, G., Casati, G., Strini, G.: Principles of Quantum Computation And Information: Basic Tools And Special Topics. World Scientific Publishing, River Edge (2007)
41. Benioff, P.: Space Searches with a Quantum Robot. AMS Contemporary Mathematics Series, vol. 305. American Mathematical Society, Providence (2002)

42. Bennett, C.H., Bernstein, E., Brassard, G., Vazirani, U.V.: Strengths and weaknesses of quantum computing. SIAM J. Comput. **26**(5), 1510–1523 (1997)
43. Bergou, J.A., Hillery, M.: Introduction to the Theory of Quantum Information Processing. Springer, New York (2013)
44. Bernard, P.-A., Chan, A., Loranger, É., Tamon, C., Vinet, L.: A graph with fractional revival. Phys. Lett. A **382**(5), 259–264 (2018)
45. Bernasconi, A., Godsil, C., Severini, S.: Quantum networks on cubelike graphs. Phys. Rev. A **78**, 052320 (2008)
46. Berry, S.D., Bourke, P., Wang, J.B.: QwViz: visualisation of quantum walks on graphs. Comput. Phys. Commun. **182**(10), 2295–2302 (2011)
47. Bhattacharya, N., van Linden van den Heuvell, H.B., Spreeuw, R.J.C., : Implementation of quantum search algorithm using classical Fourier optics. Phys. Rev. Lett. **88**, 137901 (2002)
48. Bian, Z.-H., Li, J., Zhan, X., Twamley, J., Xue, P.: Experimental implementation of a quantum walk on a circle with single photons. Phys. Rev. A **95**, 052338 (2017)
49. Biham, O., Nielsen, M.A., Osborne, T.J.: Entanglement monotone derived from Grover's algorithm. Phys. Rev. A **65**, 062312 (2002)
50. Boada, O., Novo, L., Sciarrino, F., Omar, Y.: Quantum walks in synthetic gauge fields with three-dimensional integrated photonics. Phys. Rev. A **95**, 013830 (2017)
51. Boettcher, S., Falkner, S., Portugal, R.: Renormalization group for quantum walks. J. Phys. Conf. Ser. **473**(1), 012018 (2013)
52. Boettcher, S., Li, S.: Analysis of coined quantum walks with renormalization. Phys. Rev. A **97**, 012309 (2018)
53. Bondy, A., Murty, U.S.R.: Graph Theory. Graduate Texts in Mathematics. Springer, London (2011)
54. Bose, S.: Quantum communication through an unmodulated spin chain. Phys. Rev. Lett. **91**, 207901 (2003)
55. Botsinis, P., Babar, Z., Alanis, D., Chandra, D., Nguyen, H., Ng, S.X., Hanzo, L.: Quantum error correction protects quantum search algorithms against decoherence. Sci. Rep. **6**, 38095 (2016)
56. Bougroura, H., Aissaoui, H., Chancellor, N., Kendon, V.: Quantum-walk transport properties on graphene structures. Phys. Rev. A **94**, 062331 (2016)
57. Boyer, M., Brassard, G., Høyer, P., Tapp, A.: Tight bounds on quantum searching. Forstschritte Der Physik **4**, 820–831 (1998)
58. Brandstädt, A., Le, V.B., Spinrad, J.P.: Graph Classes: A Survey. SIAM, Philadelphia (1999)
59. Brassard, G., Høyer, P., Mosca, M., Tapp, A.: Quantum amplitude amplification and estimation. Quantum Computation and Quantum Information Science. AMS Contemporary Mathematics Series, vol. 305, pp. 53–74. American Mathematical Society, Providence (2002)
60. Brassard, G., Høyer, P., Tapp, A.: Quantum cryptanalysis of hash and claw-free functions. In: Proceedings of the 3rd Latin American Symposium LATIN'98, pp. 163–169. Springer, Berlin (1998)
61. Breuer, H.P., Petruccione, F.: The Theory of Open Quantum Systems. Oxford University Press, Oxford (2002)
62. Bru, L.A., de Valcárcel, G.J., di Molfetta, G., Pérez, A., Roldán, E., Silva, F.: Quantum walk on a cylinder. Phys. Rev. A **94**, 032328 (2016)
63. Bruderer, M., Plenio, M.B.: Decoherence-enhanced performance of quantum walks applied to graph isomorphism testing. Phys. Rev. A **94**, 062317 (2016)
64. Buhrman, H., Dürr, C., Heiligman, M., Høyer, P., Magniez, F., Santha, M., de Wolf, R.: Quantum algorithms for element distinctness. SIAM J. Comput. **34**(6), 1324–1330 (2005)
65. Byrnes, T., Forster, G., Tessler, L.: Generalized Grover's algorithm for multiple phase inversion states. Phys. Rev. Lett. **120**, 060501 (2018)
66. Cáceres, M.O.: On the quantum CTRW approach. Eur. Phys. J. B **90**(4), 74 (2017)
67. Cameron, S., Fehrenbach, S., Granger, L., Hennigh, O., Shrestha, S., Tamon, C.: Universal state transfer on graphs. Linear Algebra Appl. **455**, 115–142 (2014)

68. Carteret, H.A., Ismail, M.E.H., Richmond, B.: Three routes to the exact asymptotics for the one-dimensional quantum walk. J. Phys. A: Math. Gen. **36**(33), 8775–8795 (2003)
69. Carvalho, S.L., Guidi, L.F., Lardizabal, C.F.: Site recurrence of open and unitary quantum walks on the line. Quantum Inf. Process. **16**(1), 17 (2016)
70. Cedzich, C., Geib, T., Grünbaum, F.A., Stahl, C., Velázquez, L., Werner, A.H., Werner, R.F.: The topological classification of one-dimensional symmetric quantum walks. Ann. Henri Poincaré **19**(2), 325–383 (2018)
71. Chakraborty, K., Maitra, S.: Application of Grover's algorithm to check non-resiliency of a boolean function. Cryptogr. Commun. **8**(3), 401–413 (2016)
72. Chakraborty, S., Novo, L., Di Giorgio, S., Omar, Y.: Optimal quantum spatial search on random temporal networks. Phys. Rev. Lett. **119**, 220503 (2017)
73. Chan, A., Coutinho, G., Tamon, C., Vinet, L., Zhan, H.: Quantum fractional revival on graphs (2018). arXiv:1801.09654
74. Chandrashekar, C.M., Busch, T.: Quantum percolation and transition point of a directed discrete-time quantum walk. Sci. Rep. **4**, 6583 (2014)
75. Chartrand, G., Lesniak, L., Zhang, P.: Graphs & Digraphs. Chapman & Hall/CRC, Boca Raton (2010)
76. Chiang, C.-F., Gomez, G.: Hitting time of quantum walks with perturbation. Quantum Inf. Process. **12**(1), 217–228 (2013)
77. Chiang, C.-F., Nagaj, D., Wocjan, P.: Efficient circuits for quantum walks. Quantum Inf. Comput. **10**(5–6), 420–434 (2010)
78. Childs, A.M.: Universal computation by quantum walk. Phys. Rev. Lett. **102**, 180501 (2009)
79. Childs, A.M.: On the relationship between continuous- and discrete-time quantum walk. Commun. Math. Phys. **294**(2), 581–603 (2010)
80. Childs, A.M., Eisenberg, J.M.: Quantum algorithms for subset finding. Quantum Inf. Comput. **5**(7), 593–604 (2005)
81. Childs, A.M., Farhi, E., Gutmann, S.: An example of the difference between quantum and classical random walks. Quantum Inf. Process. **1**(1), 35–43 (2002)
82. Childs, A.M., Goldstone, J.: Spatial search and the Dirac equation. Phys. Rev. A **70**, 042312 (2004)
83. Christandl, M., Datta, N., Ekert, A., Landahl, A.J.: Perfect state transfer in quantum spin networks. Phys. Rev. Lett. **92**, 187902 (2004)
84. Cohen-Tannoudji, C., Diu, B., Laloe, F.: Quantum Mechanics. Wiley-Interscience, New York (2006)
85. Connelly, E., Grammel, N., Kraut, M., Serazo, L., Tamon, C.: Universality in perfect state transfer. Linear Algebra Appl. **531**, 516–532 (2017)
86. Coutinho, G.: Quantum walks and the size of the graph. Discret. Math. (2018). arXiv:1802.08734
87. Coutinho, G., Godsil, C.: Perfect state transfer in products and covers of graphs. Linear Multilinear Algebra **64**(2), 235–246 (2016)
88. Coutinho, G., Godsil, C.: Perfect state transfer is poly-time. Quantum Inf. Comput. **17**(5–6), 495–502 (2017)
89. Coutinho, G., Portugal, R.: Discretization of continuous-time quantum walks via the staggered model with Hamiltonians. Nat. Comput. (2018). arXiv:1701.03423
90. Cover, T.M., Thomas, J.: Elements of Information Theory. Wiley, New York (1991)
91. Crespi, A., Osellame, R., Ramponi, R., Giovannetti, V., Fazio, R., Sansoni, L., De Nicola, F., Sciarrino, F., Mataloni, P.: Anderson localization of entangled photons in an integrated quantum walk. Nat. Photonics **7**(4), 322–328 (2013)
92. D'Ariano, G.M., Erba, M., Perinotti, P., Tosini, A.: Virtually abelian quantum walks. J. Phys. A: Math. Theor. **50**(3), 035301 (2017)
93. de Abreu, A.S.: Tesselações em grafos e suas aplicações em computação quântica. Master's thesis, UFRJ (2017)
94. de Abreu, A.S., Ferreira, M.M., Kowada, L.A.B., Marquezino, F.L.: QEDS: A classical simulator for quantum element distinctness. Revista de Informática Teórica e Aplicada **23**(2), 51–66 (2016)

95. Derevyanko, S.: Anderson localization of a one-dimensional quantum walker. Sci. Rep. **8**(1), 1795 (2018)
96. d'Espagnat, B.: Conceptual Foundations of Quantum Mechanics. Westview Press, Boulder (1999)
97. Desurvire, E.: Classical and Quantum Information Theory: An Introduction for the Telecom Scientist. Cambridge University Press, Cambridge (2009)
98. Dheeraj, M.N., Brun, T.A.: Continuous limit of discrete quantum walks. Phys. Rev. A **91**, 062304 (2015)
99. di Molfetta, G., Debbasch, F.: Discrete-time quantum walks: continuous limit and symmetries. J. Math. Phys. **53**(12), 123302 (2012)
100. Diao, Z., Zubairy, M.S., Chen, G.: A quantum circuit design for Grover's algorithm. Z. Naturforsch. A **57**(8), 701–708 (2002)
101. Díaz, N., Donangelo, R., Portugal, R., Romanelli, A.: Transient temperature and mixing times of quantum walks on cycles. Phys. Rev. A **94**, 012305 (2016)
102. Diestel, R.: Graph Theory. Graduate Texts in Mathematics, vol. 173. Springer, New York (2012)
103. Dodd, J.L., Ralph, T.C., Milburn, G.J.: Experimental requirements for Grover's algorithm in optical quantum computation. Phys. Rev. A **68**, 042328 (2003)
104. Domino, K., Glos, A., Ostaszewski, M.: Superdiffusive quantum stochastic walk definable on arbitrary directed graph. Quantum Info. Comput. **17**(11–12), 973–986 (2017)
105. Du, Y.-M., Lu, L.-H., Li, Y.-Q.: A rout to protect quantum gates constructed via quantum walks from noises. Sci. Rep. **8**(1), 7117 (2018)
106. Dukes, P.R.: Quantum state revivals in quantum walks on cycles. Results Phys. **4**, 189–197 (2014)
107. Dunjko, V., Briegel, H.J.: Quantum mixing of Markov chains for special distributions. New J. Phys. **17**(7), 073004 (2015)
108. Ellinas, D., Konstandakis, C.: Parametric quantum search algorithm as quantum walk: a quantum simulation. Rep. Math. Phys. **77**(1), 105–128 (2016)
109. Endo, T., Konno, N., Obuse, H., Segawa, E.: Sensitivity of quantum walks to a boundary of two-dimensional lattices: approaches based on the CGMV method and topological phases. J. Phys. A: Math. Theor. **50**(45), 455302 (2017)
110. Ermakov, V.L., Fung, B.M.: Experimental realization of a continuous version of the Grover algorithm. Phys. Rev. A **66**, 042310 (2002)
111. Falk, M.: Quantum search on the spatial grid (2013). arXiv:1303.4127
112. Falloon, P.E., Rodriguez, J., Wang, J.B.: QSWalk: a mathematica package for quantum stochastic walks on arbitrary graphs. Comput. Phys. Commun. **217**, 162–170 (2017)
113. Farhi, E., Gutmann, S.: Quantum computation and decision trees. Phys. Rev. A **58**, 915–928 (1998)
114. Feller, W.: An Introduction to Probability Theory and Its Applications. Wiley, New York (1968)
115. Foulger, I., Gnutzmann, S., Tanner, G.: Quantum walks and quantum search on graphene lattices. Phys. Rev. A **91**, 062323 (2015)
116. Fujiwara, S., Hasegawa, S.: General method for realizing the conditional phase-shift gate and a simulation of Grover's algorithm in an ion-trap system. Phys. Rev. A **71**, 012337 (2005)
117. Galiceanu, M., Strunz, W.T.: Continuous-time quantum walks on multilayer dendrimer networks. Phys. Rev. E **94**, 022307 (2016)
118. Mc Gettrick, M., Miszczak, J.A.: Quantum walks with memory on cycles. Phys. A **399**, 163–170 (2014)
119. Ghosh, J.: Simulating Anderson localization via a quantum walk on a one-dimensional lattice of superconducting qubits. Phys. Rev. A **89**, 022309 (2014)
120. Glos, A., Miszczak, J.A., Ostaszewski, M.: QSWalk.jl: Julia package for quantum stochastic walks analysis (2018). arXiv:1801.01294
121. Godsil, C., Royle, G.F.: Algebraic Graph Theory. Graduate Texts in Mathematics, vol. 207. Springer, New York (2001)

122. Gönülol, M., Aydner, E., Shikano, Y., Müstecaplolu, Ö.E.: Survival probability in a quantum walk on a one-dimensional lattice with partially absorbing traps. J. Comput. Theor. Nanosci. **10**(7), 1596–1600 (2013)
123. Gould, H.W.: Combinatorial Identities. Morgantown Printing and Binding Co., Morgantown (1972)
124. Goyal, S.K., Konrad, T., Diósi, L.: Unitary equivalence of quantum walks. Phys. Lett. A **379**(3), 100–104 (2015)
125. Graham, R.L., Knuth, D.E., Patashnik, O.: Concrete Mathematics: A Foundation for Computer Science. Addison-Wesley, Reading (1994)
126. Griffiths, D.: Introduction to Quantum Mechanics. Benjamin Cummings, Menlo Park (2005)
127. Grigoriev, D.: Karpinski, M., auf der Heide, F.M., Smolensky, R.: A lower bound for randomized algebraic decision trees. Comput. Complex. **6**(4), 357–375 (1996)
128. Grover, L.K.: A fast quantum mechanical algorithm for database search. In: Proceedings of the 28th Annual ACM Symposium on Theory of Computing, STOC '96, pp. 212–219. New York (1996)
129. Grover, L.K.: Quantum computers can search arbitrarily large databases by a single query. Phys. Rev. Lett. **79**(23), 4709–4712 (1997)
130. Grover, L.K.: Quantum mechanics helps in searching for a needle in a haystack. Phys. Rev. Lett. **79**(2), 325–328 (1997)
131. Grover, L.K.: Quantum computers can search rapidly by using almost any transformation. Phys. Rev. Lett. **80**(19), 4329–4332 (1998)
132. Grover, L.K.: Trade-offs in the quantum search algorithm. Phys. Rev. A **66**, 052314 (2002)
133. Gudder, S.: Quantum Probability. Academic Press, San Diego (1988)
134. Lo Gullo, N., Ambarish, C.V., Busch, T., Dell'Anna, L., Chandrashekar, C.M., Chandrashekar, C.M.: Dynamics and energy spectra of aperiodic discrete-time quantum walks. Phys. Rev. E **96**, 012111 (2017)
135. Hamada, M., Konno, N., Segawa, E.: Relation between coined quantum walks and quantum cellular automata. RIMS Kokyuroku **1422**, 1–11 (2005)
136. Hamilton, C.S., Barkhofen, S., Sansoni, L., Jex, I., Silberhorn, C.: Driven discrete time quantum walks. New J. Phys. **18**(7), 073008 (2016)
137. Hao, L., Li, J., Long, G.: Eavesdropping in a quantum secret sharing protocol based on Grover algorithm and its solution. Sci. China Phys. Mech. Astron. **53**(3), 491–495 (2010)
138. Harary, F.: Graph Theory. Addison-Wesley, Boston (1969)
139. Hartsfield, N., Ringel, G.: Pearls in Graph Theory: A Comprehensive Introduction. Dover Books on Mathematics. Dover Publications, New York (1994)
140. Hayashi, M., Ishizaka, S., Kawachi, A., Kimura, G., Ogawa, T.: Introduction to Quantum Information Science. Springer, Berlin (2014)
141. He, Z., Huang, Z., Li, L., Situ, H.: Coherence of one-dimensional quantum walk on cycles. Quantum Inf. Process. **16**(11), 271 (2017)
142. He, Z., Huang, Z., Li, L., Situ, H.: Coherence evolution in two-dimensional quantum walk on lattice. Int. J. Quantum Inf. **16**(02), 1850011 (2018)
143. He, Z., Huang, Z., Situ, H.: Dynamics of quantum coherence in two-dimensional quantum walk on finite lattices. Eur. Phys. J. Plus **132**(7), 299 (2017)
144. Hein, B., Tanner, G.: Quantum search algorithms on a regular lattice. Phys. Rev. A **82**(1), 012326 (2010)
145. Higuchi, Y., Konno, N., Sato, I., Segawa, E.: Spectral and asymptotic properties of Grover walks on crystal lattices. J. Funct. Anal. **267**(11), 4197–4235 (2014)
146. Hirvensalo, M.: Quantum Computing. Springer, Berlin (2010)
147. Ho, C.-L., Ide, Y., Konno, N., Segawa, E., Takumi, K.: A spectral analysis of discrete-time quantum walks related to the birth and death chains. J. Stat. Phys. **171**(2), 207–219 (2018)
148. Hoffman, K.M., Kunze, R.: Linear Algebra. Prentice Hall, New York (1971)
149. Holweck, F., Jaffali, H., Nounouh, I.: Grover's algorithm and the secant varieties. Quantum Inf. Process. **15**(11), 4391–4413 (2016)
150. Horn, R., Johnson, C.R.: Matrix Analysis. Cambridge University Press, Cambridge (1985)

151. Høyer, P.: Arbitrary phases in quantum amplitude amplification. Phys. Rev. A **62**, 052304 (2000)
152. Høyer, P., Komeili, M.: Efficient quantum walk on the grid with multiple marked elements. In: Vollmer, H., Vallée, B. (eds.) Proceedings of the 34th Symposium on Theoretical Aspects of Computer Science STACS, vol. 66, pp. 42:1–14. Dagstuhl, Germany (2017)
153. Hsu, L.-Y.: Quantum secret-sharing protocol based on Grover's algorithm. Phys. Rev. A **68**, 022306 (2003)
154. Hughes, B.D.: Random Walks and Random Environments: Voloum 1 Random Walks. Oxford University Press, Oxford (1995)
155. Hughes, B.D.: Random Walks and Random Environments: Volume 2 Random Environments. Oxford University Press, Oxford (1996)
156. Hush, M.R., Bentley, C.D.B., Ahlefeldt, R.L., James, M.R., Sellars, M.J., Ugrinovskii, V.: Quantum state transfer through time reversal of an optical channel. Phys. Rev. A **94**, 062302 (2016)
157. Ide, Y., Konno, N., Segawa, E.: Time averaged distribution of a discrete-time quantum walk on the path. Quantum Inf. Process. **11**(5), 1207–1218 (2012)
158. Innocenti, L., Majury, H., Giordani, T., Spagnolo, N., Sciarrino, F., Paternostro, M., Ferraro, A.: Quantum state engineering using one-dimensional discrete-time quantum walks. Phys. Rev. A **96**, 062326 (2017)
159. Itakura, Y.K.: Quantum algorithm for commutativity testing of a matrix set. Master's thesis, University of Waterloo, Waterloo (2005)
160. Iwai, T., Hayashi, N., Mizobe, K.: The geometry of entanglement and Grover's algorithm. J. Phys. A: Math. Theor. **41**(10), 105202 (2008)
161. Izaac, J.A., Wang, J.B.: PyCTQW: a continuous-time quantum walk simulator on distributed memory computers. Comput. Phys. Commun. **186**, 81–92 (2015)
162. Izaac, J.A., Wang, J.B.: Systematic dimensionality reduction for continuous-time quantum walks of interacting fermions. Phys. Rev. E **96**, 032136 (2017)
163. Izaac, J.A., Zhan, X., Bian, Z., Wang, K., Li, J., Wang, J.B., Xue, P.: Centrality measure based on continuous-time quantum walks and experimental realization. Phys. Rev. A **95**, 032318 (2017)
164. Jeffery, S., Magniez, F., de Wolf, R.: Optimal parallel quantum query algorithms. Algorithmica **79**(2), 509–529 (2017)
165. Jin, W., Chen, X.: A desired state can not be found with certainty for Grover's algorithm in a possible three-dimensional complex subspace. Quantum Inf. Process. **10**(3), 419–429 (2011)
166. Johnston, N., Kirkland, S., Plosker, S., Storey, R., Zhang, X.: Perfect quantum state transfer using Hadamard diagonalizable graphs. Linear Algebra Appl. **531**, 375–398 (2017)
167. Jones, J.A., Mosca, M., Hansen, R.H.: Implementation of a quantum search algorithm on a quantum computer. Nature **393**(6683), 344–346 (1998)
168. Kaplan, M.: Quantum attacks against iterated block ciphers. Mat. Vopr. Kriptogr. **7**, 71–90 (2016)
169. Kargin, V.: Bounds for mixing time of quantum walks on finite graphs. J. Phys. A: Math. Theor. **43**(33), 335302 (2010)
170. Kaye, P., Laflamme, R., Mosca, M.: An Introduction to Quantum Computing. Oxford University Press, New York (2007)
171. Kedon, V.M., Tamon, C.: Perfect state transfer in quantum walks on graphs. J. Comput. Theor. Nanosci. **8**(3), 422–433 (2011)
172. Kempe, J.: Quantum random walks - an introductory overview. Contemp. Phys. **44**(4), 302–327 (2003)
173. Kempe, J.: Discrete quantum walks hit exponentially faster. Probab. Theory Relat. Fields **133**(2), 215–235 (2005). arXiv:quant-ph/0205083
174. Kempton, M., Lippner, G., Yau, S.-T.: Perfect state transfer on graphs with a potential. Quantum Inf. Comput. **17**(3–4), 303–327 (2017)
175. Kendon, V.: Decoherence in quantum walks - a review. Math. Struct. Comput. Sci. **17**(6), 1169–1220 (2007)

176. Kendon, V., Sanders, B.C.: Complementarity and quantum walks. Phys. Rev. A **71**, 022307 (2005)
177. Kirkland, S., Severini, S.: Spin-system dynamics and fault detection in threshold networks. Phys. Rev. A **83**, 012310 (2011)
178. Kitaev, A.Y., Shen, A.H., Vyalyi, M.N.: Classical and Quantum Computation. American Mathematical Society, Boston (2002)
179. Koch, D., Hillery, M.: Finding paths in tree graphs with a quantum walk. Phys. Rev. A **97**, 012308 (2018)
180. Kollár, B., Novotný, J., Kiss, T., Jex, I.: Percolation induced effects in two-dimensional coined quantum walks: analytic asymptotic solutions. New J. Phys. **16**(2), 023002 (2014)
181. Komatsu, T., Konno, N.: Stationary amplitudes of quantum walks on the higher-dimensional integer lattice. Quantum Inf. Process. **16**(12), 291 (2017)
182. Konno, N.: Quantum random walks in one dimension. Quantum Inf. Process. **1**(5), 345–354 (2002)
183. Konno, N.: Quantum walks. In: Franz, U., Schürmann, M. (eds.) Quantum Potential Theory. Lecture Notes in Mathematics, vol. 1954, pp. 309–452. Springer, Berlin (2008)
184. Konno, N., Ide, Y., Sato, I.: The spectral analysis of the unitary matrix of a 2-tessellable staggered quantum walk on a graph. Linear Algebra Appl. **545**, 207–225 (2018)
185. Konno, N., Mitsuhashi, H., Sato, I.: The discrete-time quaternionic quantum walk on a graph. Quantum Inf. Process. **15**(2), 651–673 (2016)
186. Konno, N., Obata, N., Segawa, E.: Localization of the Grover walks on spidernets and free Meixner laws. Commun. Math. Phys. **322**(3), 667–695 (2013)
187. Konno, N., Portugal, R., Sato, I., Segawa, E.: Partition-based discrete-time quantum walks. Quantum Inf. Process. **17**(4), 100 (2018)
188. Konno, N., Sato, I.: On the relation between quantum walks and zeta functions. Quantum Inf. Process. **11**(2), 341–349 (2012)
189. Konno, N., Sato, I., Segawa, E.: The spectra of the unitary matrix of a 2-tessellable staggered quantum walk on a graph. Yokohama Math. J. **62**, 52–87 (2017)
190. Košík, J.: Two models of quantum random walk. Central Eur. J. Phys. **4**, 556–573 (2003)
191. Košík, J., Bužek, V., Hillery, M.: Quantum walks with random phase shifts. Phys. Rev. A **74**, 022310 (2006)
192. Krawec, W.O.: History dependent quantum walk on the cycle with an unbalanced coin. Phys. A **428**, 319–331 (2015)
193. Krovi, H., Brun, T.A.: Quantum walks with infinite hitting times. Phys. Rev. A **74**, 042334 (2006)
194. Krovi, H., Brun, T.A.: Quantum walks on quotient graphs. Phys. Rev. A **75**, 062332 (2007)
195. Krovi, H., Magniez, F., Ozols, M., Roland, J.: Finding is as easy as detecting for quantum walks. Automata, Languages and Programming. Lecture Notes in Computer Science, vol. 6198, pp. 540–551. Springer, Berlin (2010)
196. Kutin, S.: Quantum lower bound for the collision problem with small range. Theory Comput. **1**, 29–36 (2005)
197. Laarhoven, T., Mosca, M., van de Pol, J.: Finding shortest lattice vectors faster using quantum search. Des. Codes Cryptogr. **77**(2), 375–400 (2015)
198. Lam, H.T., Szeto, K.Y.: Ramsauer effect in a one-dimensional quantum walk with multiple defects. Phys. Rev. A **92**, 012323 (2015)
199. Lang, S.: Linear Algebra. Undergraduate Texts in Mathematics and Technology. Springer, New York (1987)
200. Lang, S.: Introduction to Linear Algebra. Undergraduate Texts in Mathematics. Springer, New York (1997)
201. Lara, P.C.S., Leão, A., Portugal, R.: Simulation of quantum walks using HPC. J. Comput. Int. Sci. **6**, 21 (2015)
202. Lehman, L.: Environment-induced mixing processes in quantum walks. Int. J. Quantum Inf. **12**(04), 1450021 (2014)

203. Leuenberger, M.N., Loss, D.: Grover algorithm for large nuclear spins in semiconductors. Phys. Rev. B **68**, 165317 (2003)
204. Li, D., Mc Gettrick, M., Gao, F., Xu, J., Wen, Q.-Y., Wen, Q.-Y.: Generic quantum walks with memory on regular graphs. Phys. Rev. A **93**, 042323 (2016)
205. Li, D., Mc Gettrick, M., Zhang, W.-W., Zhang, K.-J., Zhang, K.-J.: Quantum walks on two kinds of two-dimensional models. Int. J. Theor. Phys. **54**(8), 2771–2783 (2015)
206. Li, P., Li, S.: Phase matching in Grover's algorithm. Phys. Lett. A **366**(1), 42–46 (2007)
207. Li, P., Li, S.: Two improvements in Grover's algorithm. Chin. J. Electron. **17**(1), 100–104 (2008)
208. Lin, J.-Y., Zhu, X., Wu, S.: Limitations of discrete-time quantum walk on a one-dimensional infinite chain. Phys. Lett. A **382**(13), 899–903 (2018)
209. Lipton, R.J., Regan, K.W.: Quantum Algorithms via Linear Algebra: A Primer. MIT Press, Boston (2014)
210. Liu, C., Balu, R.: Steady states of continuous-time open quantum walks. Quantum Inf. Process. **16**(7), 173 (2017)
211. Loke, T., Tang, J.W., Rodriguez, J., Small, M., Wang, J.B.: Comparing classical and quantum pageranks. Quantum Inf. Process. **16**(1), 25 (2016)
212. Loke, T., Wang, J.B.: Efficient quantum circuits for continuous-time quantum walks on composite graphs. J. Phys. A: Math. Theor. **50**(5), 055303 (2017)
213. Loke, T., Wang, J.B.: Efficient quantum circuits for Szegedy quantum walks. Ann. Phys. **382**, 64–84 (2017)
214. Long, G.L.: Grover algorithm with zero theoretical failure rate. Phys. Rev. A **64**, 022307 (2001)
215. Lovász, L.: Random walks on graphs: a survey. Comb. Paul Erdös Eighty **2**, 1–46 (1993)
216. Lovett, N.B., Cooper, S., Everitt, M., Trevers, M., Kendon, V.: Universal quantum computation using the discrete-time quantum walk. Phys. Rev. A **81**, 042330 (2010)
217. Lovett, N.B., Everitt, M., Heath, R.M., Kendon, V.: The quantum walk search algorithm: factors affecting efficiency. Math. Struct. Comput. Sci. **67**, 1–141 (2018)
218. Lu, X., Yuan, J., Zhang, W.: Workflow of the Grover algorithm simulation incorporating CUDA and GPGPU. Comput. Phys. Commun. **184**(9), 2035–2041 (2013)
219. Ma, B.-W., Bao, W.-S., Li, T., Li, F.-G., Zhang, S., Fu, X.-Q.: A four-phase improvement of Grover's algorithm. Chin. Phys. Lett. **34**(7), 070305 (2017)
220. Machida, T., Chandrashekar, C.M.: Localization and limit laws of a three-state alternate quantum walk on a two-dimensional lattice. Phys. Rev. A **92**, 062307 (2015)
221. Machida, T., Chandrashekar, C.M., Konno, N., Busch, T.: Limit distributions for different forms of four-state quantum walks on a two-dimensional lattice. Quantum Inf. Comput. **15**(13–14), 1248–1258 (2015)
222. Mackay, T.D., Bartlett, S.D., Stephenson, L.T., Sanders, B.C.: Quantum walks in higher dimensions. J. Phys. A: Math. Gen. **35**(12), 2745 (2002)
223. Magniez, F., Nayak, A.: Quantum complexity of testing group commutativity. Algorithmica **48**(3), 221–232 (2007)
224. Magniez, F., Nayak, A., Richter, P., Santha, M.: On the hitting times of quantum versus random walks. In: Proceedings of the 20th ACM-SIAM Symposium on Discrete Algorithms (2009)
225. Magniez, F., Nayak, A., Roland, J., Santha, M.: Search via quantum walk. In: Proceedings of the 39th ACM Symposium on Theory of Computing, pp. 575–584 (2007)
226. Magniez, F., Santha, M., Szegedy, M.: Quantum algorithms for the triangle problem. SIAM J. Comput. **37**(2), 413–424 (2007)
227. Makmal, A., Tiersch, M., Ganahl, C., Briegel, H.J.: Quantum walks on embedded hypercubes: nonsymmetric and nonlocal cases. Phys. Rev. A **93**, 022322 (2016)
228. Makmal, A., Zhu, M., Manzano, D., Tiersch, M., Briegel, H.J.: Quantum walks on embedded hypercubes. Phys. Rev. A **90**, 022314 (2014)
229. Manouchehri, K., Wang, J.: Physical Implementation of Quantum Walks. Springer, New York (2014)

230. Marinescu, D.C., Marinescu, G.M.: Approaching Quantum Computing. Pearson/Prentice Hall, Michigan (2005)
231. Marquezino, F.L., Portugal, R.: The qwalk simulator of quantum walks. Comput. Phys. Commun. **179**(5), 359–369 (2008)
232. Marquezino, F.L., Portugal, R., Abal, G.: Mixing times in quantum walks on two-dimensional grids. Phys. Rev. A **82**(4), 042341 (2010)
233. Marquezino, F.L., Portugal, R., Abal, G., Donangelo, R.: Mixing times in quantum walks on the hypercube. Phys. Rev. A **77**, 042312 (2008)
234. Mermin, N.D.: Quantum Computer Science: An Introduction. Cambridge University Press, New York (2007)
235. Meyer, C.D.: Matrix Analysis and Applied Linear Algebra. SIAM, Philadelphia (2001)
236. Meyer, D.A.: From quantum cellular automata to quantum lattice gases. J. Stat. Phys. **85**(5), 551–574 (1996)
237. Meyer, D.A.: Sophisticated quantum search without entanglement. Phys. Rev. Lett. **85**, 2014–2017 (2000)
238. Meyer, D.A., Wong, T.G.: Connectivity is a poor indicator of fast quantum search. Phys. Rev. Lett. **114**, 110503 (2015)
239. Mlodinow, L., Brun, T.A.: Discrete spacetime, quantum walks, and relativistic wave equations. Phys. Rev. A **97**, 042131 (2018)
240. Moore, C., Mertens, S.: The Nature of Computation. Oxford University Press, New York (2011)
241. Moore, C., Russell, A.: Quantum walks on the hypercube. In: Proceedings of the 6th International Workshop on Randomization and Approximation Techniques RANDOM, pp. 164–178. Springer, Berlin (2002)
242. Moqadam, J.K., Portugal, R., de Oliveira, M.C.: Quantum walks on a circle with optomechanical systems. Quantum Inf. Process. **14**(10), 3595–3611 (2015)
243. Khatibi Moqadam, J., de Oliveira, M.C., Portugal, R., Portugal, R.: Staggered quantum walks with superconducting microwave resonators. Phys. Rev. B **95**, 144506 (2017)
244. Mosca, M.: Counting by quantum eigenvalue estimation. Theor. Comput. Sci. **264**(1), 139–153 (2001)
245. Motwani, R., Raghavan, P.: Randomized algorithms. ACM Comput. Surv. **28**(1), 33–37 (1996)
246. Mülken, O., Blumen, A.: Continuous-time quantum walks: models for coherent transport on complex networks. Phys. Rep. **502**(2), 37–87 (2011)
247. Nayak, A., Vishwanath, A.: Quantum walk on a line. DIMACS Technical Report 2000-43 (2000). arXiv:quant-ph/0010117
248. Nielsen, M.A., Chuang, I.L.: Quantum Computation and Quantum Information. Cambridge University Press, New York (2000)
249. Novo, L., Chakraborty, S., Mohseni, M., Neven, H., Omar, Y.: Systematic dimensionality reduction for quantum walks: optimal spatial search and transport on non-regular graphs. Sci. Rep. **5**, 13304 (2015)
250. Ohno, H.: Unitary equivalent classes of one-dimensional quantum walks. Quantum Inf. Process. **15**(9), 3599–3617 (2016)
251. Oliveira, A.C., Portugal, R., Donangelo, R.: Decoherence in two-dimensional quantum walks. Phys. Rev. A **74**, 012312 (2006)
252. Omnès, R.: Understanding Quantum Mechanics. Princeton University Press, Princeton (1999)
253. Pal, H., Bhattacharjya, B.: Perfect state transfer on gcd-graphs. Linear Multilinear Algebra **65**(11), 2245–2256 (2017)
254. Paparo, G.D., Müller, M., Comellas, F., Martin-Delgado, M.A.: Quantum Google in a complex network. Sci. Rep. **3**, 2773 (2013)
255. Parthasarathy, K.R.: The passage from random walk to diffusion in quantum probability. J. Appl. Probab. **25**, 151–166 (1988)
256. Patel, A., Raghunathan, K.S., Rungta, P.: Quantum random walks do not need a coin toss. Phys. Rev. A **71**, 032347 (2005)
257. Peres, A.: Quantum Theory: Concepts and Methods. Springer, Berlin (1995)

258. Pérez, A., Romanelli, A.: Spatially dependent decoherence and anomalous diffussion of quantum walks. J. Comput. Theor. Nanosci. **10**(7), 1591–1595 (2013)
259. Peterson, D.: Gridline graphs: a review in two dimensions and an extension to higher dimensions. Discret. Appl. Math. **126**(2), 223–239 (2003)
260. Philipp, P., Portugal, R.: Exact simulation of coined quantum walks with the continuous-time model. Quantum Inf. Process. **16**(1), 14 (2017)
261. Philipp, P., Tarrataca, L., Boettcher, S.: Continuous-time quantum search on balanced trees. Phys. Rev. A **93**, 032305 (2016)
262. Piccinini, E., Benedetti, C., Siloi, I., Paris, M.G.A., Bordone, P.: GPU-accelerated algorithms for many-particle continuous-time quantum walks. Comput. Phys. Commun. **215**, 235–245 (2017)
263. Portugal, R.: Establishing the equivalence between Szegedy's and coined quantum walks using the staggered model. Quantum Inf. Process. **15**(4), 1387–1409 (2016)
264. Portugal, R.: Staggered quantum walks on graphs. Phys. Rev. A **93**, 062335 (2016)
265. Portugal, R.: Element distinctness revisited. Quantum Inf. Process. **17**(7), 163 (2018)
266. Portugal, R., Boettcher, S., Falkner, S.: One-dimensional coinless quantum walks. Phys. Rev. A **91**, 052319 (2015)
267. Portugal, R., de Oliveira, M.C., Moqadam, J.K.: Staggered quantum walks with Hamiltonians. Phys. Rev. A **95**, 012328 (2017)
268. Portugal, R., Fernandes, T.D.: Quantum search on the two-dimensional lattice using the staggered model with Hamiltonians. Phys. Rev. A **95**, 042341 (2017)
269. Portugal, R., Santos, R.A.M., Fernandes, T.D., Gonçalves, D.N.: The staggered quantum walk model. Quantum Inf. Process. **15**(1), 85–101 (2016)
270. Portugal, R., Segawa, E.: Connecting coined quantum walks with Szegedy's model. Interdiscip. Inf. Sci. **23**(1), 119–125 (2017)
271. Preiss, P.M., Ma, R., Tai, M.E., Lukin, A., Rispoli, M., Zupancic, P., Lahini, Y., Islam, R., Greiner, M.: Strongly correlated quantum walks in optical lattices. Science **347**(6227), 1229–1233 (2015)
272. Preskill, J.: Lecture Notes on Quantum Computation (1998). http://www.theory.caltech.edu/~preskill/ph229
273. Reitzner, D., Hillery, M., Koch, D.: Finding paths with quantum walks or quantum walking through a maze. Phys. Rev. A **96**, 032323 (2017)
274. Reitzner, D., Nagaj, D., Bužek, V.: Quantum walks. Acta Phys. Slov. **61**(6), 603–725 (2011)
275. Ren, P., Aleksić, T., Emms, D., Wilson, R.C., Hancock, E.R.: Quantum walks, Ihara zeta functions and cospectrality in regular graphs. Quantum Inf. Process. **10**(3), 405–417 (2011)
276. Rieffel, E., Polak, W.: Quantum Computing, a Gentle Introduction. MIT Press, Cambridge (2011)
277. Robens, C., Alt, W., Meschede, D., Emary, C., Alberti, A.: Ideal negative measurements in quantum walks disprove theories based on classical trajectories. Phys. Rev. X **5**, 011003 (2015)
278. Rodrigues, J., Paunković, N., Mateus, P.: A simulator for discrete quantum walks on lattices. Int. J. Mod. Phys. C **28**(04), 1750055 (2017)
279. Rohde, P.P., Fedrizzi, A., Ralph, T.C.: Entanglement dynamics and quasi-periodicity in discrete quantum walks. J. Modern Opt. **59**(8), 710–720 (2012)
280. Romanelli, A., Siri, R., Abal, G., Auyuanet, A., Donangelo, R.: Decoherence in the quantum walk on the line. Phys. A **347**, 137–152 (2005)
281. Ronke, R., Estarellas, M.P., D'Amico, I., Spiller, T.P., Miyadera, T.: Anderson localisation in spin chains for perfect state transfer. Eur. Phys. J. D **70**(9), 189 (2016)
282. Rosmanis, A.: Quantum adversary lower bound for element distinctness with small range. Chic. J. Theor. Comput. Sci. **4**, 2014 (2014)
283. Rossi, M.A.C., Benedetti, C., Borrelli, M., Maniscalco, S., Paris, M.G.A.: Continuous-time quantum walks on spatially correlated noisy lattices. Phys. Rev. A **96**, 040301 (2017)
284. Rudinger, K., Gamble, J.K., Bach, E., Friesen, M., Joynt, R., Coppersmith, S.N.: Comparing algorithms for graph isomorphism using discrete- and continuous-time quantum random walks. J. Comput. Theor. Nanosci. **10**(7), 1653–1661 (2013)

285. Sadgrove, M.: Quantum amplitude amplification by phase noise. Europhys. Lett. **86**(5), 50005 (2009)
286. Sadowski, P., Miszczak, J.A., Ostaszewski, M.: Lively quantum walks on cycles. J. Phys. A: Math. Theor. **49**(37), 375302 (2016)
287. Sakurai, J.J., Napolitano, J.: Modern Quantum Mechanics. Addison-Wesley, Reading (2011)
288. Salas, P.J.: Noise effect on Grover algorithm. Eur. Phys. J. D **46**(2), 365–373 (2008)
289. Sampathkumar, E.: On the line graph of subsivision graph. J. Karnatak Univ. Sci. **17**, 259–260 (1972)
290. Santha, M.: Quantum walk based search algorithms. In: Proceedings of the 5th International Conference, TAMC 2008, Xi'an, China, 2008, pp. 31–46. Springer, Berlin (2008)
291. Santos, R.A.M.: Szegedy's quantum walk with queries. Quantum Inf. Process. **15**(11), 4461–4475 (2016)
292. Santos, R.A.M., Portugal, R.: Quantum hitting time on the complete graph. Int. J. Quantum Inf. **8**(5), 881–894 (2010)
293. Santos, R.A.M., Portugal, R., Boettcher, S.: Moments of coinless quantum walks on lattices. Quantum Inf. Process. **14**(9), 3179–3191 (2015)
294. Schmitz, A.T., Schwalm, W.A.: Simulating continuous-time hamiltonian dynamics by way of a discrete-time quantum walk. Phys. Lett. A **380**(11), 1125–1134 (2016)
295. Segawa, E.: Localization of quantum walks induced by recurrence properties of random walks. J. Comput. Theor. Nanosci. **10**(7), 1583–1590 (2013)
296. Shakeel, A., Meyer, D.A., Love, P.J.: History dependent quantum random walks as quantum lattice gas automata. J. Math. Phys. **55**(12), 122204 (2014)
297. Shenvi, N., Kempe, J., Whaley, K.B.: A quantum random walk search algorithm. Phys. Rev. A **67**(5), 052307 (2003)
298. Shi, H.-L., Liu, S.-Y., Wang, X.-H., Yang, W.-L., Yang, Z.-Y., Fan, H.: Coherence depletion in the Grover quantum search algorithm. Phys. Rev. A **95**, 032307 (2017)
299. Souza, A.M.C., Andrade, R.F.S.: Discrete time quantum walk on the Apollonian network. J. Phys. A: Math. Theor. **46**(14), 145102 (2013)
300. Souza, D.S., Marquezino, F.L., Lima, A.A.B.: Quandoop: a classical simulator of quantum walks on computer clusters. J. Comput. Int. Sci. **8**, 109–172 (2017)
301. Stefaňák, M., Skoupý, S.: Perfect state transfer by means of discrete-time quantum walk on complete bipartite graphs. Quantum Inf. Process. **16**(3), 72 (2017)
302. Stefaňák, M., Kollár, B., Kiss, T., Jex, I.: Full revivals in 2D quantum walks. Phys. Scr. **2010**(T140), 014035 (2010)
303. Stolze, J., Suter, D.: Quantum Computing, Revised and Enlarged: A Short Course from Theory to Experiment. Wiley-VCH, New York (2008)
304. Stong, R.A.: On 1-factorizability of Cayley graphs. J. Comb. Theory Ser. B **39**(3), 298–307 (1985)
305. Strang, G.: Linear Algebra and Its Applications. Brooks Cole (1988)
306. Strauch, F.W.: Connecting the discrete- and continuous-time quantum walks. Phys. Rev. A **74**(3), 030301 (2006)
307. Szegedy, M.: Quantum speed-up of Markov chain based algorithms. In: Proceedings of the 45th Annual IEEE Symposium on Foundations of Computer Science, FOCS '04, pp. 32–41. Washington (2004)
308. Szegedy, M.: Spectra of quantized walks and a $\sqrt{\delta\epsilon}$ rule (2004). arXiv:quant-ph/0401053
309. Tani, S.: Claw finding algorithms using quantum walk. Theor. Comput. Sci. **410**(50), 5285–5297 (2009)
310. Tödtli, B., Laner, M., Semenov, J., Paoli, B., Blattner, M., Kunegis, J.: Continuous-time quantum walks on directed bipartite graphs. Phys. Rev. A **94**, 052338 (2016)
311. Toyama, F.M., Van Dijk, W., Nogami, Y.: Quantum search with certainty based on modified Grover algorithms: optimum choice of parameters. Quantum Inf. Process. **12**(5), 1897–1914 (2013)
312. Travaglione, B.C., Milburn, G.J.: Implementing the quantum random walk. Phys. Rev. A **65**(3), 032310 (2002)

313. Tregenna, B., Flanagan, W., Maile, R., Kendon, V.: Controlling discrete quantum walks: coins and initial states. New J. Phys. **5**(1), 83 (2003)
314. Trudeau, R.J.: Introduction to Graph Theory. Dover Books on Mathematics. Dover Publications, Mineola (2013)
315. Tulsi, A.: Faster quantum-walk algorithm for the two-dimensional spatial search. Phys. Rev. A **78**(1), 012310 (2008)
316. Tulsi, A.: General framework for quantum search algorithms. Phys. Rev. A **86**, 042331 (2012)
317. Tulsi, A.: Robust quantum spatial search. Quantum Inf. Process. **15**(7), 2675–2683 (2016)
318. Valencia-Pabon, M., Vera, J.-C.: On the diameter of Kneser graphs. Discret. Math. **305**(1), 383–385 (2005)
319. Venegas-Andraca, S.E.: Quantum Walks for Computer Scientists. Morgan and Claypool Publishers (2008)
320. Venegas-Andraca, S.E.: Quantum walks: a comprehensive review. Quantum Inf. Process. **11**(5), 1015–1106 (2012)
321. Vieira, R., Amorim, E.P.M., Rigolin, G.: Entangling power of disordered quantum walks. Phys. Rev. A **89**, 042307 (2014)
322. Wang, C., Hao, L., Song, S.Y., Long, G.L.: Quantum direct communication based on quantum search algorithm. Int. J. Quantum Inf. **08**(03), 443–450 (2010)
323. Wang, G.: Efficient quantum algorithms for analyzing large sparse electrical networks. Quantum Inf. Comput. **17**(11&12), 987–1026 (2017)
324. Wang, Y., Shang, Y., Xue, P.: Generalized teleportation by quantum walks. Quantum Inf. Process. **16**(9), 221 (2017)
325. Waseem, M., Ahmed, R., Irfan, M., Qamar, S.: Three-qubit Grover's algorithm using superconducting quantum interference devices in cavity-QED. Quantum Inf. Process. **12**(12), 3649–3664 (2013)
326. West, D.B.: Introduction to Graph Theory. Prentice Hall, Englewood Cliffs (2000)
327. Whitfield, J.D., Rodríguez-Rosario, C.A., Aspuru-Guzik, A.: Quantum stochastic walks: a generalization of classical random walks and quantum walks. Phys. Rev. A **81**, 022323 (2010)
328. Williams, C.P.: Explorations in Quantum Computing. Springer, Berlin (2008)
329. Wong, T.G.: Quantum walk search with time-reversal symmetry breaking. J. Phys. A: Math. Theor. **48**(40), 405303 (2015)
330. Wong, T.G.: Coined quantum walks on weighted graphs. J. Phys. A: Math. Theor. **50**(47), 475301 (2017)
331. Wong, T.G.: Faster search by lackadaisical quantum walk. Quantum Inf. Process. **17**(3), 68 (2018)
332. Wong, T.G., Ambainis, A.: Quantum search with multiple walk steps per oracle query. Phys. Rev. A **92**, 022338 (2015)
333. Wong, T.G., Santos, R.A.M.: Exceptional quantum walk search on the cycle. Quantum Inf. Process. **16**(6), 154 (2017)
334. Wong, T.G., Tarrataca, L., Nahimov, N.: Laplacian versus adjacency matrix in quantum walk search. Quantum Inf. Process. **15**(10), 4029–4048 (2016)
335. Xi-Ling, X., Zhi-Hao, L., Han-Wu, C.: Search algorithm on strongly regular graphs based on scattering quantum walk. Chin. Phys. B **26**(1), 010301 (2017)
336. Xu, X.-P., Ide, Y.: Exact solutions and symmetry analysis for the limiting probability distribution of quantum walks. Ann. Phys. **373**, 682–693 (2016)
337. Xu, X.-P., Ide, Y., Konno, N.: Symmetry and localization of quantum walks induced by an extra link in cycles. Phys. Rev. A **85**, 042327 (2012)
338. Yalçinkaya, I., Gedik, Z.: Two-dimensional quantum walk under artificial magnetic field. Phys. Rev. A **92**, 042324 (2015)
339. Yalouz, S., Pouthier, V.: Continuous-time quantum walk on an extended star graph: trapping and superradiance transition. Phys. Rev. E **97**, 022304 (2018)
340. Yamaguchi, F., Milman, P., Brune, M., Raimond, J.M., Haroche, S.: Quantum search with two-atom collisions in cavity QED. Phys. Rev. A **66**, 010302 (2002)

341. Yang-Yi, H., Ping-Xing, C.: Localization of quantum walks on finite graphs. Chin. Phys. B **25**(12), 120303 (2016)
342. Yao, A.C.C.: Near-optimal time-space tradeoff for element distinctness. In: Proceedings of the 29th Annual Symposium on Foundations of Computer Science, pp. 91–97 (1988)
343. Yoon, C.S., Kang, M.S., Lim, J.I., Yang, H.J.: Quantum signature scheme based on a quantum search algorithm. Phys. Scr. **90**(1), 015103 (2015)
344. Zalka, C.: Grover's quantum searching algorithm is optimal. Phys. Rev. A **60**, 2746–2751 (1999)
345. Zeng, M., Yong, E.H.: Discrete-time quantum walk with phase disorder: localization and entanglement entropy. Sci. Rep. **7**(1), 12024 (2017)
346. Zhan, X., Qin, H., Bian, Z.-H., Li, J., Xue, P.: Perfect state transfer and efficient quantum routing: a discrete-time quantum-walk approach. Phys. Rev. A **90**, 012331 (2014)
347. Zhang, F., Chen, Y.-C., Chen, Z.: Clique-inserted-graphs and spectral dynamics of clique-inserting. J. Math. Anal. Appl. **349**(1), 211–225 (2009)
348. Zhang, R., Qin, H., Tang, B., Xue, P.: Disorder and decoherence in coined quantum walks. Chin. Phys. B **22**(11), 110312 (2013)
349. Zhang, Y.-C., Bao, W.-S., Wang, X., Fu, X.-Q.: Effects of systematic phase errors on optimized quantum random-walk search algorithm. Chin. Phys. B **24**(6), 060304 (2015)
350. Zhang, Y.-C., Bao, W.-S., Wang, X., Fu, X.-Q.: Optimized quantum random-walk search algorithm for multi-solution search. Chin. Phys. B **24**(11), 110309 (2015)
351. Zhirov, O.V., Shepelyansky, D.L.: Dissipative decoherence in the Grover algorithm. Eur. Phys. J. D **38**(2), 405–408 (2006)
352. Zhou, J., Bu, C.: State transfer and star complements in graphs. Discret. Appl. Math. **176**, 130–134 (2014)

Index

A
Abelian group, 131, 279
Absorbing state, 224
Abstract algebra, 278
Abstract search algorithm, 66
Adjacency matrix, 24, 163, 272
Adjacent, 106, 203, 225, 271
Adjoint operator, 257
Amplitude amplification technique, 41, 63–66, 183, 185, 200, 202
Arc, 23, 127, 195, 277, 285
Arc notation, 125, 128, 131, 157, 196
Argument, 135
Average distribution, 153, 155
Average position, 20
Average probability distribution, 125, 139

B
Ballistic, 30, 32
Barycentric subdivision, 275
Basis, 248
Benioff, 175
Bilinear, 263
Binary sum, 43, 106
Binary vector, 108
Binomial, 40
Binomial coefficient, 203
Binomial distribution, 20
Bipartite digraph, 223, 234
Bipartite graph, 220, 273
Bipartite multigraph, 274, 275
Bipartite quantum walk, 225
Bitwise xor, 43
Black box group, 246
Bloch sphere, 252
Block diagonal, 128
Bound, 156
Bra-ket notation, 249, 250

C
Canonical basis, 251
Cardinality, 204
Cauchy–Schwarz inequality, 55, 257
Cayley graph, 131, 278
Ceiling function, 236
Characteristic function, 169
Characteristic polynomial, 52, 230
Chebyshev polynomial, 236, 241
Chirality, 118
Chromatic index, 276
Chromatic number, 276
Class 1, 125, 127, 276
Class 2, 125, 127, 276
Classical algorithm, 62
Classical bit, 253
Classical discrete-time Markov chain, 23
Classical hitting time, 223, 227, 234
Classical Markov chain, 23, 223
Classical mixing time, 156
Classical physics, 9
Classical random robot, 175
Classical random walk, 19, 35, 40, 69, 139, 156, 281
Class NP-complete, 8
Clique, 174, 204, 205, 273
Clique cover, 274
Clique graph, 161, 274, 275
Clique–insertion operator, 275
Clique partition, 274
Cliques, 159
Closed physical system, 8
Coined model, 176, 195

© Springer Nature Switzerland AG 2018

R. Portugal, *Quantum Walks and Search Algorithms*, Quantum Science and Technology, https://doi.org/10.1007/978-3-319-97813-0

Coined quantum walk, 78, 125, 126, 128, 157, 227
Coined quantum walk model, 19, 26
Coinless, 174, 223
Coin operator, 26, 126, 128, 132
Coin space, 114
Coin-position notation, 125–127
Collapse, 12
Collision problem, 220
Colorable, 161
Coloring, 276
Commutative group, 279
Complete bipartite graph, 273
Complete graph, 24, 176, 195, 197, 223, 237, 272, 281
Completeness relation, 142, 256
Complex number, 141
Composite system, 11
Computational basis, 14, 89, 251
Computational complexity, 41
Computer Physics Communications library, 86, 87
Conjugate-linear, 248, 257, 264
Connected graph, 197, 272
Continued fraction approximation, 135
Continuous-time Markov chain, 19, 33, 35
Continuous-time model, 39, 125
Continuous-time quantum walk, 35, 39, 137
Continuous-time quantum walk model, 19
Counting algorithm, 66
Cycle, 89, 126, 143, 272

D
Dagger, 257
Decision problem, 201
Decoherence, 253
Degree, 24, 106, 128, 272, 283
Degree sum formula, 272
Derived graph, 274
Detection problem, 237
Detection time, 246
Diagonalizable, 255, 256
Diagonalize, 92
Diagonal representation, 12, 255
Diagonal state, 44, 98, 107, 114, 251, 265, 268
Diameter, 277
Diamond-free graph, 272
Diamond graph, 272
Digraph, 277
Dimension, 248
Dimensionless, 72
Dirac notation, 18, 269
Directed acyclic graph, 277
Directed cycle graph, 277
Directed edge, 277
Directed graph, 127, 277
Disconnected graph, 272
Discrete model, 26
Discrete-time classical Markov chain, 223
Discrete-time Markov chain, 40
Discrete-time quantum walk, 223
Discriminant, 227
Distance, 152
Duplication process, 223, 224, 234

E
Eccentricity, 276
Edge, 19, 127
Edge-chromatic number, 125, 126, 161, 276
Edge-colorability, 157
Edge coloring, 126, 276, 129
Eigenvalue, 228, 255
Eigenvector, 228, 255
Electron, 6
Element distinctness problem, 177, 201, 202, 245
Entangled, 11
Equilibrium distribution, 283
Euler number, 190
Evolution equation, 71, 99
Evolution operator, 44, 70, 118, 126, 128, 132, 227
Expansion, 275
Expected distance, 19, 20, 69
Expected position, 20
Expected time, 281
Expected value, 13, 84, 170, 282

F
Fidelity, 157
Finding problem, 237
Finite lattice, 126
Finite vector space, 247
Flip-flop shift operator, 81, 126, 128, 132, 196
Fortran, 29
Fourier, 81
Fourier basis, 71, 72, 91, 100, 108, 142
Fourier transform, 69, 71, 89, 91, 92, 108
Fractional revival, 137, 138, 157
Fundamental period, 134, 197

G
Gamma function, 150
Gaussian distribution, 22
Generalized Toffoli gate, 43, 59, 266
Generating matrix, 33
Generating set, 278, 279
Geodesic distance, 276
Geometric series, 242
Global phase factor, 13, 252
Global sink, 277
Global source, 277
Gram–Schmidt process, 229
Graph, 19, 125, 272, 281
Graph tessellation, 159, 160, 174
Graph tessellation cover, 159, 160, 167, 174
Graph theory, 159
Grid, 175
Group, 278
Group order, 279
Grover, 66, 81
Grover coin, 98, 106, 115
Grover matrix, 107
Grover operator, 163
Grover quantum walk, 130
Grover's algorithm, 41, 195, 197, 199

H
Hadamard, 27, 81
Hadamard coin, 70
Hajós graph, 159
Half-silvered mirror, 9
Hamiltonian walk, 38
Hamming distance, 106
Hamming weight, 110, 115, 148
Handshaking lemma, 272
Head, 127, 195, 277
Hermitian, 19
Hermitian operator, 258
H-free, 272
Hilbert space, 249
Hiperwalk, 86
Hitting time, 246, 281
Homogeneous coin, 126
Homogeneous rate, 33
Hypercube, 89, 106, 126, 143, 176, 199

I
Identity operator, 253
Imaginary unit, 35
Indegree, 277
Induced subgraph, 272
Infinitesimal, 33
Infinite vector space, 248
Inflection point, 22
Initial condition, 139
In-neighborhood, 277
Inner product, 248
Inner product matrix, 227
Instantaneous uniform mixing, 156, 157
Interchange graph, 274
Intersection graph, 273
Invariant, 83, 84
Inverse Fourier transform, 79
Isolated physical system, 7

J
Java, 29
Johnson graph, 220, 246
Julia, 29

K
Kernel, 227, 229, 253
Ket, 15
Kneser graph, 278
Kronecker delta, 250
Kronecker product, 264

L
Language C, 29
Laplacian matrix, 272
Las Vegas algorithm, 63
Latin letter, 251
Lattice, 199
Laurent series, 242
Law of excluded middle, 7
Lazy random walk, 156
Leaf, 132, 276
Learning graph, 221
Least common multiple, 135
Left singular vector, 229
Left stochastic matrix, 23
Limiting distribution, 24, 89, 96, 115, 125, 139, 153, 155, 157, 283
Limiting probability distribution, 125
Linear operator, 253
Line graph, 132, 220, 246, 274
Locality, 38, 129
Local operator, 129, 130, 162, 163
Local sink, 277
Local source, 277
Loop, 24, 195, 234, 271, 285
Loopless complete graph, 195

M
Maple, 29, 36
Marked element, 42, 64
Marked vertex, 175, 176, 178, 181, 186, 191, 192, 194, 198, 200, 223, 234, 285
Markov chain, 224
Markov's inequality, 63
Matching, 274
Mathematica, 29, 36
Matrix representation, 98, 254
Maximal clique, 159, 207, 273
Maximum degree, 125, 272
Maximum indegree, 277
Measurement, 14, 16
Metric, 152
Minimum clique cover, 274
Minimum clique partition, 274
Minimum degree, 272
Minimum indegree, 277
Mixing time, 89, 115, 125
Modified evolution operator, 177
Moment, 170
Monte Carlo algorithm, 63
Moral graph, 277
Moving shift operator, 126, 128, 191
Multigraph, 132, 273, 275
Multiple edge, 132, 271
Multiplicity, 255
Multiset, 273

N
Natural logarithm, 22
Neighbor, 130, 271
Neighborhood, 271, 283
Non-bipartite, 139
Non-homogeneous coin, 126, 191, 195, 197
Non-orthogonal projector, 258
Norm, 134, 137, 249
Normal, 257
Normal distribution, 22
Normalization condition, 70, 80, 107
Normalization constant, 72
Normalized vector, 249
Normal matrix, 227
North pole, 252
NP-complete, 276
Nullity, 253
Null operator, 253
Nullspace, 253

O
Observable, 12
Optimal algorithm, 41, 53
Optimality, 66
Oracle, 42
Orthogonal, 249
Orthogonal complement, 249, 258
Orthogonal projector, 12, 258
Orthonormal, 249
Orthonormal basis, 91
Outdegree, 223, 224, 277
Outer product, 250
Out-neighborhood, 277

P
Pair of symmetric arcs, 277
Para-line graph, 275
Parity, 95, 97
Partial inner product, 138
Partial measurement, 16
Partition, 159
Path, 272
Pauli matrices, 259
Perfect matching, 274
Perfect state transfer, 125, 137, 138, 157, 174
Periodic, 134, 197
Periodic boundary condition, 98
Perron-Frobenius theorem, 287
Persitent random walk, 87
Petersen graph, 278
Phase, 13, 135
Phase estimation, 66
Polygamma function, 190
Polygon, 160, 197
Position-coin notation, 125, 127, 196
Position standard deviation, 20
Positive definite operator, 258
Positive operator, 258
Postulate of composite systems, 11
Postulate of evolution, 8
Postulate of measurement, 12
Principal eigenvalue technique, 177, 178, 184, 187, 190, 192, 195, 198, 199, 212, 216
Probabilistic classical bit, 253
Probability amplification, 63
Probability amplitude, 70, 77
Probability distribution, 13
Probability matrix, 23, 283
Probability theory, 169
Program QWalk, 86
Projective measurement, 12, 140
Projector, 237, 243
Promise, 42

PyCTQW, 86
Python, 29

Q
Q-circuit, 266
QSWalk, 87
QSWalk.jl, 87
Quantization, 25
Quantize, 33
Quantum algorithm, 9, 19
Quantum computation, 18, 247
Quantum computer, 19
Quantum database, 41
Quantum hitting time, 223, 227, 233–235, 245, 286
Quantum mechanics, 170, 176, 248
Quantum mixing time, 155–157
Quantum query model, 201
Quantum random walk, 25
Quantum robot, 175
Quantum transport, 125
Quantum-walk-based search algorithm, 126, 176, 199
Quantum walk dynamic, 125
Quantum walks, 19
Quasi-periodic, 125, 134, 153
Quasi-periodic behavior, 125
Quasi-periodic dynamic, 133
Qubit, 11, 251
Query complexity, 45
QwViz, 86

R
Randomness, 25
Random number generator, 63
Random variable, 169
Random walk, 175, 224
Rank, 253
Rank-nullity theorem, 253
Recursive equation, 24
Reduced evolution operator, 93, 120, 142
Reflection, 227
Reflection operator, 46, 226
Register, 11, 43, 267
Regular graph, 106, 125, 126, 272
Relative phase factor, 13
Relativistic chessboard model, 39
Renormalization, 16
Renormalization group, 87
Reverse triangle inequality, 56
Reversibility, 43
Right singular vector, 229
Right stochastic matrix, 224, 283
Root graph, 274
Running time, 48, 178, 183, 220, 237

S
Sage, 29
Sample space, 169
Schrödinger equation, 9
Schrödinger's cat, 8
Search algorithm, 41
Self-adjoint operator, 258
Shift operator, 26, 70, 90, 98, 105, 106
Similar, 255
Similarity transformation, 261
Simple digraph, 277
Simple graph, 159, 271, 272
Singular value, 227, 228
Singular value decomposition, 228
Singular vector, 227, 228
Sink, 223, 224, 234, 277
Source, 277
South pole, 252
Spatial search algorithm, 177, 199
Spatial search problem, 175
Spectral decomposition, 52, 114, 134, 167, 228
Spherical Bessel function, 242
Spin, 6
Spin chain, 137
Spin down, 6
Spin up, 6
Stable set, 274
Staggered model, 125, 159, 174, 176, 220
Staggered model with Hamiltonians, 162
Staggered quantum walk, 138, 246
Staggered quantum walk model, 197, 204, 205
Standard deviation, 13, 69, 84
Standard evolution operator, 90, 99, 107
State, 5, 223, 252
State space, 7, 223
State space postulate, 7, 12, 176
State vector, 7, 252
Stationary distribution, 139, 223, 282, 283
Stirling's approximation, 22, 40
Stochastic, 26, 140
Stochastic matrix, 23, 223
Stochastic process, 223
Subdivision, 275
Subgroup, 279
Subset finding, 220, 221
Subspace, 249

Success probability, 176, 178, 183, 199, 220
Support, 253
Symmetric, 279
Symmetrical, 153
Symmetric arc, 127, 129
Symmetric bipartite digraph, 223
Symmetric bipartite graph, 223
Symmetric digraph, 125, 127, 277, 285
Symmetric directed graph, 277
Symmetric generating set, 131
Symmetric multidigraph, 132
Symmetric probability distribution, 78
Sync function, 242
Szegedy's model, 220, 286

T
Tail, 127, 195, 277
Taylor series, 34
Tensor product, 11, 263
k-tessellable, 160
k-tessellable quantum walk, 163
1-tessellable, 197
2-tessellable, 220
2-tessellable quantum walk, 132, 138
Tessellation, 138, 197
Tessellation cover, 138, 197
Tessellation cover number, 160
Three-dimensional infinite lattice, 69
Tile, 160
Time complexity, 42, 45
Time evolution, 8
Time-homogeneous Markov chain, 224
Time-independent evolution operator, 125, 133
Torus, 89, 98, 175
Total variation distance, 152
Trace, 261
Transition matrix, 23, 224, 227, 283
Transition rate, 19, 33
Transpose-conjugate, 257
Triangle finding, 220, 221
Triangle-free graph, 274, 275
Triangle inequality, 55, 153
Trivial tessellation, 160
Tulsi's modification, 183, 191, 218, 246
Two-dimensional infinite lattice, 69
Two-dimensional lattice, 89, 143, 175, 199
Two-dimensional spacetime, 39

U
Unbiased coin, 78
Uncertainty principle, 16
Uncoupled quantum walk, 82
Underlying digraph, 224
Underlying graph, 277
Underlying symmetric digraph, 157
Undirected edge, 195
Undirected labeled multigraph, 273
Uniform distribution, 282
Uniform rate, 33
Unit vector, 249, 251
Unitary operator, 257
Unitary transformation, 8
Universal gates, 41, 45, 268, 269
Universal quantum computation, 39
Unstructured search, 201

V
Vector space, 247
Vertices, 19

W
Wavefront, 95
Wave number, 72
Wheel graph, 161

X
Xor, 269

Z
Zero matrix, 254